UNIVERSIDADE DE COIMBRA

Anísio Alberto Martinho de Andrade

ONE-DIMENSIONAL MODELS FOR THE SPATIAL BEHAVIOUR OF TAPERED THIN-WALLED BARS WITH OPEN CROSS-SECTIONS: STATIC, DYNAMIC AND BUCKLING ANALYSES

A Thesis submitted to the Faculty of Sciences and Technology of the University of Coimbra in fulfillment of the requirements for the degree of Doctor of Philosophy in Civil Engineering (Structures)

July, 2012

In memoriam

Anísio Ferreira de Andrade

ABSTRACT

Tapered thin-walled bars are extensively used in the fields of civil, mechanical and aeronautical engineering. The competitiveness of tapered structural members is hindered by the fact that their spatial behaviour is still poorly understood and by the lack of rational and efficient methods for their analysis and design. The present thesis aims at providing a contribution to overcome these drawbacks, by (i) developing one-dimensional models (*i.e.*, models having a single independent spatial variable) to perform linear static, dynamic and lateral-torsional buckling analyses of tapered thin-walled bars with open cross-sections, (ii) supplying physical interpretations for the key behavioural features implied by these models and (iii) offering a detailed examination of several illustrative examples that will be useful for benchmarking purposes.

The first part of the thesis is devoted to bars whose shape allows them to resist biaxial bending by the membrane action of their walls (I-section or C-section bars, for instance). It starts with the development, based on the induced-constraint approach, of a linear one-dimensional model for the stretching, bending and twisting of tapered thin-walled bars with arbitrary open cross-sections under general static loading conditions. A two-dimensional linearly elastic membrane shell model is adopted as parent theory. The Vlasov assumptions, extended to the tapered case in such a way as to retain an intrinsic geometrical meaning, are treated consistently as internal constraints, that is, *a priori* restrictions, of a constitutive nature, on the possible deformations of the middle surface of the bar. Accordingly, (i) the membrane forces are decomposed additively into active and reactive parts, and (ii) the constitutive dependence of the active membrane forces on the membrane strains reflects the maximal symmetry compatible with the assumed internal constraints.

For a large class of tapered thin-walled bars with open cross-sections, the membrane strain and force fields implied by the internal constraints do not have the same form as in Vlasov's prismatic bar theory – they feature an extra term, involving the rate of twist. Consequently, the torsional behaviour (be it uncoupled or coupled with other modes of deformation) predicted by our tapered model is generally at odds with that obtained using a

piecewise prismatic (stepped) approach. The discrepancies may be significant, as illustrated through examples.

The developed linear model is then extended into the dynamic range. The contributions of rotatory inertia and torsion-warping inertia are fully taken into account. The inclusion of a viscous-type dissipative mechanism is briefly addressed.

Subsequently, we derive a model for the elastic lateral-torsional buckling of singly symmetric tapered thin-walled beams with arbitrary open cross-sections, loaded in the plane of greatest bending stiffness. The adopted kinematical description rules out any local or distortional phenomena. Moreover, the effect of the pre-buckling deflections is ignored. Since isolated beams with idealised support conditions are seldom found in actual design practice, an archetypal problem is used to show how the presence of out-of-plane restraints can be accommodated in the one-dimensional buckling model. The restraints may (i) have a translational, torsional, minor axis bending and/or warping character, and (ii) be either linearly elastic or perfectly rigid.

The second part of the thesis is concerned with strip members (*i.e.*, members with a narrow rectangular cross-section) exhibiting constant thickness and varying depth. It deals with three problems of increasing complexity:

(i) the elastic lateral-torsional buckling of cantilevered beams with linearly varying depth, acted at the free-end section by a conservative point load;

(ii) the elastic lateral-torsional buckling of cantilevers (ii_1) whose depth varies according to a non-increasing polygonal function of the distance to the support and (ii_2) which are subjected to an arbitrary number of independent conservative point loads;

(iii) the elastic flexural-torsional buckling of linearly tapered cantilever beam-columns, acted by axial and transverse point loads applied at the free-end section.

These three problems are tackled analytically – we obtain exact closed-form solutions to the governing differential equations and, thereby, establish exact closed-form characteristic equations for the buckling loads. However, in the third problem, the analytical approach is successful only for certain values of the ratio between the minimal and maximal depth of the strip beam-column – in the remaining cases, it is necessary to resort to a numerical procedure.

RESUMO

Modelos Unidimensionais para o Comportamento Espacial de Barras Não Prismáticas com Secção de Parede Fina Aberta – Análises Estática, Dinâmica e de Encurvadura

As barras não prismáticas de parede fina são largamente utilizadas em engenharia civil, mecânica e aeronáutica. A competitividade destes elementos estruturais é prejudicada pelo facto de o seu comportamento espacial ser ainda mal compreendido e pela falta de métodos eficientes para a sua análise e dimensionamento. Esta tese visa dar um contributo para superar estas dificuldades, através (i) do desenvolvimento de modelos unidimensionais (isto é, modelos com uma única variável espacial independente) para efectuar análises lineares, em regime estático ou dinâmico, e de encurvadura lateral por flexão-torção de barras com secção de parede fina aberta continuamente variável, (ii) da interpretação física dos aspectos essenciais do comportamento destas barras, tal como previsto por estes modelos, e (iii) do exame detalhado de alguns exemplos ilustrativos, com utilidade para efeitos de verificação e validação.

A primeira parte da tese é dedicada às barras cuja forma lhes permite resistir a flexão biaxial por acção de membrana das suas paredes (barras com secção em I ou em C, por exemplo). Começa com o desenvolvimento de um modelo linear unidimensional para a flexão e torção de barras não prismáticas com secção de parede fina aberta arbitrária, submetidas a carregamentos estáticos genéricos. Como ponto de partida, adopta-se um modelo bidimensional de membrana. As hipóteses de Vlasov, generalizadas ao caso não prismático de forma a manterem um significado intrínseco, são tratadas como constrangimentos internos, isto é, restrições de natureza constitutiva às possíveis deformações da superfície média da barra. Assim, (i) as forças de membrana são decompostas em parcelas activa e reactiva e (ii) a relação constitutiva entre as forças de membrana activas e as deformações de membrana reflecte a simetria máxima compatível com os constrangimentos internos impostos.

Em geral, os constrangimentos internos admitidos implicam que as expressões analíticas que definem os campos de deformações e forças de membrana em barras não prismáticas incluem uma parcela adicional, associada à torção, em relação às da teoria de Vlasov para barras prismáticas. Assim, o comportamento torsional previsto pelo modelo unidimensional

desenvolvido contrasta, em geral, com o obtido através de uma modelação "em escada", em que uma barra não prismática é aproximada por uma sequência de segmentos prismáticos. Os exemplos ilustrativos apresentados permitem concluir que as diferenças podem ser significativas.

O modelo linear desenvolvido é depois generalizado para o caso da análise dinâmica. As contribuições das inércias de rotação e de empenamento de torção são tomadas em consideração. Discute-se também a inclusão de um mecanismo de dissipação do tipo viscoso.

Em seguida, estabelece-se um modelo unidimensional para a encurvadura lateral por flexão-torção de vigas monossimétricas não prismáticas com secção de parede fina aberta arbitrária. A descrição cinemática adoptada exclui a consideração de fenómenos locais ou distorcionais. O efeito dos deslocamentos de pré-encurvadura é também ignorado. Uma vez que, na prática, é raro encontrar vigas isoladas e com condições de apoio ideais, mostra-se ainda, através de um problema arquétipo, como se pode ter em consideração a presença de elementos de contraventamento. Estes elementos podem (i) restringir a translação, a torção, a rotação em torno do eixo de menor inércia e/ou o empenamento por torção e (ii) ser rígidos ou exibir um comportamento elástico linear.

A segunda parte da tese diz respeito a elementos com secção rectangular fina de espessura constante e altura variável. São estudados três problemas de complexidade crescente:

(i) a encurvadura lateral por flexão-torção de consolas com altura linearmente variável e submetidas a uma carga pontual transversal aplicada na extremidade livre;
(ii) a encurvadura lateral por flexão-torção de consolas (ii_l) com variação poligonal da altura e (ii_l) submetidas a um número arbitrário de cargas pontuais transversais independentes;
(iii) a encurvadura por flexão-torção de colunas-viga em consola com altura linearmente variável, actuadas por uma carga pontual axial e outra transversal, ambas aplicadas na extremidade livre.

Estes três problemas são resolvidos analiticamente – obtêm-se soluções exactas para as equações diferenciais que os regem, o que permite estabelecer, também de forma exacta, as equações características para determinar as cargas de encurvadura. No entanto, no terceiro dos problemas elencados, a abordagem analítica só dá frutos numa determinada gama de relações entre as alturas mínima e máxima, sendo necessário recorrer a um procedimento numérico nos restantes casos.

KEYWORDS

Tapered thin-walled bars with open cross-sections

Strip beams and beam-columns

One-dimensional models

Linear static analysis

Linear dynamic analysis

Lateral-torsional buckling

Non-uniform torsion

Eigenproblems

PALAVRAS-CHAVE

Barras não prismáticas com secção de parede fina aberta

Vigas e colunas-viga de secção rectangular fina

Modelos unidimensionais

Análise estática linear

Análise dinâmica linear

Encurvadura lateral por flexão-torção

Torção não uniforme

Problemas de valores e funções próprios

ACKNOWLEDGMENTS

I would like to express my sincere gratitude to Professors Paulo Providência e Costa and Dinar Camotim for their advice and unflinching encouragement during the course of this work. Their high standards of scholarship and keen eye for detail have made this thesis a better one. Their philosophical attitude, which provided me with the freedom to pursue my own research interests, is equally appreciated.

I also wish to thank Professor Luís Cruz Simões, head of the Structural Analysis Group, for his incentive and support.

The joint work with Prof. Challamel was deeply stimulating and rewarding.

A special word of gratitude is due to my friends and colleagues Alfredo Dias and Ricardo Costa for many enjoyable discussions and helpful suggestions.

The financial support of the Portuguese Foundation for Science and Technology (FCT) through the Doctoral Grant SFRH/BD/39115/2007 is gratefully acknowledged.

It is a pleasure to thank my friend Rui Prata Ribeiro and his charming family for their enthusiastic encouragement.

My deepest gratitude goes to my family, without whose love and unconditional support this thesis would never have been completed.

TABLE OF CONTENTS

Chapter 3

A LINEAR ONE-DIMENSIONAL MODEL FOR THE STRETCHING, BENDING AND TWISTING OF TAPERED THIN-WALLED BARS WITH OPEN CROSS-SECTIONS

Chapter 4

ONE-DIMENSIONAL MODEL FOR THE LATERAL-TORSIONAL BUCKLING OF SINGLY SYMMETRIC TAPERED THIN-WALLED BEAMS WITH OPEN CROSS-SECTIONS

Chapter 5

LATERAL-TORSIONAL BUCKLING OF STRIP BEAMS WITH LINEARLY TAPERED DEPTH

Chapter 6

LIST OF FIGURES

Chapter 2

Chapter 3

Chapter 4

Chapter 5

LIST OF TABLES

Chapter 2

Chapter 3

Chapter 4

Chapter 5

LIST OF SYMBOLS

Sets and maps

$\cup$ Union

$\cap$ Intersection

$\subset$ is a subset of, is contained in

$\in$ is an element of, belongs to

$\notin$ is not an element of, does not belong to

$\forall$ universal quantifier

$\varnothing$ empty set

$\{x\}$ set having x as unique element

$\{x_1, \cdots, x_N\}$ set of elements of a finite sequence

$\{x \in X \mid P(x)\}$ set of elements of X having the property P

$\overline{X}$ closure of the set X

$X \setminus Y$ complement of Y in X

$X \times Y$ Cartesian product of the sets X and Y

(x, y) ordered pair

$X_1 \times \cdots \times X_N$ Cartesian product of N sets $X_1, \cdots, X_N$

X^N Cartesian product of N sets equal to X

$(x_1, \cdots, x_N)$ ordered N-tuple

$\mathbb{Z}$ ring of integers

$\mathbb{Z}^+$ set of positive integers

$\mathbb{Z}_0^+$ set of non-negative integers

$\mathbb{Z}_0^-$ set of non-positive integers

$\mathbb{R}$ field of real numbers

$\mathbb{R}^+$ set of positive real numbers

$\mathbb{R}_0^+$ set of non-negative real numbers

$\overline{\mathbb{R}}$ extended real line

$+\infty, -\infty$ points at infinity in $\overline{\mathbb{R}}$

$\mathbb{C}$ field of complex numbers

(x, y) open interval (resp. open segment) of $\mathbb{R}$ (resp. of $\mathbb{C}$) with extremities x and y

$[x, y]$ closed interval (resp. closed segment) of $\mathbb{R}$ (resp. of $\mathbb{C}$) with extremities x and y

$\mathrm{Re}(z)$ real part of the complex number z

$\mathrm{Im}(z)$ imaginary part of the complex number z

$|x|$ absolute value, or modulus, of the real or complex number x

$\overline{z}$ conjugate of the complex number z

$f : X \to Y$ or $x \in X \mapsto f(x) \in Y$ map, or function, from X into Y

$f(x)$ value of the map f at x

$f[A]$ direct image of $A \subset X$ by the map $f : X \to Y$

$f^{-1}[B]$ inverse image of $B \subset Y$ by the map $f : X \to Y$

$f \,|\, A$ restriction of the map f to the subset A of its domain

f^{-1} inverse of the bijective map f

$f \circ g$ composite map (f following g)

$f(\cdot, y)$ (resp. $f(x, \cdot)$) partial map $x \mapsto f(x, y)$ (resp. $y \mapsto f(x, y)$) of f

$C^0(X; Y)$ set of all continuous maps from a topological space X into a topological space Y

$C^0(X)$ $= C^0(X; \mathbb{R})$

Linear algebra and geometry

$\cdot$ inner product on a generic *n*-dimensional Euclidean vector space $\mathcal{U}$; in particular, inner product on $\mathcal{V}$

: inner product on $\mathscr{L}(\mathcal{U})$, induced by the inner product on $\mathcal{U}$

$\oplus$ direct sum of vector spaces

$\times$ cross product on $\mathcal{V}$

$\otimes$ tensor product

$\| \ \|$ norm on a generic *n*-dimensional Euclidean vector space $\mathcal{U}$; in particular, norm on $\mathcal{V}$

$\| \ \|_F$ Frobenius norm on $\mathscr{L}(\mathcal{U})$

$\| \ \|_{L^2}$ L^2 norm in the space of equivalence classes of almost everywhere equal square-integrable functions

$\mathscr{E}$ three-dimensional Euclidean point space

$\{\boldsymbol{e}_1, \boldsymbol{e}_2, \boldsymbol{e}_3\}$ fixed positive orthonormal ordered basis for $\mathcal{V}$

$\mathscr{L}(\mathbb{R}, \mathcal{V})$ space of all linear transformations from $\mathbb{R}$ into $\mathcal{V}$, identified with $\mathcal{V}$ itself

$\mathscr{L}(\mathcal{U})$ space of all linear transformations from $\mathcal{U}$ into itself

$O \in \mathscr{E}$ origin of a Cartesian frame

$\boldsymbol{R}$, $\mathfrak{Q}$ rotations

$SO(\mathcal{U})$ set of all rotations in $\mathscr{L}(\mathcal{U})$

span$\{\cdot\}$ vector space spanned by $\{\cdot\}$

tr trace

$\mathcal{U}$ generic *n*-dimensional Euclidean vector space

$\mathcal{V}$ three-dimensional Euclidean vector space associated with $\mathscr{E}$ (oriented)

$\hat{x}$ coordinate system associated with a given Cartesian frame for $\mathscr{E}$

$\hat{x}_i$ Coordinate functions of $\hat{x}$

$\delta_{\alpha\beta}$ Kronecker delta

Differential calculus

$f'(x), Df(x)$ (total) derivative of f at x

f', Df (total) derivative (as a map)

$D_i f$ Partial derivative of f with respect to the i^{th} variable

$f'', D^2 f, \cdots, f^{(p)}, D^p f$ higher-order derivatives of f

$D_i D_j f, \cdots, D_i^p D_j^q f$ higher-order partial derivatives of f

$C^n(A;Y)$ space of all n times continuously differentiable maps from a subset A of a normed vector space (or Euclidean point space) into a normed vector space (or Euclidean point space) Y

$C^n(A)$ $= C^n(A;\mathbb{R})$

δ variation

Special functions

a, b parameters of Kummer's function and Kummer's equation

$(a)_n$ Pochhammer's symbol for the rising factorial

Γ Gamma function

J_ν Bessel function of the first kind of order ν

Y_ν canonical Bessel function of the second kind of order ν

M Kummer's function

$P(m)$ indicial polynomial

U principal branch of Tricomi's function

Reference shape and differential geometry of surfaces

A cross-sectional area

A^* cross-sectional area evaluated with the reduced wall thickness t^*

$\mathcal{A}_{x_1}$ intersection of $\mathcal{B}$ and the plane $\left\{X \in \mathcal{E} \,\middle|\, \hat{x}_1(X) = x_1\right\}$, identified with a cross-section

$\mathscr{A}_0$, $\mathscr{A}_L$ end cross-sections

$\{\boldsymbol{a}_1(\theta^1,\theta^2), \boldsymbol{a}_2(\theta^1,\theta^2)\}$ covariant basis at $(\theta^1,\theta^2)\in\bar{\Omega}$ associated with the parametrisation F

$\boldsymbol{a}_3(\theta^1,\theta^2)$ unit vector orthogonal to $\{\boldsymbol{a}_1(\theta^1,\theta^2), \boldsymbol{a}_2(\theta^1,\theta^2)\}$

$a_{\alpha\beta}(\theta^1,\theta^2)$ metric coefficients

$\left[a_{\alpha\beta}(\theta^1,\theta^2)\right]$ matrix of metric coefficients

$a(\theta^1,\theta^2)$ determinant of the matrix $\left[a_{\alpha\beta}(\theta^1,\theta^2)\right]$ of metric coefficients

$\mathscr{B}$ reference (unloaded) shape of a tapered thin-walled bar with open cross-sections, identified with the bar itself

b_f flange width

b_b bottom flange width

b_t top flange width

$dS(X)$ area form at $X\in\mathscr{S}$

$F:\bar{\Omega}\to\mathscr{E}$ parametrisation of $\mathscr{S}$ $(\mathscr{S}=F[\bar{\Omega}])$

$\mathfrak{F}:\bar{\Omega}\times\left[-\frac{1}{2},\frac{1}{2}\right]\to\mathscr{E}$ canonical extension of the parametrisation F

h cross-section depth (in I- and C-section bars, h is measured between flange middle lines)

h_0 $=h(0)$

I_2 , I_3 , I_{23} cross-sectional second moments of area

I_2^* , I_3^* , I_{23}^* cross-sectional second moments of area evaluated with the reduced wall thickness t^*

$\mathrm{I}_X:T_X\mathscr{S}\to\mathbb{R}$ first fundamental form of $\mathscr{S}$ at $X\in\mathscr{S}$.

I_ω , $I_{2\omega}$, $I_{3\omega}$ cross-sectional second sectorial moments

I_{ω_S} , $I_{2\omega_S}$, $I_{3\omega_S}$ cross-sectional second sectorial moments evaluated with the sectorial coordinate ω_S (in prismatic bars)

I_ω^* , $I_{2\omega}^*$, $I_{3\omega}^*$ cross-sectional second sectorial moments evaluated with the reduced wall thickness t^*

I_ψ^*, $I_{2\psi}^*$, $I_{3\psi}^*$, $I_{\omega\psi}^*$, S_ψ^* geometrical properties concerning the taper function ψ and thus peculiar to tapered bars

L length

$\mathscr{L}_{x_1}$ intersection of $\mathscr{S}$ and the plane $\left\{X \in \mathscr{E} \,\middle|\, \hat{x}_1(X) = x_1\right\}$, identified with a cross-section middle line

$\left\{\boldsymbol{o}_{\mathrm{I}}(\theta^1,\theta^2), \boldsymbol{o}_{\mathrm{II}}(\theta^1,\theta^2)\right\}$ orthonormal ordered basis for $T_{F(\theta^1,\theta^2)}\mathscr{S}$ with $\boldsymbol{o}_{\mathrm{I}}(\theta^1,\theta^2) \in \mathscr{T}^{\perp}_{F(\theta^1,\theta^2)}$ and $\boldsymbol{o}_{\mathrm{I}}(\theta^1,\theta^2) \in \mathscr{T}_{F(\theta^1,\theta^2)}$

$\mathscr{S}$ middle surface of $\mathscr{B}$, identified with the middle surface of the bar

S_2, S_3 cross-sectional first moments of area

S_2^*, S_3^* cross-sectional first moments of area evaluated with the reduced wall thickness t^*

S_ω cross-sectional first sectorial moment

$S_{\omega_S}\ (=0)$ cross-sectional first sectorial moment evaluated with the sectorial coordinate ω_S (in prismatic bars)

S_ω^* cross-sectional first sectorial moment evaluated with the reduced wall thickness t^*

$t(\theta^1,\theta^2)$ wall thickness

$t^*(\theta^1,\theta^2)$ reduced wall thickness (defined in equation (2.5.4))

t_f flange thickness

t_b bottom flange thickness

t_t top flange thickness

t_w web thickness

$T_X\mathscr{S}$ tangent plane to $\mathscr{S}$ at the point X

$\mathscr{T}_X$ subspace of all vectors tangent at $X \in \mathscr{S}$ to the cross-section middle line passing through that point

$\mathscr{T}_X^{\perp}$ orthogonal complement of $\mathscr{T}_X$ in $T_X\mathscr{S}$

$\overline{x}_i = \hat{x}_i \circ F$ maps that assign to each $(\theta^1, \theta^2) \in \overline{\Omega}$ the Cartesian coordinates of the point $F(\theta^1, \theta^2) \in \mathscr{S}$

x_{3b} x_3-coordinate of the bottom flange middle plane

x_{3t} x_3-coordinate of the top flange middle plane

x_2^S, x_3^S coordinates defining the line of shear centres in prismatic bars

$\alpha(\theta^1, \theta^2)$ angle between the vectors $\boldsymbol{a}_1(\theta^1, \theta^2)$ and $\boldsymbol{a}_2(\theta^1, \theta^2)$

$\alpha, \alpha_b, \alpha_t, \alpha_w, \beta$ taper ratios

β_2 pismatic counterpart of β_2^*

β_2^* geometrical property of the reference shape related to its asymmetry with respect to the plane passing through the origin O and spanned by $\{\boldsymbol{e}_1, \boldsymbol{e}_2\}$

$\varphi, \varphi_b, \varphi_t$ inclinations of the flanges with respect to the planes spanned by $\{\boldsymbol{e}_1, \boldsymbol{e}_2\}$

$\boldsymbol{\kappa}_{\omega 0}$ non-dimensional ratio $= \dfrac{\pi}{L}\sqrt{\dfrac{\tilde{E}I_\omega^*(0)}{GJ(0)}}$

$\boldsymbol{\kappa}_{J0}$ non-dimensional ratio $= \dfrac{h_0\, t_w^3}{3\, J(0)}$

$\overline{\Omega}$ domain of the parametrisation F; vertically simple region of $\mathbb{R}^2$

θ^1, θ^2 Gaussian coordinates on $\mathscr{S}$ associated with the parametrisation F

θ^3 transverse variable

Kinematics

$\{d\}$ column vector of generalised displacements

$\{e\}$ column vector of generalised strains

$\boldsymbol{G}$ Non-linear membrane strain tensor field associated with a given (smooth enough) middle surface displacement field

$G_{\alpha\beta}$ covariant component fields of $\boldsymbol{G}$

$G_{\Sigma\Lambda}(\theta^1, \theta^2)$ components of $\boldsymbol{G}(\theta^1, \theta^2)$ with respect to the orthonormal ordered basis $\{\boldsymbol{o}_{\mathrm{I}}(\theta^1, \theta^2), \boldsymbol{o}_{\mathrm{II}}(\theta^1, \theta^2)\}$

$G_{\text{I-I}}^{2^{nd}\ order}(\theta^1,\theta^2)$ second-order part of the strain $G_{\text{I-I}}(\theta^1,\theta^2)$

$[L],[L_1],[L_2]$ formal linear differential operators

$[L]^{\dagger}$ formal adjoint differential operator of $[L]$

$\boldsymbol{U}$ admissible displacement field or motion of the middle surafce

$\boldsymbol{U}^{f}$ admissible displacement field of the middle surface in a fundamental equilibrium state

$\boldsymbol{u}$ incremental displacement field of the middle surface from a fundamental state

U_i Cartesian component fields of $\boldsymbol{U}$

u_i Cartesian component fields of $\boldsymbol{u}$

$v_1,v_2,v_3,\Xi_1,\Xi_2,\Xi_3,v_\omega$ generalised velocities

$\{v\}$ column vector of generalised velocities

W_1,W_2,W_3,Φ_1 generalised displacements

$\hat{W}_1,W_{S.2},W_{S.3},\Phi_1$ alternative set of generalised displacements for prismatic bars, with $W_{S.2}$ and $W_{S.3}$ referred to the line of shear centres

w_1,w_2,w_3,ϕ_1 generalised incremental displacements

$w_1,w_{S.2},w_{S.3},\phi_1$ alternative set of generalised incremental displacements for prismatic beams, with $w_{S.2}$ and $w_{S.3}$ referred to the line of shear centres

$w_{2.cr},\phi_{1.cr}$ components of critical bukling mode

$\tilde{w},\tilde{\phi}$ non-dimensional counterparts of w_2,ϕ_1

$\tilde{w}_{cr},\tilde{\phi}_{cr}$ non-dimensional counterparts of $w_{2.cr},\phi_{1.cr}$

$\varepsilon,\kappa_1,\kappa_2,\kappa_3,\Gamma$ generalised strains

$\boldsymbol{\gamma}$ linearised membrane strain tensor field associated with a given (smooth enough) displacement field $\boldsymbol{U}$

$\gamma_{\alpha\beta}$ covariant component fields of $\boldsymbol{\gamma}$

$\gamma_{\Sigma\Lambda}(\theta^1, \theta^2)$ components of $\boldsymbol{\gamma}(\theta^1, \theta^2)$ with respect to the orthonormal ordered basis $\{\boldsymbol{o}_{\mathrm{I}}(\theta^1, \theta^2), \boldsymbol{o}_{\mathrm{II}}(\theta^1, \theta^2)\}$

ω warping function; sectorial coordinate

ω_S sectorial coordinate with pole at the shear center and origin at a sectorial centroid (in prismatic bars)

ψ taper function

τ time

Loads

b applied distributed bimomental load per unit length of the line segment $\{O + \theta^1 \boldsymbol{e}_1, 0 \le \theta^1 \le L\}$, evaluated with the warping function ω

b_S Applied distributed bimomental load evaluated with the sectorial coordinate ω_S (in prismatic bars)

B_0, B_L applied concentrated bimoments at the end sections

$\boldsymbol{m}$ applied distributed moment per unit length of the line segment $\{O + \theta^1 \boldsymbol{e}_1, 0 \le \theta^1 \le L\}$

$\boldsymbol{M}_0$, $\boldsymbol{M}_L$ applied concentrated moments at the end sections

$m_{S.1}$ applied distributed torque about the line of shear centres (in prismatic bars)

$\boldsymbol{q}$ applied distributed force per unit length of the line segment $\{O + \theta^1 \boldsymbol{e}_1, 0 \le \theta^1 \le L\}$

$\{q\}$ column vector of distributed bar loads corresponding to the generalised displacements $\{d\}$,

$\boldsymbol{Q}_0$, $\boldsymbol{Q}_L$ applied concentrated forces at the end sections

x_3^q, x_3^Q x_3-coordinates of the points of application of loads

ε, ζ_Q non-dimensional load position parameters

λ, λ_n load factors

$\lambda_{cr}, \lambda_{n.cr}$ critical values of λ, λ_n

$\lambda_b^{(n)}$ buckling value of the load factor λ corresponding to the n^{th} mode

γ, γ_n non-dimensional loads

$\gamma_{cr}, \gamma_{n.cr}$ critical values of γ, γ_n

$\gamma_b^{(n)}$ buckling value of the non-dimensional load γ corresponding to the n^{th} mode

μ non-dimensional applied torque

Constitutive equations and energy functionals

$\tilde{A}$ material part of $I\tilde{I}$

$\tilde{B}$ geometrical part of $I\tilde{I}$ per unit value of the non-dimensional load γ

$\mathbb{C}$ elasticity tensor field

$\mathscr{C}_{(\theta^1,\theta^2)}$ constraint space

$\mathscr{C}^{\perp}_{(\theta^1,\theta^2)}$ orthogonal complement of $\mathscr{C}_{(\theta^1,\theta^2)}$

$\mathscr{D}$ domain of a functional

$\tilde{E}$ modified elastic modulus

E_{I} Young modulus relative to the direction $\boldsymbol{o}_{\text{I}}(\theta^1,\theta^2)$

G shear modulus

$[I]$ inertia matrix

$[K]$ stiffness matrix

k_{R1}, k_{Rf}, k_T stiffness of end restraints

$\mathfrak{L}$ Lagrangian

$\mathfrak{S}$ Hamiltonian action

T kinetic energy

U strain energy

U_m membrane strain energy

U_{SV} Strain energy associated with Saint-Venant torsion

W_e work of the external loads

$W_{e2.ref}$ second-order part of the work performed by the reference load system in the displacement $\boldsymbol{u}$

x_3^T x_3-coordinate of translational restraint

μ_d viscous damping coefficient

$\nu_{\text{I·II}}, \nu_{\text{II·I}}$ Poisson ratios relative to the ordered pairs $\left(\boldsymbol{o}_{\text{I}}(\theta^1,\theta^2), \boldsymbol{o}_{\text{II}}(\theta^1,\theta^2)\right)$ and $\left(\boldsymbol{o}_{\text{II}}(\theta^1,\theta^2), \boldsymbol{o}_{\text{I}}(\theta^1,\theta^2)\right)$ of mutually orthogonal directions

Π_2 second-order term of the change in total potential energy of the system between a fundamental equilibrium state and an adjacent state, at constant λ

$\Pi_2^{(0)}$ strain energy of the linear theory, corresponding to the incremental displacement field $\boldsymbol{u}$

$\Pi_{2.ref}^{(1)}$ work of the active membrane forces $n_{\text{I·I}.ref}^{(A)f}$ due to the second-order part of the strain $G_{\text{I·I}}$

$\tilde{\Pi}$ non-dimensional counterpart of Π_2

ϱ mass density over the reference shape (in chapter 3)

$\sigma_{R1}, \sigma_{Rf}, \sigma_T$ non-dimensional restraint stiffness parameters

ζ_T non-dimensional position parameter for translational restraint

Membrane forces and cross-sectional stress resultants

B bimoment

B_S bimoment evaluated with the sectorial coordinate ω_S (in prismatic bars)

M_1 torque about the line $\left\{O+\theta^1\boldsymbol{e}_1, 0\le\theta^1\le L\right\}$

$M_1^{(A)}$ active part of the torque M_1

$M_1^{(R)}$ reactive part of the torque M_1

$M_{S.1}$ torque about the line of shear centres (in prismatic bars)

M_2 bending moment relative to the axis through $O+\theta^1\boldsymbol{e}_1$ and spanned by $\boldsymbol{e}_2$

M_2^f bending moment M_2 in a fundamental equilibrium state

$M_{2.ref}^f$ bending moment M_2^f for a unit value of the load factor λ

M_3 bending moment relative to the axis through $O+\theta^1\boldsymbol{e}_1$ and spanned by $\boldsymbol{e}_3$

$\boldsymbol{n}$ membrane force tensor field

$\boldsymbol{n}^{(A)}$ active part of $\boldsymbol{n}$

$n_{\Sigma A}^{(A)}$ components of $\boldsymbol{n}(\theta^1,\theta^2)$ with respect to the orthonormal ordered basis $\{\boldsymbol{o}_{\mathrm{I}}(\theta^1,\theta^2),\boldsymbol{o}_{\mathrm{II}}(\theta^1,\theta^2)\}$

$n_{\mathrm{I\cdot I}.ref}^{(A)\,f}$ active membrane forces $n_{\mathrm{I\cdot I}}^{(A)}$ in the fundamental state corresponding to the reference load system ($\lambda=1$)

$\boldsymbol{n}^{(R)}$ reactive part of $\boldsymbol{n}$

N normal force

$\{s^{(A)}\}$ column vector of active stress resultants

$\{s^{(R)}\}$ column vector of reactive stress resultants

V_2 shear force parallel to $\boldsymbol{e}_2$

V_3 shear force parallel to $\boldsymbol{e}_3$

Momentum densities

$\boldsymbol{l}$ angular momentum density

l_i Cartesian components of the angular momentum density

$l_{S.1}$ axial component of the angular momentum density relative to $O+\theta^1\boldsymbol{e}_1+x_2^S\,\boldsymbol{e}_2+x_3^S\,\boldsymbol{e}_3$

$\boldsymbol{p}$ linear momentum density

p_i Cartesian components of the linear momentum density

p_ω warping momentum density

$p_{\omega S}$ warping momentum density, evaluated with the sectorial coordinate ω_S

$\{p\}$ column vector of momentum densities

Abbreviations

FTB flexural-torsional buckling

LTB lateral-torsional buckling

Chapter 1

GENERAL INTRODUCTION

They say that the first sentence in any speech is always the hardest.
Well, that one's behind me.

WISLAWA SZYMBORSKA

1.1 THE CLASSIFICATION OF STRUCTURAL ELEMENTS ACCORDING TO THEIR SPATIAL CHARACTER

It is a fitting tribute to Vlasov that we should name the opening section of this thesis, so much inspired by his work, after the opening section of his monumental treatise on thin-walled bars (VLASOV 1961).

Structural elements are commonly divided into four broad groups according to their spatial character (VLASOV 1961, ch. 1, § 1, or TRABUCHO & VIAÑO 1996, Introduction):

(i) massive bodies, whose dimensions in all three spatial directions are of the same order of magnitude;

(ii) plates and shells, which exhibit one characteristic dimension (the thickness) that is much smaller than the other two;

(iii) bars with solid cross-section, which are bodies with two characteristic dimensions of comparable magnitude (the cross-sectional dimensions), both much smaller than the third one (the length);

(iv) thin-walled bars, distinguished by the fact that their characteristic dimensions are all of different orders of magnitude – the wall thickness is small compared with the diameter of the cross-section, which, in turn, is small compared with the length.

Loosely speaking, a bar can be thought of as a three-dimensional solid occupying the volume obtained by attaching a cross-section to each point of a simple regular curve, the bar axis. Each cross-section is a planar connected region, perpendicular to the axis and whose diameter is much smaller than the length of the axis. If every cross-section can be

viewed as the slight thickening of a planar curve, then the bar is thin-walled; otherwise, it exhibits a solid cross-section. A bar is said to be prismatic whenever its axis is a straight line segment and the cross-section is uniform. Bars with a continuously varying cross-section are called tapered bars.

From the point of view of mechanical behaviour, the distinctive feature of a thin-walled bar is the fact that it resists torsion as a spatial system: the cross-sections undergo out-of-plane warping and, since this warping generally varies along the length of the bar, there arise non-negligible longitudinal normal stresses, in addition to the cross-sectional shear stresses. This challenges the validity of both Bernoulli's law of plane sections and Saint-Venant's torsion theory.

The above classification is of necessity a rather qualitative one and no sharp boundaries can be drawn between groups. "The same structure can be classified differently depending on the external loading conditions, on the manner in which the structure is to be employed in the given structural problem, and on the degree of accuracy demanded from the calculation." For instance, "a thin-walled beam which has a rigid closed cross-section can, in many cases, be considered as belonging to the class of solid beams insofar as its behaviour under combined flexure and torsion is concerned" (VLASOV 1961, p. 5).

1.2 NATURE AND PURPOSE OF ONE-DIMENSIONAL BAR MODELS

> The sciences do not try to explain, they hardly even try to interpret,
> they mainly make models. By a model is meant a mathematical construct which,
> with the addition of certain verbal interpretations, describes observed phenomena.
> The justification of such a mathematical construct is solely and precisely
> that it is expected to work.
>
> JOHN VON NEUMANN

> That is, in a specific example, the best material model of a cat is another,
> or preferably the same, cat … The situation is the same with the theoretical models.
>
> ARTURO ROSENBLUETH & NORBERT WIENER

The equations describing the mechanics of a three-dimensional continuum are formidable to solve. Even in this day and age of powerful numerical techniques and high-speed, large-capacity computers, it is not feasible to treat every solid body as a three-dimensional continuum, at least in routine applications. This dictates the need for tractable

and accurate lower-dimensional models – two-dimensional models for plates and shells, one-dimensional models for bars, either with solid cross-section or thin-walled, according to their distinctive spatial character. Massive bodies, on the other hand, are the province of the three-dimensional theories.

One-dimensional bar models, or theories of bars, can therefore be defined as characterisations of particular aspects of the mechanical behaviour of a specified class of bars by a finite set of equations having the parameter of a certain curve and, possibly, time as the only independent variables (ANTMAN 1972, § 1). Moreover, the variables entering these equations are required to have a relatively simple physical interpretation. Of course, one should not forget that any one-dimensional bar model is necessarily approximate – paraphrasing KOITER (1969, p. 93), an exact one-dimensional theory of bars cannot exist, because the actual body we have to deal with, slender as it may be, is always three-dimensional. In fact, every model is an idealisation, and thus only approximate in relation to the physical phenomena under consideration. In this respect, the difference between three-dimensional and lower-dimensional models, when formulated consistently and logically, is one of degree rather than of kind, as acutely observed by MALVERN (1969, pp. 2-3).

In the long and successful history enjoyed by one-dimensional bar models,[1] two main approaches can be discerned (ANTMAN 1972, ch. B, parts I and II): (i) the intrinsic or direct approach, often associated with the name of the brothers E. and F. Cosserat, in which the bar is conceived *ab initio* as a one-dimensional continuum endowed with some additional structure, and (ii) the induced approach from some parent higher-dimensional model, which can proceed either via asymptotic methods or by constraining the displacement, strain or stress fields to take on some particular analytical form.

One example of the use of the induced-constraint approach, of particular importance to the object of the present thesis, is the one-dimensional model derived by VLASOV (1961) for analysing the spatial behaviour of prismatic thin-walled bars with open cross-sections. In the words of TRABUCHO & VIAÑO (1996, pp. 500-501), "it is an elegant and powerful combination of mathematical analysis and mechanics [...] based on a more general and

[1] For a detailed history of the early one-dimensional bar models, see TRUESDELL 1960. A much more succinct account, which also spans the nineteenth century and the first half of the twentieth century, is given by ERICKSEN & TRUESDELL 1958, § 1.

more natural *a priori* hypotheses than Bernoulli-Navier's assumption of plane sections" – invariance of the cross-sectional shape and negligible shear deformations on the middle surface. Indeed, one can only marvel at the insight that led Vlasov to conceive his model out of purely mechanical and geometrical intuitions.

1.3 AIMS, SCOPE AND OUTLINE OF THE THESIS

Tapered thin-walled bars are extensively used in the fields of civil, mechanical and aeronautical engineering because of their unique ability to combine efficiency, economy and aesthetics – the three ideals of structural art, according to BILLINGTON (1985). The competitiveness of tapered structural members, however, is hindered by the fact that their spatial behaviour is still poorly understood and by the lack of consistent and efficient methods for their analysis and design – on the one hand, the piecewise prismatic ("stepped") approach, which replaces a tapered bar by a sequence of prismatic segments (whose number is increased until convergence is achieved), while intuitively plausible at first sight, at least for a mild taper, cannot withstand closer scrutiny (as we shall see in chapter 2) and its unqualified applicability is thus questionable;[2] on the other hand, the computational effort and post-processing difficulties implied by the use of shell or solid finite element models is prohibitive for routine applications. The present thesis aims at providing a contribution to overcome these drawbacks, by (i) developing consistent one-dimensional models to perform linear static, dynamic and lateral-torsional buckling analyses of tapered thin-walled bars with open (*i.e.*, simply connected) cross-sections, and (ii) supplying physical interpretations for the key behavioural features implied by these models, which shed light into the roles played by the various geometrical and mechanical parameters, with particular emphasis on those that are peculiar to the tapered case.

[2] As illustration of one deficiency in the stepped approach, we offer the following simple example, in anticipation of the discussion in § 2.11. Consider a doubly symmetric I-section cantilever. When twisted, its flanges bend in opposite directions. In any given cross-section, the bending moments in the flanges form a self-equilibrating pair if the web depth is uniform. However, if the web depth varies continuously, these bending moments, being orthogonal to the flanges, exhibit an axial resultant – such a contribution to the total torque cannot be accounted for by a stepped model, regardless of the number of prismatic segments it comprises.

The main body of the thesis can be divided into two largely independent parts. The first, comprising chapters 2 through 4, is devoted to bars whose shape allows them to resist biaxial bending by the membrane action of their walls (I-section or C-section bars, for instance). Members with narrow rectangular cross-section are therefore excluded.

In chapter 2, we construct a linear one-dimensional model for the stretching, bending and twisting of tapered thin-walled bars with open cross-sections under general static loading conditions. We follow mainly the induced-constraint approach, deemed the most versatile and physically meaningful, as well as being entirely consistent with the engineering quantities of interest. As parent theory, we adopt a two-dimensional linearly elastic membrane shell model. The Vlasov assumptions, extended to the tapered case in such a way as to retain an intrinsic geometrical meaning, are treated consistently as internal constraints, that is, *a priori* restrictions, of a constitutive nature, on the possible deformations of the middle surface of the bar. Accordingly, (i) the membrane forces are decomposed additively into active and reactive parts, and (ii) the constitutive dependence of the active membrane forces on the membrane strains reflects the maximal symmetry compatible with the assumed internal constraints. Despite our acknowledged debt to the work of WILDE (1968), we consider these developments and their physical interpretation new in the main.

Vlasov's model for prismatic bars is obtained as a particular case. However, for a large class of tapered thin-walled bars with open cross-sections, the membrane strain and force fields implied by the assumed internal constraints do not have the same form as in Vlasov's theory – they feature an extra term, involving the rate of twist. This result is absolutely central to this chapter and carries over to the developments in chapters 3 and 4. It explains why the torsional behaviour (be it uncoupled or coupled with other modes of deformation) predicted by our tapered model is generally at odds with that obtained with the stepped approach. The discrepancies may be significant, as illustrated through examples, and, in view of the stepped models several deficiencies (whose physical significance is pointed out in the discussion of these examples), their use to simulate the spatial behaviour of tapered thin-walled bars with open cross-sections is inadequate except in special cases.

In chapter 3, the linear static one-dimensional model is extended into the dynamic range. The contributions of rotatory inertia and torsion-warping inertia are fully taken into account. Although we shall deal mainly with undamped motions, the inclusion of a viscous-type dissipative mechanism is also briefly addressed. The chapter closes with an illustrative

example concerning the undamped free torsional motions of doubly symmetric web-tapered I-section cantilevers. The technique of separation of variables leads to an eigenproblem that provides the natural torsional frequencies and the corresponding vibration modes. A so-called "paradox" (CYWINSKI 2001) is elucidated.

Chapter 4 deals with the elastic lateral-torsional buckling of singly symmetric tapered thin-walled beams (flexural members) with open cross-sections, loaded in the plane of greatest bending stiffness (symmetry plane). Lateral-torsional buckling is a bifurcation-type instability in which (i) the fundamental equilibrium path corresponds to shapes that are symmetric with respect to the plane of loading and (ii) the buckled states are associated with non-symmetric shapes – the beam deflects laterally (out-of-plane) and twists. Due to their typically low lateral bending and torsional rigidities, thin-walled bars with open cross-sections are particularly susceptible to this phenomenon. We derive anew, in a simpler and more direct manner, the one-dimensional model originally proposed by ANDRADE & CAMOTIM (2005). The adopted kinematical description precludes the model from capturing any local or distortional phenomena. Moreover, the effect of the pre-buckling deflections is ignored. It has been shown elsewhere that the predictions of this one-dimensional model – critical buckling loads and corresponding buckling modes – correlate well with the results of shell finite element analyses (ANDRADE *et al.* 2007, ASGARIAN *et al.* 2012, ZHANG & TONG 2008). In actual design practice, beams are usually connected to other elements that may contribute significantly to their buckling strength, even when they are not primarily intended for that specific purpose. Using an archetypal problem, it is shown how the presence of out-of-plane restraints can be accommodated in the one-dimensional buckling model. The restraints may (i) have a translational, torsional, minor axis bending and/or warping character and (ii) be either linearly elastic or perfectly rigid. A parametric study is then conducted to examine in some detail (i) the effectiveness of different types of restraint, (ii) the importance of the restraint stiffness and (iii) the interplay between these two aspects and the effects of tapering. This parametric study once again highlights the differences between the predictions of tapered and stepped (piecewise prismatic) models.

The second part of the thesis, which consists of chapter 5, is concerned with strip members (*i.e.*, members with narrow rectangular cross-section) exhibiting constant thickness and varying depth (prismatic members are considered as a particular case). It deals with three problems of increasing complexity:

(i) the elastic lateral-torsional buckling of cantilevered beams with linearly varying depth, acted at the free-end section by a conservative point load;

(ii) the elastic lateral-torsional buckling of cantilevers (ii_1) whose depth varies according to a non-increasing polygonal function of the distance to the support and (ii_2) which are subjected to an arbitrary number of independent conservative point loads, all acting in the same "downward" direction;

(iii) the elastic flexural-torsional buckling of linearly tapered cantilever beam-columns, acted by axial and transverse point loads applied at the free-end section.

These three problems are tackled analytically – we aim at obtaining exact closed-form solutions to the governing differential equations and, thereby, at establishing exact closed-form characteristic equations for the buckling loads (even if these characteristic equations are transcendental and do not have closed-form solutions). For the third problem, however, the analytical approach is fruitful only for certain values of the ratio between the minimal and maximal depth of the strip beam-column; in the remaining cases, one resorts to a numerical procedure. At the expense of some unavoidable repetitions, this chapter was written as a self-contained unit within the thesis.

Variational principles are used throughout – the principle of stationary total potential energy in chapter 2, Hamilton's principle in chapter 3, the criterion of Trefftz in chapters 4 and 5. In favour of the use of variational principles, the following reasons are commonly adduced (TRUESDELL & TOUPIN 1960, § 231, FUNG 1965, p. 270):

(i) They are statements about a system as a whole, rather than the parts that it comprises.

(ii) They imply the field equations (ordinary or partial differential equations) for the problem under consideration, as well as the corresponding boundary and jump conditions.

(iii) They automatically include the effects of constraints, without requiring the corresponding reactions to be known.

(iv) The direct method of solution of variational problems is one of the most powerful tools for obtaining numerical solutions.

The first three items will be put to good use in this thesis. A fifth reason, the elegance that variational principles usually exhibit, is often added to the list, but may be largely viewed as a subjective expression of taste.

Chapters 2 through 4 rely rather heavily on a number of elementary notions from the differential geometry of curves and surfaces. Moreover, chapter 5 requires some familiarity with the rudiments of the theory of analytic maps of a real or complex variable. For the benefit of the reader, the needed prerequisites, which have been kept to a minimum, are briefly expounded at the beginning of chapters 2 and 5, making the thesis largely self-contained in this respect.

We have made an effort to keep the arguments rigorous, the word "rigour" being here understood in the sense defined by André Weil: "it does not consist in proving everything, but in maintaining a sharp distinction between what is assumed and what is proved, and in endeavouring to assume as little as possible at every stage" (*apud* TRUESDELL 1984, p. 112). In particular, it should always be clear what has to be done to check an argument, and this dictates small, explicit steps.

Some will undoubtedly reproach us with too much abstract and useless formalism. Nevertheless, the treatment is intended to illuminate the physical aspects of the theory, not merely in the narrow sense of predicting numerical results for comparison with experiments (or with simulations involving higher-dimensional models), but first and foremost for grasping a global, coherent and intelligible picture of the behaviour implied by the models. Moreover, we try to clarify the underlying structure of these models and to fit them into a unifying framework, shared with other models of structural mechanics and, indeed, of mathematical physics at large. In the same vein, the examples, which are presented in considerable detail, were chosen not as much for their immediate practical significance as for their usefulness in illustrating some of the peculiar aspects of the general models (and, therefore, for their usefulness as benchmarks). With the possible exception of the fifth chapter, it is fair to say that technique, important as it may be, never takes precedence over concept.

* * *

Each chapter is divided into a number of sections and subsections, and includes an introduction with the pertinent literature review. Moreover, each chapter has its own list of references. Equations, figures and tables are consecutively numbered within each section; footnotes are consecutively numbered within each chapter.

1.4 GENERAL REMARKS ON MATHEMATICAL NOTATION AND TERMINOLOGY

…mais qu'on ne s'y trompe pas: dans les Sciences mathématiques,
une bonne notation a la même importance philosophique
qu'une bonne classification dans les Sciences naturelles.

HENRI POINCARÉ

… for a good notation has a subtlety and suggestiveness which
at times make it seem almost like a live teacher.

BERTRAND RUSSELL

Throughout this thesis, $\mathcal{E}$ denotes a three-dimensional Euclidean point space and $\mathcal{V}$ its associated real inner-product space, oriented in one of the two possible ways.[3] The term "point" is reserved for elements of $\mathcal{E}$, the term "vector" for elements of $\mathcal{V}$. A Cartesian frame for $\mathcal{E}$ consists of a fixed origin $O \in \mathcal{E}$ and a fixed positive orthonormal ordered basis $\{\boldsymbol{e}_1, \boldsymbol{e}_2, \boldsymbol{e}_3\}$ for $\mathcal{V}$. We denote by $\hat{x} : \mathcal{E} \to \mathbb{R}^3$ the coordinate system associated with a given Cartesian frame for $\mathcal{E}$, that is, the field that assigns to each point X in $\mathcal{E}$ the ordered triplet (x_1, x_2, x_3) defined by $x_i = (X - O) \cdot \boldsymbol{e}_i$, $i = 1, 2, 3$. The scalar fields $\hat{x}_i : \mathcal{E} \to \mathbb{R}$ $(i = 1, 2, 3)$ such that $\hat{x}(X) = \big(\hat{x}_1(X), \hat{x}_2(X), \hat{x}_3(X)\big)$, for every X in $\mathcal{E}$, are called the coordinate functions of $\hat{x}$. The inner product and the cross product of two vectors $\boldsymbol{x}$, $\boldsymbol{y}$ in $\mathcal{V}$ are denoted by $\boldsymbol{x} \cdot \boldsymbol{y}$ and $\boldsymbol{x} \times \boldsymbol{y}$, respectively. The Euclidean norm or length of a vector $\boldsymbol{x}$ is written $\|\boldsymbol{x}\| = \sqrt{\boldsymbol{x} \cdot \boldsymbol{x}}$.

Unless otherwise indicated, the range of a Latin index (subscript or superscript) is the set $\{1, 2, 3\}$, that of a Greek index is the set $\{1, 2\}$. For the sake of notational brevity, Einstein's summation convention is adopted – when an index appears twice, and only twice, in the same term, a summation over the range of that index is implied (EINSTEIN 1916, § 5). A systematic exception to these rules is the index n, which is specifically used for indexing sequences and families.

The words "function", "map" and "transformation" are used as synonymous. "The all important (and characteristic) property of a map is that it associates to any «value» of the

[3] On the concept of finite-dimensional Euclidean point space, see, *e.g.*, BERGER (1987, § 9.1), BOWEN & WANG (1976, § 43), NOMIZU (1966, ch. 10) or SATAKE (1975, supplement, § 4). The orientation of a real finite-dimensional vector space is discussed at length in BERGER (1987, § 2.7.2) and GREUB (1981, ch. 4, § 8, and ch. 7, § 3).

variable a *single* element; in other words, there is no such thing as a «multiple-valued» function, despite many books to the contrary" (DIEUDONNÉ 1960, p. 1). We consider a map as a single object, just as a point or a number, and make a careful distinction between the map $f : X \to Y$, from X into Y – also written simply as f or $x \mapsto f(x)$ when the domain and codomain are clear from the context –, and the value $f(x) \in Y$ that it takes at the argument $x \in X$. However, a constant map is often identified with its value.

As a rule, when it comes to concepts of mathematical analysis (differential calculus, in particular), we adopt the notational conventions of DIEUDONNÉ (1960). Accordingly, the (total) derivative of the map f at x_0, if it exists, is written $f'(x_0)$ or, less frequently, $Df(x_0)$. Higher-order derivatives at x_0 are denoted by $f''(x_0)$, ... , $f^{(p)}(x_0)$ or by $D^2 f(x_0)$, ... , $D^p f(x_0)$. Suppose now that the map f is defined on a subset of a product of n normed spaces. The partial of f at $(x_1,\cdots,x_n)$ with respect to the i^{th} variable, if it exists, is written $D_i f(x_1,\cdots,x_n)$.[4] Higher-order partial derivatives at $(x_1,\cdots,x_n)$ are written $D_i^p D_j^q \ldots f(x_1,\cdots,x_n)$.

[4] As remarked by DIEUDONNÉ (1960, p. 171), the usual notations $f'_{x_i}(x_1,\cdots,x_n)$ or $\partial / \partial x_i \, f(x_1,\cdots,x_n)$ for $D_i f(x_1,\cdots,x_n)$ lead to hopeless confusion when substitutions are made ("what does $f'_y(y,x)$ or $f'_x(x,x)$ mean?").

REFERENCES

ANDRADE A. and CAMOTIM D. (2005). Lateral-torsional buckling of singly symmetric tapered beams: Theory and applications. *Journal of Engineering Mechanics – ASCE*, **131**(6), 586-597.

ANDRADE A., CAMOTIM D. and DINIS P.B. (2007). Lateral-torsional buckling of singly symmetric web-tapered thin-walled I-beams: 1D model vs. shell FEA. *Computers & Structures*, **85**(17-18), 1343-1359.

ANTMAN S.S. (1972). The theory of rods. *Handbuch der Physik*, Volume VIa/2, C. Truesdell (Ed.). Berlin: Springer, 641-703.

ASGARIAN B., SOLTANI M. and MOHRI F. (2012). Lateral-torsional buckling of tapered thin-walled beams with arbitrary cross-sections. *Thin-Walled Structures*, in press.

BERGER M. (1987). *Geometry I*. Berlin: Springer.

BILLINGTON D.P. (1985). *The Tower and the Bridge – The New Art of Structural Engineering*. Princeton: Princeton University Press.

BOWEN R.M. and WANG C.-C. (1976). *Introduction to Vectors and Tensors*, Volume 2: Vector and Tensor Analysis. New York: Plenum Press.

CYWINSKI Z. (2001). History of a "paradox" for thin-walled members with variable, open cross-section. *International Journal of Structural Stability and Dynamics*, **1**(1), 47-58.

DIEUDONNÉ J. (1960). *Foundations of Modern Analysis*. New York: Academic Press.

EINSTEIN A. (1916). Die Grundlage der allgemeinen Relativitätstheorie [The foundation of the general theory of relativity]. *Annalen der Physik*, **49**, 769-822. English translation by W. Perret and G.B. Jeffery (1952), *The Principle of Relativity – A Collection of Original Memoirs on the Special and General Theory of Relativity*. New York: Dover, 111-164.

ERICKSEN J.L. and TRUESDELL C. (1958). Exact theory of stress and strain in rods and shells. *Archive for Rational Mechanics and Analysis*, **1**(4), 295-323.

FUNG Y.C. (1965). *Foundations of Solid Mechanics*. Englewood Cliffs, New Jersey: Prentice-Hall.

GREUB W.H. (1981). *Linear Algebra* (4th edition). New York: Springer.

KOITER W.T. (1969). Foundations and basic equations of shell theory – A survey of recent progress. *Theory of Thin Shells*, F.I. Niordson (Ed.). Berlin: Springer, 93-105.

MALVERN L.E. (1969). *Introduction to the Mechanics of a Continuous Medium*. Englewood Cliffs, New Jersey: Prentice-Hall.

NOMIZU K. (1966). *Fundamentals of Linear Algebra*. New York: McGraw-Hill.

SATAKE I. (1975). *Linear Algebra*. New York: Marcel Dekker.

TRABUCHO L. and VIAÑO J.M. (1996). Mathematical modeling of rods. *Handbook of Numerical Analysis*, Volume 4: Finite Element Methods (Part 2) – Numerical Methods for Solids (Part 2), P.G. Ciarlet and J.L. Lions (Eds.). Amsterdam: Elsevier, 487-974.

TRUESDELL C. (1960). *The Rational Mechanics of Flexible or Elastic Bodies, 1638-1788*. Editor's Introduction to Volumes 10 and 11 of *Leonhardi Euleri Opera Omnia*, Series Secunda (Opera Mechanica et Astronomica). Zurich: Orell Füssli.

TRUESDELL C. (1984). *An Idiot's Fugitive Essays on Science – Methods, Criticism, Training, Circumstances*. New York: Springer.

TRUESDELL C. and TOUPIN R. (1960). The classical field theories. *Handbuch der Physik*, Volume III/1, S. Flügge (Ed.). Berlin: Springer, 225-793.

VLASOV V.Z. (1961). *Thin-Walled Elastic Beams* [English translation of the 2nd Russian edition of 1959]. Jerusalem: Israel Program for Scientific Translation. French translation of the said Russian edition by G. Smirnoff (1962), *Pièces Longues en Voiles Minces*. Paris: Eyrolles.

WILDE P. (1968). The torsion of thin-walled bars with variable cross-section. *Archiwum Mechaniki Stosowanej*, **4**(20), 431-443.

ZHANG L. and TONG G.S. (2008). Lateral buckling of web-tapered I-beams: A new theory. *Journal of Constructional Steel Research*, **64**(12), 1379-1393.

Chapter 2

A LINEAR ONE-DIMENSIONAL MODEL FOR THE STRETCHING, BENDING AND TWISTING OF TAPERED THIN-WALLED BARS WITH OPEN CROSS-SECTIONS

THE STATIC CASE

We shall not cease from exploration
And the end of all our exploring
Will be to arrive where we started
And know the place for the first time.

T.S. ELIOT

Car on sait par l'expérience, que lorsqu'une recherche est fort épineuse,
les premiers efforts nous en éclaircissent ordinairement fort peu;
& ce n'est que par des efforts réitérés, & envisageant la même chose
sous plusieurs points de vûe, qu'on parvient à une connoissance accomplie.

LEONHARD EULER

As I read the works on the foundations of mechanics by Euler, his teacher John Bernoulli, and John Bernoulli's teacher James Bernoulli, I discern a simple pattern.
[…]
(5) Never rest content with an imperfect or incomplete argument. If you cannot complete and perfect it yourself, lay bare its flaws for others to see.
(6) Never abandon a problem you have solved. There are always better ways. Keep searching for them, for they lead to fuller understanding. While broadening, deepen and simplify.

CLIFFORD TRUESDELL

2.1 INTRODUCTION

2.1.1 An historical sketch of the development of linear one-dimensional models for prismatic thin-walled bars with open cross-section

It is appropriate to start this chapter by discussing the various engineering approaches used heretofore to construct linear one-dimensional models for the bending and twisting of prismatic thin-walled bars with open cross-section.[1] Indeed, such a discussion provides the background against which the developments for tapered bars can best be assessed. From an historical viewpoint, we can distinguish three different, though closely related (in fact, largely equivalent), approaches, which we shall name after their initiators.

Timoshenko's approach

Only rarely can we assign an exact date to the origin of a particular question. In the case of non-uniform torsion, we can for once identify just where, when, how and by whom the problem was first stated – the place was Göttingen, the year was 1905 and the author was S.P. Timoshenko. At the suggestion of Ludwig Prandtl, Timoshenko began working on the lateral-torsional buckling of I-beams. He realised that a doubly symmetric I-beam subjected to constant torque displays markedly different behaviours, depending on whether it is free to warp (uniform torsion) or whether one of its ends is restrained from warping (non-uniform torsion or warping torsion) – see figure 2.1.1. In the latter case, torsion is accompanied by bending of the flanges in opposite directions and the beam is significantly stiffer – Saint-Venant's torsion theory is not applicable. As Timoshenko recollects in his autobiography (TIMOSHENKO 1968),

> it took me about two weeks to figure out how to allow for this bending, to realize that the torque is counterbalanced by the same stresses as in ordinary [uniform] torsion, added to the moment produced by the shear forces resulting from the buckling [bending] of the I-beam's flanges. Once this was understood, writing an equation for the torsion was no longer difficult.

[1] We will not delve into the (relatively recent) mathematical work on this subject, based on asymptotic expansion methods and Γ-convergence theory – BÉCHET *et al.* (2010), FREDDI *et al.* (2007), GRILLET *et al.* (2000, 2005), HAMDOUNI & MILLET (2011) and RODRIGUEZ & VIAÑO (1995, 1997).

The total torque is thus the sum of two parts, denoted in TIMOSHENKO (1913) as M_1 and M_2. The torque M_1 is proportional to the rate of twist φ':

$$M_1 = C\,\varphi' \ , \tag{2.1.1}$$

where C is the classical Saint-Venant torsional rigidity of the cross-section. To find the second part of the torque, Timoshenko establishes, by appealing to symmetry considerations, that each cross-section rotates about the centroidal axis of the bar. The lateral deflections of the central lines of the flanges are therefore

$$y = \pm\frac{1}{2} h\,\varphi \ , \tag{2.1.2}$$

where h is the distance between middle lines of the flanges. If the flanges are individually regarded as planar Euler-Bernoulli beams, then the curvatures $\pm\frac{1}{2} h\,\varphi''$ that they acquire due to restrained warping give rise to bending moments

$$M_f = \pm\frac{1}{2} D\,h\,\varphi'' \tag{2.1.3}$$

and shear forces

$$Q_f = \pm\frac{1}{2} D\,h\,\varphi''' \ , \tag{2.1.4}$$

where D is the major-axis flexural rigidity of each flange. The shear forces in the two flanges have the same magnitude but are oppositely directed. They thus form the couple

$$M_2 = -\frac{1}{2} D\,h^2\,\varphi''' \ . \tag{2.1.5}$$

The equation for non-uniform torsion of a doubly symmetric I-beam then becomes

$$M = M_1 + M_2 = C\,\varphi' - \frac{1}{2} D\,h^2\,\varphi''' \ . \tag{2.1.6}$$

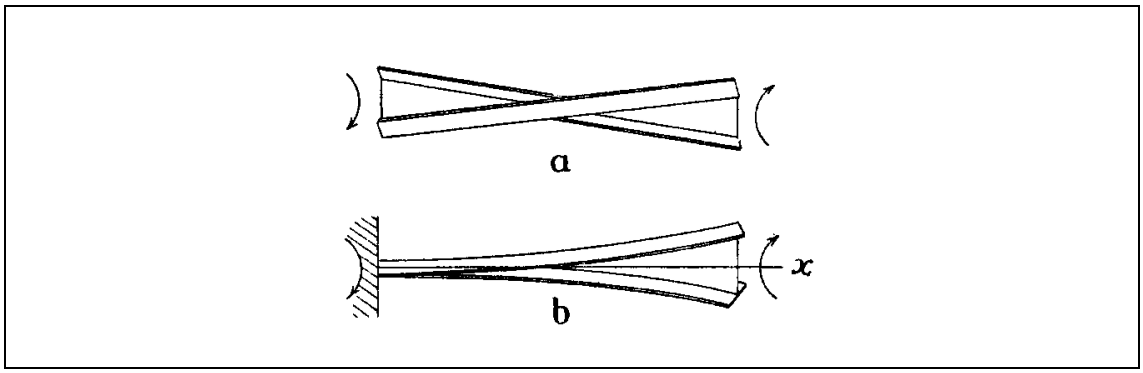

Figure 2.1.1: Uniform and non-uniform torsion of a doubly symmetric I-beam, as schematically shown in TIMOSHENKO (1913)

Today, the mechanical property $\frac{1}{2} D h^2$ is called the warping rigidity of the cross-section. Timoshenko's work, originally published in Russian, was later reported in German and French (TIMOSHENKO 1910, 1913).

Further progress along these lines had to wait for the introduction of the concept of shear centre (EGGENSCHWYLER 1920a, 1920b, 1921a, 1921b and MAILLART 1921a, 1921b, 1924a, 1924b), a surprisingly latecomer into structural mechanics,[2] and the identification of shear and twist centres by WEBER (1924), using Maxwell's theorem.[3] With this conceptual apparatus in place, WEBER (1926) extended Timoshenko's approach to the linear analysis of non-uniform torsion in prismatic bars with arbitrary (*i.e.*, singly symmetric, point symmetric or asymmetric) double-flanged open cross-sections – see figure 2.1.2. It should be noted that, in general, restrained warping gives rise to longitudinal normal stresses in all plated components (flanges and web). Moreover, in each component, these normal stresses are, in general, statically equivalent to a bending moment and an axial force. The theoretical results of Weber were found to be in agreement with the experiments performed by BACH (1909, 1910) on C-section steel bars.

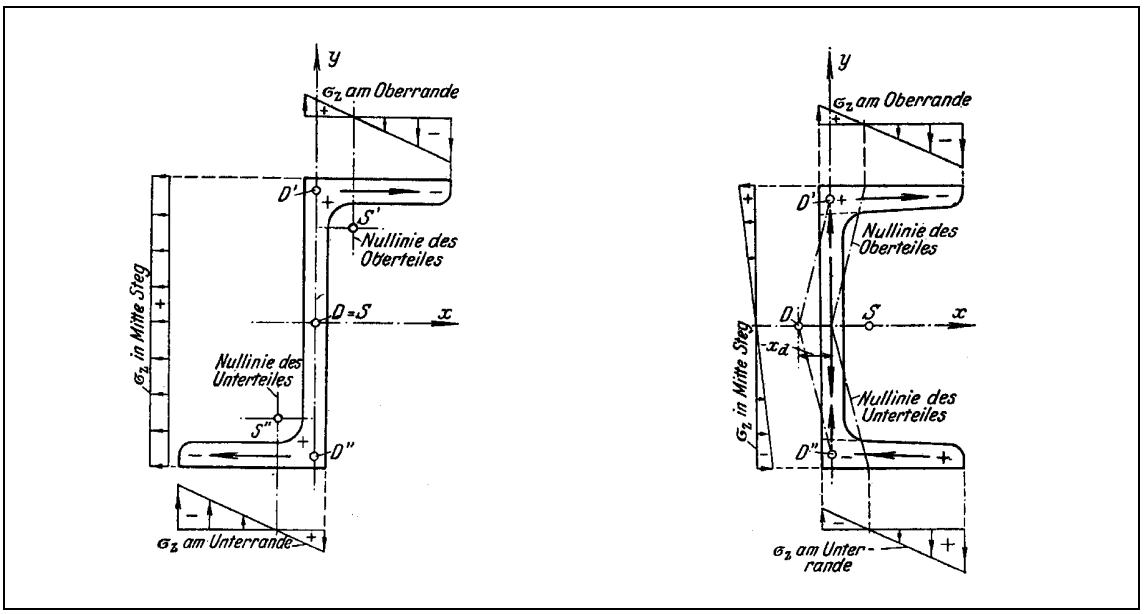

Figure 2.1.2: Two examples of double-flanged open cross-sections addressed by WEBER (1926), showing the distribution of longitudinal normal stresses due to restrained warping

[2] See BILLINGTON (1997, pp. 104-107), KURRER (2008, § 7.3.2) and REISSNER (1973) for the broader context surrounding the discovery of the shear centre.

[3] This has since become a textbook example of the application of Maxwell's theorem (*e.g.*, MASSONNET 1968, pp. 474-475, and DIAS DA SILVA 2006, p. 478).

The line of attack initiated by Timoshenko culminated with the development, by F. & H. BLEICH (1936),[4] of a general linear theory of bending and twisting of prismatic bars with open cross-section composed of an arbitrary number of thin flat plates (see figure 2.1.3). These authors assumed that the Euler-Bernoulli theory of bending remains valid for each individual plate and enforced the continuity of the longitudinal strain at the junctions between contiguous plates. As a result, "the cross-section of each plate between two consecutive corners will remain plane, although the planes may be different for two adjoining plates and the cross-section of the entire bar will be warped" (BLEICH 1952, p. 108). Unlike the preceding authors, who relied on direct equilibrium considerations, the Bleiches formulated a general expression for the total potential energy and derived the governing differential equations from the principle of stationary total potential energy.

Wagner's approach

In Saint-Venant's torsion theory, the axial displacements are given by the product of a warping function defined over the cross-section – the solution to a Neumann problem in potential theory (*e.g.*, SOKOLNIKOFF 1956, § 34) – and the (constant) rate of twist. To develop a theory of non-uniform torsion for thin-walled bars with open cross-section, WAGNER (1929)

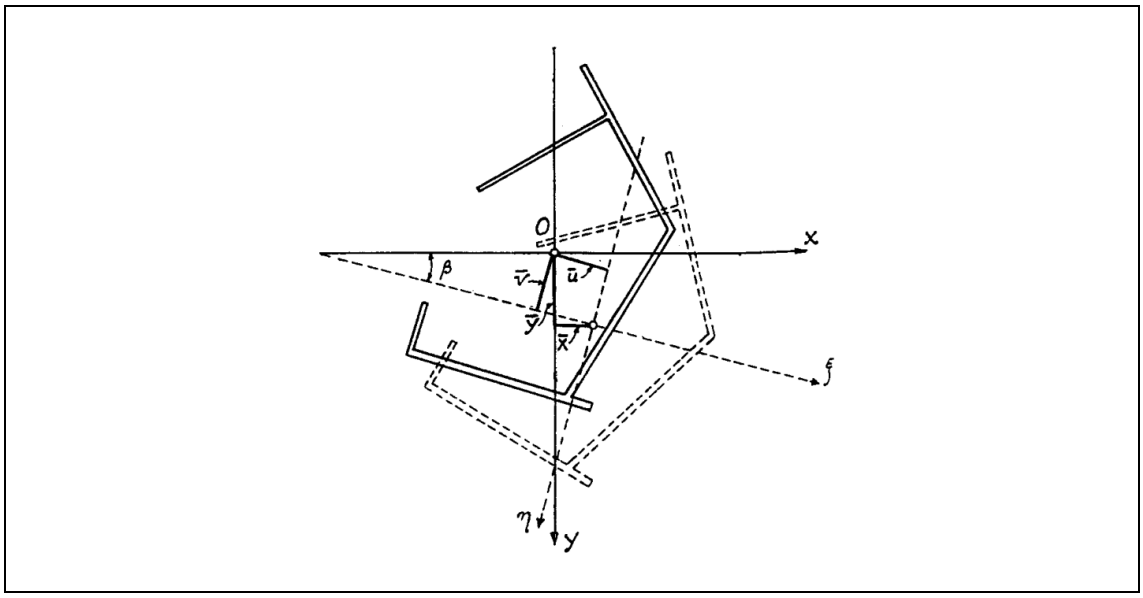

Figure 2.1.3: In-plane displacement of the cross-section of a prismatic bar composed of several thin flat plates, as considered by F. & H. BLEICH (1936)

[4] See also BLEICH (1952, ch. 3, §§ 35-38).

adopted an axial displacement field of the same form as in Saint-Venant's theory, except that the rate of twist is no longer constant.[5] Moreover, Wagner approximated Saint-Venant's warping function by a "unit warping" that is the sum of two components, w_u and w_n, the former pertaining to the middle line of the cross-section and the latter to the wall thickness.[6] Wagner's work, which does not make for easy reading, was further developed by KAPPUS (1937).

Vlasov's approach

A comprehensive theory of combined bending and twisting of thin-walled open bars was developed during the 1930s by V.Z. Vlasov and published in Russian in 1940 (see the historical sketch and literature survey in VLASOV 1961, pp. 464-472, and NOWINSKI 1959). The theory

> is based on the "lumping" of a two-dimensional continuous elastic system [membrane shell] [...] into a discrete-continuous system, *i.e.*, a system possessing a finite number of degrees of freedom in the transverse directions and an infinite number of degrees of freedom in the direction of the generator of the shell (VLASOV 1961, p. 47).

This dimensional reduction process is achieved by means of the following kinematical assumptions (VLASOV 1961, p. 7):

> a) a thin-walled beam of open section can be considered as a shell of rigid (undeformable) section;[7]
> b) the shearing deformation of the middle surface (characterizing the change in the angle between the coordinate lines $z = const$, and $s = const$) can be assumed to vanish [the coordinate systems adopted by Vlasov – a left-handed Cartesian system on the 3-dimensional ambient space and a Gaussian system on the middle surface of the beam – are shown in figure 2.1.4].

---

[5] See also WAGNER & PRETSCHNER (1934).

[6] The component w_u coincides with Vlasov's sectorial area with pole at the shear centre and origin at a sectorial zero-point (these concepts are defined below). The component w_n is associated with secondary, or through-the-thickness, warping (*e.g.*, ODEN & RIPPERGER 1981, § 7.8). It can be shown that Saint-Venant's warping function for thin-walled open sections may indeed be approximated by w_u as the thickness t tends to zero, up to $O(t)$ terms (MULLER 1983).

[7] In fact, this assumption is tacitly adopted by all the previously mentioned authors.

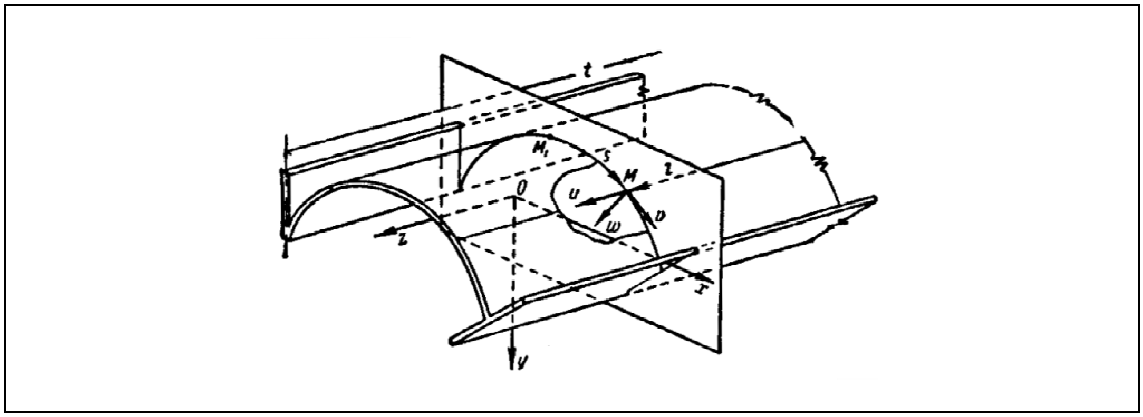

Figure 2.1.4: Coordinate systems adopted by VLASOV (1961, p. 11)

From these assumptions, Vlasov derives his "law of sectorial areas" (VLASOV 1961, p. 17):

> The longitudinal displacements $u(z,s)$ in the section $z = const$ of a thin-walled open shell of cylindrical or prismatic shape are made up of displacements linear [affine] in the Cartesian coordinates of the point on the profile line and displacements proportional to the sectorial area [see figure 2.1.5], providing there are no bending deformations of the cross-section and the middle surface is free of shear [*i.e.*, providing the assumptions a) and b) stated above hold].

The latter represent "the part of the displacement that does not obey the law of plane sections [warping] and which arises as a result of torsion." In fact, Vlasov finds that "the longitudinal displacement of any point M on the middle surface through torsional deformation only is equal to minus the product of $\theta'(z)$ [rate of twist] and the sectorial area $\omega(s)$", thus obtaining, as a proposition, Wagner's hypothesis (restricted to the middle line of the cross-section). Vlasov also proves the following statement concerning bars with open section that consist of "one or more interconnected bundles of narrow rectangular plates", which establishes a link with the work of the Bleiches (see figure 2.1.6): "the sectorial diagram varies according to the law of plane sections within the limits of [each] bundle" (VLASOV 1961, p. 26).

Since the wall thickness of a thin-walled bar is, by definition, very small compared with the other cross-sectional dimensions, of all the stresses that arise in a cross-section, Vlasov considers "only the normal stresses [σ] in the direction of the generator of the middle surface and the tangential stresses in the direction of the tangent to the profile line

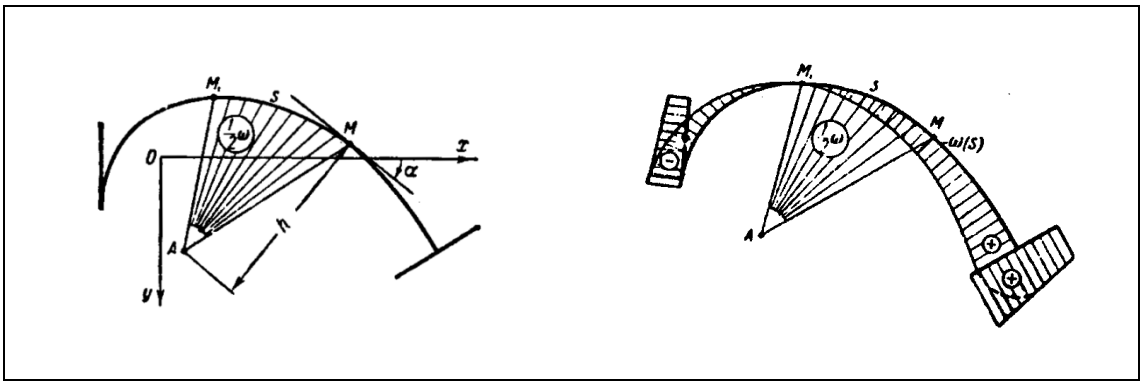

Figure 2.1.5: Sectorial area ω (VLASOV 1961, pp. 16-17)

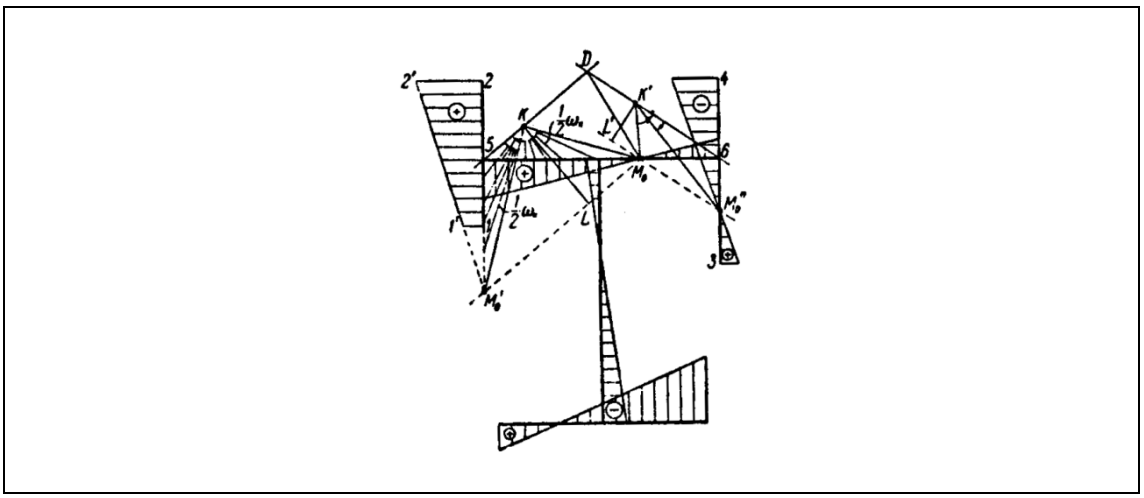

Figure 2.1.6: Sectorial area ω for beams with open cross-section consisting of narrow rectangular plates (VLASOV 1961, pp. 26)

[middle line of the cross-section]" (see figure 2.1.7(a, b)). Moreover, he assumes that "the normal stresses are constant over the thickness of the beam wall and that the tangential stresses over the beam wall vary according to a linear [affine] law", with average value τ (VLASOV 1961, p. 27). These stresses are developed owing to two distinct modes of deformation – a pure twisting of the bar, during which all sections are free to warp, and bending of the bar coupled with non-uniform warping. The first mode of deformation leads to the tangential stresses shown in figure 2.1.7(d), which vary linearly over the thickness and are zero at the middle line; the additional tangential stresses due to the second mode of deformation are uniform over the thickness, as shown in figure 2.1.7(c).

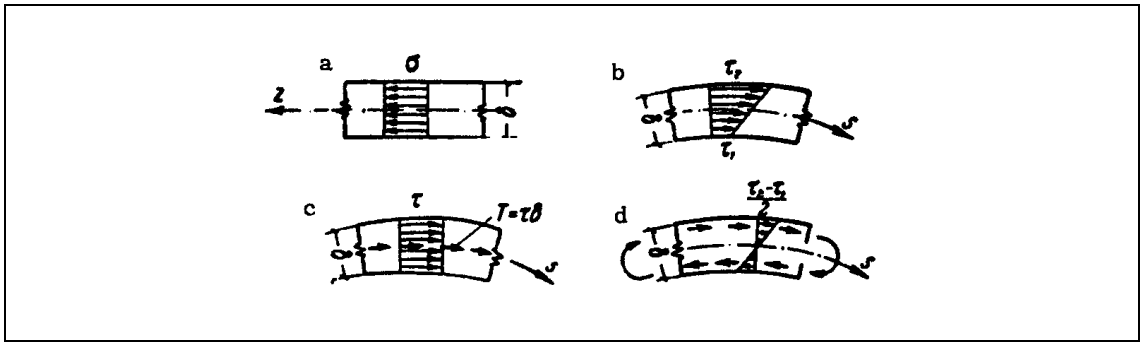

Figure 2.1.7: Cross-sectional state of stress (VLASOV 1961, p. 28)

Corresponding to the warping of the cross-section, Vlasov introduces a new cross-sectional stress resultant

$$B = \int_F \sigma\, \omega\, dF \quad , \tag{2.1.7}$$

which he calls the bimoment. "In contrast to the moment, the bimoment is a generalized balanced force system, *i.e.*, a force system statically equivalent to zero" (VLASOV 1961, p. 48).[8]

The work of Vlasov did not become generally known outside the Soviet Union until the (posthumous) second edition of his treatise was translated into English and French in the early 1960s. By then, a general theory based on similar assumptions had been independently worked out by TIMOSHENKO (1945).[9]

2.1.2 One-dimensional models for tapered thin-walled bars with open cross-sections

Naturally enough, the first attempts to develop one-dimensional models for the torsional behaviour of tapered thin-walled bars with open cross-sections were restricted to I-section bars and adopted Timoshenko's approach – LEE (1956) and LEE & SZABO (1967). The same approach was used later by KITIPORNCHAI & TRAHAIR (1972, 1975). These works, which exhibit some shortcomings, are critically examined in § 2.11 (see the remarks following equation (2.11.21)).

BAZANT (1965) and WILDE (1968) treated tapered bars of arbitrary open cross-sections under a general loading. Bazant develops his analysis by analogy with Vlasov's and

[8] This is why GJELSVIK (1981, p. v) writes that "the bimoment is particularly obscure and a feeling for what it is takes time to develop."

[9] See also TIMOSHENKO & GERE (1961, § 5.3).

assumes that "the distribution of the longitudinal normal strains and stresses in the section can be regarded as similar to the distribution for a bar with constant section." In fact, the one-dimensional model thus obtained is tantamount to replacing the actual tapered member by an assembly of prismatic segments obeying Vlasov's theory (stepped or piecewise prismatic model) and making the length of these segments tend to zero. Wilde, on the other hand, adopts a much more consistent approach. He regards a tapered bar as a membrane shell subjected to two kinematical constraints, which adapt to the tapered case the classical assumptions of Vlasov. However, in spite of these constraints, the membrane shell is treated as isotropic. WEKEZER (1984, 1990) developed a finite element formulation for Wilde's theory.

* * *

In the present chapter, we revisit Wilde's work, which is truly remarkable, and we do so in the light of the "method of internal constraints", introduced by PODIO-GUIDUGLI (1989).[10] We adopt, as parent theory, a two-dimensional linearly elastic membrane shell model. The Vlasov assumptions, suitably extended to the tapered case (as in WILDE 1968), are treated consistently as internal constraints, that is, *a priori* restrictions, of a constitutive nature, on the possible deformations of the middle surface of the bar.[11] Accordingly, (i) the membrane forces are decomposed additively into active and reactive parts, and (ii) the constitutive dependence of the active membrane forces on the membrane strains is such as to reflect the maximal symmetry compatible with the assumed internal constraints.[12] As PODIO-GUIDUGLI (1989) remarks, failure to consider the reactive forces (*i.e.*, the forces required to maintain the constraints) and an undue assumption of isotropy would lead to contradictions.

[10] Not to be confused with the method proposed by VOLTERRA (1955, 1956, 1961), in which the constraints have merely a kinematical character, without constitutive implications. This was shown to be generally incorrect by GREEN *et al.* (1967).

[11] GURTIN (1981, pp. 115-116) considers three types of constitutive assumptions, namely: (i) constraints on the possible deformations the body may undergo, (ii) assumptions on the form of the stress tensor and (iii) constitutive equations relating the stress to the motion.

[12] The method of internal constraints has been applied to obtain linear plate, shell and rod models by DAVÍ (1992, 1993), DICARLO *et al.* (2001), LEMBO (1989), LEMBO & PODIO-GUIDUGLI (1991, 2001, 2007), NARDINOCCHI & PODIO-GUIDUGLI (1994, 2001) and PODIO-GUIDUGLI (1989, 2003, 2006). A brief history of the method of internal constraints is included in PODIO-GUIDUGLI (2008). For similar ideas, developed along a somewhat different line, see MASSONNET (1982, 1983), who considers an orthotropic, transversely rigid material. In all these works, the parent theory is three-dimensional linear elasticity.

The developed one-dimensional model, which is restricted to bars whose shape allows them to resist biaxial bending by membrane action of their walls (strip members, for instance, are excluded), has one far-reaching consequence: it is shown, both analytically and *per exempla*, that the torsional behaviour predicted for a large class of tapered thin-walled bars with open cross-sections, whether uncoupled or coupled with other modes of deformation, cannot be reproduced using a stepped model, regardless of the number of prismatic segments considered. Indeed, Bazant's fundamental assumption, that "the distribution of the longitudinal normal strains and stresses in the section can be regarded as similar to the distribution for a bar with constant section", is found to be untenable within the framework of the adopted internal constraints (except in special cases). In the closing illustrative examples, we also discuss the correct use of Timoshenko's approach in the tapered case, which is shown to be entirely compatible with ours.

2.2 THE REFERENCE SHAPE OF THE BAR

2.2.1 General description

Let $\mathcal{B} \subset \mathcal{E}$ be the shape of a tapered thin-walled open-section bar in its unloaded state, which is taken as the reference shape.[13] The region $\mathcal{B}$ is assumed to be generated by the translation along a straight line segment, of length L, of a smoothly varying planar region, orthogonal to the said line segment, which can be viewed as the thickening of a smooth, simple and open curve. The length L is much larger than the length of this curve, which, in turn, is much larger than its thickening. Henceforth, the bar is identified with its reference shape $\mathcal{B}$. The middle surface of $\mathcal{B}$, denoted by $\mathcal{S}$, is identified with the middle surface of the bar (see figure 2.2.1).

Choose a Cartesian frame for $\mathcal{E}$, consisting of an origin $O \in \mathcal{E}$ and a positive orthonormal ordered basis $\{\boldsymbol{e}_1, \boldsymbol{e}_2, \boldsymbol{e}_3\}$ for $\mathcal{V}$, in such a way that (i) $\boldsymbol{e}_1$ is parallel to the straight line segment used to generate $\mathcal{B}$ and (ii) $\hat{x}_1[\mathcal{B}] = [0, L]$. The intersection of $\mathcal{B}$ (resp. $\mathcal{S}$) and the plane $\{X \in \mathcal{E} \,|\, \hat{x}_1(X) = x_1\}$, with $0 \le x_1 \le L$, is denoted by $\mathcal{A}_{x_1}$ (resp. $\mathcal{L}_{x_1}$) and is identified with a cross-section (resp. cross-section middle line) of the bar (see figure 2.2.1). We call $\mathcal{A}_0$ and $\mathcal{A}_L$ the end sections of the bar.

[13] On the concept of shape of a body, see TRUESDELL (1991, ch. 1, § 7, and ch. 2, §§ 1 and 3).

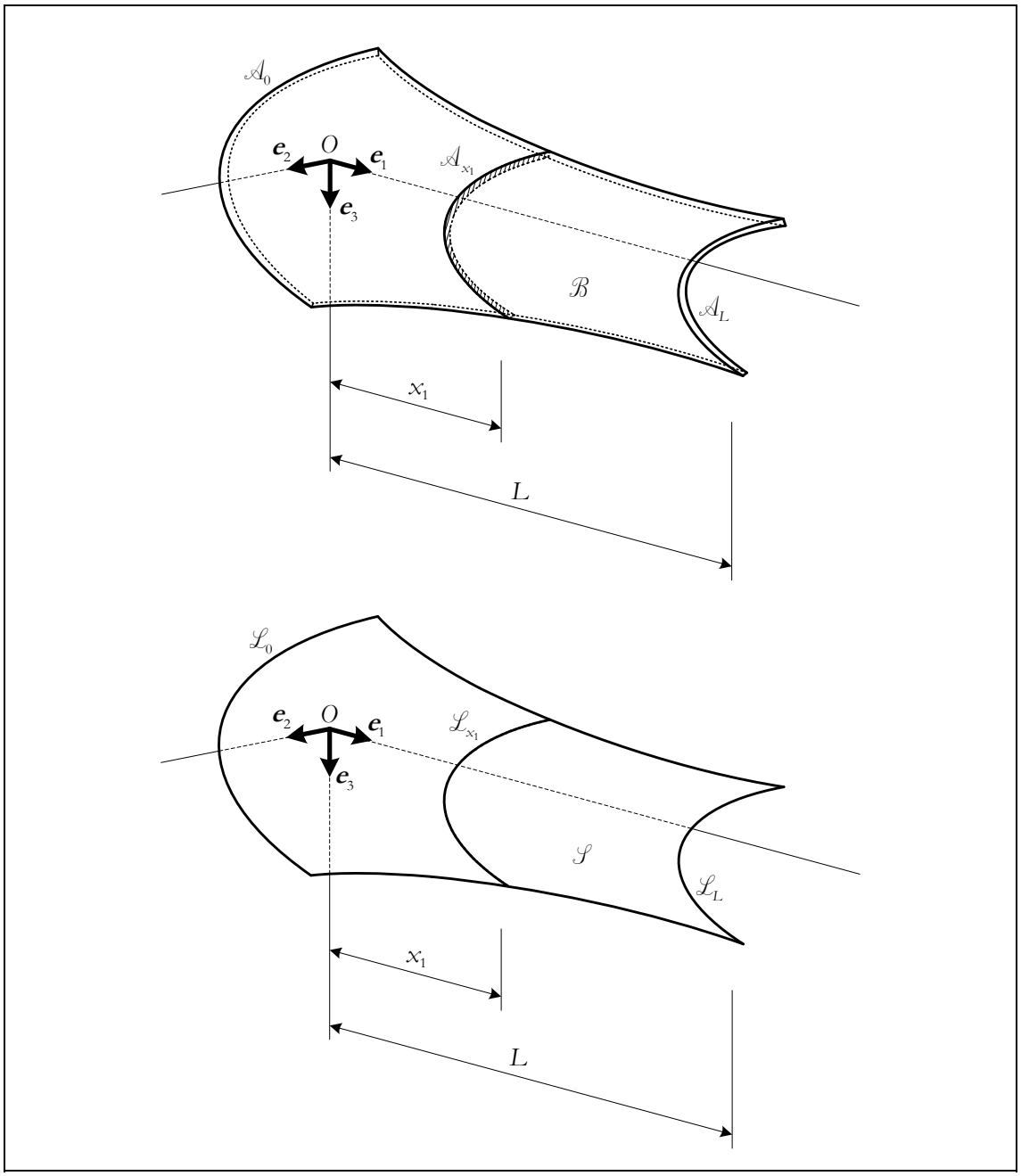

Figure 2.2.1: Reference shapes of a tapered thin-walled bar with open cross-sections and its middle surface

Clearly, this framework is not sufficiently general to include such important special cases as I-section or C-section bars. Nevertheless, it allows us to develop the one-dimensional model without being distracted by accessory details, which are best dealt with at a later stage – *vide infra*, § 2.10.

In the above description of the reference shape of a thin-walled tapered bar, we have carefully avoided any reference to a line of centroids or a line of shear centres. In general,

"it is not evident how to define [these] curve[s] conveniently and unambiguously. Were such a definition possible [..., their] actual construction from geometrical data would remain a formidable practical task" (ANTMAN 1972, p. 647).[14]

2.2.2 The parametrisation of $\mathcal{S}$

Et quia per naturam superficierum quaelibet
coordinate debet esse functio binarum variabilium.

LEONHARD EULER

Mathematically, the reference shape $\mathcal{S}$ of the middle surface of the bar is the image of the closure $\overline{\Omega}$ of a regularly open,[15] bounded, simply connected and Jordan measurable[16] subset Ω of $\mathbb{R}^2$ under an injective and smooth enough immersion[17] $F : \overline{\Omega} \to \mathcal{E}$:

$$\mathcal{S} = F\left[\overline{\Omega}\right] .^{18} \tag{2.2.1}$$

The map F is called a parametrisation of $\mathcal{S}$. The expression "smooth enough" is just a convenient way of saying that the smoothness of F is such that a given definition or argument makes sense. As a consequence, the required degree of smoothness may vary from place to place. Throughout §§ 2.2-2.5, it is assumed that $F \in C^2\left(\overline{\Omega}; \mathcal{E}\right)$.[19]

For each point $X \in \mathcal{S}$, there exists a unique ordered pair $(\theta^1, \theta^2) \in \overline{\Omega}$ such that $X = F(\theta^1, \theta^2)$ – the real numbers θ^1 and θ^2 are called the Gaussian coordinates of X in the parametrisation F. The first coordinate curve passing through $X = F(\theta^1, \theta^2) \in \mathcal{S}$ is

---

[14] See also VILLAGGIO (1997, p. 62).

[15] A subset of a topological space is said to be regularly open if it coincides with the interior of its closure (*e.g.*, NOLL & VIRGA 1988, p. 12, or WILLARD 1970, p. 29).

[16] The concept of Jordan measurability is discussed, *e.g.*, in DUISTERMAAT & KOLK (2004, § 6.3) and LIMA (1989, ch. 6, § 3). If $\Omega \subset \mathbb{R}^2$ is bounded and Jordan-measurable, then so is its closure $\overline{\Omega}$ and a continuous real-valued function defined on $\overline{\Omega}$ is Riemann integrable over $\overline{\Omega}$ (DUISTERMAAT & KOLK 2004, corollary 6.3.3 and th. 6.3.5 – *vide infra*, § 2.2.4).

[17] An immersion is a differentiable map whose derivative is everywhere injective (*e.g.*, BERGER & GOSTIAUX 1987, def. 0.2.23). The requirement that $F : \overline{\Omega} \to \mathcal{E}$ be an injective immersion guarantees the existence of the tangent plane to $\mathcal{S}$ at each of its points (*vide infra*, § 2.2.3)

[18] Following KELLEY (1985, p. 85), square brackets are used in the designation of subsets of the range or domain of a map, while parentheses occur in the designation of elements belonging to those sets.

[19] This ensures the injectivity of the canonical extension of F (*vide infra*, § 2.2.5). It also ensures the applicability of Leibniz rule to compute the partial derivative $D_1\omega$ of the map $\omega : \overline{\Omega} \to \mathbb{R}$, to be defined in § 2.3 – *vide infra*, equation (2.3.16) and note 24.

the image under F of $(\mathbb{R}\times\{\theta^2\})\cap\overline{\Omega}$ – in other words, it is the set consisting of all points in $\mathcal{S}$ having the same second Gaussian coordinate θ^2 as X. The second coordinate curve passing through X is similarly defined – see figure 2.2.2. The maps

$$\overline{x}_i = \hat{x}_i \circ F : \overline{\Omega} \to \mathbb{R} \ , \tag{2.2.2}$$

which have the same degree of smoothness as F, assign to each $(\theta^1,\theta^2)\in\overline{\Omega}$ the Cartesian coordinates of the point $F(\theta^1,\theta^2)\in\mathcal{S}$.

Of course, there is a great deal of freedom in choosing one particular parametrisation for $\mathcal{S}$. In the present work, we adopt a parametrisation $F:\overline{\Omega}\to\mathcal{E}$ with the following specific features (see figure 2.2.2):

(i) $\overline{\Omega}$ is a vertically simple region of $\mathbb{R}^2$ of the form

$$\overline{\Omega} = \left\{(\theta^1,\theta^2)\in\mathbb{R}^2 \,\middle|\, 0\le\theta^1\le L \text{ and } g_1(\theta^1)\le\theta^2\le g_2(\theta^1)\right\} \ , \tag{2.2.3}$$

where g_1 and g_2 are real-valued continuous functions on $[0,L]$ satisfying the conditions $g_1(\theta^1) < g_2(\theta^1)$ and $0\in\left[g_1(\theta^1),\, g_2(\theta^1)\right]$ for every $\theta^1\in[0,L]$.

(ii) For fixed $\theta^1\in[0,L]$, the partial map $\theta^2\mapsto F(\theta^1,\theta^2)$ defined on the interval $\left[g_1(\theta^1),\, g_2(\theta^1)\right]$ is an arc-length parametrisation of $\mathcal{L}_{\theta^1}$ (hence $\overline{x}_1(\theta^1,\theta^2)=\theta^1$ everywhere on $\overline{\Omega}$).

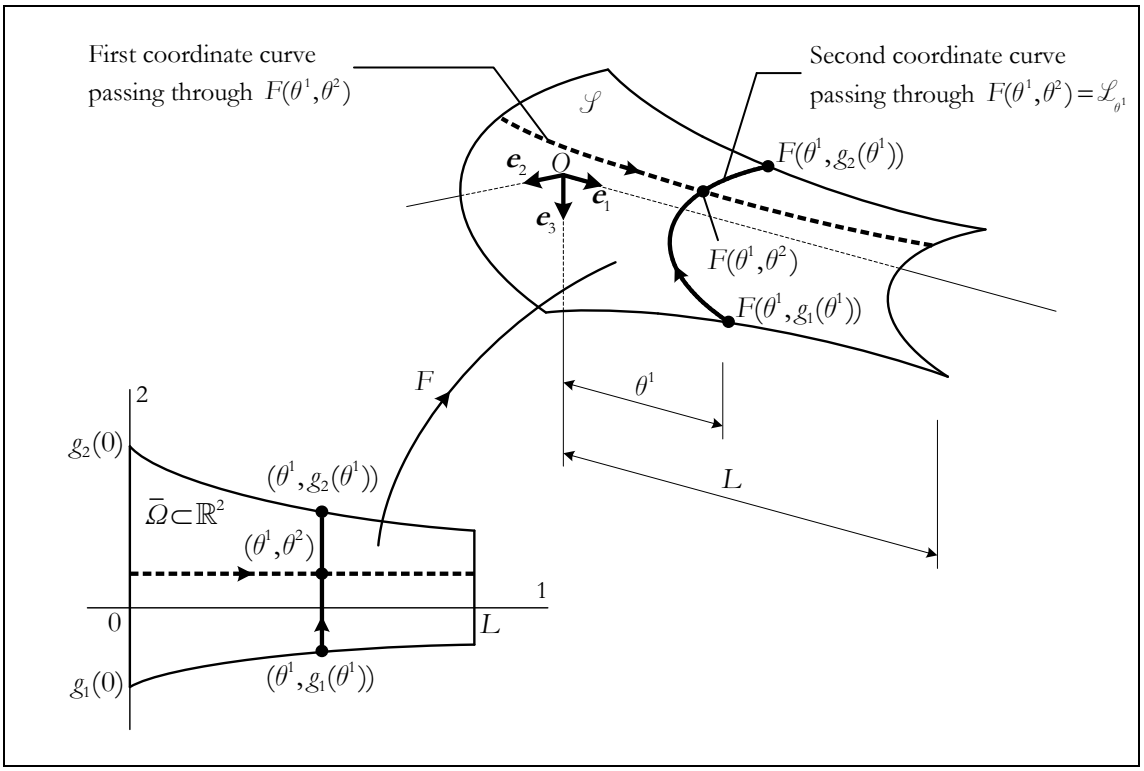

Figure 2.2.2: Parametrisation of $\mathcal{S}$

2.2.3 The tangent planes to $\mathcal{S}$

For each $(\theta^1, \theta^2) \in \overline{\Omega}$, define the vectors

$$\boldsymbol{a}_\alpha(\theta^1, \theta^2) = D_\alpha F(\theta^1, \theta^2) \ .^{20} \tag{2.2.4}$$

Since $F \in C^2\left(\overline{\Omega}; \mathcal{E}\right)$, the maps $(\theta^1, \theta^2) \in \overline{\Omega} \mapsto D_\alpha F(\theta^1, \theta^2) \in \mathcal{V}$ thus defined are continuously differentiable on $\overline{\Omega}$ (*e.g.*, ABRAHAM *et al.* 1988, prop. 2.4.12, which can be easily extended to functions whose domain is the closure of an open subset of $\mathbb{R}^2$). The vectors $\boldsymbol{a}_\alpha(\theta^1, \theta^2)$ are tangent to the coordinate curves passing through the point $F(\theta^1, \theta^2) \in \mathcal{S}$. Moreover, since F is an immersion, they are linearly independent and span a two-dimensional subspace of $\mathcal{V}$, called the tangent plane to $\mathcal{S}$ at $F(\theta^1, \theta^2)$ and denoted $T_{F(\theta^1, \theta^2)}\mathcal{S}$ (*e.g.*, BLOCH 1997, § 1.3, CARMO 1976, § 2.4, KÜHNEL 2005, p. 57, or MONTIEL & ROS 2005, § 2.5) – see figure 2.2.3.[21] The ordered basis $\left\{\boldsymbol{a}_1(\theta^1, \theta^2), \boldsymbol{a}_2(\theta^1, \theta^2)\right\}$ for $T_{F(\theta^1, \theta^2)}\mathcal{S}$ is called the covariant basis at $(\theta^1, \theta^2) \in \overline{\Omega}$ associated with the parametrisation F – *e.g.*, CIARLET (2000, p. 68), CIARLET (2005, p. 59), or the classic work of GREEN & ZERNA (1968, p. 33).

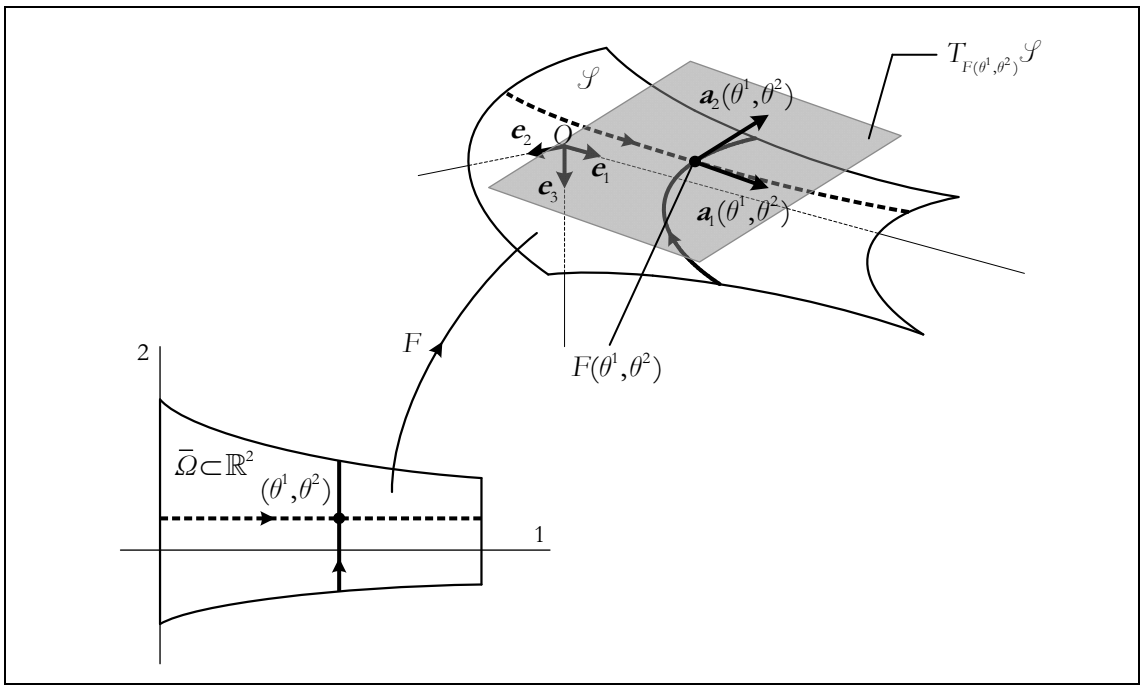

Figure 2.2.3: The tangent plane to $\mathcal{S}$ at $F(\theta^1, \theta^2)$ and the covariant basis at $(\theta^1, \theta^2) \in \overline{\Omega}$ associated with the parametrisation F

[20] The partial derivatives $D_\alpha F(\theta^1, \theta^2) \in \mathcal{L}\left(\mathbb{R}, \mathcal{V}\right)$, where $\mathcal{L}\left(\mathbb{R}, \mathcal{V}\right)$ is the space of all linear transformations from $\mathbb{R}$ into $\mathcal{V}$, have been identified with the vectors $D_\alpha F(\theta^1, \theta^2) \cdot 1 \in \mathcal{V}$ (*e.g.*, AVEZ 1983, th. A.4.1, BERGER & GOSTIAUX 1987, remark 8.2.1.2, or DIEUDONNÉ 1960, p. 149).

[21] We are committing here a convenient *abus de langage* – the tangent plane to $\mathcal{S}$ at a point $X \in \mathcal{S}$ is in fact the affine plane $\left\{X + \boldsymbol{v} \in \mathcal{E} \,\middle|\, \boldsymbol{v} \in T_X\mathcal{S}\right\}$.

In terms of the Cartesian ordered basis $\{\boldsymbol{e}_1, \boldsymbol{e}_2, \boldsymbol{e}_3\}$, the covariant base vectors are given by

$$\boldsymbol{a}_\alpha(\theta^1, \theta^2) = D_\alpha \, \overline{x}_i(\theta^1, \theta^2) \, \boldsymbol{e}_i \ . \tag{2.2.5}$$

For our specific choice of parametrisation, we have $\overline{x}_1(\theta^1, \theta^2) = \theta^1, \forall (\theta^1, \theta^2) \in \overline{\Omega}$, and hence the preceding equation specialises into

$$\boldsymbol{a}_1(\theta^1, \theta^2) = \boldsymbol{e}_1 + D_1 \, \overline{x}_2(\theta^1, \theta^2) \, \boldsymbol{e}_2 + D_1 \, \overline{x}_3(\theta^1, \theta^2) \, \boldsymbol{e}_3 \tag{2.2.6}$$

$$\boldsymbol{a}_2(\theta^1, \theta^2) = D_2 \, \overline{x}_2(\theta^1, \theta^2) \, \boldsymbol{e}_2 + D_2 \, \overline{x}_3(\theta^1, \theta^2) \, \boldsymbol{e}_3 \ . \tag{2.2.7}$$

Moreover, for fixed θ^1, the partial map $\theta^2 \mapsto F(\theta^1, \theta^2)$ is an arc-length parametrisation of $\mathscr{L}_{\theta^1}$, and so it follows that $\boldsymbol{a}_2(\theta^1, \theta^2)$ is a unit vector tangent at $F(\theta^1, \theta^2)$ to $\mathscr{L}_{\theta^1}$ – recall the second feature characterising our choice of parametrisation and see, *e.g.*, BERGER & GOSTIAUX (1987, § 8.3), KÜHNEL (2005, lemma 2.2) or MONTIEL & ROS (2005, § 1.3).

2.2.4 The first fundamental form of $\mathscr{S}$

Given a point X in $\mathscr{S} \subset \mathscr{E}$, the tangent plane $T_X\mathscr{S}$ is a two-dimensional subspace of $\mathscr{V}$. The restriction to $T_X\mathscr{S}$ of the inner product on $\mathscr{V}$ is clearly an inner product on $T_X\mathscr{S}$ (*i.e.*, a positive definite, symmetric bilinear form on $T_X\mathscr{S}$ – *e.g.*, HOFFMAN & KUNZE 1971, p. 368). To this inner product there corresponds a quadratic form $\mathrm{I}_X : T_X\mathscr{S} \to \mathbb{R}$ given by $\mathrm{I}_X(\boldsymbol{v}) = \boldsymbol{v} \cdot \boldsymbol{v} = \|\boldsymbol{v}\|^2$, called the first fundamental form of $\mathscr{S}$ at $X \in \mathscr{S}$. The first fundamental form of $\mathscr{S}$ is the map $X \mapsto \mathrm{I}_X$ that assigns to each point X in $\mathscr{S}$ the quadratic form I_X. Therefore, the first fundamental form is merely the expression of how the surface $\mathscr{S}$ inherits the inner product on $\mathscr{V}$.

The first fundamental form was defined above with no reference to a particular choice of parametrisation. Now, let $F : \overline{\Omega} \to \mathscr{E}$ be a parametrisation of $\mathscr{S}$ and let $X = F(\theta^1, \theta^2)$, $(\theta^1, \theta^2) \in \overline{\Omega}$. With respect to the covariant basis at (θ^1, θ^2), $\{\boldsymbol{a}_1(\theta^1, \theta^2), \boldsymbol{a}_2(\theta^1, \theta^2)\}$, the quadratic form I_X is entirely determined by the so-called metric coefficients

$$a_{\alpha\beta}(\theta^1, \theta^2) = \boldsymbol{a}_\alpha(\theta^1, \theta^2) \cdot \boldsymbol{a}_\beta(\theta^1, \theta^2) \ . \tag{2.2.8}$$

Indeed, for $\boldsymbol{v} = v^\alpha \, \boldsymbol{a}_\alpha(\theta^1, \theta^2) \in T_X\mathscr{S}$, one has

$$\begin{aligned} \mathrm{I}_X(\boldsymbol{v}) &= \left(v^\alpha \, \boldsymbol{a}_\alpha(\theta^1, \theta^2)\right) \cdot \left(v^\beta \, \boldsymbol{a}_\beta(\theta^1, \theta^2)\right) = v^\alpha \, v^\beta \, \boldsymbol{a}_\alpha(\theta^1, \theta^2) \cdot \boldsymbol{a}_\beta(\theta^1, \theta^2) \\ &= v^\alpha \, v^\beta \, a_{\alpha\beta}(\theta^1, \theta^2) \ . \end{aligned} \tag{2.2.9}$$

The metric coefficients satisfy

$$a_{\alpha\beta}(\theta^1,\theta^2)=a_{\beta\alpha}(\theta^1,\theta^2) \tag{2.2.10}$$

$$a_{11}(\theta^1,\theta^2)=\left\|\boldsymbol{a}_1(\theta^1,\theta^2)\right\|^2>0 \tag{2.2.11}$$

$$a_{22}(\theta^1,\theta^2)=\left\|\boldsymbol{a}_2(\theta^1,\theta^2)\right\|^2>0 \tag{2.2.12}$$

$$a_{11}(\theta^1,\theta^2)\,a_{22}(\theta^1,\theta^2)-\left(a_{12}(\theta^1,\theta^2)\right)^2>0\ , \tag{2.2.13}$$

the last property being a direct consequence of the Cauchy-Schwartz inequality (*e.g.*, HOFFMAN & KUNZE 1971, pp. 277-278), together with the fact that the vectors $\boldsymbol{a}_1(\theta^1,\theta^2)$ and $\boldsymbol{a}_2(\theta^1,\theta^2)$ are linearly independent. In brief, the matrix

$$\left[a_{\alpha\beta}(\theta^1,\theta^2)\right]=\begin{bmatrix} a_{11}(\theta^1,\theta^2) & a_{12}(\theta^1,\theta^2)\\ a_{21}(\theta^1,\theta^2) & a_{22}(\theta^1,\theta^2)\end{bmatrix} \tag{2.2.14}$$

is symmetric and positive definite (*e.g.*, MAGALHÃES 2003, th. 6.32). Moreover, if $F\in C^2\left(\overline{\Omega};\mathcal{E}\right)$, then the real-valued maps $(\theta^1,\theta^2)\mapsto a_{\alpha\beta}(\theta^1,\theta^2)$ and $(\theta^1,\theta^2)\mapsto a(\theta^1,\theta^2)=\det\left[a_{\alpha\beta}(\theta^1,\theta^2)\right]$ are of class C^1. Specifically, in view of (2.2.6)-(2.2.7),

$$a_{11}(\theta^1,\theta^2)=1+\left(D_1\,\overline{x}_2(\theta^1,\theta^2)\right)^2+\left(D_1\,\overline{x}_3(\theta^1,\theta^2)\right)^2 \tag{2.2.15}$$

$$a_{12}(\theta^1,\theta^2)=a_{21}(\theta^1,\theta^2)=D_1\,\overline{x}_2(\theta^1,\theta^2)\,D_2\,\overline{x}_2(\theta^1,\theta^2)+D_1\,\overline{x}_3(\theta^1,\theta^2)\,D_2\,\overline{x}_3(\theta^1,\theta^2) \tag{2.2.16}$$

$$a_{22}(\theta^1,\theta^2)=\left(D_2\,\overline{x}_2(\theta^1,\theta^2)\right)^2+\left(D_2\,\overline{x}_3(\theta^1,\theta^2)\right)^2=1 \tag{2.2.17}$$

$$a(\theta^1,\theta^2)=1+\left(D_1\,\overline{x}_2(\theta^1,\theta^2)\,D_2\,\overline{x}_3(\theta^1,\theta^2)-D_2\,\overline{x}_2(\theta^1,\theta^2)\,D_1\,\overline{x}_3(\theta^1,\theta^2)\right)^2\ . \tag{2.2.18}$$

The first fundamental form allows us to make measurements on the surface – length of curves, angles between intersecting curves, areas of regions – without referring back to the ambient space $\mathcal{E}$ where the surface lies. For instance, the angle between the coordinate curves at $X=F(\theta^1,\theta^2)\in\mathcal{S}$ is defined to be the angle between the vectors $\boldsymbol{a}_1(\theta^1,\theta^2)$ and $\boldsymbol{a}_2(\theta^1,\theta^2)$ and, therefore, is given by

$$\cos\alpha(\theta^1,\theta^2)=\frac{a_{12}(\theta^1,\theta^2)}{\sqrt{a_{11}(\theta^1,\theta^2)\,a_{22}(\theta^1,\theta^2)}}\ . \tag{2.2.19}$$

Accordingly, the coordinate curves are orthogonal at X if and only if $a_{12}(\theta^1,\theta^2)=0$. In view of (2.2.16), this is not necessarily the case for our specific choice of parametrisation, a fact that cannot be overemphasised.

The area form $dS(X)$ at $X=F(\theta^1,\theta^2)\in\mathcal{S}$ is defined as (CIARLET 2000, th. 2.1-1, or CIARLET 2005, th. 2.3-1)

$$dS(X) = \sqrt{a(\theta^1, \theta^2)}\, d\theta^1 d\theta^2 \ . \tag{2.2.20}$$

The integrals of continuous real-valued functions defined on $\mathcal{S}$ can now be computed by referring them back to $\overline{\Omega}$:

$$\int_{\mathcal{S}} f(X)\, dS(X) = \int_{\overline{\Omega}} \big(f \circ F\big)(\theta^1, \theta^2) \sqrt{a(\theta^1, \theta^2)}\, d\theta^1 d\theta^2 \ . \tag{2.2.21}$$

Observe that the integrand on the right-hand side of (2.2.21) is continuous on the compact (*i.e.*, closed and bounded) and Jordan measurable set $\overline{\Omega} \subset \mathbb{R}^2$, and is thus Riemann integrable over $\overline{\Omega}$ (*vide supra*, note 16). In particular, the area of $\mathcal{S}$ is

$$\int_{\mathcal{S}} dS(X) = \int_{\overline{\Omega}} \sqrt{a(\theta^1, \theta^2)}\, d\theta^1 d\theta^2 \ . \tag{2.2.22}$$

Moreover, $\overline{\Omega}$ was specifically chosen as a vertically simple region of $\mathbb{R}^2$, and consequently the integral on the right-hand side of (2.2.21) can be written as an iterated integral (DUISTERMAAT & KOLK 2004, th. 6.4.5):

$$\int_{\overline{\Omega}} \big(f \circ F\big)(\theta^1, \theta^2) \sqrt{a(\theta^1, \theta^2)}\, d\theta^1 d\theta^2 = \int_0^L \left[\int_{g_1(\theta^1)}^{g_2(\theta^1)} \big(f \circ F\big)(\theta^1, \theta^2) \sqrt{a(\theta^1, \theta^2)}\, d\theta^2 \right] d\theta^1 \ . \tag{2.2.23}$$

* * *

Given a point X in $\mathcal{S}$, the tangent space $T_X\mathcal{S}$ can be written as the direct sum of (i) the subspace $\mathcal{T}_X$ of all vectors tangent at X to the cross-section middle line passing through that point and (ii) the orthogonal complement of $\mathcal{T}_X$, denoted by $\mathcal{T}_X^{\perp}$:

$$T_X\mathcal{S} = \mathcal{T}_X \oplus \mathcal{T}_X^{\perp} \ . \tag{2.2.24}$$

This direct-sum decomposition of $T_X\mathcal{S}$ has an intrinsic geometrical meaning (independent of the choice of parametrisation for $\mathcal{S}$). It is therefore natural to consider an orthonormal basis for $T_X\mathcal{S}$ with one member in $\mathcal{T}_X$ and the other in $\mathcal{T}_X^{\perp}$.

If we insist on viewing $\mathcal{S}$ through the parametrisation $F : \overline{\Omega} \to \mathcal{E}$, the point $X \in \mathcal{S}$ is identified with its Gaussian coordinates $(\theta^1, \theta^2) \in \overline{\Omega}$ (relative to F) and

$$\mathcal{T}_X = \operatorname{span}\big\{\boldsymbol{a}_2(\theta^1, \theta^2)\big\} \ . \tag{2.2.25}$$

For definiteness, the desired orthonormal ordered basis for $T_{F(\theta^1, \theta^2)}\mathcal{S}$, which we shall denote by $\big\{\boldsymbol{o}_{\mathrm{I}}(\theta^1, \theta^2), \boldsymbol{o}_{\mathrm{II}}(\theta^1, \theta^2)\big\}$,[22] is constructed so as to exhibit the following properties:

[22] To distinguish between the two ordered bases for $T_{F(\theta^1, \theta^2)}\mathcal{S}$, $\big\{\boldsymbol{a}_1(\theta^1, \theta^2), \boldsymbol{a}_2(\theta^1, \theta^2)\big\}$ and $\big\{\boldsymbol{o}_{\mathrm{I}}(\theta^1, \theta^2), \boldsymbol{o}_{\mathrm{II}}(\theta^1, \theta^2)\big\}$, we shall employ upper-case Greek letters and Roman numerals for the indices pertaining to the orthonormal basis, which therefore take values in the set $\{\mathrm{I}, \mathrm{II}\}$. The summation convention applies, as usual, to twice-repeated upper-case Greek indices.

(i) $\boldsymbol{o}_{\mathrm{II}}(\theta^1,\theta^2)=\boldsymbol{a}_2(\theta^1,\theta^2)$ and (ii) the new basis and the covariant basis have the same orientation. A trivial application of the Gram-Schmidt process (*e.g.*, HOFFMAN & KUNZE 1971, pp. 280-281) yields

$$\boldsymbol{o}_{\Sigma}(\theta^1,\theta^2)=C_{\Sigma}^{\cdot\alpha}(\theta^1,\theta^2)\,\boldsymbol{a}_{\alpha}(\theta^1,\theta^2)\ , \tag{2.2.26}$$

with

$$\begin{aligned} C_{\mathrm{I}}^{\cdot 1}(\theta^1,\theta^2)&=\frac{1}{\sqrt{1+\left(D_1\,\overline{x}_2(\theta^1,\theta^2)\,D_2\,\overline{x}_3(\theta^1,\theta^2)-D_2\,\overline{x}_2(\theta^1,\theta^2)\,D_1\,\overline{x}_3(\theta^1,\theta^2)\right)^2}}\\ &=\frac{1}{\sqrt{a(\theta^1,\theta^2)}} \end{aligned} \tag{2.2.27}$$

$$\begin{aligned} C_{\mathrm{I}}^{\cdot 2}(\theta^1,\theta^2)&=-\frac{D_1\,\overline{x}_2(\theta^1,\theta^2)\,D_2\,\overline{x}_2(\theta^1,\theta^2)+D_1\,\overline{x}_3(\theta^1,\theta^2)\,D_2\,\overline{x}_3(\theta^1,\theta^2)}{\sqrt{1+\left(D_1\,\overline{x}_2(\theta^1,\theta^2)\,D_2\,\overline{x}_3(\theta^1,\theta^2)-D_2\,\overline{x}_2(\theta^1,\theta^2)\,D_1\,\overline{x}_3(\theta^1,\theta^2)\right)^2}}\\ &=-\frac{a_{12}(\theta^1,\theta^2)}{\sqrt{a(\theta^1,\theta^2)}} \end{aligned} \tag{2.2.28}$$

$$C_{\mathrm{II}}^{\cdot 1}(\theta^1,\theta^2)=0 \tag{2.2.29}$$

$$C_{\mathrm{II}}^{\cdot 2}(\theta^1,\theta^2)=1\ . \tag{2.2.30}$$

2.2.5 Through-the-thickness description

To each $(\theta^1,\theta^2)\in\overline{\Omega}$ we can easily assign a unit vector $\boldsymbol{a}_3(\theta^1,\theta^2)$ orthogonal to $T_{F(\theta^1,\theta^2)}\mathscr{S}$ by setting

$$\begin{aligned} \boldsymbol{a}_3(\theta^1,\theta^2)&=\frac{\boldsymbol{a}_1(\theta^1,\theta^2)\times\boldsymbol{a}_2(\theta^1,\theta^2)}{\left\|\boldsymbol{a}_1(\theta^1,\theta^2)\times\boldsymbol{a}_2(\theta^1,\theta^2)\right\|}=\frac{\boldsymbol{a}_1(\theta^1,\theta^2)\times\boldsymbol{a}_2(\theta^1,\theta^2)}{\sqrt{a(\theta^1,\theta^2)}}\\ &=\boldsymbol{o}_{\mathrm{I}}(\theta^1,\theta^2)\times\boldsymbol{o}_{\mathrm{II}}(\theta^1,\theta^2)\ . \end{aligned} \tag{2.2.31}$$

Except for negligible inaccuracies near the end sections $\mathscr{A}_0$ and $\mathscr{A}_L$, the reference shape $\mathscr{B}\subset\mathscr{E}$ of the tapered thin-walled bar with open cross-sections can now be described as the image of the set $\overline{\Omega}\times\left[-\frac{1}{2},\frac{1}{2}\right]\subset\mathbb{R}^3$ under the map given by

$$\mathfrak{F}(\theta^1,\theta^2,\theta^3)=F(\theta^1,\theta^2)+\theta^3\,t(\theta^1,\theta^2)\,\boldsymbol{a}_3(\theta^1,\theta^2)\ , \tag{2.2.32}$$

where the map $(\theta^1,\theta^2)\in\overline{\Omega}\mapsto t(\theta^1,\theta^2)\in\mathbb{R}^+$, assumed to be continuous, defines the wall thickness at each point $F(\theta^1,\theta^2)$ of the middle surface $\mathscr{S}$. The map $\mathfrak{F}:\overline{\Omega}\times\left[-\frac{1}{2},\frac{1}{2}\right]\to\mathscr{E}$ given by equation (2.2.32) is called the canonical extension of the parametrisation F (CIARLET 2000, p. 144) and the coordinate $\theta^3\in\left[-\frac{1}{2},\frac{1}{2}\right]$ is called the transverse variable.

Since $F \in C^2\left(\overline{\Omega}; \mathcal{E}\right)$, it can be shown that its canonical extension $\mathfrak{F}$ is injective provided that $t_{\max} = \max_{(\theta^1,\theta^2)\in\overline{\Omega}} \left\{t(\theta^1,\theta^2)\right\}$ is small enough (CIARLET 2000, th. 3.1-1), a fact that will be taken for granted. The geometrical description of $\mathcal{B}$ embodied in equation (2.2.32) is therefore a meaningful one, in the sense that to each point $X \in \mathcal{B}$ there corresponds a unique ordered triplet $(\theta^1,\theta^2,\theta^3) \in \overline{\Omega}\times\left[-\tfrac{1}{2},\tfrac{1}{2}\right]$ such that $X = \mathfrak{F}(\theta^1,\theta^2,\theta^3)$.

2.3 KINEMATICS

The one-dimensional model developed in this chapter rests upon regarding a tapered thin-walled bar with open cross-sections as a membrane shell that is subjected to the following internal constraints:

(V1) To within the first-order, each cross-section middle line does not deform in its own plane.

(V2) On the middle surface of the bar, the linearised shear strain $\gamma_{\text{I·II}} = \gamma_{\text{II·I}}$ vanishes.

These constraints are clearly an extension to the tapered case of the hypotheses underpinning the classical theory of Vlasov for prismatic thin-walled open beams (VLASOV 1961, p. 7).

Let the smooth enough map $\boldsymbol{U} : \overline{\Omega} \to \mathcal{V}$ represent a displacement field of the middle surface $\mathcal{S} = F\left[\overline{\Omega}\right]$ of the bar, *i.e.*, for each $(\theta^1,\theta^2) \in \overline{\Omega}$, the vector $\boldsymbol{U}(\theta^1,\theta^2)$ is the displacement of the (material) point (whose reference place is) $F(\theta^1,\theta^2) \in \mathcal{S}$.[23] In this section, we shall examine the restrictions placed on $\boldsymbol{U}$ by the constraints (V1)-(V2).

According to (V1), the displacement of an arbitrary cross-section middle line $\mathcal{L}_{\theta^1}$, $\theta^1 \in \left[0, L\right]$ – that is, the restriction to $\{\theta^1\}\times\left[g_1(\theta^1), g_2(\theta^1)\right]$ of $\boldsymbol{U} : \overline{\Omega} \to \mathcal{V}$ – can be broken down into (i) an infinitesimal rigid displacement (GURTIN 1972, pp. 30-32, GURTIN 1981, pp. 55-56)

$$\boldsymbol{W}(\theta^1) + \boldsymbol{\Phi}(\theta^1)\times\left(\overline{x}_2(\theta^1,\theta^2)\,\boldsymbol{e}_2 + \overline{x}_3(\theta^1,\theta^2)\,\boldsymbol{e}_3\right), \tag{2.3.1}$$

specified by the vectors $\boldsymbol{W}(\theta^1) = W_i(\theta^1)\,\boldsymbol{e}_i$ and $\boldsymbol{\Phi}(\theta^1) = \Phi_i(\theta^1)\,\boldsymbol{e}_i$, (ii) followed by an out-of-plane warping displacement $f(\theta^1,\theta^2)$ normal to the plane of the rotated middle line (*i.e.*, along $\boldsymbol{e}_1 + \boldsymbol{\Phi}(\theta^1)\times\boldsymbol{e}_1$), which, upon retaining only first-order terms, reduces to

[23] This approach is not entirely intrinsic, since we are viewing the displacement field $\boldsymbol{U}$ through the parametrisation F and not as an object defined on the surface $\mathcal{S}$ itself. With the usual identification of $\mathcal{L}\left(\mathbb{R},\mathcal{V}\right)$ with $\mathcal{V}$ (*vide supra*, note 20), the partial derivatives $D_\alpha\boldsymbol{U}$ are again maps from $\overline{\Omega}$ into $\mathcal{V}$. We will loosely refer to maps defined on $\overline{\Omega}$ as fields.

$$f(\theta^1,\theta^2)\,\boldsymbol{e}_1\ . \tag{2.3.2}$$

Therefore, a displacement field $\boldsymbol{U}:\overline{\Omega}\to\mathcal{V}$ consistent with the constraint (V1) admits the representation (cf. SIMO & VU-QUOC 1991, eq. 10)

$$\boldsymbol{U}(\theta^1,\theta^2)=\boldsymbol{W}(\theta^1)+\boldsymbol{\Phi}(\theta^1)\times\left(\overline{x}_2(\theta^1,\theta^2)\,\boldsymbol{e}_2+\overline{x}_3(\theta^1,\theta^2)\,\boldsymbol{e}_3\right)+f(\theta^1,\theta^2)\,\boldsymbol{e}_1 \tag{2.3.3}$$

or, in terms of Cartesian components,

$$U_1(\theta^1,\theta^2)=\boldsymbol{U}(\theta^1,\theta^2)\cdot\boldsymbol{e}_1=W_1(\theta^1)+\overline{x}_3(\theta^1,\theta^2)\Phi_2(\theta^1)-\overline{x}_2(\theta^1,\theta^2)\Phi_3(\theta^1)+f(\theta^1,\theta^2) \tag{2.3.4}$$

$$U_2(\theta^1,\theta^2)=\boldsymbol{U}(\theta^1,\theta^2)\cdot\boldsymbol{e}_2=W_2(\theta^1)-\overline{x}_3(\theta^1,\theta^2)\Phi_1(\theta^1) \tag{2.3.5}$$

$$U_3(\theta^1,\theta^2)=\boldsymbol{U}(\theta^1,\theta^2)\cdot\boldsymbol{e}_3=W_3(\theta^1)+\overline{x}_2(\theta^1,\theta^2)\Phi_1(\theta^1)\ . \tag{2.3.6}$$

In the representation (2.3.4) for the displacement component along $\boldsymbol{e}_1$, the sum $W_1(\theta^1)+f(\theta^1,\theta^2)$ is well-defined, but the individual terms $W_1(\theta^1)$ and $f(\theta^1,\theta^2)$ are not. This undesirable feature is circumvented by appending the condition

$$f(\theta^1,0)=0,\ \forall\theta^1\in[0,L]\ . \tag{2.3.7}$$

We now turn to the examination of the constraint (V2). Let $\boldsymbol{\gamma}$ denote the linearised membrane strain tensor field (or linearised change of metric tensor field) associated with a given (smooth enough) displacement field $\boldsymbol{U}$. The corresponding covariant component fields are given by (BLOUZA & LE DRET 1999, lemma 2, CIARLET 2000, th. 2.4-1, CIARLET 2005, th. 4.2-1)

$$\begin{aligned}\gamma_{\alpha\beta}(\theta^1,\theta^2)&=\boldsymbol{a}_\alpha(\theta^1,\theta^2)\cdot\boldsymbol{\gamma}(\theta^1,\theta^2)\,\boldsymbol{a}_\beta(\theta^1,\theta^2)\\&=\frac{1}{2}\left(\boldsymbol{a}_\alpha(\theta^1,\theta^2)\cdot D_\beta\boldsymbol{U}(\theta^1,\theta^2)+\boldsymbol{a}_\beta(\theta^1,\theta^2)\cdot D_\alpha\boldsymbol{U}(\theta^1,\theta^2)\right)\ .\end{aligned} \tag{2.3.8}$$

The substitution of (2.2.6)-(2.2.7) and (2.3.5)-(2.3.6) into this definition yields, after routine calculations,

$$\begin{aligned}\gamma_{11}(\theta^1,\theta^2)&=D_1U_1(\theta^1,\theta^2)+D_1\overline{x}_2(\theta^1,\theta^2)\left(W_2'(\theta^1)-\overline{x}_3(\theta^1,\theta^2)\Phi_1'(\theta^1)\right)\\&\quad+D_1\overline{x}_3(\theta^1,\theta^2)\left(W_3'(\theta^1)+\overline{x}_2(\theta^1,\theta^2)\Phi_1'(\theta^1)\right)\end{aligned} \tag{2.3.9}$$

$$\begin{aligned}\gamma_{12}(\theta^1,\theta^2)=\gamma_{21}(\theta^1,\theta^2)&=\frac{1}{2}\Big[D_2U_1(\theta^1,\theta^2)+D_2\overline{x}_2(\theta^1,\theta^2)\left(W_2'(\theta^1)-\overline{x}_3(\theta^1,\theta^2)\Phi_1'(\theta^1)\right)\\&\quad+D_2\overline{x}_3(\theta^1,\theta^2)\left(W_3'(\theta^1)+\overline{x}_2(\theta^1,\theta^2)\Phi_1'(\theta^1)\right)\Big]\end{aligned} \tag{2.3.10}$$

$$\gamma_{22}(\theta^1,\theta^2)=0\ . \tag{2.3.11}$$

In view of (2.2.26), the components of $\boldsymbol{\gamma}(\theta^1,\theta^2)$ with respect to the orthonormal ordered basis $\{\boldsymbol{o}_{\mathrm{I}}(\theta^1,\theta^2),\boldsymbol{o}_{\mathrm{II}}(\theta^1,\theta^2)\}$ are related to the above covariant components via

$$\begin{aligned}\gamma_{\Sigma\Lambda}(\theta^1,\theta^2) &= \boldsymbol{o}_{\Sigma}(\theta^1,\theta^2)\cdot\boldsymbol{\gamma}(\theta^1,\theta^2)\,\boldsymbol{o}_{\Lambda}(\theta^1,\theta^2)\\ &= C_{\Sigma}^{\cdot\alpha}(\theta^1,\theta^2)\,C_{\Lambda}^{\cdot\beta}(\theta^1,\theta^2)\,\gamma_{\alpha\beta}(\theta^1,\theta^2)\ .\end{aligned}\tag{2.3.12}$$

In particular, one finds

$$\gamma_{\mathrm{I}\cdot\mathrm{II}}(\theta^1,\theta^2)=\gamma_{\mathrm{II}\cdot\mathrm{I}}(\theta^1,\theta^2)=\left(C_{\mathrm{I}}^{\cdot 1}(\theta^1,\theta^2)C_{\mathrm{II}}^{\cdot 2}(\theta^1,\theta^2)+C_{\mathrm{I}}^{\cdot 2}(\theta^1,\theta^2)C_{\mathrm{II}}^{\cdot 1}(\theta^1,\theta^2)\right)\gamma_{12}(\theta^1,\theta^2),\tag{2.3.13}$$

and hence the constraint (V2), requiring that $\gamma_{\mathrm{I}\cdot\mathrm{II}}(\theta^1,\theta^2)=0,\ \forall(\theta^1,\theta^2)\in\overline{\Omega}$, is in fact equivalent to $\gamma_{12}(\theta^1,\theta^2)=0,\ \forall(\theta^1,\theta^2)\in\overline{\Omega}$.

It now follows from (2.3.10) that

$$\begin{aligned}D_2U_1(\theta^1,\theta^2) &= -D_2\overline{x}_2(\theta^1,\theta^2)\left(W_2'(\theta^1)-\overline{x}_3(\theta^1,\theta^2)\Phi_1'(\theta^1)\right)\\ &\quad -D_2\overline{x}_3(\theta^1,\theta^2)\left(W_3'(\theta^1)+\overline{x}_2(\theta^1,\theta^2)\Phi_1'(\theta^1)\right)\end{aligned}\tag{2.3.14}$$

and, after integration with respect to the second Gaussian coordinate, one finds

$$\begin{aligned}U_1(\theta^1,\theta^2) &= U_1(\theta^1,0)+\overline{x}_2(\theta^1,0)W_2'(\theta^1)+\overline{x}_3(\theta^1,0)W_3'(\theta^1)\\ &\quad -\overline{x}_2(\theta^1,\theta^2)W_2'(\theta^1)-\overline{x}_3(\theta^1,\theta^2)W_3'(\theta^1)-\omega(\theta^1,\theta^2)\Phi_1'(\theta^1)\ ,\end{aligned}\tag{2.3.15}$$

with

$$\omega(\theta^1,\theta^2)=\int_0^{\theta^2}\left(\overline{x}_2(\theta^1,s)D_2\overline{x}_3(\theta^1,s)-\overline{x}_3(\theta^1,s)D_2\overline{x}_2(\theta^1,s)\right)ds\ .\tag{2.3.16}$$

For fixed $\theta^1\in[0,L]$, the restriction of ω to $\{\theta^1\}\times[g_1(\theta^1),g_2(\theta^1)]$ represents a sectorial coordinate on $\mathscr{L}_{\theta^1}$ (viewed through the parametrisation F, of course), with origin at $F(\theta^1,0)$ and pole at $O+\theta^1\boldsymbol{e}_1$ (VLASOV 1961, p. 16) – see figure 2.3.1 for a geometrical interpretation. Moreover, by definition, $\omega(\theta^1,0)=0,\ \forall\theta^1\in[0,L]$. The field $\omega:\overline{\Omega}\to\mathbb{R}$ is continuous on $\overline{\Omega}$, with continuous partial derivative $D_1\omega$.[24]

[24] Let $(\theta^1,\theta^2)\in\Omega$. Using Leibniz rule to differentiate under the integral sign (*e.g.*, BARTLE 1967, th. 23.10),

$$\begin{aligned}D_1\omega(\theta^1,\theta^2) &= \int_0^{\theta^2}\left(D_1\overline{x}_2(\theta^1,s)D_2\overline{x}_3(\theta^1,s)+\overline{x}_2(\theta^1,s)D_1D_2\overline{x}_3(\theta^1,s)\right.\\ &\quad \left.-D_1\overline{x}_3(\theta^1,s)D_2\overline{x}_2(\theta^1,s)-\overline{x}_3(\theta^1,s)D_1D_2\overline{x}_2(\theta^1,s)\right)ds\ .\end{aligned}$$

Since the integrand is continuous and bounded on Ω, this result extends continuously to $\overline{\Omega}$ – the extended map is also written as $D_1\omega$. The author is indebted to Prof. Isabel N. Figueiredo for suggesting the use of Leibniz rule.

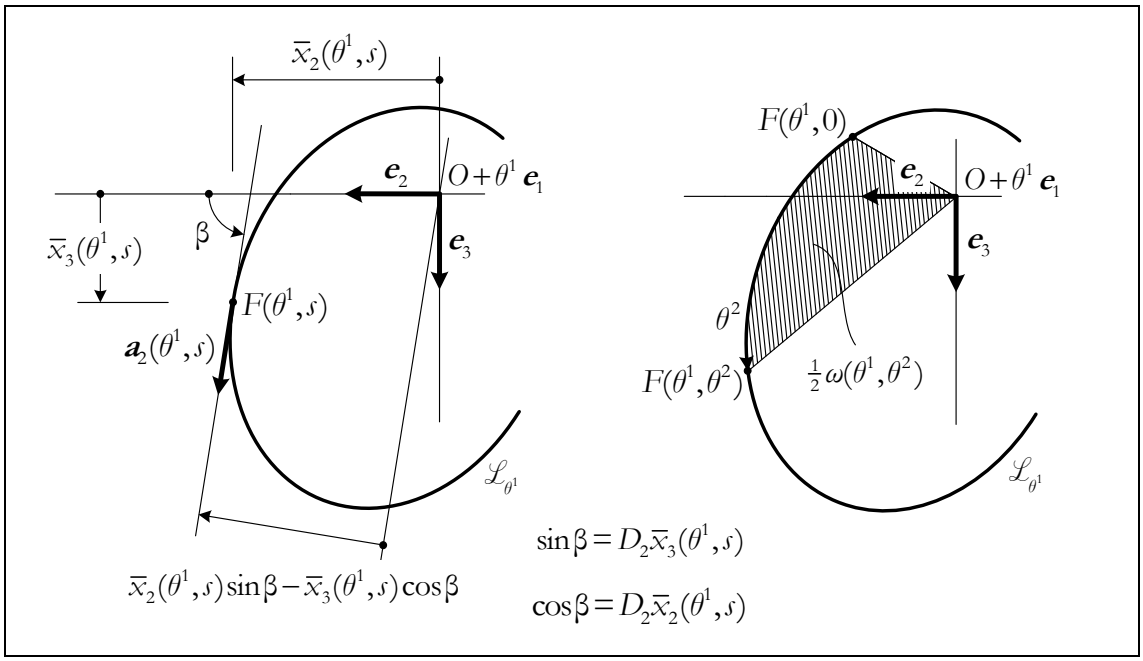

Figure 2.3.1: Restriction of ω to $\{\theta^1\}\times\left[g_1(\theta^1),\,g_2(\theta^1)\right]$ – Geometrical interpretation

Bearing in mind (2.3.7), the comparison of (2.3.4) with (2.3.15) provides

$$W_1(\theta^1)=U_1(\theta^1,0)+\bar{x}_2(\theta^1,0)W_2'(\theta^1)+\bar{x}_3(\theta^1,0)W_3'(\theta^1) \tag{2.3.17}$$

$$\Phi_2(\theta^1)=-W_3'(\theta^1) \tag{2.3.18}$$

$$\Phi_3(\theta^1)=W_2'(\theta^1)\ , \tag{2.3.19}$$

$$f(\theta^1,\theta^2)=-\omega(\theta^1,\theta^2)\Phi_1'(\theta^1) \tag{2.3.20}$$

and so we may write

$$U_1(\theta^1,\theta^2)=W_1(\theta^1)-\bar{x}_2(\theta^1,\theta^2)W_2'(\theta^1)-\bar{x}_3(\theta^1,\theta^2)W_3'(\theta^1)-\omega(\theta^1,\theta^2)\Phi_1'(\theta^1)\ . \tag{2.3.21}$$

The constraint (V2) is thus seen to place the following restrictions on a displacement field of the form (2.3.3):

(i) The (infinitesimal) rotations Φ_2 and Φ_3, about axes parallel to $\boldsymbol{e}_2$ and $\boldsymbol{e}_3$, are identified with the derivatives of W_3 and W_2 (up to sign), as in the Euler-Bernoulli beam theory.[25]

(ii) For each cross-section middle line (*i.e.*, for fixed θ^1 in the interval $[0,L]$), the out-of-plane warping displacements are given by the product of (ii$_1$) minus the rate of twist $\Phi_1'(\theta^1)$, which defines the warping amplitude, by (ii$_2$) the sectorial coordinate

[25] Observe that

$$\Phi_2(\theta^1)=-\left(\boldsymbol{\Phi}(\theta^1)\times\boldsymbol{e}_1\right)\cdot\boldsymbol{e}_3$$
$$\Phi_3(\theta^1)=\left(\boldsymbol{\Phi}(\theta^1)\times\boldsymbol{e}_1\right)\cdot\boldsymbol{e}_2\ .$$

$\omega\left|\{\theta^1\}\times\left[g_1(\theta^1),\, g_2(\theta^1)\right]\right.$, of a purely geometrical character, which provides the unit-amplitude distribution of warping displacements over the middle line $\mathscr{L}_{\theta^1}$.

In other words, Vlasov's "law of sectorial areas" for the longitudinal displacement U_1 (VLASOV 1961, p. 17) remains valid in the case of tapered members.

A displacement field $\boldsymbol{U}:\overline{\Omega}\to\mathcal{V}$ of the middle surface is called admissible if it can be represented in the form

$$\boldsymbol{U}(\theta^1,\theta^2)=\boldsymbol{W}(\theta^1)+\boldsymbol{\Phi}(\theta^1)\times\left(\overline{x}_2(\theta^1,\theta^2)\,\boldsymbol{e}_2+\overline{x}_3(\theta^1,\theta^2)\,\boldsymbol{e}_3\right)-\omega(\theta^1,\theta^2)\,\Phi_1'(\theta^1)\,\boldsymbol{e}_1\ , \tag{2.3.22}$$

$$\boldsymbol{W}(\theta^1)=W_i(\theta^1)\,\boldsymbol{e}_i \tag{2.3.23}$$

$$\boldsymbol{\Phi}(\theta^1)=\Phi_1(\theta^1)\,\boldsymbol{e}_1-W_3'(\theta^1)\,\boldsymbol{e}_2+W_2'(\theta^1)\,\boldsymbol{e}_3\ , \tag{2.3.24}$$

with (i) W_1 continuously differentiable on $[0,L]$ and (ii) W_2, W_3 and Φ_1 twice continuously differentiable on the same interval. The maps W_i $(i=1,2,3)$ and Φ_1 are collectively called the generalised displacements. In the same vein, a linearised membrane strain tensor field $\boldsymbol{\gamma}$ associated with an admissible displacement field $\boldsymbol{U}$ is labelled "admissible" as well. In the light of the previous discussion, the only non-vanishing covariant component field of an admissible $\boldsymbol{\gamma}$ is given by

$$\begin{aligned}\gamma_{11}(\theta^1,\theta^2)=W_1'(\theta^1)-\overline{x}_2(\theta^1,\theta^2)\,W_2''(\theta^1)-\overline{x}_3(\theta^1,\theta^2)\,W_3''(\theta^1)-\omega(\theta^1,\theta^2)\,\Phi_1''(\theta^1)\\ -\psi(\theta^1,\theta^2)\,\Phi_1'(\theta^1)\ ,\end{aligned} \tag{2.3.25}$$

where

$$\psi(\theta^1,\theta^2)=D_1\omega(\theta^1,\theta^2)+\overline{x}_3(\theta^1,\theta^2)\,D_1\overline{x}_2(\theta^1,\theta^2)-\overline{x}_2(\theta^1,\theta^2)\,D_1\overline{x}_3(\theta^1,\theta^2)\ . \tag{2.3.26}$$

The real-valued field ψ defined on $\overline{\Omega}$ by (2.3.26) is continuous,[26] and so is the field $\gamma_{11}:\overline{\Omega}\to\mathbb{R}$. Introducing the generalised strains

$$\varepsilon(\theta^1)=W_1'(\theta^1) \tag{2.3.27}$$

$$\kappa_1(\theta^1)=\Phi_1'(\theta^1) \tag{2.3.28}$$

$$\kappa_2(\theta^1)=-W_3''(\theta^1) \tag{2.3.29}$$

$$\kappa_3(\theta^1)=-W_2''(\theta^1) \tag{2.3.30}$$

$$\Gamma(\theta^1)=-\Phi_1''(\theta^1)\ , \tag{2.3.31}$$

equation (2.3.25) becomes

[26] *Vide supra*, note 24.

$$\gamma_{11}(\theta^1,\theta^2)=\varepsilon(\theta^1)+\overline{x}_2(\theta^1,\theta^2)\kappa_3(\theta^1)+\overline{x}_3(\theta^1,\theta^2)\kappa_2(\theta^1)+\omega(\theta^1,\theta^2)\Gamma(\theta^1)$$
$$-\psi(\theta^1,\theta^2)\kappa_1(\theta^1)\ . \tag{2.3.32}$$

The generalised strains have a clear physical meaning: (i) ε, κ_2 and κ_3 are the linearised extension and curvature components of the line segment $\left\{O+\theta^1\boldsymbol{e}_1,\,0\le\theta^1\le L\right\}$ – which, in general, is not identifiable with a material line –, upon being carried into $\left\{O+\theta^1\boldsymbol{e}_1+\boldsymbol{W}(\theta^1),\,0\le\theta^1\le L\right\}$, (ii) κ_1 is the rate of twist and (iii) Γ is the derivative of the warping amplitude (*i.e.*, the derivative of the rate of twist).

Finally, using (2.3.12) and (2.2.27), one finds that

$$\begin{aligned}\gamma_{\mathrm{I\text{-}I}}(\theta^1,\theta^2)&=\left(C_{\mathrm{I}}^{\cdot 1}(\theta^1,\theta^2)\right)^2\gamma_{11}(\theta^1,\theta^2)+2C_{\mathrm{I}}^{\cdot 1}(\theta^1,\theta^2)C_{\mathrm{I}}^{\cdot 2}(\theta^1,\theta^2)\gamma_{12}(\theta^1,\theta^2)\\&\quad+\left(C_{\mathrm{I}}^{\cdot 2}(\theta^1,\theta^2)\right)^2\gamma_{22}(\theta^1,\theta^2)\\&=\left(C_{\mathrm{I}}^{\cdot 1}(\theta^1,\theta^2)\right)^2\gamma_{11}(\theta^1,\theta^2)=\frac{\gamma_{11}(\theta^1,\theta^2)}{a(\theta^1,\theta^2)}\\&=\frac{\varepsilon(\theta^1)+\overline{x}_2(\theta^1,\theta^2)\kappa_3(\theta^1)+\overline{x}_3(\theta^1,\theta^2)\kappa_2(\theta^1)+\omega(\theta^1,\theta^2)\Gamma(\theta^1)-\psi(\theta^1,\theta^2)\kappa_1(\theta^1)}{1+\left(D_1\overline{x}_2(\theta^1,\theta^2)D_2\overline{x}_3(\theta^1,\theta^2)-D_2\overline{x}_2(\theta^1,\theta^2)D_1\overline{x}_3(\theta^1,\theta^2)\right)^2}\end{aligned} \tag{2.3.33}$$

is the only non-vanishing component field of an admissible $\boldsymbol{\gamma}$ with respect to the orthonormal ordered basis field $(\theta^1,\theta^2)\in\overline{\Omega}\mapsto\left\{\boldsymbol{o}_{\mathrm{I}}(\theta^1,\theta^2),\boldsymbol{o}_{\mathrm{II}}(\theta^1,\theta^2)\right\}$. Clearly, $\gamma_{\mathrm{I\text{-}I}}:\overline{\Omega}\to\mathbb{R}$ is continuous and can be thought of as the superposition of five basic strain modes, namely

$$\frac{1}{a}\qquad\frac{\overline{x}_2}{a}\qquad\frac{\overline{x}_3}{a}\qquad\frac{\omega}{a}\qquad-\frac{\psi}{a}\ , \tag{2.3.34}$$

whose amplitudes are modulated by the generalised strains.

2.4 MEMBRANE FORCES, ACTIVE AND REACTIVE. CONSTITUTIVE EQUATION

As shown in the preceding section, the internal constraints (V1)-(V2) restrict the value at $(\theta^1,\theta^2)\in\overline{\Omega}$ of the linearised membrane strain tensor field $\boldsymbol{\gamma}$ to lie in the space

$$\mathscr{C}_{(\theta^1,\theta^2)}=\mathrm{span}\left\{\boldsymbol{o}_{\mathrm{I}}(\theta^1,\theta^2)\otimes\boldsymbol{o}_{\mathrm{I}}(\theta^1,\theta^2)\right\}\subset Sym\left(T_{F(\theta^1,\theta^2)}\mathcal{S}\right),^{27} \tag{2.4.1}$$

[27] Let $\mathcal{U}$ be a *n*-dimensional Euclidean vector space and write $\mathscr{L}(\mathcal{U})$ for the real vector space of all linear transformations from $\mathcal{U}$ into itself, with addition and multiplication by scalars defined in the usual pointwise manner. The elements of $\mathscr{L}(\mathcal{U})$ are identified with (second-order) tensors. When there is no

called the constraint space (PODIO-GUIDUGLI 2000, § 17.2, PODIO-GUIDUGLI & VIANELLO 1992). The value at $(\theta^1, \theta^2) \in \overline{\Omega}$ of the membrane force tensor field $\boldsymbol{n}$ is then split into active (or determinate) and reactive (or latent) parts, denoted $\boldsymbol{n}^{(A)}(\theta^1, \theta^2)$ and $\boldsymbol{n}^{(R)}(\theta^1, \theta^2)$, as follows:[28]

$$\boldsymbol{n}(\theta^1, \theta^2) = \boldsymbol{n}^{(A)}(\theta^1, \theta^2) + \boldsymbol{n}^{(R)}(\theta^1, \theta^2) \tag{2.4.2}$$

$$\boldsymbol{n}^{(A)}(\theta^1, \theta^2) \in \mathscr{C}_{(\theta^1, \theta^2)} \tag{2.4.3}$$

---

danger of confusion, the value of $\boldsymbol{A}$ at $\boldsymbol{x}$ is written multiplicatively as $\boldsymbol{A}\,\boldsymbol{x}$. Composition of tensors is also denoted multiplicatively:

$$(\boldsymbol{A}\boldsymbol{B})\boldsymbol{a} = \boldsymbol{A}(\boldsymbol{B}\boldsymbol{a}), \forall \boldsymbol{a} \in \mathcal{U}.$$

To each ordered pair $(\boldsymbol{u}, \boldsymbol{v}) \in \mathcal{U} \times \mathcal{U}$ there corresponds a tensor $\boldsymbol{u} \otimes \boldsymbol{v} \in \mathcal{L}(\mathcal{U})$, called the tensor product or dyad of $\boldsymbol{u}$ and $\boldsymbol{v}$, which sends each $\boldsymbol{a} \in \mathcal{U}$ to $(\boldsymbol{v} \cdot \boldsymbol{a})\boldsymbol{u} \in \mathcal{U}$:

$$(\boldsymbol{u} \otimes \boldsymbol{v})\boldsymbol{a} = (\boldsymbol{v} \cdot \boldsymbol{a})\boldsymbol{u}, \forall \boldsymbol{a} \in \mathcal{U}.$$

Given a basis $\{\boldsymbol{u}_1, \cdots, \boldsymbol{u}_n\}$ for $\mathcal{U}$, the set $\{\boldsymbol{u}_i \otimes \boldsymbol{u}_j, i, j = 1, \cdots, n\}$ is a basis for $\mathcal{L}(\mathcal{U})$.

The transpose of $\boldsymbol{A} \in \mathcal{L}(\mathcal{U})$ is the tensor $\boldsymbol{A}^T$ uniquely defined by

$$\boldsymbol{A}\boldsymbol{u} \cdot \boldsymbol{v} = \boldsymbol{u} \cdot \boldsymbol{A}^T\boldsymbol{v}, \forall \boldsymbol{u}, \boldsymbol{v} \in \mathcal{U}.$$

In particular,

$$(\boldsymbol{u} \otimes \boldsymbol{v})^T = \boldsymbol{v} \otimes \boldsymbol{u}.$$

A tensor $\boldsymbol{S}$ is said to be symmetric if $\boldsymbol{S} = \boldsymbol{S}^T$. The set

$$Sym(\mathcal{U}) = \left\{ \boldsymbol{S} \in \mathcal{L}(\mathcal{U}) \,\middle|\, \boldsymbol{S} = \boldsymbol{S}^T \right\}$$

forms a $\frac{1}{2}n(n+1)$-dimensional subspace of $\mathcal{L}(\mathcal{U})$. Given a basis $\{\boldsymbol{u}_1, \cdots, \boldsymbol{u}_n\}$ for $\mathcal{U}$, then a basis for $Sym(\mathcal{U})$ is provided by

$$\boldsymbol{u}_i \otimes \boldsymbol{u}_j + \boldsymbol{u}_j \otimes \boldsymbol{u}_i, i \le j.$$

The trace is the linear functional on $\mathcal{L}(\mathcal{U})$ that assigns to each tensor $\boldsymbol{A}$ the scalar $\mathrm{tr}(\boldsymbol{A})$ satisfying

$$\mathrm{tr}(\boldsymbol{u} \otimes \boldsymbol{v}) = \boldsymbol{u} \cdot \boldsymbol{v}, \forall \boldsymbol{u}, \boldsymbol{v} \in \mathcal{U}.$$

This definition implies that the trace of a tensor is equal to the sum of the diagonal entries of its matrix representation with respect to an arbitrarily chosen ordered basis for $\mathcal{U}$.

The inner product on $\mathcal{U}$ induces an inner product on $\mathcal{L}(\mathcal{U})$, denoted by two dots, via

$$(\boldsymbol{u} \otimes \boldsymbol{v}) : (\boldsymbol{w} \otimes \boldsymbol{x}) = (\boldsymbol{u} \cdot \boldsymbol{w})(\boldsymbol{v} \cdot \boldsymbol{x}), \forall \boldsymbol{u}, \boldsymbol{v}, \boldsymbol{w}, \boldsymbol{x} \in \mathcal{U},$$

so that

$$\boldsymbol{A} : \boldsymbol{B} = \mathrm{tr}(\boldsymbol{A}\boldsymbol{B}^T) = \mathrm{tr}(\boldsymbol{A}^T\boldsymbol{B}).$$

With this definition, $\mathcal{L}(\mathcal{U})$ becomes an Euclidean vector space in its own right.

The norm corresponding to the induced inner product on $\mathcal{L}(\mathcal{U})$, often called the Frobenius norm, is defined in the usual way as

$$\|\boldsymbol{A}\|_F = \sqrt{\boldsymbol{A} : \boldsymbol{A}} = \sqrt{\mathrm{tr}(\boldsymbol{A}\boldsymbol{A}^T)}.$$

[28] Cf. the "principle of determinism for simple materials subjected to internal constraints" laid down in TRUESDELL (1991, ch. 4, § 7) or TRUESDELL & NOLL (2004, § 30). Cf. also ANTMAN & MARLOW (1991).

$$\boldsymbol{n}^{(R)}(\theta^1,\theta^2)\in\mathscr{C}^{\perp}_{(\theta^1,\theta^2)}=\operatorname{span}\left\{\boldsymbol{o}_{\mathrm{II}}(\theta^1,\theta^2)\otimes\boldsymbol{o}_{\mathrm{II}}(\theta^1,\theta^2),\right.$$
$$\left.\boldsymbol{o}_{\mathrm{I}}(\theta^1,\theta^2)\otimes\boldsymbol{o}_{\mathrm{II}}(\theta^1,\theta^2)+\boldsymbol{o}_{\mathrm{II}}(\theta^1,\theta^2)\otimes\boldsymbol{o}_{\mathrm{I}}(\theta^1,\theta^2)\right\}. \quad (2.4.4)$$

In (2.4.4), $\mathscr{C}^{\perp}_{(\theta^1,\theta^2)}$ denotes the orthogonal complement of $\mathscr{C}_{(\theta^1,\theta^2)}$ in $Sym\left(T_{F(\theta^1,\theta^2)}\mathscr{S}\right)$. The reactive part $\boldsymbol{n}^{(R)}(\theta^1,\theta^2)$, being orthogonal to $\mathscr{C}_{(\theta^1,\theta^2)}$, performs no work in any admissible deformation. Its role is that of maintaining the constraints. Assuming that the reference placement corresponds to a natural state (CIARLET 1988, p. 118), the active part $\boldsymbol{n}^{(A)}(\theta^1,\theta^2)$ is obtained from the strain $\boldsymbol{\gamma}(\theta^1,\theta^2)$ through a linearly elastic constitutive equation of the form

$$\boldsymbol{n}^{(A)}(\theta^1,\theta^2)=\mathbb{C}(\theta^1,\theta^2)\,\boldsymbol{\gamma}(\theta^1,\theta^2)\ , \quad (2.4.5)$$

where the elasticity tensor $\mathbb{C}(\theta^1,\theta^2)$ is a linear transformation from $\mathscr{C}_{(\theta^1,\theta^2)}$ into itself.

Our immediate task is to obtain a suitable definition for $\mathbb{C}(\theta^1,\theta^2)$. We start by associating with the constraint space $\mathscr{C}_{(\theta^1,\theta^2)}$ the subgroup of all rotations $\boldsymbol{\varrho}\in SO\left(T_{F(\theta^1,\theta^2)}\mathscr{S}\right)$ such that

$$\boldsymbol{\varrho}\,\boldsymbol{\gamma}(\theta^1,\theta^2)\,\boldsymbol{\varrho}^T\in\mathscr{C}_{(\theta^1,\theta^2)} \quad (2.4.6)$$

whenever $\boldsymbol{\gamma}(\theta^1,\theta^2)\in\mathscr{C}_{(\theta^1,\theta^2)}$ (*i.e.*, that leave $\mathscr{C}_{(\theta^1,\theta^2)}$ invariant).[29] This subgroup specifies the maximal material symmetry that is compatible with the constraint space $\mathscr{C}_{(\theta^1,\theta^2)}$ (PODIO-GUIDUGLI 2000, § 18, PODIO-GUIDUGLI & VIANELLO 1992). Since

$$\boldsymbol{\varrho}\left(\boldsymbol{o}_{\mathrm{I}}(\theta^1,\theta^2)\otimes\boldsymbol{o}_{\mathrm{I}}(\theta^1,\theta^2)\right)\boldsymbol{\varrho}^T=\left(\boldsymbol{\varrho}\,\boldsymbol{o}_{\mathrm{I}}(\theta^1,\theta^2)\right)\otimes\left(\boldsymbol{\varrho}\,\boldsymbol{o}_{\mathrm{I}}(\theta^1,\theta^2)\right), \quad (2.4.7)$$

$\boldsymbol{\varrho}$ must be either the identity or the central inversion in order to meet the requirement (2.4.6). Therefore, the maximal material symmetry compatible with the constraints (V1)-(V2) is that of an orthotropic membrane, with orthotropy directions $\boldsymbol{o}_{\mathrm{I}}(\theta^1,\theta^2)$ and $\boldsymbol{o}_{\mathrm{II}}(\theta^1,\theta^2)$ at $F(\theta^1,\theta^2)\in\mathscr{S}$.[30] Then, a straightforward application of the constrained representation

---

[29] Let $\mathcal{U}$ and $\mathcal{L}(\mathcal{U})$ be as in note 27. A (second-order) tensor $\boldsymbol{Q}\in\mathcal{L}(\mathcal{U})$ is orthogonal if it preserves the inner product of vectors, that is to say

$$(\boldsymbol{Q}\boldsymbol{u})\cdot(\boldsymbol{Q}\boldsymbol{v})=\boldsymbol{u}\cdot\boldsymbol{v},\ \forall\boldsymbol{u},\boldsymbol{v}\in\mathcal{U}\ .$$

It can be shown that a tensor $\boldsymbol{Q}$ is orthogonal if and only if $\boldsymbol{Q}^{-1}=\boldsymbol{Q}^T$, from which follows that $\det(\boldsymbol{Q})=\pm1$. If $\det(\boldsymbol{Q})=1$, the orthogonal tensor $\boldsymbol{Q}$ is called a rotation. The set of all rotations in $\mathcal{L}(\mathcal{U})$ forms a group under composition, called the special orthogonal group $SO(\mathcal{U})$.

[30] This is a particular case of curvilinear anisotropy, a kind of anisotropy discussed by SAINT-VENANT (1865) – see also LEKHNITSKII (1963, § 9) and LOVE (1944, § 110). We are thus able to assign a precise meaning to Wilde's rather cryptic remark that "the membrane is not isotropic under the assumed approximations [(V1)-(V2)]", made just after having used an isotropic constitutive relation (WILDE 1968).

theorem of PODIO-GUIDUGLI & VIANELLO (1992) to the elasticity tensor of an unconstrained orthotropic membrane (LEKHNITSKII 1963, ch. 1) yields

$$\begin{aligned}\mathbb{C}(\theta^1,\theta^2) &= \frac{E_{\mathrm{I}}\, t(\theta^1,\theta^2)}{1-\nu_{\mathrm{I\cdot II}}\,\nu_{\mathrm{II\cdot I}}}\boldsymbol{P}_{\mathrm{I}}(\theta^1,\theta^2)\otimes\boldsymbol{P}_{\mathrm{I}}(\theta^1,\theta^2)\\ &= \tilde{E}\, t(\theta^1,\theta^2)\,\boldsymbol{P}_{\mathrm{I}}(\theta^1,\theta^2)\otimes\boldsymbol{P}_{\mathrm{I}}(\theta^1,\theta^2)\ ,\end{aligned} \tag{2.4.8}$$

where E_{I} is the Young modulus relative to the direction $\boldsymbol{o}_{\mathrm{I}}(\theta^1,\theta^2)$, $\nu_{\mathrm{I\cdot II}}$ and $\nu_{\mathrm{II\cdot I}}$ are the Poisson ratios relative to the ordered pairs $\left(\boldsymbol{o}_{\mathrm{I}}(\theta^1,\theta^2),\boldsymbol{o}_{\mathrm{II}}(\theta^1,\theta^2)\right)$ and $\left(\boldsymbol{o}_{\mathrm{II}}(\theta^1,\theta^2),\boldsymbol{o}_{\mathrm{I}}(\theta^1,\theta^2)\right)$ of mutually orthogonal directions, and

$$\boldsymbol{P}_{\mathrm{I}}(\theta^1,\theta^2)=\boldsymbol{o}_{\mathrm{I}}(\theta^1,\theta^2)\otimes\boldsymbol{o}_{\mathrm{I}}(\theta^1,\theta^2) \tag{2.4.9}$$

is the perpendicular projection onto the span of $\boldsymbol{o}_{\mathrm{I}}(\theta^1,\theta^2)$ (*e.g.*, TRUESDELL 1991, pp. 314-315). It is assumed that the modified elastic modulus

$$\tilde{E}=\frac{E_{\mathrm{I}}}{1-\nu_{\mathrm{I\cdot II}}\,\nu_{\mathrm{II\cdot I}}} \tag{2.4.10}$$

is independent of the point in $\mathscr{S}$ under consideration.[31]

From (2.4.5) it now follows

$$\begin{aligned}\boldsymbol{n}^{(\mathcal{A})}(\theta^1,\theta^2) &= n^{(\mathcal{A})}_{\mathrm{I\cdot I}}(\theta^1,\theta^2)\,\boldsymbol{o}_{\mathrm{I}}(\theta^1,\theta^2)\otimes\boldsymbol{o}_{\mathrm{I}}(\theta^1,\theta^2)\\ &= \tilde{E}\, t(\theta^1,\theta^2)\,\gamma_{\mathrm{I\cdot I}}(\theta^1,\theta^2)\,\boldsymbol{o}_{\mathrm{I}}(\theta^1,\theta^2)\otimes\boldsymbol{o}_{\mathrm{I}}(\theta^1,\theta^2)\end{aligned} \tag{2.4.11}$$

and the field $n^{(\mathcal{A})}_{\mathrm{I\cdot I}}:\overline{\Omega}\to\mathbb{R}$ is clearly continuous.

2.5 TOTAL POTENTIAL ENERGY

2.5.1 Strain energy

Let $\boldsymbol{U}:\overline{\Omega}\to\mathcal{V}$ be an admissible displacement field of the middle surface $\mathscr{S}=F[\overline{\Omega}]$, specified by the generalised displacements $W_i,\Phi_1:[0,L]\to\mathbb{R}$, and let $\boldsymbol{\gamma}$ and $\boldsymbol{n}^{(\mathcal{A})}=\mathbb{C}\boldsymbol{\gamma}$ be the associated membrane strain and active membrane force tensor fields. The membrane strain energy corresponding to $\boldsymbol{U}$ is defined as (recall equation (2.2.20))

$$U_m=\frac{1}{2}\int_{\overline{\Omega}}\boldsymbol{n}^{(\mathcal{A})}(\theta^1,\theta^2):\boldsymbol{\gamma}(\theta^1,\theta^2)\sqrt{a(\theta^1,\theta^2)}\;d\theta^1 d\theta^2\ , \tag{2.5.1}$$

[31] This assumption is obviously not essential and it would have been a simple matter to consider $\tilde{E}$ as a function of the Gaussian coordinates θ^1, θ^2.

where $\boldsymbol{n}^{(A)}(\theta^1,\theta^2):\boldsymbol{\gamma}(\theta^1,\theta^2)=\mathrm{tr}\left(\boldsymbol{n}^{(A)}(\theta^1,\theta^2)\boldsymbol{\gamma}(\theta^1,\theta^2)^T\right)$ and $a(\theta^1,\theta^2)$ is given by equation (2.2.18).[32] In view of our previous results concerning the components of $\boldsymbol{n}^{(A)}(\theta^1,\theta^2)$ and $\boldsymbol{\gamma}(\theta^1,\theta^2)$, U_m reduces to

$$U_m=\frac{1}{2}\int_{\bar{\Omega}} n_{\mathrm{I\text{-}I}}^{(A)}(\theta^1,\theta^2)\,\gamma_{\mathrm{I\text{-}I}}(\theta^1,\theta^2)\sqrt{a(\theta^1,\theta^2)}\,d\theta^1 d\theta^2\ . \tag{2.5.2}$$

Then, using the constitutive equation (2.4.11), relating $n_{\mathrm{I\text{-}I}}^{(A)}(\theta^1,\theta^2)$ to $\gamma_{\mathrm{I\text{-}I}}(\theta^1,\theta^2)$, and equations (2.3.33), (2.3.27)-(2.3.31), relating $\gamma_{\mathrm{I\text{-}I}}(\theta^1,\theta^2)$ to the generalised displacements W_i and Φ_1, one obtains

$$\begin{aligned}U_m=\frac{\tilde{E}}{2}\int_{\bar{\Omega}}\Big(&W_1'(\theta^1)-\bar{x}_2(\theta^1,\theta^2)W_2''(\theta^1)-\bar{x}_3(\theta^1,\theta^2)W_3''(\theta^1)\\&-\omega(\theta^1,\theta^2)\Phi_1''(\theta^1)-\psi(\theta^1,\theta^2)\Phi_1'(\theta^1)\Big)^2\,t^*(\theta^1,\theta^2)\,d\theta^1\,d\theta^2\ ,\end{aligned} \tag{2.5.3}$$

where

$$\begin{aligned}t^*(\theta^1,\theta^2)&=\frac{t(\theta^1,\theta^2)}{\sqrt{\left(a(\theta^1,\theta^2)\right)^3}}\\&=\frac{t(\theta^1,\theta^2)}{\left[1+\left(D_1\bar{x}_2(\theta^1,\theta^2)D_2\bar{x}_3(\theta^1,\theta^2)-D_2\bar{x}_2(\theta^1,\theta^2)D_1\bar{x}_3(\theta^1,\theta^2)\right)^2\right]^{\frac{3}{2}}}\end{aligned} \tag{2.5.4}$$

can be thought of as a reduced wall thickness – indeed, $0<t^*(\theta^1,\theta^2)\le t(\theta^1,\theta^2)$, $\forall(\theta^1,\theta^2)\in\bar{\Omega}$, with equality holding if and only if $a(\theta^1,\theta^2)=1$.

The integral in equation (2.5.3) is well-defined and can be written as an iterated integral (*vide supra*, § 2.2.4):

$$\begin{aligned}U_m=\frac{\tilde{E}}{2}\int_0^L\Bigg[\int_{g_1(\theta^1)}^{g_2(\theta^1)}\Big(&W_1'(\theta^1)-\bar{x}_2(\theta^1,\theta^2)W_2''(\theta^1)-\bar{x}_3(\theta^1,\theta^2)W_3''(\theta^1)\\&-\omega(\theta^1,\theta^2)\Phi_1''(\theta^1)-\psi(\theta^1,\theta^2)\Phi_1'(\theta^1)\Big)^2\,t^*(\theta^1,\theta^2)\,d\theta^2\Bigg]d\theta^1\end{aligned} \tag{2.5.5}$$

Introducing the continuous[33] real-valued maps defined on $[0,L]$ by

$$A^*(\theta^1)=\int_{g_1(\theta^1)}^{g_2(\theta^1)}t^*(\theta^1,\theta^2)\,d\theta^2 \tag{2.5.6}$$

$$S_2^*(\theta^1)=\int_{g_1(\theta^1)}^{g_2(\theta^1)}\bar{x}_3(\theta^1,\theta^2)\,t^*(\theta^1,\theta^2)\,d\theta^2 \tag{2.5.7}$$

---

[32] *Vide supra*, note 27.

[33] See DUISTERMAAT & KOLK (2004, proof of th. 6.4.5).

$$S_3^*(\theta^1) = \int_{g_1(\theta^1)}^{g_2(\theta^1)} \overline{x}_2(\theta^1,\theta^2)\, t^*(\theta^1,\theta^2)\, d\theta^2 \tag{2.5.8}$$

$$S_\omega^*(\theta^1) = \int_{g_1(\theta^1)}^{g_2(\theta^1)} \omega(\theta^1,\theta^2)\, t^*(\theta^1,\theta^2)\, d\theta^2 \tag{2.5.9}$$

$$S_\psi^*(\theta^1) = \int_{g_1(\theta^1)}^{g_2(\theta^1)} \psi(\theta^1,\theta^2)\, t^*(\theta^1,\theta^2)\, d\theta^2 \tag{2.5.10}$$

$$I_2^*(\theta^1) = \int_{g_1(\theta^1)}^{g_2(\theta^1)} \overline{x}_3^2(\theta^1,\theta^2)\, t^*(\theta^1,\theta^2)\, d\theta^2 \tag{2.5.11}$$

$$I_3^*(\theta^1) = \int_{g_1(\theta^1)}^{g_2(\theta^1)} \overline{x}_2^2(\theta^1,\theta^2)\, t^*(\theta^1,\theta^2)\, d\theta^2 \tag{2.5.12}$$

$$I_\omega^*(\theta^1) = \int_{g_1(\theta^1)}^{g_2(\theta^1)} \omega^2(\theta^1,\theta^2)\, t^*(\theta^1,\theta^2)\, d\theta^2 \tag{2.5.13}$$

$$I_\psi^*(\theta^1) = \int_{g_1(\theta^1)}^{g_2(\theta^1)} \psi^2(\theta^1,\theta^2)\, t^*(\theta^1,\theta^2)\, d\theta^2 \tag{2.5.14}$$

$$I_{23}^*(\theta^1) = \int_{g_1(\theta^1)}^{g_2(\theta^1)} \overline{x}_2(\theta^1,\theta^2)\, \overline{x}_3(\theta^1,\theta^2)\, t^*(\theta^1,\theta^2)\, d\theta^2 \tag{2.5.15}$$

$$I_{2\omega}^*(\theta^1) = \int_{g_1(\theta^1)}^{g_2(\theta^1)} \overline{x}_3(\theta^1,\theta^2)\, \omega(\theta^1,\theta^2)\, t^*(\theta^1,\theta^2)\, d\theta^2 \tag{2.5.16}$$

$$I_{3\omega}^*(\theta^1) = \int_{g_1(\theta^1)}^{g_2(\theta^1)} \overline{x}_2(\theta^1,\theta^2)\, \omega(\theta^1,\theta^2)\, t^*(\theta^1,\theta^2)\, d\theta^2 \tag{2.5.17}$$

$$I_{2\psi}^*(\theta^1) = \int_{g_1(\theta^1)}^{g_2(\theta^1)} \overline{x}_3(\theta^1,\theta^2)\, \psi(\theta^1,\theta^2)\, t^*(\theta^1,\theta^2)\, d\theta^2 \tag{2.5.18}$$

$$I_{3\psi}^*(\theta^1) = \int_{g_1(\theta^1)}^{g_2(\theta^1)} \overline{x}_2(\theta^1,\theta^2)\, \psi(\theta^1,\theta^2)\, t^*(\theta^1,\theta^2)\, d\theta^2 \tag{2.5.19}$$

$$I_{\omega\psi}^*(\theta^1) = \int_{g_1(\theta^1)}^{g_2(\theta^1)} \omega(\theta^1,\theta^2)\, \psi(\theta^1,\theta^2)\, t^*(\theta^1,\theta^2)\, d\theta^2 \quad , \tag{2.5.20}$$

U_m is finally brought into the form

$$\begin{aligned} U_m = \frac{\tilde{E}}{2}\int_0^L \Big[& A^*(\theta^1)\left(W_1'(\theta^1)\right)^2 - 2\,S_3^*(\theta^1)\,W_1'(\theta^1)\,W_2''(\theta^1) - 2\,S_2^*(\theta^1)\,W_1'(\theta^1)\,W_3''(\theta^1) \\ & -2\,S_\omega^*(\theta^1)\,W_1'(\theta^1)\,\Phi_1''(\theta^1) - 2\,S_\psi^*(\theta^1)\,W_1'(\theta^1)\,\Phi_1'(\theta^1) + I_3^*(\theta^1)\left(W_2''(\theta^1)\right)^2 \\ & +2\,I_{23}^*(\theta^1)\,W_2''(\theta^1)\,W_3''(\theta^1) + 2\,I_{3\omega}^*(\theta^1)\,W_2''(\theta^1)\,\Phi_1''(\theta^1) \\ & +2\,I_{3\psi}^*(\theta^1)\,W_2''(\theta^1)\,\Phi_1'(\theta^1) + I_2^*(\theta^1)\left(W_3''(\theta^1)\right)^2 + 2\,I_{2\omega}^*(\theta^1)\,W_3''(\theta^1)\,\Phi_1''(\theta^1) \\ & +2\,I_{2\psi}^*(\theta^1)\,W_3''(\theta^1)\,\Phi_1'(\theta^1) + I_\omega^*(\theta^1)\left(\Phi_1''(\theta^1)\right)^2 \\ & +2\,I_{\omega\psi}^*(\theta^1)\,\Phi_1''(\theta^1)\,\Phi_1'(\theta^1) + I_\psi^*(\theta^1)\left(\Phi_1'(\theta^1)\right)^2 \Big]\, d\theta^1 \ . \end{aligned} \tag{2.5.21}$$

Notice that the integrands in (2.5.6)-(2.5.20) consist of products of pairs of the basic strain modes (2.3.34), multiplied by the additional factor $t\sqrt{a}$.

So far, the bar has been treated as a membrane shell, that is, it has been reduced to its middle surface, on which the shear strain $\gamma_{\mathrm{I\cdot II}} = \gamma_{\mathrm{II\cdot I}}$ is constrained to vanish. In order to account, in an approximate way, for a variation of shear deformation over each cross-section (with a zero value at the middle line), the term

$$U_{\mathrm{SV}} = \frac{G}{2}\int_0^L J(\theta^1)\left(\Phi_1'(\theta^1)\right)^2 d\theta^1 \ , \tag{2.5.22}$$

where G is the shear modulus[34] and $J(\theta^1)$ is the torsion constant of a prismatic bar with cross-section $\mathcal{A}_{\theta^1}$ (FÖPPL 1917a, 1917b), is added to the membrane strain energy.[35] Therefore, the total strain energy stored in the bar is

$$U = U_m + U_{\mathrm{SV}} \ . \tag{2.5.23}$$

2.5.2 Work of the external loads

The middle surface of the bar is subjected to a system of dead surface and edge loads,[36] which are referred to as shell loads (GJELSVIK 1981, pp. 15-16). This load system is deemed smooth enough so that there exist (i) continuous maps $\boldsymbol{q}, \boldsymbol{m} : [0, L] \to \mathcal{V}$ and $b : [0, L] \to \mathbb{R}$, (ii) vectors $\boldsymbol{Q}_0$, $\boldsymbol{Q}_L$, $\boldsymbol{M}_0$, and $\boldsymbol{M}_L$ and (iii) real numbers B_0 and B_L, collectively referred to as bar loads (GJELSVIK 1981, pp. 25-27), such that the work performed in an admissible displacement field $\boldsymbol{U} : \overline{\Omega} \to \mathcal{V}$ of the middle surface (defined in equations (2.3.22)-(2.3.24)) can be written in the form

$$\begin{aligned} W_e = &\int_0^L \left(\boldsymbol{q}(\theta^1)\cdot\boldsymbol{W}(\theta^1) + \boldsymbol{m}(\theta^1)\cdot\boldsymbol{\Phi}(\theta^1) - b(\theta^1)\,\Phi_1'(\theta^1)\right) d\theta^1 \\ &+\boldsymbol{Q}_0\cdot\boldsymbol{W}(0) + \boldsymbol{Q}_L\cdot\boldsymbol{W}(L) + \boldsymbol{M}_0\cdot\boldsymbol{\Phi}(0) + \boldsymbol{M}_L\cdot\boldsymbol{\Phi}(L) \\ &-B_0\,\Phi_1'(0) - B_L\,\Phi_1'(L) \ . \end{aligned} \tag{2.5.24}$$

In terms of Cartesian components, we write

$$\boldsymbol{q}(\theta^1) = q_i(\theta^1)\,\boldsymbol{e}_i \tag{2.5.25}$$

$$\boldsymbol{m}(\theta^1) = m_i(\theta^1)\,\boldsymbol{e}_i \tag{2.5.26}$$

---

[34] As remarked by MASSONNET (1982, 1983), there is no reason to adopt different shear moduli.

[35] A more consistent model, without this *ad hoc* approximation, would require more sophisticated constraints on the displacement field (of the whole bar and not merely of the middle surface) – in so far as only prismatic bars are concerned, see GJELSVIK (1981, ch. 1).

[36] On the concept of dead loads, see CIARLET (1988, § 2.7).

$$\boldsymbol{Q}_0 = Q_{0.i}\,\boldsymbol{e}_i \tag{2.5.27}$$

$$\boldsymbol{Q}_L = Q_{L.i}\,\boldsymbol{e}_i \tag{2.5.28}$$

$$\boldsymbol{M}_0 = M_{0.i}\,\boldsymbol{e}_i \tag{2.5.29}$$

$$\boldsymbol{M}_L = M_{L.i}\,\boldsymbol{e}_i \tag{2.5.30}$$

and equation (2.5.24) becomes

$$\begin{aligned} W_e = \int_0^L \Big(& q_i(\theta^1) W_i(\theta^1) + m_1(\theta^1)\Phi_1(\theta^1) - m_2(\theta^1) W_3'(\theta^1) \\ & + m_3(\theta^1) W_2'(\theta^1) - b(\theta^1)\Phi_1'(\theta^1) \Big) d\theta^1 \\ & + Q_{0.i}\, W_i(0) + Q_{L.i}\, W_i(L) \\ & + M_{0.1}\,\Phi_1(0) - M_{0.2}\, W_3'(0) + M_{0.3}\, W_2'(0) \\ & + M_{L.1}\,\Phi_1(L) - M_{L.2}\, W_3'(L) + M_{L.3}\, W_2'(L) \\ & - B_0\,\Phi_1'(0) - B_L\,\Phi_1'(L)\ . \end{aligned} \tag{2.5.31}$$

The physical significance of the bar loads is clear: (i) the maps $\boldsymbol{q}$, $\boldsymbol{m}$ and b represent the applied distributed force, moment and bimoment per unit length of the line segment $\{O + \theta^1 \boldsymbol{e}_1,\ 0 \le \theta^1 \le L\}$, while (ii) $\boldsymbol{Q}_0$, $\boldsymbol{M}_0$, B_0 and $\boldsymbol{Q}_L$, $\boldsymbol{M}_L$, B_L are applied concentrated forces, moments and bimoments at the end points O and $O + L\,\boldsymbol{e}_1$. The bimomental loads are directly tied to the warping of the cross-sections[37] and depend only on the shell loads acting along $\boldsymbol{e}_1$.

It should be noticed that the longitudinal shell loads cannot merely be replaced by a statically equivalent system of bar loads, an observation that applies to tapered and prismatic bars alike. Indeed, the condition of static equivalence is not sufficient to characterise fully the system of bar loads – this system must also be complete, in the sense that the equality between the work performed by the shell loads and the work performed by the bar loads, as expressed in equations (2.5.24) or (2.5.31), is required to hold for every admissible displacement field of the middle surface. This point, which is missed by MURRAY (1986, § 2.3.1), is clearly illustrated by the example in figure 2.5.1, taken from VLASOV (1961, pp. 10-11).[38] The applied longitudinal force in (a) is statically equivalent to the sum of the systems of forces shown in (b), (c) and (d), which cause stretching (b) and bending in the principal planes of inertia (c, d). The system (e) is statically equivalent to zero

[37] In fact, they are called warping loads by GJELSVIK (1981, p. 27).

[38] For a similar example, see ODEN & RIPPERGER (1981, § 7.1).

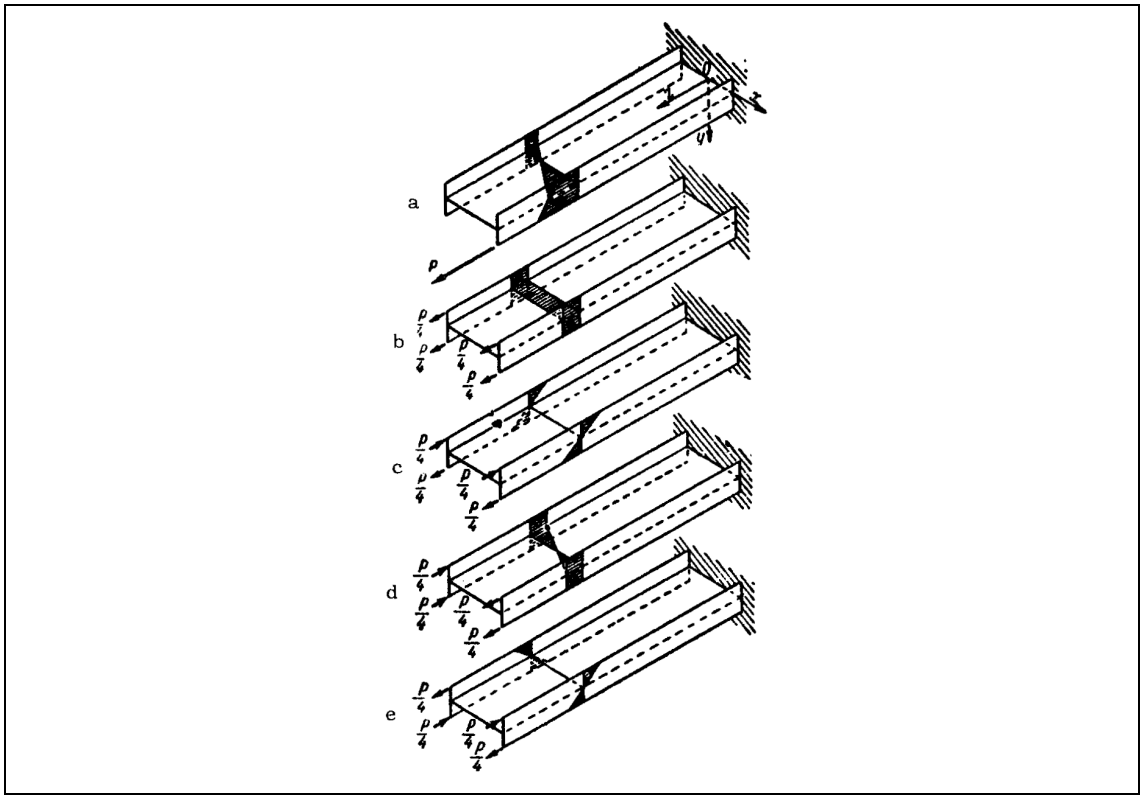

Figure 2.5.1: I-section cantilever acted by eccentric longitudinal force (VLASOV 1961, p. 10)

force and zero moment (*i.e.*, it is self-equilibrating), but nevertheless causes bending of the flanges in opposite directions – this effect is not just local, instead it exhibits a slow rate of decay with increasing distance from the section where the self-equilibrating external forces are applied.[39] As a result, the thin-walled bar is twisted.

2.5.3 Total potential energy

The total potential energy Π of the bar-load system is now given by the sum of the strain energy U and the potential of the external loads, the latter being the negative of the work W_e they perform:

[39] According to Saint-Venant's principle, or "principle of the elastic equivalence of statically equipollent systems of load", the strains and stresses that are produced in a body by the application, to a small part of its surface, of a system of forces statically equivalent to zero force and zero couple, are of negligible magnitude at distances which are large compared with the linear dimensions of the part (LOVE 1944, § 89). The justification of this principle is largely empirical and, as such, its applicability is not entirely clear. However, as FUNG (1965, p. 309) remarks, "Saint-Venant's principle works only if there is a possibility for it to work; in other words, only if there exist paths for the internal forces to follow in order to balance one another within a short distance of the region at which a group of self-equilibrating external forces is applied". This is generally not the case in thin-walled open bars, and certainly not the case in the example of figure 2.5.1.

$$\Pi = U - W_e = U_m + U_{\mathrm{SV}} - W_e \ . \tag{2.5.32}$$

Inserting (2.5.21), (2.5.22) and (2.5.31) into the above equation, one obtains the total potential energy Π as a quadratic functional defined on some appropriate subset of the linear space $C^1[0,L]\times C^2[0,L]\times C^2[0,L]\times C^2[0,L]$ of all ordered quadruplets (W_1, W_2, W_3, Φ_1) – henceforth shortened to (W_i, Φ_1) – of generalised displacements.

2.6 THE BOUNDARY VALUE PROBLEM FOR THE GENERALISED DISPLACEMENTS

> Cum enim Mundi universi fabrica sit perfectissima,
> atque a Creatore sapientisssimo absoluta, nihil omnino in mundo contingit,
> in quo non maximi minimive ratio quaepiam eluceat:
> quamobrem dubium prorsus est nullum, quin omnes Mundi effectus ex causis finalibus,
> ope Methodi maximorum & minimorum aeque feliciter determinari queant,
> atque ex ipsis causis efficientibus.
>
> LEONHARD EULER

With a view to establishing the Euler-Lagrange equations associated with the total potential energy functional (2.5.32), we make the following smoothness assumptions on the data (geometry and loading):

(i) The maps A^*, S_ψ^*, I_ψ^* and J, as well as m_2, m_3 and b, are continuously differentiable on $[0,L]$.

(ii) S_2^*, S_3^*, S_ω^*, I_2^*, I_3^*, I_ω^*, I_{23}^*, $I_{2\omega}^*$, $I_{3\omega}^*$, $I_{2\psi}^*$, $I_{3\psi}^*$ and $I_{\omega\psi}^*$ are twice continuously differentiable on $[0,L]$.

Moreover, the domain $\mathcal{D}$ of the functional Π is specified to be the set of all ordered quadruplets (W_i, Φ_1) of real-valued maps defined on the interval $[0,L]$ that satisfy:

(i) The smoothness requirements

- $W_1 \in C^3[0,L]$,
- $W_2, W_3, \Phi_1 \in C^4[0,L]$.

(ii) The essential (*i.e.*, kinematical) boundary conditions prescribed for the particular problem under consideration.[40]

[40] The rule for distinguishing between essential and natural boundary conditions is the following: if derivatives of order up to k of a given dependent variable are involved in the definition of the functional Π, then the essential boundary conditions on that variable are those that involve only derivatives of order less that k; those involving derivatives of order k or higher, up to $2k-1$, are natural boundary conditions (*e.g.*, AXELSSON & BARKER 1984, ch. 2, or STRANG & FIX 1973, ch. 1).

Let $(\delta W_i, \delta\Phi_1)$ denote the difference between two members of $\mathcal{D}$ – the maps $\delta W_i, \delta\Phi_1 : [0, L] \to \mathbb{R}$ are then collectively called admissible variations of the generalised displacements. Notice that these admissible variations (i) exhibit the same degree of smoothness as the generalised displacements themselves and (ii) satisfy the homogeneous form of the essential boundary conditions – they are thus elements of a linear space. The first variation of Π at $(W_i, \Phi_1) \in \mathcal{D}$ in the direction of $(\delta W_i, \delta\Phi_1)$ is defined as

$$\delta\Pi(W_i, \Phi_1)[\delta W_i, \delta\Phi_1] = \frac{d}{da}\Pi(W_i + a\,\delta W_i, \Phi_1 + a\,\delta\Phi_1)\bigg|_{a=0} \quad (a \in \mathbb{R}) \,. \tag{2.6.1}$$

Using Leibniz rule to differentiate under the integral sign (*e.g.*, BARTLE 1967, th. 23.10), one gets

$$\begin{aligned}
&\delta\Pi(W_i, \Phi_1)[\delta W_i, \delta\Phi_1] = \\
&= \int_0^L \Big[\Big(\tilde{E}A^*(\theta^1) W_1'(\theta^1) - \tilde{E}S_3^*(\theta^1) W_2''(\theta^1) - \tilde{E}S_2^*(\theta^1) W_3''(\theta^1) - \tilde{E}S_\omega^*(\theta^1) \Phi_1''(\theta^1) \\
&\qquad - \tilde{E}S_\psi^*(\theta^1) \Phi_1'(\theta^1) \Big) \delta W_1'(\theta^1) \\
&\quad + \Big(-\tilde{E}S_3^*(\theta^1) W_1'(\theta^1) + \tilde{E}I_3^*(\theta^1) W_2''(\theta^1) + \tilde{E}I_{23}^*(\theta^1) W_3''(\theta^1) + \tilde{E}I_{3\omega}^*(\theta^1) \Phi_1''(\theta^1) \\
&\qquad + \tilde{E}I_{3\psi}^*(\theta^1) \Phi_1'(\theta^1) \Big) \delta W_2''(\theta^1) \\
&\quad + \Big(-\tilde{E}S_2^*(\theta^1) W_1'(\theta^1) + \tilde{E}I_{23}^*(\theta^1) W_2''(\theta^1) + \tilde{E}I_2^*(\theta^1) W_3''(\theta^1) + \tilde{E}I_{2\omega}^*(\theta^1) \Phi_1''(\theta^1) \\
&\qquad + \tilde{E}I_{2\psi}^*(\theta^1) \Phi_1'(\theta^1) \Big) \delta W_3''(\theta^1) \\
&\quad + \Big(-\tilde{E}S_\omega^*(\theta^1) W_1'(\theta^1) + \tilde{E}I_{3\omega}^*(\theta^1) W_2''(\theta^1) + \tilde{E}I_{2\omega}^*(\theta^1) W_3''(\theta^1) + \tilde{E}I_\omega^*(\theta^1) \Phi_1''(\theta^1) \\
&\qquad + \tilde{E}I_{\omega\psi}^*(\theta^1) \Phi_1'(\theta^1) \Big) \delta\Phi_1''(\theta^1) \\
&\quad + \Big(-\tilde{E}S_\psi^*(\theta^1) W_1'(\theta^1) + \tilde{E}I_{3\psi}^*(\theta^1) W_2''(\theta^1) + \tilde{E}I_{2\psi}^*(\theta^1) W_3''(\theta^1) + \tilde{E}I_{\omega\psi}^*(\theta^1) \Phi_1''(\theta^1) \\
&\qquad + GJ(\theta^1) \Phi_1'(\theta^1) + \tilde{E}I_\psi^*(\theta^1) \Phi_1'(\theta^1) \Big) \delta\Phi_1'(\theta^1) \Big] d\theta^1 \\
&- \int_0^L \Big(q_1(\theta^1) \delta W_1(\theta^1) + q_2(\theta^1) \delta W_2(\theta^1) + q_3(\theta^1) \delta W_3(\theta^1) + m_1(\theta^1) \delta\Phi_1(\theta^1) \\
&\qquad - m_2(\theta^1) \delta W_3'(\theta^1) + m_3(\theta^1) \delta W_2'(\theta^1) - b(\theta^1) \delta\Phi_1'(\theta^1) \Big) d\theta^1 \\
&- Q_{0.1} \delta W_1(0) - Q_{0.2} \delta W_2(0) - Q_{0.3} \delta W_3(0) - M_{0.1} \delta\Phi_1(0) \\
&+ M_{0.2} \delta W_3'(0) - M_{0.3} \delta W_2'(0) + B_0 \delta\Phi_1'(0) \\
&- Q_{L.1} \delta W_1(L) - Q_{L.2} \delta W_2(L) - Q_{L.3} \delta W_3(L) - M_{L.1} \delta\Phi_1(L) \\
&+ M_{L.2} \delta W_3'(L) - M_{L.3} \delta W_2'(L) + B_L \delta\Phi_1'(L) \,.
\end{aligned} \tag{2.6.2}$$

Integration by parts, which is permissible in view of the smoothness of the maps involved (*e.g.*, CAMPOS FERREIRA 1987, ch. 5, § 1, th. 18), now yields[41]

$$
\begin{aligned}
&\delta\Pi(W_i, \Phi_1)[\delta W_i, \delta\Phi_1] = \\
&= -\int_0^L \Big[\left(\tilde{E}A^* W_1' - \tilde{E}S_3^* W_2'' - \tilde{E}S_2^* W_3'' - \tilde{E}S_\omega^* \Phi_1'' - \tilde{E}S_\psi^* \Phi_1' \right)' (\theta^1) + q_1(\theta^1) \Big] \delta W_1(\theta^1)\, d\theta^1 \\
&\quad + \Big[\Big(\tilde{E}A^*(\theta^1) W_1'(\theta^1) - \tilde{E}S_3^*(\theta^1) W_2''(\theta^1) - \tilde{E}S_2^*(\theta^1) W_3''(\theta^1) - \tilde{E}S_\omega^*(\theta^1) \Phi_1''(\theta^1) \\
&\qquad - \tilde{E}S_\psi^*(\theta^1) \Phi_1'(\theta^1) \Big) \delta W_1(\theta^1) \Big]_0^L - Q_{0.1}\, \delta W_1(0) - Q_{L.1}\, \delta W_1(L) \\
&\quad + \int_0^L \Big[\left(-\tilde{E}S_3^* W_1' + \tilde{E}I_3^* W_2'' + \tilde{E}I_{23}^* W_3'' + \tilde{E}I_{3\omega}^* \Phi_1'' + \tilde{E}I_{3\psi}^* \Phi_1' \right)'' (\theta^1) \\
&\qquad - q_2(\theta^1) + m_3'(\theta^1) \Big] \delta W_2(\theta^1)\, d\theta^1 \\
&\quad + \Big[\Big(-\tilde{E}S_3^*(\theta^1) W_1'(\theta^1) + \tilde{E}I_3^*(\theta^1) W_2''(\theta^1) + \tilde{E}I_{23}^*(\theta^1) W_3''(\theta^1) + \tilde{E}I_{3\omega}^*(\theta^1) \Phi_1''(\theta^1) \\
&\qquad + \tilde{E}I_{3\psi}^*(\theta^1) \Phi_1'(\theta^1) \Big) \delta W_2'(\theta^1) \Big]_0^L - M_{0.3}\, \delta W_2'(0) - M_{L.3}\, \delta W_2'(L) \\
&\quad - \Big[\Big\{ \left(-\tilde{E}S_3^* W_1' + \tilde{E}I_3^* W_2'' + \tilde{E}I_{23}^* W_3'' + \tilde{E}I_{3\omega}^* \Phi_1'' + \tilde{E}I_{3\psi}^* \Phi_1' \right)' (\theta^1) + m_3(\theta^1) \Big\} \delta W_2(\theta^1) \Big]_0^L \\
&\qquad - Q_{0.2}\, \delta W_2(0) - Q_{L.2}\, \delta W_2(L) \\
&\quad + \int_0^L \Big[\left(-\tilde{E}S_2^* W_1' + \tilde{E}I_{23}^* W_2'' + \tilde{E}I_2^* W_3'' + \tilde{E}I_{2\omega}^* \Phi_1'' + \tilde{E}I_{2\psi}^* \Phi_1' \right)'' (\theta^1) \\
&\qquad - q_3(\theta^1) - m_2'(\theta^1) \Big] \delta W_3(\theta^1)\, d\theta^1 \\
&\quad + \Big[\Big(-\tilde{E}S_2^*(\theta^1) W_1'(\theta^1) + \tilde{E}I_{23}^*(\theta^1) W_2''(\theta^1) + \tilde{E}I_2^*(\theta^1) W_3''(\theta^1) + \tilde{E}I_{2\omega}^*(\theta^1) \Phi_1''(\theta^1) \\
&\qquad + \tilde{E}I_{2\psi}^*(\theta^1) \Phi_1'(\theta^1) \Big) \delta W_3'(\theta^1) \Big]_0^L + M_{0.2}\, \delta W_3'(0) + M_{L.2}\, \delta W_3'(L) \\
&\quad - \Big[\Big\{ \left(-\tilde{E}S_2^* W_1' + \tilde{E}I_{23}^* W_2'' + \tilde{E}I_2^* W_3'' + \tilde{E}I_{2\omega}^* \Phi_1'' + \tilde{E}I_{2\psi}^* \Phi_1' \right)' (\theta^1) - m_2(\theta^1) \Big\} \delta W_3(\theta^1) \Big]_0^L \\
&\qquad - Q_{0.3}\, \delta W_3(0) - Q_{L.3}\, \delta W_3(L)
\end{aligned}
$$

[41] To assist in the reading of the lengthy expression that follows, an increased line spacing is used to separate the terms pertaining to the variation of different generalised displacements.

$$
\begin{aligned}
&+\int_0^L \Big\{ \Big(-\tilde{E}S_\omega^* W_1' + \tilde{E}I_{3\omega}^* W_2'' + \tilde{E}I_{2\omega}^* W_3'' + \tilde{E}I_\omega^* \Phi_1'' + \tilde{E}I_{\omega\psi}^* \Phi_1' \Big)'' (\theta^1) \\
&\qquad - \Big[-\tilde{E}S_\psi^* W_1' + \tilde{E}I_{3\psi}^* W_2'' + \tilde{E}I_{2\psi}^* W_3'' + \tilde{E}I_{\omega\psi}^* \Phi_1'' + \Big(GJ + \tilde{E}I_\psi^* \Big) \Phi' \Big]' (\theta^1) \\
&\qquad - m_1(\theta^1) - b'(\theta^1) \Big\} \, \delta\Phi_1(\theta^1) \, d\theta^1 \\
&+ \Big[\Big(-\tilde{E}S_\omega^*(\theta^1) W_1'(\theta^1) + \tilde{E}I_{3\omega}^*(\theta^1) W_2''(\theta^1) + \tilde{E}I_{2\omega}^*(\theta^1) W_3''(\theta^1) + \tilde{E}I_\omega^*(\theta^1) \Phi_1''(\theta^1) \\
&\qquad + \tilde{E}I_{\omega\psi}^*(\theta^1) \Phi_1'(\theta^1) \Big) \delta\Phi_1'(\theta^1) \Big]_0^L + B_0 \, \delta\Phi_1'(0) + B_L \, \delta\Phi_1'(L) \\
&- \Big[\Big\{ \Big(-\tilde{E}S_\omega^* W_1' + \tilde{E}I_{3\omega}^* W_2'' + \tilde{E}I_{2\omega}^* W_3'' + \tilde{E}I_\omega^* \Phi_1'' + \tilde{E}I_{\omega\psi}^* \Phi_1' \Big)' (\theta^1) \\
&\qquad + \tilde{E}S_\psi^*(\theta^1) W_1'(\theta^1) - \tilde{E}I_{3\psi}^*(\theta^1) W_2''(\theta^1) - \tilde{E}I_{2\psi}^*(\theta^1) W_3''(\theta^1) \\
&\qquad - \tilde{E}I_{\omega\psi}^*(\theta^1) \Phi_1''(\theta^1) - \Big(GJ(\theta^1) + \tilde{E}I_\psi^*(\theta^1) \Big) \Phi_1'(\theta^1) - b(\theta^1) \Big\} \delta\Phi_1(\theta^1) \Big]_0^L \\
&- M_{0.1} \, \delta\Phi_1(0) - M_{L.1} \, \delta\Phi_1(L) \; . \qquad (2.6.3)
\end{aligned}
$$

By the principle of stationary total potential energy (*e.g.*, MASON 1980, §§ 8.1.1 and 8.2.1), the ordered quadruplet of generalised displacements $(W_i, \Phi_1) \in \mathcal{D}$ specifies the actual equilibrium shape of the bar if and only if

$$\delta\Pi(W_i, \Phi_1)[\delta W_i, \delta\Phi_1] = 0 \qquad (2.6.4)$$

for every admissible variations δW_i, $\delta\Phi_1$. By virtue of the fundamental lemma of the calculus of variations (*e.g.*, DACOROGNA 2004, th. 1.24), this variational identity leads to the classical or strong form of the structural problem, which may be phrased as follows:

Find real-valued maps W_1, W_2, W_3 and Φ_1 defined on the interval $[0, L]$, with

- $W_1 \in C^3[0, L]$ and
- $W_2, W_3, \Phi_1 \in C^4[0, L]$,

satisfying the differential equations

$$\Big(\tilde{E}A^* W_1' - \tilde{E}S_3^* W_2'' - \tilde{E}S_2^* W_3'' - \tilde{E}S_\omega^* \Phi_1'' - \tilde{E}S_\psi^* \Phi_1' \Big)' (\theta^1) + q_1(\theta^1) = 0 \qquad (2.6.5)$$

$$\Big(\tilde{E}S_3^* W_1' - \tilde{E}I_3^* W_2'' - \tilde{E}I_{23}^* W_3'' - \tilde{E}I_{3\omega}^* \Phi_1'' - \tilde{E}I_{3\psi}^* \Phi_1' \Big)'' (\theta^1) + q_2(\theta^1) - m_3'(\theta^1) = 0 \qquad (2.6.6)$$

$$\Big(\tilde{E}S_2^* W_1' - \tilde{E}I_{23}^* W_2'' - \tilde{E}I_2^* W_3'' - \tilde{E}I_{2\omega}^* \Phi_1'' - \tilde{E}I_{2\psi}^* \Phi_1' \Big)'' (\theta^1) + q_3(\theta^1) + m_2'(\theta^1) = 0 \qquad (2.6.7)$$

$$\left(\tilde{E}S^*_{\omega}W_1' - \tilde{E}I^*_{3\omega}W_2'' - \tilde{E}I^*_{2\omega}W_3'' - \tilde{E}I^*_{\omega}\Phi_1'' - \tilde{E}I^*_{\omega\psi}\Phi_1'\right)''(\theta^1)$$
$$+\left[-\tilde{E}S^*_{\psi}W_1' + \tilde{E}I^*_{3\psi}W_2'' + \tilde{E}I^*_{2\psi}W_3'' + \tilde{E}I^*_{\omega\psi}\Phi_1'' + \left(GJ + \tilde{E}I^*_{\psi}\right)\Phi_1'\right]'(\theta^1)$$
$$+b'(\theta^1) + m_1(\theta^1) = 0 \qquad (2.6.8)$$

on the open interval $(0, L)$,[42] together with the appropriate boundary conditions at $\theta^1 = 0$ and $\theta^1 = L$, to be selected from table 2.6.1 (from each row of the table, select one, and only one, boundary condition).[43]

2.7 CROSS-SECTIONAL STRESS RESULTANTS, ACTIVE AND REACTIVE. EQUILIBRIUM

The natural boundary conditions in table 2.6.1 prompt the following definitions for the cross-sectional stress resultants (or generalised stresses) – see figure 2.7.1:

(i) Normal force

$$N(\theta^1) = \tilde{E}A^*(\theta^1)W_1'(\theta^1) - \tilde{E}S^*_3(\theta^1)W_2''(\theta^1) - \tilde{E}S^*_2(\theta^1)W_3''(\theta^1)$$
$$-\tilde{E}S^*_{\omega}(\theta^1)\Phi_1''(\theta^1) - \tilde{E}S^*_{\psi}(\theta^1)\Phi_1'(\theta^1)\ . \qquad (2.7.1)$$

(ii) Shear forces

$$V_2(\theta^1) = \left(\tilde{E}S^*_3W_1' - \tilde{E}I^*_3W_2'' - \tilde{E}I^*_{23}W_3'' - \tilde{E}I^*_{3\omega}\Phi_1'' - \tilde{E}I^*_{3\psi}\Phi_1'\right)'(\theta^1) - m_3(\theta^1) \qquad (2.7.2)$$

$$V_3(\theta^1) = \left(\tilde{E}S^*_2W_1' - \tilde{E}I^*_{23}W_2'' - \tilde{E}I^*_2W_3'' - \tilde{E}I^*_{2\omega}\Phi_1'' - \tilde{E}I^*_{2\psi}\Phi_1'\right)'(\theta^1) + m_2(\theta^1)\ . \qquad (2.7.3)$$

(iii) Bending moments (relative to the axes through $O + \theta^1\boldsymbol{e}_1$ and spanned by $\boldsymbol{e}_2$ and $\boldsymbol{e}_3$)

$$M_2(\theta^1) = \tilde{E}S^*_2(\theta^1)W_1'(\theta^1) - \tilde{E}I^*_{23}(\theta^1)W_2''(\theta^1) - \tilde{E}I^*_2(\theta^1)W_3''(\theta^1)$$
$$-\tilde{E}I^*_{2\omega}(\theta^1)\Phi_1''(\theta^1) - \tilde{E}I^*_{2\psi}(\theta^1)\Phi_1'(\theta^1) \qquad (2.7.4)$$

$$M_3(\theta^1) = \tilde{E}S^*_3(\theta^1)W_1'(\theta^1) - \tilde{E}I^*_3(\theta^1)W_2''(\theta^1) - \tilde{E}I^*_{23}(\theta^1)W_3''(\theta^1)$$
$$-\tilde{E}I^*_{3\omega}(\theta^1)\Phi_1''(\theta^1) - \tilde{E}I^*_{3\psi}(\theta^1)\Phi_1'(\theta^1)\ . \qquad (2.7.5)$$

---

[42] These are the Euler-Lagrange equations associated with the functional Π, which form a mixed-order system of linear ordinary differential equations.

[43] Therefore, there are exactly seven boundary conditions at each end of the bar.

	Natural boundary conditions		Essential boundary conditions
Either	$\tilde{E}A^*(0)W_1'(0) - \tilde{E}S_3^*(0)W_2''(0) - \tilde{E}S_2^*(0)W_3''(0) - \tilde{E}S_\omega^*(0)\Phi_1''(0) - \tilde{E}S_\psi^*(0)\Phi_1'(0) = -Q_{0.1}$	or	$W_1(0)$ prescribed (*i.e.*, $\delta W_1(0) = 0$)
	$\tilde{E}A^*(L)W_1'(L) - \tilde{E}S_3^*(L)W_2''(L) - \tilde{E}S_2^*(L)W_3''(L) - \tilde{E}S_\omega^*(L)\Phi_1''(L) - \tilde{E}S_\psi^*(L)\Phi_1'(L) = Q_{L.1}$		$W_1(L)$ prescribed (*i.e.*, $\delta W_1(L) = 0$)
	$\left(\tilde{E}S_3^* W_1' - \tilde{E}I_3^* W_2'' - \tilde{E}I_{23}^* W_3'' - \tilde{E}I_{3\omega}^* \Phi_1'' - \tilde{E}I_{3\psi}^* \Phi_1'\right)'(0) - m_3(0) = -Q_{0.2}$		$W_2(0)$ prescribed (*i.e.*, $\delta W_2(0) = 0$)
	$\left(\tilde{E}S_3^* W_1' - \tilde{E}I_3^* W_2'' - \tilde{E}I_{23}^* W_3'' - \tilde{E}I_{3\omega}^* \Phi_1'' - \tilde{E}I_{3\psi}^* \Phi_1'\right)'(L) - m_3(L) = Q_{L.2}$		$W_2(L)$ prescribed (*i.e.*, $\delta W_2(L) = 0$)
	$\tilde{E}S_3^*(0)W_1'(0) - \tilde{E}I_3^*(0)W_2''(0) - \tilde{E}I_{23}^*(0)W_3''(0) - \tilde{E}I_{3\omega}^*(0)\Phi_1''(0) - \tilde{E}I_{3\psi}^*(0)\Phi_1'(0) = M_{0.3}$		$W_2'(0)$ prescribed (*i.e.*, $\delta W_2'(0) = 0$)
	$\tilde{E}S_3^*(L)W_1'(L) - \tilde{E}I_3^*(L)W_2''(L) - \tilde{E}I_{23}^*(L)W_3''(L) - \tilde{E}I_{3\omega}^*(L)\Phi_1''(L) - \tilde{E}I_{3\psi}^*(L)\Phi_1'(L) = -M_{L.3}$		$W_2'(L)$ prescribed (*i.e.*, $\delta W_2'(L) = 0$)
	$\left(\tilde{E}S_2^* W_1' - \tilde{E}I_{23}^* W_2'' - \tilde{E}I_2^* W_3'' - \tilde{E}I_{2\omega}^* \Phi_1'' - \tilde{E}I_{2\psi}^* \Phi_1'\right)'(0) + m_2(0) = -Q_{0.3}$		$W_3(0)$ prescribed (*i.e.*, $\delta W_3(0) = 0$)
	$\left(\tilde{E}S_2^* W_1' - \tilde{E}I_{23}^* W_2'' - \tilde{E}I_2^* W_3'' - \tilde{E}I_{2\omega}^* \Phi_1'' - \tilde{E}I_{2\psi}^* \Phi_1'\right)'(L) + m_2(L) = Q_{L.3}$		$W_3(L)$ prescribed (*i.e.*, $\delta W_3(L) = 0$)

Table 2.6.1: Natural and essential boundary conditions

	Natural boundary conditions		Essential boundary conditions
Either	$\tilde{E}S_2^*(0)W_1'(0)-\tilde{E}I_{23}^*(0)W_2''(0)-\tilde{E}I_2^*(0)W_3''(0)-\tilde{E}I_{2\omega}^*(0)\Phi_1''(0)-\tilde{E}I_{2\psi}^*(0)\Phi_1'(0)=-M_{0.2}$	or	$W_3'(0)$ prescribed (*i.e.*, $\delta W_3'(0)=0$)
	$\tilde{E}S_2^*(L)W_1'(L)-\tilde{E}I_{23}^*(L)W_2''(L)-\tilde{E}I_2^*(L)W_3''(L)-\tilde{E}I_{2\omega}^*(L)\Phi_1''(L)-\tilde{E}I_{2\psi}^*(L)\Phi_1'(L)=M_{L.2}$		$W_3'(L)$ prescribed (*i.e.*, $\delta W_3'(L)=0$)
	$\left(\tilde{E}S_\omega^* W_1'-\tilde{E}I_{3\omega}^* W_2''-\tilde{E}I_{2\omega}^* W_3''-\tilde{E}I_\omega^* \Phi_1''-\tilde{E}I_{\omega\psi}^* \Phi_1'\right)'(0)$ $-\tilde{E}S_\psi^*(0)W_1'(0)+\tilde{E}I_{3\psi}^*(0)W_2''(0)+\tilde{E}I_{2\psi}^*(0)W_3''(0)$ $+\tilde{E}I_{\omega\psi}^*(0)\Phi_1''(0)+\left(GJ(0)+\tilde{E}I_\psi^*(0)\right)\Phi_1'(0)+b(0)=-M_{0.1}$		$\Phi_1(0)$ prescribed (*i.e.*, $\delta\Phi_1(0)=0$)
	$\left(\tilde{E}S_\omega^* W_1'-\tilde{E}I_{3\omega}^* W_2''-\tilde{E}I_{2\omega}^* W_3''-\tilde{E}I_\omega^* \Phi_1''-\tilde{E}I_{\omega\psi}^* \Phi_1'\right)'(L)$ $-\tilde{E}S_\psi^*(L)W_1'(L)+\tilde{E}I_{3\psi}^*(L)W_2''(L)+\tilde{E}I_{2\psi}^*(L)W_3''(L)$ $+\tilde{E}I_{\omega\psi}^*(L)\Phi_1''(L)+\left(GJ(L)+\tilde{E}I_\psi^*(L)\right)\Phi_1'(L)+b(L)=M_{L.1}$		$\Phi_1(L)$ prescribed (*i.e.*, $\delta\Phi_1(L)=0$)
	$\tilde{E}S_\omega^*(0)W_1'(0)-\tilde{E}I_{3\omega}^*(0)W_2''(0)-\tilde{E}I_{2\omega}^*(0)W_3''(0)-\tilde{E}I_\omega^*(0)\Phi_1''(0)-\tilde{E}I_{\omega\psi}^*(0)\Phi_1'(0)=-B_0$		$\Phi_1'(0)$ prescribed (*i.e.*, $\delta\Phi_1'(0)=0$)
	$\tilde{E}S_\omega^*(L)W_1'(L)-\tilde{E}I_{3\omega}^*(L)W_2''(L)-\tilde{E}I_{2\omega}^*(L)W_3''(L)-\tilde{E}I_\omega^*(L)\Phi_1''(L)-\tilde{E}I_{\omega\psi}^*(L)\Phi_1'(L)=B_L$		$\Phi_1'(L)$ prescribed (*i.e.*, $\delta\Phi_1'(L)=0$)

Table 2.6.1 (continued): Natural and essential boundary conditions

(iv) Torque (about the line $\{O+\theta^1\boldsymbol{e}_1,\, 0\le\theta^1\le L\}$)

$$\begin{aligned} M_1(\theta^1) = &\left(\tilde{E}S^*_\omega W_1' - \tilde{E}I^*_{3\omega} W_2'' - \tilde{E}I^*_{2\omega} W_3'' - \tilde{E}I^*_\omega \Phi_1'' - \tilde{E}I^*_{\omega\psi} \Phi_1'\right)'(\theta^1) \\ &-\tilde{E}S^*_\psi(\theta^1) W_1'(\theta^1) + \tilde{E}I^*_{3\psi}(\theta^1) W_2''(\theta^1) + \tilde{E}I^*_{2\psi}(\theta^1) W_3''(\theta^1) \\ &+\tilde{E}I^*_{\omega\psi}(\theta^1)\Phi_1''(\theta^1) + \left(GJ(\theta^1) + \tilde{E}I^*_\psi(\theta^1)\right)\Phi_1'(\theta^1) + b(\theta^1)\ . \end{aligned} \tag{2.7.6}$$

(v) Bimoment (represented by a three-headed arrow in figure 2.7.1 – GJELSVIK 1981, p. 25)

$$\begin{aligned} B(\theta^1) = &\tilde{E}S^*_\omega(\theta^1) W_1'(\theta^1) - \tilde{E}I^*_{3\omega}(\theta^1) W_2''(\theta^1) - \tilde{E}I^*_{2\omega}(\theta^1) W_3''(\theta^1) \\ &-\tilde{E}I^*_\omega(\theta^1)\Phi_1''(\theta^1) - \tilde{E}I^*_{\omega\psi}(\theta^1)\Phi_1'(\theta^1)\ . \end{aligned} \tag{2.7.7}$$

Indeed, with these definitions, the natural boundary conditions amount to prescribing the stress resultants at the bar ends as follows:

$$N(0) = -Q_{0.1} \qquad N(L) = Q_{L.1} \tag{2.7.8}$$

$$V_2(0) = -Q_{0.2} \qquad V_2(L) = Q_{L.2} \tag{2.7.9}$$

$$V_3(0) = -Q_{0.3} \qquad V_3(L) = Q_{L.3} \tag{2.7.10}$$

$$M_1(0) = -M_{0.1} \qquad M_1(L) = M_{L.1} \tag{2.7.11}$$

$$M_2(0) = -M_{0.2} \qquad M_2(L) = M_{L.2} \tag{2.7.12}$$

$$M_3(0) = M_{0.3} \qquad M_3(L) = -M_{L.3} \tag{2.7.13}$$

$$B(0) = -B_0 \qquad B(L) = B_L\ . \tag{2.7.14}$$

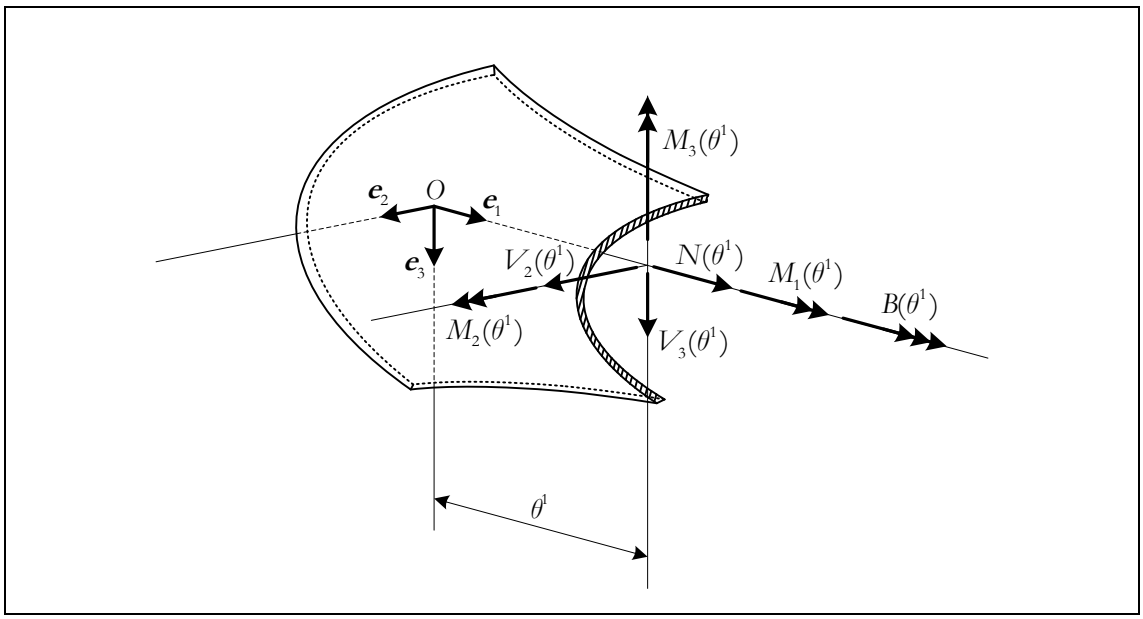

Figure 2.7.1: Cross-sectional stress resultants

According to the smoothness assumptions stated at the beginning of § 2.6, the real-valued maps $\theta^1 \mapsto N(\theta^1)$, $\theta^1 \mapsto V_2(\theta^1)$, $\theta^1 \mapsto V_3(\theta^1)$ and $\theta^1 \mapsto M_1(\theta^1)$ are continuously differentiable on $[0, L]$, while $\theta^1 \mapsto M_2(\theta^1)$, $\theta^1 \mapsto M_3(\theta^1)$ and $\theta^1 \mapsto B(\theta^1)$ are twice continuously differentiable on the same interval.

As in the case of the membrane forces, the cross-sectional stress resultants (2.7.1)-(2.7.7) are divided into active and reactive categories. The normal force, bending moments and bimoment are clearly active, as they can be obtained from the sole active membrane force $n_{\mathrm{I}\cdot\mathrm{I}}^{(A)}$ through integration over the interval $\left[g_1(\theta^1), g_2(\theta^1)\right]$ (*i.e.*, over $\mathscr{L}_{\theta^1}$, viewed through the parametrisation F):

$$N(\theta^1) = \int_{g_1(\theta^1)}^{g_2(\theta^1)} n_{\mathrm{I}\cdot\mathrm{I}}^{(A)}(\theta^1, \theta^2)\, \boldsymbol{o}_{\mathrm{I}}(\theta^1, \theta^2) \cdot \boldsymbol{e}_1 \, d\theta^2 \tag{2.7.15}$$

$$M_2(\theta^1) = \int_{g_1(\theta^1)}^{g_2(\theta^1)} \overline{x}_3(\theta^1, \theta^2)\, n_{\mathrm{I}\cdot\mathrm{I}}^{(A)}(\theta^1, \theta^2)\, \boldsymbol{o}_{\mathrm{I}}(\theta^1, \theta^2) \cdot \boldsymbol{e}_1 \, d\theta^2 \tag{2.7.16}$$

$$M_3(\theta^1) = \int_{g_1(\theta^1)}^{g_2(\theta^1)} \overline{x}_2(\theta^1, \theta^2)\, n_{\mathrm{I}\cdot\mathrm{I}}^{(A)}(\theta^1, \theta^2)\, \boldsymbol{o}_{\mathrm{I}}(\theta^1, \theta^2) \cdot \boldsymbol{e}_1 \, d\theta^2 \tag{2.7.17}$$

$$B(\theta^1) = \int_{g_1(\theta^1)}^{g_2(\theta^1)} \omega(\theta^1, \theta^2)\, n_{\mathrm{I}\cdot\mathrm{I}}^{(A)}(\theta^1, \theta^2)\, \boldsymbol{o}_{\mathrm{I}}(\theta^1, \theta^2) \cdot \boldsymbol{e}_1 \, d\theta^2 \ . \tag{2.7.18}$$

On the other hand, the shear forces are obviously reactive, being related to the active cross-sectional stress resultants by

$$V_2(\theta^1) = M_3'(\theta^1) - m_3(\theta^1) \tag{2.7.19}$$

$$V_3(\theta^1) = M_2'(\theta^1) + m_2(\theta^1) \ . \tag{2.7.20}$$

As for the torque $M_1(\theta^1)$, it can be split into an active part $M_1^{(A)}(\theta^1)$ and a reactive part $M_1^{(R)}(\theta^1)$. The active part is given by

$$\begin{aligned} M_1^{(A)}(\theta^1) &= -\int_{g_1(\theta^1)}^{g_2(\theta^1)} \psi(\theta^1, \theta^2)\, n_{\mathrm{I}\cdot\mathrm{I}}^{(A)}(\theta^1, \theta^2)\, \boldsymbol{o}_{\mathrm{I}}(\theta^1, \theta^2) \cdot \boldsymbol{e}_1 \, d\theta^2 + GJ(\theta^1)\Phi_1'(\theta^1) \\ &= -\tilde{E}S_{\psi}^*(\theta^1) W_1'(\theta^1) + \tilde{E}I_{3\psi}^*(\theta^1) W_2''(\theta^1) + \tilde{E}I_{2\psi}^*(\theta^1) W_3''(\theta^1) \\ &\quad + \tilde{E}I_{\omega\psi}^*(\theta^1)\Phi_1''(\theta^1) + \left(GJ(\theta^1) + \tilde{E}I_{\psi}^*(\theta^1)\right)\Phi_1'(\theta^1) \ . \end{aligned} \tag{2.7.21}$$

The reactive part is simply

$$\begin{aligned} M_1^{(R)}(\theta^1) &= B'(\theta^1) + b(\theta^1) \\ &= \left(\tilde{E}S_{\omega}^* W_1' - \tilde{E}I_{3\omega}^* W_2'' - \tilde{E}I_{2\omega}^* W_3'' - \tilde{E}I_{\omega}^* \Phi_1'' - \tilde{E}I_{\omega\psi}^* \Phi'\right)'(\theta^1) + b(\theta^1) \ . \end{aligned} \tag{2.7.22}$$

With this distinction between active and reactive cross-sectional stress resultants, the strain energy functional (2.5.23) can be rewritten concisely in the form

$$U = \frac{1}{2}\int_0^L \Big(N(\theta^1)\,\varepsilon(\theta^1) + M_1^{(A)}(\theta^1)\,\kappa_1(\theta^1) + M_2(\theta^1)\,\kappa_2(\theta^1) + M_3(\theta^1)\,\kappa_3(\theta^1) + B(\theta^1)\,\Gamma(\theta^1)\Big)\, d\theta^1 \ , \tag{2.7.23}$$

where ε, κ_1, κ_2, κ_3 and Γ are the generalised strains introduced in (2.3.27)-(2.3.31), which are thus seen to be conjugate to the active stress resultants. The reactive cross-sectional stress resultants, that is, the forces maintaining the constraints (V1)-(V2), do no work in any deformation satisfying these constraints and are thereby absent in equation (2.7.23).

The incorporation of the definitions (2.7.1) and (2.7.4)-(2.7.6) into the differential equations (2.6.5)-(2.6.8) yields the classical local form of the equilibrium equations on $(0, L)$:

$$N'(\theta^1) + q_1(\theta^1) = 0 \tag{2.7.24}$$

$$M_3''(\theta^1) - m_3'(\theta^1) + q_2(\theta^1) = 0 \tag{2.7.25}$$

$$M_2''(\theta^1) + m_2'(\theta^1) + q_3(\theta^1) = 0 \tag{2.7.26}$$

$$M_1'(\theta^1) + m_1(\theta^1) = 0 \ . \tag{2.7.27}$$

Concerning the second term on the left-hand side of equations (2.7.25)-(2.7.26), we remark that a continuously differentiable moment distribution $\theta^1 \mapsto m_3(\theta^1)\,\boldsymbol{e}_3$ (resp. $\theta^1 \mapsto m_2(\theta^1)\,\boldsymbol{e}_2$) per unit length of the line segment $\{O + \theta^1 \boldsymbol{e}_1,\, 0 \le \theta^1 \le L\}$ is statically equivalent to (i) a distributed force $\theta^1 \mapsto -m_3'(\theta^1)\,\boldsymbol{e}_2$ (resp. $\theta^1 \mapsto m_2'(\theta^1)\,\boldsymbol{e}_3$) per unit length of the same line segment plus (ii) concentrated forces $-m_3(0)\,\boldsymbol{e}_2$ and $m_3(L)\,\boldsymbol{e}_2$ (resp. $m_2(0)\,\boldsymbol{e}_3$ and $-m_2(L)\,\boldsymbol{e}_3$) at the end points O and $O + L\,\boldsymbol{e}_1$. Finally, notice that equation (2.7.27) may be written exclusively in terms of active cross-sectional stress resultants as

$$B''(\theta^1) + M_1^{(A)\prime}(\theta^1) + b'(\theta^1) + m_1(\theta^1) = 0 \ . \tag{2.7.28}$$

2.8 A SUMMARY OF THE FIELD EQUATIONS OF THE ONE-DIMENSIONAL MODEL

At this point, it is convenient to present a systematic summary of the field equations of the one-dimensional model developed in this chapter. The objective is threefold:

(i) To offer an overall, sweeping view of the model, which was admittedly difficult to convey so far due to the considerable amount of detail involved in the derivations.

(ii) To underscore the basic ingredients – the building blocks, so to speak – and mathematical structure of the one-dimensional model, which are shared with other linear models of structural mechanics (of bars, plates and shells alike), as well as with linear elastostatics and many other physical theories, concerning widely different physical contents (TONTI 1972a, 1972b).

(iii) To draw attention to some particular features of the model that stem from the constraints that are imposed on the higher-dimensional parent theory, which have not yet received the appropriate emphasis.

In the one-dimensional model, we can single out the following four sets of dependent variables (which are all real-valued maps of a single real variable, defined on the interval $[0, L]$):

(i) The generalised displacements, grouped in the column vector

$$\{d\} = \begin{Bmatrix} W_1 \\ W_2 \\ W_3 \\ \Phi_1 \end{Bmatrix} . \tag{2.8.1}$$

(ii) The generalised strains, collected in the column vector

$$\{e\} = \begin{Bmatrix} \varepsilon \\ \kappa_1 \\ \kappa_2 \\ \kappa_3 \\ \Gamma \end{Bmatrix} . \tag{2.8.2}$$

(iii) The active cross-sectional stress resultants, which are conjugate to the generalised strains, arranged in the column vector

$$\{s^{(A)}\} = \begin{Bmatrix} N \\ M_1^{(A)} \\ M_2 \\ M_3 \\ B \end{Bmatrix} , \tag{2.8.3}$$

so that the strain energy stored in the bar is

$$\frac{1}{2}\int_0^L \{s^{(A)}(\theta^1)\}^T \{e(\theta^1)\}\, d\theta^1 \quad . \tag{2.8.4}$$

(iv) The distributed bar loads corresponding to the generalised displacements $\{d\}$, arranged in the column vector

$$\{q\} = \begin{Bmatrix} q_1 \\ -m_3' + q_2 \\ m_2' + q_3 \\ b' + m_1 \end{Bmatrix} . \tag{2.8.5}$$

This definition, which may seem odd at first sight, stems from the requirement that the work of the distributed bar loads – *i.e.*, the integral on the right-hand side of (2.5.24) or (2.5.31) – be equal to

$$\int_0^L \{q(\theta^1)\}^T \{d(\theta^1)\} d\theta^1 + \text{boundary terms} . \tag{2.8.6}$$

It should be noted that the bar loads m_2, m_3 and b are associated with derivatives of generalised displacements and not with independent generalised displacements in their own right. This is a direct consequence of the internal constraints upon which the one-dimensional model is based and which imply the conditions (2.3.18)-(2.3.20).

The generalised displacements $\{d\}$ and the generalised strains $\{e\}$ are connected by the compatibility equation

$$\{e\} = [L]\{d\} , \tag{2.8.7}$$

where

$$[L] = \begin{bmatrix} D & \cdot & \cdot & \cdot \\ \cdot & \cdot & \cdot & D \\ \cdot & \cdot & -D^2 & \cdot \\ \cdot & -D^2 & \cdot & \cdot \\ \cdot & \cdot & \cdot & -D^2 \end{bmatrix} \tag{2.8.8}$$

is a formal linear differential operator.[44]

The active cross-sectional stress resultants $\{s^{(A)}\}$ are given in terms of the generalised strains $\{e\}$ by the constitutive relation

$$\{s^{(A)}\} = [K]\{e\} , \tag{2.8.9}$$

where $[K]$ is the (symmetric) stiffness matrix

[44] The word "formal" just means that the domain of the operator is not specified.

$$[K]=\begin{bmatrix} \tilde{E}A^* & -\tilde{E}S_\psi^* & \tilde{E}S_2^* & \tilde{E}S_3^* & \tilde{E}S_\omega^* \\ -\tilde{E}S_\psi^* & \left(GJ+\tilde{E}I_\psi^*\right) & -\tilde{E}I_{2\psi}^* & -\tilde{E}I_{3\psi}^* & -\tilde{E}I_{\omega\psi}^* \\ \tilde{E}S_2^* & -\tilde{E}I_{2\psi}^* & \tilde{E}I_2^* & \tilde{E}I_{23}^* & \tilde{E}I_{2\omega}^* \\ \tilde{E}S_3^* & -\tilde{E}I_{3\psi}^* & \tilde{E}I_{23}^* & \tilde{E}I_3^* & \tilde{E}I_{3\omega}^* \\ \tilde{E}S_\omega^* & -\tilde{E}I_{\omega\psi}^* & \tilde{E}I_{2\omega}^* & \tilde{E}I_{3\omega}^* & \tilde{E}I_\omega^* \end{bmatrix}, \tag{2.8.10}$$

whose entries are known real-valued maps defined on $[0,L]$.

The distributed bar loads $\{q\}$ are related to the active cross-sectional stress resultants $\{s^{(A)}\}$ via the equilibrium conditions

$$[L]^\dagger\{s^{(A)}\}=\{q\}\ , \tag{2.8.11}$$

where

$$[L]^\dagger=\begin{bmatrix} -D & \cdot & \cdot & \cdot & \cdot \\ \cdot & \cdot & \cdot & -D^2 & \cdot \\ \cdot & \cdot & -D^2 & \cdot & \cdot \\ \cdot & -D & \cdot & \cdot & -D^2 \end{bmatrix} \tag{2.8.12}$$

is the formal adjoint differential operator of $[L]$ (*e.g.*, LANCZOS 1996, §§ 4.10-4.12, or SEWELL 1987, § 3.3).

The three equations (2.8.7), (2.8.9) and (2.8.11) can be combined to yield

$$[L]^\dagger[K][L]\{d\}=\{q\}\ , \tag{2.8.13}$$

which are none other than the governing equations (2.6.5)-(2.6.8), written in compact matrix form. The process is summarised in figure 2.8.1 by means of a Tonti diagram (TONTI 1972a, 1972b, 1975, 1976).

To the four sets of dependent variables already described, one now adds the reactive cross-sectional stress resultants, collected in the column vector

$$\{s^{(R)}\}=\begin{Bmatrix} V_2 \\ V_3 \\ M_1^{(R)} \end{Bmatrix}. \tag{2.8.14}$$

These reactive cross-sectional stress resultants satisfy the equilibrium conditions

$$\begin{Bmatrix} V_2 \\ V_3 \\ M_1^{(R)} \end{Bmatrix}=\begin{Bmatrix} M_3' \\ M_2' \\ B' \end{Bmatrix}+\begin{Bmatrix} -m_3 \\ m_2 \\ b \end{Bmatrix}\ , \tag{2.8.15}$$

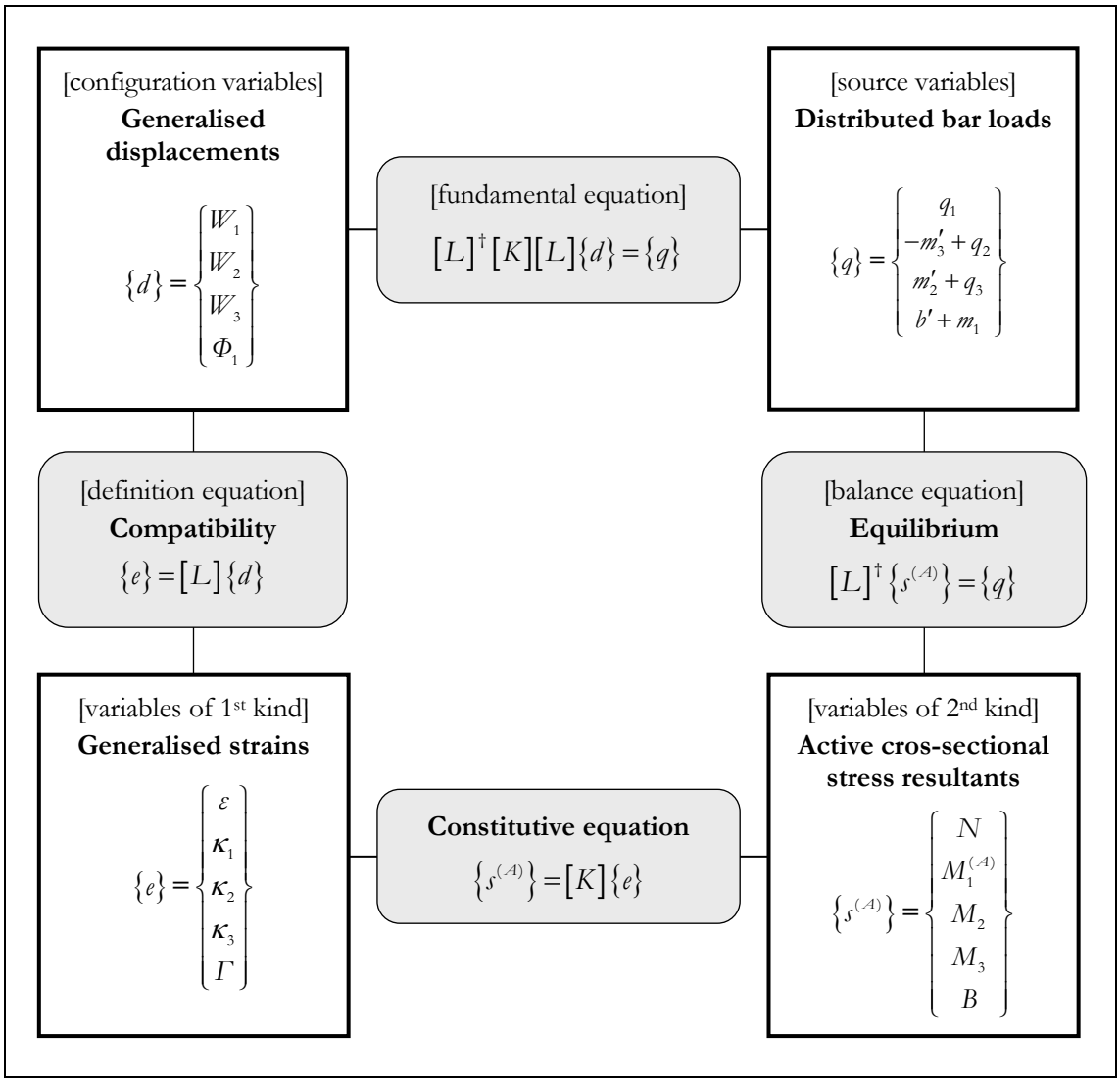

Figure 2.8.1: Tonti diagram (Tonti's usual terminology is given between square brackets)

and can therefore be thought of as arising from internal causes (constraints) and external causes (loading) – see GJELSVIK 1981, p. 30. Moreover, observe that m_2, m_3 and b are precisely the bar loads whose derivatives appear in the definition of the column vector $\{q\}$. Finally, equations (2.7.2), (2.7.3) and (2.7.22) are recovered after inserting the constitutive and compatibility equations (2.8.9) and (2.8.7) into the equilibrium equation (2.8.15):

$$\begin{Bmatrix} V_2 \\ V_3 \\ M_1^{(\mathrm{R})} \end{Bmatrix} = \left(\begin{bmatrix} \tilde{E}S_3^* & -\tilde{E}I_{3\psi}^* & \tilde{E}I_{23}^* & \tilde{E}I_3^* & \tilde{E}I_{3\omega}^* \\ \tilde{E}S_2^* & -\tilde{E}I_{2\psi}^* & \tilde{E}I_2^* & \tilde{E}I_{23}^* & \tilde{E}I_{2\omega}^* \\ \tilde{E}S_\omega^* & -\tilde{E}I_{\omega\psi}^* & \tilde{E}I_{2\omega}^* & \tilde{E}I_{3\omega}^* & \tilde{E}I_\omega^* \end{bmatrix} \begin{Bmatrix} W_1' \\ \Phi_1' \\ -W_3'' \\ -W_2'' \\ -\Phi_1'' \end{Bmatrix} \right)' + \begin{Bmatrix} -m_3 \\ m_2 \\ b \end{Bmatrix} . \qquad (2.8.16)$$

2.9 A STUDY OF SOME PARTICULAR CASES

2.9.1 Bars with a longitudinal plane of symmetry

Let the reference shape $\mathcal{B}$ of the bar be symmetric with respect to the plane passing through the origin O and spanned by the Cartesian base vectors $\boldsymbol{e}_1$ and $\boldsymbol{e}_3$. The reference shape $\mathcal{S}$ of the middle surface of the bar is itself symmetric with respect to the said plane and it is thus possible to choose $\overline{\Omega}$ with $g_1 = -g_2$, so that the region $\overline{\Omega}$ is symmetric with respect to the θ^1-axis (see figure 2.9.1). The image of $[0, L] \times \{0\}$ under the parametrisation F is the intersection of $\mathcal{S}$ with the symmetry plane. Moreover, for each $(\theta^1, \theta^2) \in \overline{\Omega}$, one has $t(\theta^1, \theta^2) = t(\theta^1, -\theta^2)$.

For fixed $\theta^1 \in [0, L]$, the map $\theta^2 \mapsto \overline{x}_2(\theta^1, \theta^2)$ (resp. $\theta^2 \mapsto \overline{x}_3(\theta^1, \theta^2)$) from $\left[-g_2(\theta^1), g_2(\theta^1)\right]$ into $\mathbb{R}$ is odd (resp. even), *i.e.*,

$$\overline{x}_2(\theta^1, \theta^2) = -\overline{x}_2(\theta^1, -\theta^2) \tag{2.9.1}$$

$$\overline{x}_3(\theta^1, \theta^2) = \overline{x}_3(\theta^1, -\theta^2)) \,, \tag{2.9.2}$$

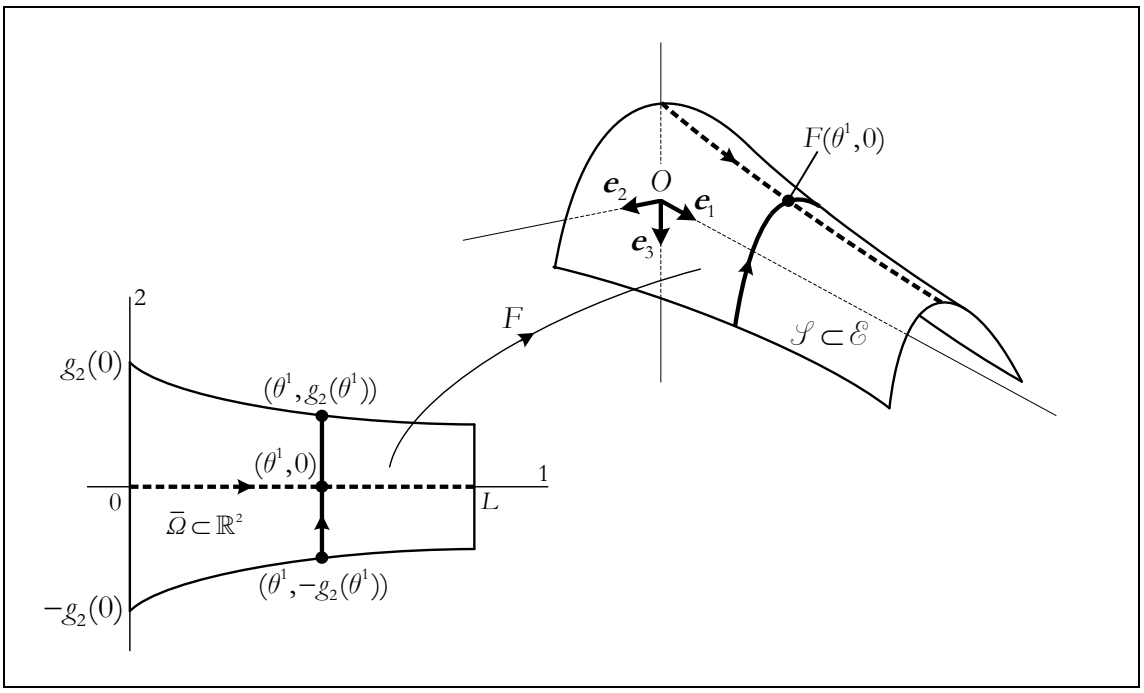

Figure 2.9.1: Bars with a longitudinal plane of symmetry – Parametrisation of the reference shape $\mathcal{S}$ of the middle surface

$\forall \theta^2 \in \left[-g_2(\theta^1), g_2(\theta^1)\right]$. Consequently, the map $\theta^2 \mapsto D_2\overline{x}_2(\theta^1, \theta^2)$ (resp. $\theta^2 \mapsto D_2\overline{x}_3(\theta^1, \theta^2)$) is even (resp. odd), *i.e.*,

$$D_2\overline{x}_2(\theta^1, \theta^2) = D_2\overline{x}_2(\theta^1, -\theta^2) \tag{2.9.3}$$

$$D_2\overline{x}_3(\theta^1, \theta^2) = -D_2\overline{x}_3(\theta^1, -\theta^2) \ , \tag{2.9.4}$$

$\forall \theta^2 \in \left[-g_2(\theta^1), g_2(\theta^1)\right]$. It now follows from the definition (2.3.16) that, for each $\theta^1 \in \left[0, L\right]$, $\theta^2 \mapsto \omega(\theta^1, \theta^2)$ is an odd map – indeed, by the change of variable theorem (*e.g.*, CAMPOS FERREIRA 1987, th. 19, § 5.1.2), one has

$$\begin{aligned}
\omega(\theta^1, -\theta^2) &= \int_0^{-\theta^2} \left(\overline{x}_2(\theta^1, s)\, D_2\overline{x}_3(\theta^1, s) - \overline{x}_3(\theta^1, s)\, D_2\overline{x}_2(\theta^1, s)\right) ds \\
&= \int_0^{\theta^2} \left(\overline{x}_2(\theta^1, -t)\, D_2\overline{x}_3(\theta^1, -t) - \overline{x}_3(\theta^1, -t)\, D_2\overline{x}_2(\theta^1, -t)\right)(-1)\, dt \\
&= -\int_0^{\theta^2} \left(\overline{x}_2(\theta^1, t)\, D_2\overline{x}_3(\theta^1, t) - \overline{x}_3(\theta^1, t)\, D_2\overline{x}_2(\theta^1, t)\right) dt \\
&= -\omega(\theta^1, \theta^2) \ .
\end{aligned} \tag{2.9.5}$$

Consider now an arbitrary point (θ^1, θ^2) in Ω. The first coordinate lines through the points $F(\theta^1, \theta^2)$ and $F(\theta^1, -\theta^2)$ are symmetric with respect to the plane defined by O and $\{\boldsymbol{e}_1, \boldsymbol{e}_3\}$. Therefore,

$$D_1\overline{x}_2(\theta^1, \theta^2) = \boldsymbol{a}_1(\theta^1, \theta^2)\cdot\boldsymbol{e}_2 = -\boldsymbol{a}_1(\theta^1, -\theta^2)\cdot\boldsymbol{e}_2 = -D_1\overline{x}_2(\theta^1, -\theta^2) \tag{2.9.6}$$

$$D_1\overline{x}_3(\theta^1, \theta^2) = \boldsymbol{a}_1(\theta^1, \theta^2)\cdot\boldsymbol{e}_3 = \boldsymbol{a}_1(\theta^1, -\theta^2)\cdot\boldsymbol{e}_3 = D_1\overline{x}_3(\theta^1, -\theta^2) \ . \tag{2.9.7}$$

By continuity, these identities extend to $\overline{\Omega}$ (see the "principle of extension of identities" in BOURBAKI 2007, p. 53, or DIEUDONNÉ 1960, th. 3.15.2). Together with previous results, they imply $t^*(\theta^1, \theta^2) = t^*(\theta^1, -\theta^2)$, $\forall (\theta^1, \theta^2) \in \overline{\Omega}$. Likewise, one has

$$D_1\omega(\theta^1, \theta^2) = -D_1\omega(\theta^1, -\theta^2) \tag{2.9.8}$$

$$\psi(\theta^1, \theta^2) = -\psi(\theta^1, -\theta^2) \tag{2.9.9}$$

on $\overline{\Omega}$.

In the light of the above, it is obvious that S_3^*, S_ω^*, S_ψ^*, I_{23}^*, $I_{2\omega}^*$ and $I_{2\psi}^*$ are identically zero. The governing differential equations (2.6.5)-(2.6.8) on the interval $\left(0, L\right)$ then reduce to

$$\left(\tilde{E}A^*\, W_1' - \tilde{E}S_2^*\, W_3''\right)'(\theta^1) + q_1(\theta^1) = 0 \tag{2.9.10}$$

$$-\left(\tilde{E}I_3^*\, W_2'' + \tilde{E}I_{3\omega}^*\, \Phi_1'' + \tilde{E}I_{3\psi}^*\, \Phi_1'\right)''(\theta^1) + q_2(\theta^1) - m_3'(\theta^1) = 0 \tag{2.9.11}$$

$$\left(\tilde{E}S_2^*\,W_1' - \tilde{E}I_2^*\,W_3''\right)''(\theta^1) + q_3(\theta^1) + m_2'(\theta^1) = 0 \tag{2.9.12}$$

$$-\left(\tilde{E}I_{3\omega}^*\,W_2'' + \tilde{E}I_{\omega}^*\,\Phi_1'' + \tilde{E}I_{\omega\psi}^*\,\Phi_1'\right)''(\theta^1) + \left[\tilde{E}I_{3\psi}^*\,W_2'' + \tilde{E}I_{\omega\psi}^*\,\Phi_1'' + \left(GJ + \tilde{E}I_{\psi}^*\right)\Phi'\right]'(\theta^1)$$

$$+b'(\theta^1) + m_1(\theta^1) = 0\ , \tag{2.9.13}$$

while the cross-sectional stress resultants (2.7.1)-(2.7.7) become simply

$$N(\theta^1) = \tilde{E}A^*(\theta^1)\,W_1'(\theta^1) - \tilde{E}S_2^*(\theta^1)\,W_3''(\theta^1) \tag{2.9.14}$$

$$V_2(\theta^1) = -\left(\tilde{E}I_3^*\,W_2'' + \tilde{E}I_{3\omega}^*\,\Phi_1''(\theta^1) + \tilde{E}I_{3\psi}^*\,\Phi_1'\right)'(\theta^1) - m_3(\theta^1) \tag{2.9.15}$$

$$V_3(\theta^1) = \left(\tilde{E}S_2^*\,W_1' - \tilde{E}I_2^*\,W_3''\right)'(\theta^1) + m_2(\theta^1) \tag{2.9.16}$$

$$M_2(\theta^1) = \tilde{E}S_2^*(\theta^1)\,W_1'(\theta^1) - \tilde{E}I_2^*(\theta^1)\,W_3''(\theta^1) \tag{2.9.17}$$

$$M_3(\theta^1) = -\tilde{E}I_3^*(\theta^1)\,W_2''(\theta^1) - \tilde{E}I_{3\omega}^*(\theta^1)\,\Phi_1''(\theta^1) - \tilde{E}I_{3\psi}^*(\theta^1)\,\Phi_1'(\theta^1) \tag{2.9.18}$$

$$M_1(\theta^1) = -\left(\tilde{E}I_{3\omega}^*\,W_2'' + \tilde{E}I_{\omega}^*\,\Phi_1'' + \tilde{E}I_{\omega\psi}^*\,\Phi_1'\right)'(\theta^1) + \tilde{E}I_{3\psi}^*(\theta^1)\,W_2''(\theta^1)$$

$$+\tilde{E}I_{\omega\psi}^*(\theta^1)\,\Phi_1''(\theta^1) + \left(GJ(\theta^1) + \tilde{E}I_{\psi}^*(\theta^1)\right)\Phi_1'(\theta^1) + b(\theta^1) \tag{2.9.19}$$

$$B(\theta^1) = -\tilde{E}I_{3\omega}^*(\theta^1)\,W_2''(\theta^1) - \tilde{E}I_{\omega}^*(\theta^1)\,\Phi_1''(\theta^1) - \tilde{E}I_{\omega\psi}^*(\theta^1)\,\Phi_1'(\theta^1)\ . \tag{2.9.20}$$

Note the couplings (i) between W_1 and W_3, introduced by $\tilde{E}S_2^*$, and (ii) between W_2 and Φ_1, introduced by $\tilde{E}I_{3\omega}^*$ and $\tilde{E}I_{3\psi}^*$.

2.9.2 Prismatic bars

For a prismatic bar, the reference shape $\mathscr{S}$ of the middle surface is a cylindrical surface. Therefore, it admits a parametrisation of the form (OPREA 2007, p. 75)

$$F : \bar{\Omega} = [0, L] \times [a, b] \to \mathscr{E}\ ,\quad F(\theta^1, \theta^2) = C(\theta^2) + \theta^1\,\boldsymbol{e}_1\ , \tag{2.9.21}$$

where $C : [a, b] \to \mathscr{E}$ is an arc-length parametrisation of the middle line $\mathscr{L}_0$ (which is a directrix of $\mathscr{S}$) and it is required that $0 \in [a, b]$. For such a parametrisation, the coordinate curves form an orthogonal grid (see figure 2.9.2) and the identities

$$\boldsymbol{a}_1(\theta^1, \theta^2) = D_1\,F(\theta^1, \theta^2) = \boldsymbol{o}_1(\theta^1, \theta^2) = \boldsymbol{e}_1 \tag{2.9.22}$$

$$a_{\alpha\beta}(\theta^1, \theta^2) = \boldsymbol{a}_\alpha(\theta^1, \theta^2) \cdot \boldsymbol{a}_\beta(\theta^1, \theta^2) = \delta_{\alpha\beta} \tag{2.9.23}$$

$$a(\theta^1, \theta^2) = \det\left[a_{\alpha\beta}(\theta^1, \theta^2)\right] = 1\ , \tag{2.9.24}$$

where $\delta_{\alpha\beta}$ denotes the Kronecker delta, hold everywhere on the rectangle $\bar{\Omega} = [0, L] \times [a, b]$. Moreover, the maps $\bar{x}_2, \bar{x}_3 : \bar{\Omega} \to \mathbb{R}$ do not depend on the Gaussian coordinate θ^1 – indeed,

$$\bar{x}_2(\theta^1,\theta^2) = \hat{x}_2\left(F(\theta^1,\theta^2)\right) = \left[\left(C(\theta^2)+\theta^1\,\boldsymbol{e}_1\right)-O\right]\cdot\boldsymbol{e}_2 = \left(C(\theta^2)-O\right)\cdot\boldsymbol{e}_2 \qquad (2.9.25)$$

$$\bar{x}_3(\theta^1,\theta^2) = \hat{x}_3\left(F(\theta^1,\theta^2)\right) = \left[\left(C(\theta^2)+\theta^1\,\boldsymbol{e}_1\right)-O\right]\cdot\boldsymbol{e}_3 = \left(C(\theta^2)-O\right)\cdot\boldsymbol{e}_3\ . \qquad (2.9.26)$$

It follows at once that ω also does not depend on θ^1 and ψ is identically zero on $\bar{\Omega}$ (recall the definitions (2.3.16) and (2.3.26)). In view of (2.9.24), the reduced wall thickness t^*, defined by (2.5.4), coincides with the actual thickness t, which is also a function of θ^2 alone. Throughout the remainder of the analysis of the prismatic case, we will regard $\bar{x}_2$, $\bar{x}_3$, ω and t as maps defined on the interval $[a,b]$, a very convenient and harmless notational abuse.

From the above discussion, one concludes that the real-valued maps defined by (2.5.6)-(2.5.20) are constant maps. In particular, S^*_ψ, I^*_ψ, $I^*_{2\psi}$, $I^*_{3\psi}$ and $I^*_{\omega\psi}$ are identically zero. The constant values of the remaining ones are denoted by the same symbol as the map itself, but without the asterisk. They represent standard cross-sectional geometrical properties – area A, first moments of area S_2 and S_3, first sectorial moment S_ω, second moments of area I_2, I_3 and I_{23} and second sectorial moments I_ω, $I_{2\omega}$ and $I_{3\omega}$ –, under the usual simplifying assumption of considering the wall thickness as if "collapsed" on the cross-section middle line.[45] Similarly, the map $\theta^1 \mapsto J(\theta^1)$ is constant and, for the sake of convenience, the same symbol is used to denote the map and its constant value.

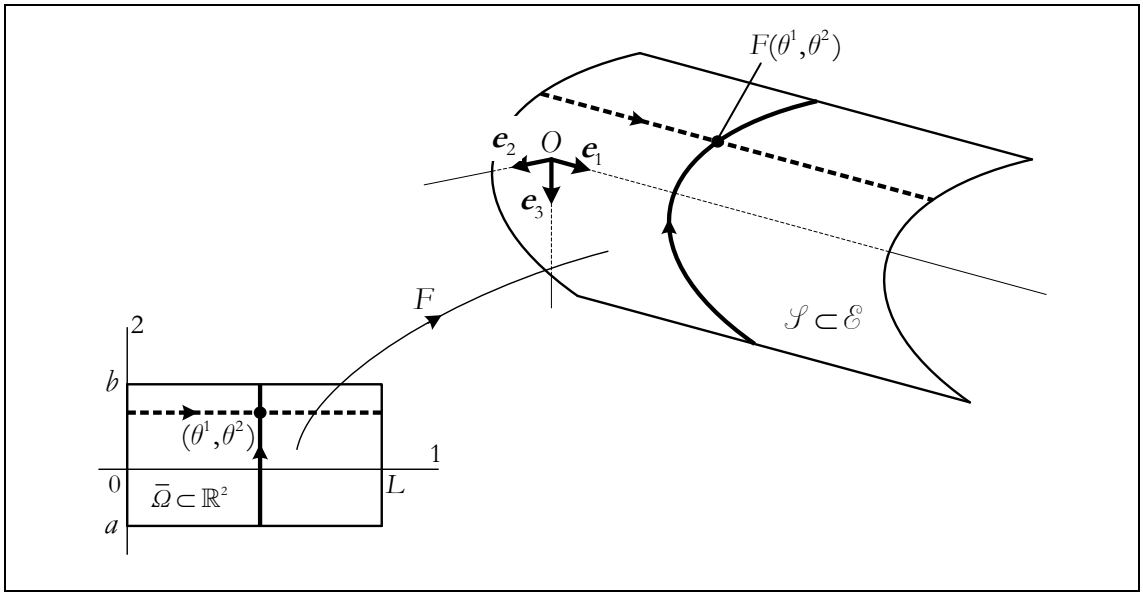

Figure 2.9.2: Prismatic bars – Parametrisation of the reference shape $\mathcal{S}$ of the middle surface

[45] GJELSVIK (1981, eqs. (1.64)) presents more accurate expressions for the second area and sectorial moments, which take proper account of the wall-thickness.

Suppose now that the Cartesian frame $\left(O,\{\boldsymbol{e}_1,\boldsymbol{e}_2,\boldsymbol{e}_3\}\right)$ is chosen so that

$$S_2 = S_3 = 0 \tag{2.9.27}$$

$$I_{23} = 0 \tag{2.9.28}$$

(*i.e.*, (i) the centroidal line of the bar $\mathcal{B}$ lies on the axis defined by the origin O and $\boldsymbol{e}_1$ and (ii) the axes defined by O and $\boldsymbol{e}_2$ and by O and $\boldsymbol{e}_3$ are principal central axes for the cross-section $\mathcal{A}_0$). The governing differential equations (2.6.5)-(2.6.8) on the interval $\left(0,L\right)$ then simplify to

$$\tilde{E}\mathcal{A}W_1''(\theta^1) - \tilde{E}S_\omega \Phi_1'''(\theta^1) + q_1(\theta^1) = 0 \tag{2.9.30}$$

$$-\tilde{E}I_3 W_2^{(4)}(\theta^1) - \tilde{E}I_{3\omega}\Phi_1^{(4)}(\theta^1) + q_2(\theta^1) - m_3'(\theta^1) = 0 \tag{2.9.31}$$

$$-\tilde{E}I_2 W_3^{(4)}(\theta^1) - \tilde{E}I_{2\omega}\Phi_1^{(4)}(\theta^1) + q_3(\theta^1) + m_2'(\theta^1) = 0 \tag{2.9.32}$$

$$\tilde{E}S_\omega W_1''(\theta^1) - \tilde{E}I_{3\omega}W_2^{(4)}(\theta^1) - \tilde{E}I_{2\omega}W_3^{(4)}(\theta^1) - \tilde{E}I_\omega \Phi_1^{(4)}(\theta^1) + GJ\Phi_1''(\theta^1) + b'(\theta^1) + m_1(\theta^1) = 0 \tag{2.9.33}$$

while the cross-sectional stress resultants (2.7.1)-(2.7.7) are given simply by

$$N(\theta^1) = \tilde{E}\mathcal{A}W_1'(\theta^1) - \tilde{E}S_\omega \Phi_1''(\theta^1) \tag{2.9.34}$$

$$V_2(\theta^1) = -\tilde{E}I_3 W_2'''(\theta^1) - \tilde{E}I_{3\omega}\Phi_1'''(\theta^1) - m_3(\theta^1) \tag{2.9.35}$$

$$V_3(\theta^1) = -\tilde{E}I_2 W_3'''(\theta^1) - \tilde{E}I_{2\omega}\Phi_1'''(\theta^1) + m_2(\theta^1) \tag{2.9.36}$$

$$M_2(\theta^1) = -\tilde{E}I_2 W_3''(\theta^1) - \tilde{E}I_{2\omega}\Phi_1''(\theta^1) \tag{2.9.37}$$

$$M_3(\theta^1) = -\tilde{E}I_3 W_2''(\theta^1) - \tilde{E}I_{3\omega}\Phi_1''(\theta^1) \tag{2.9.38}$$

$$M_1(\theta^1) = \tilde{E}S_\omega W_1''(\theta^1) - \tilde{E}I_{3\omega}W_2'''(\theta^1) - \tilde{E}I_{2\omega}W_3'''(\theta^1) - \tilde{E}I_\omega \Phi_1'''(\theta^1) + GJ\,\Phi_1'(\theta^1) + b(\theta^1) \tag{2.9.39}$$

$$B(\theta^1) = \tilde{E}S_\omega W_1'(\theta^1) - \tilde{E}I_{3\omega}W_2''(\theta^1) - \tilde{E}I_{2\omega}W_3''(\theta^1) - \tilde{E}I_\omega \Phi_1''(\theta^1)\ . \tag{2.9.40}$$

This is not, however, the "simplest form" in which the equations for prismatic bars can be written – the one in which they usually appear in the literature. To arrive at such "simplest form" – in essence, a process of orthogonalisation –, we keep the above choice of Cartesian frame and rewrite the admissible displacement field of the (cylindrical) middle surface as

$$U_1(\theta^1,\theta^2) = \hat{W}_1(\theta^1) - \overline{x}_2(\theta^2)W_{S.2}'(\theta^1) - \overline{x}_3(\theta^2)W_{S.3}'(\theta^1) - \omega_S(\theta^2)\Phi_1'(\theta^1) \tag{2.9.41}$$

$$U_2(\theta^1,\theta^2) = W_{S.2}(\theta^1) - \left(\overline{x}_3(\theta^2) - x_3^S\right)\Phi_1(\theta^1) \tag{2.9.42}$$

$$U_3(\theta^1,\theta^2) = W_{S.3}(\theta^1) + \left(\overline{x}_2(\theta^2) - x_2^S\right)\Phi_1(\theta^1)\ , \tag{2.9.43}$$

where the coordinates

$$x_2^S = \frac{I_{2\omega}}{I_2} \tag{2.9.44}$$

$$x_3^S = -\frac{I_{3\omega}}{I_3} \tag{2.9.45}$$

define the line of shear centres (TREFFTZ 1935, WEINSTEIN 1947, VLASOV 1961, ch 1, § 9)[46],

$$W_{S.2}(\theta^1) = W_2(\theta^1) - x_3^S \Phi_1(\theta^1) \tag{2.9.46}$$

$$W_{S.3}(\theta^1) = W_3(\theta^1) + x_2^S \Phi_1(\theta^1) \tag{2.9.47}$$

are the displacements, along $\boldsymbol{e}_2$ and $\boldsymbol{e}_3$, of the line of shear centres,

$$\begin{aligned}\omega_S(\theta^2) &= \int_0^{\theta^2} \left[\left(\overline{x}_2(s) - x_2^S \right) \overline{x}_3'(s) - \left(\overline{x}_3(s) - x_3^S \right) \overline{x}_2'(s) \right] ds \\ &= \omega(\theta^2) + x_3^S \left(\overline{x}_2(\theta^2) - \overline{x}_2(0) \right) - x_2^S \left(\overline{x}_3(\theta^2) - \overline{x}_3(0) \right)\end{aligned} \tag{2.9.48}$$

is the sectorial coordinate on $\mathscr{L}_{\theta^1}$ with pole at the shear centre and origin at $C(0) + \theta^1 \boldsymbol{e}_1$ (for arbitrary θ^1 in $[0, L]$),[47] and

$$\hat{W}_1(\theta^1) = W_1(\theta^1) - \left(x_3^S \overline{x}_2(0) - x_2^S \overline{x}_3(0) \right) \Phi_1'(\theta^1) \ . \tag{2.9.49}$$

The smoothness requirements on the new generalised displacement $\hat{W}_1 : [0, L] \to \mathbb{R}$ (resp. $W_{S.2}, W_{S.3} : [0, L] \to \mathbb{R}$) are the same as those previously placed on W_1 (resp. W_2, W_3).

The first and second sectorial moments evaluated with ω_S are given by

$$S_{\omega_S} = \int_a^b \omega_S(\theta^2)\, t(\theta^2)\, d\theta^2 = S_\omega - \left(x_3^S \overline{x}_2(0) - x_2^S \overline{x}_3(0) \right) A \tag{2.9.50}$$

$$I_{2\omega_S} = \int_a^b \omega_S(\theta^2)\, \overline{x}_3(\theta^2)\, t(\theta^2)\, d\theta^2 = I_{2\omega} - x_2^S I_2 = 0 \tag{2.9.51}$$

$$I_{3\omega_S} = \int_a^b \omega_S(\theta^2)\, \overline{x}_2(\theta^2)\, t(\theta^2)\, d\theta^2 = I_{3\omega} + x_3^S I_3 = 0 \tag{2.9.52}$$

$$\begin{aligned}I_{\omega_S} = \int_a^b \omega_S^2(\theta^2)\ t(\theta^2)\, d\theta^2 &= I_\omega - (x_2^S)^2 \left(I_2 - \overline{x}_3^2(0)\, A \right) - (x_3^S)^2 \left(I_3 - \overline{x}_2^2(0)\, A \right) \\ &\quad + 2 x_2^S \overline{x}_3(0) S_\omega - 2 x_3^S \overline{x}_2(0) S_\omega - 2 x_2^S x_3^S \overline{x}_2(0) \overline{x}_3(0) A \ .\end{aligned} \tag{2.9.53}$$

If the origin of the sectorial coordinate ω_S is chosen so that the condition

$$S_{\omega_S} = 0 \tag{2.9.54}$$

---

[46] See also REISSNER & TSAI (1972) and REISSNER (1979). For an elementary discussion of the concept(s) of shear centre, see FUNG (1993, app. 1).

[47] Hence ω_S and ω have different poles – the cross-section shear centre and the centroid, respectively –, but the same origin.

is fulfilled (that is, if the origin of ω_S is placed at a sectorial centroid[48]), then equation (2.9.53) reduces to

$$I_{\omega_S} = I_\omega - (x_2^S)^2 I_2 - (x_3^S)^2 I_3 - \frac{S_\omega^2}{A} \tag{2.9.55}$$

and one obtains from (2.9.30)-(2.9.33) the uncoupled differential equations

$$\tilde{E} A \hat{W}_1''(\theta^1) + q_1(\theta^1) = 0 \tag{2.9.56}$$

$$-\tilde{E} I_3 W_{S.2}^{(4)}(\theta^1) + q_2(\theta^1) - m_3'(\theta^1) = 0 \tag{2.9.57}$$

$$-\tilde{E} I_2 W_{S.3}^{(4)}(\theta^1) + q_3(\theta^1) + m_2'(\theta^1) = 0 \tag{2.9.58}$$

$$-\tilde{E} I_{\omega_S} \Phi_1^{(4)}(\theta^1) + GJ \Phi_1''(\theta^1) + b_S'(\theta^1) + m_{S.1}(\theta^1) = 0 \ . \tag{2.9.59}$$

In the last-written equation,

$$m_{S.1}(\theta^1) = m_1(\theta^1) + x_3^S q_2(\theta^1) - x_2^S q_3(\theta^1) \tag{2.9.60}$$

is the applied distributed torque about the line of shear centres and

$$b_S(\theta^1) = b(\theta^1) - \frac{S_\omega}{A} q_1(\theta^1) - x_2^S m_2(\theta^1) - x_3^S m_3(\theta^1) \tag{2.9.61}$$

is the distributed bimomental load evaluated with the sectorial coordinate ω_S. As for the cross-sectional stress resultants, the normal force (2.9.34), shear forces (2.9.35)-(2.9.36) and bending moments (2.9.37)-(2.9.38) are given in terms of the new generalised displacements simply by

$$N(\theta^1) = \tilde{E} A \hat{W}_1'(\theta^1) \tag{2.9.62}$$

$$V_2(\theta^1) = -\tilde{E} I_3 W_{S.2}'''(\theta^1) - m_3(\theta^1) \tag{2.9.63}$$

$$V_3(\theta^1) = -\tilde{E} I_2 W_{S.3}'''(\theta^1) + m_2(\theta^1) \tag{2.9.64}$$

$$M_2(\theta^1) = -\tilde{E} I_2 W_{S.3}''(\theta^1) \tag{2.9.65}$$

$$M_3(\theta^1) = -\tilde{E} I_3 W_{S.2}''(\theta^1) \ . \tag{2.9.66}$$

The bimoment, when evaluated with the sectorial coordinate ω_S, reduces to

$$B_S(\theta^1) = \int_a^b \omega_S(\theta^2) n_{1.1}(\theta^1, \theta^2) d\theta^2 = -\tilde{E} I_{\omega_S} \Phi_1''(\theta^1) \ . \tag{2.9.67}$$

It is related to the bimoment of equation (2.9.40), evaluated with the sectorial coordinate ω, through the relationship

---

[48] This is the terminology adopted by ODEN & RIPPERGER (1981, p. 217). VLASOV (1961, p. 45) uses instead the expression "sectorial zero-point".

$$B_{S}(\theta^1) = B(\theta^1) - \left(x_3^S \, \bar{x}_2(0) - x_2^S \, \bar{x}_3(0) \right) N(\theta^1) - x_2^S \, M_2(\theta^1) + x_3^S \, M_3(\theta^1) \ . \tag{2.9.68}$$

Finally, the torque about the line of shear centres is

$$M_{S.1}(\theta^1) = -\tilde{E} I_{\omega_S} \, \Phi_1'''(\theta^1) + GJ \, \Phi_1'(\theta^1) + b_S(\theta^1) \ , \tag{2.9.69}$$

which is obviously related to the torque about the line of centroids of equation (2.9.39) by (see figure 2.9.3)

$$M_{S.1}(\theta^1) = M_1(\theta^1) + x_3^S \, V_2(\theta^1) - x_2^S \, V_3(\theta^1) \ . \tag{2.9.70}$$

(Since the torque $M_{S.1}$ is referred to the line of shear centres, the shear forces V_2 and V_3 act through this line.)

The boundary conditions that complement the differential system (2.9.56)-(2.9.59) are indicated in table 2.9.1 (once again, select one, and only one, boundary condition from each row of the table).

Except for the definition of the elastic modulus $\tilde{E}$, the above prismatic bar equations are in agreement with those presented by GJELSVIK (1981, eqs. (1.68) and (1.89), tables 1.4-1.5) and VLASOV (1961, ch. 1, §§ 7-8).[49]

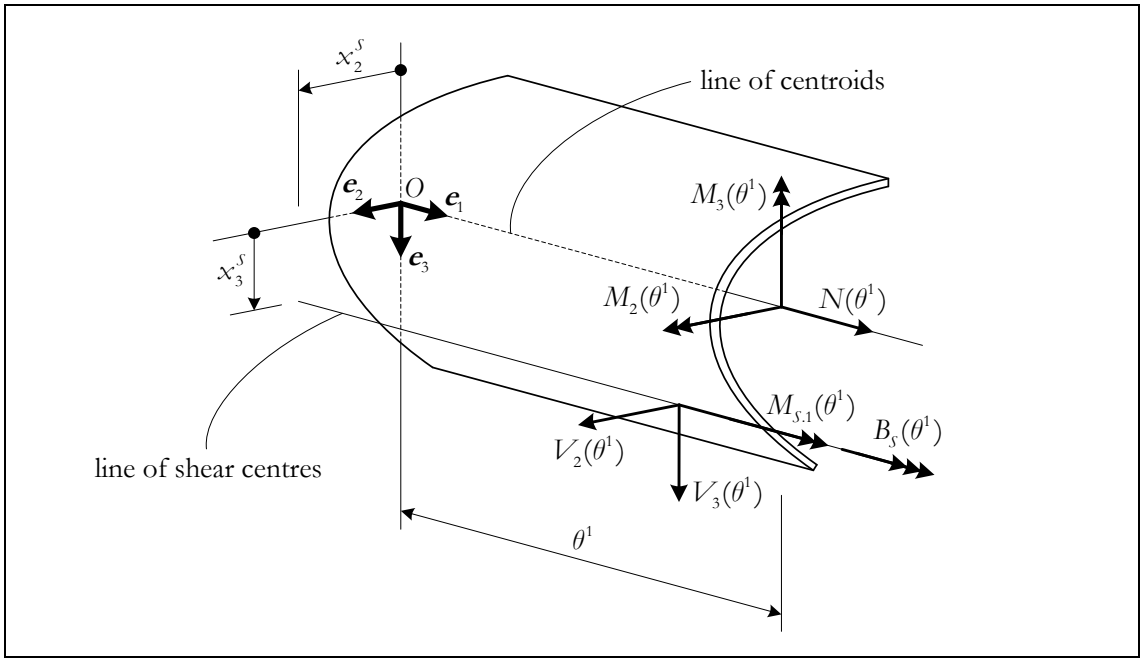

Figure 2.9.3: Prismatic bars – Cross-sectional stress resultants

[49] Concerning the latter reference, there is also the difference in the definitions of the second area and sectorial moments mentioned in note 45.

	Natural boundary conditions		Essential boundary conditions
Either	$\tilde{E}A\hat{W}_1'(0) = -Q_{0.1}$	or	$\hat{W}_1(0)$ prescribed
	$\tilde{E}A\hat{W}_1'(L) = Q_{L.1}$		$\hat{W}_1(L)$ prescribed
	$-\tilde{E}I_3 W_{S.2}'''(0) - m_3(0) = -Q_{0.2}$		$W_{S.2}(0)$ prescribed
	$-\tilde{E}I_3 W_{S.2}'''(L) - m_3(L) = Q_{L.2}$		$W_{S.2}(L)$ prescribed
	$-\tilde{E}I_3 W_{S.2}''(0) = M_{0.3}$		$W_{S.2}'(0)$ prescribed
	$-\tilde{E}I_3 W_{S.2}''(L) = -M_{L.3}$		$W_{S.2}'(L)$ prescribed
	$-\tilde{E}I_2 W_{S.3}'''(0) + m_2(0) = -Q_{0.3}$		$W_{S.3}(0)$ prescribed
	$-\tilde{E}I_2 W_{S.3}'''(L) + m_2(L) = Q_{L.3}$		$W_{S.3}(L)$ prescribed
	$-\tilde{E}I_2 W_{S.3}''(0) = -M_{0.2}$		$W_{S.3}'(0)$ prescribed
	$-\tilde{E}I_2 W_{S.3}''(L) = M_{L.2}$		$W_{S.3}'(L)$ prescribed
	$-\tilde{E}I_{\omega_S} \Phi_1'''(0) + GJ\,\Phi_1'(0) + b_S(0) = -M_{0.1} - x_3^S Q_{0.2} + x_2^S Q_{0.3}$		$\Phi_1(0)$ prescribed
	$-\tilde{E}I_{\omega_S} \Phi_1'''(L) + GJ\,\Phi_1'(L) + b_S(L) = M_{L.1} + x_3^S Q_{L.2} - x_2^S Q_{L.3}$		$\Phi_1(L)$ prescribed
	$-\tilde{E}I_{\omega_S} \Phi_1''(0) = -B_0 + \left(x_3^S \bar{x}_2(0) - x_2^S \bar{x}_3(0)\right) Q_{0.1} + x_2^S M_{0.2} + x_3^S M_{0.3}$		$\Phi_1'(0)$ prescribed
	$-\tilde{E}I_{\omega_S} \Phi_1''(L) = B_L - \left(x_3^S \bar{x}_2(0) - x_2^S \bar{x}_3(0)\right) Q_{L.1} - x_2^S M_{L.2} - x_3^S M_{L.3}$		$\Phi_1'(L)$ prescribed

Table 2.9.1: Prismatic bars – Natural and essential boundary conditions

* * *

One now turns to the discussion of the main differences between the full one-dimensional model for tapered thin-walled bars with open-sections and its prismatic special case. Clearly, the main qualitative difference resides in the map ψ, of a geometrical nature, which is identically zero for prismatic bars, but not necessarily so when dealing with a tapered bar. This map has a dual role. On the kinematics side, it provides an additional basic strain mode (recall (2.3.34)), whose amplitude is the rate of twist $\kappa_1 = \Phi_1'$ and without

which the strain field $\gamma_{\mathrm{I\cdot I}}$ cannot fully incorporate the taper effect whenever torsion is involved. On the statics side, it provides, by means of equation (2.7.21), the contribution of the membrane forces $n_{\mathrm{I\cdot I}}^{(A)}$ to the torque M_1 (this contribution obviously vanishes in prismatic bars, whose middle surface is cylindrical). It gives rise to a number of non-standard geometrical properties – equations (2.5.10), (2.5.14) and (2.5.18)-(2.5.20) – in the membrane strain energy and in the boundary value problem for the generalised displacements. In prismatic bars, these non-standard properties vanish.

A second difference between the full model and its prismatic special case, more of a quantitative character, lies in the field a, the determinant of the matrix (2.2.14) of metric coefficients of $\mathcal{S}$, which is everywhere equal to one for prismatic bars, but generally not so for tapered ones. The field a appears in the area form on $\mathcal{S}$, given by (2.2.20), and in the definition of the five basic strain modes (2.3.34). Ultimately, it leads to the use of a reduced wall thickness t^* in the definition of the geometrical properties (2.5.6)-(2.5.20). In prismatic bars, the reduced wall thickness t^* and the actual wall thickness t coincide.

Of course, it is perfectly possible to have a tapered bar with $\psi(\theta^1,\theta^2)=0$ and $a(\theta^1,\theta^2)=1$ everywhere on $\overline{\Omega}$, as when the middle surface of the tapered bar is cut out from a cylindrical surface.

Consider a tapered bar for which $\psi\neq 0$. In a stepped (*i.e.*, piecewise prismatic) model for such a bar, it would be a simple matter to use the reduced wall thickness t^* to compute the (standard) cross-sectional rigidities of the prismatic segments. Moreover, the torsional rigidity GJ could easily be replaced by $GJ+\tilde{E}I_{\psi}^{*}$. However, the effects associated with the remaining (non-standard) rigidities cannot be accommodated in the stepped model. It follows that the torsional behaviour of the tapered bar, whether uncoupled or coupled with other modes of deformation, cannot be adequately predicted by the stepped model, regardless of the number of segments considered and even if its properties are modified according to the above indications.[50]

[50] YAU (2008) has recently proposed the use of stepped models in the predictor phase of an iterative strategy for the torsional analysis of web-tapered I-beams. The corrector phase, however, requires the accurate computation of the cross-sectional stress results, taking the effects of taper in due account.

2.10 BARS WITH IRREGULAR MIDDLE SURFACE

In § 2.2, we considered bars whose middle surface reference shape $\mathcal{S}$ was given by a single, smooth enough parametrisation $F : \overline{\Omega} \to \mathcal{E}$. This too restrictive framework is now extended to what we shall call irregular middle surfaces, made up of several surface elements, each defined via a single, smooth enough parametrisation, joined along longitudinal edges.

Let us consider, as a prototypical example, the case depicted in figure 2.10.1, where the middle surface $\mathcal{S}$ is made up of two surface elements, $\mathcal{S}_1$ and $\mathcal{S}_2$, rigidly joined along the longitudinal edge $\mathcal{J}$:

$$\mathcal{S} = \mathcal{S}_1 \cup \mathcal{S}_2 \tag{2.10.1}$$

$$\mathcal{J} = \mathcal{S}_1 \cap \mathcal{S}_2 \tag{2.10.2}$$

$$\hat{x}_1[\mathcal{J}] = [0, L] \ . \tag{2.10.3}$$

The surface elements $\mathcal{S}_1$ and $\mathcal{S}_2$ are parametrised by the maps $F_1 : \overline{\Omega}_1 \to \mathcal{E}$ and $F_2 : \overline{\Omega}_2 \to \mathcal{E}$, each satisfying the conditions laid down in § 2.2.2. In particular, F_1 and F_2 are smooth injective immersions and their domains $\overline{\Omega}_1$ and $\overline{\Omega}_2$ are vertically simple regions of $\mathbb{R}^2$ of the form

$$\overline{\Omega}_n = \left\{ (\theta^1, \theta^2) \in \mathbb{R}^2 \,\middle|\, 0 \le \theta^1 \le L \text{ and } g_{1.n}(\theta^1) \le \theta^2 \le g_{2.n}(\theta^1) \right\} \ , \quad n = 1, 2 \ , \tag{2.10.4}$$

where $g_{1.n}$ and $g_{2.n}$ are real-valued continuous functions on $[0, L]$, with $g_{1.n}(\theta^1) < g_{2.n}(\theta^1)$ and $0 \in \left[g_{1.n}(\theta^1), g_{2.n}(\theta^1) \right]$ for every $\theta^1 \in [0, L]$. Without loss of generality, we assume that (see figure 2.10.1)

$$F_1(\theta^1, g_{2.1}(\theta^1)) = F_2(\theta^1, g_{1.2}(\theta^1)) \ , \quad \forall \theta^1 \in [0, L] \ . \tag{2.10.5}$$

That being the case, we make the additional requirement that $g_{2.1}$ and $g_{1.2}$ have the same minimum degree of smoothness as F_1 and F_2 – *i.e.*, we require that $g_{2.1}$ and $g_{1.2}$ be at least twice continuously differentiable on $[0, L]$.

Since $\overline{\Omega}_1$ and $\overline{\Omega}_2$ are vertically simple regions, their interiors can be "juxtaposed" as follows (see figure 2.10.2):

$$\underset{\sim}{\Omega}_1 = \Omega_1 \tag{2.10.6}$$

$$\underset{\sim}{\Omega}_2 = \left\{ (\theta^1, \theta^2) \in \mathbb{R}^2 \,\middle|\, 0 < \theta^1 < L \text{ and } g_{2.1}(\theta^1) \le \theta^2 \le g_{2.1}(\theta^1) + g_{2.2}(\theta^1) - g_{1.2}(\theta^1) \right\} \tag{2.10.7}$$

$$\underset{\sim}{\Omega} = \underset{\sim}{\Omega}_1 \cup \underset{\sim}{\Omega}_2 \ . \tag{2.10.8}$$

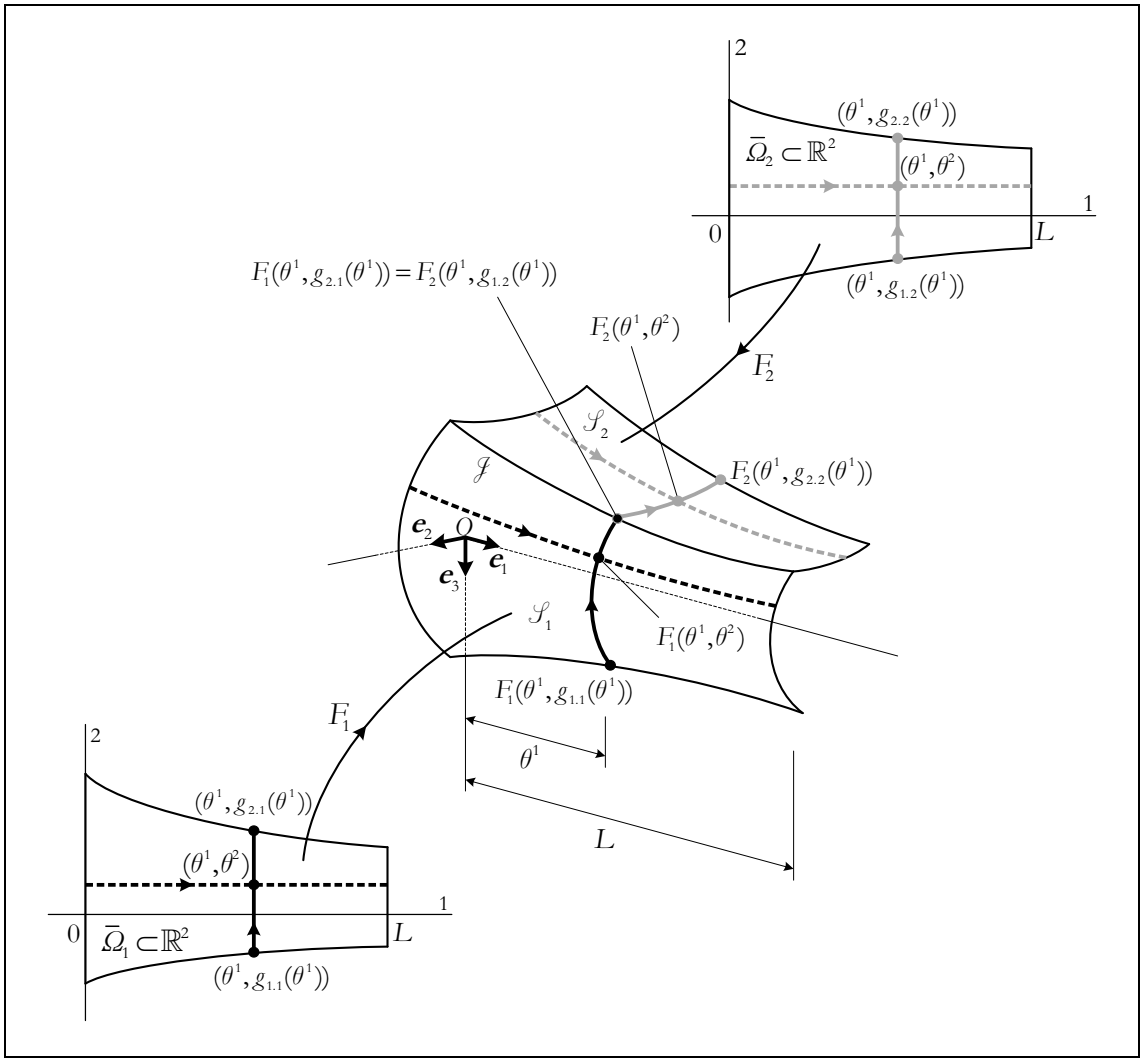

Figure 2.10.1: Irregular middle surface made up of two surface elements, $\mathscr{S}_1$ and $\mathscr{S}_2$, rigidly joined along the longitudinal edge $\mathscr{J}$

The restrictions of F_1 and F_2 to the interior of their domains can be similarly "juxtaposed" to form the single map $\underset{\sim}{F} : \underset{\sim}{\Omega} \to \mathscr{E}$ defined by

$$\underset{\sim}{F}(\theta^1, \theta^2) = \begin{cases} F_1(\theta^1, \theta^2) & \text{if } (\theta^1, \theta^2) \in \underset{\sim}{\Omega}_1 \\ F_2(\theta^1, \theta^2 - g_{2.1}(\theta^1) + g_{1.2}(\theta^1)) & \text{if } (\theta^1, \theta^2) \in \underset{\sim}{\Omega}_2 \end{cases} . \tag{2.10.9}$$

Clearly, the restrictions of $\underset{\sim}{F}$ to $\underset{\sim}{\Omega}_1$ and $\underset{\sim}{\Omega}_2$ are injective immersions with the same minimum degree of smoothness as F_1 and F_2. Moreover, for fixed $\theta^1 \in]0, L[$, the map $\theta^2 \mapsto \underset{\sim}{F}(\theta^1, \theta^2)$ is a piecewise arc-length parametrisation of the (reference shape of the) cross-section middle line $\mathscr{L}_{\theta^1}$ minus the end points $F_1(\theta^1, g_{1.1}(\theta^1))$ and $F_2(\theta^1, g_{2.2}(\theta^1))$ and the junction point $F_1(\theta^1, g_{2.1}(\theta^1)) = F_2(\theta^1, g_{1.2}(\theta^1))$.

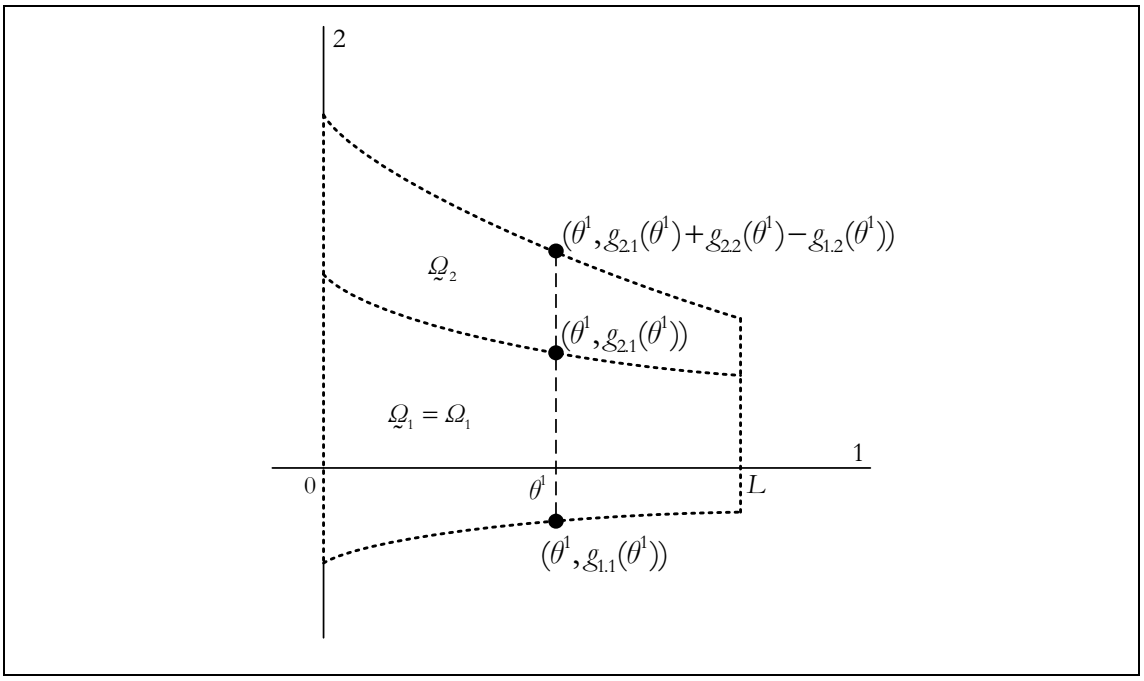

Figure 2.10.2: Bars with irregular middle surface – "Juxtaposition" of Ω_1 and Ω_2 to form the open set $\underset{\sim}{\Omega} = \underset{\sim}{\Omega}_1 \cup \underset{\sim}{\Omega}_2$

We can now define the underscored counterparts of the maps (2.2.2), (2.2.4), (2.2.8) and (2.2.18) in the obvious way:

$$\underset{\sim}{\overline{x}}_i = \hat{x}_i \circ \underset{\sim}{F} : \underset{\sim}{\Omega} \to \mathbb{R} \tag{2.10.10}$$

$$\underset{\sim}{\boldsymbol{a}}_\alpha = D_\alpha \underset{\sim}{F} : \underset{\sim}{\Omega} \to \mathcal{V} \tag{2.10.11}$$

$$\underset{\sim}{a}_{\alpha\beta} = \underset{\sim}{\boldsymbol{a}}_\alpha \cdot \underset{\sim}{\boldsymbol{a}}_\beta : \underset{\sim}{\Omega} \to \mathbb{R} \tag{2.10.12}$$

$$\underset{\sim}{a} = \det\left[\underset{\sim}{a}_{\alpha\beta}\right] : \underset{\sim}{\Omega} \to \mathbb{R}^+ \ . \tag{2.10.13}$$

Moreover, for each $(\theta^1, \theta^2) \in \underset{\sim}{\Omega}$, we define the orthonormal ordered basis $\left\{\underset{\sim}{\boldsymbol{o}}_{\mathrm{I}}(\theta^1, \theta^2), \underset{\sim}{\boldsymbol{o}}_{\mathrm{II}}(\theta^1, \theta^2)\right\}$ for $T_{\underset{\sim}{F}(\theta^1, \theta^2)}\mathcal{S}$ such that (i) it exhibits the same orientation as the covariant basis $\left\{\underset{\sim}{\boldsymbol{a}}_1(\theta^1, \theta^2), \underset{\sim}{\boldsymbol{a}}_2(\theta^1, \theta^2)\right\}$ associated with $\underset{\sim}{F}$ and (ii) $\underset{\sim}{\boldsymbol{o}}_{\mathrm{II}}(\theta^1, \theta^2) = \underset{\sim}{\boldsymbol{a}}_2(\theta^1, \theta^2)$.

The wall thickness is given by the continuous maps $t_n : \overline{\Omega}_n \to \mathbb{R}^+$, $n = 1, 2$, with small enough $t_{n.\max} = \max_{(\theta^1, \theta^2) \in \overline{\Omega}_n} \left\{t_n(\theta^1, \theta^2)\right\}$.[51] We introduce the map $\underset{\sim}{t} : \underset{\sim}{\Omega} \to \mathbb{R}^+$ defined by

$$\underset{\sim}{t}(\theta^1, \theta^2) = \begin{cases} t_1(\theta^1, \theta^2) & \text{if } (\theta^1, \theta^2) \in \underset{\sim}{\Omega}_1 \\ t_2(\theta^1, \theta^2 - g_{2.1}(\theta^1) + g_{1.2}(\theta^1)) & \text{if } (\theta^1, \theta^2) \in \underset{\sim}{\Omega}_2 \end{cases} \ . \tag{2.10.14}$$

[51] It is not required that $t_1(\theta^1, g_{2.1}(\theta^1)) = t_2(\theta^1, g_{1.2}(\theta^1))$, $0 \le \theta^1 \le L$.

With the obvious replacements of non-underscored symbols with their underscored counterparts,[52] the kinematic and constitutive developments in §§ 2.3-2.4 remain entirely valid. Only the adaptation of the definition (2.3.16) requires some elaboration – it is generalised as follows:

$$\underset{\sim}{\omega}(\theta^1, \theta^2) = \int_0^{\theta^2} \left(\overline{\underset{\sim}{x}}_2(\theta^1, s)\, D_2 \overline{\underset{\sim}{x}}_3(\theta^1, s) - \overline{\underset{\sim}{x}}_3(\theta^1, s)\, D_2 \overline{\underset{\sim}{x}}_2(\theta^1, s) \right) ds \tag{2.10.15}$$

if $(\theta^1, \theta^2) \in \underset{\sim}{\Omega}_{(1)}$ and

$$\begin{aligned} \underset{\sim}{\omega}(\theta^1, \theta^2) = & \int_0^{g_{2.1}(\theta^1)} \left(\overline{\underset{\sim}{x}}_2(\theta^1, s)\, D_2 \overline{\underset{\sim}{x}}_3(\theta^1, s) - \overline{\underset{\sim}{x}}_3(\theta^1, s)\, D_2 \overline{\underset{\sim}{x}}_2(\theta^1, s) \right) ds \\ & + \int_{g_{2.1}(\theta^1)}^{\theta^2} \left(\overline{\underset{\sim}{x}}_2(\theta^1, s)\, D_2 \overline{\underset{\sim}{x}}_3(\theta^1, s) - \overline{\underset{\sim}{x}}_3(\theta^1, s)\, D_2 \overline{\underset{\sim}{x}}_2(\theta^1, s) \right) ds \quad . \end{aligned} \tag{2.10.16}$$

if $(\theta^1, \theta^2) \in \underset{\sim}{\Omega}_2$. Observe that the integrand is continuous and bounded on $\underset{\sim}{\Omega}$, since its restriction to $\underset{\sim}{\Omega}_1$ (resp. $\underset{\sim}{\Omega}_2$) admits a continuous extension to $\overline{\underset{\sim}{\Omega}}_1$ (resp. $\overline{\underset{\sim}{\Omega}}_2$) – *e.g.*, DIEUDONNÉ (1960, th. 3.17.10). Therefore, the above definition is a meaningful one (see LIMA 1989, ch. 6, § 3).[53]

The membrane strain energy can now be obtained as in (2.5.1), replacing the integral over $\overline{\Omega}$ with an integral over $\underset{\sim}{\Omega}$ (hence, by the sum of two integrals, over $\underset{\sim}{\Omega}_1$ and over $\underset{\sim}{\Omega}_2$). Once again, we remark that the integrand is continuous and bounded on $\underset{\sim}{\Omega}$. Then, *mutatis mutandis*, the remainder of the discussion in §§ 2.5-2.9 retains its validity.[54]

The above ideas can be readily extended to more general situations. In particular, we may consider more junctions, as in the case of tapered I-section bars to which we now turn. For the sake of notational simplicity, the underscored notation is dropped, since it will always be clear from the context when we are dealing with irregular middle surfaces.

---

[52] It is understood that the underscored counterpart of the closed set $\overline{\Omega}$ is the open set $\underset{\sim}{\Omega} = \underset{\sim}{\Omega}_1 \cup \underset{\sim}{\Omega}_2$. Observe that the boundary of a bounded and Jordan measurable subset of $\mathbb{R}^2$, such as $\overline{\Omega}$ or $\underset{\sim}{\Omega}$, is negligible (DUISTERMAAT & KOLK 2004, th 6.3.2).

[53] A more general version of Leibniz rule than the one used in note 24 is now required to obtain a formula for $D_1\omega$ – see, *e.g.*, BARTLE (1967, th. 23.11).

[54] For instance, in the geometrical properties (2.5.6)-(2.5.20), the integrals over $\left[g_1(\theta^1), g_2(\theta^1) \right]$ are replaced with the sum of two integrals, over $\left(g_{1.1}(\theta^1), g_{2.1}(\theta^1) \right)$ and over $\left(g_{2.1}(\theta^1), g_{2.1}(\theta^1) + g_{2.2}(\theta^1) - g_{1.2}(\theta^1) \right)$.

2.10.1 An important special case: I-section bars with linearly varying web depth and/or flange width

> Research in engineering science cannot be considered
> to be completed until […] the results have been presented
> in a form accessible to other engineers.
>
> WARNER T. KOITER

Tapered I-section bars with linearly varying web depth and/or flange width can be fabricated by (i) reassembling split rolled profiles or (ii) welding flat plates cut to trapezoidal form (KREFELD *et al.* 1959). If the web of a rolled I-section profile having the desired span length is cut diagonally and the separated parts are reversed, the depth will be increased at one end and decreased at the other. Split rolled bars provide constant flange width and tapered web depth. The fabrication consists of a web weld at mid-depth of the tapered bar. The built-up bars assembled from plates cut to provide the desired taper of the web and/or flanges require flange-to-web welds.

Figure 2.10.3 shows (i) the reference shape of the most general I-section bar that we shall consider and (ii) the adopted Cartesian reference frame, with the plane containing the origin O and spanned by $\{\boldsymbol{e}_1, \boldsymbol{e}_3\}$ being a plane of symmetry for the reference shape. The width of the flanges and the depth of the web (measured between flange middle lines) are described by the affine maps (from $[0, L]$ into $\mathbb{R}^+$)

$$b_t(x_1) = \left[1 - \left(1 - \frac{b_{t.L}}{b_{t.0}}\right)\frac{x_1}{L}\right] b_{t.0} = \left[1 - (1 - \alpha_t)\frac{x_1}{L}\right] b_{t.0} \ , \quad \alpha_t = \frac{b_{t.L}}{b_{t.0}} \tag{2.10.17}$$

$$b_b(x_1) = \left[1 - \left(1 - \frac{b_{b.L}}{b_{b.0}}\right)\frac{x_1}{L}\right] b_{b.0} = \left[1 - (1 - \alpha_b)\frac{x_1}{L}\right] b_{b.0} \ , \quad \alpha_b = \frac{b_{b.L}}{b_{b.0}} \tag{2.10.18}$$

$$h(x_1) = \left[1 - \left(1 - \frac{h_L}{h_0}\right)\frac{x_1}{L}\right] h_0 = \left[1 - (1 - \alpha_w)\frac{x_1}{L}\right] h_0 \ , \quad \alpha_w = \frac{h_L}{h_0} \tag{2.10.19}$$

(the subscripts 0 and L indicate dimensions at $x_1 = 0$ and $x_1 = L$, respectively). These plated components exhibit constant thicknesses t_t, t_b and t_w. The x_3-coordinate of the top flange middle plane is given by

$$x_{3t}(x_1) = x_{3t.0} + \frac{x_{3t.L} - x_{3t.0}}{L} x_1 \ . \tag{2.10.20}$$

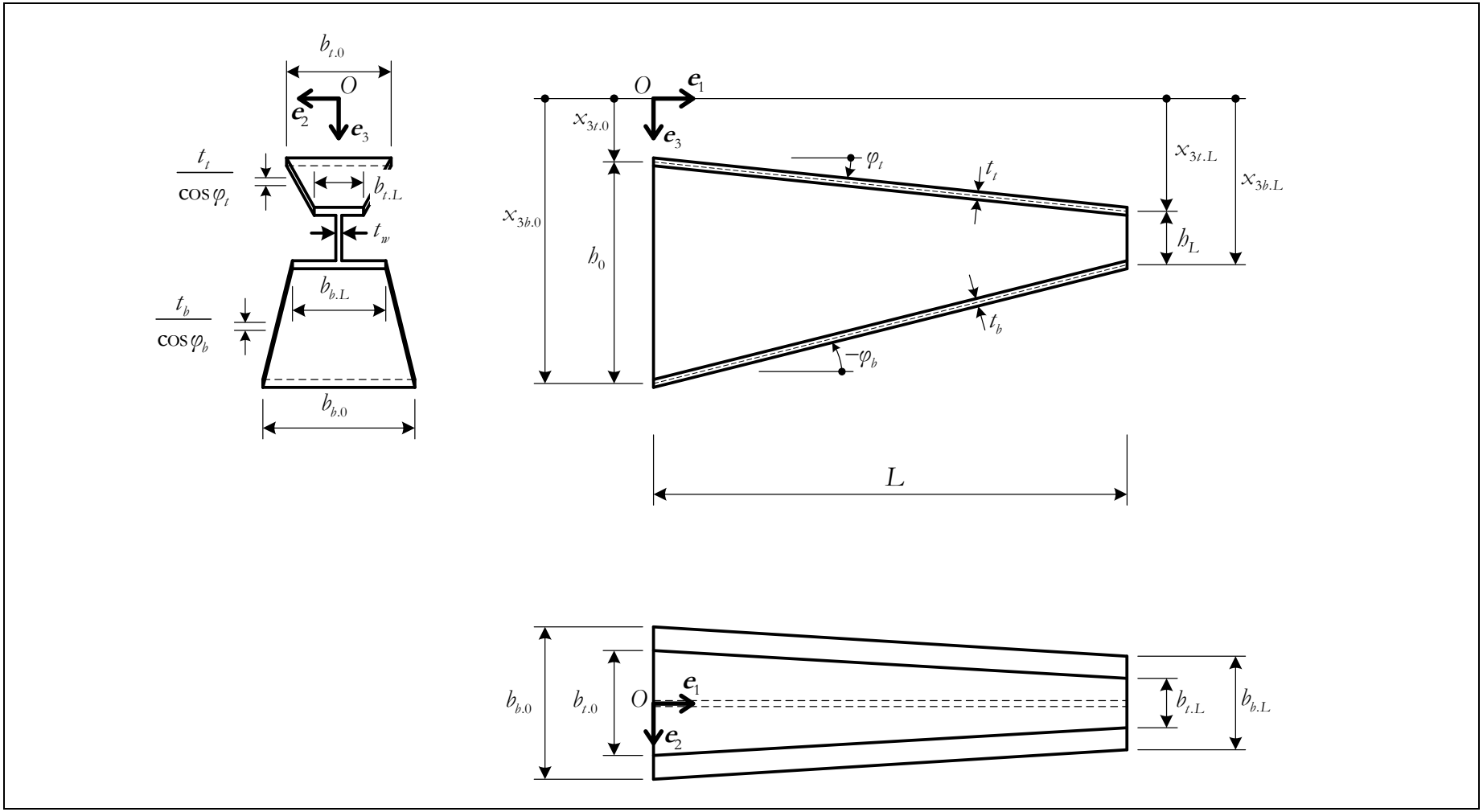

Fig. 2.10.3: Tapered I-section bar – Reference shape

Accordingly, the x_3-coordinate of the bottom flange middle plane reads

$$x_{3b}(x_1) = x_{3t}(x_1) + h(x_1) = (x_{3t.0} + h_0) + \frac{(x_{3t.L} + h_L) - (x_{3t.0} + h_0)}{L} x_1 \ . \tag{2.10.21}$$

The inclinations of the top and bottom flanges with respect to the planes spanned by $\{\boldsymbol{e}_1, \boldsymbol{e}_2\}$ are

$$\varphi_t = \arctan \frac{x_{3t.L} - x_{3t.0}}{L} \tag{2.10.22}$$

$$\varphi_b = \arctan \frac{x_{3b.L} - x_{3b.0}}{L} \ ; \tag{2.10.23}$$

observe that $-\pi/2 \ll \varphi_t, \varphi_b \ll \pi/2$.

The scheme adopted for the parametrisation of (the reference shape of) the middle surface is summarised in figure 2.10.4 and in table 2.10.1. The latter also provides all the geometrical features that are required to compute the properties (2.5.6)-(2.5.20). One obtains:

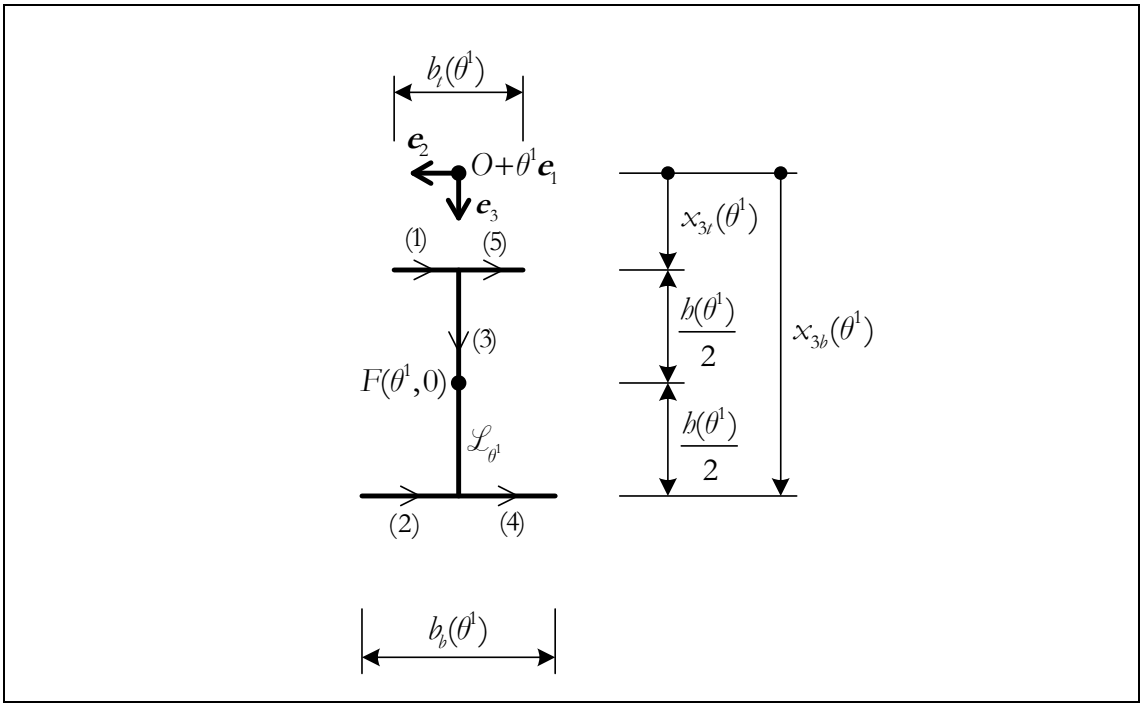

Fig. 2.10.4: Tapered I-section bar – Parametrisation of the middle surface

	range of θ^2	$\bar{x}_2(\theta^1,\theta^2)$	$\bar{x}_3(\theta^1,\theta^2)$	$a(\theta^1,\theta^2)$	$t^*(\theta^1,\theta^2)$
Ω_1	$-\frac{h(\theta^1)}{2}-\frac{b_t(\theta^1)}{2}-\frac{b_b(\theta^1)}{2}<\theta^2<-\frac{h(\theta^1)}{2}-\frac{b_b(\theta^1)}{2}$	$-\left(\theta^2+\frac{h(\theta^1)}{2}+\frac{b_b(\theta^1)}{2}\right)$	$x_{3t}(\theta^1)$	$1+\tan^2\varphi_t$	$t_t\cos^3\varphi_t$
Ω_2	$-\frac{h(\theta^1)}{2}-\frac{b_b(\theta^1)}{2}<\theta^2<-\frac{h(\theta^1)}{2}$	$-\left(\theta^2+\frac{h(\theta^1)}{2}\right)$	$x_{3b}(\theta^1)$	$1+\tan^2\varphi_b$	$t_b\cos^3\varphi_b$
Ω_3	$-\frac{h(\theta^1)}{2}<\theta^2<\frac{h(\theta^1)}{2}$	0	$\theta^2+x_{3t}(\theta^1)+\frac{h(\theta^1)}{2}$	1	t_w
Ω_4	$\frac{h(\theta^1)}{2}<\theta^2<\frac{h(\theta^1)}{2}+\frac{b_b(\theta^1)}{2}$	$-\left(\theta^2-\frac{h(\theta^1)}{2}\right)$	$x_{3b}(\theta^1)$	$1+\tan^2\varphi_b$	$t_b\cos^3\varphi_b$
Ω_5	$\frac{h(\theta^1)}{2}+\frac{b_b(\theta^1)}{2}<\theta^2<\frac{h(\theta^1)}{2}+\frac{b_t(\theta^1)}{2}+\frac{b_b(\theta^1)}{2}$	$-\left(\theta^2-\frac{h(\theta^1)}{2}-\frac{b_b(\theta^1)}{2}\right)$	$x_{3t}(\theta^1)$	$1+\tan^2\varphi_t$	$t_t\cos^3\varphi_t$

Table 2.10.1: Tapered I-section bar – Geometrical features

	range of θ^2	$\omega(\theta^1,\theta^2)$	$\psi(\theta^1,\theta^2)$
Ω_1	$-\frac{h(\theta^1)}{2}-\frac{b_t(\theta^1)}{2}-\frac{b_b(\theta^1)}{2}<\theta^2<-\frac{h(\theta^1)}{2}-\frac{b_b(\theta^1)}{2}$	$x_{3t}(\theta^1)\left(\theta^2+\frac{h(\theta^1)}{2}+\frac{b_b(\theta^1)}{2}\right)$	$2\tan\varphi_t\left(\theta^2+\frac{h(\theta^1)}{2}+\frac{b_b(\theta^1)}{2}\right)$
Ω_2	$-\frac{h(\theta^1)}{2}-\frac{b_b(\theta^1)}{2}<\theta^2<-\frac{h(\theta^1)}{2}$	$x_{3b}(\theta^1)\left(\theta^2+\frac{h(\theta^1)}{2}\right)$	$2\tan\varphi_b\left(\theta^2+\frac{h(\theta^1)}{2}\right)$
Ω_3	$-\frac{h(\theta^1)}{2}<\theta^2<\frac{h(\theta^1)}{2}$	0	0
Ω_4	$\frac{h(\theta^1)}{2}<\theta^2<\frac{h(\theta^1)}{2}+\frac{b_b(\theta^1)}{2}$	$x_{3b}(\theta^1)\left(\theta^2-\frac{h(\theta^1)}{2}\right)$	$2\tan\varphi_b\left(\theta^2-\frac{h(\theta^1)}{2}\right)$
Ω_5	$\frac{h(\theta^1)}{2}+\frac{b_b(\theta^1)}{2}<\theta^2<\frac{h(\theta^1)}{2}+\frac{b_t(\theta^1)}{2}+\frac{b_b(\theta^1)}{2}$	$x_{3t}(\theta^1)\left(\theta^2-\frac{h(\theta^1)}{2}-\frac{b_b(\theta^1)}{2}\right)$	$2\tan\varphi_t\left(\theta^2-\frac{h(\theta^1)}{2}-\frac{b_b(\theta^1)}{2}\right)$

Table 2.10.1 (continued): Tapered I-section bar – Geometrical features

$$A^*(\theta^1) = h(\theta^1)t_w + b_t(\theta^1)t_t\cos^3\varphi_t + b_b(\theta^1)t_b\cos^3\varphi_b \tag{2.10.24}$$

$$S_2^*(\theta^1) = \left(\frac{h(\theta^1)}{2} + x_{3t}(\theta^1)\right)h(\theta^1)t_w + x_{3t}(\theta^1)b_t(\theta^1)t_t\cos^3\varphi_t + x_{3b}(\theta^1)b_b(\theta^1)t_b\cos^3\varphi_b \tag{2.10.25}$$

$$I_2^*(\theta^1) = \frac{h(\theta^1)^3 t_w}{12} + \left(\frac{h(\theta^1)}{2} + x_{3t}(\theta^1)\right)^2 h(\theta^1)t_w + x_{3t}(\theta^1)^2 b_t(\theta^1)t_t\cos^3\varphi_t + x_{3b}(\theta^1)^2 b_b(\theta^1)t_b\cos^3\varphi_b \tag{2.10.26}$$

$$I_3^*(\theta^1) = \frac{1}{12}b_t(\theta^1)^3 t_t\cos^3\varphi_t + \frac{1}{12}b_b(\theta^1)^3 t_b\cos^3\varphi_b \tag{2.10.27}$$

$$I_\omega^*(\theta^1) = \frac{1}{12}x_{3t}(\theta^1)^2 b_t(\theta^1)^3 t_t\cos^3\varphi_t + \frac{1}{12}x_{3b}(\theta^1)^2 b_b(\theta^1)^3 t_b\cos^3\varphi_b \tag{2.10.28}$$

$$I_\psi^*(\theta^1) = \frac{1}{3}b_t(\theta^1)^3\tan^2\varphi_t\, t_t\cos^3\varphi_t + \frac{1}{3}b_b(\theta^1)^3\tan^2\varphi_b\, t_b\cos^3\varphi_b \tag{2.10.29}$$

$$I_{3\omega}^*(\theta^1) = -\frac{1}{12}x_{3t}(\theta^1)b_t(\theta^1)^3 t_t\cos^3\varphi_t - \frac{1}{12}x_{3b}(\theta^1)b_b(\theta^1)^3 t_b\cos^3\varphi_b \tag{2.10.30}$$

$$I_{3\psi}^*(\theta^1) = -\frac{1}{6}b_t(\theta^1)^3\tan\varphi_t\, t_t\cos^3\varphi_t - \frac{1}{6}b_b(\theta^1)^3\tan\varphi_b\, t_b\cos^3\varphi_b \tag{2.10.31}$$

$$I_{\omega\psi}^*(\theta^1) = \frac{1}{6}x_{3t}(\theta^1)b_t(\theta^1)^3\tan\varphi_t\, t_t\cos^3\varphi_t + \frac{1}{6}x_{3b}(\theta^1)b_b(\theta^1)^3\tan\varphi_b\, t_b\cos^3\varphi_b\ . \tag{2.10.32}$$

Due to symmetry, S_3^*, S_ω^*, S_ψ^*, I_{23}^*, $I_{2\omega}^*$ and $I_{2\psi}^*$ are identically zero (*vide supra*, § 2.9.1). Moreover,

$$J(\theta^1) = \frac{1}{3}\left[h(\theta^1)t_w^3 + b_t(\theta^1)\left(\frac{t_t}{\cos\varphi_t}\right)^3 + b_b(\theta^1)\left(\frac{t_b}{\cos\varphi_b}\right)^3\right]. \tag{2.10.33}$$

This formula for J is approximate and presupposes that each plated component (web and flanges) exhibits a sufficiently large width-to-thickness ratio throughout the whole length of the bar (*e.g.*, TIMOSHENKO & GOODIER 1970, §§ 108-109).

Finally, figure 2.10.5 gives schematic representations of the maps ω and ψ.

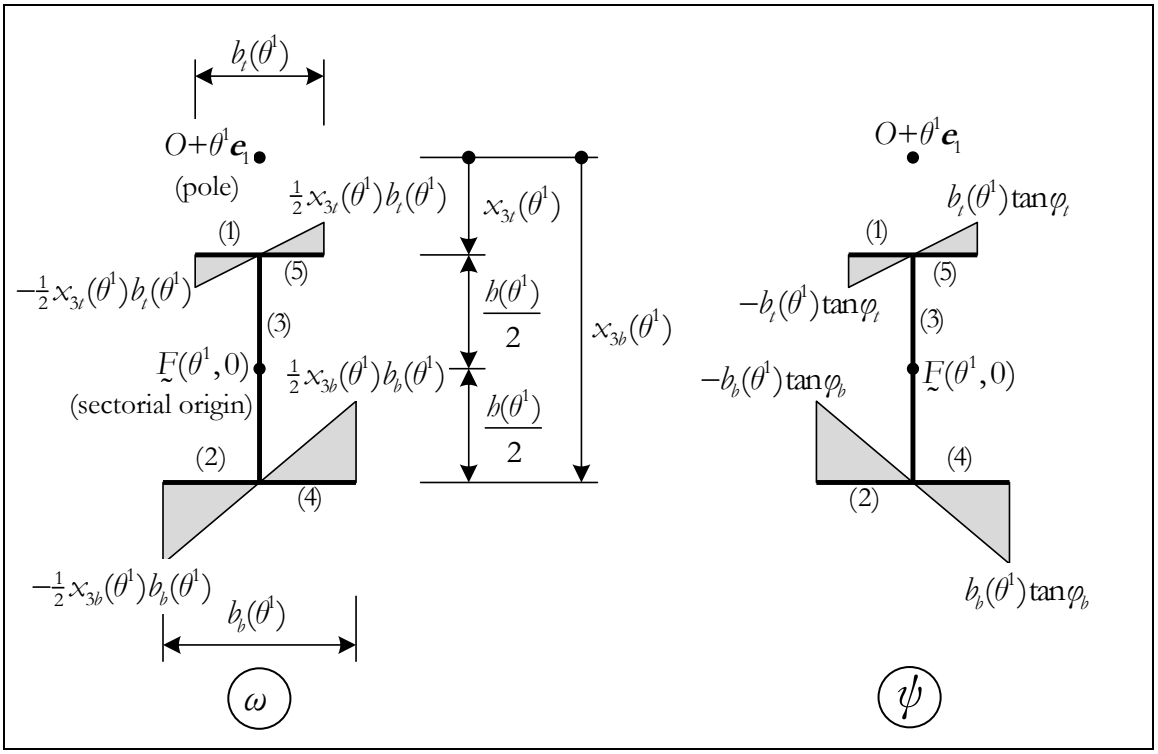

Fig. 2.10.5: Tapered I-section bar – Schematic representations of the maps ω and ψ

2.11 ILLUSTRATIVE EXAMPLES

Man muss immer mit den einfachsten Beispielen anfangen.

DAVID HILBERT

Illustrative example 1

As a first illustration of the one-dimensional model developed in this chapter, consider the family of doubly symmetric web-tapered I-section cantilevers whose reference shape is shown in figure 2.11.1. The adopted Cartesian reference frame is also shown in this figure and is such that the planes containing the origin O and spanned by $\{\boldsymbol{e}_1,\boldsymbol{e}_2\}$ and by $\{\boldsymbol{e}_1,\boldsymbol{e}_3\}$ are the longitudinal planes of symmetry of the reference shape. The flanges are uniform, with thickness t_f and width b_f. The web has constant thickness t_w and its depth h, measured between flange middle lines, varies according to the affine law

$$h(x_1)=\left(1-(1-\alpha)\frac{x_1}{L}\right)h_0\ , \tag{2.11.1}$$

with $0<\alpha\leq 1$. The parameter α will be called the web taper ratio (or simply the taper ratio). Observe that $\alpha=1$ corresponds to a prismatic beam. The flanges exhibit symmetrical slopes $\pm\tan\varphi$ with respect to the planes spanned by $\{\boldsymbol{e}_1,\boldsymbol{e}_2\}$, where $\tan\varphi=(1-\alpha)\,h_0/(2L)$. The cantilever is clamped at its larger end ($\mathscr{A}_0$) and free at the smaller end ($\mathscr{A}_L$), where a concentrated torque M_{L1} is applied.

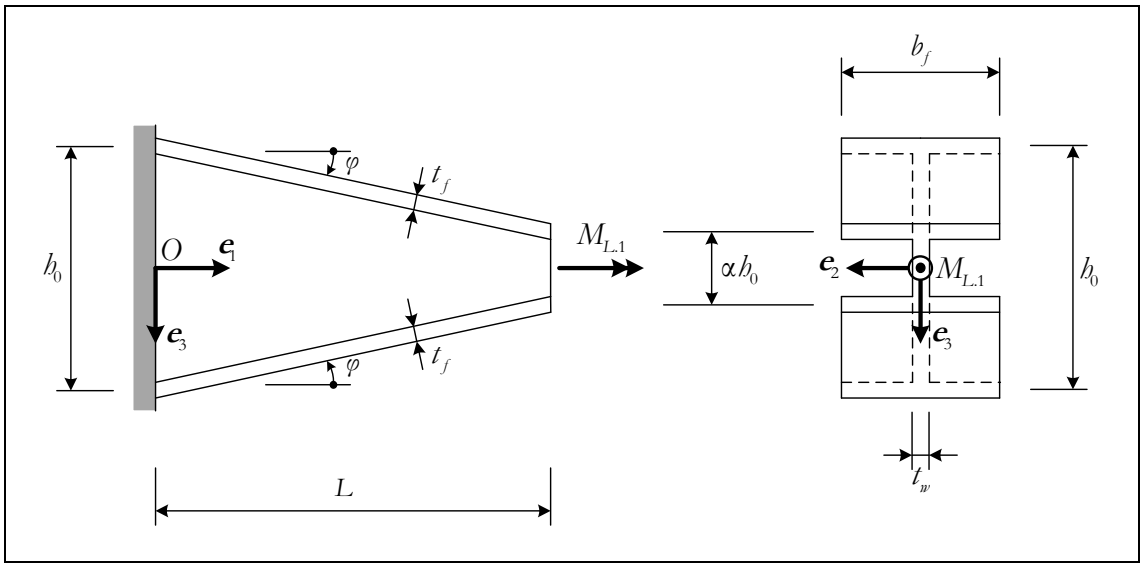

Figure 2.11.1: Illustrative example 1 – Reference shape, support conditions and applied torque

From the analysis in § 2.9.1, applied to each of the two longitudinal symmetry planes, or by appropriate specialisation of the results given in § 2.10.1, one readily concludes that the boundary value problem for the generalised displacements of § 2.6 is entirely uncoupled. In view of the applied loading, it follows at once that W_1, W_2 and W_3 are all identically zero and we are just left with the following problem:

Illustrative example 1.

Find $\Phi_1 : [0, L] \to \mathbb{R}$, with $\Phi_1 \in C^4[0, L]$, satisfying the ordinary differential equation

$$-\left(\tilde{E}I^*_\omega \Phi_1'' + \tilde{E}I^*_{\omega\psi} \Phi_1'\right)''(\theta^1) + \left[\tilde{E}I^*_{\omega\psi} \Phi_1'' + \left(GJ + \tilde{E}I^*_\psi\right)\Phi_1'\right]'(\theta^1) = 0 \qquad (2.11.2)$$

on the open interval $(0, L)$, together with the boundary conditions

$$\Phi_1(0) = 0 \qquad (2.11.3)$$

$$\Phi_1'(0) = 0 \qquad (2.11.4)$$

$$-\left(\tilde{E}I^*_\omega \Phi_1'' + \tilde{E}I^*_{\omega\psi} \Phi_1'\right)'(L) + \tilde{E}I^*_{\omega\psi}(L)\Phi_1''(L) + \left(GJ(L) + \tilde{E}I^*_\psi(L)\right)\Phi_1'(L) = M_{L.1} \qquad (2.11.5)$$

$$\tilde{E}I^*_\omega(L)\Phi_1''(L) + \tilde{E}I^*_{\omega\psi}(L)\Phi_1'(L) = 0\ . \qquad (2.11.6)$$

In these equations,

$$I_{\omega}^{*}(\theta^1)=\frac{1}{24}\,h(\theta^1)^2\,b_f^3\,t_f\cos^3\varphi=\frac{1}{24}\left(1-(1-\alpha)\frac{\theta^1}{L}\right)^2 h_0^2\,b_f^3\,t_f\cos^3\varphi$$

$$=\left(1-(1-\alpha)\frac{\theta^1}{L}\right)^2 I_{\omega}^{*}(0) \tag{2.11.7}$$

$$I_{\omega\psi}^{*}(\theta^1)=-\frac{1}{6}h(\theta^1)\,b_f^3\tan\varphi\,t_f\cos^3\varphi=-\frac{1-\alpha}{12\,L}\left(1-(1-\alpha)\frac{\theta^1}{L}\right)h_0^2\,b_f^3\,t_f\cos^3\varphi$$

$$=-\frac{2}{L}(1-\alpha)\left(1-(1-\alpha)\frac{\theta^1}{L}\right)I_{\omega}^{*}(0) \tag{2.11.8}$$

$$I_{\psi}^{*}(\theta^1)=\frac{2}{3}b_f^3\tan^2\varphi\,t_f\cos^3\varphi=\frac{1}{6}\left(\frac{1-\alpha}{L}\right)^2 h_0^2\,b_f^3\,t_f\cos^3\varphi=\frac{4}{L^2}(1-\alpha)^2\,I_{\omega}^{*}(0) \tag{2.11.9}$$

$$J(\theta^1)=\frac{2\,b_f}{3}\left(\frac{t_f}{\cos\varphi}\right)^3+\frac{h(\theta^1)\,t_w^3}{3}=\left(1-\frac{h_0\,t_w^3}{3\,J(0)}(1-\alpha)\frac{\theta^1}{L}\right)J(0)\ .^{55} \tag{2.11.10}$$

Observe that the differential equation (2.11.2) has polynomial coefficients (which become constant coefficients when $\alpha=1$). The coefficient $\tilde{E}I_{\omega}^{*}$ of the leading term does not vanish on $(0,L)$. Moreover, it should be noticed that

$$I_{\omega\psi}^{*}(\theta^1)=I_{\omega}^{*\prime}(\theta^1) \tag{2.11.11}$$

$$I_{\psi}^{*}(\theta^1)=2\,I_{\omega}^{*\prime\prime}(\theta^1)=2\,I_{\omega\psi}^{*\prime}(\theta^1) \tag{2.11.12}$$

(it goes without saying that the validity of these identities is restricted to the particular bar geometry considered in this illustrative example).

In an effort to gain further understanding of the nature of the tapered one-dimensional model, we contrast in figures 2.11.2-2.11.7 the warping-torsion behaviours of prismatic ($\alpha=1$) and linearly depth-tapered ($0<\alpha<1$) doubly symmetric I-section bars (ANDRADE *et al.* 2010). The following facts are worthy of notice:

(i) In both cases, the internal constraints (V1)-(V2), together with symmetry considerations, imply qualitatively similar displacement fields for the cross-section middle line at a distance θ^1 from the origin (figure 2.11.2): (i_1) the middle line rotates about the centroidal axis through an angle $\Phi_1(\theta^1)$ and (i_2) the flanges warp out of the plane by rotating $\pm\frac{h(\theta^1)}{2}\Phi_1'(\theta^1)$ about their major axes. However, one must not forget that in the web-tapered case the displacements along $\boldsymbol{e}_3$ are obviously *not* orthogonal to the middle planes of the flanges.

[55] The order of the differential equation (2.11.2) and the number of accompanying boundary conditions could have been lowered from 4 to 3. We chose not to do so to keep a more direct link with the general boundary value problem of § 2.6.

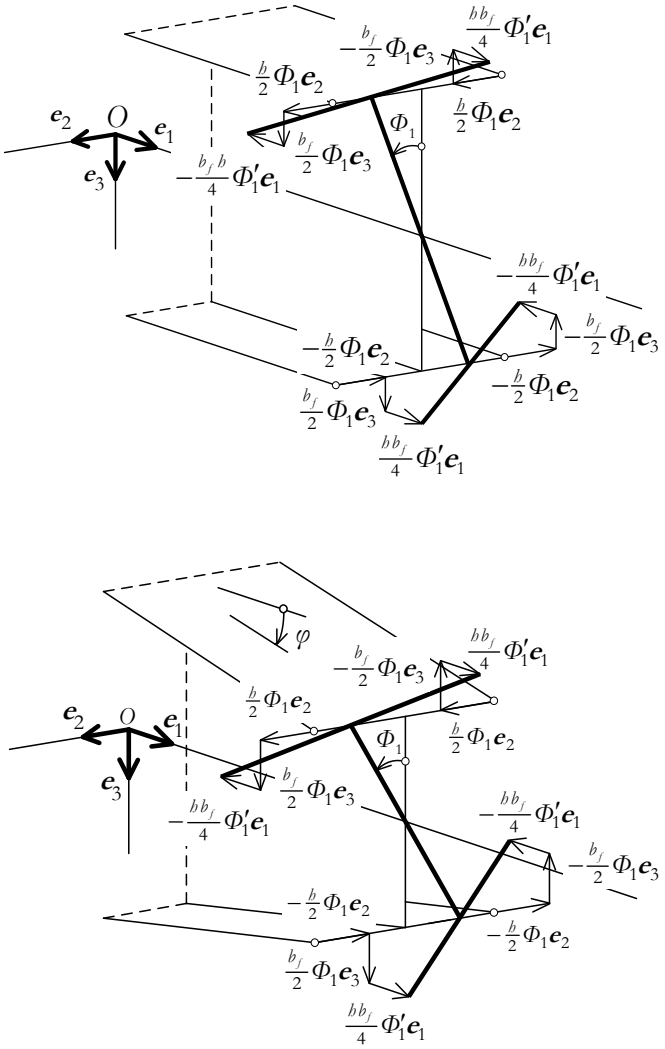

Figure 2.11.2: Contrasting the warping-torsion behaviours of prismatic and web-tapered doubly symmetric I-section bars – Displacement field of cross-section middle line

(ii) The displacement fields discussed above can now be used to find the membrane strains $\gamma_{1\cdot1}$ in the flanges by direct computation (figure 2.11.3). Comparing the ensuing strain-displacement relations for prismatic and web-tapered bars, one readily sees that the latter contains an additional term and a scaling factor ($\cos^2\varphi$).[56] Now, by specialising the results summarised in table 2.10.1 and figure 2.10.5, one readily sees that this additional term is none other than $-\psi\,\Phi_1'$ and the scaling factor is $\frac{1}{a}$ (recall

[56] This particular strain distribution is identical to that one obtained by CYWINSKI & KOLLBRUNNER (1971, § 3, eq. 13). However, in subsequent developments, these authors adopted the approximation $\cos^2\varphi \cong 1$.

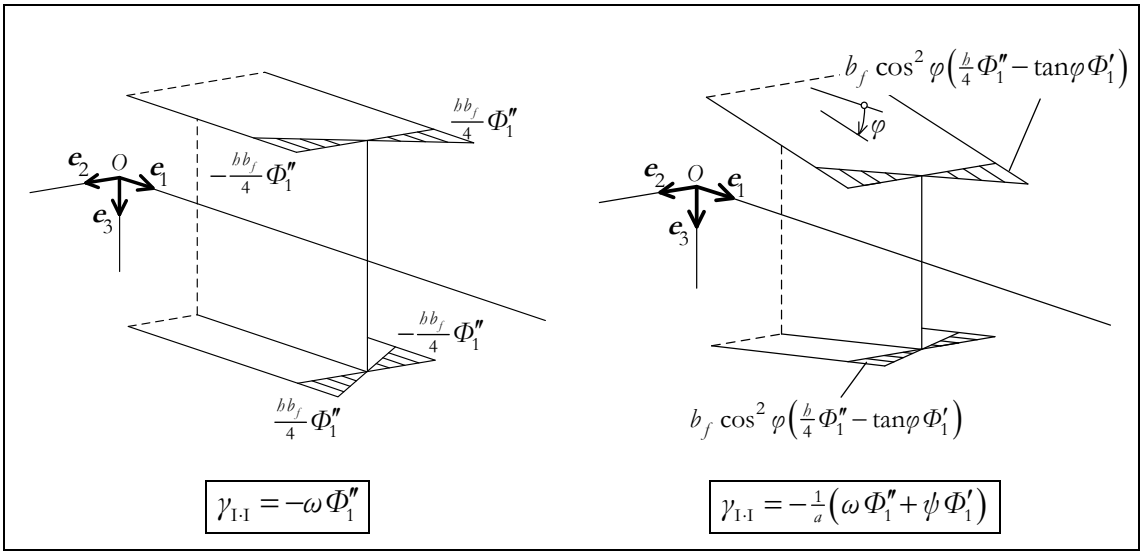

Figure 2.11.3: Contrasting the warping-torsion behaviours of prismatic and web-tapered doubly symmetric I-section bars – Membrane strains $\gamma_{\mathrm{I\cdot I}}$

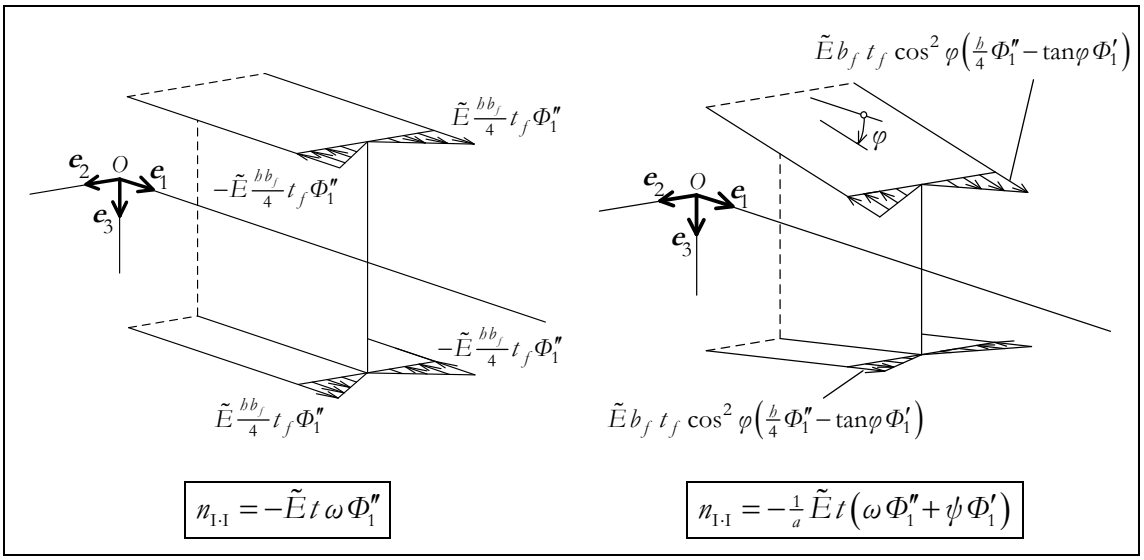

Figure 2.11.4: Contrasting the warping-torsion behaviours of prismatic and web-tapered doubly symmetric I-section bars – Membrane forces $n_{\mathrm{I\cdot I}}$ (active)

the basic strain modes (2.3.34)). These remarks also apply to the (active) membrane forces $n_{\mathrm{I\cdot I}}$ in the flanges, as shown in figure 2.11.4.

(iii) The membrane forces $n_{\mathrm{I\cdot II}}$ shown in figure 2.11.5, which have a reactive character, may be found by considering the equilibrium of a "flange slice" acted by the previously obtained membrane forces $n_{\mathrm{I\cdot I}}$, as ordinarily done in standard textbooks on strength of materials (*e.g.*, MASSONNET 1968, §§ 7.3-7.4, or DIAS DA SILVA 2006, §§ 8.2 and 8.3.c).

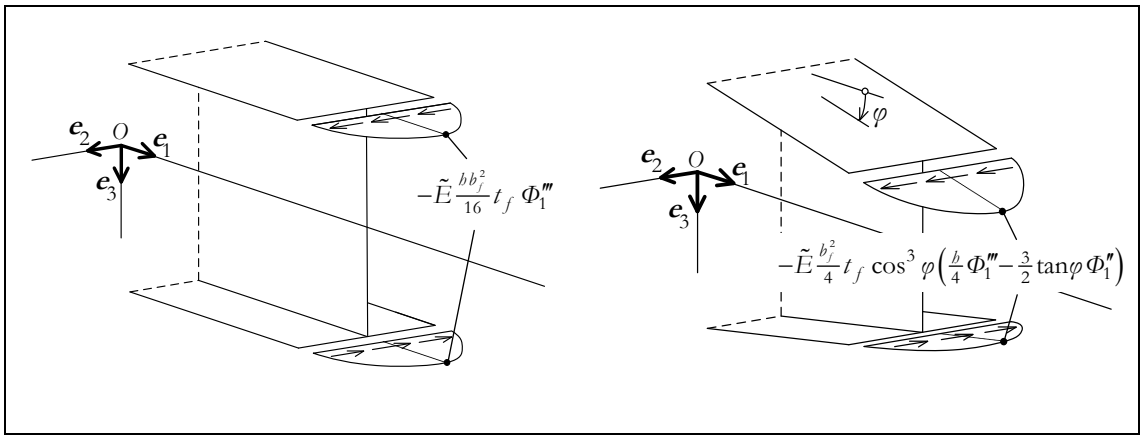

Figure 2.11.5: Contrasting the warping-torsion behaviours of prismatic and web-tapered doubly symmetric I-section bars – Membrane forces $n_{\text{I-II}}$ (reactive)

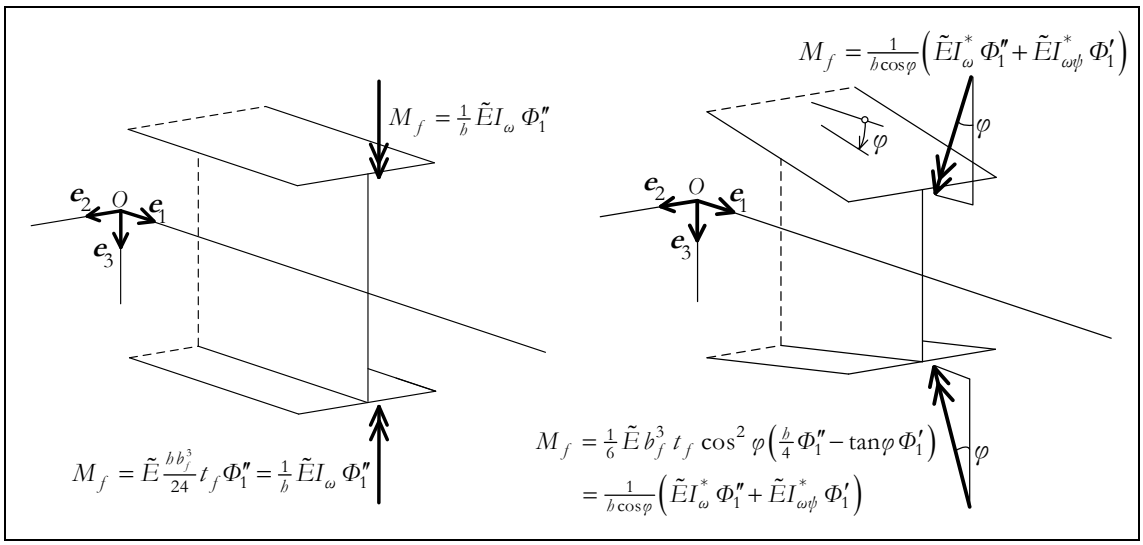

Figure 2.11.6: Contrasting the warping-torsion behaviours of prismatic and web-tapered doubly symmetric I-section bars – Bending moments M_f in the flanges

(iv) The membrane forces $n_{\text{I-I}}$ (resp. $n_{\text{I-II}}$) are statically equivalent to a bending moment $M_f(\theta^1)$ (resp. shear force $V_f(\theta^1)$) in each flange (figures 2.11.6-2.11.7). In the web-tapered case, the modified warping stiffness $\tilde{E}I_\omega^*(\theta^1)$, calculated with the reduced flange thickness $t_f\cos^3\varphi$, and the non-standard mechanical property $\tilde{E}I_{\omega\psi}^*(\theta^1)$ arise naturally in this process:

$$M_f(\theta^1) = \frac{1}{6}\tilde{E}\,b_f^3\,t_f\cos^2\varphi\left(\frac{h(\theta^1)}{4}\Phi_1''(\theta^1) - \tan\varphi\,\Phi_1'(\theta^1)\right)$$

$$= \frac{1}{h(\theta^1)\cos\varphi}\left(\tilde{E}I_\omega^*(\theta^1)\,\Phi_1''(\theta^1) + \tilde{E}I_{\omega\psi}^*(\theta^1)\,\Phi_1'(\theta^1)\right) \qquad (2.11.13)$$

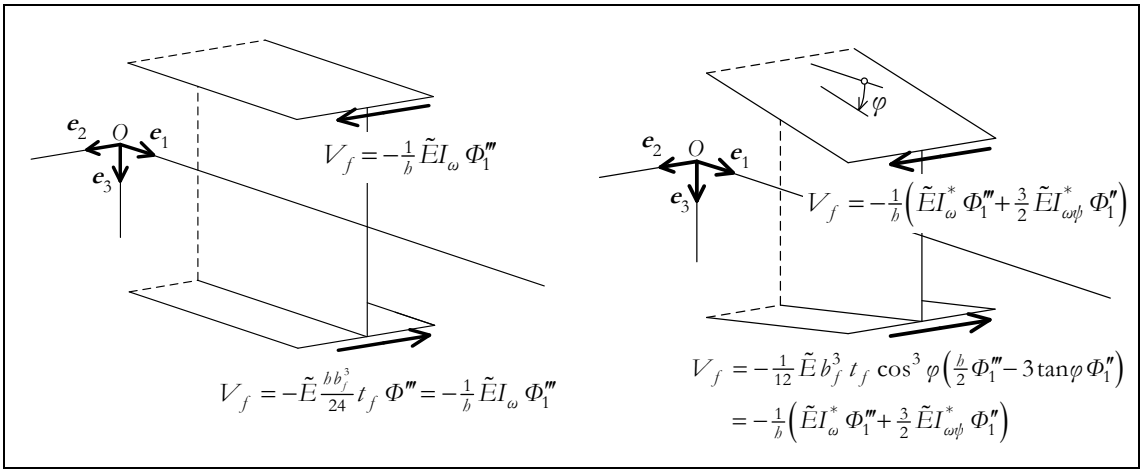

Figure 2.11.7: Contrasting the warping-torsion behaviours of prismatic and web-tapered doubly symmetric I-section bars – Shear forces V_f in the flanges

$$V_f(\theta^1) = -\frac{1}{12}\tilde{E}b_f^3 t_f \cos^3\varphi\left(\frac{h(\theta^1)}{2}\Phi_1'''(\theta^1) - 3\tan\varphi\,\Phi_1''(\theta^1)\right)$$

$$= -\frac{1}{h(\theta^1)}\left(\tilde{E}I_\omega^*(\theta^1)\Phi_1'''(\theta^1) + \frac{3}{2}\tilde{E}I_{\omega\psi}^*(\theta^1)\Phi_1''(\theta^1)\right) . \qquad (2.11.14)$$

Observe that

$$M_f(\theta^1) = \tilde{E}\frac{b_f^3 t_f}{12}\cos^2\varphi\left(\frac{h}{2}\Phi_1\right)''(\theta^1) . \qquad (2.11.15)$$

$$V_f(\theta^1) = -\cos\varphi\, M_f'(\theta^1) . \qquad (2.11.16)$$

We can thus look at each flange as an Euler-Bernoulli beam undergoing deflections $\pm\frac{h}{2}\Phi_1$. However, a word of caution is in order: when dealing with web-tapered bars, one must carefully distinguish between derivatives with respect to θ^1 and derivatives with respect to the arc length of the flange centroidal lines, whence the appearance of $\cos\varphi$ in equations (2.11.15)-(2.11.16).[57]

(v) In web-tapered bars, the flange bending moments have an axial component, featuring $\tilde{E}I_{\omega\psi}^*$ and $\tilde{E}I_\psi^*$, which totals

$$-2\sin\varphi\, M_f(\theta^1)\boldsymbol{e}_1 = -\frac{2\tan\varphi}{h(\theta^1)}\left(\tilde{E}I_\omega^*(\theta^1)\Phi_1''(\theta^1) + \tilde{E}I_{\omega\psi}^*(\theta^1)\Phi_1'(\theta^1)\right)\boldsymbol{e}_1$$

$$= \frac{1}{2}\left(\tilde{E}I_{\omega\psi}^*(\theta^1)\Phi_1''(\theta^1) + \tilde{E}I_\psi^*(\theta^1)\Phi_1'(\theta^1)\right)\boldsymbol{e}_1 . \qquad (2.11.17)$$

[57] Clearly, a stepped model, regardless of the number of prismatic segments it comprises, cannot capture the second term on the right-hand side of $\frac{1}{2}\left(h\Phi_1\right)''(\theta^1) = \frac{1}{2}h(\theta^1)\Phi_1''(\theta^1) + h'(\theta^1)\Phi_1'(\theta^1)$, nor can it capture the factor $\cos\varphi$.

In complete agreement with the general definition (2.7.6), the torque is thus given by

$$M_1(\theta^1) = -2\sin\varphi\, M_f(\theta^1) + V_f(\theta^1)\, h(\theta^1) + GJ(\theta^1)\,\Phi_1'(\theta^1)$$

$$= -\tilde{E}I_\omega^*(\theta^1)\,\Phi_1'''(\theta^1) - \tilde{E}I_{\omega\psi}^*(\theta^1)\,\Phi_1''(\theta^1) + \left(GJ(\theta^1) + \frac{1}{2}\,\tilde{E}I_\psi^*(\theta^1) \right)\Phi_1'(\theta^1) \ . \quad (2.11.18)$$

Obviously, the contribution of the flange bending moments to the torque (i) is absent in prismatic bars and (ii) cannot be captured by stepped models. Finally, notice that

$$\cos\varphi\, M_f(\theta^1) = \frac{1}{h(\theta^1)} \left(\tilde{E}I_\omega^*(\theta^1)\,\Phi_1''(\theta^1) + \tilde{E}I_{\omega\psi}^*(\theta^1)\,\Phi_1'(\theta^1) \right) = -\frac{B(\theta^1)}{h(\theta^1)} \ . \quad (2.11.19)$$

(vi) The splitting of the torque (2.11.18) into active and reactive parts is rather subtle. By plugging (2.11.19) into (2.11.16), one obtains

$$V_f(\theta^1) = \frac{1}{h(\theta^1)} \left(B'(\theta^1) + \frac{2\tan\varphi}{h(\theta^1)}\, B(\theta^1) \right) . \quad (2.11.20)$$

Then, the active and reactive parts of the torque are

$$M_1^{(A)}(\theta^1) = -2\sin\varphi\, M_f(\theta^1) + \frac{2\tan\varphi}{h(\theta^1)}\, B(\theta^1) + GJ(\theta^1)\,\Phi_1'(\theta^1)$$

$$= \tilde{E}I_{\omega\psi}^*(\theta^1)\,\Phi_1''(\theta^1) + \left(GJ(\theta^1) + \tilde{E}I_\psi^*(\theta^1) \right)\Phi_1'(\theta^1) \quad (2.11.21)$$

$$M_1^{(R)}(\theta^1) = B'(\theta^1) = -\left(\tilde{E}I_\omega^*\,\Phi_1'' + \tilde{E}I_{\omega\psi}^*\,\Phi_1' \right)'(\theta^1) \ , \quad (2.11.22)$$

in accordance with the general definitions (2.7.21)-(2.7.22).

LEE (1956) and KITIPORNCHAI & TRAHAIR (1972) have also provided a physical explanation for the warping-torsion behaviour of doubly symmetric web-tapered I-section bars, by regarding each flange as an individual Euler-Bernoulli beam in bending, with deflections $\pm\frac{h}{2}\Phi_1$. However, their analysis is marred by the fact that they fail to distinguish between derivatives with respect to the longitudinal coordinate of the bar and derivatives with respect to the arc length of the flange centroidal lines. This prevents them from arriving at the reduced flange thickness $t_f \cos^3\varphi$. Moreover, Kitipornchai and Trahair allow for doubly symmetric I-section bars with curved flanges (that is, bars whose depth is described by a smooth non-affine map), in which case the equation used to relate bending moments in the flanges to the rotation about the beam axis – equation (14) in the cited paper – is incomplete. In particular, it leads to the conclusion that a rigid infinitesimal rotation of the beam about its axis causes bending moments in the flanges, which is

obviously absurd. The term responsible for this conclusion, which features $b''\Phi_1$ and is "neglected as being small [...] for most structural beams", would not have arisen in the first place if the complete equation for a curved rectangular beam (*e.g.*, equation (7.2.28) in YANG & KUO 1994, p. 400) had been used. The same kind of oversight is present in LEE & SZABO (1967).

After this brief, and hopefully enlightening, digression, let us now return to the boundary value problem (2.11.2)-(2.11.10). By an appropriate change of independent variable, this problem may be posed on a fixed reference domain (*i.e.*, independent of the cantilever length L) and written in non-dimensional form. Indeed, consider the real analytic diffeomorphism $f:[0,L]\to[0,1]$ defined by $\theta^1 \mapsto \frac{\theta^1}{L}$ and let $s = f(\theta^1)$ denote the associated change of independent variable. Moreover, define $\tilde{\Phi}:[0,1]\to\mathbb{R}$ such that $\Phi_1 = \tilde{\Phi}\circ f$ (that is, $\tilde{\Phi} = \Phi_1 \circ f^{-1}$). Clearly, Φ_1 is four times continuously differentiable on $[0,L]$ if and only if $\tilde{\Phi}$ is four times continuously differentiable on $[0,1]$, with the chain rule yielding (*e.g.*, RUDIN 1976, th. 5.5)

$$\Phi_1^{(n)}(\theta^1) = \frac{1}{L^n}\tilde{\Phi}^{(n)}(s) - \quad , \quad n = 1,\cdots,4 \quad . \tag{2.11.23}$$

Then, with the introduction of the non-dimensional ratios

$$\kappa_{\omega 0} = \frac{\pi}{L}\sqrt{\frac{\tilde{E}I_\omega^*(0)}{GJ(0)}} \tag{2.11.24}$$

$$\kappa_{J0} = \frac{b_0\, t_w^3}{3\, J(0)} \tag{2.11.25}$$

$$\mu = \frac{M_{L.1}\, L}{GJ(0)} \quad , \tag{2.11.26}$$

the illustrative example 1 is brought into the following form:

Illustrative example 1 (non-dimensional version).

Find $\tilde{\Phi}:[0,1]\to\mathbb{R}$, with $\tilde{\Phi}\in C^4[0,1]$, satisfying the ordinary differential equation

$$-\big(1-(1-\alpha)s\big)^2\left(\frac{\kappa_{\omega 0}}{\pi}\right)^2\tilde{\Phi}^{(4)}(s) + 4(1-\alpha)\big(1-(1-\alpha)s\big)\left(\frac{\kappa_{\omega 0}}{\pi}\right)^2\tilde{\Phi}'''(s)$$
$$+\big(1-\kappa_{J0}(1-\alpha)s\big)\tilde{\Phi}''(s) - \kappa_{J0}(1-\alpha)\tilde{\Phi}'(s) = 0 \tag{2.11.27}$$

on the open interval $(0,1)$, together with the boundary conditions

$$\tilde{\Phi}(0)=0 \tag{2.11.28}$$

$$\tilde{\Phi}'(0)=0 \tag{2.11.29}$$

$$\begin{aligned}-\alpha^2\left(\frac{\kappa_{\omega 0}}{\pi}\right)^2\tilde{\Phi}'''(1)+2\alpha(1-\alpha)\left(\frac{\kappa_{\omega 0}}{\pi}\right)^2\tilde{\Phi}''(1)\\ +\left[1+2(1-\alpha)^2\left(\frac{\kappa_{\omega 0}}{\pi}\right)^2-\kappa_{J0}(1-\alpha)\right]\tilde{\Phi}'(1)=\mu\end{aligned} \tag{2.11.30}$$

$$\alpha\tilde{\Phi}''(1)-2(1-\alpha)\tilde{\Phi}'(1)=0\ . \tag{2.11.31}$$

We remark that $\{\alpha,\kappa_{\omega 0},\kappa_{J0},\mu\}$ constitutes a complete set of independent non-dimensional parameters characterising the linear torsional behaviour of the family of cantilevers depicted in figure 2.11.1. This conclusion could also have been reached through Vaschy-Buckingham's theorem (VASCHY 1892, 1896, ch. 0, §§ 11-12, and BUCKINGHAM 1914, 1915, 1921), the fundamental result that "summarizes the entire theory of dimensional analysis" (LANGHAAR 1951, p. 19).[58] Moreover, observe that the parameter κ_{J0} is not required in the analysis of prismatic bars, as it always appears in the governing equations multiplied by $(1-\alpha)$. In design practice, $\kappa_{\omega 0}$ ranges from 0.1 to 2.5, with low (resp. high) values of this parameter corresponding to long (resp. short) cantilevers and/or compact (resp. slender) cross-sections at the support (KITIPORNCHAI & TRAHAIR 1980). As for κ_{J0}, which measures the relative contribution of the web to the Saint-Venant torsional rigidity of the clamped cross-section, it lies in the open interval $(0,1)$ – the limiting values $\kappa_{J0}=0$ and $\kappa_{J0}=1$, not addressed here, are associated with two degenerate cases: webless and narrow rectangular beams, respectively.

In the prismatic case ($\alpha=1$), the solution to the non-dimensional version of the illustrative example 1 is (*e.g.*, CHEN & ATSUTA 1977, p. 48)

$$\begin{aligned}\tilde{\Phi}(s)=\mu\frac{\kappa_{\omega 0}}{\pi}\left(-\tanh\left(\frac{\pi}{\kappa_{\omega 0}}\right)+\tanh\left(\frac{\pi}{\kappa_{\omega 0}}\right)\cosh\left(\frac{\pi}{\kappa_{\omega 0}}s\right)\right.\\ \left.-\sinh\left(\frac{\pi}{\kappa_{\omega 0}}s\right)+\frac{\pi}{\kappa_{\omega 0}}s\right),\quad 0\le s\le 1\ .\end{aligned} \tag{2.11.32}$$

[58] Several different proofs of this theorem, with varying degrees of generality and complexity, can be found in BIRKHOFF (1960, §§ 63-64), BLUMAN & ANCO (2002, § 1.2), BOYLING (1979), BRAND (1957), BRIDGMAN (1931, ch. 4), CORRSIN (1951), CURTIS *et al.* (1982), GIBBINGS (2011, ch. 3) LANGHAAR (1951, ch. 4), LOGAN (2006, § 1.1), MENDOZA (1996), POBEDRYA & GEORGIEVSKII (2006) and SEDOV (1993, ch. 1, § 6).

In the tapered case ($0<\alpha<1$), no closed-form solution is available. The mathematical software package Mathematica (WOLFRAM RESEARCH, INC. 2006) was used to obtain numerical solutions for selected values of the parameters $\kappa_{\omega 0}$ and α – since the parameter κ_{J0} is found to be relatively unimportant, we always set $\kappa_{J0}=0.1$.[59] These solutions are plotted in figure 2.11.8. For prismatic cantilevers, it can be seen that the non-dimensional "twistature"[60] $s \mapsto \tilde{\Phi}''(s)$ is a strictly decreasing map that vanishes at $s=1$, as required by the boundary condition (2.11.31). For web-tapered bars, on the other hand, the non-dimensional "twistature" $\tilde{\Phi}''$ exhibits an increase near the free end – this boundary effect is all the more noticeable as $\kappa_{\omega 0}$ increases and as α decreases.

Another interesting difference in the warping-torsion behaviours of prismatic and web-tapered cantilevers is revealed in figure 2.11.9, which displays the lateral deflection $\Phi_1 h/2$ of the top flange centroidal line per unit torque $M_{L.1}$, rendered non-dimensional by the factor $GJ(0)/(L h_0)$:

$$\frac{\tilde{\Phi}(s)}{2\mu}\big(1-(1-\alpha)s\big)=\frac{\Phi_1(sL)h(sL)}{2M_{L.1}}\frac{GJ(0)}{Lh_0}\ . \tag{2.11.33}$$

Regarded as Euler-Bernoulli beams, the flanges in a prismatic bar exhibit single curvature bending, while in a tapered bar they undergo double curvature bending. In the latter case, the inflection point moves to the left, *i.e.*, away from the free end and towards the support, as the taper ratio α decreases. Such a behavioural feature is also clearly visible in figure 2.11.10, which displays the non-dimensional bimoment distribution

$$\begin{aligned} s \mapsto \beta(s) &= \frac{B(sL)}{GJ(0)} \\ &= -\big(1-(1-\alpha)s\big)^2\left(\frac{\kappa_{\omega 0}}{\pi}\right)^2\tilde{\Phi}''(s)+2(1-\alpha)\big(1-(1-\alpha)s\big)\left(\frac{\kappa_{\omega 0}}{\pi}\right)^2\tilde{\Phi}'(s) \end{aligned} \tag{2.11.34}$$

per unit non-dimensional torque μ – the reader should bear in mind the identity (2.11.19), relating the bending moment in the flanges to the bimoment. Inspection of the graphs in figure 2.11.10 also shows that, for low $\kappa_{\omega 0}$, the bimoment distribution is essentially localised in a small region adjacent to the support; for high $\kappa_{\omega 0}$, on the contrary, it has appreciable values over the entire length of the bars – this observation applies to prismatic and tapered bars alike.

---

[59] As an indication, members with $h_0 \cong 2b$ and $t_f \cong 2t_w$ exhibit $\kappa_{J0} \cong 0.1$.

[60] A neologism coined by TRAHAIR (1993, p. 39).

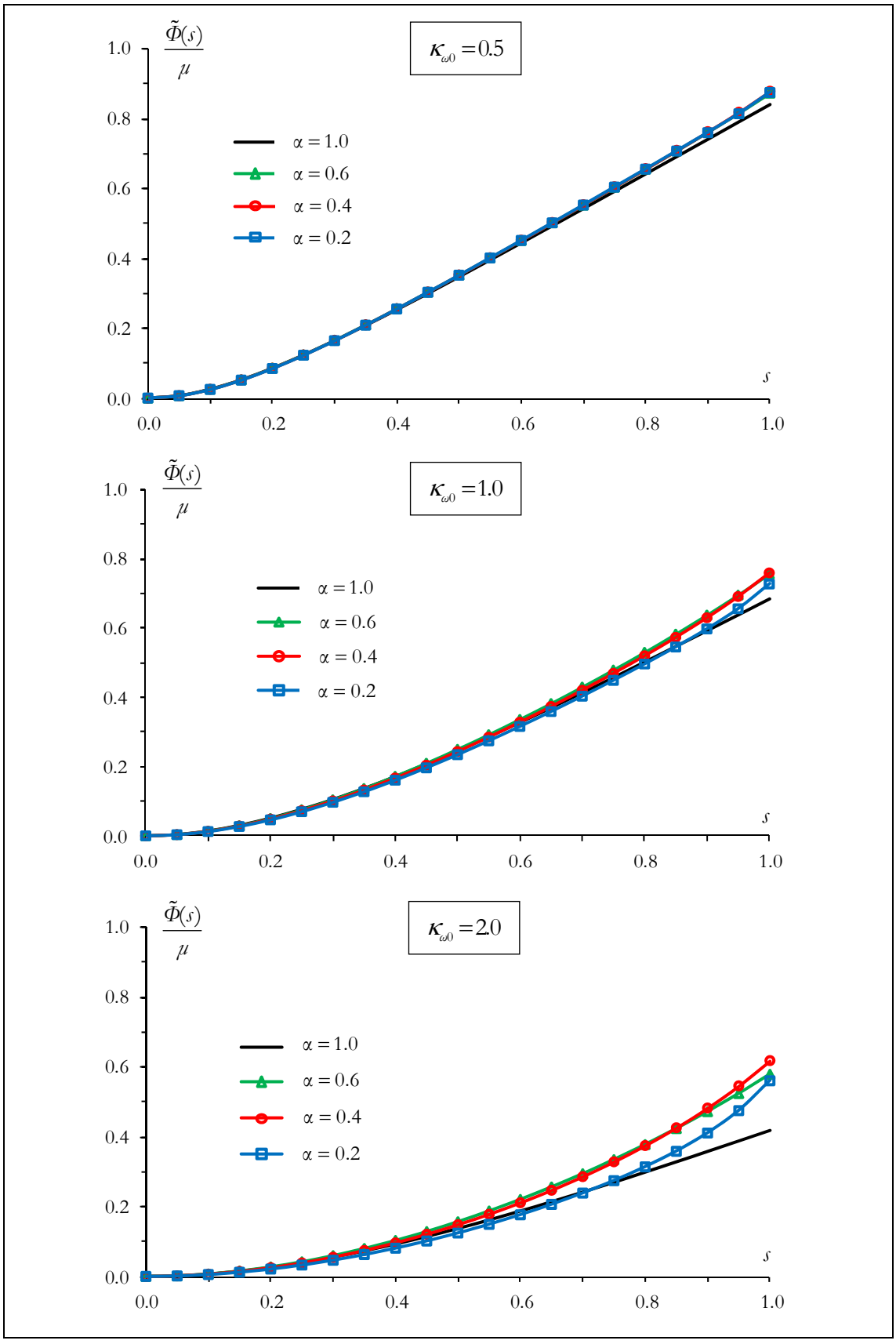

Fig. 2.11.8: Illustrative example 1 ($\kappa_{J0} = 0.1$) – Solutions $s \mapsto \tilde{\Phi}(s)$ to the non-dimensional version of the boundary value problem per unit non-dimensional torque μ

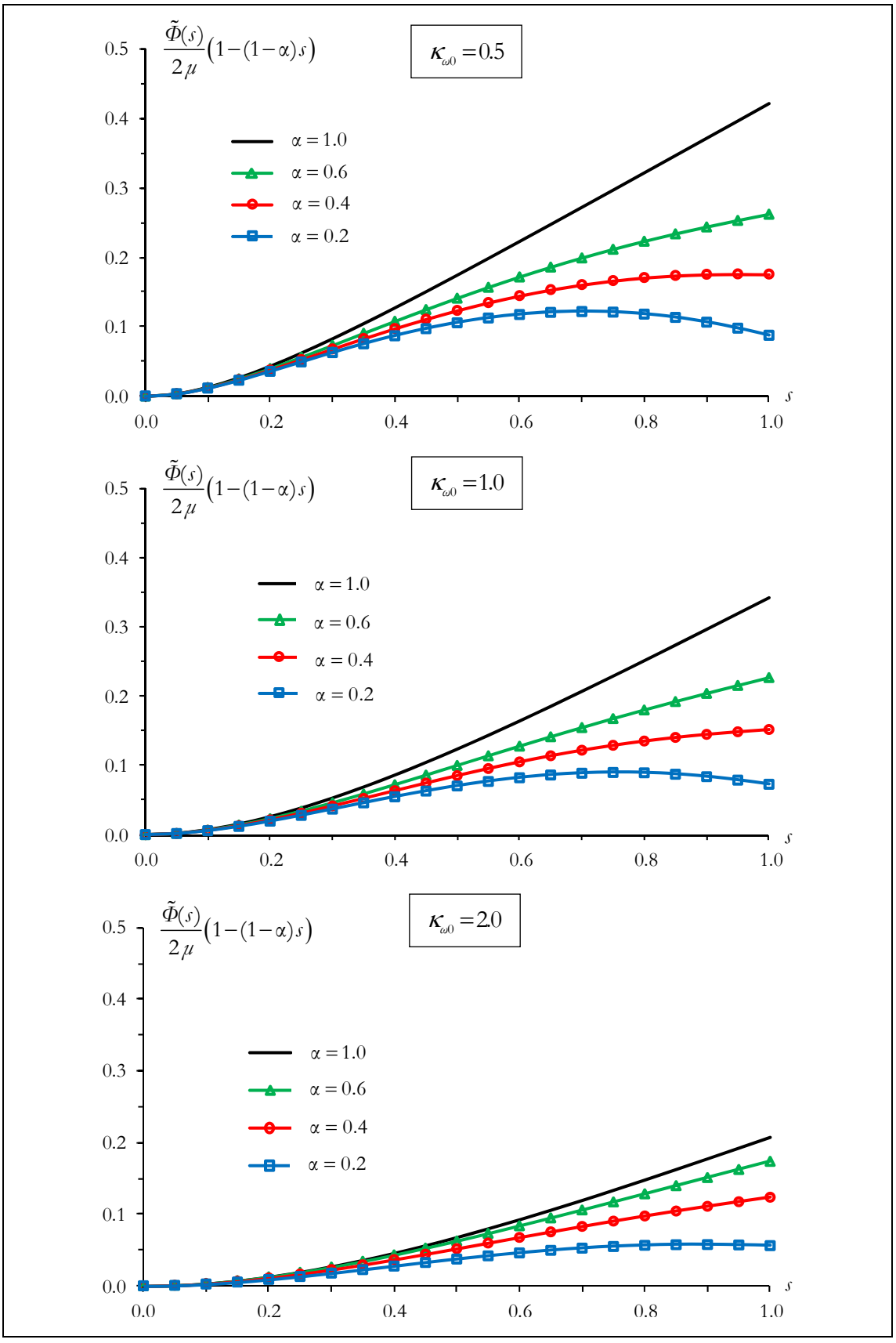

Fig. 2.11.9: Illustrative example 1 ($\kappa_{J0}=0.1$) – Lateral deflections of the top flange centroidal line per unit torque in non-dimensional form

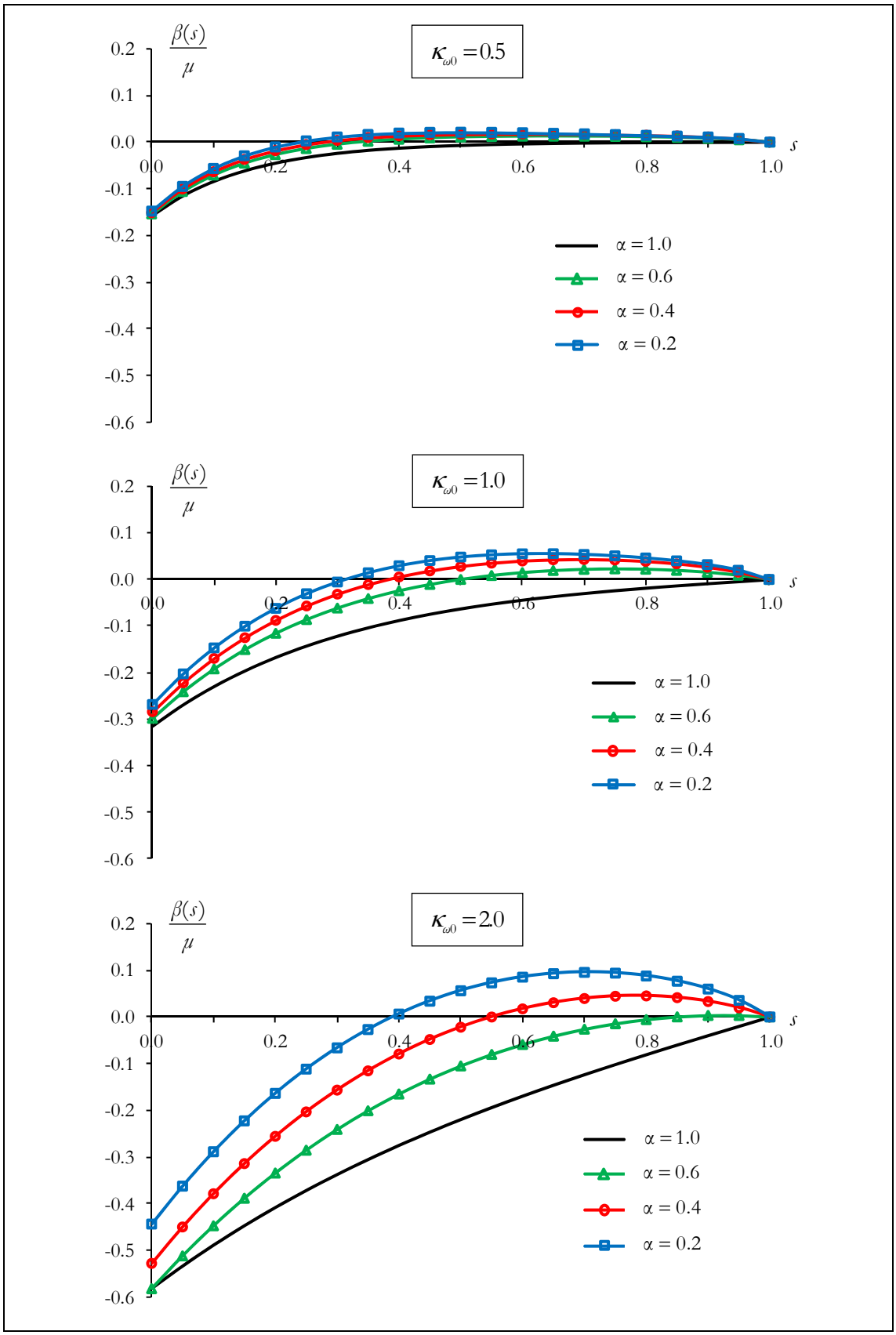

Fig. 2.11.10: Illustrative example 1 ($\kappa_{J0} = 0.1$) – Non-dimensional bimoment distributions $s \mapsto \beta(s)$ per unit non-dimensional torque μ

Figure 2.11.11 shows the non-dimensional flange shear force distribution

$$s \mapsto \varpi(s) = \frac{V_f(sL)\,h_0\,L}{GJ(0)} = -\left(1-(1-\alpha)s\right)\left(\frac{\kappa_{\omega 0}}{\pi}\right)^2 \tilde{\Phi}'''(s) + 3(1-\alpha)\left(\frac{\kappa_{\omega 0}}{\pi}\right)^2 \tilde{\Phi}''(s) \quad (2.11.35)$$

per unit non-dimensional torque μ. We can notice here another boundary effect. For most of their length, there are no significant differences between prismatic and tapered bars (especially for low $\kappa_{\omega 0}$). However, near the free end, the shear forces in the flanges of tapered bars change sign and, as α decreases, their absolute value exhibits a gradually sharper increase. For $\alpha = 0.2$, in particular, we have $|\varpi(1)| > \varpi(0)$, with the difference becoming larger as $\kappa_{\omega 0}$ increases.

The differences in warping-torsion behaviour between prismatic and web-tapered I-section cantilevers can be further illustrated by considering the non-dimensional torsional stiffness $\mu/\tilde{\Phi}(1)$, plotted in figure 2.11.12 *versus* the taper ratio α (solid lines, labelled "tapered model"). Contrary to intuition (which is often misleading), $\mu/\tilde{\Phi}(1)$ is not a monotonic increasing function of α. Instead, it reaches a minimum for an intermediate value of α, dependent on $\kappa_{\omega 0}$. This is explained by the specific taper effects that were discussed in connection with figures 2.11.2-2.11.7 and which are embodied predominantly in the field $\psi\,(\neq 0)$ and, to a much lesser extent, in the field $a\,(\neq 1)$ of the general one-dimensional model. Indeed, if one sets $\psi = 0$ and $a = 1$ – in other words, if one represents a tapered bar by an assembly of prismatic segments obeying Vlasov's theory and makes the length of the segments tend to zero –, then one obtains the dashed lines shown in figure 2.11.12 with the label "stepped model", which are practically straight and have a positive slope. The difference between solid and dashed lines (that is, between tapered and stepped models) becomes more pronounced as $\kappa_{\omega 0}$ increases, reflecting the growing importance of restrained warping to torsional stiffness. For reference purposes, figure 2.11.12 also presents the non-dimensional torsional stiffness of prismatic cantilevers with the largest and the smallest cross-sectional dimensions, *i.e.*, with constant web depth h_0 and αh_0, respectively (dotted lines, labelled "prismatic, largest section" and "prismatic, smallest section"). As expected, the dotted lines form an envelope within which the solid lines lie for $\alpha < 1$ (dotted and solid lines obviously coincide for $\alpha = 1$).

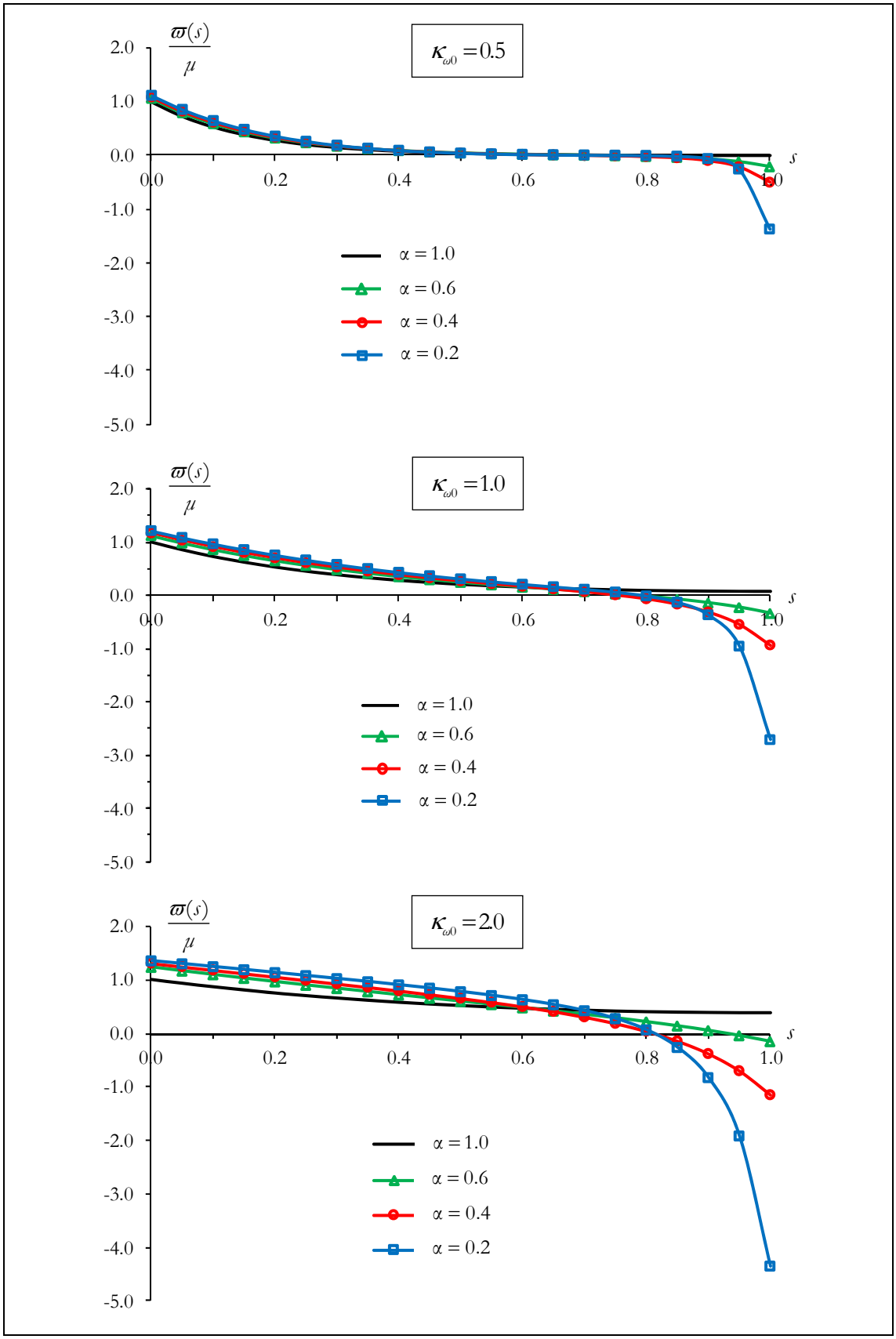

Fig. 2.11.11: Illustrative example 1 ($\kappa_{J0}=0.1$) – Non-dimensional flange shear force distributions $s \mapsto \varpi(s)$ per unit non-dimensional torque μ

To shed further light on the peculiar features of the torsional behaviour of web-tapered bars, we now investigate how the three individual contributions to the total torque singled out in equation (2.11.18), namely $-2\sin\varphi M_f$, $V_f h$ and $GJ\Phi_1'$, vary along the cantilever length. To this end, we plot in figure 2.11.13, for different values of the taper ratio α, the non-dimensional distributions

$$s \mapsto \mu_{M_f}(s) = -\frac{2\sin\varphi M_f(sL)L}{GJ(0)}$$

$$= -(1-\alpha)\left(1-(1-\alpha)s\right)\left(\frac{\kappa_{\omega 0}}{\pi}\right)^2 \tilde{\Phi}''(s) + 2(1-\alpha)^2\left(\frac{\kappa_{\omega 0}}{\pi}\right)^2 \tilde{\Phi}'(s) \qquad (2.11.36)$$

$$s \mapsto \mu_{V_f}(s) = \frac{V_f(sL)h(sL)L}{GJ(0)}$$

$$= -\left(1-(1-\alpha)s\right)^2\left(\frac{\kappa_{\omega 0}}{\pi}\right)^2 \tilde{\Phi}'''(s) + 3(1-\alpha)\left(1-(1-\alpha)s\right)\left(\frac{\kappa_{\omega 0}}{\pi}\right)^2 \tilde{\Phi}''(s) \qquad (2.11.37)$$

$$s \mapsto \mu_{\mathrm{SV}}(s) = \frac{GJ(sL)\tilde{\Phi}'(s)L}{GJ(0)} = \left(1-\kappa_{J0}(1-\alpha)s\right)\tilde{\Phi}'(s) \qquad (2.11.38)$$

per unit non-dimensional torque μ (needless to say, μ_{M_f} is identically zero in prismatic bars). We restrict attention to the case $\kappa_{\omega 0} = 2.0$, for which the differences between tapered and stepped models are significant. For tapered bars, and in very broad strokes, we see that (i) close to the clamped end, the negative contribution of the axial component of the bending moments in the flanges is matched by an increase in the positive contribution of the shear forces in the flanges and (ii) near the free end, the sharp rise in the contribution of the Saint-Venant component is compensated by an equally sharp fall in the contribution of the shear forces in the flanges, which eventually becomes negative.

Illustrative example 2

Consider now the family of singly symmetric web-tapered C-section cantilevers whose reference shape is shown in figure 2.11.14. The adopted Cartesian reference frame, also shown in this figure, is such that (i) the plane containing the origin O and spanned by $\{\boldsymbol{e}_1, \boldsymbol{e}_2\}$ is the longitudinal plane of symmetry for the reference shape and (ii) the web middle surface lies in the plane through O and spanned by $\{\boldsymbol{e}_1, \boldsymbol{e}_3\}$. The flanges are uniform, with thickness t_f and width b_f (measured from their tip to the web middle line).

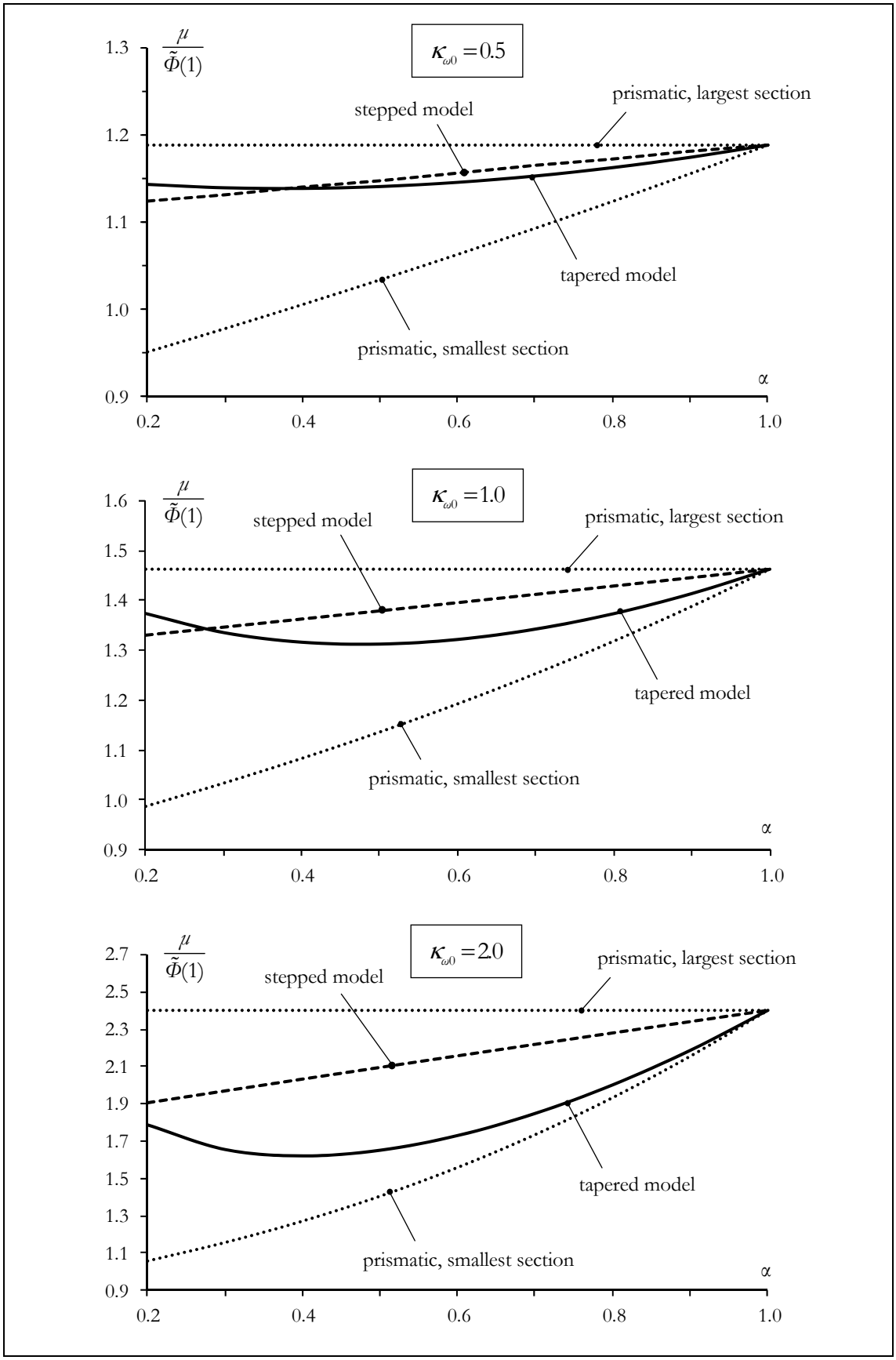

Fig. 2.11.12: Illustrative example 1 ($\kappa_{J0} = 0.1$) – Non-dimensional torsional stiffness $\mu / \tilde{\Phi}(1)$ *versus* the taper ratio α

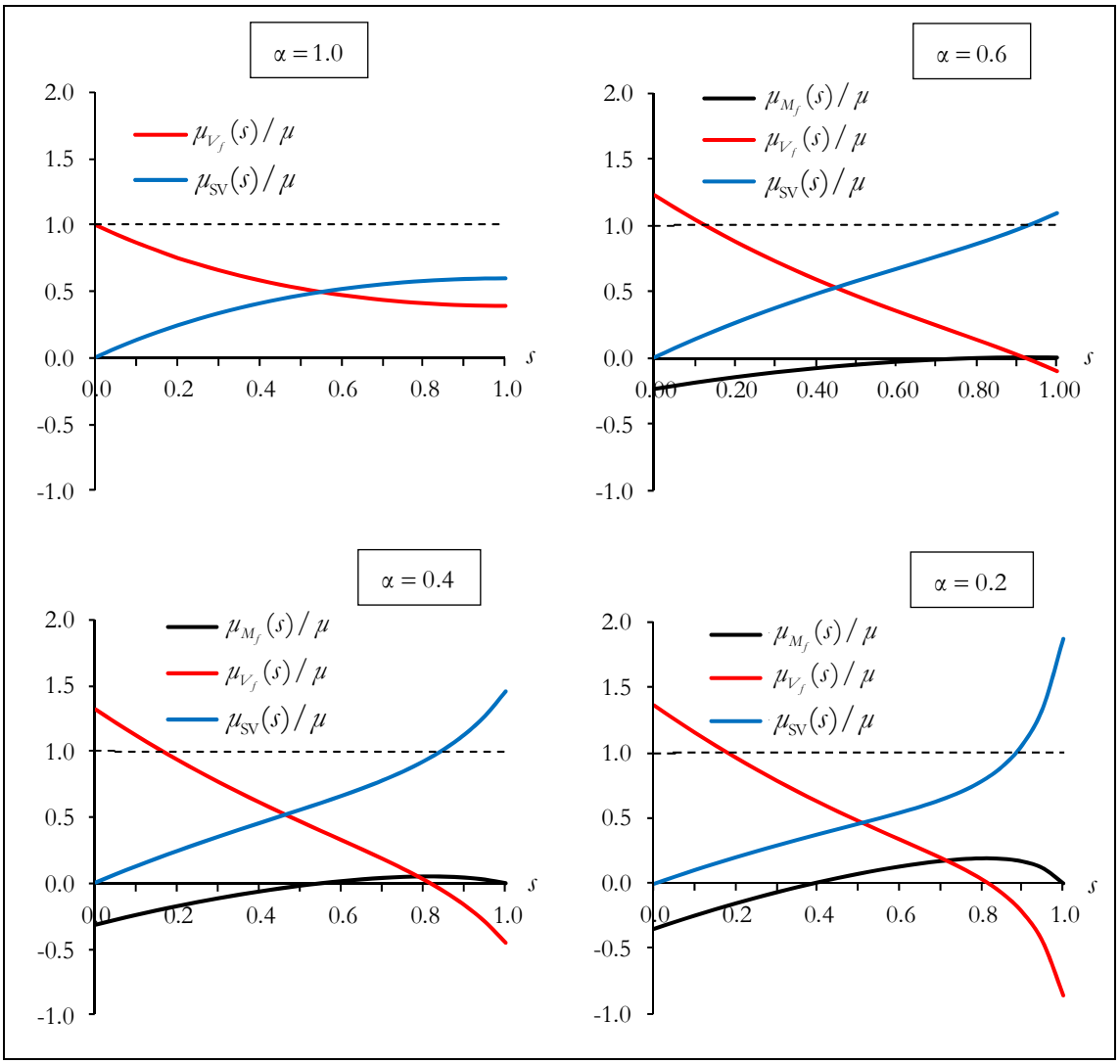

Fig. 2.11.13: Illustrative example 1 ($\kappa_{\omega 0} = 2.0$, $\kappa_{J0} = 0.1$) – Non-dimensional distributions $s \mapsto \mu_{M_f}(s)$, $s \mapsto \mu_{V_f}(s)$ and $s \mapsto \mu_{SV}(s)$ per unit non-dimensional torque μ

The web has constant thickness t_w and its depth h, measured between flange middle lines, varies according to the affine law (2.11.1), with $0 < \alpha \leq 1$. Once again, the parameter α is called the (web) taper ratio. The flanges exhibit symmetrical slopes $\pm\tan\varphi$ with respect to the planes spanned by $\{\boldsymbol{e}_1, \boldsymbol{e}_2\}$, where $\tan\varphi = (1-\alpha)h_0/(2L)$. The cantilever is clamped at its larger end ($\mathscr{A}_0$) and free at the smaller end ($\mathscr{A}_L$), where a point load $Q_{L.3}\,\boldsymbol{e}_3$ is applied (at the point $O + L\,\boldsymbol{e}_1$).

The middle surface is made up of three surface elements, numbered as shown in figure 2.11.15. The scheme adopted for its parametrisation is also indicated in this figure. All the required geometrical features are summarised in table 2.11.1. Moreover, the maps ω and ψ are plotted schematically in figure 2.11.16, directly upon the middle line of a generic cross-section, for a better grasp of their significance.

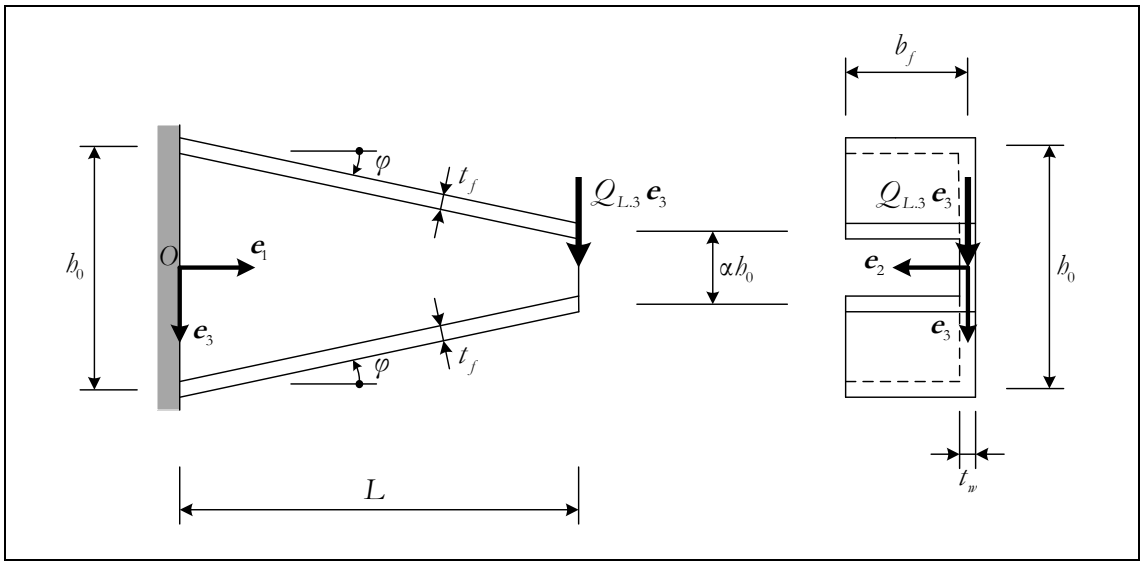

Figure 2.11.14: Illustrative example 2 – Reference shape, support conditions and applied load

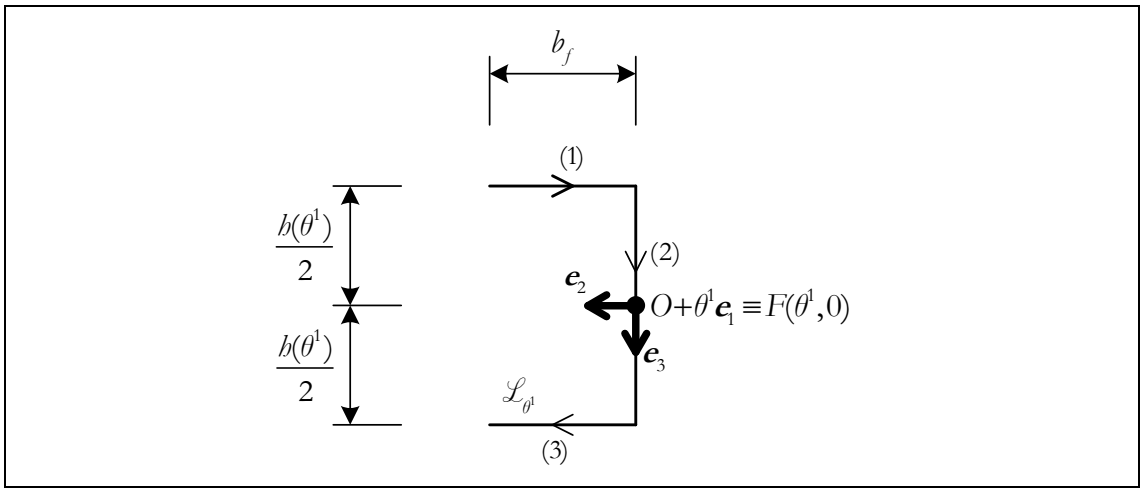

Fig. 2.11.15: Illustrative example 2 – Parametrisation of the middle surface

The geometrical properties (2.5.6)-(2.5.20) are given by

$$A^*(\theta^1) = h(\theta^1)\,t_w + 2\,b_f\,t_f\cos^3\varphi \tag{2.11.39}$$

$$S_2^*(\theta^1) = 0 \tag{2.11.40}$$

$$S_3^*(\theta^1) = b_f^2\,t_f\cos^3\varphi \tag{2.11.41}$$

$$S_\omega^*(\theta^1) = 0 \tag{2.11.42}$$

$$S_\psi^*(\theta^1) = 0 \tag{2.11.43}$$

$$I_2^*(\theta^1) = \frac{h(\theta^1)^3\,t_w}{12} + \frac{h(\theta^1)^2}{2}\,b_f\,t_f\cos^3\varphi \tag{2.11.44}$$

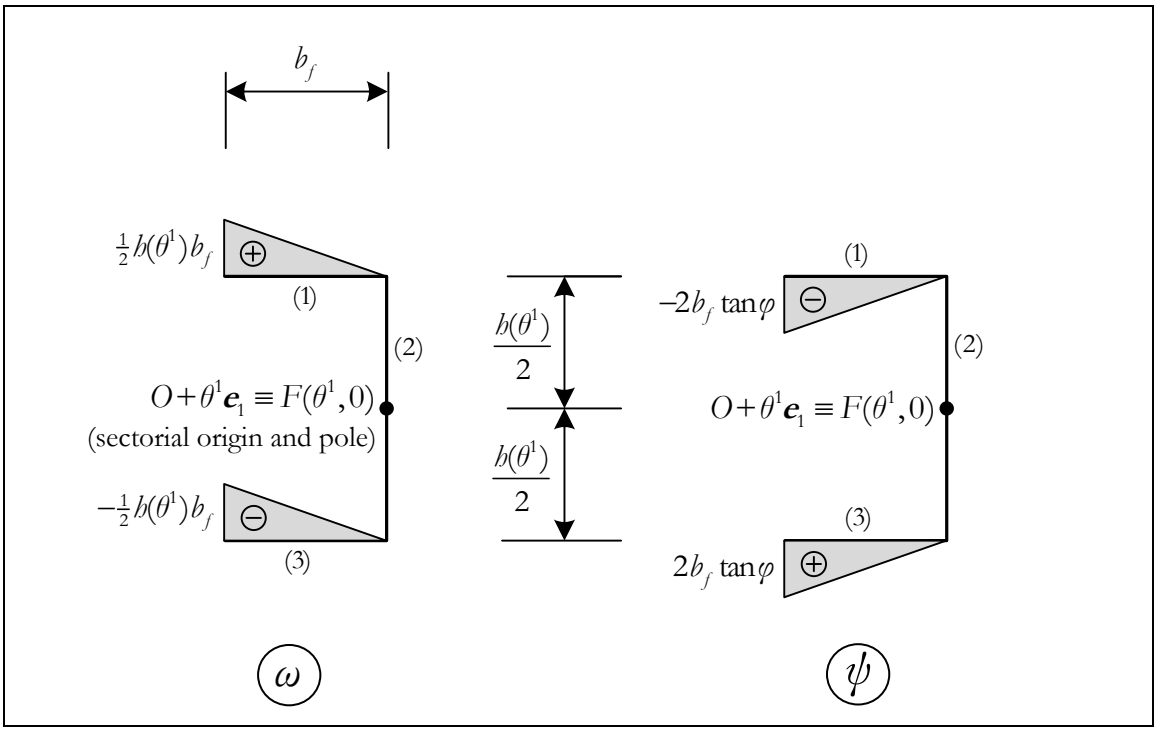

Fig. 2.11.16: Illustrative example 2 – Schematic representations of the maps ω and ψ

$$I_3^*(\theta^1) = \frac{2}{3} b_f^3 t_f \cos^3\varphi \tag{2.11.45}$$

$$I_\omega^*(\theta^1) = \frac{1}{6} h(\theta^1)^2 b_f^3 t_f \cos^3\varphi \tag{2.11.46}$$

$$I_\psi^*(\theta^1) = \frac{8}{3} b_f^3 \tan^2\varphi\, t_f \cos^3\varphi \tag{2.11.47}$$

$$I_{23}^*(\theta^1) = 0 \tag{2.11.48}$$

$$I_{2\omega}^*(\theta^1) = -\frac{1}{4} h(\theta^1)^2 b_f^2 t_f \cos^3\varphi \tag{2.11.49}$$

$$I_{3\omega}^*(\theta^1) = 0 \tag{2.11.50}$$

$$I_{2\psi}^*(\theta^1) = h(\theta^1) b_f^2 \tan\varphi\, t_f \cos^3\varphi \tag{2.11.51}$$

$$I_{3\psi}^*(\theta^1) = 0 \tag{2.11.52}$$

$$I_{\omega\psi}^*(\theta^1) = -\frac{2}{3} h(\theta^1) b_f^3 \tan\varphi\, t_f \cos^3\varphi \ . \tag{2.11.53}$$

	range of θ^2	$\overline{x}_2(\theta^1,\theta^2)$	$\overline{x}_3(\theta^1,\theta^2)$	$a(\theta^1,\theta^2)$	$t^*(\theta^1,\theta^2)$	$\omega(\theta^1,\theta^2)$	$\psi(\theta^1,\theta^2)$
Ω_1	$-\frac{h(\theta^1)}{2}-b_f<\theta^2<-\frac{h(\theta^1)}{2}$	$-\left(\theta^2+\frac{h(\theta^1)}{2}\right)$	$-\frac{h(\theta^1)}{2}$	$1+\tan^2\varphi$	$t_f\cos^3\varphi$	$-\frac{h(\theta^1)}{2}\left(\theta^2+\frac{h(\theta^1)}{2}\right)$	$2\tan\varphi\left(\theta^2+\frac{h(\theta^1)}{2}\right)$
Ω_2	$-\frac{h(\theta^1)}{2}<\theta^2<\frac{h(\theta^1)}{2}$	0	θ^2	1	t_w	0	0
Ω_3	$\frac{h(\theta^1)}{2}<\theta^2<\frac{h(\theta^1)}{2}+b_f$	$\theta^2-\frac{h(\theta^1)}{2}$	$\frac{h(\theta^1)}{2}$	$1+\tan^2\varphi$	$t_f\cos^3\varphi$	$-\frac{h(\theta^1)}{2}\left(\theta^2-\frac{h(\theta^1)}{2}\right)$	$2\tan\varphi\left(\theta^2-\frac{h(\theta^1)}{2}\right)$

Table 2.11.1: Singly symmetric web-tapered C-section bar – Geometrical features

Observe that

$$I^*_{2\psi}(\theta^1) = I^{*\prime}_{2\omega}(\theta^1) \tag{2.11.54}$$

$$I^*_{\omega\psi}(\theta^1) = I^{*\prime}_{\omega}(\theta^1) \tag{2.11.55}$$

$$I^*_{\psi}(\theta^1) = 2\, I^{*\prime\prime}_{\omega}(\theta^1) = 2\, I^{*\prime}_{\omega\psi}(\theta^1)\ . \tag{2.11.56}$$

As for J, it is assumed that the width-to-thickness ratio of each plated component is always sufficiently large for the approximation

$$J(\theta^1) = \frac{1}{3}\left(h(\theta^1) t_w^3 + 2\, b_f \left(\frac{t_f}{\cos\varphi} \right)^3 \right) \tag{2.11.57}$$

to be legitimate.

From the symmetry of the reference shape and support conditions, and from the skew-symmetry of the loading, one infers at once, by virtue of Curies's principle (CURIE 1894), that W_1 and W_2 are identically zero. We are thus left with the problem of finding W_3 and Φ_1, which can be phrased as follows:

Illustrative example 2.

Find $W_3, \Phi_1 : [0, L] \to \mathbb{R}$, with $W_3, \Phi_1 \in C^4[0, L]$, satisfying the ordinary differential equations

$$\left(\tilde{E} I^*_2\, W_3'' + \tilde{E} I^*_{2\omega}\, \Phi_1'' + \tilde{E} I^*_{2\psi}\, \Phi_1' \right)'' (\theta^1) = 0 \tag{2.11.58}$$

$$-\left(\tilde{E} I^*_{2\omega}\, W_3'' + \tilde{E} I^*_{\omega}\, \Phi_1'' + \tilde{E} I^*_{\omega\psi}\, \Phi_1' \right)'' (\theta^1)$$

$$+\left[\tilde{E} I^*_{2\psi}\, W_3'' + \tilde{E} I^*_{\omega\psi}\, \Phi_1'' + \left(GJ + \tilde{E} I^*_{\psi} \right) \Phi_1' \right]' (\theta^1) = 0 \tag{2.11.59}$$

on the open interval $(0, L)$, together with the boundary conditions

$$W_3(0) = 0 \tag{2.11.60}$$

$$W_3'(0) = 0 \tag{2.11.61}$$

$$-\left(\tilde{E} I^*_2\, W_3'' + \tilde{E} I^*_{2\omega}\, \Phi_1'' + \tilde{E} I^*_{2\psi}\, \Phi_1' \right)' (L) = \mathcal{Q}_{L.3} \tag{2.11.62}$$

$$\tilde{E} I^*_2(L) W_3''(L) + \tilde{E} I^*_{2\omega}(L) \Phi_1''(L) + \tilde{E} I^*_{2\psi}(L) \Phi_1'(L) = 0\ . \tag{2.11.63}$$

$$\Phi_1(0) = 0 \tag{2.11.64}$$

$$\Phi_1'(0) = 0 \tag{2.11.65}$$

$$-\left(\tilde{E}I^*_{2\omega}\,W_3'' + \tilde{E}I^*_{\omega}\,\Phi_1'' + \tilde{E}I^*_{\omega\psi}\,\Phi_1'\right)'(L) + \tilde{E}I^*_{2\psi}(L)W_3''(L)$$

$$+\tilde{E}I^*_{\omega\psi}(L)\Phi_1''(L) + \left(GJ(L) + \tilde{E}I^*_{\psi}(L)\right)\Phi_1'(L) = 0 \qquad (2.11.66)$$

$$\tilde{E}I^*_{2\omega}(L)W_3''(L) + \tilde{E}I^*_{\omega}(L)\Phi_1''(L) + \tilde{E}I^*_{\omega\psi}(L)\Phi_1'(L) = 0\ . \qquad (2.11.67)$$

Before addressing the solution of this boundary value problem, it is once again enlightening to contrast the flexural-torsional behaviours of prismatic ($\alpha = 1$) and linearly depth-tapered ($0 < \alpha < 1$) bars:

(i) By virtue of the constraint (V1), the displacements along $\boldsymbol{e}_2$ and $\boldsymbol{e}_3$ of the cross-section middle line at a distance θ^1 from the origin, for prismatic and web-tapered bars alike, are given by the superposition of (i_1) an infinitesimal rotation $\Phi_1(\theta^1)$ about the (oriented) axis defined by the origin O and the Cartesian base vector $\boldsymbol{e}_1$, and (i_2) a translation $W_3(\theta^1)\boldsymbol{e}_3$ (see figure 2.11.17). The constraint (V2) then provides the displacements along $\boldsymbol{e}_1$, which stem from (i_3) an infinitesimal rotation $-W_3'(\theta^1)$ about the (oriented) axis defined by the point $O+\theta^1\boldsymbol{e}_1$ and the Cartesian base vector $\boldsymbol{e}_2$, and (i_4) torsion-warping of the cross-section middle line (again, see figure 2.11.17).

(ii) By direct computation, one obtains the membrane strains $\gamma_{1\cdot1}$ shown schematically in figure 2.11.18. As in the first illustrative example, the strain-displacement relation in the web-tapered case exhibits an additional term ($-\psi\,\Phi_1'$) and a scaling factor ($\frac{1}{a}$) which are absent in the prismatic case. The same is true of the (active) membrane forces $n_{1\cdot1}$, as shown in figure 2.11.19.

(iii) Figure 2.11.20 shows a force system statically equivalent to the membrane forces $n_{1\cdot1}$ in the web and in the flanges. It comprises a web bending moment

$$M_w(\theta^1) = \tilde{E}\frac{h(\theta^1)^3\,t_w}{12}W_3''(\theta^1) \qquad (2.11.68)$$

and, in each flange, a bending moment-normal force pair

$$M_f(\theta^1) = -\tilde{E}\frac{h(\theta^1)}{4}b_f^2\,t_f\cos^2\varphi\,W_3'' + \frac{2}{3}\tilde{E}\,b_f^3\,t_f\cos^2\varphi\left(\frac{h(\theta^1)}{4}\Phi_1''(\theta^1) - \tan\varphi\,\Phi_1'(\theta^1)\right)$$

$$= \frac{1}{h(\theta^1)\cos\varphi}\left(\tilde{E}I^*_{2\omega}(\theta^1)W_3''(\theta^1) + \tilde{E}I^*_{\omega}(\theta^1)\Phi_1''(\theta^1) + \tilde{E}I^*_{\omega\psi}(\theta^1)\Phi_1'(\theta^1)\right) \qquad (2.11.69)$$

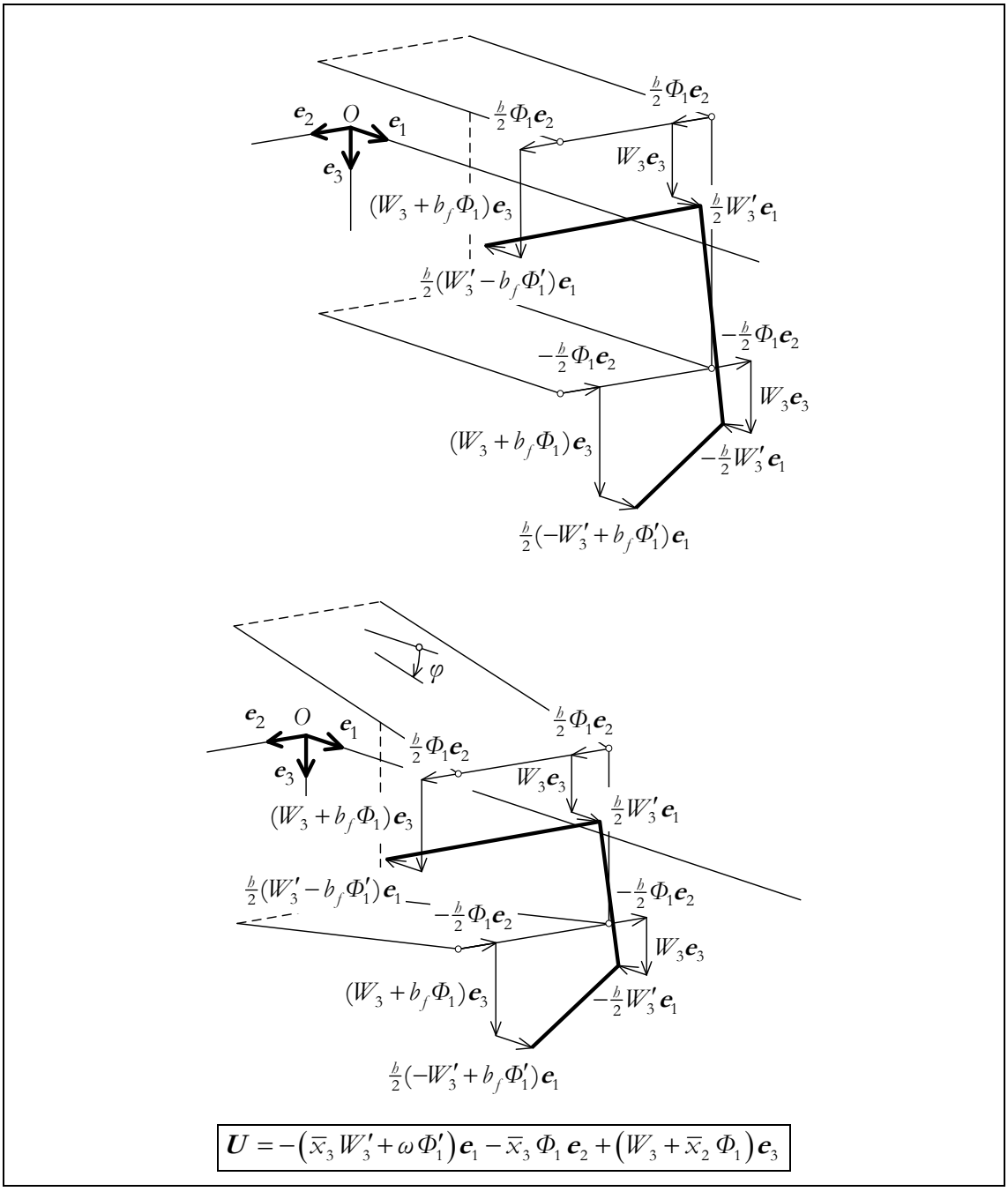

Figure 2.11.17: Contrasting the flexural-torsional behaviours of prismatic and web-tapered singly symmetric C-section bars – Displacement field of cross-section middle line

$$N_f(\theta^1) = \tilde{E}\frac{h(\theta^1)}{2} b_f\, t_f \cos^2\varphi\, W_3''(\theta^1) - \tilde{E}\, b_f^2\, t_f \cos^2\varphi\left(\frac{h(\theta^1)}{4}\Phi_1''(\theta^1) - \tan\varphi\,\Phi_1'(\theta^1)\right)$$

$$= \tilde{E}\frac{h(\theta^1)}{2} b_f\, t_f \cos^2\varphi\, W_3''(\theta^1)$$

$$+ \frac{1}{h(\theta^1)\cos\varphi}\left(\tilde{E} I_{2\omega}^*(\theta^1)\Phi_1''(\theta^1) + \tilde{E} I_{2\psi}^*(\theta^1)\Phi_1'(\theta^1)\right), \qquad (2.11.70)$$

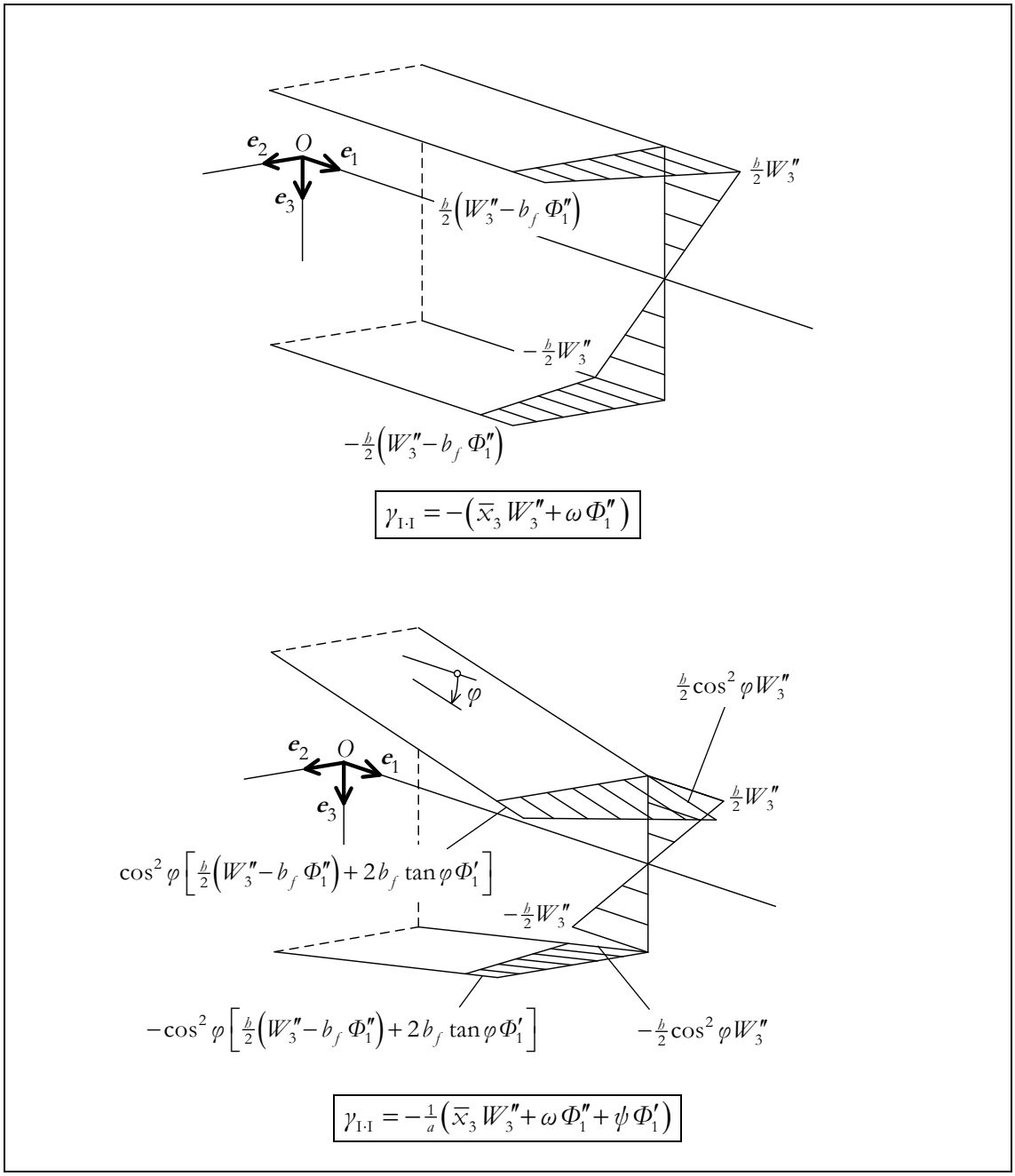

Figure 2.11.18: Contrasting the flexural-torsional behaviours of prismatic and web-tapered singly symmetric C-section bars – Membrane strains $\gamma_{\mathrm{I\cdot I}}$

with N_f acting along the junctions between the web and the flanges. Observe that

$$M_w(\theta^1)+\cos\varphi\,N_f(\theta^1)\,h(\theta^1)=\tilde{E}I_2^*(\theta^1)W_3''(\theta^1)+\tilde{E}I_{2\omega}^*(\theta^1)\Phi_1''(\theta^1)+\tilde{E}I_{2\psi}^*(\theta^1)\Phi_1'(\theta^1)$$
$$=-M_2(\theta^1) \tag{2.11.71}$$

$$M_f(\theta^1)=\tilde{E}\frac{b_f^3\,t_f}{12}\cos^2\varphi\left(\frac{h}{2}\Phi_1\right)''(\theta^1)-\frac{b_f}{2}N_f(\theta^1)\ . \tag{2.11.72}$$

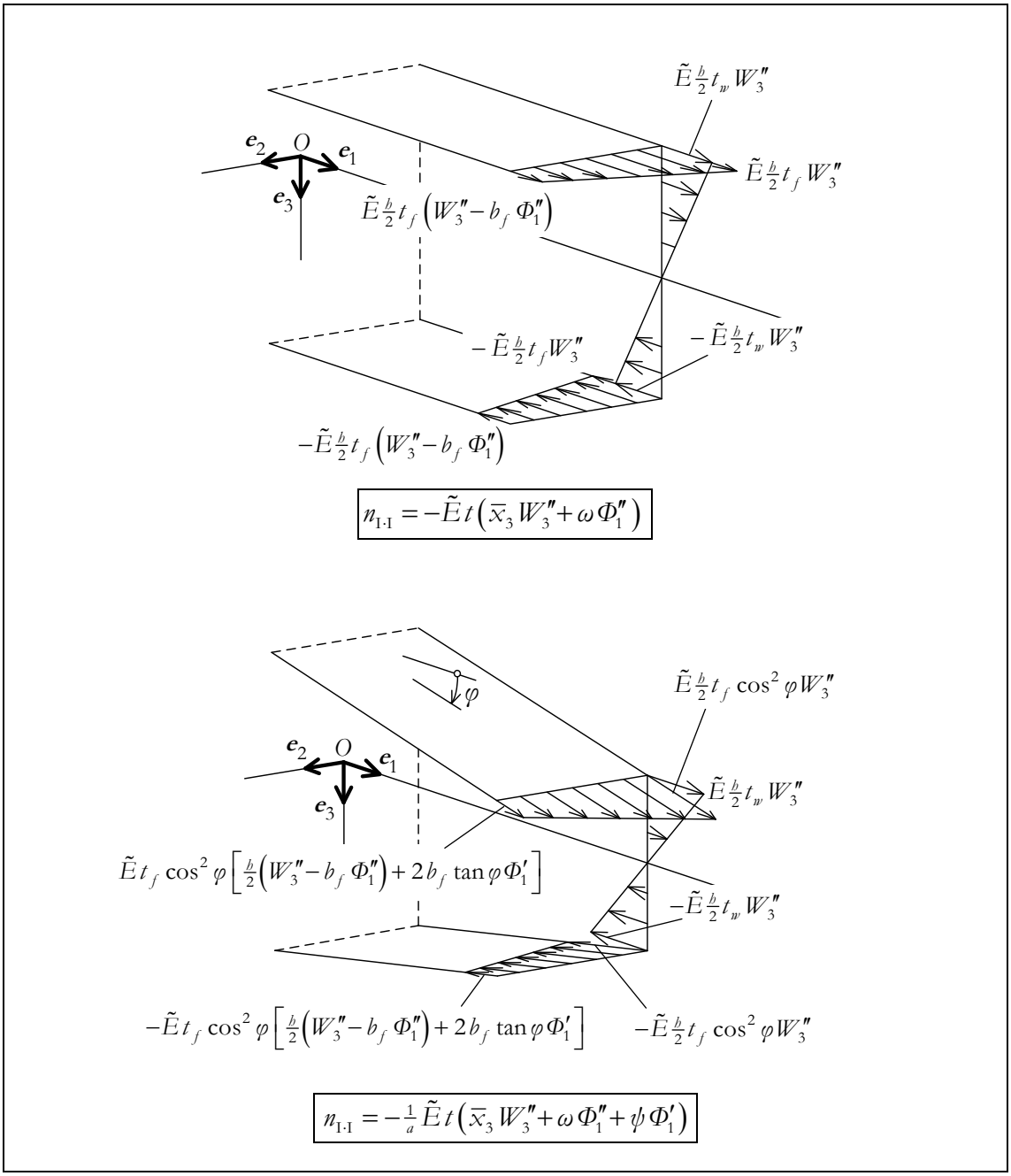

Figure 2.11.19: Contrasting the flexural-torsional behaviours of prismatic and web-tapered singly symmetric C-section bars – Membrane forces $n_{1\cdot\mathrm{I}}$ (active)

(iv) The shear forces developed in the web and in each flange can now be found by equilibrium considerations. Indeed, one must have (see figure 2.11.21)

$$V_w(\theta^1)+2\sin\varphi\, N_f(\theta^1)=V_3(\theta^1)=M_2'(\theta^1) \tag{2.11.73}$$

$$V_f(\theta^1)=\cos\varphi\, M_f'(\theta^1)\ , \tag{2.11.74}$$

whence

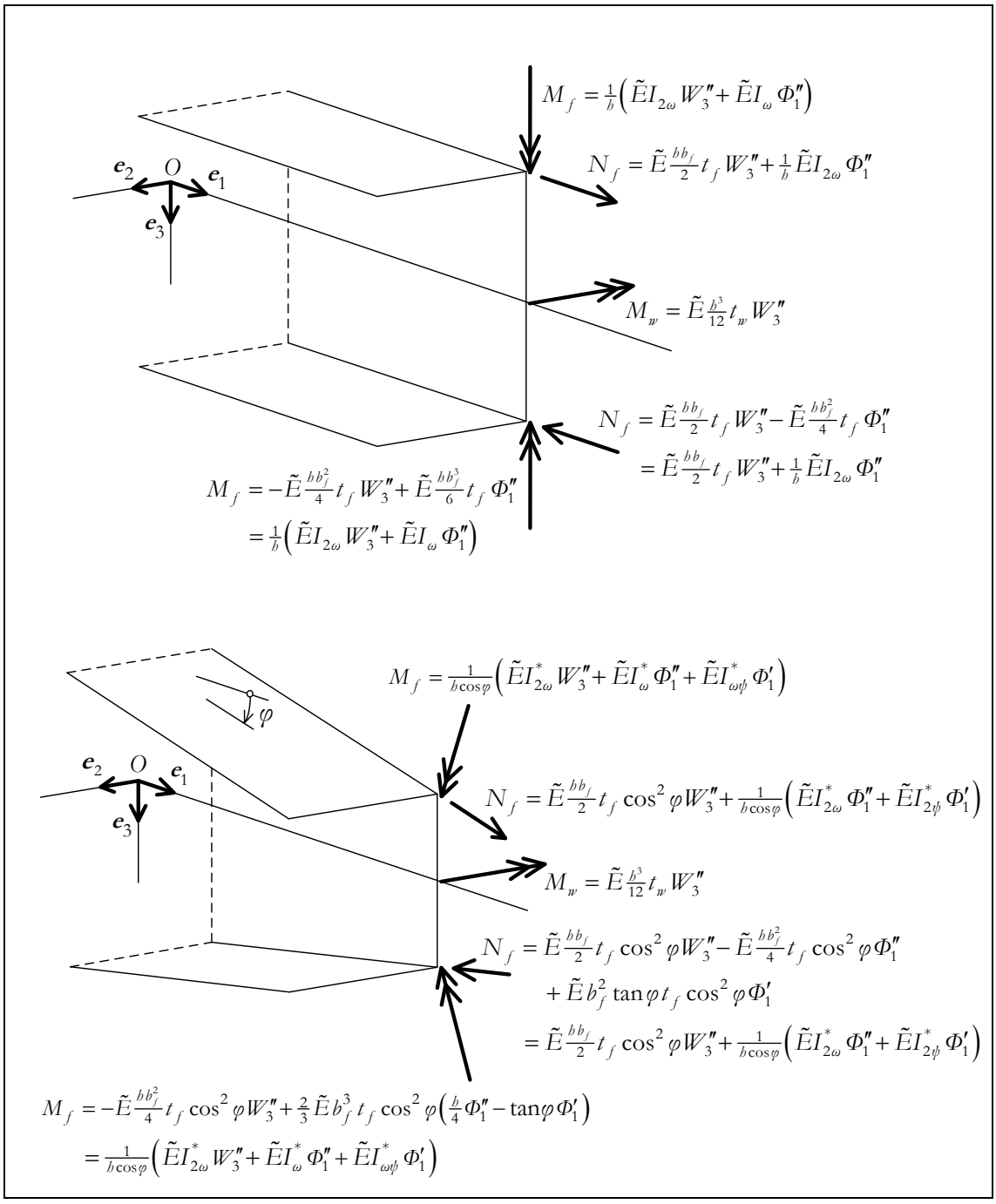

Figure 2.11.20: Contrasting the flexural-torsional behaviours of prismatic and web-tapered singly symmetric C-section bars – Force system statically equivalent to the membrane forces $n_{1\cdot1}$ in the web and in the flanges

$$V_w(\theta^1) = -\tilde{E}I_2^*(\theta^1)W_3'''(\theta^1) + \tilde{E}\left(\frac{h(\theta^1)^2}{2}\tan\varphi\, t_w + h(\theta^1)b_f \tan\varphi\, t_f \cos^3\varphi\right)W_3''(\theta^1)$$

$$-\tilde{E}I_{2\omega}^*(\theta^1)\Phi_1'''(\theta^1) - \frac{3}{2}\tilde{E}I_{2\psi}^*(\theta^1)\Phi_1''(\theta^1) \qquad (2.11.75)$$

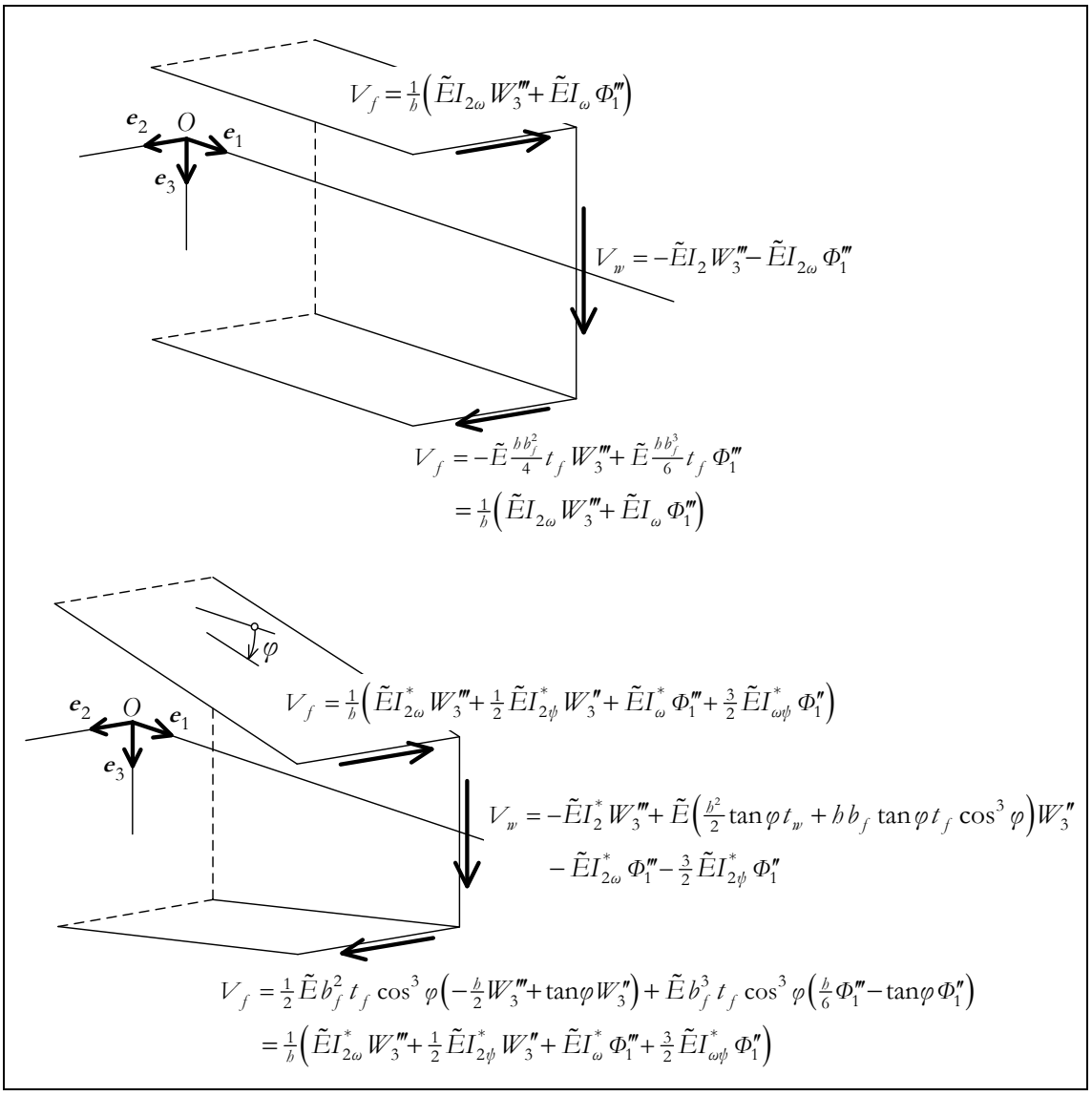

Figure 2.11.21: Contrasting the flexural-torsional behaviours of prismatic and web-tapered singly symmetric C-section bars – Shear forces in the flanges (V_f) and in the web (V_w)

$$
\begin{aligned}
V_f(\theta^1) &= \frac{1}{2}\tilde{E}b_f^2 t_f \cos^3\varphi\left(-\frac{h(\theta^1)}{2}W_3'''(\theta^1) + \tan\varphi\, W_3''(\theta^1)\right) \\
&\quad + \tilde{E}b_f^3 t_f \cos^3\varphi\left(\frac{h(\theta^1)}{6}\Phi_1'''(\theta^1) - \tan\varphi\,\Phi_1''(\theta^1)\right) \\
&= \frac{1}{h(\theta^1)}\left(\tilde{E}I^*_{2\omega}(\theta^1)W_3'''(\theta^1) + \frac{1}{2}\tilde{E}I^*_{2\psi}(\theta^1)W_3''(\theta^1)\right. \\
&\quad \left. + \tilde{E}I^*_{\omega}(\theta^1)\Phi_1'''(\theta^1) + \frac{3}{2}\tilde{E}I^*_{\omega\psi}(\theta^1)\Phi_1''(\theta^1)\right) .
\end{aligned}
\tag{2.11.76}
$$

(v) In web-tapered bars, the flange bending moments have an axial component that totals

$$-2\sin\varphi\, M_f(\theta^1)\,\boldsymbol{e}_1 = -\frac{2\tan\varphi}{h(\theta^1)}\left(\tilde{E}I^*_{2\omega}(\theta^1)W_3''(\theta^1)+\tilde{E}I^*_{\omega}(\theta^1)\Phi_1''(\theta^1)+\tilde{E}I^*_{\omega\psi}(\theta^1)\Phi_1'(\theta^1)\right)\boldsymbol{e}_1$$

$$=-\frac{1}{2}\left(\tilde{E}I^*_{2\psi}(\theta^1)W_3''(\theta^1)+\tilde{E}I^*_{\omega\psi}(\theta^1)\Phi_1''(\theta^1)+\tilde{E}I^*_{\psi}(\theta^1)\Phi_1'(\theta^1)\right)\boldsymbol{e}_1\,. \quad (2.11.77)$$

In complete agreement with the general definition (2.7.6), the torque is thus given by

$$M_1(\theta^1) = -2\sin\varphi\, M_f(\theta^1) - V_f(\theta^1)h(\theta^1) + GJ(\theta^1)\Phi_1'(\theta^1)$$

$$=-\tilde{E}I^*_{2\omega}(\theta^1)W_3'''(\theta^1)-\tilde{E}I^*_{\omega}(\theta^1)\Phi_1'''(\theta^1)-\tilde{E}I^*_{\omega\psi}(\theta^1)\Phi_1''(\theta^1)$$

$$+\left(GJ(\theta^1)+\frac{1}{2}\tilde{E}I^*_{\psi}(\theta^1)\right)\Phi_1'(\theta^1)\ . \quad (2.11.78)$$

Obviously, the contribution of the flange bending moments to the torque is absent in prismatic bars. Finally, notice that

$$\cos\varphi\, M_f(\theta^1) = \frac{1}{h(\theta^1)}\left(\tilde{E}I^*_{2\omega}(\theta^1)W_3''(\theta^1)+\tilde{E}I^*_{\omega}(\theta^1)\Phi_1''(\theta^1)+\tilde{E}I^*_{\omega\psi}(\theta^1)\Phi_1'(\theta^1)\right)$$

$$=-\frac{B(\theta^1)}{h(\theta^1)}\ , \quad (2.11.79)$$

exactly as in the first illustrative example.

(vi) To split the torque (2.11.78) into active and reactive parts, we start by plugging (2.11.79) into (2.11.74), thus obtaining

$$V_f(\theta^1) = -\frac{1}{h(\theta^1)}\left(B'(\theta^1)+\frac{2\tan\varphi}{h(\theta^1)}B(\theta^1)\right)\,. \quad (2.11.80)$$

The active and reactive parts of the torque are then given by

$$M_1^{(A)}(\theta^1) = -2\sin\varphi\, M_f(\theta^1)+\frac{2\tan\varphi}{h(\theta^1)}B(\theta^1)+GJ(\theta^1)\Phi_1'(\theta^1)$$

$$=\tilde{E}I^*_{2\psi}(\theta^1)W_3''(\theta^1)+\tilde{E}I^*_{\omega\psi}(\theta^1)\Phi_1''(\theta^1)+\left(GJ(\theta^1)+\tilde{E}I^*_{\psi}(\theta^1)\right)\Phi_1'(\theta^1) \quad (2.11.81)$$

$$M_1^{(R)}(\theta^1) = B'(\theta^1) = -\left(\tilde{E}I^*_{2\omega}W_3''+\tilde{E}I^*_{\omega}\Phi_1''+\tilde{E}I^*_{\omega\psi}\Phi_1'\right)'(\theta^1)\ , \quad (2.11.82)$$

in accordance with the general definitions (2.7.21)-(2.7.22).

Let us now return to the boundary value problem (2.11.58)-(2.11.67). From the differential equation (2.11.58), one obtains by successive integration

$$\left(\tilde{E}I_2^* W_3'' + \tilde{E}I_{2\omega}^* \Phi_1'' + \tilde{E}I_{2\psi}^* \Phi_1'\right)'(\theta^1) = c_1 \tag{2.11.83}$$

$$\tilde{E}I_2^*(\theta^1) W_3''(\theta^1) + \tilde{E}I_{2\omega}^*(\theta^1) \Phi_1''(\theta^1) + \tilde{E}I_{2\psi}^*(\theta^1) \Phi_1'(\theta^1) = c_1 \theta^1 + c_2 \ , \tag{2.11.84}$$

with $0 < \theta^1 < L$ and $c_1, c_2 \in \mathbb{R}$. Since W_3 and Φ_1 are required to be four times continuously differentiable on $[0, L]$, it follows from the "principle of extension of identities" (BOURBAKI 2007, p. 53, or DIEUDONNÉ 1960, th. 3.15.2) that these equations hold at the end points $\theta^1 = 0$ and $\theta^1 = L$ as well. The boundary conditions (2.11.62)-(2.11.63) then imply

$$c_1 = -Q_{L.3} \tag{2.11.85}$$

$$c_2 = L\, Q_{L.3} \ . \tag{2.11.86}$$

Consequently, we may write

$$W_3''(\theta^1) = -\frac{1}{\tilde{E}I_2^*(\theta^1)}\left(\tilde{E}I_{2\omega}^*(\theta^1) \Phi_1''(\theta^1) + \tilde{E}I_{2\psi}^*(\theta^1) \Phi_1'(\theta^1) + Q_{L.3}(\theta^1 - L)\right), \ 0 \le \theta^1 \le L, \tag{2.11.87}$$

Similarly, from (2.11.59) and (2.11.66), together with continuity considerations, we conclude that

$$\begin{aligned} &-\left(\tilde{E}I_{2\omega}^* W_3'' + \tilde{E}I_{\omega}^* \Phi_1'' + \tilde{E}I_{\omega\psi}^* \Phi_1'\right)'(\theta^1) + \tilde{E}I_{2\psi}^*(\theta^1) W_3''(\theta^1) \\ &\quad + \tilde{E}I_{\omega\psi}^*(\theta^1) \Phi_1''(\theta^1) + \left(GJ(\theta^1) + \tilde{E}I_{\psi}^*(\theta^1)\right) \Phi_1'(\theta^1) = 0 \ , \ 0 \le \theta^1 \le L \ . \end{aligned} \tag{2.11.88}$$

In fact, these two equations are merely the specialisation of (2.7.4) and (2.7.6). In particular, equation (2.11.87) puts us in a position to eliminate W_3 and formulate the illustrative example in terms of the single dependent variable Φ_1. Bearing in mind (2.11.54)-(2.11.56), we have:

Illustrative example 2 (reduced version).

Find $\Phi_1 : [0, L] \to \mathbb{R}$, with $\Phi_1 \in C^4[0, L]$, satisfying, on the open interval $(0, L)$, the ordinary differential equation

$$\begin{aligned} &\tilde{E}I_{2\omega}^*(\theta^1)\left[\frac{1}{\tilde{E}I_2^*}\left(\tilde{E}I_{2\omega}^* \Phi_1'' + \tilde{E}I_{2\psi}^* \Phi_1' + M_2\right)\right]'(\theta^1) \\ &\quad - \tilde{E}I_{\omega}^*(\theta^1) \Phi_1'''(\theta^1) - \tilde{E}I_{\omega\psi}^*(\theta^1) \Phi_1''(\theta^1) + \left(GJ(\theta^1) + \frac{1}{2}\tilde{E}I_{\psi}^*(\theta^1)\right) \Phi_1'(\theta^1) = 0 \end{aligned} \tag{2.11.89}$$

where $M_2(\theta^1) = Q_{L.3}(\theta^1 - L)$, together with the boundary conditions

$$\Phi_1(0) = 0 \tag{2.11.90}$$

$$\Phi_1'(0) = 0 \tag{2.11.91}$$

$$-\frac{\tilde{E}I^*_{2\omega}(L)}{\tilde{E}I^*_{2}(L)}\left(\tilde{E}I^*_{2\omega}(L)\Phi_1''(L)+\tilde{E}I^*_{2\psi}(L)\Phi_1'(L)\right)$$

$$+\tilde{E}I^*_{\omega}(L)\Phi_1''(L)+\tilde{E}I^*_{\omega\psi}(L)\Phi_1'(L)=0\ . \qquad (2.11.92)$$

Once Φ_1 is known, W_3 can be obtained by solving the *initial* value problem defined by (2.11.87) and (2.11.60)-(2.11.61).

In the prismatic case ($\alpha=1$), the solution to the illustrative example 2 is (*e.g.*, CHEN & ATSUTA 1977, p. 48)

$$\Phi_1(\theta^1)=\frac{Q_{L.3}\,d}{GJ}\sqrt{\frac{\tilde{E}I_{\omega_S}}{GJ}}\left[-\tanh\left(\sqrt{\frac{GJ\,L^2}{\tilde{E}I_{\omega_S}}}\right)+\tanh\left(\sqrt{\frac{GJ\,L^2}{\tilde{E}I_{\omega_S}}}\right)\cosh\left(\sqrt{\frac{GJ}{\tilde{E}I_{\omega_S}}}\,\theta^1\right)\right.$$

$$\left.-\sinh\left(\sqrt{\frac{GJ}{\tilde{E}I_{\omega_S}}}\,\theta^1\right)+\sqrt{\frac{GJ}{\tilde{E}I_{\omega_S}}}\,\theta^1\right] \qquad (2.11.93)$$

$$W_3(\theta^1)=\frac{Q_{L.3}\,L}{2\,\tilde{E}I_2}\left(1-\frac{\theta^1}{3L}\right)(\theta^1)^2+d\,\Phi_1(\theta^1)\ ,\quad 0\le\theta^1\le L\ , \qquad (2.11.94)$$

where

$$d=\frac{3\,b_f^2\,t_f}{h_0\,t_w+6\,b_f\,t_f} \qquad (2.11.95)$$

is the distance from the web middle line to the shear centre and

$$I_{\omega_S}=\frac{h_0^2\,b_f^3\,t_f}{12}\,\frac{2\,h_0\,t_w+3\,b_f\,t_f}{h_0\,t_w+6\,b_f\,t_f} \qquad (2.11.96)$$

is the sectorial moment of inertia for the sectorial coordinate ω_S with pole at the shear centre and origin at the corresponding sectorial centroid (midpoint of the web middle line) – *e.g.*, ODEN & RIPPERGER (1981, table 7.1) or VLASOV (1961, p. 61).

In the tapered case ($0<\alpha<1$), no closed-form solution is available. We considered

$L=4500\,\text{mm}$ $\quad h_0=500\,\text{mm}$ $\quad t_w=12\,\text{mm}$ $\quad b_f=150\,\text{mm}$ $\quad t_f=18\,\text{mm}$

$\tilde{E}=210\,\text{GPa}$ $\quad G=80.77\,\text{GPa}$

and used the mathematical software package Mathematica (WOLFRAM RESEARCH, INC. 2006) to obtain numerical solutions for selected values of the web taper ratio α, ranging from 0.4 to 1.0. The results are plotted in figure 2.11.22 (solid lines). For comparison purposes, the results obtained by adopting a stepped model are also presented (dashed lines).

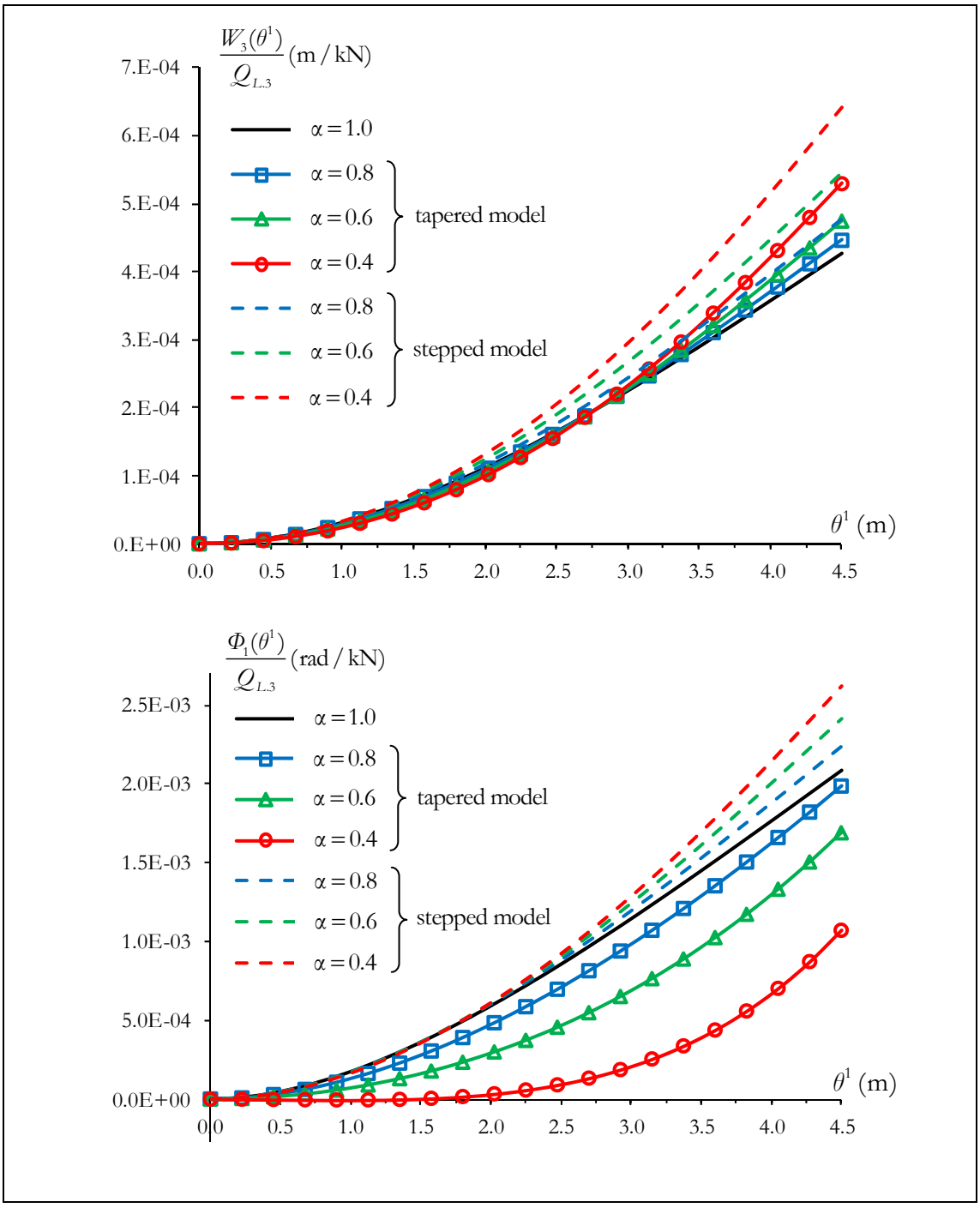

Fig. 2.11.22: Illustrative example 2 – Vertical deflections $\theta^1 \mapsto W_3(\theta^1)$ and twists $\theta^1 \mapsto \Phi_1(\theta^1)$ per unit load $Q_{L.3}$

For fixed θ^1 in the interval $(0, L]$, the tapered model yields decreasing values of $\Phi_1(\theta^1) / Q_{L.3}$ with decreasing α – this is the most striking feature about the plots in figure 2.11.22. In particular, the stiffness $Q_{L.3} / \Phi_1(L)$ is a strictly decreasing function of α, as shown in figure 2.11.23, and falls outside the dotted-line envelope corresponding to prismatic

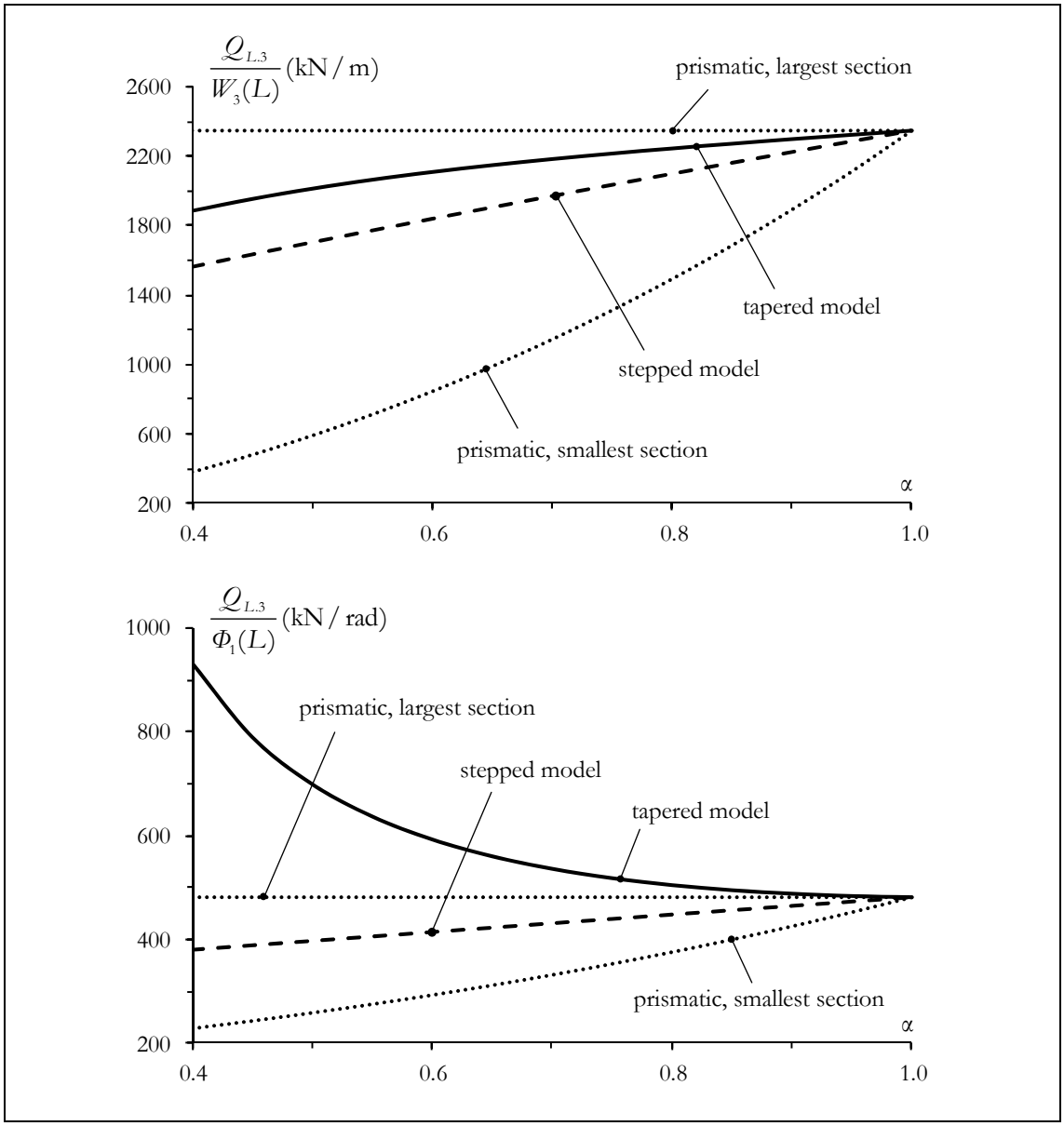

Fig. 2.11.23: Illustrative example 2 – Stiffnesses $Q_{L.3} / W_3(L)$ and $Q_{L.3} / \Phi_1(L)$ *versus* the taper ratio α

cantilevers with the largest and the smallest cross-sectional dimensions, *i.e.*, with web depth h_0 and αh_0, respectively. This surprising, if not paradoxical, result can be explained by observing that $\Phi_1'(\theta^1) / Q_{L.3}$, which provides the warping amplitude per unit load $Q_{L.3}$, also decreases with decreasing α over a considerable length – a reversal in this trend is only noticeable near the tip of the cantilever. In fact, for $\alpha = 0.4$, we have $\Phi_1'(\theta^1) / Q_{L.3} \cong 0$ – *i.e.*, warping is effectively prevented – over the first quarter-span. The depth taper thus acts as an internal warping restraint over much of the span, the effectiveness of which increases as the flanges become more steeply inclined. Such a physical interpretation is consistent with the bimoment distributions per unit load $Q_{L.3}$ shown in figure 2.11.24, which exhibit

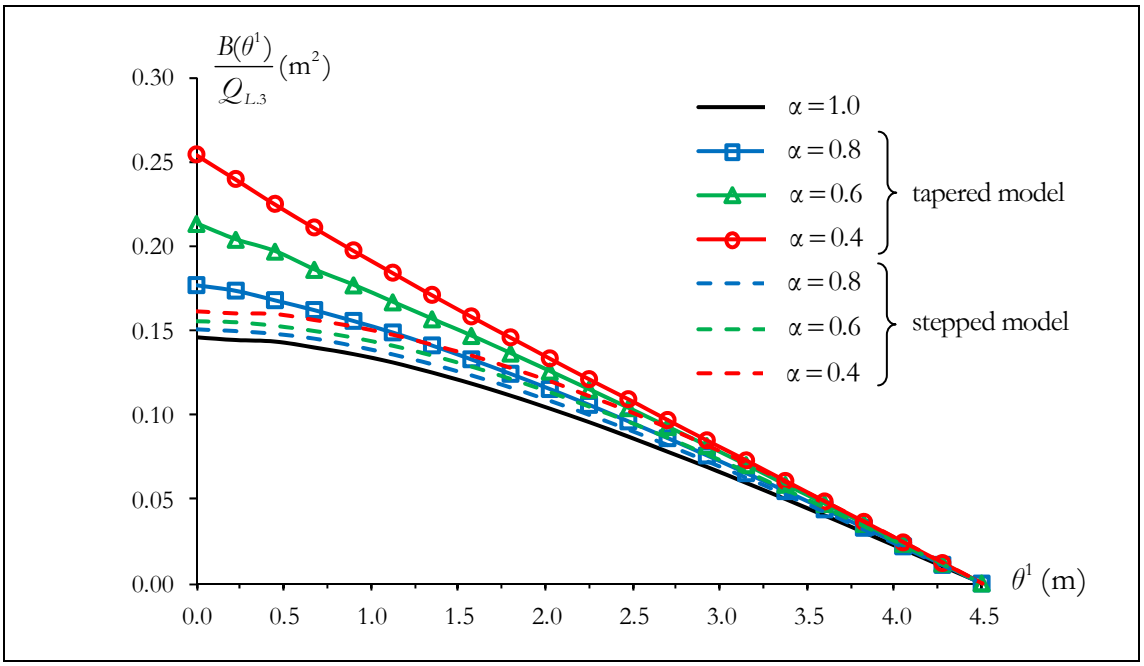

Fig. 2.11.24: Illustrative example 2 – Bimoment distributions $\theta^1 \mapsto B(\theta^1)$ per unit load $Q_{L.3}$

a marked increase at the clamped end as α decreases. The stepped model is notoriously incapable of capturing this internal warping restraint. Indeed, near the clamped end, the twist $\Phi_1(\theta^1)$ and its derivative $\Phi_1'(\theta^1)$ per unit $Q_{L.3}$ as provided by the stepped model are practically independent of α and coincident with the prismatic solution ($\alpha = 1.0$).

REFERENCES

ABRAHAM R., MARSDEN J.E. and RATIU T. (1988). *Manifolds, Tensor Analysis, and Applications* (2nd edition). New York: Springer.

ANDRADE A., PROVIDÊNCIA P. and CAMOTIM D. (2010). Elastic lateral-torsional buckling of restrained web-tapered I-beams. *Computers & Structures*, **88**(21-22), 1179-1196.

ANTMAN S.S. (1972). The theory of rods. *Handbuch der Physik*, Volume VIa/2, C. Truesdell (Ed.). Berlin: Springer, 641-703.

ANTMAN S.S. and MARLOW R.S. (1991). Material constraints, Lagrange multipliers, and compatibility – Applications to rod and shell theories. *Archive for Rational Mechanics and Analysis*, **116**(3), 257-299.

AVEZ A. (1983). *Calcul Différentiel* [Differential Calculus]. Paris: Masson.

AXELSSON O. and BARKER V.A. (1984). *Finite Element Solution of Boundary Value Problems – Theory and Computation*. Orlando, Florida: Academic Press.

BACH C. (1909). Versuche über die tatsächliche Widerstandsfähigkeit von Balken mit C-förmigem Querschnitt [Experiments on the actual strength of beams with C-shaped cross-section]. *Zeitschrift des Vereines deutscher Ingenieure*, **53**, 1790-1795.

BACH C. (1910). Versuche über die tatsächliche Widerstandsfähigkeit von Trägern mit C-förmigem Querschnitt [Experiments on the actual strength of beams with C-shaped cross-section]. *Zeitschrift des Vereines deutscher Ingenieure*, **54**, 382-387.

BARTLE R.G. (1967). *The Elements of Real Analysis*. New York: Wiley.

BAZANT Z.P. (1965). Non uniform torsion of thin walled bars of variable section. *IABSE Publications*, **25**, 17-39.

BÉCHET F., MILLET O. and SANCHEZ-PALENCIA E. (2010). Limit behavior of Koiter model for long cylindrical shells and Vlassov model. *International Journal of Solids and Structures*, **47**(3-4), 365–373.

BERGER M. and GOSTIAUX B. (1987). *Géométrie Différentielle: Variétés, Courbes et Surfaces*. Paris: Presses Universitaires de France. English translation by S. Levy (1988), *Differential Geometry: Manifolds, Curves, and Surfaces*. New York: Springer.

BILLINGTON D.P. (1997). *Robert Maillart – Builder, Designer, and Artist*. Cambridge: Cambridge University Press.

BIRKHOFF G. (1960). *Hydrodynamics – A Study in Logic, Fact and Similitude*. Princeton, New Jersey: Princeton University Press.

BLEICH F. (1952). *Buckling Strength of Metal Structures*, H.H. Bleich (Ed.). New York: McGraw-Hill.

BLEICH F. and BLEICH H. (1936). Bending, torsion and buckling of bars composed of thin walls. *IABSE Congress Report*, Volume 2, 871-894.

BLOCH E.D. (1997). *A First Course in Geometric Topology and Differential Geometry*. Boston: Birkhäuser.

BLOUZA A. and LE DRET H. (1999). Existence and uniqueness for the linear Koiter model for shells with little regularity. *Quarterly of Applied Mathematics*, **57**(2), 317-337.

BLUMAN G.W. and ANCO S.C. (2002). *Symmetry and Integration Methods for Differential Equations*. New York: Springer.

BOURBAKI N. (2007). *Éléments de Mathématique – Topologie Générale (Chapitres 1 à 4)* [Elements of Mathematics – General Topology (Chapters 1 to 4)]. Berlin: Springer.

BOYLING J.B. (1979). A short proof of the Pi theorem of dimensional analysis. *Zeitschrift für angewandte Mathematik und Physik*, **30**(3), 531-533.

BRAND L. (1957). The pi-theorem of dimensional analysis. *Archive for Rational Mechanics and Analysis*, **1**(1), 35-45.

BRIDGMAN P.W. (1931). *Dimensional Analysis* (2nd edition). New Haven, Connecticut: Yale University Press.

BUCKINGHAM E. (1914). On physically similar systems; illustrations of the use of dimensional equations. *Physical Review*, **4**(4), 345-376.

BUCKINGHAM E. (1915). Model experiments and the forms of empirical equations. *Transactions of the ASME*, **37**, 263-296.

BUCKINGHAM E. (1921). Notes on the method of dimensions. *Philosophical Magazine* (Series 6), **42**(251), 696-719.

CAMPOS FERREIRA J. (1987). *Introdução à Análise Matemática* [Introduction to Mathematical Analysis]. Lisboa: Fundação Calouste Gulbenkian.

CARMO M.P. (1976). *Differential Geometry of Curves and Surfaces*. Englewood Cliffs, New Jersey: Prentice-Hall.

CHEN W.F. and ATSUTA T. (1977). *Theory of Beam-Columns*, Volume 2: Space Behavior and Design. New York: McGraw-Hill.

CIARLET P.G. (1988). *Mathematical Elasticity*, Volume 1: Three-Dimensional Elasticity. Amsterdam: Elsevier.

CIARLET P.G. (2000). *Mathematical Elasticity*, Volume 3: Theory of Shells. Amsterdam: Elsevier.

CIARLET P.G. (2005). An introduction to differential geometry with applications to elasticity. *Journal of Elasticity*, **78-79**(1-3), 1-215.

CORRSIN S. (1951). A simple geometrical proof of Buckingham's π-theorem. *American Journal of Physics*, **19**(3), 180-181.

CURIE P. (1894). Sur la symétrie des phénomènes physiques: Symétrie d'un champ électrique et d'un champ magnétique [On symmetry in physical phenomena: Symmetry of an electric field and of a magnetic field]. *Journal de Physique*, 3^{e} Série, 393-415.

CURTIS W.D., LOGAN J.D. and PARKER W.A. (1982). Dimensional analysis and the pi theorem. *Linear Algebra and Its Applications*, **47**, 117-126.

CYWINSKI Z. and KOLLBRUNNER C.F. (1971). *Drillknicken dünnwandiger I-Stäbe mit veränderlichen, doppelt-symmetrischen Querschnitten* [Torsional buckling of thin-walled I-bars with variable, doubly symmetric cross-sections]. Institut für Bauwissenschaftliche Forschung, Zürich.

DACOROGNA B. (2004). *Introduction to the Calculus of Variations*. London: Imperial College Press.

DAVÍ F. (1992). The theory of Kirchhoff rods as an exact consequence of three-dimensional elasticity. *Journal of Elasticity*, **29**(3), 243-262.

DAVÍ F. (1993). On the constraint and scaling methods to derive the equations of linearly elastic rods. *Meccanica*, **28**(3), 203-208.

DIAS DA SILVA V. (2006). *Mechanics and Strength of Materials*. Berlin: Springer.

DICARLO A., PODIO-GUIDUGLI P. and WILLIAMS W.O. (2001). Shells with thickness distension. *International Journal of Solids and Structures*, **38**(6-7), 1201-1225.

DIEUDONNÉ J. (1960). *Foundations of Modern Analysis*. New York: Academic Press.

DUISTERMAAT J.J. and KOLK J.A.C. (2004). *Multidimensional Real Analysis II: Integration*. Cambridge: Cambridge University Press.

EGGENSCHWYLER A. (1920a). Zur Festigkeitslehre [On strength of materials]. *Schweizerische Bauzeitung*, **76**(18), 206–208.

EGGENSCHWYLER A. (1920b). Zur Festigkeitslehre [On strength of materials]. *Schweizerische Bauzeitung*, **76**(23), 266.

EGGENSCHWYLER A. (1921a). *Über die Festigkeitsberechnung von Schiebetoren und ähnlichen Bauwerken* [On the Strength Calculation of Sliding Locks and Similar Structures]. Ph.D. Thesis, Eidgenössischen Technischen Hochschulein Zürich.

EGGENSCHWYLER A. (1921b). Über die Drehungsbeanspruchung von dünnwandigen symmetrischen C-förmigen Querschnitten [On torsional stresses in thin-walled symmetric C-shaped cross-sections]. *Der Eisenbau*, **12**(9), 207–215.

FÖPPL A. (1917a). Über den elastischen Verdrehungswinkel eines Stabes [On the elastic angle of twist of a rod]. *Sitzungsberichte der mathematisch-physikalischen Klasse der Bayerischen Akademie der Wissenschaften zu Munich*, 5–31.

FÖPPL A. (1917b). Der Drillungswiderstand von Walzeisenträgern [The torsion resistance of rolled steel beams]. *Zeitschrift des Vereines deutscher Ingenieure*, **60**(33), pp. 694–695.

FREDDI L., MORASSI A. and PARONI R. (2007). Thin-walled beams: A derivation of Vlassov theory via Γ-convergence. *Journal of Elasticity*, **86**(3), 263-296.

FUNG Y.C. (1965). *Foundations of Solid Mechanics*. Englewood Cliffs, New Jersey: Prentice-Hall.

FUNG Y.C. (1993). *An Introduction to the Theory of Aeroelasticity*. New York: Dover.

GIBBINGS J.C. (2011). *Dimensional Analysis*. London: Springer.

GJELSVIK A. (1981). *The Theory of Thin Walled Bars*. New York: Wiley.

GREEN A.E., LAWS N. and NAGHDI P.M. (1967). A linear theory of straight elastic rods. *Archive for Rational Mechanics and Analysis*, **25**(4), 285-298.

GREEN A.E. and ZERNA W. (1968). *Theoretical Elasticity* (2nd edition). London: Oxford University Press.

GRILLET L., HAMDOUNI A. and ALLERY C. (2000). Modèle asymptotique linéaire de poutres voiles fortement courbés [Linear asymptotic model for thin-walled beams with strongly curved cross-section profile]. *Comptes Rendus de l'Académie des Sciences – Série IIb*, **328**(8), 587-592.

GRILLET L., HAMDOUNI A. and MILLET O. (2005). Justification of the kinematic assumptions for thin-walled rods with shallow profile. *Comptes Rendus Mécanique*, **333**(6), 493-498.

GURTIN M.E. (1972). The linear theory of elasticity. *Handbuch der Physik*, Volume VIa/2, C. Truesdell (Ed.). Berlin: Springer, 1-295.

GURTIN M.E. (1981). *An Introduction to Continuum Mechanics*. New York: Academic Press.

HAMDOUNI A. and MILLET O. (2011). An asymptotic linear thin-walled rod model coupling twist and bending. *International Applied Mechanics*, **46**(9), 1072-1092.

HOFFMAN K. and KUNZE R. (1971). *Linear Algebra* (2nd edition). Englewood Cliffs, New Jersey: Prentice-Hall.

KAPPUS R. (1937). Drillknicken zentrisch gedrückter Stäbe mit offenen Profil im elastischen Bereich. *Luftfahrtforschung*, **14**(9), 444-457. English translation by J. Vanier (1938), *Twisting Failure of Centrally Loaded Open-Section Columns in the Elastic Range*, National Advisory Committee for Aeronautics (NACA), Technical Memorandum n. 851.

KELLEY J.L. (1985). *General Topology*. New York: Springer.

KITIPORNCHAI S. and TRAHAIR N.S. (1972). Elastic stability of tapered I-beams. *Journal of the Structural Division – ASCE*, **98**(3), 713-728.

KITIPORNCHAI S. and TRAHAIR N.S. (1975). Elastic behavior of tapered monosymmetric I-beams. *Journal of the Structural Division – ASCE*, **101**(8), 1661-1678.

KITIPORNCHAI S. and TRAHAIR N.S. (1980). Buckling properties of monosymmetric I-beams. *Journal of the Structural Division – ASCE*, **106**(5), 941-957.

KREFELD W.J., BUTLER D.J. and ANDERSON G.B. (1959). Welded cantilever wedge beams. *Welding Journal Research Supplement*, **38**(3), 97s-112s.

KÜHNEL W. (2005). *Differential Geometry: Curves – Surfaces – Manifolds* (2nd edition). Providence, Rhode Island: American Mathematical Society.

KURRER K.-E. (2008). *The History of the Theory of Structures – From Arch Analysis to Computational Mechanics*. Berlin: Ernst & Sohn.

LANCZOS C. (1996). *Linear Differential Operators*. Philadelphia: Society for Industrial and Applied Mathematics (SIAM).

LANGHAAR H.L. (1951). *Dimensional Analysis and Theory of Models*. New York: Wiley.

LEE G.C. and SZABO B.A. (1967). Torsional response of tapered I-girders. *Journal of the Structural Division – ASCE*, **93**(5), 233-252.

LEE L.H.N. (1956). Non uniform torsion of tapered I-beams. *Journal of the Franklin Institute*, **262**(July), 37-44.

LEKHNITSKII S.G. (1963). *Theory of Elasticity of an Anisotropic Elastic Body*. San Francisco: Holden-Day.

LEMBO M. (1989). The membranal and flexural equations of thin elastic plates deduced exactly from the three-dimensional theory. *Meccanica*, **24**(2), 93-97.

LEMBO M. and PODIO-GUIDUGLI P. (1991). Plate theory as na exact consequence of three-dimensional elasticity. *European Journal of Mechanics – A/Solids*, **10**(5), 485-516.

LEMBO M. and PODIO-GUIDUGLI P. (2001). Internal constraints, reactive stresses, and the Timoshenko beam theory. *Journal of Elasticity*, **65**(1-3), 131-148.

LEMBO M. and PODIO-GUIDUGLI P. (2007). How to use reactive stresses to improve plate-theory approximations of the stress field in a linearly elastic plate-like body. *International Journal of Solids and Structures*, **44**(5), 1337-1369.

LIMA E.L. (1989). *Curso de Análise* [A Course in Analysis], Volume 2 (3rd edition). Rio de Janeiro: Instituto de Matemática Pura e Aplicada.

LOGAN J.D. (2006). *Applied Mathematics* (3rd edition). Hoboken, New Jersey: Wiley.

LOVE A.E.H. (1944). *A Treatise on the Mathematical Theory of Elasticity* (4th edition). New York: Dover.

MAGALHÃES L.T. (2003). *Álgebra Linear como Introdução à Matemática Aplicada* [Linear Algebra as an Introduction to Applied Mathematics] (9th edition). Lisboa: Texto Editora.

MAILLART R. (1921a). Zur Frage der Biegung [On the problem of bending]. *Schweizerische Bauzeitung*, **77**(18), 195-197.

MAILLART R. (1921b). Bemerkungen zur Frage der Biegung [Comments on the problem of bending]. *Schweizerische Bauzeitung*, **78**(2), 18-19.

MAILLART R. (1924a). Der Schubmittelpunkt [The shear centre]. *Schweizerische Bauzeitung*, **83**(10), 109-111.

MAILLART R. (1924b). Le centre de glissement [The shear centre]. *Bulletin Technique de la Suisse Romande*, **50**, 158-162.

MASON J. (1980). *Variational, Incremental and Energy Methods in Solid Mechanics and Shell Theory*. Amsterdam: Elsevier.

MASSONNET C. (1968). *Résistance des Matériaux* [Strength of Materials], Volume 1 (2nd edition). Paris: Dunod.

MASSONNET C.E. (1982). Théorie perfectionnée des poutres droites à parois minces [Improved theory for thin-walled straight bars]. *IABSE Proceedings*, **P-55**, 81-95.

MASSONNET C.E. (1983). A new approach (including shear lag) to elementary mechanics of materials. *International Journal of Solids and Structures*, **19**(1), 33-54.

MENDOZA C. (1996). Yet another proof of the π-theorem. *Mechanics Research Communications*, **23**(3), 299-303.

MONTIEL S. and ROS A. (2005). *Curves and Surfaces*. Providence, Rhode Island: American Mathematical Society.

MULLER P. (1983). Torsional-flexural waves in thin-walled open beams. *Journal of Sound and Vibration*, **87**(1), 115-141.

MURRAY N.W. (1986). *Introduction to the Theory of Thin-Walled Structures*. Oxford: Oxford University Press.

NARDINOCCHI P. and PODIO-GUIDUGLI P. (1994). The equations of Reissner-Mindlin plates obtained by the method of internal constraints. *Meccanica*, **29**(2), 143-157.

NARDINOCCHI P. and PODIO-GUIDUGLI P. (2001). Angle plates. *Journal of Elasticity*, **63**(1), 19–53.

NOLL W. and VIRGA E.G. (1988). Fit regions and functions of bounded variation. *Archive for Rational Mechanics and Analysis*, **102**(1), 1-21.

NOWINSKI J. (1959). Theory of thin-walled bars. *Applied Mechanics Reviews*, **12**(4), 219-227.

ODEN J.T. and RIPPERGER E.A. (1981). *Mechanics of Elastic Structures* (2nd edition). Washington: Hemisphere Publishing Corporation.

OPREA J. (2007). *Differential Geometry and Its Applications*. Washington, D.C.: The Mathematical Association of America.

POBEDRYA B.E. and GEORGIEVSKII D.V. (2006). On the proof of the π-theorem in dimension theory. *Russian Journal of Mathematical Physics*, **13**(4), 431-437.

PODIO-GUIDUGLI P. (1989). An exact derivation of the thin plate equation. *Journal of Elasticity*, **22**(2-3), 121-133.

PODIO-GUIDUGLI P. (2000). A primer in elasticity. *Journal of Elasticity*, **58**(1), 1-104.

PODIO-GUIDUGLI P. (2003). A new quasilinear model for plate buckling. *Journal of Elasticity*, **71**(1-3), 157–182.

PODIO-GUIDUGLI P. (2006). On structure thinness, mechanical and variational. *Variational Formulations in Mechanics: Theory and Applications*, E. Taroco, E.A. de Souza Neto and A.A. Novotny (Eds.), Barcelona: CIMNE, 227-242.

PODIO-GUIDUGLI P. (2008). Concepts in the mechanics of thin structures. *Classical and Advanced Theories of Thin Structures – Mechanical and Mathematical Aspects*, CISM Courses and Lectures n. 503, A. Morassi and R. Paroni (Eds.). Wien: Springer, 77-109.

PODIO-GUIDUGLI P. and VIANELLO M. (1992). The representation problem of constrained linear elasticity. *Journal of Elasticity*, **28**(3), 271-276.

REISSNER E. (1973). A History of the center-of-shear concept: Maillart's work and ramifications. *Proceedings of the 2nd National Conference on Civil Engineering: History, Heritage and the Humanities* (Princeton), D.P. Billington, R. Mark and J.F. Abel (Eds.). Princeton, New Jersey: Department of Civil Engineering, Princeton University, 77-96.

REISSNER E. (1979). Some considerations on the problem of torsion and flexure of prismatical beams. *International Journal of Solids and Structures*, **15**(1), 41-53.

REISSNER E. and TSAI W.T. (1972). On the determination of the centers of twist and of shear for cylindrical shell beams. *Journal of Applied Mechanics – Transactions of the ASME*, **39**(4), 1098-1102.

RODRÍGUEZ J.M. and VIAÑO J.M. (1995). Asymptotic general bending and torsion models for thin-walled elastic beams. *Asymptotic Methods for Elastic Structures*, P.G. Ciarlet, L. Trabucho and J.M. Viaño (Eds.). Berlin: Walter de Gruyer, 255-274.

RODRÍGUEZ J.M. and VIAÑO J.M. (1997). Asymptotic derivation of a general linear model for thin-walled elastic rods. *Computer Methods in Applied Mechanics and Engineering*, **147**(3-4), 287-321.

RUDIN W. (1976). *Principles of Mathematical Analysis* (3rd edition). Tokyo: McGraw-Hill.

SAINT-VENANT A.J.C.B. (1865). Sur les divers genres d'homogénéité des corps solides, et principalement sur l'homogénéité semi-polaire ou cylindrique, et sur les homogénéités polaires ou sphériconique et sphérique [On the different types of homogeneity of solid bodies, and chiefly on the semi-polar or cylindrical homogeneity, and on the polar or spherical-conical and spherical homogeneities]. *Journal de Mathématiques Pures et Appliquées* (2ème Série), **10**, 297-349.

SEDOV L.I. (1993). *Similarity and Dimensional Methods in Mechanics* (10th edition). Boca Raton, Florida: CRC Press.

SEWELL M.J. (1987). *Maximum and Minimum Principles – A Unified Approach, with Applications*. Cambridge: Cambridge University Press.

SIMO J.C. and VU-QUOC L. (1991). A geometrically-exact rod model incorporating shear and torsion-warping deformation. *International Journal of Solids and Structures*, **27**(3), 371-393.

SOKOLNIKOFF I.S. (1956). *Mathematical Theory of Elasticity* (2nd edition). New York: McGraw-Hill.

STRANG G. and FIX G.J. (1973). *An Analysis of the Finite Element Method*. Englewood Cliffs, New Jersey: Prentice-Hall.

TIMOSHENKO S.P. (1910). Einige Stabilitätsprobleme der Elastizitätstheorie [Some stability problems in the theory of elasticity]. *Zeitschrift für Mathematik und Physik*, **58**, 337-385. Reprinted in *The Collected Papers of Stephen P. Timoshenko*, 1953. New York: McGraw-Hill, 1-50.

TIMOSHENKO S.P. (1913). Sur la stabilité des systems élastiques [On the stability of elastic systems]. *Annales des Ponts et Chaussées*, 9e Série, Tome XV, Volume 3, 496-566; Tome XVI, Volume 4, 73-132; Tome XVII, Volume 5, 372-412. Reprinted in *The Collected Papers of Stephen P. Timoshenko*, 1953. New York: McGraw-Hill, 92-224.

TIMOSHENKO S.P. (1945). Theory of bending, torsion and buckling of thin-walled members of open cross section. *Journal of the Franklin Institute*, **239**(3, 4 and 5), 201-219, 249-268 and 243-361. Reprinted in *The Collected Papers of Stephen P. Timoshenko*, 1953. New York: McGraw-Hill, 559-609.

TIMOSHENKO S.P. (1968). *As I Remember*. Princeton, New Jersey: Van Nostrand.

TIMOSHENKO S.P. and GERE J.M. (1961). *Theory of Elastic Stability* (2nd edition). New York: McGraw-Hill.

TIMOSHENKO S.P. and GOODIER J.N. (1970). *Theory of Elasticity* (3rd edition). New-York: McGraw-Hill.

TONTI E. (1972a). On the mathematical structure of a large class of physical theories. *Rendiconti della Classe di Scienze Fisiche, Matematiche e Naturali – Accademia Nazionale dei Lincei*, Serie 8, **52**(1), 48-56.

TONTI E. (1972b). A mathematical model for physical theories. *Rendiconti della Classe di Scienze Fisiche, Matematiche e Naturali – Accademia Nazionale dei Lincei*, Serie 8, **52**(2-3), 176-181.

TONTI E. (1975). *On the Formal Structure of Physical Theories*. Milano: Quaderno dei Gruppi di Ricerca Matemática del Consiglio Nazionale delle Ricerche.

TONTI E. (1976). The reason for analogies between physical theories. *Applied Mathematical Modelling*, **1**(1), 37-50.

TRAHAIR N.S. (1993). *Flexural-Torsional Buckling of Structures*. London: E & FN Spon.

TREFFTZ E. (1935). Über den Schubmittelpunkt in einem durch eine Einzellast gebogenen Balken [On the shear centre of a bar bent by a concentrated load]. *Zeitschrift für angewandte Mathematik und Mechanik*, **15**(4), 220-225.

TRUESDELL C. (1991). *A First Course in Rational Continuum Mechanics*, Volume 1: General Concepts (2nd edition). San Diego, California: Academic Press.

TRUESDELL C. and NOLL W. (2004). *The Non-Linear Field Theories of Mechanics* (3rd edition), S.S. Antman (Ed.). Berlin: Springer.

VASCHY A. (1892). Sur les lois de similitude en physique [On the laws of similarity in physics]. *Annales Télégraphiques*, **19**, 25-28.

VASCHY A. (1896). *Théorie de l'Électricité: Exposé des Phénomènes Électriques et Magnétiques Fondé Uniquement sur l'Expérience et le Raisonnement* [Theory of Electricity: Presentation of Electrical and Magnetic Phenomena Based Solely on Experience and Reasoning]. Paris: Librairie Polytechnique, Baudry et C.ie.

VILLAGGIO P. (1997). *Mathematical Models for Elastic Structures*. Cambridge: Cambridge University Press.

VLASOV V.Z. (1961). *Thin-Walled Elastic Beams* [English translation of the 2nd Russian edition of 1959]. Jerusalem: Israel Program for Scientific Translation. French translation of the said Russian edition by G. Smirnoff (1962), *Pièces Longues en Voiles Minces*. Paris: Eyrolles.

VOLTERRA E. (1955). The equations of motion for curved elastic bars deduced by the use of the "method of internal constraints". *Archive of Applied Mechanics*, **23**(6), 402-409.

VOLTERRA E. (1956). The equations of motion for curved and twisted elastic bars deduced by the use of the "method of internal constraints". *Archive of Applied Mechanics*, **24**(6), 392-400.

VOLTERRA E. (1961). Second approximation of the method of internal constraints and its applications. *International Journal of Mechanical Sciences*, **3**(1-2), 47-67.

WAGNER H. (1929). Verdrehung und Knickung von offenen Profilen. *Veröffentlichung zum 25jährigen Jubiläum, Technische Hochschule Danzig, 1904-1929*. Danzig: Verlag A.W. Kaffemann, 329-343. English translation by S. Reiss (1936), *Torsion and Buckling of Open Sections*, Technical Memorandum n. 807, National Advisory Committee for Aeronautics (NACA).

WAGNER H. and PRETSCHNER W. (1934). Verdrehung und Knickung von offenen Profilen. *Luftfahrtforschung*, **11**(6), 174-180. English translation by J. Vanier (1936), *Torsion and Buckling of Open Sections*, Technical Memorandum n. 784, National Advisory Committee for Aeronautics (NACA).

WEBER C. (1924). Biegung und Schub im geraden Balken [Bending and shear in straight beams]. *Zeitschrift für angewandte Mathematik und Mechanik*, **4**(4), 334-348.

WEBER C. (1926). Übertragung des Drehmoments in Balken mit doppelflanschigem Querschnitt [Transmission of torque in bars with double-flanged cross-section]. *Zeitschrift für angewandte Mathematik und Mechanik*, **6**(2), 85-97.

WEINSTEIN A. (1947). The center of shear and the center of twist. *Quarterly of Applied Mathematics*, **5**(1), 97-99.

WEKEZER J.W. (1984). Elastic torsion of thin walled bars of variable cross sections. *Computers & Structures*, **19**(3), 401-407.

WEKEZER J.W. (1990). A thin-walled bar element as a special case of a shell with internal constraints. *Finite Element Applications to Thin-Walled Structures*, J.W. Bull (Ed.). London: Elsevier, 41-62.

WILDE P. (1968). The torsion of thin-walled bars with variable cross-section. *Archiwum Mechaniki Stosowanej*, **4**(20), 431-443.

WILLARD S. (1970). *General Topology*. Reading, Massachusetts: Addison-Wesley.

WOLFRAM RESEARCH, INC. (2006). *Wolfram Mathematica 6.2*. Champaign, Illinois.

YANG Y.-B. and KUO S.-R. (1994). *Theory and Analysis of Nonlinear Framed Structures*. Englewood Cliffs, New Jersey: Prentice Hall.

YAU J.-D. (2008). An iterative approach to linear torsion analysis of web-tapered I-beams using a uniform I-beam element. *International Journal of Structural Stability and Dynamics*, **8**(3), 521-529.

Chapter 3

A LINEAR ONE-DIMENSIONAL MODEL FOR THE STRETCHING, BENDING AND TWISTING OF TAPERED THIN-WALLED BARS WITH OPEN CROSS-SECTIONS

THE DYNAMIC CASE

3.1 INTRODUCTION

The linear dynamic behaviour of prismatic thin-walled bars with open cross-section has been extensively studied since the pioneering works of FEDERHOFER (1947), GERE (1954a, 1954b), GERE & LIN (1958) and VLASOV (1961, ch. 9), and is by now well understood. However, the same cannot be said about the tapered bar case.

When attempting to extend Vlasov's (or Gere's) dynamic equations to tapered bars, some authors merely replace constant dimensions with variable ones in the expressions for the relevant geometrical properties, without adding any extra terms (*e.g.*, EISENBERGER 1997). The works of AMBROSINI *et al.* (1995, 2000) and AMBROSINI (2009), which include the effect of shear flexibility (not considered in Gere's or Vlasov's models), also fall in this category as far as the cross-section variation is concerned. As seen in the preceding chapter, taper affects the stiffness in ways that cannot be accounted for, in general, by such a perfunctory procedure.

RAO & MIRZA (1988) investigated the torsional vibration behaviour of doubly symmetric tapered I-section cantilevers.[1] To this end, they combined d'Alembert's principle with what we have dubbed "Timoshenko's approach" in chapter 2. Their analysis fails to

[1] Oddly enough, these authors took the clamped end to be the smaller one.

include the inertia torque due to warping of the cross-sections (that is, the term $\varrho D_1(I_\omega D_1 D_2^2 \Phi_1)$ in equations (3.4.7) and (3.9.1) below). They also fail to distinguish between derivatives with respect to the longitudinal coordinate of the bar and derivatives with respect to the arc length of the flange centroidal lines – a common oversight when applying Timoshenko's approach to tapered bars, as we have seen before, in the static case.

Building on previous work by WILDE (1968), WEKEZER (1987) formulated the eigenproblem providing the natural frequencies and corresponding vibration modes of tapered thin-walled bars with generic open cross-sections. The bars are regarded as membrane shells subjected to internal constraints, but these constraints have a mere kinematical character, with no constitutive repercussions. Moreover, Wekezer seems not to have grasped the peculiar torsional behavioural features implied by the constraints in tapered bars, for in a subsequent paper he writes: "Regardless of the number of finite elements chosen, the present method, which was developed for constant cross-sectional elements, does not seem capable of predicting torsional frequencies for variable cross-sections and should be used cautiously" (WEKEZER 1989).

Due to this state of affairs, it is worthwhile to extend into the dynamic range the linear static one-dimensional model developed in the preceding chapter. Accordingly, the proposed model rests upon regarding the bars under consideration as membrane shells subjected, at each time instant, to the internal constraints (V1)-(V2) stated at the beginning of § 2.3. The constitutive implications of these internal constraints are consistently dealt with by resorting to Podio-Guidugli's method. The (undamped) equations of motion and the general form of the boundary conditions are derived by means of Hamilton's principle, taking into account the contributions of rotatory inertia and torsion-warping inertia. Moreover, the inclusion in the proposed model of a viscous-type dissipative mechanism, with damping force proportional to the velocity, is also briefly addressed. As in the static case addressed in the preceding chapter, the tapered nature of the bars, in general, gives rise to non-standard stiffness terms associated with the torsional behaviour (whether uncoupled or coupled with other modes of deformation). The presence of these additional, non-standard terms renders the use of stepped models inadequate whenever torsional effects are involved, regardless of the number of prismatic segments considered. The chapter closes with an illustrative example concerning the undamped free torsional motions of two series of doubly symmetric web-tapered I-section cantilevers (one series with narrow

flanges and the other with wide flanges). The technique of separation of variables leads to an eigenproblem, consisting of an ordinary differential equation and the accompanying boundary conditions, which provides the natural torsional frequencies and the corresponding vibration modes.

Some remarks on notation and terminology

Throughout this chapter, the symbol τ will always denote time. By a time interval we mean an interval of the form $(0,\tau_0)$ or $[0,\tau_0]$, with $\tau_0 > 0$. If f is a map on the Cartesian product $[0,L]\times[0,\tau_0]$, we write $f(\cdot,\tau)$ for the partial map $\theta^1 \mapsto f(\theta^1,\tau)$ on $[0,L]$ obtained by holding $\tau \in [0,\tau_0]$ fixed, and $f(\theta^1,\cdot)$ for the partial map $\tau \mapsto f(\theta^1,\tau)$ on $[0,\tau_0]$ obtained by holding $\theta^1 \in [0,L]$ fixed (see DIEUDONNÉ 1960, ch. 1, § 5). Let M and N be non-negative integers. Following GURTIN (1972, § 9), we say that the map f is of class $C^{M,N}$ on the open set $(0,L)\times(0,\tau_0)$ if f is continuous on $(0,L)\times(0,\tau_0)$ and the partial derivatives

$$D_1^m D_2^n f \ , \quad m \in \{0,1,\cdots,M\} \ , \quad n \in \{0,1,\cdots,N\} \ , \quad m+n \le \max\{M,N\} \ , \tag{3.1.1}$$

exist and are continuous on $(0,L)\times(0,\tau_0)$. We say that f is of class $C^{M,N}$ on $[0,L]\times[0,\tau_0]$ if it is continuous on $[0,L]\times[0,\tau_0]$, of class $C^{M,N}$ on $(0,L)\times(0,\tau_0)$ and each of the partial derivatives $D_1^m D_2^n f$ has a continuous extension to $[0,L]\times[0,\tau_0]$ – in this case, we also write $D_1^m D_2^n f$ for the extended map. Finally, we write C^N for $C^{N,N}$.

3.2 MOTIONS

> Ainsi, tout modèle comporte *a priori* deux parties:
> une cinématique, dont l'objet est de paramétrer les formes ou les états du processus considéré;
> une dynamique, dont l'objet est de d'écrire l'évolution temporelle entre ces formes.
>
> RENÉ THOM

Let us consider a tapered thin-walled bar with open cross-sections and regular middle surface, as described in § 2.2. The generalisation to bars with irregular middle surfaces can be done along the lines indicated in § 2.10 and warrants no further explanation. Moreover, let us choose a fixed Cartesian frame for $\mathcal{E}$ (inertial frame) as in § 2.2.1.

An admissible motion of the middle surface of the bar in the time interval $[0,\tau_0]$ is a map $\boldsymbol{U} : \bar{\Omega}\times[0,\tau_0] \to \mathcal{V}$ of the form

$$\boldsymbol{U}(\theta^1,\theta^2,\tau)=U_i(\theta^1,\theta^2,\tau)\,\boldsymbol{e}_i$$
$$=\boldsymbol{W}(\theta^1,\tau)+\boldsymbol{\Phi}(\theta^1,\tau)\times\left(\bar{x}_2(\theta^1,\theta^2)\,\boldsymbol{e}_2+\bar{x}_3(\theta^1,\theta^2)\,\boldsymbol{e}_3\right)-\omega(\theta^1,\theta^2)\,D_1\Phi_1(\theta^1,\tau)\,\boldsymbol{e}_1\ , \quad (3.2.1)$$

$$\boldsymbol{W}(\theta^1,\tau)=W_i(\theta^1,\tau)\,\boldsymbol{e}_i \quad (3.2.2)$$

$$\boldsymbol{\Phi}(\theta^1,\tau)=\Phi_1(\theta^1,\tau)\,\boldsymbol{e}_1-D_1W_3(\theta^1,\tau)\,\boldsymbol{e}_2+D_1W_2(\theta^1,\tau)\,\boldsymbol{e}_3\ , \quad (3.2.3)$$

with (i) W_1 of class $C^{1,2}$ on $[0,L]\times[0,\tau_0]$ and (ii) W_2, W_3 and Φ_1 of class C^2 on $[0,L]\times[0,\tau_0]$. The map $\omega:\bar{\Omega}\to\mathbb{R}$ appearing in equation (3.2.1) is defined by (2.3.16). Vector $\boldsymbol{U}(\theta^1,\theta^2,\tau)$ is the displacement, at time τ, of the (material) point (whose reference place is) $F(\theta^1,\theta^2)\in\mathcal{S}$. Therefore, an admissible motion of the middle surface is a smooth one-parameter family of admissible displacement fields (as defined in § 2.3), time τ being the parameter. Consequently, in an admissible motion the constraints (V1)-(V2), defined at the beginning of § 2.3, are satisfied for all τ in $[0,\tau_0]$. With the usual identification of $\mathcal{L}(\mathbb{R},\mathcal{V})$ with $\mathcal{V}$ (*vide supra*, ch. 2, note 20), the velocity $D_3\boldsymbol{U}$ and acceleration $D_3^2\boldsymbol{U}$ are vector fields on $\bar{\Omega}\times[0,\tau_0]$.

As in § 2.3, the maps W_i $(i=1,2,3)$ and Φ_1, from $[0,L]\times[0,\tau_0]$ into $\mathbb{R}$, are collectively called the generalised displacements. For later convenience, we define the generalised velocities to be the real-valued maps defined on $[0,L]\times[0,\tau_0]$ by

$$v_i(\theta^1,\tau)=D_2W_i(\theta^1,\tau) \quad (3.2.4)$$

$$\Xi_1(\theta^1,\tau)=D_2\Phi_1(\theta^1,\tau) \quad (3.2.5)$$

$$\Xi_2(\theta^1,\tau)=-D_1D_2W_3(\theta^1,\tau) \quad (3.2.6)$$

$$\Xi_3(\theta^1,\tau)=D_1D_2W_2(\theta^1,\tau) \quad (3.2.7)$$

$$v_\omega(\theta^1,\tau)=-D_1D_2\Phi_1(\theta^1,\tau)\ . \quad (3.2.8)$$

While the Ξ_i are angular velocities, v_ω can be fittingly called the warping velocity – it is the derivative, with respect to time, of the warping amplitude $-D_1\Phi_1$.

To an admissible motion $\boldsymbol{U}:\bar{\Omega}\times[0,\tau_0]\to\mathcal{V}$ of the middle surface there corresponds a one-parameter family $\boldsymbol{\gamma}$ of admissible linearised membrane strain tensor fields, whose single non-vanishing covariant component is given by

$$\gamma_{11}(\theta^1,\theta^2,\tau)=\boldsymbol{a}_1(\theta^1,\theta^2)\cdot\boldsymbol{\gamma}(\theta^1,\theta^2,\tau)\,\boldsymbol{a}_1(\theta^1,\theta^2)$$
$$=D_1W_1(\theta^1,\tau)-\bar{x}_2(\theta^1,\theta^2)\,D_1^2W_2(\theta^1,\tau)-\bar{x}_3(\theta^1,\theta^2)\,D_1^2W_3(\theta^1,\tau)$$
$$-\omega(\theta^1,\theta^2)\,D_1^2\Phi_1(\theta^1,\tau)-\psi(\theta^1,\theta^2)\,D_1\Phi_1(\theta^1,\tau)\ . \quad (3.2.9)$$

The map $\psi : \bar{\Omega} \to \mathbb{R}$ appearing in this equation is defined by (2.3.26). The generalised strains

$$\varepsilon(\theta^1, \tau) = D_1 W_1(\theta^1, \tau) \tag{3.2.10}$$

$$\boldsymbol{\kappa}_1(\theta^1, \tau) = D_1 \Phi_1(\theta^1, \tau) \tag{3.2.11}$$

$$\boldsymbol{\kappa}_2(\theta^1, \tau) = -D_1^2 W_3(\theta^1, \tau) \tag{3.2.12}$$

$$\boldsymbol{\kappa}_3(\theta^1, \tau) = -D_1^2 W_2(\theta^1, \tau) \tag{3.2.13}$$

$$\Gamma(\theta^1, \tau) = -D_1^2 \Phi_1(\theta^1, \tau) \ , \tag{3.2.14}$$

whose physical significance was discussed in § 2.3, enable us to rewrite (3.2.9) in the form

$$\begin{aligned} \gamma_{11}(\theta^1, \theta^2, \tau) = {} & \varepsilon(\theta^1, \tau) + \bar{x}_2(\theta^1, \theta^2)\, \boldsymbol{\kappa}_3(\theta^1, \tau) + \bar{x}_3(\theta^1, \theta^2)\, \boldsymbol{\kappa}_2(\theta^1, \tau) \\ & + \omega(\theta^1, \theta^2)\, \Gamma(\theta^1, \tau) - \psi(\theta^1, \theta^2)\, \boldsymbol{\kappa}_1(\theta^1, \tau) \ . \end{aligned} \tag{3.2.15}$$

Relative to the orthonormal ordered basis field $(\theta^1, \theta^2) \in \bar{\Omega} \mapsto \left\{ \boldsymbol{o}_{\mathrm{I}}(\theta^1, \theta^2), \boldsymbol{o}_{\mathrm{II}}(\theta^1, \theta^2) \right\}$, we have

$$\boldsymbol{\gamma}(\theta^1, \theta^2, \tau) = \gamma_{\mathrm{I\text{-}I}}(\theta^1, \theta^2, \tau)\, \boldsymbol{o}_{\mathrm{I}}(\theta^1, \theta^2) \otimes \boldsymbol{o}_{\mathrm{I}}(\theta^1, \theta^2) \tag{3.2.16}$$

$$\gamma_{\mathrm{I\text{-}I}}(\theta^1, \theta^2, \tau) = \frac{\gamma_{11}(\theta^1, \theta^2, \tau)}{a(\theta^1, \theta^2)} \ , \tag{3.2.17}$$

where $a(\theta^1, \theta^2)$ is the determinant of the symmetric and positive definite matrix (2.2.14) of metric coefficients.

3.3 THE LAGRANGIAN

3.3.1 Kinetic energy

For a given admissible motion $\boldsymbol{U} : \bar{\Omega} \times [0, \tau_0] \to \mathcal{V}$ of the middle surface, the kinetic energy of the bar at time $\tau \in [0, \tau_0)$ is given by

$$T = \frac{\varrho}{2} \int_{\bar{\Omega}} \left\| D_3 \boldsymbol{U}(\theta^1, \theta^2, \tau) \right\|^2 t(\theta^1, \theta^2) \sqrt{a(\theta^1, \theta^2)}\, d\theta^1\, d\theta^2 \ , \tag{3.3.1}$$

where ϱ is the mass density over the reference shape (TRUESDELL 1991, ch. 2, § 2), assumed to be constant.[2]

---

[2] For each τ in $[0, \tau_0]$, the map $(\theta^1, \theta^2) \mapsto \left\| D_3 \boldsymbol{U}(\theta^1, \theta^2, \tau) \right\|$ is continuous on $\bar{\Omega}$ (on the continuity of $(\theta^1, \theta^2) \mapsto D_3 \boldsymbol{U}(\theta^1, \theta^2, \tau)$, see DIEUDONNÉ 1960, th. 3.20.14; on the continuity of the norm, see ABRAHAM *et al.* 1988, p. 45; finally, on the continuity of the composition of continuous maps, see DIEUDONNÉ 1960, th. 3.11.5). The integral in equation (3.3.1) is thus well-defined.

The assumption of a constant mass density ϱ is obviously not essential and it would have been a simple matter to consider ϱ as a function of the Gaussian coordinates θ^1, θ^2.

Inserting (3.2.1)-(3.2.3) into (3.3.1) and writing the integral over $\overline{\Omega}$ as an iterated integral, one obtains

$$T = \frac{\varrho}{2}\int_0^L \left\{ \int_{g_1(\theta^1)}^{g_2(\theta^1)} \Big[\Big(D_2 W_1(\theta^1,\tau) - \overline{x}_2(\theta^1,\theta^2)\, D_1 D_2 W_2(\theta^1,\tau) - \overline{x}_3(\theta^1,\theta^2)\, D_1 D_2 W_3(\theta^1,\tau) \right.$$
$$\left. - \omega(\theta^1,\theta^2)\, D_1 D_2 \Phi_1(\theta^1,\tau) \Big)^2 + \Big(D_2 W_2(\theta^1,\tau) - \overline{x}_3(\theta^1,\theta^2)\, D_2 \Phi_1(\theta^1,\tau) \Big)^2 \right.$$
$$\left. + \Big(D_2 W_3(\theta^1,\tau) + \overline{x}_2(\theta^1,\theta^2)\, D_2 \Phi_1(\theta^1,\tau) \Big)^2 \Big] t(\theta^1,\theta^2) \sqrt{a(\theta^1,\theta^2)}\, d\theta^1 \right\} d\theta^2 \quad . (3.3.2)$$

Then, introducing the continuous real-valued maps defined on $[0,L]$ by

$$A(\theta^1) = \int_{g_1(\theta^1)}^{g_2(\theta^1)} t(\theta^1,\theta^2) \sqrt{a(\theta^1,\theta^2)}\, d\theta^2 \tag{3.3.3}$$

$$S_2(\theta^1) = \int_{g_1(\theta^1)}^{g_2(\theta^1)} \overline{x}_3(\theta^1,\theta^2)\, t(\theta^1,\theta^2) \sqrt{a(\theta^1,\theta^2)}\, d\theta^2 \tag{3.3.4}$$

$$S_3(\theta^1) = \int_{g_1(\theta^1)}^{g_2(\theta^1)} \overline{x}_2(\theta^1,\theta^2)\, t(\theta^1,\theta^2) \sqrt{a(\theta^1,\theta^2)}\, d\theta^2 \tag{3.3.5}$$

$$S_\omega(\theta^1) = \int_{g_1(\theta^1)}^{g_2(\theta^1)} \omega(\theta^1,\theta^2)\, t(\theta^1,\theta^2) \sqrt{a(\theta^1,\theta^2)}\, d\theta^2 \tag{3.3.6}$$

$$I_2(\theta^1) = \int_{g_1(\theta^1)}^{g_2(\theta^1)} \overline{x}_3^{\,2}(\theta^1,\theta^2)\, t(\theta^1,\theta^2) \sqrt{a(\theta^1,\theta^2)}\, d\theta^2 \tag{3.3.7}$$

$$I_3(\theta^1) = \int_{g_1(\theta^1)}^{g_2(\theta^1)} \overline{x}_2^{\,2}(\theta^1,\theta^2)\, t(\theta^1,\theta^2) \sqrt{a(\theta^1,\theta^2)}\, d\theta^2 \tag{3.3.8}$$

$$I_\omega(\theta^1) = \int_{g_1(\theta^1)}^{g_2(\theta^1)} \omega^2(\theta^1,\theta^2)\, t(\theta^1,\theta^2) \sqrt{a(\theta^1,\theta^2)}\, d\theta^2 \tag{3.3.9}$$

$$I_{23}(\theta^1) = \int_{g_1(\theta^1)}^{g_2(\theta^1)} \overline{x}_2(\theta^1,\theta^2)\, \overline{x}_3(\theta^1,\theta^2)\, t(\theta^1,\theta^2) \sqrt{a(\theta^1,\theta^2)}\, d\theta^2 \tag{3.3.10}$$

$$I_{2\omega}(\theta^1) = \int_{g_1(\theta^1)}^{g_2(\theta^1)} \overline{x}_3(\theta^1,\theta^2)\, \omega(\theta^1,\theta^2)\, t(\theta^1,\theta^2) \sqrt{a(\theta^1,\theta^2)}\, d\theta^2 \tag{3.3.11}$$

$$I_{3\omega}(\theta^1) = \int_{g_1(\theta^1)}^{g_2(\theta^1)} \overline{x}_2(\theta^1,\theta^2)\, \omega(\theta^1,\theta^2)\, t(\theta^1,\theta^2) \sqrt{a(\theta^1,\theta^2)}\, d\theta^2 \quad ,^3 \tag{3.3.12}$$

---

[3] Observe that $t(\theta^1,\theta^1)\sqrt{a(\theta^1,\theta^1)}$ is the wall thickness at $F(\theta^1,\theta^1) \in \mathscr{S}$ measured in the plane of the cross-section $\mathscr{A}_{\theta^1}$. Indeed, the orthogonal projection of $\boldsymbol{a}_3(\theta^1,\theta^1)$ on the subspace spanned by $\{\boldsymbol{e}_2,\boldsymbol{e}_3\}$ is (SANTANA & QUEIRÓ 2010, th. 10.16)

$$\begin{aligned} \mathrm{proj}_{\mathrm{span}\{\boldsymbol{e}_2,\boldsymbol{e}_3\}}\, \boldsymbol{a}_3(\theta^1,\theta^1) &= \big(\boldsymbol{a}_3(\theta^1,\theta^1)\cdot\boldsymbol{e}_2\big)\boldsymbol{e}_2 + \big(\boldsymbol{a}_3(\theta^1,\theta^1)\cdot\boldsymbol{e}_3\big)\boldsymbol{e}_3 \\ &= \frac{1}{\sqrt{a(\theta^1,\theta^1)}} \big(-D_2\overline{x}_3(\theta^1,\theta^1)\,\boldsymbol{e}_2 + D_2\overline{x}_2(\theta^1,\theta^1)\,\boldsymbol{e}_3 \big) \,. \end{aligned}$$

The angle $\vartheta(\theta^1,\theta^1)$ between $\boldsymbol{a}_3(\theta^1,\theta^1)$ and $\mathrm{span}\{\boldsymbol{e}_2,\boldsymbol{e}_3\}$ is therefore defined by

the kinetic energy is cast in the form

$$
\begin{aligned}
T = \frac{\varrho}{2}\int_0^L \Big\{ & A(\theta^1)\Big[\big(D_2 W_1(\theta^1,\tau)\big)^2 + \big(D_2 W_2(\theta^1,\tau)\big)^2 + \big(D_2 W_3(\theta^1,\tau)\big)^2\Big] \\
& -2\,S_3(\theta^1)\big(D_2 W_1(\theta^1,\tau)\,D_1 D_2 W_2(\theta^1,\tau) - D_2 W_3(\theta^1,\tau)\,D_2\Phi_1(\theta^1,\tau)\big) \\
& -2\,S_2(\theta^1)\big(D_2 W_1(\theta^1,\tau)\,D_1 D_2 W_3(\theta^1,\tau) + D_2 W_2(\theta^1,\tau)\,D_2\Phi_1(\theta^1,\tau)\big) \\
& -2\,S_\omega(\theta^1)\,D_2 W_1(\theta^1,\tau)\,D_1 D_2\Phi_1(\theta^1,\tau) \\
& +I_3(\theta^1)\Big[\big(D_1 D_2 W_2(\theta^1,\tau)\big)^2 + \big(D_2\Phi_1(\theta^1,\tau)\big)^2\Big] \\
& +I_2(\theta^1)\Big[\big(D_1 D_2 W_3(\theta^1,\tau)\big)^2 + \big(D_2\Phi_1(\theta^1,\tau)\big)^2\Big] \\
& +I_\omega(\theta^1)\big(D_1 D_2\Phi_1(\theta^1,\tau)\big)^2 + 2\,I_{23}(\theta^1)\,D_1 D_2 W_2(\theta^1,\tau)\,D_1 D_2 W_3(\theta^1,\tau) \\
& +2\,I_{3\omega}(\theta^1)\,D_1 D_2 W_2(\theta^1,\tau)\,D_1 D_2\Phi_1(\theta^1,\tau) \\
& +2\,I_{2\omega}(\theta^1)\,D_1 D_2 W_3(\theta^1,\tau)\,D_1 D_2\Phi_1(\theta^1,\tau)\Big\}\,d\theta^1 \ . \qquad (3.3.13)
\end{aligned}
$$

Notice that there is no conflict between the notation in (3.3.3)-(3.3.12) and that adopted in § 2.9.2 for prismatic bars – in the latter case, $a(\theta^1,\theta^2)=1$ everywhere on $\overline{\Omega}$. For the special case of the tapered I-section bars discussed in § 2.10.1 (see, in particular, figure 2.10.3 and table 2.10.1), one has

$$
A(\theta^1) = h(\theta^1)\,t_w + b_t(\theta^1)\frac{t_t}{\cos\varphi_t} + b_b(\theta^1)\frac{t_b}{\cos\varphi_b} \qquad (3.3.14)
$$

$$
S_2(\theta^1) = \left(\frac{h(\theta^1)}{2} + x_{3t}(\theta^1)\right) h(\theta^1)\,t_w + x_{3t}(\theta^1)\,b_t(\theta^1)\frac{t_t}{\cos\varphi_t} + x_{3b}(\theta^1)\,b_b(\theta^1)\frac{t_b}{\cos\varphi_b} \qquad (3.3.15)
$$

$$
\begin{aligned}
I_2(\theta^1) = {} & \frac{h(\theta^1)^3\,t_w}{12} + \left(\frac{h(\theta^1)}{2} + x_{3t}(\theta^1)\right)^2 h(\theta^1)\,t_w + x_{3t}(\theta^1)^2\,b_t(\theta^1)\frac{t_t}{\cos\varphi_t} \\
& + x_{3b}(\theta^1)^2\,b_b(\theta^1)\frac{t_b}{\cos\varphi_b} \qquad (3.3.16)
\end{aligned}
$$

$$
\cos^2\vartheta(\theta^1,\theta^1) = \frac{\Big(\boldsymbol{a}_3(\theta^1,\theta^1)\cdot \mathrm{proj}_{\mathrm{span}\{\boldsymbol{e}_2,\boldsymbol{e}_3\}}\,\boldsymbol{a}_3(\theta^1,\theta^1)\Big)^2}{\Big\|\mathrm{proj}_{\mathrm{span}\{\boldsymbol{e}_2,\boldsymbol{e}_3\}}\,\boldsymbol{a}_3(\theta^1,\theta^1)\Big\|^2} = \frac{1}{a(\theta^1,\theta^1)} \ , \ 0 \le \vartheta(\theta^1,\theta^1) \ll \frac{\pi}{2} \ .
$$

This gives

$$
\frac{t(\theta^1,\theta^1)}{\cos\vartheta(\theta^1,\theta^1)} = t(\theta^1,\theta^1)\sqrt{a(\theta^1,\theta^1)}
$$

for the wall thickness at $F(\theta^1,\theta^1)$ measured in the plane of $\mathcal{A}_{\theta^1}$, as asserted above.

$$I_3(\theta^1) = \frac{1}{12} b_t(\theta^1)^3 \frac{t_t}{\cos\varphi_t} + \frac{1}{12} b_b(\theta^1)^3 \frac{t_b}{\cos\varphi_b} \tag{3.3.17}$$

$$I_\omega(\theta^1) = \frac{1}{12} \varkappa_{3t}(\theta^1)^2\, b_t(\theta^1)^3 \frac{t_t}{\cos\varphi_t} + \frac{1}{12} \varkappa_{3b}(\theta^1)^2\, b_b(\theta^1)^3 \frac{t_b}{\cos\varphi_b} \tag{3.3.18}$$

$$I_{3\omega}(\theta^1) = -\frac{1}{12} \varkappa_{3t}(\theta^1) b_t(\theta^1)^3 \frac{t_t}{\cos\varphi_t} - \frac{1}{12} \varkappa_{3b}(\theta^1) b_b(\theta^1)^3 \frac{t_b}{\cos\varphi_b}\ , \tag{3.3.19}$$

which makes perfect sense, while, due to symmetry, S_3, S_ω, I_{23} and $I_{2\omega}$ are identically zero.

A more elegant and compact expression for the kinetic energy can be achieved if one defines the linear momentum density

$$\boldsymbol{p}(\theta^1,\tau) = \varrho \int_{g_1(\theta^1)}^{g_2(\theta^1)} D_3\boldsymbol{U}(\theta^1,\theta^2,\tau)\, t(\theta^1,\theta^2) \sqrt{a(\theta^1,\theta^2)}\, d\theta^2 = p_i(\theta^1,\tau)\, \boldsymbol{e}_i \tag{3.3.20}$$

$$\begin{aligned} p_1(\theta^1,\tau) &= \varrho \int_{g_1(\theta^1)}^{g_2(\theta^1)} D_3 U_1(\theta^1,\theta^2,\tau)\, t(\theta^1,\theta^2) \sqrt{a(\theta^1,\theta^2)}\, d\theta^2 \\ &= \varrho \Big(A(\theta^1) D_2 W_1(\theta^1,\tau) - S_3(\theta^1) D_1 D_2 W_2(\theta^1,\tau) \\ &\qquad - S_2(\theta^1) D_1 D_2 W_3(\theta^1,\tau) - S_\omega(\theta^1) D_1 D_2 \Phi_1(\theta^1,\tau) \Big) \end{aligned} \tag{3.3.21}$$

$$\begin{aligned} p_2(\theta^1,\tau) &= \varrho \int_{g_1(\theta^1)}^{g_2(\theta^1)} D_3 U_2(\theta^1,\theta^2,\tau)\, t(\theta^1,\theta^2) \sqrt{a(\theta^1,\theta^2)}\, d\theta^2 \\ &= \varrho \Big(A(\theta^1) D_2 W_2(\theta^1,\tau) - S_2(\theta^1) D_2 \Phi_1(\theta^1,\tau) \Big) \end{aligned} \tag{3.3.22}$$

$$\begin{aligned} p_3(\theta^1,\tau) &= \varrho \int_{g_1(\theta^1)}^{g_2(\theta^1)} D_3 U_3(\theta^1,\theta^2,\tau)\, t(\theta^1,\theta^2) \sqrt{a(\theta^1,\theta^2)}\, d\theta^2 \\ &= \varrho \Big(A(\theta^1) D_2 W_3(\theta^1,\tau) + S_3(\theta^1) D_2 \Phi_1(\theta^1,\tau) \Big)\ , \end{aligned} \tag{3.3.23}$$

the angular momentum density (relative to $O + \theta^1 \boldsymbol{e}_1$)

$$\begin{aligned} \boldsymbol{l}(\theta^1,\tau) &= \varrho \int_{g_1(\theta^1)}^{g_2(\theta^1)} \Big(\overline{x}_2(\theta^1,\theta^2)\, \boldsymbol{e}_2 + \overline{x}_3(\theta^1,\theta^2)\, \boldsymbol{e}_3 \Big) \times D_3\boldsymbol{U}(\theta^1,\theta^2,\tau)\, t(\theta^1,\theta^2) \sqrt{a(\theta^1,\theta^2)}\, d\theta^2 \\ &= l_i(\theta^1,\tau)\, \boldsymbol{e}_i \end{aligned} \tag{3.3.24}$$

$$\begin{aligned} l_1(\theta^1,\tau) &= \varrho \int_{g_1(\theta^1)}^{g_2(\theta^1)} \Big(\overline{x}_2(\theta^1,\theta^2) D_3 U_3(\theta^1,\theta^2,\tau) - \overline{x}_3(\theta^1,\theta^2) D_3 U_2(\theta^1,\theta^2,\tau) \Big) t(\theta^1,\theta^2) \sqrt{a(\theta^1,\theta^2)}\, d\theta^2 \\ &= \varrho \Big[-S_2(\theta^1) D_2 W_2(\theta^1,\tau) + S_3(\theta^1) D_2 W_3(\theta^1,\tau) + \Big(I_2(\theta^1) + I_3(\theta^1) \Big) D_2 \Phi_1(\theta^1,\tau) \Big] \end{aligned} \tag{3.3.25}$$

$$l_2(\theta^1,\tau) = \varrho \int_{g_1(\theta^1)}^{g_2(\theta^1)} \overline{x}_3(\theta^1,\theta^2)\, D_3 U_1(\theta^1,\theta^2,\tau)\, t(\theta^1,\theta^2)\, \sqrt{a(\theta^1,\theta^2)}\; d\theta^2$$

$$= \varrho \Big(S_2(\theta^1)\, D_2 W_1(\theta^1,\tau) - I_{23}(\theta^1)\, D_1 D_2 W_2(\theta^1,\tau)$$

$$- I_2(\theta^1)\, D_1 D_2 W_3(\theta^1,\tau) - I_{2\omega}(\theta^1)\, D_1 D_2 \Phi_1(\theta^1,\tau) \Big) \qquad (3.3.26)$$

$$l_3(\theta^1,\tau) = -\varrho \int_{g_1(\theta^1)}^{g_2(\theta^1)} \overline{x}_2(\theta^1,\theta^2)\, D_3 U_1(\theta^1,\theta^2,\tau)\, t(\theta^1,\theta^2)\, \sqrt{a(\theta^1,\theta^2)}\; d\theta^2$$

$$= \varrho \Big(-S_3(\theta^1)\, D_2 W_1(\theta^1,\tau) + I_3(\theta^1)\, D_1 D_2 W_2(\theta^1,\tau)$$

$$+ I_{23}(\theta^1)\, D_1 D_2 W_3(\theta^1,\tau) + I_{3\omega}(\theta^1)\, D_1 D_2 \Phi_1(\theta^1,\tau) \Big) \qquad (3.3.27)$$

and the warping momentum density

$$p_\omega(\theta^1,\tau) = \varrho \int_{g_1(\theta^1)}^{g_2(\theta^1)} \omega(\theta^1,\theta^2)\, D_3 U_1(\theta^1,\theta^2,\tau)\, t(\theta^1,\theta^2)\, \sqrt{a(\theta^1,\theta^2)}\; d\theta^2$$

$$= \varrho \Big(S_\omega(\theta^1)\, D_2 W_1(\theta^1,\tau) - I_{3\omega}(\theta^1)\, D_1 D_2 W_2(\theta^1,\tau)$$

$$- I_{2\omega}(\theta^1)\, D_1 D_2 W_3(\theta^1,\tau) - I_\omega(\theta^1)\, D_1 D_2 \Phi_1(\theta^1,\tau) \Big) \; . \qquad (3.3.28)$$

With these definitions, together with the generalised velocities (3.2.4)-(3.2.8), the kinetic energy becomes simply

$$T = \frac{1}{2} \int_0^L \Big(p_i(\theta^1,\tau)\, v_i(\theta^1,\tau) + l_i(\theta^1,\tau)\, \Xi_i(\theta^1,\tau) + p_\omega(\theta^1,\tau)\, v_\omega(\theta^1,\tau) \Big)\, d\theta^1 \; .^4 \qquad (3.3.29)$$

3.3.2 Strain energy

Let $\boldsymbol{U} : \overline{\Omega} \times [0,\tau_0] \to \mathcal{V}$ be an admissible motion of the middle surface and $\boldsymbol{\gamma}$ be the corresponding one-parameter family of admissible linearised membrane strain tensor fields. Then, the membrane strain energy at time $\tau \in [0,\tau_0]$ is

$$U_m = \frac{1}{2} \int_{\overline{\Omega}} \Big(\mathbb{C}(\theta^1,\theta^2)\, \boldsymbol{\gamma}(\theta^1,\theta^2,\tau) \Big) : \boldsymbol{\gamma}(\theta^1,\theta^2,\tau) \sqrt{a(\theta^1,\theta^2)}\; d\theta^1 d\theta^2 \quad , \qquad (3.3.30)$$

where $\mathbb{C}(\theta^1,\theta^2)$ is the elasticity tensor defined in equation (2.4.8). Using previous results, one obtains

---

[4] If the kinetic energy T is regarded as a quadratic functional of the generalised velocities v_i, Ξ_i and v_ω, then

$$\frac{\partial T}{\partial v_i} = \int_0^L p_i \, d\theta^1 \qquad \frac{\partial T}{\partial \Xi_i} = \int_0^L l_i \, d\theta^1 \qquad \frac{\partial T}{\partial v_\omega} = \int_0^L p_\omega \, d\theta^1 \; .$$

This is consistent with the usual definition of generalised momenta in the classical mechanics of point masses (for a velocity-independent generalised potential) – *e.g.*, GREENWOOD (1997, p. 39) and LANCZOS (1970, pp. 120-122).

$$U_m = \frac{\tilde{E}}{2}\int_{\bar{\Omega}}\Big(D_1 W_1(\theta^1,\tau) - \overline{x}_2(\theta^1,\theta^2)\, D_1^2 W_2(\theta^1,\tau) - \overline{x}_3(\theta^1,\theta^2)\, D_1^2 W_3(\theta^1,\tau) \\ -\omega(\theta^1,\theta^2)\, D_1^2\Phi_1(\theta^1,\tau) - \psi(\theta^1,\theta^2)\, D_1\Phi_1(\theta^1,\tau)\Big)^2\, t^*(\theta^1,\theta^2)\, d\theta^1\, d\theta^2 \ , \quad (3.3.31)$$

where $t^*(\theta^1,\theta^2)$ is the reduced wall thickness (2.5.4). Writing the integral over $\bar{\Omega}$ as an iterated integral and using the geometrical properties (2.5.6)-(2.5.20), one obtains

$$\begin{aligned} U_m = \frac{\tilde{E}}{2}\int_0^L \Big[& A^*(\theta^1)\Big(D_1 W_1(\theta^1,\tau)\Big)^2 - 2\, S_3^*(\theta^1)\, D_1 W_1(\theta^1,\tau)\, D_1^2 W_2(\theta^1,\tau) \\ & -2\, S_2^*(\theta^1)\, D_1 W_1(\theta^1,\tau)\, D_1^2 W_3(\theta^1,\tau) - 2\, S_\omega^*(\theta^1)\, D_1 W_1(\theta^1,\tau)\, D_1^2\Phi_1(\theta^1,\tau) \\ & -2\, S_\psi^*(\theta^1)\, D_1 W_1(\theta^1,\tau)\, D_1\Phi_1(\theta^1,\tau) + I_3^*(\theta^1)\Big(D_1^2 W_2(\theta^1,\tau)\Big)^2 \\ & +2\, I_{23}^*(\theta^1)\, D_1^2 W_2(\theta^1,\tau)\, D_1^2 W_3(\theta^1,\tau) + 2\, I_{3\omega}^*(\theta^1)\, D_1^2 W_2(\theta^1,\tau)\, D_1^2\Phi_1(\theta^1,\tau) \\ & +2\, I_{3\psi}^*(\theta^1)\, D_1^2 W_2(\theta^1,\tau)\, D_1\Phi_1(\theta^1,\tau) + I_2^*(\theta^1)\Big(D_1^2 W_3(\theta^1,\tau)\Big)^2 \\ & +2\, I_{2\omega}^*(\theta^1)\, D_1^2 W_3(\theta^1,\tau)\, D_1^2\Phi_1(\theta^1,\tau) + 2\, I_{2\psi}^*(\theta^1)\, D_1^2 W_3(\theta^1,\tau)\, D_1\Phi_1(\theta^1,\tau) \\ & +I_\omega^*(\theta^1)\Big(D_1^2\Phi_1(\theta^1,\tau)\Big)^2 + 2\, I_{\omega\psi}^*(\theta^1)\, D_1^2\Phi_1(\theta^1,\tau)\, D_1\Phi_1(\theta^1,\tau) \\ & +I_\psi^*(\theta^1)\Big(D_1\Phi_1(\theta^1,\tau)\Big)^2\Big]\, d\theta^1 \ . \end{aligned} \quad (3.3.32)$$

As in the static case (see § 2.5.1), we make the *ad hoc* addition of

$$U_{\mathrm{SV}} = \frac{G}{2}\int_0^L J(\theta^1)\Big(D_1\Phi_1(\theta^1,\tau)\Big)^2\, d\theta^1 \quad (3.3.33)$$

to the membrane strain energy, so that the total strain energy stored in the bar is

$$U = U_m + U_{\mathrm{SV}} \ . \quad (3.3.34)$$

3.3.3 Work of the external loads

We prescribe a system of monogenic[5] bar loads comprising:

(i) a distributed force

$$\boldsymbol{q} : [0,L]\times[0,\tau_0] \to \mathcal{V} \ , \quad (3.3.35)$$

(ii) a distributed moment

$$\boldsymbol{m} : [0,L]\times[0,\tau_0] \to \mathcal{V} \ , \quad (3.3.36)$$

[5] The word "monogenic" (literally, "single-generated") is used here in the sense of LANCZOS (1970, ch. 1, § 7) – see also ARGYRIS & SYMEONIDIS (1981, § 1.1.2) and GOLDSTEIN *et al.* (2001, p. 34). MEIROVITCH (1970, p. 17) uses instead the word "lamellar".

(iii) a distributed bimomental load

$$b:[0,L]\times[0,\tau_0]\to\mathbb{R}\ , \tag{3.3.37}$$

defined per unit length of the line segment $\{O+\theta^1\boldsymbol{e}_1,\ 0\le\theta^1\le L\}$, and

(iv) concentrated forces

$$\boldsymbol{Q}_0,\boldsymbol{Q}_L:[0,\tau_0]\to\mathcal{V}\ , \tag{3.3.38}$$

(v) concentrated moments

$$\boldsymbol{M}_0,\boldsymbol{M}_L:[0,\tau_0]\to\mathcal{V}\ , \tag{3.3.39}$$

(vi) concentrated bimoments

$$B_0,B_L:[0,\tau_0]\to\mathbb{R} \tag{3.3.40}$$

at the end points O and $O+L\,\boldsymbol{e}_1$. All the above maps are assumed to be continuous. In terms of Cartesian components, we write

$$\boldsymbol{q}(\theta^1,\tau)=q_i(\theta^1,\tau)\boldsymbol{e}_i \tag{3.3.41}$$

$$\boldsymbol{m}(\theta^1,\tau)=m_i(\theta^1,\tau)\boldsymbol{e}_i \tag{3.3.42}$$

$$\boldsymbol{Q}_0(\tau)=Q_{0.i}(\tau)\boldsymbol{e}_i \tag{3.3.43}$$

$$\boldsymbol{Q}_L(\tau)=Q_{L.i}(\tau)\boldsymbol{e}_i \tag{3.3.44}$$

$$\boldsymbol{M}_0(\tau)=M_{0.i}(\tau)\boldsymbol{e}_i \tag{3.3.45}$$

$$\boldsymbol{M}_L(\tau)=M_{L.i}(\tau)\boldsymbol{e}_i\ . \tag{3.3.46}$$

In a given admissible motion $\boldsymbol{U}:\bar{\Omega}\times[0,\tau_0]\to\mathcal{V}$ of the middle surface (recall (3.2.1)-(3.2.3)), the (time-dependent) work performed by these bar loads is

$$\begin{aligned}W_e=\int_0^L\Big(&\boldsymbol{q}(\theta^1,\tau)\cdot\boldsymbol{W}(\theta^1,\tau)+\boldsymbol{m}(\theta^1,\tau)\cdot\boldsymbol{\Phi}(\theta^1,\tau)-b(\theta^1,\tau)\,D_1\Phi_1(\theta^1,\tau)\Big)d\theta^1\\&+\boldsymbol{Q}_0(\tau)\cdot\boldsymbol{W}(0,\tau)+\boldsymbol{Q}_L(\tau)\cdot\boldsymbol{W}(L,\tau)+\boldsymbol{M}_0(\tau)\cdot\boldsymbol{\Phi}(0,\tau)+\boldsymbol{M}_L(\tau)\cdot\boldsymbol{\Phi}(L,\tau)\\&-B_0(\tau)\,D_1\Phi_1(0,\tau)-B_L(\tau)\,D_1\Phi_1(L,\tau)\end{aligned} \tag{3.3.47}$$

or, alternatively,

$$\begin{aligned}W_e=\int_0^L\Big(&q_i(\theta^1,\tau)W_i(\theta^1,\tau)+m_1(\theta^1,\tau)\Phi_1(\theta^1,\tau)-m_2(\theta^1,\tau)\,D_1W_3(\theta^1,\tau)\\&+m_3(\theta^1,\tau)\,D_1W_2(\theta^1,\tau)-b(\theta^1,\tau)\,D_1\Phi_1(\theta^1,\tau)\Big)d\theta^1\\&+Q_{0.i}(\tau)W_i(0,\tau)+Q_{L.i}(\tau)W_i(L,\tau)\\&+M_{0.1}(\tau)\Phi_1(0,\tau)-M_{0.2}(\tau)\,D_1W_3(0,\tau)+M_{0.3}(\tau)\,D_1W_2(0,\tau)\\&+M_{L.1}(\tau)\Phi_1(L,\tau)-M_{L.2}(\tau)\,D_1W_3(L,\tau)+M_{L.3}(\tau)\,D_1W_2(L,\tau)\\&-B_0(\tau)\,D_1\Phi_1(0,\tau)-B_L(\tau)\,D_1\Phi_1(L,\tau)\ .\end{aligned} \tag{3.3.48}$$

3.3.4 The Lagrangian

The Lagrangian $\mathfrak{L}$ of the bar-load system reads

$$\mathfrak{L} = T - U + W_e \ . \tag{3.3.49}$$

For a given admissible motion of the middle surface, the quantities $\mathfrak{L}$, T, U and W_e are functions of time alone – this was the viewpoint adopted in §§ 3.3.1-3.3.3. However, they can also be considered functions of the generalised displacements (which completely specify the admissible motions of the middle surface) and time. Henceforth, the latter viewpoint shall be adopted.

3.4 THE INITIAL-BOUNDARY VALUE PROBLEM FOR THE GENERALISED DISPLACEMENTS

> The unifying quality of a variational principle is truly remarkable. Although the modern development of physics deviates essentially from the older course on account of relativity and quantum theory, yet the idea of deriving the basic equations of nature from a variational principle has never been abandoned, and both the equations of relativity and the equations of wave mechanics share with the older equations of physics the common feature that they are derivable from a "principle of least action." It is only the Lagrangian function L which has to be defined in a different manner.
>
> CORNELIUS LANCZOS

Let $\mathcal{D}$ be the set of all ordered quadruplets (W_1, W_2, W_3, Φ_1) – henceforth shortened to (W_i, Φ_1) – of generalised displacements that satisfy the essential boundary conditions for the particular problem under consideration and such that:

(i) W_1 is of class $\in C^{3,2}$ on $[0, L] \times [0, \tau_0]$.

(ii) W_2, W_3 and Φ_1 are of class $\in C^{4,2}$ on $[0, L] \times [0, \tau_0]$.

(iii) The partial maps $W_i(\cdot, 0)$, $W_i(\cdot, \tau_0)$, $\Phi_1(\cdot, 0)$, and $\Phi_1(\cdot, \tau_0)$, whose domain is $[0, L]$, are prescribed.

The Hamiltonian action is the functional $\mathfrak{S} : \mathcal{D} \to \mathbb{R}$ defined by

$$\mathfrak{S}(W_i, \Phi_1) = \int_0^{\tau_0} \mathfrak{L}(W_i, \Phi_1, \tau)\, d\tau \ . \tag{3.4.1}$$

Let $(\delta W_i, \delta \Phi_1)$ denote the difference between two members of $\mathcal{D}$ – the maps $\delta W_i, \delta \Phi_1 : [0, L] \times [0, \tau_0] \to \mathbb{R}$ are then collectively called admissible variations of the generalised displacements. Notice that these admissible variations (i) exhibit the same

degree of smoothness as the generalised displacements themselves and (ii) satisfy the homogeneous form of the essential boundary conditions. Moreover, the partial maps $\delta W_i(\cdot,0)$, $\delta W_i(\cdot,\tau_0)$, $\delta\Phi_1(\cdot,0)$, and $\delta\Phi_1(\cdot,\tau_0)$ are identically zero. The first variation of $\mathfrak{S}$ at $(W_i,\Phi_1)\in\mathcal{D}$ in the direction of $(\delta W_i,\delta\Phi_1)$ is defined as

$$\delta\mathfrak{S}(W_i,\Phi_1)[\delta W_i,\delta\Phi_1]=\frac{d}{da}\mathfrak{S}(W_i+a\,\delta W_i,\Phi_1+a\,\delta\Phi_1)\Big|_{a=0}\quad(a\in\mathbb{R})\,. \tag{3.4.2}$$

By Hamilton's principle, or principle of stationary action,[6] $(W_i,\Phi_1)\in\mathcal{D}$ specifies the actual motion of the bar in the time interval $[0,\tau_0]$ if and only if

$$\delta\mathfrak{S}(W_i,\Phi_1)[\delta W_i,\delta\Phi_1]=0 \tag{3.4.3}$$

for every admissible variations δW_i, $\delta\Phi_1$ (*e.g.*, ABRAHAM & MARSDEN 1987, § 3.8, FUNG 1965, §§ 11.1-11.2, GELFAND & FOMIN 1963, § 36, LANCZOS 1970, ch. 5, § 1, LANGHAAR 1962, § 7.2, LOVE 1944, § 115, MEIROVITCH 1970, § 2.7, TRUESDELL & TOUPIN 1960, § 236, or WASHIZU 1975, pp. 2-3). The partial differential equations of motion and the corresponding boundary conditions can now be conveniently obtained from this variational statement.[7] When these are supplemented by the initial conditions, the resulting initial-boundary value problem may be phrased as follows:

Find real-valued maps W_1, W_2, W_3 and Φ_1 defined on $[0,L]\times[0,\tau_0]$, with

- W_1 of class $C^{3,2}$ on $[0,L]\times[0,\tau_0]$ and
- W_2, W_3, Φ_1 of class $C^{4,2}$ on $[0,L]\times[0,\tau_0]$,

satisfying the partial differential equations of motion

$$\begin{aligned}&D_1\left(\tilde{E}A^*\,D_1W_1-\tilde{E}S_3^*\,D_1^2W_2-\tilde{E}S_2^*\,D_1^2W_3-\tilde{E}S_\omega^*\,D_1^2\Phi_1-\tilde{E}S_\psi^*\,D_1\Phi_1\right)(\theta^1,\tau)\\&\quad-\varrho\,A(\theta^1)\,D_2^2W_1(\theta^1,\tau)+\varrho\,S_3(\theta^1)\,D_1D_2^2W_2(\theta^1,\tau)+\varrho\,S_2(\theta^1)\,D_1D_2^2W_3(\theta^1,\tau)\\&\quad+\varrho\,S_\omega(\theta^1)\,D_1D_2^2\Phi_1(\theta^1,\tau)+q_1(\theta^1,\tau)=0\end{aligned} \tag{3.4.4}$$

[6] Not necessarily *least* action – see GALLAVOTTI (1983, § 2.24 and § 3.4), GRAY & TAYLOR (2007) and LANDAU & LIFSCHITZ (2000, p. 2).

[7] This entails (i) the use of Leibniz rule to differentiate under the integral sign (*e.g.*, BARTLE 1967, th. 23.10), (ii) the interchange of the order of integration (*e.g.*, BARTLE 1967, th. 23.12), (iii) integration by parts (*e.g.*, CAMPOS FERREIRA 1987, ch. 5, § 1, th. 18) and (iv) an appeal to the fundamental lemma of the calculus of variations (*e.g.*, DACOROGNA 2004, th. 1.24). It is assumed that the data (geometry and loading) are sufficiently smooth so as to render legitimate the use of these theorems.

$$D_1^2\left(\tilde{E}S_3^*\,D_1W_1-\tilde{E}I_3^*\,D_1^2W_2-\tilde{E}I_{23}^*\,D_1^2W_3-\tilde{E}I_{3\omega}^*\,D_1^2\Phi_1-\tilde{E}I_{3\psi}^*\,D_1\Phi_1\right)(\theta^1,\tau)$$
$$+D_1\left(-\varrho\,S_3\,D_2^2W_1+\varrho\,I_3\,D_1D_2^2W_2+\varrho\,I_{23}\,D_1D_2^2W_3+\varrho\,I_{3\omega}\,D_1D_2^2\Phi_1-m_3\right)(\theta^1,\tau)$$
$$-\varrho\,A(\theta^1)\,D_2^2W_2(\theta^1,\tau)+\varrho\,S_2(\theta^1)\,D_2^2\Phi_1(\theta^1,\tau)+q_2(\theta^1,\tau)=0 \tag{3.4.5}$$

$$D_1^2\left(\tilde{E}S_2^*\,D_1W_1-\tilde{E}I_{23}^*\,D_1^2W_2-\tilde{E}I_2^*\,D_1^2W_3-\tilde{E}I_{2\omega}^*\,D_1^2\Phi_1-\tilde{E}I_{2\psi}^*\,D_1\Phi_1\right)(\theta^1,\tau)$$
$$+D_1\left(-\varrho\,S_2\,D_2^2W_1+\varrho\,I_{23}\,D_1D_2^2W_2+\varrho\,I_2\,D_1D_2^2W_3+\varrho\,I_{2\omega}\,D_1D_2^2\Phi_1+m_2\right)(\theta^1,\tau)$$
$$-\varrho\,A(\theta^1)\,D_2^2W_3(\theta^1,\tau)-\varrho\,S_3(\theta^1)\,D_2^2\Phi_1(\theta^1,\tau)+q_3(\theta^1,\tau)=0 \tag{3.4.6}$$

$$D_1^2\left(\tilde{E}S_\omega^*\,D_1W_1-\tilde{E}I_{3\omega}^*\,D_1^2W_2-\tilde{E}I_{2\omega}^*\,D_1^2W_3-\tilde{E}I_\omega^*\,D_1^2\Phi_1-\tilde{E}I_{\omega\psi}^*\,D_1\Phi_1\right)(\theta^1,\tau)$$
$$+D_1\Big[-\tilde{E}S_\psi^*\,D_1W_1+\tilde{E}I_{3\psi}^*\,D_1^2W_2+\tilde{E}I_{2\psi}^*\,D_1^2W_3$$
$$+\tilde{E}I_{\omega\psi}^*\,D_1^2\Phi_1+\left(GJ+\tilde{E}I_\psi^*\right)D_1\Phi_1\Big](\theta^1,\tau)$$
$$+D_1\left(-\varrho\,S_\omega\,D_2^2W_1+\varrho\,I_{3\omega}\,D_1D_2^2W_2+\varrho\,I_{2\omega}\,D_1D_2^2W_3+\varrho\,I_\omega\,D_1D_2^2\Phi_1+b\right)(\theta^1,\tau)$$
$$+\varrho\,S_2(\theta^1)\,D_2^2W_2(\theta^1,\tau)-\varrho\,S_3(\theta^1)\,D_2^2W_3(\theta^1,\tau)-\varrho\left(I_2(\theta^1)+I_3(\theta^1)\right)D_2^2\Phi_1(\theta^1,\tau)$$
$$+m_1(\theta^1,\tau)=0 \tag{3.4.7}$$

on $(0,L)\times(0,\tau_0)$, together with (i) the appropriate boundary conditions, to be selected from table 3.4.1 (from each row of the table, select one, and only one, boundary condition), and (ii) the initial conditions

$$W_1(\theta^1,0)=W_{1.0}(\theta^1) \qquad D_2W_1(\theta^1,0)=\dot{W}_{1.0}(\theta^1) \tag{3.4.8}$$

$$W_2(\theta^1,0)=W_{2.0}(\theta^1) \qquad D_2W_2(\theta^1,0)=\dot{W}_{2.0}(\theta^1) \tag{3.4.9}$$

$$W_3(\theta^1,0)=W_{3.0}(\theta^1) \qquad D_2W_3(\theta^1,0)=\dot{W}_{3.0}(\theta^1) \tag{3.4.10}$$

$$\Phi_1(\theta^1,0)=\Phi_{1.0}(\theta^1) \qquad D_2\Phi_1(\theta^1,0)=\dot{\Phi}_{1.0}(\theta^1)\ , \tag{3.4.11}$$

where $W_{i.0}$, $\dot{W}_{i.0}$, $\Phi_{1.0}$ and $\dot{\Phi}_{1.0}$ are given real-valued functions on $[0,L]$.[8]

[8] The superposed dot notation in (3.4.8)-(3.4.11) is symbolic rather than operational.

	Natural boundary conditions		Essential boundary conditions
Either	$\tilde{E}A^*(0)D_1W_1(0,\tau)-\tilde{E}S_3^*(0)D_1^2W_2(0,\tau)-\tilde{E}S_2^*(0)D_1^2W_3(0,\tau)-\tilde{E}S_\omega^*(0)D_1^2\Phi_1(0,\tau)-\tilde{E}S_\psi^*(0)D_1\Phi_1(0,\tau)=-Q_{0.1}(\tau)$	or	$W_1(0,\tau)$ prescribed
	$\tilde{E}A^*(L)D_1W_1(L,\tau)-\tilde{E}S_3^*(L)D_1^2W_2(L,\tau)-\tilde{E}S_2^*(L)D_1^2W_3(L,\tau)-\tilde{E}S_\omega^*(L)D_1^2\Phi_1(L,\tau)-\tilde{E}S_\psi^*(L)D_1\Phi_1(L,\tau)=Q_{L.1}(\tau)$		$W_1(L,\tau)$ prescribed
	$D_1\left(\tilde{E}S_3^*D_1W_1-\tilde{E}I_3^*D_1^2W_2-\tilde{E}I_{23}^*D_1^2W_3-\tilde{E}I_{3\omega}^*D_1^2\Phi_1-\tilde{E}I_{3\psi}^*D_1\Phi_1\right)(0,\tau)$ $-\varrho S_3(0)D_2^2W_1(0,\tau)+\varrho I_3(0)D_1D_2^2W_2(0,\tau)+\varrho I_{23}(0)D_1D_2^2W_3(0,\tau)+\varrho I_{3\omega}(0)D_1D_2^2\Phi_1(0,\tau)-m_3(0,\tau)=-Q_{0.2}(\tau)$		$W_2(0,\tau)$ prescribed
	$D_1\left(\tilde{E}S_3^*D_1W_1-\tilde{E}I_3^*D_1^2W_2-\tilde{E}I_{23}^*D_1^2W_3-\tilde{E}I_{3\omega}^*D_1^2\Phi_1-\tilde{E}I_{3\psi}^*D_1\Phi_1\right)(L,\tau)$ $-\varrho S_3(L)D_2^2W_1(L,\tau)+\varrho I_3(L)D_1D_2^2W_2(L,\tau)+\varrho I_{23}(L)D_1D_2^2W_3(L,\tau)+\varrho I_{3\omega}(L)D_1D_2^2\Phi_1(L,\tau)-m_3(L,\tau)=Q_{L.2}(\tau)$		$W_2(L,\tau)$ prescribed
	$\tilde{E}S_3^*(0)D_1W_1(0,\tau)-\tilde{E}I_3^*(0)D_1^2W_2(0,\tau)-\tilde{E}I_{23}^*(0)D_1^2W_3(0,\tau)-\tilde{E}I_{3\omega}^*(0)D_1^2\Phi_1(0,\tau)-\tilde{E}I_{3\psi}^*(0)D_1\Phi_1(0,\tau)=M_{0.3}(\tau)$		$D_1W_2(0,\tau)$ prescribed
	$\tilde{E}S_3^*(L)D_1W_1(L,\tau)-\tilde{E}I_3^*(L)D_1^2W_2(L,\tau)-\tilde{E}I_{23}^*(L)D_1^2W_3(L,\tau)-\tilde{E}I_{3\omega}^*(L)D_1^2\Phi_1(L,\tau)-\tilde{E}I_{3\psi}^*(L)D_1\Phi_1(L,\tau)=-M_{L.3}(\tau)$		$D_1W_2(L,\tau)$ prescribed
	$D_1\left(\tilde{E}S_2^*D_1W_1-\tilde{E}I_{23}^*D_1^2W_2(\theta^1)-\tilde{E}I_2^*D_1^2W_3-\tilde{E}I_{2\omega}^*D_1^2\Phi_1-\tilde{E}I_{2\psi}^*D_1\Phi_1\right)(0,\tau)$ $-\varrho S_2(0)D_2^2W_1(0,\tau)+\varrho I_{23}(0)D_1D_2^2W_2(0,\tau)+\varrho I_2(0)D_1D_2^2W_3(0,\tau)+\varrho I_{2\omega}(0)D_1D_2^2\Phi_1(0,\tau)+m_2(0,\tau)=-Q_{0.3}(\tau)$		$W_3(0,\tau)$ prescribed
	$D_1\left(\tilde{E}S_2^*D_1W_1-\tilde{E}I_{23}^*D_1^2W_2-\tilde{E}I_2^*D_1^2W_3-\tilde{E}I_{2\omega}^*D_1^2\Phi_1-\tilde{E}I_{2\psi}^*D_1\Phi_1\right)(L,\tau)$ $-\varrho S_2(L)D_2^2W_1(L,\tau)+\varrho I_{23}(L)D_1D_2^2W_2(L,\tau)+\varrho I_2(L)D_1D_2^2W_3(L,\tau)+\varrho I_{2\omega}(L)D_1D_2^2\Phi_1(L,\tau)+m_2(L,\tau)=Q_{L.3}(\tau)$		$W_3(L,\tau)$ prescribed

Table 3.4.1: Boundary conditions $(0 \le \tau \le \tau_0)$

	Natural boundary conditions		Essential boundary conditions
Either	$\tilde{E}S^*_2(0)\,D_1W_1(0,\tau)-\tilde{E}I^*_{23}(0)\,D_1^2W_2(0,\tau)-\tilde{E}I^*_2(0)\,D_1^2W_3(0,\tau)-\tilde{E}I^*_{2\omega}(0)\,D_1^2\Phi_1(0,\tau)-\tilde{E}I^*_{2\psi}(0)\,D_1\Phi_1(0,\tau)=-M_{0.2}(\tau)$	or	$D_1W_3(0,\tau)$ prescribed
	$\tilde{E}S^*_2(L)\,D_1W_1(L,\tau)-\tilde{E}I^*_{23}(L)\,D_1^2W_2(L,\tau)-\tilde{E}I^*_2(L)\,D_1^2W_3(L,\tau)-\tilde{E}I^*_{2\omega}(L)\,D_1^2\Phi_1(L,\tau)-\tilde{E}I^*_{2\psi}(L,\tau)\,D_1\Phi_1(L)=M_{L.2}(\tau)$		$D_1W_3(L,\tau)$ prescribed
	$D_1\left(\tilde{E}S^*_\omega\,D_1W_1-\tilde{E}I^*_{3\omega}\,D_1^2W_2-\tilde{E}I^*_{2\omega}\,D_1^2W_3-\tilde{E}I^*_\omega\,D_1^2\Phi_1-\tilde{E}I^*_{\omega\psi}\,D_1\Phi_1\right)(0,\tau)$ $-\tilde{E}S^*_\psi(0)\,D_1W_1(0,\tau)+\tilde{E}I^*_{3\psi}(0)\,D_1^2W_2(0,\tau)+\tilde{E}I^*_{2\psi}(0)\,D_1^2W_3(0,\tau)+\tilde{E}I^*_{\omega\psi}(0)\,D_1^2\Phi_1(0,\tau)+\left(GJ(0)+\tilde{E}I^*_\psi(0)\right)D_1\Phi_1(0,\tau)$ $-\varrho S_\omega(0)\,D_2^2W_1(0,\tau)+\varrho I_{3\omega}(0)\,D_1D_2^2W_2(0,\tau)+\varrho I_{2\omega}(0)\,D_1D_2^2W_3(0,\tau)+\varrho I_\omega(0)\,D_1D_2^2\Phi_1(0,\tau)+b(0,\tau)=-M_{0.1}(\tau)$		$\Phi_1(0,\tau)$ prescribed
	$D_1\left(\tilde{E}S^*_\omega\,D_1W_1-\tilde{E}I^*_{3\omega}\,D_1^2W_2-\tilde{E}I^*_{2\omega}\,D_1^2W_3-\tilde{E}I^*_\omega\,D_1^2\Phi_1-\tilde{E}I^*_{\omega\psi}\,D_1\Phi_1\right)(L,\tau)$ $-\tilde{E}S^*_\psi(L)\,D_1W_1(L,\tau)+\tilde{E}I^*_{3\psi}(L)\,D_1^2W_2(L,\tau)+\tilde{E}I^*_{2\psi}(L)\,D_1^2W_3(L,\tau)+\tilde{E}I^*_{\omega\psi}(L)\,D_1^2\Phi_1(L,\tau)+\left(GJ(L)+\tilde{E}I^*_\psi(L)\right)D_1\Phi_1(L,\tau)$ $-\varrho S_\omega(L)\,D_2^2W_1(L,\tau)+\varrho I_{3\omega}(L)\,D_1D_2^2W_2(L,\tau)+\varrho I_{2\omega}(L)\,D_1D_2^2W_3(L,\tau)+\varrho I_\omega(L)\,D_1D_2^2\Phi_1(L,\tau)+b(L,\tau)=M_{L.1}(\tau)$		$\Phi_1(L,\tau)$ prescribed
	$\tilde{E}S^*_\omega(0)\,D_1W_1(0,\tau)-\tilde{E}I^*_{3\omega}(0)\,D_1^2W_2(0,\tau)-\tilde{E}I^*_{2\omega}(0)\,D_1^2W_3(0,\tau)-\tilde{E}I^*_\omega(0)\,D_1^2\Phi_1(0,\tau)-\tilde{E}I^*_{\omega\psi}(0)\,D_1\Phi_1(0,\tau)=-B_0(\tau)$		$D_1\Phi_1(0,\tau)$ prescribed
	$\tilde{E}S^*_\omega(L)\,D_1W_1(L,\tau)-\tilde{E}I^*_{3\omega}(L)\,D_1^2W_2(L,\tau)-\tilde{E}I^*_{2\omega}(L)\,D_1^2W_3(L,\tau)-\tilde{E}I^*_\omega(L)\,D_1^2\Phi_1(L,\tau)-\tilde{E}I^*_{\omega\psi}(L)\,D_1\Phi_1(L,\tau)=B_L(\tau)$		$D_1\Phi_1(L,\tau)$ prescribed

Table 3.4.1 (continued): Boundary conditions $(0 \le \tau \le \tau_0)$

3.5 CROSS-SECTIONAL STRESS RESULTANTS. EQUATIONS OF BALANCE

The natural boundary conditions in table 3.4.1 lead to the following definitions for the cross-sectional stress resultants (or generalised stresses) – see figure 2.7.1:

(i) Normal force

$$N(\theta^1,\tau) = \tilde{E}A^*(\theta^1)\,D_1W_1(\theta^1,\tau) - \tilde{E}S_3^*(\theta^1)\,D_1^2W_2(\theta^1,\tau) - \tilde{E}S_2^*(\theta^1)\,D_1^2W_3(\theta^1,\tau)$$
$$-\tilde{E}S_\omega^*(\theta^1)\,D_1^2\Phi_1(\theta^1,\tau) - \tilde{E}S_\psi^*(\theta^1)\,D_1\Phi_1(\theta^1,\tau)\ . \tag{3.5.1}$$

(ii) Shear forces

$$V_2(\theta^1,\tau) = D_1\left(\tilde{E}S_3^*\,D_1W_1 - \tilde{E}I_3^*\,D_1^2W_2 - \tilde{E}I_{23}^*\,D_1^2W_3 - \tilde{E}I_{3\omega}^*\,D_1^2\Phi_1 - \tilde{E}I_{3\psi}^*\,D_1\Phi_1\right)(\theta^1,\tau)$$
$$-\varrho\,S_3(\theta^1)\,D_2^2W_1(\theta^1,\tau) + \varrho\,I_3(\theta^1)\,D_1D_2^2W_2(\theta^1,\tau) + \varrho\,I_{23}(\theta^1)\,D_1D_2^2W_3(\theta^1,\tau)$$
$$+\varrho\,I_{3\omega}(\theta^1)\,D_1D_2^2\Phi_1(\theta^1,\tau) - m_3(\theta^1,\tau) \tag{3.5.2}$$

$$V_3(\theta^1,\tau) = D_1\left(\tilde{E}S_2^*\,D_1W_1 - \tilde{E}I_{23}^*\,D_1^2W_2 - \tilde{E}I_2^*\,D_1^2W_3 - \tilde{E}I_{2\omega}^*\,D_1^2\Phi_1 - \tilde{E}I_{2\psi}^*\,D_1\Phi_1\right)(\theta^1,\tau)$$
$$-\varrho\,S_2(\theta^1)\,D_2^2W_1(\theta^1,\tau) + \varrho\,I_{23}(\theta^1)\,D_1D_2^2W_2(\theta^1,\tau) + \varrho\,I_2(\theta^1)\,D_1D_2^2W_3(\theta^1,\tau)$$
$$+\varrho\,I_{2\omega}(\theta^1)\,D_1D_2^2\Phi_1(\theta^1,\tau) + m_2(\theta^1,\tau)\ . \tag{3.5.3}$$

(iii) Bending moments (relative to the axes through $O+\theta^1\boldsymbol{e}_1$ and spanned by $\boldsymbol{e}_2$ and $\boldsymbol{e}_3$)

$$M_2(\theta^1,\tau) = \tilde{E}S_2^*(\theta^1)\,D_1W_1(\theta^1,\tau) - \tilde{E}I_{23}^*(\theta^1)\,D_1^2W_2(\theta^1,\tau) - \tilde{E}I_2^*(\theta^1)\,D_1^2W_3(\theta^1,\tau)$$
$$-\tilde{E}I_{2\omega}^*(\theta^1)\,D_1^2\Phi_1(\theta^1,\tau) - \tilde{E}I_{2\psi}^*(\theta^1)\,D_1\Phi_1(\theta^1,\tau) \tag{3.5.4}$$

$$M_3(\theta^1,\tau) = \tilde{E}S_3^*(\theta^1)\,D_1W_1(\theta^1,\tau) - \tilde{E}I_3^*(\theta^1)\,D_1^2W_2(\theta^1,\tau) - \tilde{E}I_{23}^*(\theta^1)\,D_1^2W_3(\theta^1,\tau)$$
$$-\tilde{E}I_{3\omega}^*(\theta^1)\,D_1^2\Phi_1(\theta^1,\tau) - \tilde{E}I_{3\psi}^*(\theta^1)\,D_1\Phi_1(\theta^1,\tau)\ . \tag{3.5.5}$$

(iv) Torque (about the line $\left\{O+\theta^1\boldsymbol{e}_1,\ 0\le\theta^1\le L\right\}$)

$$M_1(\theta^1,\tau) = D_1\left(\tilde{E}S_\omega^*\,D_1W_1 - \tilde{E}I_{3\omega}^*\,D_1^2W_2 - \tilde{E}I_{2\omega}^*\,D_1^2W_3 - \tilde{E}I_\omega^*\,D_1^2\Phi_1 - \tilde{E}I_{\omega\psi}^*\,D_1\Phi_1\right)(\theta^1,\tau)$$
$$-\tilde{E}S_\psi^*(\theta^1)\,D_1W_1(\theta^1,\tau) + \tilde{E}I_{3\psi}^*(\theta^1)\,D_1^2W_2(\theta^1,\tau) + \tilde{E}I_{2\psi}^*(\theta^1)\,D_1^2W_3(\theta^1,\tau)$$
$$+\tilde{E}I_{\omega\psi}^*(\theta^1)\,D_1^2\Phi_1(\theta^1,\tau) + \left(GJ(\theta^1) + \tilde{E}I_\psi^*(\theta^1)\right)D_1\Phi_1(\theta^1,\tau)$$
$$-\varrho\,S_\omega(\theta^1)\,D_2^2W_1(\theta^1,\tau) + \varrho\,I_{3\omega}(\theta^1)\,D_1D_2^2W_2(\theta^1,\tau) + \varrho\,I_{2\omega}(\theta^1)\,D_1D_2^2W_3(\theta^1,\tau)$$
$$+\varrho\,I_\omega(\theta^1)\,D_1D_2^2\Phi_1(\theta^1,\tau) + b(\theta^1,\tau)\ . \tag{3.5.6}$$

(v) Bimoment (represented by a three-headed arrow in figure 2.7.1)

$$B(\theta^1,\tau) = \tilde{E}S^*_{\omega}(\theta^1)\,D_1W_1(\theta^1,\tau) - \tilde{E}I^*_{3\omega}(\theta^1)\,D_1^2W_2(\theta^1,\tau) - \tilde{E}I^*_{2\omega}(\theta^1)\,D_1^2W_3(\theta^1,\tau)$$
$$-\tilde{E}I^*_{\omega}(\theta^1)\,D_1^2\Phi_1(\theta^1,\tau) - \tilde{E}I^*_{\omega\psi}(\theta^1)\,D_1\Phi_1(\theta^1,\tau)\ . \tag{3.5.7}$$

Indeed, with these definitions, the natural boundary conditions amount to prescribing, at each time τ in $[0,\tau_0]$, the stress resultants at the bar ends.

As discussed in § 2.7, the normal force, bending moments and bimoment have an active character. On the other hand, the shear forces are clearly reactive and satisfy the equations of balance

$$V_2(\theta^1,\tau) = D_1M_3(\theta^1,\tau) - m_3(\theta^1,\tau) + D_2l_3(\theta^1,\tau) \tag{3.5.8}$$

$$V_3(\theta^1,\tau) = D_1M_2(\theta^1,\tau) + m_2(\theta^1,\tau) - D_2l_2(\theta^1,\tau)\ , \tag{3.5.9}$$

which are the dynamic counterparts of the static equilibrium equations (2.7.19)-(2.7.20). As for the torque $M_1(\theta^1,\tau)$, it splits additively into an active part

$$M_1^{(A)}(\theta^1,\tau) = -\tilde{E}S^*_{\psi}(\theta^1)\,D_1W_1(\theta^1,\tau) + \tilde{E}I^*_{3\psi}(\theta^1)\,D_1^2W_2(\theta^1,\tau) + \tilde{E}I^*_{2\psi}(\theta^1)\,D_1^2W_3(\theta^1,\tau)$$
$$+\tilde{E}I^*_{\omega\psi}(\theta^1)\,D_1^2\Phi_1(\theta^1,\tau) + \left(GJ(\theta^1) + \tilde{E}I^*_{\psi}(\theta^1)\right)D_1\Phi_1(\theta^1,\tau) \tag{3.5.10}$$

and a reactive part

$$M_1^{(R)}(\theta^1,\tau) = D_1B(\theta^1,\tau) + b(\theta^1,\tau) - D_2p_{\omega}(\theta^1,\tau)\ . \tag{3.5.11}$$

The incorporation of the definitions (3.5.1) and (3.5.4)-(3.5.6) into the equations of motion (3.4.4)-(3.4.7) yields the following equations of balance on $(0,L)\times(0,\tau_0)$:

$$D_1N(\theta^1,\tau) + \left(q_1(\theta^1,\tau) - D_2p_1(\theta^1,\tau)\right) = 0 \tag{3.5.12}$$

$$D_1^2M_3(\theta^1,\tau) - D_1\left(m_3 - D_2l_3\right)(\theta^1,\tau) + \left(q_2(\theta^1,\tau) - D_2p_2(\theta^1,\tau)\right) = 0 \tag{3.5.13}$$

$$D_1^2M_2(\theta^1,\tau) + D_1\left(m_2 - D_2l_2\right)(\theta^1,\tau) + \left(q_3(\theta^1,\tau) - D_2p_3(\theta^1,\tau)\right) = 0 \tag{3.5.14}$$

$$D_1M_1(\theta^1,\tau) + \left(m_1(\theta^1,\tau) - D_2l_1(\theta^1,\tau)\right) = 0\ . \tag{3.5.15}$$

By virtue of (3.5.11), the last-written equation is equivalent to

$$D_1^2B(\theta^1,\tau) + D_1M_1^{(A)}(\theta^1,\tau) + D_1\left(b - D_2p_{\omega}\right)(\theta^1,\tau) + \left(m_1(\theta^1,\tau) - D_2l_1(\theta^1,\tau)\right) = 0\ , \tag{3.5.16}$$

which makes it clear that $-D_2p_{\omega}$ is a distributed inertial bimoment, just as $-D_2p_i$ and $-D_2l_i$, $i=1,2,3$, are distributed inertial forces and moments, respectively.

3.6 A SUMMARY OF THE FIELD EQUATIONS OF THE ONE-DIMENSIONAL MODEL

This seems a convenient moment to reconsider the one-dimensional model, or at any rate its field equations, as a whole. We seek to relate the generalised displacements, arranged in the column vector

$$\{d\} = \begin{Bmatrix} W_1 \\ W_2 \\ W_3 \\ \Phi_1 \end{Bmatrix} , \tag{3.6.1}$$

to the distributed bar loads, collected in the column vector

$$\{q\} = \begin{Bmatrix} q_1 \\ -m_3' + q_2 \\ m_2' + q_3 \\ b' + m_1 \end{Bmatrix} . \tag{3.6.2}$$

(We recall that this particular definition of $\{q\}$ stems from the requirement that the work of the distributed bar loads be equal to

$$\int_0^L \{q(\theta^1,\tau)\}^T \{d(\theta^1,\tau)\}\, d\theta^1 + \text{boundary terms} .) \tag{3.6.3}$$

As shown next, the sought relation arises as the combination of three kinds of basic equations.

First, one derives two sets of intermediate variables (variables of first kind, according to Tonti's terminology – TONTI 1972) from the generalised displacements – the generalised strains

$$\{e\} = \begin{Bmatrix} \varepsilon \\ \kappa_1 \\ \kappa_2 \\ \kappa_3 \\ \Gamma \end{Bmatrix} \tag{3.6.4}$$

and generalised velocities

$$\{v\} = \begin{Bmatrix} v_1 \\ v_2 \\ v_3 \\ \Xi_1 \\ \Xi_2 \\ \Xi_3 \\ v_\omega \end{Bmatrix} , \tag{3.6.5}$$

by means of the kinematic equations

$$\{e\} = [L_1]\{d\} \tag{3.6.6}$$

$$\{v\} = [L_2]\{d\} \ , \tag{3.6.7}$$

where

$$[L_1] = \begin{bmatrix} D_1 & \cdot & \cdot & \cdot \\ \cdot & \cdot & \cdot & D_1 \\ \cdot & \cdot & -D_1^2 & \cdot \\ \cdot & -D_1^2 & \cdot & \cdot \\ \cdot & \cdot & \cdot & -D_1^2 \end{bmatrix} \tag{3.6.8}$$

$$[L_2] = \begin{bmatrix} D_2 & \cdot & \cdot & \cdot \\ \cdot & D_2 & \cdot & \cdot \\ \cdot & \cdot & D_2 & \cdot \\ \cdot & \cdot & \cdot & D_2 \\ \cdot & \cdot & -D_1 D_2 & \cdot \\ \cdot & D_1 D_2 & \cdot & \cdot \\ \cdot & \cdot & \cdot & -D_1 D_2 \end{bmatrix} \tag{3.6.9}$$

are formal linear differential operators.

Second, two further sets of intermediate variables (variables of second kind), the active stress resultants

$$\{s^{(A)}\} = \begin{Bmatrix} N \\ M_1^{(A)} \\ M_2 \\ M_3 \\ B \end{Bmatrix} \tag{3.6.10}$$

and momentum densities

$$\{p\} = \begin{Bmatrix} p_1 \\ p_2 \\ p_3 \\ l_1 \\ l_2 \\ l_3 \\ p_\omega \end{Bmatrix} , \tag{3.6.11}$$

are obtained from the generalised displacements and velocities by means of the constitutive equations (TONTI & ZARANTONELLO 2010)

$$\left\{s^{(A)}\right\} = [K]\{e\} \tag{3.6.12}$$

$$\{p\} = [I]\{v\} \ , \tag{3.6.13}$$

where $[K]$ is the (symmetric) stiffness matrix

$$[K] = \begin{bmatrix} \tilde{E}A^* & -\tilde{E}S_\psi^* & \tilde{E}S_2^* & \tilde{E}S_3^* & \tilde{E}S_\omega^* \\ -\tilde{E}S_\psi^* & \left(GJ + \tilde{E}I_\psi^*\right) & -\tilde{E}I_{2\psi}^* & -\tilde{E}I_{3\psi}^* & -\tilde{E}I_{\omega\psi}^* \\ \tilde{E}S_2^* & -\tilde{E}I_{2\psi}^* & \tilde{E}I_2^* & \tilde{E}I_{23}^* & \tilde{E}I_{2\omega}^* \\ \tilde{E}S_3^* & -\tilde{E}I_{3\psi}^* & \tilde{E}I_{23}^* & \tilde{E}I_3^* & \tilde{E}I_{3\omega}^* \\ \tilde{E}S_\omega^* & -\tilde{E}I_{\omega\psi}^* & \tilde{E}I_{2\omega}^* & \tilde{E}I_{3\omega}^* & \tilde{E}I_\omega^* \end{bmatrix} \tag{3.6.14}$$

and $[I]$ is the (symmetric) inertia matrix

$$[I] = \begin{bmatrix} \varrho A & \cdot & \cdot & \cdot & \varrho S_2 & -\varrho S_3 & \varrho S_\omega \\ \cdot & \varrho A & \cdot & -\varrho S_2 & \cdot & \cdot & \cdot \\ \cdot & \cdot & \varrho A & \varrho S_3 & \cdot & \cdot & \cdot \\ \cdot & -\varrho S_2 & \varrho S_3 & \varrho\left(I_2 + I_3\right) & \cdot & \cdot & \cdot \\ \varrho S_2 & \cdot & \cdot & \cdot & \varrho I_2 & -\varrho I_{23} & \varrho I_{2\omega} \\ -\varrho S_3 & \cdot & \cdot & \cdot & -\varrho I_{23} & \varrho I_3 & -\varrho I_{3\omega} \\ \varrho S_\omega & \cdot & \cdot & \cdot & \varrho I_{2\omega} & -\varrho I_{3\omega} & \varrho I_\omega \end{bmatrix} , \tag{3.6.15}$$

the entries of which are known real-valued maps defined on $[0, L]$.

Finally, the active stress resultants $\left\{s^{(A)}\right\}$ and momentum densities $\{p\}$ are related to the distributed bar loads $\{q\}$ via the equations of balance

$$[L_1]^\dagger \left\{s^{(A)}\right\} - [L_2]^\dagger \{p\} = \{q\} \ , \tag{3.6.16}$$

where

$$[L_1]^\dagger = \begin{bmatrix} -D_1 & \cdot & \cdot & \cdot & \cdot \\ \cdot & \cdot & \cdot & -D_1^2 & \cdot \\ \cdot & \cdot & -D_1^2 & \cdot & \cdot \\ \cdot & -D_1 & \cdot & \cdot & -D_1^2 \end{bmatrix} \tag{3.6.17}$$

$$[L_2]^\dagger = \begin{bmatrix} -D_2 & \cdot & \cdot & \cdot & \cdot & \cdot & \cdot \\ \cdot & -D_2 & \cdot & \cdot & \cdot & D_1 D_2 & \cdot \\ \cdot & \cdot & -D_2 & \cdot & -D_1 D_2 & \cdot & \cdot \\ \cdot & \cdot & \cdot & -D_2 & \cdot & \cdot & -D_1 D_2 \end{bmatrix} \tag{3.6.18}$$

are the formal adjoint operators of $[L_1]$ and $[L_2]$, respectively.

The kinematic, constitutive and balance equations now combine to yield

$$\left([L_1]^\dagger [K][L_1] - [L_2]^\dagger [I][L_2]\right)\{d\} = \{q\} \ , \tag{3.6.19}$$

which are none other than the equations of motion (3.4.4)-(3.4.7) written in compact matrix form. The process is summarised in figure 3.6.1 by means of a Tonti diagram (TONTI 1972).

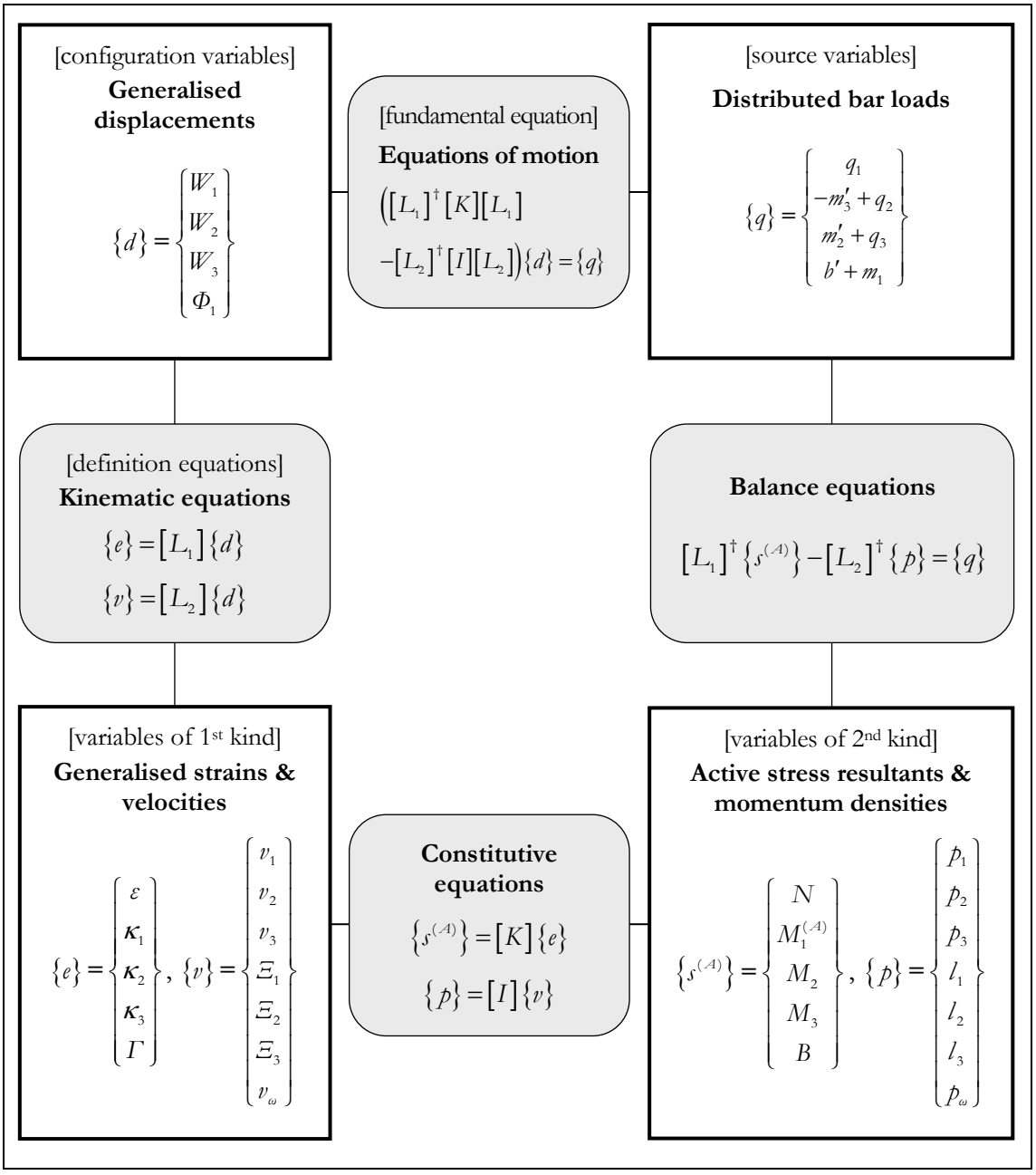

Figure 3.6.1: Tonti diagram (Tonti's usual terminology is given between square brackets)

To complete the above apparatus, all that remains to be done is to introduce the reactive cross-sectional stress resultants, collected in the column vector

$$\left\{ s^{(\mathrm{R})} \right\} = \left\{ \begin{array}{c} V_2 \\ V_3 \\ M_1^{(\mathrm{R})} \end{array} \right\} . \tag{3.6.20}$$

These reactive stress resultants satisfy the equations of balance

$$\left\{ \begin{array}{c} V_2 \\ V_3 \\ M_1^{(\mathrm{R})} \end{array} \right\} = D_1 \left\{ \begin{array}{c} M_3 \\ M_2 \\ B \end{array} \right\} + \left\{ \begin{array}{c} -m_3 \\ m_2 \\ b \end{array} \right\} - D_2 \left\{ \begin{array}{c} -l_3 \\ l_2 \\ p_\omega \end{array} \right\} \tag{3.6.21}$$

and are thus expressible in terms of the generalised displacements as follows:

$$\begin{aligned} \left\{ \begin{array}{c} V_2 \\ V_3 \\ M_1^{(\mathrm{R})} \end{array} \right\} = D_1 \left(\left[\begin{array}{cccc} \tilde{E} S_3^* & -\tilde{E} I_{3\psi}^* & \tilde{E} I_{23}^* & \tilde{E} I_3^* & \tilde{E} I_{3\omega}^* \\ \tilde{E} S_2^* & -\tilde{E} I_{2\psi}^* & \tilde{E} I_2^* & \tilde{E} I_{23}^* & \tilde{E} I_{2\omega}^* \\ \tilde{E} S_\omega^* & -\tilde{E} I_{\omega\psi}^* & \tilde{E} I_{2\omega}^* & \tilde{E} I_{3\omega}^* & \tilde{E} I_\omega^* \end{array} \right] \left\{ \begin{array}{c} D_1 W_1 \\ D_1 \Phi_1 \\ -D_1^2 W_3 \\ -D_1^2 W_2 \\ -D_1^2 \Phi_1 \end{array} \right\} \right) + \left\{ \begin{array}{c} -m_3 \\ m_2 \\ b \end{array} \right\} \\ - \left[\begin{array}{cccc} \varrho S_3 & \varrho I_{23} & -\varrho I_3 & \varrho I_{3\omega} \\ \varrho S_2 & \varrho I_2 & -\varrho I_{23} & \varrho I_{2\omega} \\ \varrho S_\omega & \varrho I_{2\omega} & -\varrho I_{3\omega} & \varrho I_\omega \end{array} \right] D_2^2 \left\{ \begin{array}{c} W_1 \\ -D_1 W_3 \\ D_1 W_2 \\ -D_1 \Phi_1 \end{array} \right\} . \end{aligned} \tag{3.6.22}$$

3.7 PRISMATIC BARS

We now consider a prismatic bar, with its middle surface parametrised as in § 2.9.2. Moreover, the inertial frame $\left(O, \{\boldsymbol{e}_1, \boldsymbol{e}_2, \boldsymbol{e}_3\}\right)$ is chosen to conform with the conditions (2.9.27)-(2.9.28). Adopting the notational conventions of the aforementioned section, the partial differential equations of motion (3.4.4)-(3.4.7) reduce to

$$\begin{aligned} &\tilde{E} A D_1^2 W_1(\theta^1,\tau) - \tilde{E} S_\omega D_1^3 \Phi_1(\theta^1,\tau) - \varrho A D_2^2 W_1(\theta^1,\tau) \\ &\qquad + \varrho S_\omega(\theta^1) D_1 D_2^2 \Phi_1(\theta^1,\tau) + q_1(\theta^1,\tau) = 0 \end{aligned} \tag{3.7.1}$$

$$\begin{aligned} &-\tilde{E} I_3 D_1^4 W_2(\theta^1,\tau) - \tilde{E} I_{3\omega} D_1^4 \Phi_1(\theta^1,\tau) + \varrho I_3 D_1^2 D_2^2 W_2(\theta^1,\tau) + \varrho I_{3\omega} D_1^2 D_2^2 \Phi_1(\theta^1,\tau) \\ &\qquad - D_1 m_3(\theta^1,\tau) - \varrho A D_2^2 W_2(\theta^1,\tau) + q_2(\theta^1,\tau) = 0 \end{aligned} \tag{3.7.2}$$

$$\begin{aligned} &-\tilde{E} I_2 D_1^4 W_3(\theta^1,\tau) - \tilde{E} I_{2\omega} D_1^4 \Phi_1(\theta^1,\tau) + \varrho I_2 D_1^2 D_2^2 W_3(\theta^1,\tau) + \varrho I_{2\omega} D_1^2 D_2^2 \Phi_1(\theta^1,\tau) \\ &\qquad + D_1 m_2(\theta^1,\tau) - \varrho A D_2^2 W_3(\theta^1,\tau) + q_3(\theta^1,\tau) = 0 \end{aligned} \tag{3.7.3}$$

$$\tilde{E}S_{\omega}\,D_1^3W_1(\theta^1,\tau)-\tilde{E}I_{3\omega}\,D_1^4W_2(\theta^1,\tau)-\tilde{E}I_{2\omega}\,D_1^4W_3(\theta^1,\tau)-\tilde{E}I_{\omega}\,D_1^4\Phi_1(\theta^1,\tau)$$
$$+GJ\,D_1^2\Phi_1(\theta^1,\tau)-\varrho S_{\omega}\,D_1D_2^2W_1(\theta^1,\tau)+\varrho I_{3\omega}\,D_1^2D_2^2W_2(\theta^1,\tau)$$
$$+\varrho I_{2\omega}\,D_1^2D_2^2W_3(\theta^1,\tau)+\varrho I_{\omega}\,D_1^2D_2^2\Phi_1(\theta^1,\tau)+D_1b(\theta^1,\tau)$$
$$-\varrho(I_2+I_3)D_2^2\Phi_1(\theta^1,\tau)+m_1(\theta^1,\tau)=0\ . \tag{3.7.4}$$

The momentum densities (3.3.21)-(3.3.23) and (3.3.25)-(3.3.28) become simply

$$p_1(\theta^1,\tau)=\varrho A\,D_2W_1(\theta^1,\tau)-\varrho S_{\omega}\,D_1D_2\Phi_1(\theta^1,\tau) \tag{3.7.5}$$

$$p_2(\theta^1,\tau)=\varrho A\,D_2W_2(\theta^1,\tau) \tag{3.7.6}$$

$$p_3(\theta^1,\tau)=\varrho A\,D_2W_3(\theta^1,\tau) \tag{3.7.7}$$

$$l_1(\theta^1,\tau)=\varrho\left(I_2+I_3\right)D_2\Phi_1(\theta^1,\tau) \tag{3.7.8}$$

$$l_2(\theta^1,\tau)=-\varrho I_2\,D_1D_2W_3(\theta^1,\tau)-\varrho I_{2\omega}\,D_1D_2\Phi_1(\theta^1,\tau) \tag{3.7.9}$$

$$l_3(\theta^1,\tau)=\varrho I_3\,D_1D_2W_2(\theta^1,\tau)+\varrho I_{3\omega}\,D_1D_2\Phi_1(\theta^1,\tau) \tag{3.7.10}$$

$$p_{\omega}(\theta^1,\tau)=\varrho S_{\omega}\,D_2W_1(\theta^1,\tau)-\varrho I_{3\omega}\,D_1D_2W_2(\theta^1,\tau)-\varrho I_{2\omega}\,D_1D_2W_3(\theta^1,\tau)-\varrho I_{\omega}\,D_1D_2\Phi_1(\theta^1,\tau), \tag{3.7.11}$$

while the stress resultants (3.5.1)-(3.5.7) read

$$N(\theta^1,\tau)=\tilde{E}A\,D_1W_1(\theta^1,\tau)-\tilde{E}S_{\omega}\,D_1^2\Phi_1(\theta^1,\tau) \tag{3.7.12}$$

$$V_2(\theta^1,\tau)=-\tilde{E}I_3\,D_1^3W_2(\theta^1,\tau)-\tilde{E}I_{3\omega}\,D_1^3\Phi_1(\theta^1,\tau)+\varrho I_3\,D_1D_2^2W_2(\theta^1,\tau)$$
$$+\varrho I_{3\omega}\,D_1D_2^2\Phi_1(\theta^1,\tau)-m_3(\theta^1,\tau) \tag{3.7.13}$$

$$V_3(\theta^1,\tau)=-\tilde{E}I_2\,D_1^3W_3(\theta^1,\tau)-\tilde{E}I_{2\omega}\,D_1^3\Phi_1(\theta^1,\tau)+\varrho I_2\,D_1D_2^2W_3(\theta^1,\tau)$$
$$+\varrho I_{2\omega}(\theta^1)\,D_1D_2^2\Phi_1(\theta^1,\tau)+m_2(\theta^1,\tau) \tag{3.7.14}$$

$$M_2(\theta^1,\tau)=-\tilde{E}I_2\,D_1^2W_3(\theta^1,\tau)-\tilde{E}I_{2\omega}\,D_1^2\Phi_1(\theta^1,\tau) \tag{3.7.15}$$

$$M_3(\theta^1,\tau)=-\tilde{E}I_3\,D_1^2W_2(\theta^1,\tau)-\tilde{E}I_{3\omega}\,D_1^2\Phi_1(\theta^1,\tau) \tag{3.7.16}$$

$$M_1(\theta^1,\tau)=\tilde{E}S_{\omega}\,D_1^2W_1(\theta^1,\tau)-\tilde{E}I_{3\omega}\,D_1^3W_2(\theta^1,\tau)-\tilde{E}I_{2\omega}\,D_1^3W_3(\theta^1,\tau)-\tilde{E}I_{\omega}\,D_1^3\Phi_1(\theta^1,\tau)$$
$$+GJD_1\Phi_1(\theta^1,\tau)-\varrho S_{\omega}\,D_2^2W_1(\theta^1,\tau)+\varrho I_{3\omega}\,D_1D_2^2W_2(\theta^1,\tau)$$
$$+\varrho I_{2\omega}\,D_1D_2^2W_3(\theta^1,\tau)+\varrho I_{\omega}\,D_1D_2^2\Phi_1(\theta^1,\tau)+b(\theta^1,\tau) \tag{3.7.17}$$

$$B(\theta^1,\tau)=\tilde{E}S_{\omega}\,D_1W_1(\theta^1,\tau)-\tilde{E}I_{3\omega}\,D_1^2W_2(\theta^1,\tau)-\tilde{E}I_{2\omega}\,D_1^2W_3(\theta^1,\tau)-\tilde{E}I_{\omega}\,D_1^2\Phi_1(\theta^1,\tau)\ . \tag{3.7.18}$$

For the purpose of comparison with the literature, it is useful to replace the generalised displacements W_1, W_2 and W_3 with (cf. equations (2.9.49) and (2.9.46)-(2.9.47))

$$\hat{W}_1(\theta^1,\tau) = W_1(\theta^1,\tau) - \left(x_3^S\, \overline{x}_2(0) - x_2^S\, \overline{x}_3(0) \right) D_1\Phi_1(\theta^1,\tau) \tag{3.7.19}$$

$$W_{S.2}(\theta^1,\tau) = W_2(\theta^1,\tau) - x_3^S\, \Phi_1(\theta^1,\tau) \tag{3.7.20}$$

$$W_{S.3}(\theta^1,\tau) = W_3(\theta^1,\tau) + x_2^S\, \Phi_1(\theta^1,\tau)\ , \tag{3.7.21}$$

where x_2^S and x_3^S are the shear centre coordinates, given by (2.9.44)-(2.9.45). Accordingly, the admissible motions $\boldsymbol{U} : [0,L]\times[a,b]\times[0,\tau_0] \to \mathcal{V}$ of the middle surface are rewritten in the form

$$\boldsymbol{U}(\theta^1,\theta^2,\tau) = U_i(\theta^1,\theta^2,\tau)\,\boldsymbol{e}_i \tag{3.7.22}$$

$$U_1(\theta^1,\theta^2,\tau) = \hat{W}_1(\theta^1,\tau) - \overline{x}_2(\theta^2)\, D_1 W_{S.2}(\theta^1,\tau) - \overline{x}_3(\theta^2)\, D_1 W_{S.3}(\theta^1,\tau) - \omega_S(\theta^2)\, D_1\Phi_1(\theta^1,\tau) \tag{3.7.23}$$

$$U_2(\theta^1,\theta^2,\tau) = W_{S.2}(\theta^1,\tau) - \left(\overline{x}_3(\theta^2) - x_3^S \right) \Phi_1(\theta^1,\tau) \tag{3.7.24}$$

$$U_3(\theta^1,\theta^2,\tau) = W_{S.3}(\theta^1,\tau) + \left(\overline{x}_2(\theta^2) - x_2^S \right) \Phi_1(\theta^1,\tau)\ , \tag{3.7.25}$$

where ω_S is the sectorial coordinate defined in equation (2.9.48), with pole at the shear centre. Moreover, if the origin of ω_S is chosen to coincide with a sectorial centroid, then conditions (2.9.54)-(2.9.55) hold and, under such circumstances, the equations of motion take on the form

$$\tilde{E} A\, D_1^2 \hat{W}_1(\theta^1,\tau) - \varrho\, A\, D_2^2 \hat{W}_1(\theta^1,\tau) + q_1(\theta^1,\tau) = 0 \tag{3.7.26}$$

$$\begin{aligned} &-\tilde{E} I_3\, D_1^4 W_{S.2}(\theta^1,\tau) + \varrho\, I_3\, D_1^2 D_2^2 W_{S.2}(\theta^1,\tau) - \varrho\, A\, D_2^2 W_{S.2}(\theta^1,\tau) \\ &\qquad - \varrho\, x_3^S\, A\, D_2^2 \Phi_1(\theta^1,\tau) - D_1 m_3(\theta^1,\tau) + q_2(\theta^1,\tau) = 0 \end{aligned} \tag{3.7.27}$$

$$\begin{aligned} &-\tilde{E} I_2\, D_1^4 W_{S.3}(\theta^1,\tau) + \varrho\, I_2\, D_1^2 D_2^2 W_{S.3}(\theta^1,\tau) - \varrho\, A\, D_2^2 W_{S.3}(\theta^1,\tau) \\ &\qquad + \varrho\, x_2^S\, A\, D_2^2 \Phi_1(\theta^1,\tau) + D_1 m_2(\theta^1,\tau) + q_3(\theta^1,\tau) = 0 \end{aligned} \tag{3.7.28}$$

$$\begin{aligned} &-\varrho\, x_3^S\, A\, D_2^2 W_{S.2}(\theta^1,\tau) + \varrho\, x_2^S\, A\, D_2^2 W_{S.3}(\theta^1,\tau) - \tilde{E} I_{\omega_S}\, D_1^4 \Phi_1(\theta^1,\tau) + \varrho\, I_{\omega_S}\, D_1^2 D_2^2 \Phi_1(\theta^1,\tau) \\ &\quad + GJ\, D_1^2 \Phi_1(\theta^1,\tau) - \varrho \left(I_2 + I_3 + (x_2^S)^2 A + (x_3^S)^2 A \right) D_2^2 \Phi_1(\theta^1,\tau) \\ &\quad + D_1 b_S(\theta^1,\tau) + m_{S.1}(\theta^1,\tau) = 0 \end{aligned} \tag{3.7.29}$$

In the last equation,

$$m_{S.1}(\theta^1,\tau) = m_1(\theta^1,\tau) + x_3^S\, q_2(\theta^1,\tau) - x_2^S\, q_3(\theta^1,\tau) \tag{3.7.30}$$

is the applied distributed torque about the line of shear centres and

$$b_S(\theta^1,\tau) = b(\theta^1,\tau) - \frac{S_\omega}{A} q_1(\theta^1,\tau) - x_2^S\, m_2(\theta^1,\tau) - x_3^S\, m_3(\theta^1,\tau) \tag{3.7.31}$$

is the distributed bimomental load evaluated with the sectorial coordinate ω_S. Moreover, $I_2 + I_3 + (x_2^S)^2 A + (x_3^S)^2 A$ is the cross-section polar second moment of area relative to the

shear centre. Observe that the partial differential equations of motion (3.7.27)-(3.7.29) become uncoupled if $x_2^S = x_3^S = 0$, that is, if the centroid and shear centre coincide.

The above prismatic equations coincide with those obtained by PROKIC (2005), using the principle of virtual displacements. When specialized to the free vibration problem, they are also in full agreement with those derived by VLASOV (1961, ch. 9, § 1), using d'Alembert's principle.[9] In equations (3.7.27)-(3.7.28), the terms $\varrho I_3 D_1^2 D_2^2 W_{S.2}(\theta^1, \tau)$ and $\varrho I_2 D_1^2 D_2^2 W_{S.3}(\theta^1, \tau)$ represent the distributed transverse inertial forces due to the bending rotations of the cross-sections. As for the term $\varrho I_{\omega_S} D_1^2 D_2^2 \Phi_1(\theta^1, \tau)$ in equation (3.7.29), it represents the distributed inertial moment about the line of shear centres due to the torsion warping of the cross-sections. If these three terms are neglected, as often done in structural applications, then equations (3.7.27)-(3.7.29) reduce to those obtained by GERE (1954a) – see also GERE & LIN (1958) and TSO (1964, ch. 1).

In terms of the new set of generalised displacements ($\hat{W}_1$, $W_{S.2}$, $W_{S.3}$ and Φ_1), the components, in the ordered basis $\{\boldsymbol{e}_1, \boldsymbol{e}_2, \boldsymbol{e}_3\}$, of the linear momentum density are given by

$$p_1(\theta^1, \tau) = \varrho A D_2 \hat{W}_1(\theta^1, \tau) \tag{3.7.32}$$

$$p_2(\theta^1, \tau) = \varrho A D_2 W_{S.2}(\theta^1, \tau) + \varrho x_3^S A D_2 \Phi_1(\theta^1, \tau) \tag{3.7.33}$$

$$p_3(\theta^1, \tau) = \varrho A D_2 W_{S.3}(\theta^1, \tau) - \varrho x_2^S A D_2 \Phi_1(\theta^1, \tau) \ , \tag{3.7.34}$$

while the transverse components, l_2 and l_3, of the angular momentum density relative to $O + \theta^1 \boldsymbol{e}_1$ read

$$l_2(\theta^1, \tau) = -\varrho I_2 D_1 D_2 W_{S.3}(\theta^1, \tau) \tag{3.7.35}$$

$$l_3(\theta^1, \tau) = \varrho I_3 D_1 D_2 W_{S.2}(\theta^1, \tau) \ . \tag{3.7.36}$$

The warping momentum density, when evaluated with the sectorial coordinate ω_S, reduces to

$$p_{\omega_S}(\theta^1, \tau) = -\varrho I_{\omega_S} D_1 D_2 \Phi_1(\theta^1, \tau) \ . \tag{3.7.37}$$

It is related to the warping momentum density of equation (3.7.11), evaluated with the sectorial coordinate ω, through the relationship

$$p_{\omega_S}(\theta^1, \tau) = p_\omega(\theta^1, \tau) - \frac{S_\omega}{A} p_1(\theta^1, \tau) - x_2^S l_2(\theta^1, \tau) - x_3^S l_3(\theta^1, \tau) \ . \tag{3.7.38}$$

Finally, the axial component of the angular momentum density relative to $O + \theta^1 \boldsymbol{e}_1 + x_2^S \boldsymbol{e}_2 + x_3^S \boldsymbol{e}_3$ reads

[9] ARPACI *et al.* (2003) do not include the term $\varrho I_{\omega_S} D_1^2 D_2^2 \Phi_1(\theta^1, \tau)$ in equation (3.7.29).

$$l_{S.1}(\theta^1,\tau) = \varrho \int_a^b \left[\left(\overline{x}_2(\theta^2) - x_2^S \right) D_3 U_3(\theta^1,\theta^2,\tau) - \left(\overline{x}_3(\theta^2) - x_2^S \right) D_3 U_2(\theta^1,\theta^2,\tau) \right] \iota(\theta^2)\, d\theta^2$$

$$= \varrho\, x_3^S\, A\, D_2 W_{S.2}(\theta^1,\tau) - \varrho\, x_2^S\, A\, D_2 W_{S.3}(\theta^1,\tau)$$

$$+ \varrho \left(I_2 + I_3 + (x_2^S)^2 A + (x_3^S)^2 A \right) D_2 \Phi_1(\theta^1,\tau) \tag{3.7.39}$$

and is related to the axial component l_1 of the angular momentum density relative to $O + \theta^1 \boldsymbol{e}_1$ (defined in equation (3.7.8)) through

$$l_{S.1}(\theta^1,\tau) = l_1(\theta^1,\tau) + x_3^S\, p_2(\theta^1,\tau) - x_2^S\, p_3(\theta^1,\tau) \ . \tag{3.7.40}$$

As for the stress resultants, the normal force (3.7.12), shear forces (3.7.13)-(3.7.14) and bending moments (3.7.15)-(3.7.16) are given in terms of the new generalised displacements simply by

$$N(\theta^1,\tau) = \tilde{E} A\, D_1 \hat{W}_1(\theta^1,\tau) \tag{3.7.41}$$

$$V_2(\theta^1,\tau) = -\tilde{E} I_3\, D_1^3 W_{S.2}(\theta^1,\tau) + \varrho\, I_3\, D_1 D_2^2 W_{S.2}(\theta^1,\tau) - m_3(\theta^1,\tau) \tag{3.7.42}$$

$$V_3(\theta^1,\tau) = -\tilde{E} I_2\, D_1^3 W_{S.3}(\theta^1,\tau) + \varrho\, I_2\, D_1 D_2^2 W_{S.3}(\theta^1,\tau) + m_2(\theta^1,\tau) \tag{3.7.43}$$

$$M_2(\theta^1,\tau) = -\tilde{E} I_2\, D_1^2 W_{S.3}(\theta^1,\tau) \tag{3.7.44}$$

$$M_3(\theta^1,\tau) = -\tilde{E} I_3\, D_1^2 W_{S.2}(\theta^1,\tau) \ . \tag{3.7.45}$$

The bimoment, when evaluated with the sectorial coordinate ω_S, reduces to

$$B_S(\theta^1,\tau) = -\tilde{E} I_{\omega_S}\, D_1^2 \Phi_1(\theta^1,\tau) \tag{3.7.46}$$

and is related to the bimoment of equation (3.7.18), evaluated with the sectorial coordinate ω, through the relationship

$$B_S(\theta^1,\tau) = B(\theta^1,\tau) - \left(x_3^S\, \overline{x}_2(0) - x_2^S\, \overline{x}_3(0) \right) N(\theta^1,\tau) - x_2^S\, M_2(\theta^1,\tau) + x_3^S\, M_3(\theta^1,\tau) \ . \tag{3.7.47}$$

Finally, the torque about the line of shear centres is

$$M_{S.1}(\theta^1,\tau) = -\tilde{E} I_{\omega_S}\, D_1^3 \Phi_1(\theta^1,\tau) + GJ D_1 \Phi_1(\theta^1,\tau) + \varrho\, I_{\omega_S}\, D_1 D_2^2 \Phi_1(\theta^1,\tau) + b_S(\theta^1,\tau) \tag{3.7.48}$$

and the relation

$$M_{S.1}(\theta^1,\tau) = M_1(\theta^1,\tau) + x_3^S\, V_2(\theta^1,\tau) - x_2^S\, V_3(\theta^1,\tau) \ , \tag{3.7.49}$$

where M_1 is the torque about the line of centroids defined in equation (3.7.17), holds.

For the sake of completeness, the boundary conditions that complement the differential system (3.7.26)-(3.7.29) are indicated in table 3.7.1 (once again, select one, and only one, boundary condition from each row of the table). The initial conditions are entirely analogous to (3.4.8)-(3.4.11) and read

$$\hat{W}_1(\theta^1,0)=\hat{W}_{1.0}(\theta^1) \qquad D_2\hat{W}_1(\theta^1,0)=\dot{\hat{W}}_{1.0}(\theta^1) \tag{3.7.50}$$

$$W_{S.2}(\theta^1,0)=W_{S.2.0}(\theta^1) \qquad D_2W_{S.2}(\theta^1,0)=\dot{W}_{S.2.0}(\theta^1) \tag{3.7.51}$$

$$W_{S.3}(\theta^1,0)=W_{S.3.0}(\theta^1) \qquad D_2W_{S.3}(\theta^1,0)=\dot{W}_{S.3.0}(\theta^1) \tag{3.7.52}$$

$$\Phi_1(\theta^1,0)=\Phi_{1.0}(\theta^1) \qquad D_2\Phi_1(\theta^1,0)=\dot{\Phi}_{1.0}(\theta^1)\ , \tag{3.7.53}$$

with the right-hand sides consisting of given real-valued functions on $[0,L]$.

	Natural boundary conditions		**Essential boundary conditions**
Either	$\tilde{E}A\,D_1\hat{W}_1(0,\tau)=-Q_{0.1}(\tau)$	or	$\hat{W}_1(0,\tau)$ prescribed
	$\tilde{E}A\,D_1\hat{W}_1(L,\tau)=Q_{L.1}(\tau)$		$\hat{W}_1(L,\tau)$ prescribed
	$-\tilde{E}I_3\,D_1^3W_{S.2}(0,\tau)+\varrho I_3\,D_1D_2^2W_{S.2}(0,\tau)-m_3(0,\tau)=-Q_{0.2}(\tau)$		$W_{S.2}(0,\tau)$ prescribed
	$-\tilde{E}I_3\,D_1^3W_{S.2}(L,\tau)+\varrho I_3\,D_1D_2^2W_{S.2}(L,\tau)-m_3(L,\tau)=Q_{L.2}(\tau)$		$W_{S.2}(L,\tau)$ prescribed
	$-\tilde{E}I_3\,D_1^2W_{S.2}(0,\tau)=M_{0.3}(\tau)$		$D_1W_{S.2}(0,\tau)$ prescribed
	$-\tilde{E}I_3\,D_1^2W_{S.2}(L,\tau)=-M_{L.3}(\tau)$		$D_1W_{S.2}(L,\tau)$ prescribed
	$-\tilde{E}I_2\,D_1^3W_{S.3}(0,\tau)+\varrho I_2\,D_1D_2^2W_{S.3}(0,\tau)+m_2(0,\tau)=-Q_{0.3}(\tau)$		$W_{S.3}(0,\tau)$ prescribed
	$-\tilde{E}I_2\,D_1^3W_{S.3}(L,\tau)+\varrho I_2\,D_1D_2^2W_{S.3}(L,\tau)+m_2(L,\tau)=Q_{L.3}(\tau)$		$W_{S.3}(L,\tau)$ prescribed
	$-\tilde{E}I_2\,D_1^2W_{S.3}(0,\tau)=-M_{0.2}(\tau)$		$D_1W_{S.3}(0,\tau)$ prescribed
	$-\tilde{E}I_2\,D_1^2W_{S.3}(L,\tau)=M_{L.2}(\tau)$		$D_1W_{S.3}(L,\tau)$ prescribed
	$-\tilde{E}I_{\omega_S}\,D_1^3\Phi_1(0,\tau)+GJD_1\Phi_1(0,\tau)+\varrho I_{\omega_S}\,D_1D_2^2\Phi_1(0,\tau)$ $+b_S(0,\tau)=-M_{0.1}(\tau)-x_3^S\,Q_{0.2}(\tau)+x_2^S\,Q_{0.3}(\tau)$		$\Phi_1(0,\tau)$ prescribed
	$-\tilde{E}I_{\omega_S}\,D_1^3\Phi_1(L,\tau)+GJD_1\Phi_1(L,\tau)+\varrho I_{\omega_S}\,D_1D_2^2\Phi_1(L,\tau)$ $+b_S(L,\tau)=M_{L.1}(\tau)+x_3^S\,Q_{L.2}(\tau)-x_2^S\,Q_{L.3}(\tau)$		$\Phi_1(L,\tau)$ prescribed
	$-\tilde{E}I_{\omega_S}\,D_1^2\Phi_1(0,\tau)=-B_0(\tau)+\left(x_3^S\,\bar{x}_2(0)-x_2^S\,\bar{x}_3(0)\right)Q_{0.1}(\tau)$ $+x_2^S\,M_{0.2}(\tau)+x_3^S\,M_{0.3}(\tau)$		$D_1\Phi_1(0,\tau)$ prescribed
	$-\tilde{E}I_{\omega_S}\,D_1^2\Phi_1(L,\tau)=B_L(\tau)-\left(x_3^S\,\bar{x}_2(0)-x_2^S\,\bar{x}_3(0)\right)Q_{L.1}(\tau)$ $-x_2^S\,M_{L.2}(\tau)-x_3^S\,M_{L.3}(\tau)$		$D_1\Phi_1(L,\tau)$ prescribed

Table 3.7.1: Prismatic bars – Boundary conditions $(0\le\tau\le\tau_0)$

3.8 VISCOUS DAMPING

The dynamic response of structural systems is inevitably affected by damping. However, due to the variety and complexity of the energy-dissipating mechanisms that may be present, damping is not as easily definable a characteristic as the elastic and inertial forces in a body.[10] As a result, damping is usually described mathematically in a highly idealised manner. Indeed, quoting SCANLAN (1970), "we do not in general pretend that a given mathematical model for damping is more than a poor crutch, yielding perhaps acceptable results in limited ranges, but certainly not implying any detailed explanation of the underlying physics", which is often only qualitatively or superficially understood.

A viscous-type dissipative mechanism, with damping force proportional to the velocity, can be readily accommodated in the one-dimensional model. To this end, the first variation (3.4.2) of the Hamiltonian action $\mathfrak{S}$ is augmented by the velocity-dependent term

$$-\mu_d \, \mathrm{Q} \int_0^{\tau_0} \int_{\bar{\Omega}} D_3 \boldsymbol{U}(\theta^1,\theta^2,\tau) \cdot \delta \boldsymbol{U}(\theta^1,\theta^2,\tau)\, t(\theta^1,\theta^2) \sqrt{a(\theta^1,\theta^2)}\; d\theta^1\, d\theta^2\, d\tau \;, \tag{3.8.1}$$

where μ_d is the viscous damping coefficient, taken to be constant,[11] and

$$\delta \boldsymbol{U}(\theta^1,\theta^2,\tau) = \delta U_i(\theta^1,\theta^2,\tau)\, \boldsymbol{e}_i \tag{3.8.2}$$

$$\begin{aligned} \delta U_1(\theta^1,\theta^2,\tau) = {} & \delta W_1(\theta^1,\tau) - \bar{x}_2(\theta^1,\theta^2)\, D_1 \delta W_2(\theta^1,\tau) \\ & - \bar{x}_3(\theta^1,\theta^2)\, D_1 \delta W_3(\theta^1,\tau) - \omega(\theta^1,\theta^2)\, D_1 \delta \Phi_1(\theta^1,\tau) \end{aligned} \tag{3.8.3}$$

$$\delta U_2(\theta^1,\theta^2,\tau) = \delta W_2(\theta^1,\tau) - \bar{x}_3(\theta^1,\theta^2)\, \delta \Phi_1(\theta^1,\tau) \tag{3.8.4}$$

$$\delta U_3(\theta^1,\theta^2,\tau) = \delta W_3(\theta^1,\tau) + \bar{x}_2(\theta^1,\theta^2)\, \delta \Phi_1(\theta^1,\tau) \;. \tag{3.8.5}$$

---

[10] In broad terms, structural damping mechanisms can be divided into three classes (*e.g.*, ARGYRIS & MLEJNEK 1991, p. 243, VAN KOTEN 1977 or WOODHOUSE 1998):

(i) Energy dissipation distributed throughout the bulk material making up the structure (material damping).

(ii) Dissipation associated with junctions or interfaces between parts of the structure (boundary damping).

(iii) Dissipation associated with a fluid in contact with the structure, involving either local viscous effects or radiation away into the fluid.

[11] It has long been recognised that linear viscous damping models generally have their most correct application in small, restricted frequency ranges. In these ranges, the damping coefficient is usually taken at that constant value which yields an energy loss-per-cycle equivalent, in some sense, to that of the actual structural system being modelled. As observed by SCANLAN (1970), "in overall use, then, the damping coefficient must be considered only as an average «local constant», which is appropriately changed for different frequency ranges of the system under study. No single constant is really appropriate for a response covering a large range of frequencies."

Such a dissipative mechanism is often referred to in the literature as mass-proportional viscous damping (SIMO & VU-QUOC 1986) or viscous air damping (BANKS & INMAN 1991).

The additional term (3.8.1) may be rewritten in the form

$$\begin{aligned}\int_0^{\tau_0}\int_0^{L}\Big(\boldsymbol{f}_d(\theta^1,\tau)\cdot\delta\boldsymbol{W}(\theta^1,\tau)+\boldsymbol{m}_d(\theta^1,\tau)\cdot\delta\boldsymbol{\Phi}(\theta^1,\tau)-b_d(\theta^1,\tau)\,D_1\delta\Phi_1(\theta^1,\tau)\Big)\,d\theta^1\,d\tau\\ =\int_0^{\tau_0}\int_0^{L}\Big(f_{d.i}(\theta^1,\tau)\,\delta W_i(\theta^1,\tau)+m_{d.1}(\theta^1,\tau)\cdot\delta\Phi_1(\theta^1,\tau)-m_{d.2}(\theta^1,\tau)\,D_1\delta W_3(\theta^1,\tau)\\ +m_{d.3}(\theta^1,\tau)\,D_1\delta W_2(\theta^1,\tau)-b_d(\theta^1,\tau)\,D_1\delta\Phi_1(\theta^1,\tau)\Big)\,d\theta^1\,d\tau\ ,\end{aligned}\tag{3.8.6}$$

where

$$\begin{aligned}f_{d.1}(\theta^1,\tau)&=-\mu_d\,\varrho\Big(A(\theta^1)\,D_2W_1(\theta^1,\tau)-S_3(\theta^1)\,D_1D_2W_2(\theta^1,\tau)\\ &\qquad -S_2(\theta^1)\,D_1D_2W_3(\theta^1,\tau)-S_\omega(\theta^1)\,D_1D_2\Phi_1(\theta^1,\tau)\Big)\\ &=-\mu_d\,p_1(\theta^1,\tau)\end{aligned}\tag{3.8.7}$$

$$\begin{aligned}f_{d.2}(\theta^1,\tau)&=-\mu_d\,\varrho\Big(A(\theta^1)\,D_2W_2(\theta^1,\tau)-S_2(\theta^1)\,D_2\Phi_1(\theta^1,\tau)\Big)\\ &=-\mu_d\,p_2(\theta^1,\tau)\end{aligned}\tag{3.8.8}$$

$$\begin{aligned}f_{d.3}(\theta^1,\tau)&=-\mu_d\,\varrho\Big(A(\theta^1)\,D_2W_3(\theta^1,\tau)+S_3(\theta^1)\,D_2\Phi_1(\theta^1,\tau)\Big)\\ &=-\mu_d\,p_3(\theta^1,\tau)\end{aligned}\tag{3.8.9}$$

$$\begin{aligned}m_{d.1}(\theta^1,\tau)&=-\mu_d\,\varrho\Big[-S_2(\theta^1)\,D_2W_2(\theta^1,\tau)+S_3(\theta^1)\,D_2W_3(\theta^1,\tau)\\ &\qquad +\Big(I_2(\theta^1)+I_3(\theta^1)\Big)\,D_2\Phi_1(\theta^1,\tau)\Big]\\ &=-\mu_d\,l_1(\theta^1,\tau)\end{aligned}\tag{3.8.10}$$

$$\begin{aligned}m_{d.2}(\theta^1,\tau)&=-\mu_d\,\varrho\Big(S_2(\theta^1)\,D_2W_1(\theta^1,\tau)-I_{23}(\theta^1)\,D_1D_2W_2(\theta^1,\tau)\\ &\qquad -I_2(\theta^1)\,D_1D_2W_3(\theta^1,\tau)-I_{2\omega}(\theta^1)\,D_1D_2\Phi_1(\theta^1,\tau)\Big)\\ &=-\mu_d\,l_2(\theta^1,\tau)\end{aligned}\tag{3.8.11}$$

$$\begin{aligned}m_{d.3}(\theta^1,\tau)&=-\mu_d\,\varrho\Big(-S_3(\theta^1)\,D_2W_1(\theta^1,\tau)+I_3(\theta^1)\,D_1D_2W_2(\theta^1,\tau)\\ &\qquad +I_{23}(\theta^1)\,D_1D_2W_3(\theta^1,\tau)+I_{3\omega}(\theta^1)\,D_1D_2\Phi_1(\theta^1,\tau)\Big)\\ &=-\mu_d\,l_3(\theta^1,\tau)\end{aligned}\tag{3.8.12}$$

are the components, relative to the ordered basis $\{\boldsymbol{e}_1,\boldsymbol{e}_2,\boldsymbol{e}_3\}$, of the viscous force and moment, which are proportional to the corresponding components of the linear and angular momentum densities, and

$$b_d(\theta^1,\tau) = -\mu_d \varrho \Big(S_\omega(\theta^1)\, D_2 W_1(\theta^1,\tau) - I_{3\omega}(\theta^1)\, D_1 D_2 W_2(\theta^1,\tau) - I_{2\omega}(\theta^1)\, D_1 D_2 W_3(\theta^1,\tau) - I_\omega(\theta^1)\, D_1 D_2 \Phi_1(\theta^1,\tau) \Big)$$
$$= -\mu_d\, p_\omega(\theta^1,\tau) \tag{3.8.13}$$

is the viscous bimoment, which is proportional to the warping momentum density.

With the inclusion of the viscous loads, the equations of balance become

$$D_1 N(\theta^1,\tau) + \Big(q_1(\theta^1,\tau) - D_2 p_1(\theta^1,\tau) - \mu_d\, p_1(\theta^1,\tau) \Big) = 0 \tag{3.8.14}$$

$$D_1^2 M_3(\theta^1,\tau) - D_1 \Big(m_3 - D_2 l_3 - \mu_d\, l_3(\theta^1,\tau) \Big)(\theta^1,\tau) + \Big(q_2(\theta^1,\tau) - D_2 p_2(\theta^1,\tau) - \mu_d\, p_2(\theta^1,\tau) \Big) = 0 \tag{3.8.15}$$

$$D_1^2 M_2(\theta^1,\tau) + D_1 \Big(m_2 - D_2 l_2 - \mu_d\, l_2(\theta^1,\tau) \Big)(\theta^1,\tau) + \Big(q_3(\theta^1,\tau) - D_2 p_3(\theta^1,\tau) - \mu_d\, p_3(\theta^1,\tau) \Big) = 0 \tag{3.8.16}$$

$$D_1^2 B(\theta^1,\tau) + D_1 M_1^{(\mathcal{A})}(\theta^1,\tau) + D_1 \Big(b - D_2 p_\omega - \mu_d\, p_\omega(\theta^1,\tau) \Big)(\theta^1,\tau) + \Big(m_1(\theta^1,\tau) - D_2 l_1(\theta^1,\tau) - \mu_d\, l_1(\theta^1,\tau) \Big) = 0 \ , \tag{3.8.17}$$

which should be compared with their undamped counterparts (3.5.12)-(3.5.14) and (3.5.16).

Alternative dissipative mechanisms typically involve inelastic (*e.g.*, viscoelastic) constitutive behaviour and are beyond the scope of this thesis.

3.9 ILLUSTRATIVE EXAMPLE

Vibrations are everywhere … and so too are the eigenvalues associated with them.

BERESFORD N. PARLETT

As a simple (and partial) illustration of the model developed in this chapter, we will look at the undamped free motion of the family of doubly symmetric web-tapered I-section cantilevers whose reference shape is shown in figure 3.9.1 (identical with the one analysed in § 2.11). The chosen inertial frame, also shown in this figure, is such that the planes containing the origin O and spanned by $\{\boldsymbol{e}_1, \boldsymbol{e}_2\}$ and by $\{\boldsymbol{e}_1, \boldsymbol{e}_3\}$ are the longitudinal planes of symmetry of the reference shape. The bar is clamped at its larger end ($\mathcal{A}_0$) and free at the smaller end ($\mathcal{A}_L$).

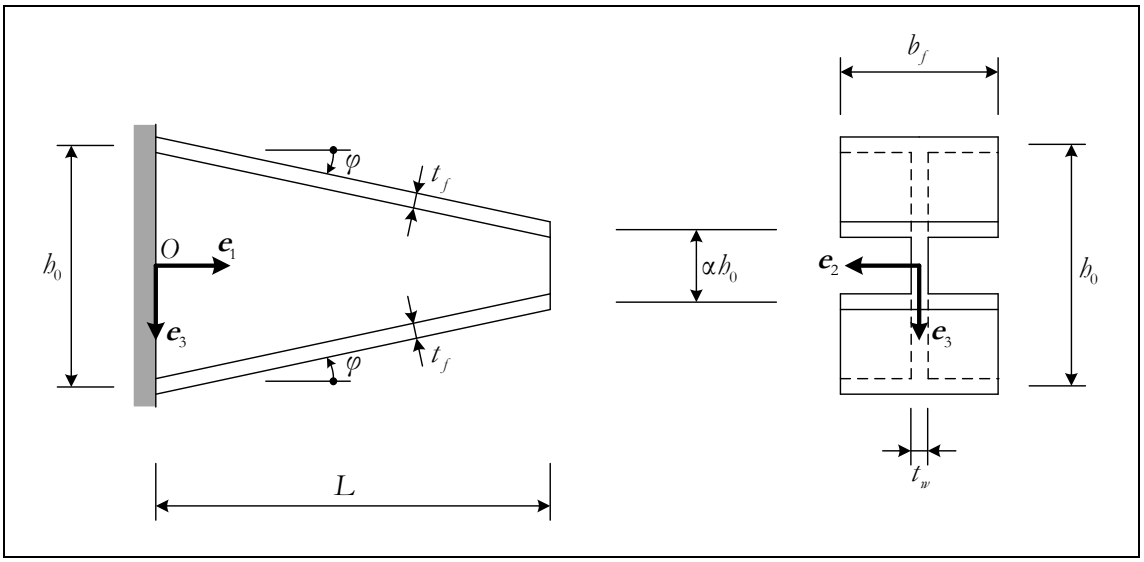

Figure 3.9.1: Illustrative example – Reference shape and support conditions

In this particular example, the initial-boundary value problem for the generalised displacements of § 3.4 is entirely uncoupled due to symmetry and we will restrict attention to the torsional motion, *i.e.*, we will be dealing with the following problem:

Illustrative example (initial-boundary value problem).

Find $\Phi_1 : [0,L]\times[0,\tau_0] \to \mathbb{R}$, with $\Phi_1 \in C^{4,2}[0,L]\times[0,\tau_0]$, satisfying the partial differential equation

$$-D_1^2\left(\tilde{E}I_\omega^*\, D_1^2\Phi_1 + \tilde{E}I_{\omega\psi}^*\, D_1\Phi_1\right)(\theta^1,\tau) + D_1\left[\tilde{E}I_{\omega\psi}^*\, D_1^2\Phi_1 + \left(GJ + \tilde{E}I_\psi^*\right)D_1\Phi_1\right](\theta^1,\tau)$$
$$+\varrho\, D_1\left(I_\omega\, D_1 D_2^2\Phi_1\right)(\theta^1,\tau) - \varrho\left(I_2(\theta^1) + I_3(\theta^1)\right)D_2^2\Phi_1(\theta^1,\tau) = 0 \qquad (3.9.1)$$

on $(0,L)\times(0,\tau_0)$, together with the boundary conditions

$$\Phi_1(0,\tau) = 0\ ,\quad 0 \le \tau \le \tau_0 \qquad (3.9.2)$$

$$D_1\Phi_1(0,\tau) = 0\ ,\quad 0 \le \tau \le \tau_0 \qquad (3.9.3)$$

$$-D_1\left(\tilde{E}I_\omega^*\, D_1^2\Phi_1 + \tilde{E}I_{\omega\psi}^*\, D_1\Phi_1\right)(\theta^1,\tau) - \tilde{E}I_{\omega\psi}^*(L)\, D_1^2\Phi_1(L,\tau)$$
$$+\left(GJ(L) + \tilde{E}I_\psi^*(L)\right)D_1\Phi_1(L,\tau) + \varrho\, I_\omega(L)\, D_1 D_2^2\Phi_1(L,\tau) = 0\ ,\quad 0 \le \tau \le \tau_0 \qquad (3.9.4)$$

$$-\tilde{E}I_\omega^*(L)\, D_1^2\Phi_1(L,\tau) - \tilde{E}I_{\omega\psi}^*(L)\, D_1\Phi_1(L,\tau) = 0\ ,\quad 0 \le \tau \le \tau_0 \qquad (3.9.5)$$

and the initial conditions

$$\Phi_1(\theta^1,0) = \Phi_{1.0}(\theta^1)\ ,\quad 0 \le \theta^1 \le L \qquad (3.9.6)$$

$$D_2\Phi_1(\theta^1,0) = \dot{\Phi}_{1.0}(\theta^1)\ ,\quad 0 \le \theta^1 \le L\ . \qquad (3.9.7)$$

In these equations, I_ω^*, $I_{\omega\psi}^*$, I_ψ^* and J are given by (2.11.7)-(2.11.10), and, by specialisation of (3.3.16)-(3.3.18),

$$I_2(\theta^1)=\left(1-(1-\alpha)\frac{\theta^1}{L}\right)^3\frac{h_0^3\,t_w}{12}+\left(1-(1-\alpha)\frac{\theta^1}{L}\right)^2\frac{h_0^2\,b_f}{2}\frac{t_f}{\cos\varphi} \tag{3.9.8}$$

$$I_3(\theta^1)=\frac{b_f^3\,t_f}{6\cos\varphi} \tag{3.9.9}$$

$$I_\omega(\theta^1)=\left(1-(1-\alpha)\frac{\theta^1}{L}\right)^2\frac{h_0^2\,b_f^3}{24}\frac{t_f}{\cos\varphi}\quad . \tag{3.9.10}$$

The physical significance of the inertial terms $\varrho I_\omega D_1D_2^2\Phi_1$ and $-\varrho(I_2+I_3)D_2^2\Phi_1$ in equation (3.9.1) – a distributed bimoment and a distributed torque, both defined per unit length of the line segment $\left\{O+\theta^1\boldsymbol{e}_1,\,0\le\theta^1\le L\right\}$ – is detailed in figures 3.9.2-3.94.

In the following, we shall ignore the initial conditions and look for a very specific type of (non-trivial) solution, namely a product of two functions, one depending only on θ^1 and four times continuously differentiable, and the other depending only on τ and twice continuously differentiable:

$$\Phi_1(\theta^1,\tau)=\boldsymbol{\phi}(\theta^1)\,f(\tau)\ ,\quad 0\le\theta^1\le L\ ,\quad 0\le\tau\le\tau_0\ . \tag{3.9.11}$$

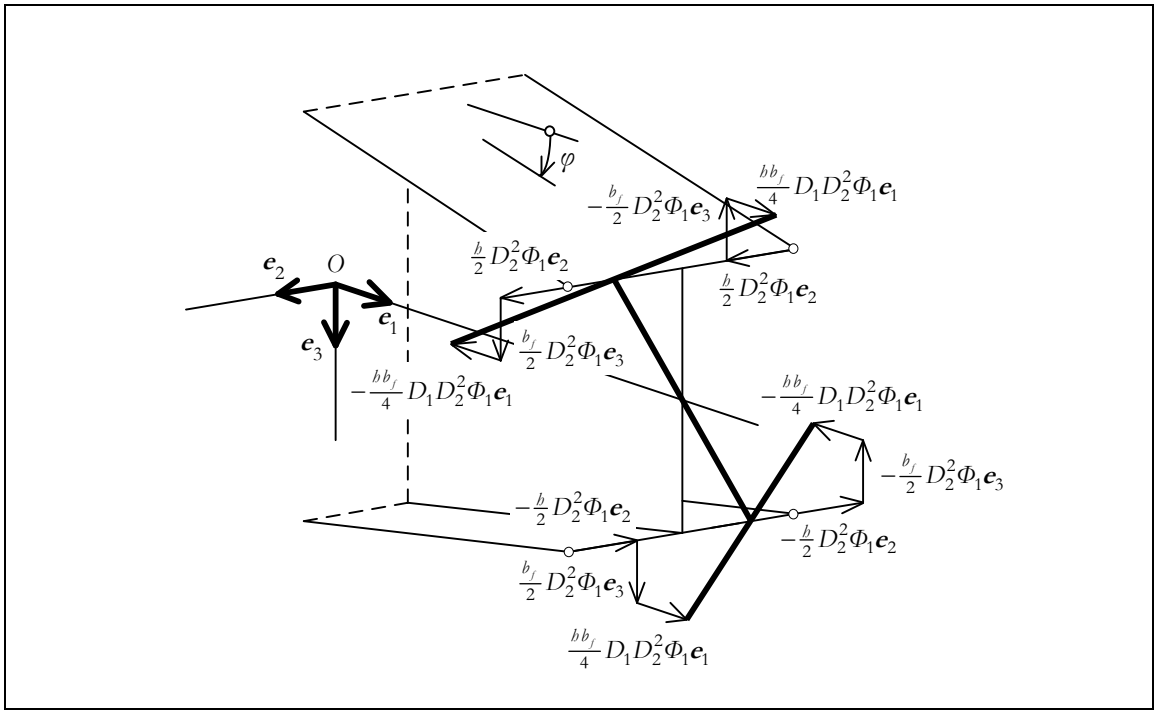

Figure 3.9.2: Illustrative example – Acceleration field $D_3^2\boldsymbol{U}$ of cross-section middle line

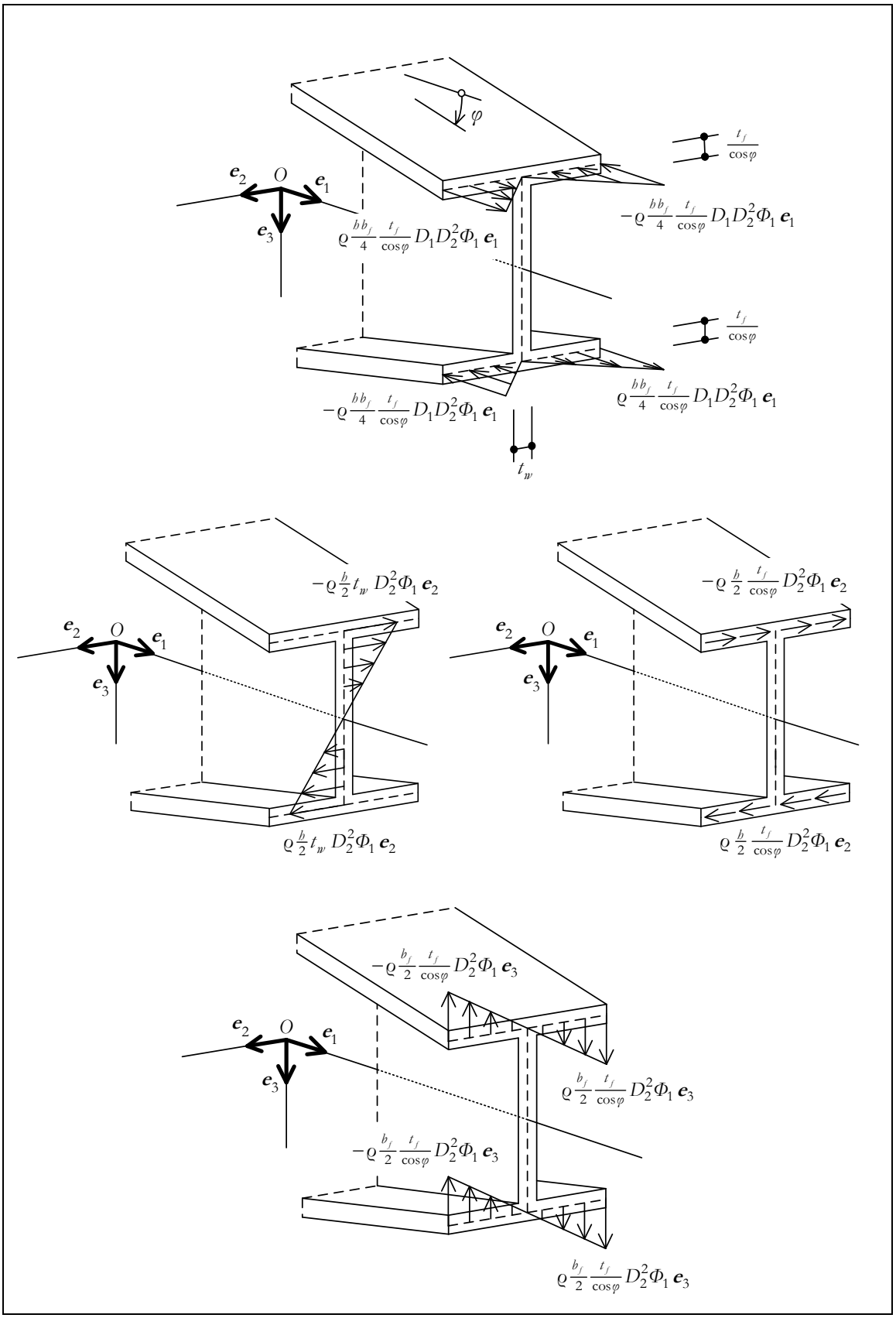

Figure 3.9.3: Illustrative example – Inertial forces $-\varrho D_3^2 \boldsymbol{U}\sqrt{a}\,t$ in the web and in the flanges

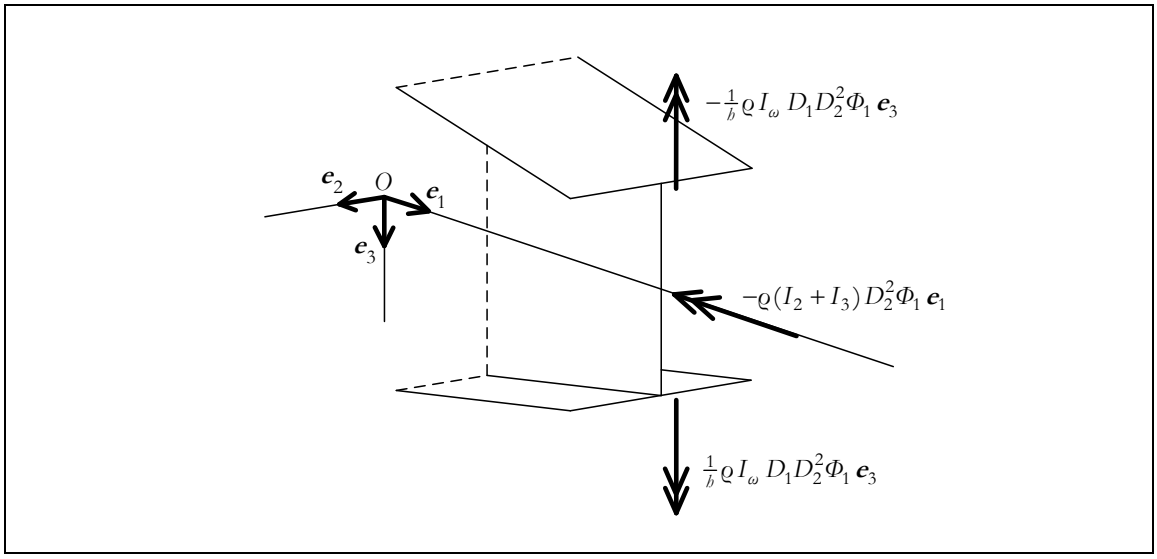

Figure 3.9.4: Illustrative example – Resultants of the inertial forces, defined per unit length of the line segment $\{O+\theta^1\boldsymbol{e}_1, 0\le\theta^1\le L\}$

(In other words, we apply the technique of separation of variables – *e.g.*, BOYCE & DIPRIMA 2009, ch. 10, EVANS 2010, § 4.1, MYINT-U & DEBNATH 2007, ch. 7, STRAUSS 1992, ch. 4, or WEINBERGER 1965, § 14.) The physical implication of (3.9.11) is that the bar undergoes a synchronous motion (MEIROVITCH 1980, p. 239).

Substituting (3.9.11) into equation (3.9.1) and bearing in mind (2.11.11)-(2.11.12), one obtains

$$\Big[-\tilde{E}I_\omega^*(\theta^1)\phi^{(4)}(\theta^1)-2\tilde{E}I_\omega^{*\prime}(\theta^1)\phi'''(\theta^1)+GJ(\theta^1)\phi''(\theta^1)+GJ'(\theta^1)\phi'(\theta^1)\Big]f(\tau)$$
$$+\Big[\varrho I_\omega(\theta^1)\phi''(\theta^1)+\varrho I_\omega'(\theta^1)\phi'(\theta^1)-\varrho\big(I_2(\theta^1)+I_3(\theta^1)\big)\phi(\theta^1)\Big]f''(\tau)=0\ . \quad (3.9.12)$$

Similarly, the boundary conditions (3.9.2)-(3.9.5) become

$$\phi(0)f(\tau)=0\ ,\ 0\le\tau\le\tau_0 \quad (3.9.13)$$

$$\phi'(0)f(\tau)=0\ ,\ 0\le\tau\le\tau_0 \quad (3.9.14)$$

$$\Big[-\tilde{E}I_\omega^*(L)\phi'''(L)-\tilde{E}I_\omega^{*\prime}(L)\phi''(L)+\Big(GJ(L)+\frac{1}{2}\tilde{E}I_\hbar^*(L)\Big)\phi'(L)\Big]f(\tau)$$
$$+\varrho I_\omega(L)\phi'(L)f''(\tau)=0\ ,\ 0\le\tau<\tau_0 \quad (3.9.15)$$

$$\big(-\tilde{E}I_\omega^*(L)\phi''(L)-\tilde{E}I_{\omega\hbar}^*(L)\phi'(L)\big)f(\tau)=0\ ,\ 0\le\tau\le\tau_0 \quad (3.9.16)$$

From equation (3.9.12), we find

$$\frac{\tilde{E}I_{\omega}^{*}(\theta^1)\phi^{(4)}(\theta^1)+2\tilde{E}I_{\omega}^{*\prime}(\theta^1)\phi'''(\theta^1)-GJ(\theta^1)\phi''(\theta^1)-GJ'(\theta^1)\phi'(\theta^1)}{\varrho I_{\omega}(\theta^1)\phi''(\theta^1)+\varrho I_{\omega}'(\theta^1)\phi'(\theta^1)-\varrho\left(I_2(\theta^1)+I_3(\theta^1)\right)\phi(\theta^1)}=\frac{f''(\tau)}{f(\tau)} \qquad (3.9.17)$$

for all $\theta^1 \in (0, L)$ and $\tau \in (0, \tau_0)$ such that

$$\left[\varrho I_{\omega}(\theta^1)\phi''(\theta^1)+\varrho I_{\omega}'(\theta^1)\phi'(\theta^1)-\varrho\left(I_2(\theta^1)+I_3(\theta^1)\right)\phi(\theta^1)\right] f(\tau) \neq 0 \ . \qquad (3.9.18)$$

Clearly, the left-hand side of (3.9.17) depends only on θ^1, while the right-hand side depends only on τ. Hence, the two sides of (3.9.17) are equal to a real constant (called the separation constant), say

$$\frac{\tilde{E}I_{\omega}^{*}(\theta^1)\phi^{(4)}(\theta^1)+2\tilde{E}I_{\omega}^{*\prime}(\theta^1)\phi'''(\theta^1)-GJ(\theta^1)\phi''(\theta^1)-GJ'(\theta^1)\phi'(\theta^1)}{\varrho I_{\omega}(\theta^1)\phi''(\theta^1)+\varrho I_{\omega}'(\theta^1)\phi'(\theta^1)-\varrho\left(I_2(\theta^1)+I_3(\theta^1)\right)\phi(\theta^1)}=\frac{f''(\tau)}{f(\tau)}=-\lambda \ .^{12} \qquad (3.9.19)$$

Therefore, the partial differential equation (3.9.1) separates into the following pair of ordinary differential equations:

$$\tilde{E}I_{\omega}^{*}(\theta^1)\phi^{(4)}(\theta^1)+2\tilde{E}I_{\omega}^{*\prime}(\theta^1)\phi'''(\theta^1)-GJ(\theta^1)\phi''(\theta^1)-GJ'(\theta^1)\phi'(\theta^1)$$
$$+\lambda\varrho\left[I_{\omega}(\theta^1)\phi''(\theta^1)+I_{\omega}'(\theta^1)\phi'(\theta^1)-\left(I_2(\theta^1)+I_3(\theta^1)\right)\phi(\theta^1)\right]=0 \ , \ 0<\theta^1<L \qquad (3.9.20)$$

$$f''(\tau)+\lambda f(\tau)=0 \ , \ 0<\tau<\tau_0 \ . \qquad (3.9.21)$$

The latter equation is linear and homogeneous, with constant coefficients, and so it can be readily solved for any value of λ:

(i) If $\lambda = 0$, its general solution is of the form

$$f(\tau)=c_1+c_2\tau \ , \text{ with } c_1, c_2 \in \mathbb{R} \ . \qquad (3.9.22)$$

(ii) If $\lambda < 0$, the general solution is

$$f(\tau)=c_1 e^{\sqrt{-\lambda}\,\tau}+c_2 e^{-\sqrt{-\lambda}\,\tau} \ , \text{ with } c_1, c_2 \in \mathbb{R} \ . \qquad (3.9.23)$$

(iii) If $\lambda > 0$, we set $\lambda = k^2$ and the general solution of (3.9.21) takes on the form

$$f(\tau)=c_1 e^{ik\tau}+c_2 e^{-ik\tau} \ , \text{ with } c_1, c_2 \in \mathbb{C} \ . \qquad (3.9.24)$$

Moreover, since $f(\tau)$ must be real, it follows that $c_2 = \overline{c_1}$.

Only case (iii), which corresponds to a harmonic oscillation with angular frequency k, is consistent with vibration in the neighbourhood of stable equilibrium. Hence we conclude that if synchronous motion is possible, then the time dependency is harmonic.

[12] It will be seen presently that the separation constant $-\lambda$ must be negative and it is convenient to exhibit the minus sign explicitly.

Now, for the boundary conditions (3.9.13)-(3.9.16) to be satisfied with $f \neq 0$, we must require that

$$\phi(0) = 0 \tag{3.9.25}$$

$$\phi'(0) = 0 \tag{3.9.26}$$

$$-\tilde{E}I_{\omega}^{*}(L)\phi'''(L) - \tilde{E}I_{\omega}^{*\prime}(L)\phi''(L) + \left(GJ(L) + \frac{1}{2}\tilde{E}I_{\psi}^{*}(L) - k^2 \varrho I_{\omega}(L) \right)\phi'(L) = 0 \tag{3.9.27}$$

$$-\tilde{E}I_{\omega}^{*}(L)\phi''(L) - \tilde{E}I_{\omega\psi}^{*}(L)\phi'(L) = 0 \ . \tag{3.9.28}$$

These conditions, together with the ordinary differential equation (3.9.20), form an eigenproblem, which can be phrased as follows:

> **Illustrative example (eigenproblem).**
> Find $\lambda = k^2 > 0$ and $\phi : [0, L] \to \mathbb{R}$, with $\phi \in C^4[0, L]$ and $\phi \neq 0$, satisfying equations (3.9.20) and (3.9.25)-(3.9.28).

The eigenvalues are the squares of the torsional natural frequencies of the bar; the corresponding eigenfunctions are the torsional vibration modes.

Among the structural engineering community, the finite element method, in one of its several versions, is unquestionably the most popular choice for solving such an eigenproblem. The finite element method is based on a variational (or weak) form of the problem, which involves derivatives of lower order than those appearing in the classical (or strong) form and, therefore, poses less stringent smoothness requirements. Moreover, the finite element procedures are very simple and flexible when it comes to (i) describe irregularly shaped multi-dimensional domains and (ii) specify boundary conditions. However, these two features, responsible for the key role played by the finite element method in solving boundary value problems for partial differential equations, are not essential in the case of ordinary differential equations: the construction of a high-order B-spline basis, for instance, is more or less straightforward (*e.g.*, DE BOOR 1978 or SCHUMAKER 2007) and no particular geometrical flexibility is required. In fact, the method of choice advocated for abstract one-dimensional eigenproblems in the numerical analysis literature, particularly when only a small number of eigenvalues and eigenfunctions is sought, consists in their reformulation so that they can be solved using a general-purpose code for boundary value problems in ordinary differential equations (ASCHER *et al.* 1995, BRAMLEY *et al.* 1991 and KELLER 1984). As SEYDEL (2010, p. 263) puts it, we "stay in the «infinite-dimensional space» of ODEs [ordinary differential

equations] and let standard software take care of the transition to the finite-dimensional world of numerical approximation." This approach was successfully applied to prismatic beam vibration problems by YUAN (1991) and will be adopted next.

The basic idea is to convert the original eigenproblem, defined by the differential equation (3.9.20) and the boundary conditions (3.9.25)-(3.9.28), into an inhomogeneous two-point boundary value problem exhibiting the "standard" form required by the software, for which the desired eigenpair corresponds to an isolated solution. This conversion can be achieved in a variety of ways. Our choice was to supplement the original problem with the first-order differential equations

$$\phi_0'(\theta^1) = (k^2)' = 0 \tag{3.9.29}$$

$$\vartheta'(\theta^1) = \phi(\theta^1)^2 \ , \ 0 < \theta^1 < L \ , \tag{3.9.30}$$

and the boundary conditions

$$\vartheta(0) = 0 \tag{3.9.31}$$

$$\vartheta(L) = 1 \ . \tag{3.9.32}$$

The first additional differential equation is just an implicit statement of the fact that each eigenvalue k^2, formally interpreted as a function of θ^1, is a constant. The second one, together with the added boundary conditions, is equivalent to the normalisation condition

$$\int_0^L \phi(\theta^1)^2 \, d\theta^1 = 1 \tag{3.9.33}$$

and makes the eigenfunctions unique (up to sign). It should be noticed that (i) the enlarged boundary value problem is non-linear and (ii) the boundary conditions remain separated.

The problem can now be solved using standard software developed for two-point boundary value problems. In this work, we use the collocation code COLNEW (BADER & ASCHER 1987), ranked among the state-of-the-art codes for the numerical solution of non-linear multi-point boundary value problems for mixed-order systems of ordinary differential equations and separated boundary conditions (CASH 2004, CASH & MAZZIA 2011). It is an improved version of the package COLSYS (ASCHER *et al.* 1981) and both codes are freely available from the ODE library at the NETLIB repository, managed by the University of Tennessee at Knoxville and the Oak Ridge National Laboratory (the current URL is `http://www.netlib.org`). A brief overview of COLNEW and COLSYS is given in Appendix 1, at the end of this chapter.

Numerical results were obtained for the first (lowest) and second torsional natural frequencies and corresponding normalised vibration modes of two series of cantilevers that share the geometrical and material properties

$$L = 4572\,\text{mm} \qquad h_0 = 554.2\,\text{mm} \qquad t_w = 11.4\,\text{mm} \qquad t_f = 17.8\,\text{mm}$$

$$\tilde{E} = 206.8\,\text{GPa} \qquad G = 79.5\,\text{GPa} \qquad \varrho = 7997.4\,\text{kg/m}^3$$

and differ in the width of the flanges: the cantilevers in the first series exhibit $b_f = 203\,\text{mm}$ (narrow flanges), while those in the second series exhibit $b_f = 350\,\text{mm}$ (wide flanges). In both series, the web taper ratio α varies between 0.2 and 1.0. It is worth pointing out that one has $\kappa_{\omega 0} \cong 1.1$ and $\kappa_{\omega 0} \cong 2.0$ for the cantilevers in the first series and second series, respectively – recall the definition of the non-dimensional ratio $\kappa_{\omega 0}$ in (2.11.24).

The first torsional natural frequency, denoted k_1, is shown in figure 3.9.5 as a function of α (solid lines, labelled "tapered model"). The result for $b_f = 203\,\text{mm}$ and $\alpha = 0.378$, namely $k_1 = 125.1\,\text{rad/s}$, is in perfect agreement with the one reported by WEKEZER (1989) – RAJASEKARAN (1994) obtained the slightly lower value of $120.3\,\text{rad/s}$, which amounts to a -3.8% relative difference. If one represents the tapered cantilevers by an assembly of prismatic segments obeying Vlasov's theory and then makes the length of the segments tend to zero (that is, if one sets $\psi = 0$ and $a = 1$ in the general one-dimensional model), one obtains the dashed lines shown in figure 3.9.5 with the label "stepped model". For the first series ($b_f = 203\,\text{mm}$), the solid and dashed lines are close to each other. In contrast, the two lines deviate considerably from each other in the second series ($b_f = 350\,\text{mm}$), with the stepped model delivering higher frequencies for $0.3 < \alpha < 1.0$. Indeed, tapered and stepped models share the same inertial characteristics but exhibit different stiffnesses and, as seen in the first illustrative example of chapter 2 (see figure 2.11.12 in particular), the differences in stiffness increase with $\kappa_{\omega 0}$. For reference purposes, figure 3.9.5 also presents the first torsional frequencies of prismatic cantilevers with the same length and material properties and with the largest or smallest cross-sectional dimensions, *i.e.*, with constant web depth $h_0 = 554.2\,\text{mm}$ or αh_0, respectively (dotted lines, labelled "prismatic, largest section" and "prismatic, smallest section"). It can be seen that the frequencies k_1 of tapered cantilevers fall outside the envelope defined by the dotted lines. According to CYWINSKI (2001), this fact "goes against the conventional engineering intuition, thus becoming a «paradox»". However, one must also observe that the frequencies

yielded by the stepped model also fall outside the said envelope (except for $\alpha < 0.3$ in the first series). In fact, since the natural frequencies depend on the relation between stiffness and inertia, it cannot be anticipated that the frequency k_1 of a tapered cantilever will always be located in-between the values obtained for similar prismatic cantilevers with the largest and smallest cross-sectional dimensions. If sometimes it does not, there is nothing necessarily "paradoxical" about it.

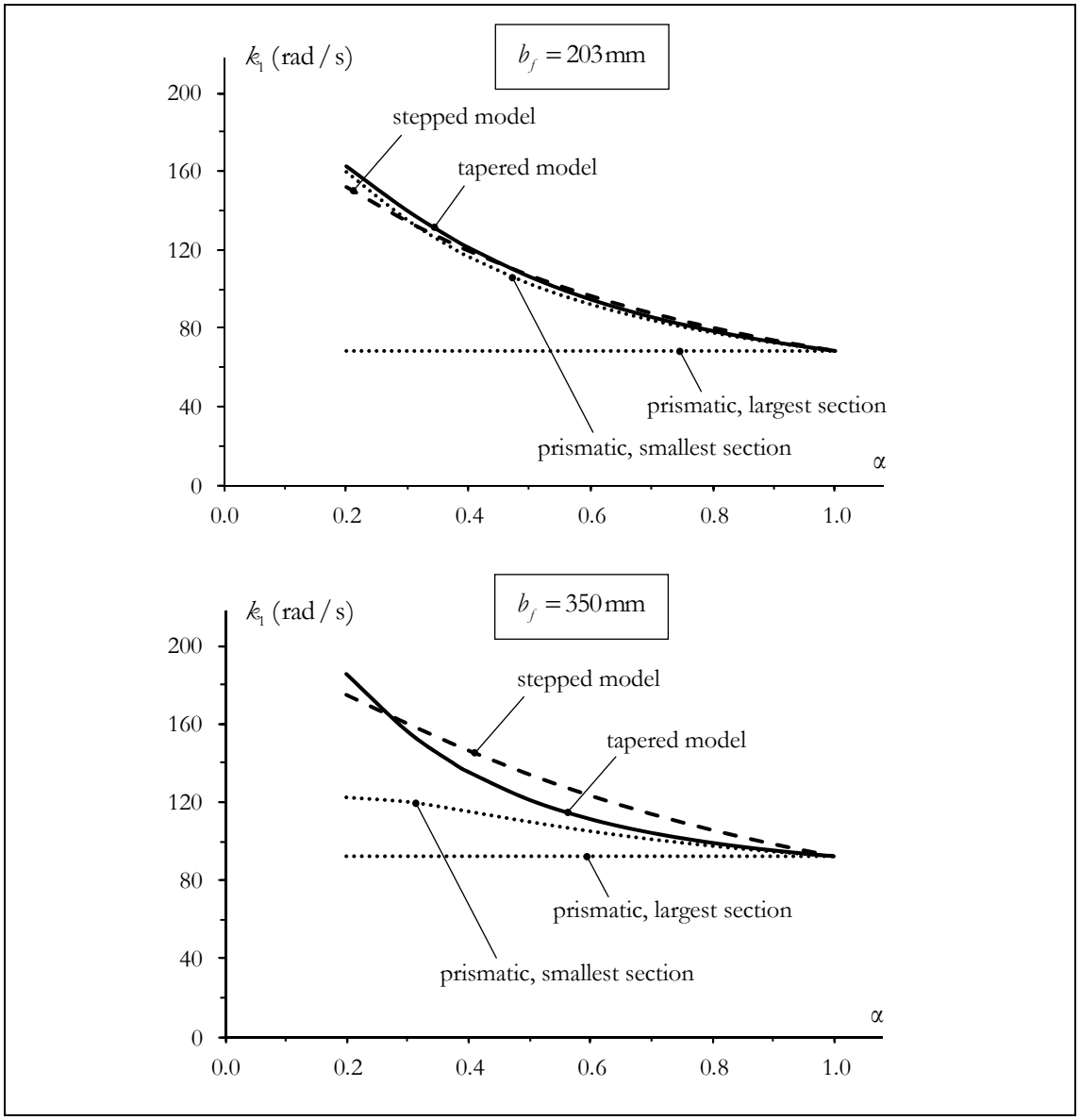

Fig. 3.9.5: Illustrative example – First (lowest) torsional natural frequency k_1 *versus* the taper ratio α

Figure 3.9.6 is analogous to figure 3.9.5 but it concerns the second torsional natural frequency k_2. Finally, figure 3.9.7 illustrates the shapes of the first and second torsional vibration modes of prismatic and tapered cantilevers (drawn with the mathematical software package Mathematica – WOLFRAM RESEARCH, INC. 2006). In the first mode, each flange of the prismatic bar exhibits a single curvature, whereas the flanges of the tapered bar exhibit double curvature. For prismatic and tapered bars alike, the second vibration modes exhibit one node in the open interval $(0, L)$, whereas the first modes exhibit none.

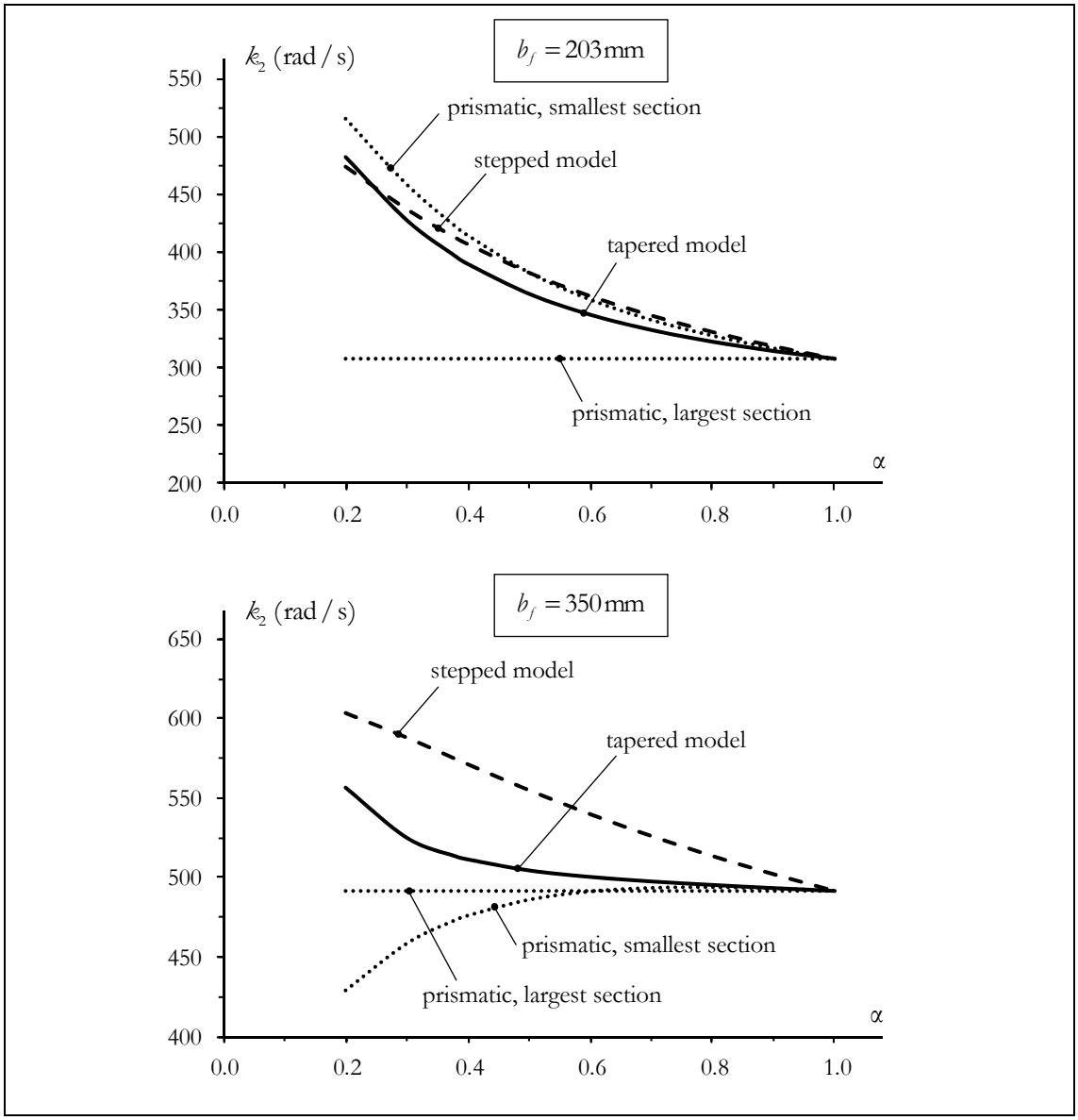

Fig. 3.9.6: Illustrative example – Second torsional natural frequency k_2 *versus* the taper ratio α

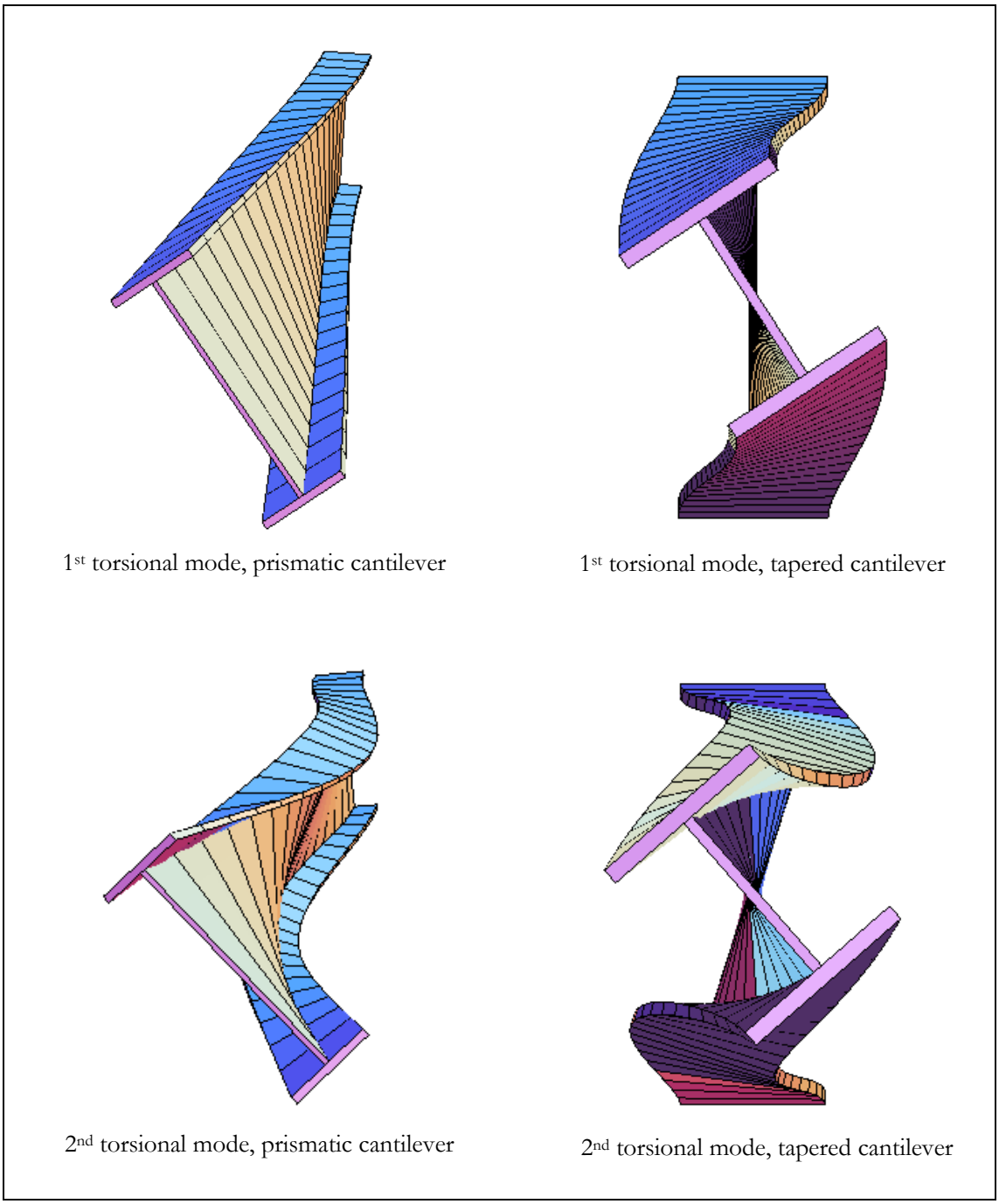

Fig. 3.9.7: Illustrative example – Shapes of the first and second torsional vibration modes of prismatic ($\alpha = 1$) and tapered ($\alpha = 0.4$) cantilevers with $b_f = 203\text{mm}$

APPENDIX 1

The code COLSYS, developed by Ascher, Christiansen and Russell, and its newer version COLNEW, written by Bader and Ascher, are general-purpose codes capable of solving linear and non-linear multi-point boundary value problems comprising a mixed-order system of ordinary differential equations and separated boundary conditions. The improvements incorporated into COLNEW – a different basis representation and several modifications in the linear algebraic equation solver and in the control of the damped Newton iteration process – resulted in a code somewhat more efficient and robust than COLSYS, although the gains in performance vary widely from problem to problem. Both codes have enjoyed considerable success. In this appendix, the numerical techniques used in COLSYS and COLNEW are briefly described. A thorough discussion of the relevant mathematical background and implementation issues can be found in ASCHER (1980), ASCHER *et al.* (1979a, 1979b, 1981, 1995), BADER & ASCHER (1987) and references therein.

Problem specification

The general class of boundary value problems handled by COLSYS and COLNEW consists of:

(i) A system of d non-linear ordinary differential equations of orders $m_1 \le \cdots \le m_d \le 4$

$$\begin{aligned} D^{m_j} y_j &= F_j\left(x; y_1, Dy_1, \cdots, D^{m_1-1} y_1, \cdots, y_d, Dy_d, \cdots, D^{m_d-1} y_d\right) \\ &\equiv F_j\left(x; \boldsymbol{z}(\boldsymbol{y})\right) \ , \quad a < x < b \ , \quad j = 1, \cdots, d \ , \end{aligned} \tag{A1.1}$$

where D denotes differentiation with respect to the independent variable x,

$$\boldsymbol{y} = \left(y_1, \cdots, y_d\right)^T \tag{A1.2}$$

is the sought solution vector and

$$\boldsymbol{z}(\boldsymbol{y}) = \left(y_1, y_1', \cdots, y_1^{(m_1-1)}, y_2, y_2', \cdots, y_2^{(m_2-1)}, \cdots, y_d, y_d', \cdots, y_d^{(m_d-1)}\right)^T \tag{A1.3}$$

is the vector of unknowns that would stem from converting (A1.1) into a first-order system.

(ii) $m^* = \sum_{j=1}^{d} m_j$ non-linear separated boundary conditions of the form

$$g_p\left(s_p; \boldsymbol{z}(\boldsymbol{y})\right) = 0 \ , \quad p = 1, \cdots, m^* \ , \tag{A1.4}$$

where s_p is the location of the p^{th} boundary condition, with $a \le s_1 \le s_2 \le \cdots \le s_{m^*} \le b$.

Solution of linear problems

The numerical method used in COLSYS and COLNEW is piecewise polynomial collocation at Gaussian points – given a mesh $\Pi : a = x_1 < x_2 < \cdots < x_{n+1} = b$ and an integer $M > \max\{m_1, \cdots, m_d\}$, the collocation approximation to the solution of (A1.1) and (A1.4) is a vector-valued function $\boldsymbol{y}_\Pi = (y_{\Pi.1}, \cdots, y_{\Pi.d})^T$ such that:

(C1) $y_{\Pi.j}$ is a polynomial of order $M + m_j$ (degree $< M + m_j$) on each sub-interval $[x_i, x_{i+1}]$;

(C2) $y_{\Pi.j}$ and its first $m_j - 1$ derivatives are continuous on $[a, b]$;

(C3) $\boldsymbol{y}_\Pi$ satisfies the d differential equations (A3.1) at the nM collocation points

$$x_{ir} = x_i + (x_{i+1} - x_i)\varrho_r \ , \ r = 1, \cdots, M \ , \ i = 1, \cdots, n \ , \tag{A1.5}$$

where ϱ_r are the Gauss-Legendre points in $[0,1]$;

(C4) $\boldsymbol{y}_\Pi$ satisfies the m^* boundary conditions (A1.4).

Since any representation of $y_{\Pi.j}$ satisfying (C1) contains $n(M + m_j)$ free parameters, there are a total of $n(Md + m^*)$ unknowns, which are determined by imposing the $n(Md + m^*)$ linear conditions (C2)-(C4), either explicitly or implicitly. In COLSYS, the piecewise polynomial approximate solution is expressed in terms of a B-spline basis (*e.g.*, DE BOOR 1978 or SCHUMAKER 2007), in which the continuity conditions are already embedded – only conditions (C3)-(C4) need to be explicitly satisfied. COLNEW, on the other hand, adopts a local monomial Runge-Kutta basis representation, for which continuity is not built in.

Solution of non-linear problems

The solution of non-linear problems is based on a modified (damped) Newton iteration with quasi-linearisation. Specifically, given an approximation $\boldsymbol{y}^l$ to an isolated solution of (A1.1) and (A1.4), a new (and hopefully better) approximation $\boldsymbol{y}^{l+1}$ is defined by

$$\boldsymbol{y}^{l+1} = \boldsymbol{y}^l + \zeta_l \boldsymbol{w}^l \ , \tag{A1.6}$$

where (i) the Newton correction $\boldsymbol{w}^l$ is the collocation solution of the linear problem

$$D^{m_j} w_j^l = \sum_{r=1}^{m^*} \frac{\partial F_j\left(x; \boldsymbol{z}(\boldsymbol{y}^l)\right)}{\partial z_r} z_r(\boldsymbol{w}^l) + F_j\left(x; \boldsymbol{z}(\boldsymbol{y}^l)\right) - D^{m_j} y_j^l \ ,$$

$$a < x < b \ , \ j = 1, \cdots, d \tag{A1.7}$$

$$\sum_{r=1}^{m^*} \frac{\partial g_p\left(s_p\,;\boldsymbol{z}(\boldsymbol{y}^{\,l})\right)}{\partial z_r} z_r(\boldsymbol{w}^{\,l})(s_p) + g_p\left(s_p\,;\boldsymbol{z}(\boldsymbol{y}^{\,l})\right) = 0 \;,\quad p = 1,\cdots,m^* \tag{A1.8}$$

and (ii) ζ_l is the relaxation (or damping) factor ($0 < \zeta_l \le 1$), which is chosen dynamically to improve convergence.

If the problem is specified by the user as "regular" (instead of "sensitive") and convergence on a given mesh is achieved, then the cautious procedure described above is dropped on the subsequent mesh and the computation proceeds with full Newton steps and holding the Jacobian fixed, provided that the norm of the residual decreases monotonically at a sufficiently rapid rate. Indeed, the converged solution on the former mesh usually constitutes a very good initial approximation, and it is found that the damped Newton method, with careful control of the relaxation factor, is often used only for the first mesh – typically, no adequate initial approximation is then available.

Error estimation and mesh selection

Given a user-specified set of tolerances tol_j and pointers $ltol_j$ ($1 \le ltol_j \le m^*$, $j = 1,\cdots,ntol \le m^*$), COLSYS and COLNEW seek to ensure that

$$\left\| z_l(\boldsymbol{y}) - z_l(\boldsymbol{y}_\Pi) \right\|_{(i)} \le tol_j + \left\| z_l(\boldsymbol{y}_\Pi) \right\|_{(i)} tol_j \;,$$
$$l = ltol_j \;,\quad j = 1,\cdots,ntol \;,\quad i = 1,\cdots,n \;, \tag{A1.9}$$

a mixed absolute/relative control where, for any appropriate function f, the norm

$$\left\| f \right\|_{(i)} = \max_{x \in [x_i, x_{i+1}]} \left| f(x) \right| \tag{A1.10}$$

is evaluated approximately. Therefore, the problem is solved on a sequence of meshes until (A1.9) is deemed satisfied. The codes incorporate reliable algorithms for error estimation and adaptive mesh selection (essentially the same in both versions), with the aim of generating an acceptable solution with the least possible number of mesh points.

Finally, it is important to note that the error estimation algorithm attempts to control the error in a continuous solution, *i.e.*, everywhere within the domain of integration and not only at the mesh points.

REFERENCES

ABRAHAM R. and MARSDEN J.E. (1987). *Foundations of Mechanics* (2nd edition). Redwood City, California: Addison-Wesley.

ABRAHAM R., MARSDEN J.E. and RATIU T. (1988). *Manifolds, Tensor Analysis, and Applications* (2nd edition). New York: Springer.

AMBROSINI D. (2009). On free vibration of nonsymmetrical thin-walled beams. *Thin-Walled Structures*, **47**(6-7), 629-636.

AMBROSINI R.D., RIERA J.D. and DANESI R.F. (1995). Dynamic analysis of thin-walled and variable open section beams with shear flexibility. *International Journal for Numerical Methods in Engineering*, **38**(17), 2867-2885.

AMBROSINI R.D., RIERA J.D. and DANESI R.F. (2000). A modified Vlasov theory for dynamic analysis of thin-walled and variable open section beams. *Engineering Structures*, **22**(8), 890-900.

ARGYRIS J.H. and MLEJNEK H.-P. (1991). *Dynamics of Structures*. Amsterdam: North-Holland.

ARGYRIS J.H. and SYMEONIDIS Sp. (1981). Nonlinear finite element analysis of elastic systems under nonconservative loading – Natural formulation. Part 1: Quasistatic problems. *Computer Methods in Applied Mechanics and Engineering*, **26**(1), 75-123.

ARPACI A., BOZDAG S.E. and SUNBULOGLU E. (2003). Triply coupled vibrations of thin-walled open cross-section beams including rotary inertia effects. *Journal of Sound and Vibration*, **260**(5), 889–900.

ASCHER U. (1980). Solving boundary-value problems with a spline-collocation code. *Journal of Computational Physics*, **34**(3), 401-413.

ASCHER U., CHRISTIANSEN J. and RUSSELL R.D. (1979a). A collocation solver for mixed order systems of boundary value problems. *Mathematics of Computation*, **33**(146), 659-679.

ASCHER U., CHRISTIANSEN J. and RUSSELL R.D. (1979b). COLSYS – A collocation code for boundary-value problems. *Codes for Boundary-Value Problems in Ordinary Differential Equations*, Lecture Notes in Computer Science 76, B. Childs, M. Scott, J.W. Daniel, E. Denman and P. Nelson (Eds.). Berlin: Springer, 164-185.

ASCHER U., CHRISTIANSEN J. and RUSSELL R.D. (1981). Collocation software for boundary-value ODEs. *ACM Transactions on Mathematical Software*, **7**(2), 209-222.

ASCHER U., MATTHEIJ R.M. and RUSSELL R.D. (1995). *Numerical Solution of Boundary Value Problems for Ordinary Differential Equations*. Philadelphia: Society for Industrial and Applied Mathematics (SIAM).

BADER G. and ASCHER U. (1987). A new basis implementation for a mixed order boundary value ODE solver. *SIAM Journal on Scientific and Statistical Computing*, **8**(4), 483-500.

BANKS H.T. and INMAN D.J. (1991). On damping mechanisms in beams. *Journal of Applied Mechanics – Transactions of the ASME*, **58**(3), 716-723.

BARTLE R.G. (1967). *The Elements of Real Analysis*. New York: Wiley.

DE BOOR C. (1978). *A Practical Guide to Splines*. New York: Springer.

BOYCE W.E. and DIPRIMA R.C. (2009). *Elementary Differential Equations and Boundary Value Problems* (9th edition). Hoboken, New Jersey: Wiley.

BRAMLEY S., DIECI L. and RUSSELL R.D. (1991). Numerical solution of eigenvalue problems for linear boundary value ODEs. *Journal of Computational Physics*, **94**(2), 382-402.

CAMPOS FERREIRA J. (1987). *Introdução à Análise Matemática* [Introduction to Mathematical Analysis]. Lisboa: Fundação Calouste Gulbenkian.

CASH J.R. (2004). A survey of some global methods for solving two-point BVPs. *Applied Numerical Analysis & Computational Mathematics*, **1**(1), 7-17.

CASH J.R. and MAZZIA F. (2011). Efficient global methods for the numerical solution of nonlinear systems of two point boundary value problems. *Recent Advances in Computational and Applied Mathematics*, T.E. Simos (Ed.). Dordrecht, The Netherlands: Springer, 23-39.

CYWINSKI Z. (2001). History of a "paradox" for thin-walled members with variable, open cross-section. *International Journal of Structural Stability and Dynamics*, **1**(1), 47-58.

DACOROGNA B. (2004). *Introduction to the Calculus of Variations*. London: Imperial College Press.

DIEUDONNÉ J. (1960). *Foundations of Modern Analysis*. New York: Academic Press.

EISENBERGER M. (1997). Torsional vibrations of open and variable cross-section bars. *Thin-Walled Structures*, **28**(3-4), 269-278.

EVANS L.C. (2010). *Partial Differential Equations* (2nd edition). Providence, Rhode Island: American Mathematical Society.

FEDERHOFER K. (1947). Eigenschwingungen von geraden Stäben mit dünnwandigen und offenen Querschnitten [Natural vibrations of straight bars with thin-walled and open sections]. *Sitzungsberichte der Akademie der Wissenschaften in Wien*, **156**, 393-416.

FUNG Y.C. (1965). *Foundations of Solid Mechanics*. Englewood Cliffs, New Jersey: Prentice-Hall.

GALLAVOTTI G. (1983). *The Elements of Mechanics*. New York: Springer.

GELFAND I.M. and FOMIN S.V. (1963). *Calculus of Variations*. Englewood Cliffs, New Jersey: Prentice-Hall.

GERE J.M. (1954a). *Bending and Torsional Vibrations of Thin-Walled Bars of Open Cross-Section*. Ph.D. Thesis, Stanford University.

GERE J.M. (1954b). Torsional vibration of beams of thin-walled open sections. *Journal of Applied Mechanics – Transactions of the ASME*, **21**(4), 381-387.

GERE J.M. and LIN Y.K. (1958). Coupled vibrations of thin-walled beams of open cross section. *Journal of Applied Mechanics – Transactions of the ASME*, **25**(3), 373-378.

GOLDSTEIN H., POOLE C. and SAFKO J. (2001). *Classical Mechanics* (3rd edition). San Francisco: Addison-Wesley.

GRAY C.G. and TAYLOR E.F. (2007). When action is not least. *American Journal of Physics*, **75**(5), 434-458.

GREENWOOD D.T. (1997). *Classical Dynamics*. Mineola, New York: Dover.

GURTIN M.E. (1972). The linear theory of elasticity. *Handbuch der Physik*, Volume VIa/2, C. Truesdell (Ed.). Berlin: Springer, 1-295.

KELLER H.B. (1984). *Numerical Solution of Two Point Boundary Value Problems*. Philadelphia: Society for Industrial and Applied Mathematics (SIAM).

VAN KOTEN H. (1977). Structural damping. *Heron*, **22**(4), 4-68.

LANCZOS C. (1970). *The Variational Principles of Mechanics* (4th edition). Toronto: University of Toronto Press.

LANDAU L.D. and LIFSCHITZ E.M. (2000). *Mechanics* (3rd edition). Course of Theoretical Physics, Volume 1. Oxford: Butterworth Heinemann.

LANGHAAR H.L. (1962). *Energy Methods in Applied Mechanics*. New York: Wiley.

LOVE A.E.H. (1944). *A Treatise on the Mathematical Theory of Elasticity* (4th edition). New York: Dover.

MEIROVITCH L. (1970). *Methods of Analytical Dynamics*. New York: McGraw-Hill.

MEIROVITCH L. (1980). *Computational Methods in Structural Dynamics*. Alphen aan den Rijn, The Netherlands: Sijthoff & Noordhoff.

MYINT-U T. and DEBNATH L. (2007). *Linear Partial Differential Equations for Scientists and Engineers* (4th edition). Boston: Birkhäuser.

PROKIC A. (2005). On triply coupled vibrations of thin-walled beams with arbitrary cross-section. *Journal of Sound and Vibration*, **279**(3-5), 723-737.

RAJASEKARAN S. (1994). Instability of tapered thin-walled beams of generic section. *Journal of Engineering Mechanics – ASCE*, **120**(8), 1630-1640.

RAO C.K. and MIRZA S. (1988). Free torsional vibrations of tapered cantilever I-beams. *Journal of Sound and Vibration*, **124**(3), 489-496.

SANTANA A.P. and QUEIRÓ J.F. (2010). *Introdução à Álgebra Linear* [Introduction to Linear Algebra]. Lisboa: Gradiva.

SCANLAN R.H. (1970). Linear damping models and causality in vibrations. *Journal of Sound and Vibration*, **13**(4), 499-503.

SCHUMAKER L.L. (2007). *Spline Functions: Basic Theory* (3rd edition). Cambridge: Cambridge University Press.

SEYDEL R. (2010). *Practical Bifurcation and Stability Analysis* (3rd edition). New York: Springer.

SIMO J.C. and VU-QUOC L. (1986). On the dynamics of flexible beams under large overall motions – The plane case: Part I. *Journal of Applied Mechanics – Transactions of the ASME*, **53**(4), 849-854.

STRAUSS W.A. (1992). *Partial Differential Equations – An Introduction*. New York: Wiley.

TONTI E. (1972). On the mathematical structure of a large class of physical theories. *Rendiconti della Classe di Scienze Fisiche, Matematiche e Naturali – Accademia Nazionale dei Lincei*, Serie 8, **52**(1), 48-56.

TONTI E. and ZARANTONELLO F. (2010). Algebraic formulation of elastodynamics: The cell method. *CMES – Computer Modeling in Engineering & Sciences*, **64**(1), 37-70.

TRUESDELL C. (1991). *A First Course in Rational Continuum Mechanics*, Volume 1: General Concepts (2nd edition). San Diego, California: Academic Press.

TRUESDELL C. and TOUPIN R. (1960). The classical field theories. *Handbuch der Physik*, Volume III/1, S. Flügge (Ed.). Berlin: Springer, 225-793.

TSO W.K. (1964). *Dynamics of Thin-Walled Beams of Open Section*. Ph.D. Thesis, California Institute of Technology.

VLASOV V.Z. (1961). *Thin-Walled Elastic Beams* [English translation of the 2nd Russian edition of 1959]. Jerusalem: Israel Program for Scientific Translation. French translation of the said Russian edition by G. Smirnoff (1962), *Pièces Longues en Voiles Minces*. Paris: Eyrolles.

WASHIZU K. (1975). *Variational Methods in Elasticity and Plasticity* (2nd edition). Oxford: Pergamon Press.

WEINBERGER H.F. (1965). *A First Course in Partial Differential Equations – With Complex Variables and Transform Methods*. New York: Dover.

WEKEZER J.W. (1987). Free vibrations of thin-walled bars with open cross sections. *Journal of Engineering Mechanics – ASCE*, **113**(10), 1441-1453.

WEKEZER J.W. (1989). Vibrational analysis of thin-walled bars with open cross sections. *Journal of Structural Engineering – ASCE*, **115**(12), 2965-2978.

WILDE P. (1968). The torsion of thin-walled bars with variable cross-section. *Archiwum Mechaniki Stosowanej*, **4**(20), 431-443.

WOLFRAM RESEARCH, INC. (2006). *Wolfram Mathematica 6.2*. Champaign, Illinois.

WOODHOUSE J. (1998). Linear damping models for structural vibration. *Journal of Sound and Vibration*, **215**(3), 547-569.

YUAN S. (1991). ODE conversion techniques and their applications in computational mechanics. *Acta Mechanica Sinica*, **7**(3), 283-288.

Chapter 4

ONE-DIMENSIONAL MODEL FOR THE LATERAL-TORSIONAL BUCKLING OF SINGLY SYMMETRIC TAPERED THIN-WALLED BEAMS WITH OPEN CROSS-SECTIONS

Todo o mundo é composto de mudança,
Tomando sempre novas qualidades.
Continuamente vemos novidades,
Diferentes em tudo da esperança.

LUÍS VAZ DE CAMÕES

4.1 INTRODUCTION

Beams (that is, slender flexural members) loaded in the plane of greatest bending stiffness may buckle out of that plane by deflecting laterally and twisting, a bifurcation-type instability known as lateral-torsional buckling (LTB). Due to their typically low lateral bending and torsional rigidities, thin-walled bars with open cross-sections are particularly susceptible to this phenomenon.

The first tapered beams whose LTB behaviour was investigated were the strip ones (*i.e.*, those having narrow rectangular cross-sections with varying depth and/or thickness). The discussion of this subject is postponed to the next chapter. Then came the I-section beams with varying web depth and/or flange width. CULVER & PREG (1968) investigated the elastic LTB behaviour of doubly symmetric I-beams with linear homothetic tapering and acted by unequal end moments. They used Bernoulli-Euler's bending theory and Lee's non uniform torsion equation (LEE 1956) to establish adjacent equilibrium equations and presented some numerical results, obtained by means of a finite difference approach. A similar analysis was undertaken by DUBAS (1984) for doubly symmetric I-beams with linearly

varying depth. His numerical results, however, are not to be trusted, due to the unjustified neglect of certain terms – precisely those that are peculiar to web-tapered I-beams. KITIPORNCHAI & TRAHAIR (1972) also addressed the buckling of doubly symmetric I-beams, but they considered more general tapering configurations and loading conditions. A few years later, they extended the analysis to singly symmetric I-beams (KITIPORNCHAI & TRAHAIR 1975). The numerical results reported by the last-mentioned authors, obtained by means of the finite integral method, were shown to correlate rather well with experimental values. More recently, BRAHAM (1997) employed the method of Galerkin to solve the buckling equations derived by Kitipornchai and Trahair. We recall that the cited works of Lee and Kitipornchai & Trahair were critically examined in § 2.11. Those criticisms carry over, word by word, to the LTB case.

Finite element formulations to perform linear buckling analyses of tapered I-beams were developed by YANG & YAU (1987), for doubly symmetric beams, and by BRADFORD & CUK (1988) and BOISSONNADE & MUZEAU (2001), for singly symmetric web-tapered I-beams. These investigations adopt (more or less) hidden assumptions and unstated approximations.

WEKEZER (1985) appears to have been the first researcher to study the LTB of thin-walled tapered beams with arbitrary cross-section and loading. He used a finite element formulation, in which (i) the walls are treated as membranes and (ii) both the in-plane cross-section deformations and the middle surface shear strains are neglected. However, this formulation is not fully consistent, partly because the internal constraints have only a kinematical character, without constitutive implications, and partly because the cross-section shear centre locations are not properly handled (in general, the location of the shear centre varies along the beam longitudinal axis). About a decade later, RAJASEKARAN (1994a) derived non linear equilibrium equations also valid for tapered beams with arbitrary cross-section, which were then solved by means of the finite element method (RAJASEKARAN 1994b). However, his derivation of the non linear strain-displacement relations is inconsistent, since it omits terms having the same order of magnitude as others which are retained.

Finally, RONAGH *et al.* (2000a, b) developed a general theory that can be used to obtain the expressions of the first and second variations of the total potential energy of thin-walled tapered beams, again with arbitrary cross-section and loading. Once again, constraints are imposed upon a membrane shell model, but these constraints are not treated as having a constitutive character. Moreover, it is not clear that the constraints have an intrinsic geometrical meaning, independent of the choice of parametrisation for the middle surface.

For the sake of completeness, this brief literature review on the LTB of tapered thin-walled beams with open cross-sections must also include a reference to the investigations that used either (i) the prismatic beam strain-displacement relationships to analyse tapered beams (as Bazant had done in the linear static case – recall § 2.1.2) or (ii) a discretisation with prismatic beam finite elements (*i.e.*, stepped models) – *e.g.*, BAZANT & EL NIMEIRI (1973), BRAHAM & HANIKENNE (1993), BROWN (1981), CHAN (1990), GALÉA (1986), GUPTA *et al.* (1996), NETHERCOT (1973) and TEBEDGE (1972). As mentioned earlier, these procedures are, in general, conceptually incorrect, because they fail to capture relevant aspects of the torsional behaviour that stem from the cross-section variation.

In this chapter, we derive anew, in a simpler and more direct manner, the one-dimensional model originally proposed by ANDRADE & CAMOTIM (2005) for the elastic lateral-torsional buckling of singly symmetric tapered thin-walled beams with open cross-sections. The adopted kinematical description precludes the model from capturing any local or distortional phenomena. Moreover, the effect of the pre-buckling deflections is ignored. The classical model of VLASOV (1961, ch. 6, § 3) for singly symmetric prismatic beams is obtained as a special case. It is then shown, using an archetypal problem, how the presence of out-of-plane restraints can be accommodated in the one-dimensional buckling model. The ensuing parametric study once again highlights the differences between the predictions of tapered and stepped (piecewise prismatic) models, which are given a physical explanation.

4.2 THE LINEARISED LATERAL-TORSIONAL BUCKLING PROBLEM

4.2.1 Statement of the problem

Let us consider a tapered thin-walled bar with open cross-sections, a regular middle surface and a longitudinal plane of symmetry, as described in § 2.9.1. The generalisation to bars with irregular middle surfaces can be done along the lines proposed in § 2.10 and warrants no further elaboration. Moreover, let us choose a fixed Cartesian frame for $\mathcal{E}$ and a parametrisation for the middle surface as in § 2.9.1. In particular, the reader should bear in mind that

$$\overline{x}_2(\theta^1,\theta^2) = -\overline{x}_2(\theta^1,-\theta^2) \tag{4.2.1}$$

$$\overline{x}_3(\theta^1,\theta^2) = \overline{x}_3(\theta^1,-\theta^2)) \tag{4.2.2}$$

$$t^*(\theta^1,\theta^2) = t^*(\theta^1,-\theta^2) \tag{4.2.3}$$

$$\omega(\theta^1,\theta^2) = -\omega(\theta^1,-\theta^2) \tag{4.2.4}$$

$$\psi(\theta^1,\theta^2) = -\psi(\theta^1,-\theta^2) \tag{4.2.5}$$

for every (θ^1,θ^2) in $\overline{\Omega}$. Consequently, the geometrical properties S_3^*, S_ω^*, S_ψ^*, I_{23}^*, $I_{2\omega}^*$ and $I_{2\psi}^*$ are all identically zero.

The longitudinal plane of symmetry of the bar – the plane through the origin O and spanned by $\{\boldsymbol{e}_1,\boldsymbol{e}_3\}$ – is assumed to be its plane of greatest bending stiffness. We prescribe a system of conservative bar loads, initially acting in this plane and comprising:

(i) a distributed force, described by the continuous map $\boldsymbol{q} = q_3\,\boldsymbol{e}_3 : [0,L] \to \mathcal{V}$, applied at the (constant) level $x_3 = x_3^q$;[1]

(ii) concentrated forces $\boldsymbol{Q}_0 = \mathcal{Q}_{0.3}\,\boldsymbol{e}_3$ and $\boldsymbol{Q}_L = \mathcal{Q}_{L.3}\,\boldsymbol{e}_3$, applied at the points $O + x_3^{\mathcal{Q}_0}\,\boldsymbol{e}_3$ and $O + L\,\boldsymbol{e}_1 + x_3^{\mathcal{Q}_L}\,\boldsymbol{e}_3$, respectively;

(iii) concentrated moments $\boldsymbol{M}_0 = M_{0.2}\,\boldsymbol{e}_2$ and $\boldsymbol{M}_L = M_{L.2}\,\boldsymbol{e}_2$ at the end sections $\mathcal{A}_0$ and $\mathcal{A}_L$, respectively.

The magnitudes of all these loads are deemed proportional to a single load factor λ, and so we write $q_3 = \lambda\, q_{ref}$, $\mathcal{Q}_{0.3} = \lambda\, \mathcal{Q}_{0.ref}$, $\mathcal{Q}_{L.3} = \lambda\, \mathcal{Q}_{L.ref}$, $M_{0.2} = \lambda\, M_{0.ref}$ and $M_{L.2} = \lambda\, M_{L.ref}$, where the subscript *"ref"* indicates a reference magnitude. When $\lambda = 1$, we speak of the reference load system.

---

[1] The assumption of a constant x_3^q is not essential and it would have been a simple matter to consider it as a continuous (or even piecewise continuous) real-valued function on $[0,L]$.

The specific nature of the conservative applied end moments (*i.e.*, their generating mechanism) needs to be specified (*e.g.*, ANDRADE *et al.* 2010a or SIMITSES & HODGES 2006, § 9.2). For definiteness, both end moments are taken to be of the quasi-tangential type,[2] each being generated by a pair of opposite conservative forces, parallel to $\boldsymbol{e}_1$ and applied to the ends of a rigid lever, rigidly attached to the bar. These levers are initially parallel to $\boldsymbol{e}_3$ and lie in the plane defined by the origin O and $\{\boldsymbol{e}_1, \boldsymbol{e}_3\}$, as shown in figure 4.2.1.

In a fundamental equilibrium state, the beam is subjected solely to bending in its plane of greatest flexural stiffness and the corresponding shape is symmetric with respect to this plane. The lateral-torsional buckled states, on the other hand, are associated with non-symmetric shapes – the beam deflects laterally (out-of-plane) and twists. It is required to find those values of λ, called buckling load factors, for which LTB occurs and the associated buckling modes.

4.2.2 Non-linear kinematics

For a given load factor λ, let the fundamental equilibrium shape of the middle surface be specified by the admissible displacement field $(\theta^1, \theta^2) \in \bar{\Omega} \mapsto \boldsymbol{U}^f(\theta^1, \theta^2, \lambda) \in \mathcal{V}$. Moreover, let $\boldsymbol{u} = u_i\, \boldsymbol{e}_i : \bar{\Omega} \to \mathcal{V}$ specify the transition from this fundamental state to an adjacent state, at the same load level λ.

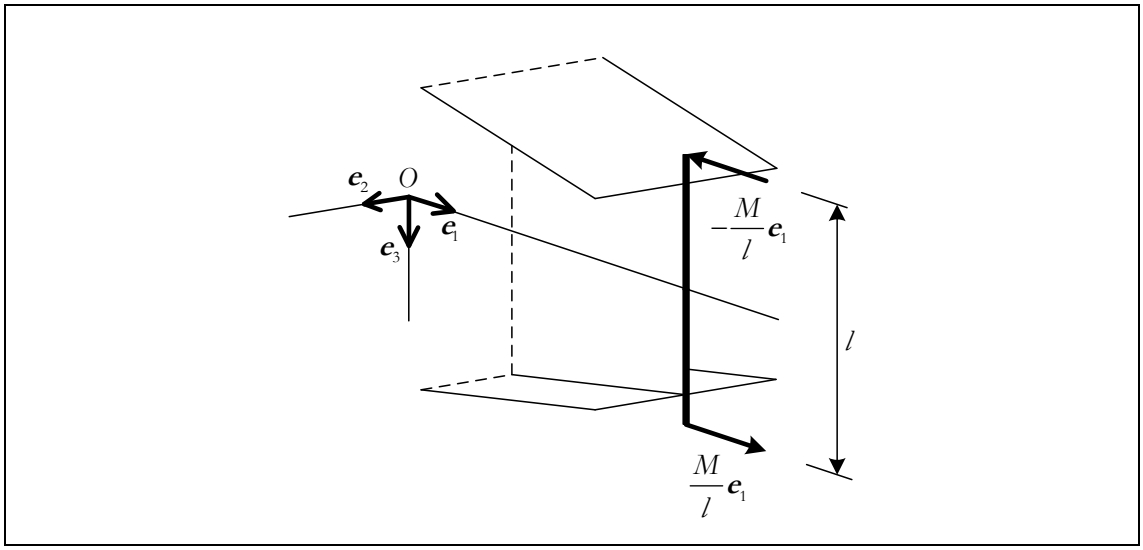

Figure 4.2.1: Quasi-tangential applied moment

[2] This is the terminology adopted by ARGYRIS *et al.* (1978a, b). ZIEGLER (1952, 1953, 1956, 1968) uses instead the term "pseudo-tangential".

With the aim of linearising the LTB problem, we ignore the change in shape between the reference and the fundamental equilibrium states, *i.e.*, we introduce the hypothesis that the pre-buckling displacements are negligible (PIGNATARO *et al.* 1991, p. 230).

Following ATTARD (1986), GHOBARAH & TSO (1971) and DE VILLE DE GOYET (1989, § 4.3), the fact that each cross-section middle line is constrained not to deform in its own plane[3] is approximately interpreted as implying expressions of the form

$$u_2(\theta^1,\theta^2) = w_2(\theta^1) - \overline{x}_2(\theta^1,\theta^2)\left(1-\cos\phi_1(\theta^1)\right) - \overline{x}_3(\theta^1,\theta^2)\sin\phi_1(\theta^1) \tag{4.2.6}$$

$$u_3(\theta^1,\theta^2) = w_3(\theta^1) + \overline{x}_2(\theta^1,\theta^2)\sin\phi_1(\theta^1) - \overline{x}_3(\theta^1,\theta^2)\left(1-\cos\phi_1(\theta^1)\right) \tag{4.2.7}$$

for the $\boldsymbol{e}_2$ - and $\boldsymbol{e}_3$-components of the incremental displacement field $\boldsymbol{u}$. These components are thus completely determined by the generalised displacements $w_2, w_3, \phi_1 : [0,L] \to \mathbb{R}$, which, for the moment, are taken to be twice continuously differentiable. The assumption of small deflections, combined with the possibility of a large twist, are implicit in (4.2.6)-(4.2.7).[4]

The covariant components of the Green membrane strain tensor field associated with the displacement field $\boldsymbol{u}$ are given by (CIARLET 2000, th. 9.1.1)

$$\begin{aligned} G_{\alpha\beta}(\theta^1,\theta^2) &= \boldsymbol{a}_\alpha(\theta^1,\theta^2)\cdot\boldsymbol{G}(\theta^1,\theta^2)\,\boldsymbol{a}_\beta(\theta^1,\theta^2) \\ &= \frac{1}{2}\Big(\boldsymbol{a}_\alpha(\theta^1,\theta^2)\cdot D_\beta\boldsymbol{u}(\theta^1,\theta^2) + \boldsymbol{a}_\beta(\theta^1,\theta^2)\cdot D_\alpha\boldsymbol{u}(\theta^1,\theta^2) \\ &\qquad + D_\alpha\boldsymbol{u}(\theta^1,\theta^2)\cdot D_\beta\boldsymbol{u}(\theta^1,\theta^2)\Big)\,. \end{aligned} \tag{4.2.8}$$

Neglecting $D_1u_1(\theta^1,\theta^2)$ in the presence of unity (in accordance with the assumption of small deflections – *e.g.*, ARANTES E OLIVEIRA 1999, § 3.4), we have

$$\begin{aligned} G_{11}(\theta^1,\theta^2) &= D_1u_1(\theta^1,\theta^2) - \overline{x}_2(\theta^1,\theta^2)\Big(w_2'(\theta^1)\sin\phi_1(\theta^1) - w_3'(\theta^1)\cos\phi_1(\theta^1)\Big)\phi_1'(\theta^1) \\ &\quad - \overline{x}_3(\theta^1,\theta^2)\Big(w_2'(\theta^1)\cos\phi_1(\theta^1) + w_3'(\theta^1)\sin\phi_1(\theta^1)\Big)\phi_1'(\theta^1) \\ &\quad + D_1\overline{x}_2(\theta^1,\theta^2)\Big(w_2'(\theta^1)\cos\phi_1(\theta^1) + w_3'(\theta^1)\sin\phi_1(\theta^1) - \overline{x}_3(\theta^1,\theta^2)\phi_1'(\theta^1)\Big) \\ &\quad - D_1\overline{x}_3(\theta^1,\theta^2)\Big(w_2'(\theta^1)\sin\phi_1(\theta^1) - w_3'(\theta^1)\cos\phi_1(\theta^1) - \overline{x}_2(\theta^1,\theta^2)\phi_1'(\theta^1)\Big) \\ &\quad + \frac{1}{2}\Big[\Big(w_2'(\theta^1)\Big)^2 + \Big(w_3'(\theta^1)\Big)^2 + \Big(\overline{x}_2(\theta^1,\theta^2)^2 + \overline{x}_3(\theta^1,\theta^2)^2\Big)\Big(\phi_1'(\theta^1)\Big)^2\Big] \end{aligned} \tag{4.2.9}$$

---

[3] It cannot be overemphasised that this constraint precludes the present one-dimensional model from capturing any local or distortional phenomena – the beam is "forced" to buckle in a pure global mode.

[4] In terms of simplicity of subsequent calculations, there is nothing to be gained from the adoption of the second-order approximations $\cos\phi_1 \cong 1-\frac{1}{2}\phi_1^2$ and $\sin\phi_1 \cong \phi_1$, which would be entirely adequate for the purpose of lateral-torsional buckling analysis (*e.g.*, PI & BRADFORD 2001).

$$G_{12}(\theta^1,\theta^2)=\frac{1}{2}\Big[\,D_2u_1(\theta^1,\theta^2)+D_2\overline{x}_2(\theta^1,\theta^2)\Big(w_2'(\theta^1)\cos\phi_1(\theta^1)+w_3'(\theta^1)\sin\phi_1(\theta^1)\Big)$$
$$-D_2\overline{x}_3(\theta^1,\theta^2)\Big(w_2'(\theta^1)\sin\phi_1(\theta^1)-w_3'(\theta^1)\cos\phi_1(\theta^1)\Big)$$
$$+\Big(\overline{x}_2(\theta^1,\theta^2)\,D_2\overline{x}_3(\theta^1,\theta^2)-\overline{x}_3(\theta^1,\theta^2)\,D_2\overline{x}_2(\theta^1,\theta^2)\Big)\phi_1'(\theta^1)\Big]\ . \qquad (4.2.10)$$

Moreover,

$$G_{22}(\theta^1,\theta^2)=\frac{1}{2}\Big(D_2u_1(\theta^1,\theta^2)\Big)^2\ , \qquad (4.2.11)$$

but we shall regard this result as spurious, stemming from the approximate nature of (4.2.6)-(4.2.7), and consider throughout $G_{22}=G_{\mathrm{II}\cdot\mathrm{II}}$ as being identically zero. Accordingly,

$$G_{\mathrm{I}\cdot\mathrm{I}}(\theta^1,\theta^2)=\boldsymbol{o}_{\mathrm{I}}(\theta^1,\theta^2)\cdot\boldsymbol{G}(\theta^1,\theta^2)\,\boldsymbol{o}_{\mathrm{I}}(\theta^1,\theta^2)=\frac{G_{11}(\theta^1,\theta^2)}{a(\theta^1,\theta^2)} \qquad (4.2.12)$$

$$G_{\mathrm{I}\cdot\mathrm{II}}(\theta^1,\theta^2)=\boldsymbol{o}_{\mathrm{I}}(\theta^1,\theta^2)\cdot\boldsymbol{G}(\theta^1,\theta^2)\,\boldsymbol{o}_{\mathrm{II}}(\theta^1,\theta^2)=\frac{G_{12}(\theta^1,\theta^2)}{\sqrt{a(\theta^1,\theta^2)}}=G_{\mathrm{II}\cdot\mathrm{I}}(\theta^1,\theta^2)\ , \qquad (4.2.13)$$

where $a(\theta^1,\theta^2)$ is the determinant of the matrix (2.2.14) of metric coefficients on the middle surface $\mathscr{S}$.

The shear strain field $G_{\mathrm{I}\cdot\mathrm{II}}=G_{\mathrm{II}\cdot\mathrm{I}}$ is now constrained to vanish. In view of (4.2.13), this amounts to equating to zero the right-hand side of (4.2.10). Integration with respect to the second Gaussian coordinate then yields

$$u_1(\theta^1,\theta^2)=w_1(\theta^1)-\overline{x}_2(\theta^1,\theta^2)\Big(w_2'(\theta^1)\cos\phi_1(\theta^1)+w_3'(\theta^1)\sin\phi_1(\theta^1)\Big)$$
$$+\overline{x}_3(\theta^1,\theta^2)\Big(w_2'(\theta^1)\sin\phi_1(\theta^1)-w_3'(\theta^1)\cos\phi_1(\theta^1)\Big)-\omega(\theta^1,\theta^2)\phi_1'(\theta^1)\ , \qquad (4.2.14)$$

where $\omega:\overline{\Omega}\to\mathbb{R}$ is the field defined in (2.3.16) and (recall that $\overline{x}_2(\theta^1,0)=0$, as implied by (4.2.1))

$$w_1(\theta^1)=u_1(\theta^1,0)-\overline{x}_3(\theta^1,0)\Big(w_2'(\theta^1)\sin\phi_1(\theta^1)-w_3'(\theta^1)\cos\phi_1(\theta^1)\Big) \qquad (4.2.15)$$

is an additional generalised displacement, which is taken to be continuously differentiable. Finally, inserting (4.2.9) and (4.2.14) into (4.2.12) provides

$$G_{\mathrm{I}\cdot\mathrm{I}}(\theta^1,\theta^2)=\frac{1}{a(\theta^1,\theta^2)}\Big\{w_1'(\theta^1)-\overline{x}_2(\theta^1,\theta^2)\Big(w_2''(\theta^1)\cos\phi_1(\theta^1)+w_3''(\theta^1)\sin\phi_1(\theta^1)\Big)$$
$$+\overline{x}_3(\theta^1,\theta^2)\Big(w_2''(\theta^1)\sin\phi_1(\theta^1)-w_3''(\theta^1)\cos\phi_1(\theta^1)\Big)$$
$$+\frac{1}{2}\Big[\Big(w_2'(\theta^1)\Big)^2+\Big(w_3'(\theta^1)\Big)^2+\Big(\overline{x}_2(\theta^1,\theta^2)^2+\overline{x}_3(\theta^1,\theta^2)^2\Big)\Big(\phi_1'(\theta^1)\Big)^2\Big]$$
$$-\omega(\theta^1,\theta^2)\phi_1''(\theta^1)-\psi(\theta^1,\theta^2)\phi_1'(\theta^1)\Big\}\ , \qquad (4.2.16)$$

where $\psi:\overline{\Omega}\to\mathbb{R}$ is the taper function defined in (2.3.26).

4.2.3 The eigenproblem for the buckling load factors and buckling modes

The second-order term of the change in total potential energy of the system between (i) the (trivial) fundamental equilibrium state corresponding to λ and (ii) an adjacent state specified by the incremental displacement field $\boldsymbol{u}$ is given by (COMO 1969, DUPUIS 1969, KOITER 1965, PIGNATARO *et al.* 1991, p. 230, REIS 1977, § 2.3)

$$\Pi_2 = \Pi_2^{(0)} + \lambda \left(\Pi_{2.ref}^{(1)} - W_{e2.ref} \right) . \tag{4.2.17}$$

In this expression, $\Pi_2^{(0)}$, $\Pi_{2.ref}^{(1)}$ and $W_{e2.ref}$ are homogeneous functionals of degree 2, with the following significance:

(i) $\Pi_2^{(0)}$ is the strain energy of the linear theory, corresponding to the displacement field $\boldsymbol{u}$. Recalling (2.5.21)-(2.5.23), we have

$$\begin{aligned}
\Pi_2^{(0)}(w_1, w_2, w_3, \phi_1) &= U(w_1, w_2, w_3, \phi_1) \\
&= \frac{1}{2}\int_0^L \Big[\tilde{E}A^*(\theta^1)\left(w_1'(\theta^1)\right)^2 - 2\,\tilde{E}S_2^*(\theta^1)\, w_1'(\theta^1)\, w_3''(\theta^1) \\
&\quad + \tilde{E}I_3^*(\theta^1)\left(w_2''(\theta^1)\right)^2 + 2\,\tilde{E}I_{3\omega}^*(\theta^1)\, w_2''(\theta^1)\, \phi_1''(\theta^1) \\
&\quad + 2\,\tilde{E}I_{3\psi}^*(\theta^1)\, w_2''(\theta^1)\, \phi_1'(\theta^1) + \tilde{E}I_2^*(\theta^1)\left(w_3''(\theta^1)\right)^2 \\
&\quad + \tilde{E}I_\omega^*(\theta^1)\left(\phi_1''(\theta^1)\right)^2 + 2\,I_{\omega\psi}^*(\theta^1)\, \phi_1''(\theta^1)\, \phi_1'(\theta^1) \\
&\quad + \left(\tilde{E}I_\psi^*(\theta^1) + GJ(\theta^1)\right)\left(\phi_1'(\theta^1)\right)^2 \Big] d\theta^1 ,
\end{aligned} \tag{4.2.18}$$

with the by now familiar non-standard geometrical properties $I_{3\psi}^*$, $I_{\omega\psi}^*$ and I_ψ^*.

(ii) $\Pi_{2.ref}^{(1)}$ represents the work of the active membrane forces in the fundamental state corresponding to the reference load system ($\lambda = 1$), denoted by $n_{\mathrm{I\cdot I}.ref}^{(A)\,f}$, due to the second-order part of the strain $G_{\mathrm{I\cdot I}}$, denoted by $G_{\mathrm{I\cdot I}}^{2^{nd}\,order}$:

$$\Pi_{2.ref}^{(1)}(w_2, \phi_1) = \int_0^L \left[\int_{-g_2(\theta^1)}^{g_2(\theta^1)} n_{\mathrm{I\cdot I}.ref}^{(A)\,f}(\theta^1, \theta^2)\, G_{\mathrm{I\cdot I}}^{2^{nd}\,order}(\theta^1, \theta^2) \sqrt{a(\theta^1, \theta^2)}\, d\theta^2 \right] d\theta^1 . \tag{4.2.19}$$

In view of (4.2.16), we have

$$\begin{aligned}
G_{\mathrm{I\cdot I}}^{2^{nd}\,order}(\theta^1, \theta^2) = \frac{1}{a(\theta^1, \theta^2)} \Big\{ & -\overline{x}_2(\theta^1, \theta^2)\, w_3''(\theta^1)\, \phi_1(\theta^1) + \overline{x}_3(\theta^1, \theta^2)\, w_2''(\theta^1)\, \phi_1(\theta^1) \\
& + \frac{1}{2}\Big[\left(w_2'(\theta^1)\right)^2 + \left(w_3'(\theta^1)\right)^2 \\
& + \left(\overline{x}_2(\theta^1, \theta^2)^2 + \overline{x}_3(\theta^1, \theta^2)^2\right)\left(\phi_1'(\theta^1)\right)^2 \Big] \Big\} .
\end{aligned} \tag{4.2.20}$$

Moreover, since the normal force is identically zero in any fundamental state, one obtains

$$n^{(A)\,f}_{\text{I-I}.ref}(\theta^1,\theta^2)=\frac{t(\theta^1,\theta^2)}{a(\theta^1,\theta^2)}\left(\overline{x}_3(\theta^1,\theta^2)-\frac{S_2^*(\theta^1)}{A^*(\theta^1)}\right)\frac{M^f_{2.ref}(\theta^1)}{I_2^*(\theta^1)-\dfrac{\left(S_2^*(\theta^1)\right)^2}{A^*(\theta^1)}}\ , \tag{4.2.21}$$

where $\theta^1\mapsto M^f_{2.ref}(\theta^1)$ is the first-order bending moment distribution associated with the reference load system. Equation (4.2.19) therefore becomes

$$\Pi^{(1)}_{2.ref}(w_2,\phi_1)=\int_0^L M^f_{2.ref}(\theta^1)\left[w_2''(\theta^1)\phi_1(\theta^1)+\frac{1}{2}\beta_2^*(\theta^1)\left(\phi_1'(\theta^1)\right)^2\right]d\theta^1\ , \tag{4.2.22}$$

where $\beta_2^*:[0,L]\to\mathbb{R}$ is a geometrical property of the reference shape related to its asymmetry with respect to the plane passing through the origin O and spanned by $\{\boldsymbol{e}_1,\boldsymbol{e}_2\}$. This property is given by the somewhat clumsy expression

$$\beta_2^*(\theta^1)=\frac{1}{I_2^*(\theta^1)-\dfrac{\left(S_2^*(\theta^1)\right)^2}{A^*(\theta^1)}}\left[\int_{-g_2(\theta^1)}^{g_2(\theta^1)}\left(\overline{x}_2(\theta^1,\theta^2)^2+\overline{x}_3(\theta^1,\theta^2)^2\right)\overline{x}_3(\theta^1,\theta^2)\,t^*(\theta^1,\theta^2)\,d\theta^2\right.$$
$$\left.-\frac{S_2^*(\theta^1)}{A^*(\theta^1)}\left(I_2^*(\theta^1)+I_3^*(\theta^1)\right)\right]\ .^{5} \tag{4.2.23}$$

(iii) $W_{e2.ref}$ is the second-order part of the work performed by the reference load system in the displacement $\boldsymbol{u}$, given by

$$W_{e2.ref}(w_2,\phi_1)=-\frac{x_3^q}{2}\int_0^L q_{ref}(\theta^1)\phi_1(\theta^1)^2\,d\theta^1-\frac{x_3^{Q_0}}{2}Q_{0.ref}\,\phi_1(0)^2-\frac{x_3^{Q_L}}{2}Q_{L.ref}\,\phi_1(L)^2$$
$$+M_{0.ref}\,w_2'(0)\phi_1(0)+M_{L.ref}\,w_2'(L)\phi_1(L)\ . \tag{4.2.24}$$

With a view to establishing the Euler-Lagrange equations, the admissible generalised displacements in the functional Π_2 are required to satisfy:

---

[5] In particular, for the I-section beam whose reference shape is shown in figure 2.10.3, the integral on the right-hand side of equation (4.2.23) reads

$$\int_{-g_2(\theta^1)}^{g_2(\theta^1)}\left(\overline{x}_2(\theta^1,\theta^2)^2+\overline{x}_3(\theta^1,\theta^2)^2\right)\overline{x}_3(\theta^1,\theta^2)\,t^*(\theta^1,\theta^2)\,d\theta^2=\frac{t_w}{4}\left(x_{3b}(\theta^1)^4-x_{3t}(\theta^1)^4\right)$$
$$+\left(\frac{b_t(\theta^1)^2}{12}+x_{3t}(\theta^1)^2\right)b_t(\theta^1)x_{3t}(\theta^1)t_t\cos^3\varphi_t$$
$$+\left(\frac{b_b(\theta^1)^2}{12}+x_{3b}(\theta^1)^2\right)b_b(\theta^1)x_{3b}(\theta^1)t_b\cos^3\varphi_b\ .$$

(i) The smoothness conditions

- $w_1 \in C^3[0,L]$,
- $w_2, w_3, \phi_1 \in C^4[0,L]$.

(ii) The homogeneous form of the essential boundary conditions prescribed for the particular problem under consideration.

Let δw_i and $\delta\phi_1$ denote admissible variations of w_i $(i=1,2,3)$ and ϕ_1. As usual, the first variation of Π_2 at $(w_1, w_2, w_3, \phi_1, \lambda)$ in the direction of $(\delta w_1, \delta w_2, \delta w_3, \delta\phi_1, 0)$ is defined as

$$\delta\Pi_2(w_1, w_2, w_3, \phi_1, \lambda)[\delta w_1, \delta w_2, \delta w_3, \delta\phi_1, 0]$$

$$= \frac{d}{da}\Pi_2(w_1 + a\,\delta w_1, w_2 + a\,\delta w_2, w_3 + a\,\delta w_3, \phi_1 + a\,\delta\phi_1, \lambda)\Big|_{a=0} \quad (a \in \mathbb{R}). \quad (4.2.25)$$

Upon using Leibniz rule to differentiate under the integral sign, integrating by parts and appealing to the fundamental lemma of the calculus of variations, the vanishing of $\delta\Pi_2$ for all admissible δw_i and $\delta\phi_1$ – often referred to in the literature as the criterion of Trefftz (TREFFTZ 1930, 1933)[6] – leads to the classical or strong form of the LTB problem, which may be phrased as follows:

Find $\lambda \in \mathbb{R}$ and real-valued maps

- $w_1 \in C^3[0,L]$
- $w_2, w_3, \phi_1 \in C^4[0,L]$,

with $w_2 \neq 0$ or $\phi_1 \neq 0$, satisfying the differential equations

$$\left(\tilde{E}\mathcal{A}^*\, w_1' - \tilde{E}S_2^*\, w_3''\right)'(\theta^1) = 0 \quad (4.2.26)$$

$$\left(\tilde{E}I_3^*\, w_2'' + \tilde{E}I_{3\omega}^*\,\phi_1'' + \tilde{E}I_{3\psi}^*\,\phi_1'\right)''(\theta^1) + \lambda\left(M_{2.ref}^f\,\phi_1\right)''(\theta^1) = 0 \quad (4.2.27)$$

$$\left(\tilde{E}S_2^*\, w_1' - \tilde{E}I_2^*\, w_3''\right)''(\theta^1) = 0 \quad (4.2.28)$$

$$\left(\tilde{E}I_{3\omega}^*\, w_2'' + \tilde{E}I_{\omega}^*\,\phi_1'' + \tilde{E}I_{\omega\psi}^*\,\phi_1'\right)''(\theta^1) - \left[\tilde{E}I_{3\psi}^*\, w_2'' + \tilde{E}I_{\omega\psi}^*\,\phi_1'' + \left(\tilde{E}I_{\psi}^* + GJ\right)\phi_1'\right]'(\theta^1)$$
$$+ \lambda\left[M_{2.ref}^f(\theta^1)\, w_2''(\theta^1) - \left(M_{2.ref}^f\,\beta_2^*\,\phi_1'\right)'(\theta^1) + x_3^q\, q_{ref}(\theta^1)\,\phi_1(\theta^1)\right] = 0 \quad (4.2.29)$$

on the open interval $(0,L)$, together with the appropriate boundary, to be selected from table 4.2.1.

[6] See also KOITER (1963, pp. 257-259) and WEMPNER (1972).

	Natural boundary conditions		**Essential boundary conditions**
Either	$\tilde{E}A^*(0)\,w_1'(0)-\tilde{E}S_2^*(0)\,w_3''(0)=0$	or	$w_1(0)=0$
	$\tilde{E}A^*(L)\,w_1'(L)-\tilde{E}S_2^*(L)\,w_3''(L)=0$		$w_1(L)=0$
	$\left(\tilde{E}I_3^*\,w_2''+\tilde{E}I_{3\omega}^*\,\phi_1''+\tilde{E}I_{3\psi}^*\,\phi_1'\right)'(0)+\lambda\left(M_{2.ref}^f\,\phi_1\right)'(0)=0$		$w_2(0)=0$
	$\left(\tilde{E}I_3^*\,w_2''+\tilde{E}I_{3\omega}^*\,\phi_1''+\tilde{E}I_{3\psi}^*\,\phi_1'\right)'(L)+\lambda\left(M_{2.ref}^f\,\phi_1\right)'(L)=0$		$w_2(L)=0$
	$\tilde{E}I_3^*(0)\,w_2''(0)+\tilde{E}I_{3\omega}^*(0)\,\phi_1''(0)+\tilde{E}I_{3\psi}^*(0)\,\phi_1'(0)=0$		$w_2'(0)=0$
	$\tilde{E}I_3^*(L)\,w_2''(L)+\tilde{E}I_{3\omega}^*(L)\,\phi_1''(L)+\tilde{E}I_{3\psi}^*(L)\,\phi_1'(L)=0$		$w_2'(L)=0$
	$\left(S_2^*\,w_1'-\tilde{E}I_2^*\,w_3''\right)'(0)=0$		$w_3(0)=0$
	$\left(S_2^*\,w_1'-\tilde{E}I_2^*\,w_3''\right)'(L)=0$		$w_3(L)=0$
	$S_2^*(0)\,w_1'(0)-\tilde{E}I_2^*(0)\,w_3''(0)=0$		$w_3'(0)=0$
	$S_2^*(L)\,w_1'(L)-\tilde{E}I_2^*(L)\,w_3''(L)=0$		$w_3'(L)=0$
	$-\left(\tilde{E}I_{3\omega}^*\,w_2''+\tilde{E}I_{\omega}^*\,\phi_1''+\tilde{E}I_{\omega\psi}^*\,\phi_1'\right)'(0)+\tilde{E}I_{3\psi}^*(0)\,w_2''(0)+\tilde{E}I_{\omega\psi}^*(0)\,\phi_1''(0)+\left(GJ(0)+\tilde{E}I_{\psi}^*(0)\right)\phi_1'(0)+\lambda\left[M_{0.ref}\left(-\beta_2^*(0)\,\phi_1'(0)+w_2'(0)\right)-x_3^{Q_0}\,Q_{0.ref}\,\phi_1(0)\right]=0$		$\phi_1(0)=0$
	$-\left(\tilde{E}I_{3\omega}^*\,w_2''+\tilde{E}I_{\omega}^*\,\phi_1''+\tilde{E}I_{\omega\psi}^*\,\phi_1'\right)'(L)+\tilde{E}I_{3\psi}^*(L)\,w_2''(L)+\tilde{E}I_{\omega\psi}^*(L)\,\phi_1''(L)+\left(GJ(L)+\tilde{E}I_{\psi}^*(L)\right)\phi_1'(L)+\lambda\left[M_{L.ref}\left(\beta_2^*(L)\,\phi_1'(L)-w_2'(L)\right)+x_3^{Q_L}\,Q_{L.ref}\,\phi_1(L)\right]=0$		$\phi_1(L)=0$
	$\tilde{E}I_{3\omega}^*(0)\,w_2''(0)+\tilde{E}I_{\omega}^*(0)\,\phi_1''(0)+\tilde{E}I_{\omega\psi}^*(0)\,\phi_1'(0)=0$		$\phi_1'(0)=0$
	$\tilde{E}I_{3\omega}^*(L)\,w_2''(L)+\tilde{E}I_{\omega}^*(L)\,\phi_1''(L)+\tilde{E}I_{\omega\psi}^*(L)\,\phi_1'(L)=0$		$\phi_1'(L)=0$

Table 4.2.1: Lateral-torsional buckling of singly symmetric tapered beams – Natural and essential boundary conditions

The equations involving w_1 and w_3 can be solve separately and are irrelevant for the purpose of obtaining the buckling load factors. They need not be considered further. We are then left with a Steklov-type eigenproblem (BABUSKA & OSBORN 1991, p. 649). The eigenvalues are the buckling load factors $\lambda_b^{(n)}$, with $n \in \mathbb{Z} \setminus \{0\}$, which are labelled so as to have $\cdots < \lambda_b^{(-2)} < \lambda_b^{(-1)} < 0 < \lambda_b^{(1)} < \lambda_b^{(2)} < \cdots$. The associated eigenfunctions are the buckling modes $(w_{2.b}^{(n)}, \phi_{1.b}^{(n)})$ and we put forward the conjecture (reminiscent of a classical result in Sturm-Liouville theory – *e.g.*, BIRKHOFF & ROTA 1989, ch. 10, th. 5, or CODDINGTON & LEVINSON 1955, ch. 8, th. 2.1) that $\phi_{1.b}^{(n)}$ has exactly $|n|-1$ zeros in the open interval $(0, L)$. In particular, the lowest positive eigenvalue is termed the critical load factor and we use the special notation $\lambda_b^{(1)} = \lambda_{cr}$ – accordingly, the corresponding buckling mode is denoted by $(w_{2.cr}, \phi_{1.cr})$ and is termed critical as well. We also speak of the critical moment, defined as

$$M_{cr} = \lambda_{cr} \max\left\{\left|M_{2.ref}^{f}(\theta^1)\right|, 0 \le \theta^1 \le L\right\} . \tag{4.2.30}$$

* * *

An assessment of the performance of the proposed one-dimensional LTB model was carried out in ANDRADE *et al.* (2007a). The study involved the critical load factors and modes of several prismatic and linearly web-tapered I-section cantilevers and simply supported beams, with equal or unequal uniform flanges, acted by point loads applied at various locations of the free end (cantilevers) or mid-span section (simply supported beams). The predictions of the one-dimensional model were compared with the results of shell finite element analyses, performed with the commercial code ABAQUS. It was found that, as long as the beams are not too short, the one-dimensional model yields reasonably accurate estimates of the critical load factors and modes. Moreover, the accuracy of these estimates gradually increases with the beam length, a trend that reflects the decreasing relevance of cross-sectional distortion (in-plane deformations). As for the considerable differences between the one-dimensional and shell finite element models recorded for the shorter beams, it was found that they are mainly due to either (i) significant web and/or flange distortion or (ii) a localised web buckling phenomenon, which occurs in the neighbourhood of the load point of application – as stressed above, none of these phenomena can be captured by the one-dimensional model. Indeed, the addition of transverse stiffners to the shell models significantly reduced the gap between the shell and the one-dimensional models. The shell finite element results reported by ASGARIAN *et al.* (2012) and ZHANG & TONG (2008), which

concern web-tapered I-section beams as well, were also found to be in good agreement with the predictions of the present one-dimensional model.

4.3 SINGLY SYMMETRIC PRISMATIC BEAMS AS A SPECIAL CASE

Let us now pause to consider in some detail the prismatic special case. The Cartesian frame and the parametrisation of the middle surface are assumed to combine the features stipulated in §§ 2.9.1 and 2.9.2. Moreover, we adhere to the notational conventions and abuses of § 2.9.2.

Under the above circumstances, the line of shear centres is defined by the coordinates

$$x_2^S = 0 \tag{4.3.1}$$

$$x_3^S = -\frac{I_{3\omega}}{I_3} \ . \tag{4.3.2}$$

We introduce the sectorial coordinate

$$\begin{aligned} \omega_S(\theta^2) &= \int_0^{\theta^2} \left[\overline{x}_2(s)\,\overline{x}_3'(s) - \left(\overline{x}_3(s) - x_3^S\right)\overline{x}_2'(s) \right] ds \\ &= \omega(\theta^2) + x_3^S\,\overline{x}_2(\theta^2) \ , \end{aligned} \tag{4.3.3}$$

with pole at the shear centre and origin at the intersection of the cross-section middle line with the longitudinal plane of symmetry. By specialisation of (2.9.50)-(2.9.53) – or by direct computation –, one finds

$$S_{\omega_S} = \int_{-b}^{b} \omega_S(\theta^2)\,t(\theta^2)\,d\theta^2 = S_\omega = 0 \tag{4.3.4}$$

$$I_{2\omega_S} = \int_{-b}^{b} \omega_S(\theta^2)\,\overline{x}_3(\theta^2)\,t(\theta^2)\,d\theta^2 = I_{2\omega} = 0 \tag{4.3.5}$$

$$I_{3\omega_S} = \int_{-b}^{b} \omega_S(\theta^2)\,\overline{x}_2(\theta^2)\,t(\theta^2)\,d\theta^2 = I_{3\omega} + x_3^S\,I_3 = 0 \tag{4.3.6}$$

$$I_{\omega_S} = \int_{-b}^{b} \omega_S^2(\theta^2)\ t(\theta^2)\,d\theta^2 = I_\omega - (x_3^S)^2\,I_3 \ . \tag{4.3.7}$$

This completes the setting of the stage.

To obtain the prismatic beam equations in their usual form, one starts by rewriting the Cartesian components of the incremental displacement field $\boldsymbol{u} : \overline{\Omega} \to \mathcal{V}$ as

$$\begin{aligned} u_1(\theta^1,\theta^2) = {} & w_1(\theta^1) - \overline{x}_2(\theta^2)\left(w_{S.2}'(\theta^1)\cos\phi_1(\theta^1) + w_{S.3}'(\theta^1)\sin\phi_1(\theta^1)\right) \\ & + \overline{x}_3(\theta^2)\left(w_{S.2}'(\theta^1)\sin\phi_1(\theta^1) - w_{S.3}'(\theta^1)\cos\phi_1(\theta^1)\right) - \omega_S(\theta^2)\,\phi_1'(\theta^1) \end{aligned} \tag{4.3.8}$$

$$u_2(\theta^1,\theta^2) = w_{S.2}(\theta^1) - \overline{x}_2(\theta^2)\left(1-\cos\phi_1(\theta^1)\right) - \left(\overline{x}_3(\theta^2) - x_3^S\right)\sin\phi_1(\theta^1) \tag{4.3.9}$$

$$u_3(\theta^1,\theta^2) = w_{S.3}(\theta^1) + \overline{x}_2(\theta^2)\sin\phi_1(\theta^1) - \left(\overline{x}_3(\theta^2) - x_3^S\right)\left(1-\cos\phi_1(\theta^1)\right)\ , \tag{4.3.10}$$

where the new generalised displacements $w_{S.2}$ and $w_{S.3}$, which replace w_2 and w_3, are referred to the line of shear centres:

$$w_{S.2}(\theta^1) = w_2(\theta^1) - x_3^S\sin\phi_1(\theta^1) \tag{4.3.11}$$

$$w_{S.3}(\theta^1) = w_3(\theta^1) - x_3^S\left(1-\cos\phi_1(\theta^1)\right)\ . \tag{4.3.12}$$

Using (4.3.8)-(4.3.10), the strain field $G_{\text{I·I}} = G_{11}$ reads

$$\begin{aligned} G_{\text{I·I}}(\theta^1,\theta^2) = {} & w_1'(\theta^1) - \overline{x}_2(\theta^2)\left(w_{S.2}''(\theta^1)\cos\phi_1(\theta^1) + w_{S.3}''(\theta^1)\sin\phi_1(\theta^1)\right) \\ & + \overline{x}_3(\theta^2)\left(w_{S.2}''(\theta^1)\sin\phi_1(\theta^1) - w_{S.3}''(\theta^1)\cos\phi_1(\theta^1)\right) - \omega_S(\theta^2)\phi_1''(\theta^1) \\ & + \frac{1}{2}\left\{\left(w_{S.2}'(\theta^1)\right)^2 + \left(w_{S.3}'(\theta^1)\right)^2 + \left[\overline{x}_2(\theta^2)^2 + \left(\overline{x}_3(\theta^2) - x_3^S\right)^2\right]\left(\phi_1'(\theta^1)\right)^2\right\} \\ & + x_3^S\left(w_{S.2}'(\theta^1)\cos\phi_1(\theta^1) + w_{S.3}'(\theta^1)\sin\phi_1(\theta^1)\right)\phi_1'(\theta^1)\ . \end{aligned} \tag{4.3.13}$$

Identical expressions were derived by ATTARD (1986, eq. 34) and DE VILLE DE GOYET (1989, eq. 4.15), while ACHOUR & ROBERTS (2000, eq. 21) obtained an extra term, namely $-\omega_S(\theta^2)\left(w_{S.2}'''(\theta^1)w_{S.3}'(\theta^1) - w_{S.2}'(\theta^1)w_{S.3}'''(\theta^1)\right)$, which stems from a second-order contribution to the rate of twist (the adoption of (4.3.8)-(4.3.10) automatically precludes the emergence of such a contribution).

In terms of the new set of generalised displacements (w_1, $w_{S.2}$, $w_{S.3}$ and ϕ_1), the energy functionals $\Pi_2^{(0)}$, $\Pi_{2.ref}^{(1)}$ and $W_{e2.ref}$ are given by

$$\begin{aligned} \Pi_2^{(0)}(w_1,w_{S.2},w_{S.3},\phi_1) = {} & \frac{1}{2}\int_0^L \left(\tilde{E}A\,w_1'(\theta^1)^2 + \tilde{E}I_3\,w_{S.2}''(\theta^1)^2 + \tilde{E}I_2\,w_{S.3}''(\theta^1)^2\right. \\ & \left. + \tilde{E}I_{\omega_S}\,\phi_1''(\theta^1)^2 + GJ\,\phi_1'(\theta^1)^2\right)d\theta^1 \end{aligned} \tag{4.3.14}$$

$$\Pi_{2.ref}^{(1)}(w_{S.2},\phi_1) = \int_0^L M_{2.ref}^f(\theta^1)\left(w_{S.2}''(\theta^1)\phi_1(\theta^1) + \frac{1}{2}\beta_2\,\phi_1'(\theta^1)^2\right)d\theta^1 \tag{4.3.15}$$

$$\begin{aligned} W_{e2.ref}(w_{S.2},\phi_1) = {} & -\frac{x_3^q - x_3^S}{2}\int_0^L q_{ref}(\theta^1)\,\phi_1(\theta^1)^2\,d\theta^1 \\ & - \frac{x_3^{Q_0} - x_3^S}{2}Q_{0.ref}\,\phi_1(0)^2 - \frac{x_3^{Q_L} - x_3^S}{2}Q_{L.ref}\,\phi_1(L)^2 \\ & + M_{0.ref}\,w_{S.2}'(0)\phi_1(0) + M_{L.ref}\,w_{S.2}'(L)\phi_1(L)\ , \end{aligned} \tag{4.3.16}$$

where

$$\beta_2 = \frac{1}{I_2}\int_{-b}^{b}\left[\overline{x}_2(\theta^2)^2 + \left(\overline{x}_3(\theta^2) - x_3^S\right)^2\right]\overline{x}_3(\theta^2)\,t(\theta^2)\,d\theta^2 \quad . \tag{4.3.17}$$

Accordingly, the Euler-Lagrange equations associated with Π_2 simplify to

$$\tilde{E}A\,w_1''(\theta^1) = 0 \tag{4.3.18}$$

$$\tilde{E}I_3\,w_{S.2}^{(4)}(\theta^1) + \lambda\left(M_{2.ref}^f\,\phi_1\right)''(\theta^1) = 0 \tag{4.3.19}$$

$$\tilde{E}I_3\,w_{S.3}^{(4)}(\theta^1) = 0 \tag{4.3.20}$$

$$\begin{aligned}\tilde{E}I_{\omega_S}\,\phi_1^{(4)}(\theta^1) - GJ\,\phi_1''(\theta^1) + \lambda\Big[& M_{2.ref}^f(\theta^1)\,w_{S.2}''(\theta^1) \\ & -\beta_2\left(M_{2.ref}^f\,\phi_1'\right)'(\theta^1) + \left(x_3^q - x_3^S\right)q_{ref}(\theta^1)\,\phi_1(\theta^1)\Big] = 0 \quad .\end{aligned} \tag{4.3.21}$$

The accompanying boundary conditions are indicated in table 4.3.1.

Once again, the equations involving w_1 and $w_{S.3}$ can be solve separately and are irrelevant for the purpose of obtaining the buckling load factors. They need not be considered further.[7] Except for the definition of the elastic modulus $\tilde{E}$, the remaining equations are in agreement with the ones derived by GJELSVIK (1981, § 7.5), TRAHAIR (1993, §§ 2.8.4 and 17.4), DE VILLE DE GOYET (1989, § 4.8) and VLASOV (1961, ch. 6, § 3).[8] In particular, the terms featuring the asymmetry property β_2 reflect an effective change in the Saint-Venant rigidity, from GJ to $GJ + \beta_2\,\lambda\,M_{2.ref}^f$, brought about by the pre-buckling membrane forces $\lambda\,n_{\text{I-I}.ref}^{(A)\,f}$. They are commonly named after H. Wagner, who described an analogous effect in connection with the torsional and flexural-torsional buckling of thin-walled columns (WAGNER 1929, WAGNER & PRETSCHNER 1934). Wagner's analysis was later extended to beam-columns by GOODIER (1942) – for a detailed discussion of Wagner's

[7] An assumption analogous to that of inextensional column buckling (*e.g.*, TRAHAIR 1993, p. 354) is thus seen to be unwarranted.

[8] None of these authors considers the action of quasi-tangential moments $\boldsymbol{M}_0$ and $\boldsymbol{M}_L$ applied at the end sections. Trahair does consider applied end moments, but assumes that they "remain parallel to their original directions" (TRAHAIR 1993, p. 348) – such axial moments are generally non-conservative, and may only be considered conservative for particular constraint conditions imposed at the member ends (ZIEGLER 1968, p. 119). Moreover, GJELSVIK (1981, eq. (6.6b)) presents a slightly different expression for the cross-sectional property β_2 (K_x in this author's notation), in which the wall thickness is more accurately taken into account.

	Natural boundary conditions		Essential boundary conditions
Either	$\tilde{E}A\,w_1'(0)=0$	or	$w_1(0)=0$
	$\tilde{E}A\,w_1'(L)=0$		$w_1(L)=0$
	$\tilde{E}I_3\,w_{S.2}'''(0)+\lambda\left(M_{2.ref}^{f}\,\phi_1\right)'(0)=0$		$w_{S.2}(0)=0$
	$\tilde{E}I_3\,w_{S.2}'''(L)+\lambda\left(M_{2.ref}^{f}\,\phi_1\right)'(L)=0$		$w_{S.2}(L)=0$
	$\tilde{E}I_3\,w_{S.2}''(0)=0$		$w_{S.2}'(0)=0$
	$\tilde{E}I_3\,w_{S.2}''(L)=0$		$w_{S.2}'(L)=0$
	$\tilde{E}I_2\,w_{S.3}'''(0)=0$		$w_{S.3}(0)=0$
	$\tilde{E}I_2\,w_{S.3}'''(L)=0$		$w_{S.3}(L)=0$
	$\tilde{E}I_2\,w_{S.3}''(0)=0$		$w_{S.3}'(0)=0$
	$\tilde{E}I_2\,w_{S.3}''(L)=0$		$w_{S.3}'(L)=0$
	$-\tilde{E}I_{\omega_S}\,\phi_1'''(0)+GJ\,\phi_1'(0)-\lambda\Big[M_{0.ref}\left(\beta_2\,\phi_1'(0)-w_{S.2}'(0)\right)+\left(x_3^{Q_0}-x_3^{S}\right)Q_{0.ref}\,\phi_1(0)\Big]=0$		$\phi_1(0)=0$
	$-\tilde{E}I_{\omega_S}\,\phi_1'''(L)+GJ\,\phi_1'(L)+\lambda\Big[M_{L.ref}\left(\beta_2\,\phi_1'(L)-w_{S.2}'(L)\right)+\left(x_3^{Q_L}-x_3^{S}\right)Q_{L.ref}\,\phi_1(L)\Big]=0$		$\phi_1(L)=0$
	$\tilde{E}I_{\omega_S}\,\phi_1''(0)=0$		$\phi_1'(0)=0$
	$\tilde{E}I_{\omega_S}\,\phi_1''(L)=0$		$\phi_1'(L)=0$

Table 4.3.1: Lateral-torsional buckling of singly symmetric prismatic beams – Natural and essential boundary conditions

effect in beam LTB problems, including an assessment of the available experimental evidence, see ANDERSON & TRAHAIR (1972) and TRAHAIR (2011).[9]

[9] The correctness of Wagner's terms has been repeatedly questioned by OJALVO (1981, 1983, 1987, 1989, 1990a, 1990b, 2002, 2007). This stirred a lively debate, the outcome of which was the convincing rebuttal of Ojalvo's objections and the universal acceptance (Ojalvo excepted) of the classical Wagner-Goodier-Vlasov theory (ALWIS & WANG 1996, GOTO & CHEN 1989, KANG *et al.* 1992, KITIPORNCHAI & DUX 1982, KITIPORNCHAI *et al.* 1987, SILVA 1990, TRAHAIR 1982).

4.4 RESTRAINED BEAMS

Up to this point, only isolated beams with idealised support conditions have been considered. Such circumstances are seldom found in actual design practice – indeed, beams are usually connected to other elements that may contribute significantly to their buckling strength, even when they are not primarily intended for that specific purpose.

Since the pioneering work of FLINT (1951) (see also KERENSKY *et al.* 1956 and AUSTIN *et al.* 1957), there have been extensive studies on the effect of restraints on the elastic lateral-torsional buckling behaviour of prismatic beams. Broad surveys on this subject, as well as detailed references to the literature, can be found in LINDNER (1996), TRAHAIR (1993), TRAHAIR & NETHERCOT (1984), YURA (2001) and ZIEMIAN (2010). On the contrary, there is little information available on the lateral-torsional buckling behaviour of tapered beams with elastic or rigid restraints. In fact, to the author's best knowledge the only publications on this subject are due to BUTLER (1966) and to BRADFORD (1988). The former reported an experimental investigation aimed at studying the influence of lateral and torsional braces on the elastic buckling strength of tip-loaded tapered cantilever I-beams – unfortunately, these experiments are insufficiently documented to be of any real value. The latter extended the tapered beam-column finite element formulation of BRADFORD & CUK (1988) to include the effects of continuous elastic restraints.

Using an archetypal problem that is intended to "contain all the germs of generality" (to quote David Hilbert), it is shown in this section how the presence of out-of-plane restraints can be accommodated in the one-dimensional LTB beam model. The archetypal problem consists of a perfectly straight doubly symmetric web-tapered I-section cantilever, acted by a tip load and exhibiting end restraints that may (i) have a translational, torsional, minor axis bending and/or warping character, and (ii) be either linearly elastic or perfectly rigid.

The resulting eigenproblem is cast in non-dimensional form over a fixed reference domain, and a complete set of independent non-dimensional parameters is identified. For its numerical solution, we use the collocation package COLNEW – this requires, as we have already seen in chapter 3, the previous reformulation of the eigenproblem as a standard inhomogeneous boundary value problem. A parametric study is then conducted in order to examine in some detail (i) the effectiveness of different types of restraint, (ii) the importance of the restraint stiffness and (iii) the interplay between these two aspects and

the degree of web tapering. Some seemingly paradoxical results are given a physical explanation.

Although only doubly symmetric web-tapered I-beams with discrete restraints are dealt with in this work, the consideration of other beam geometries (possibly with a single plane of symmetry) and the inclusion of continuous restraints are straightforward matters. Finally, we are not concerned with the forces developing in the restraining elements, which are always assumed to have adequate strength – such an analysis would necessarily require the consideration of the imperfections of the restrained beam.

This work was reported in ANDRADE *et al.* (2010b).

4.4.1 The archetypal problem

As an archetypal problem, we consider the lateral-torsional buckling of a perfectly straight doubly symmetric web-tapered I-section cantilever, with length L and acted by point load applied at the tip – see figure 4.4.1. The Cartesian frame, also shown in this figure, is chosen so that the reference shape of the cantilever is symmetrical relative to the planes passing through the origin O and spanned by $\{\boldsymbol{e}_1,\boldsymbol{e}_3\}$ and $\{\boldsymbol{e}_1,\boldsymbol{e}_2\}$. The flanges are uniform, with thickness t_f and width b. The web has constant thickness t_w and its depth h, measured between flange middle lines, varies along the length according to the affine law, expressed in terms of the web taper ratio $\alpha=\frac{h(L)}{h_0}$, reads

$$h(x_1)=\left(1-(1-\alpha)\frac{x_1}{L}\right)h_0\ , \tag{4.4.1}$$

with $0<\alpha\le 1$. As usual, the parameter $\alpha=\frac{h(L)}{h_0}$ will be referred to as the web taper ratio (or simply the taper ratio); $\alpha=1$ is associated with a prismatic beam. The flanges exhibit symmetrical slopes $\pm\tan\varphi$ with respect to the planes spanned by $\{\boldsymbol{e}_1,\boldsymbol{e}_2\}$, where $\tan\varphi=(1-\alpha)h_0/(2L)$.

The cantilever, supported at its larger end ($\mathcal{A}_0$), is acted by a conservative point load $\boldsymbol{Q}=Q\,\boldsymbol{e}_3$ applied to the material point whose reference place is $O+L\,\boldsymbol{e}_1+x_3^Q\,\boldsymbol{e}_3$. The magnitude Q of the applied load is deemed proportional to a single factor λ – we thus write $Q=Q_{ref}\,\lambda$, where Q_{ref} is a positive reference magnitude. The load remains parallel to $\boldsymbol{e}_3$ throughout the whole deformation process.

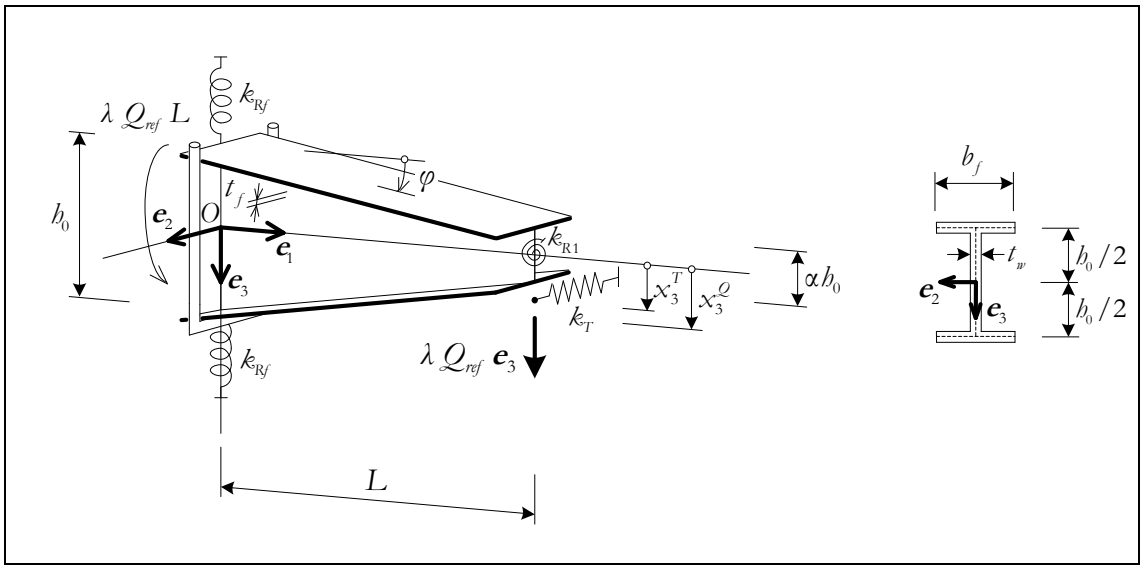

Figure 4.4.1: Archetypal problem – Reference shape, support conditions and applied load

More often than not, in actual engineering practice, such a cantilever exhibits some kind of bracing at the tip. While the actual bracing arrangement may vary significantly (figure 4.4.2(a) shows some typical details), it can usually be modelled by means of (i) a translational spring with stiffness k_T $(0 \le k_T \le +\infty)$, parallel to $\boldsymbol{e}_2$ and located at the level $x_3 = x_3^T$, and/or (ii) a torsional spring with stiffness k_{R1} $(0 \le k_{R1} \le +\infty)$. On the other hand, a cantilever is frequently just the overhanging portion of a beam extending beyond an end support, as illustrated in figure 4.4.2(b). In such case, the assumption of a built-in support may lead to a considerable overestimation of the buckling strength (see the prismatic beam results reported by ANDRADE *et al.* 2007b and TRAHAIR 1983) – a more realistic description of the actual support conditions is achieved by considering, in each flange, equal rotational springs about $\boldsymbol{e}_3$, with stiffness k_{Rf} $(0 \le k_{Rf} \le +\infty)$. They simulate the warping and lateral bending restraints provided by the adjacent span, while the torsional rotation (about $\boldsymbol{e}_1$) and the lateral displacement are kept fully prevented. In fact, this very simple and physically meaningful procedure is closely related to the warping spring concept introduced by YANG & MCGUIRE (1984) to analyze space frames made of prismatic members with partial warping restraint. If $k_{Rf} = k_T = 0$, the cantilever may rotate freely about $\boldsymbol{e}_3$ in a rigid-body mode – in order to rule out this possibility, k_{Rf} and k_T are required to satisfy $0 < k_{Rf} + k_T\, L^2 \le +\infty$ (*i.e.*, they cannot be simultaneously zero).

Our aim is to compute the buckling load factors and the corresponding buckling modes for this beam-load structural system.

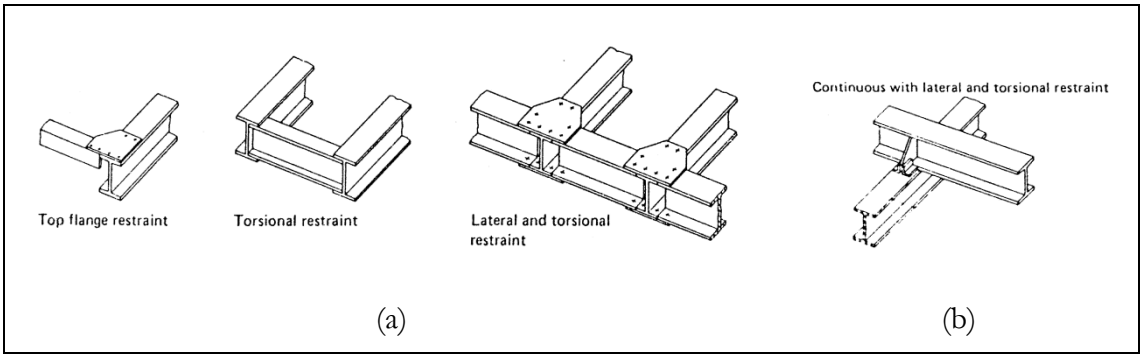

Figure 4.4.2: Some typical bracing and support details (adapted from BRITISH STANDARDS INSTITUTION 2001)

4.4.2 Mathematical formulation of the archetypal problem

In the absence of elastic restraints, the energy functional for the lateral-torsional buckling analysis of this particular beam-load system is given by[10]

$$\begin{aligned}\Pi_2(w_2,\phi_1,\lambda) = &\frac{1}{2}\int_0^L \tilde{E}I_3^*(\theta^1)\,w_2''(\theta^1)^2\,d\theta^1 + \frac{1}{2}\int_0^L \tilde{E}I_\omega^*(\theta^1)\,\phi_1''(\theta^1)^2\,d\theta^1 \\ &+\int_0^L \tilde{E}I_{\omega\psi}^*(\theta^1)\,\phi_1''(\theta^1)\,\phi_1'(\theta^1)\,d\theta^1 + \frac{1}{2}\int_0^L \left(GJ(\theta^1)+\tilde{E}I_\psi^*(\theta^1)\right)\phi_1'(\theta^1)^2\,d\theta^1 \\ &+\lambda\int_0^L M_{2.ref}^f(\theta^1)\,w_2''(\theta^1)\,\phi_1(\theta^1)\,d\theta^1 + \frac{1}{2}\varkappa_3^Q\,\lambda\,Q_{ref}\,\phi_1(L)^2\ ,\end{aligned} \tag{4.4.2}$$

where the first-order bending moment distribution associated with the reference load $Q_{ref}\,\boldsymbol{e}_3$ is

$$M_{2.ref}^f(\theta^1) = -(L-\theta^1)\,Q_{ref} \tag{4.4.3}$$

and the geometrical properties I_3^*, I_ω^*, $I_{\omega\psi}^*$, I_ψ^* and J of the reference shape are defined by

$$I_3^*(\theta^1) = \frac{1}{6}\,b_f^3\,t_f\cos^3\varphi = I_3^*(0) \tag{4.4.4}$$

and (2.11.7)-(2.11.10).

We still have to consider the end restraints and, in particular, to distinguish between the elastic (non-rigid) and rigid cases. In order to account for the presence of elastic restraints (see figure 4.4.1), the energy functional (4.4.2) must be supplemented with the terms

[10] Since w_1 and w_3 are known to be irrelevant, they were dropped.

$$\frac{1}{2}k_{Rf}\left(w_2'(0)+\frac{h_0}{2}\phi_1'(0)\right)^2+\frac{1}{2}k_{Rf}\left(w_2'(0)-\frac{h_0}{2}\phi_1'(0)\right)^2$$

$$+\frac{1}{2}k_{R1}\phi_1(L)^2+\frac{1}{2}k_T\left(w_2(L)-x_3^T\phi_1(L)\right)^2$$

$$=k_{Rf}\left(w_2'(0)^2+\frac{h_0^2}{4}\phi_1'(0)^2\right)+\frac{1}{2}k_{R1}\phi_1(L)^2+\frac{1}{2}k_T\left(w_2(L)-x_3^T\phi_1(L)\right)^2\ , \qquad (4.4.5)$$

which provide the strain energy stored in the restraints during buckling – it follows from the kinematical hypotheses underlying the one-dimensional model that the flange rotations about an axis parallel to $\boldsymbol{e}_3$ are given by $w_2'\pm\frac{h}{2}\phi_1'$ (regarding the term $\pm\frac{h}{2}\phi_1'$, recall figure 2.11.2). Of course, when a restraint is taken as perfectly rigid, it does not store any strain energy and thus there is no additional contribution to consider in the energy functional – however, relative to the unrestrained or elastically restrained cases, the admissible functions must satisfy additional essential boundary conditions, as will be seen presently.

The first term on the right-hand side of (4.3.5) can be rewritten in the form

$$\frac{1}{2}k_{R3}\,w_2'(0)^2+\frac{1}{2}k_\omega\,\phi_1'(0)^2\ , \qquad (4.4.6)$$

where

$$k_{R3}=2\,k_{Rf} \qquad (4.4.7)$$

$$k_\omega=\frac{h_0^2}{4}2k_{Rf}\ . \qquad (4.4.8)$$

This rearrangement clearly suggests the possibility of considering independently the minor axis bending and warping elastic restraints – simply replace the first term on the right-hand side of (4.4.5) with (4.3.6) and adopt two unrelated parameters, k_{R3} and k_ω, instead of the single parameter k_{Rf}. In fact, such a generalization is needed to deal with several situations of practical interest. For instance, if the warping restraint is "internal" to the beam – provided by such devices as end plates (LINDNER & GIETZELT 1983, PI & TRAHAIR 2000, VACHARAJITTIPHAN & TRAHAIR 1974), batten plates (HOTCHKISS 1966, TAKABATAKE 1988, VACHARAJITTIPHAN & TRAHAIR 1974, PI & TRAHAIR 2000) or box stiffeners (OJALVO 1975, OJALVO & CHAMBERS 1977, PI & TRAHAIR 2000, PLUM & SVENSSON 1993) –, then it is not coupled with a minor axis bending restraint (we would have $k_\omega>0$, but $k_{R3}=0$).

Suppose now that $k_{Rf}, k_{R1}, k_T \neq +\infty$ and let δw_2 and $\delta\phi_1$ be admissible variations of w_2 and ϕ_1. Upon integration by parts, the first variation of the energy functional Π_2, defined by (4.4.2)+(4.4.5), at (w_2, ϕ_1, λ) and in the direction of $(\delta w_2, \delta\phi_1, 0)$, reads

$$
\begin{aligned}
&\delta\Pi_2(w_2,\phi_1,\lambda)[\delta w_2,\delta\phi_1,0] = \\
&= \int_0^L \left[\tilde{E}I_3^*(0)\, w_2^{(4)}(\theta^1) - \lambda\, Q_{ref} \left((L-\theta^1)\phi_1''(\theta^1) - 2\phi_1'(\theta^1) \right) \right] \delta w_2(\theta^1)\, d\theta^1 \\
&+ \int_0^L \left[\left(1-(1-\alpha)\frac{\theta^1}{L} \right)^2 \tilde{E}I_\omega^*(0)\phi_1^{(4)}(\theta^1) - \frac{4}{L}(1-\alpha)\left(1-(1-\alpha)\frac{\theta^1}{L} \right) \tilde{E}I_\omega^*(0)\phi_1'''(\theta^1) \right. \\
&\qquad - \left(1-\frac{h_0\, t_w^3}{3J(0)}(1-\alpha)\frac{\theta^1}{L} \right) GJ(0)\phi_1''(\theta^1) + \frac{h_0\, t_w^3}{3J(0)}\frac{1-\alpha}{L} GJ(0)\phi_1'(\theta^1) \\
&\qquad \left. - \lambda\, Q_{ref}\, (L-\theta^1)\, w_2''(\theta^1) \right] \delta\phi(\theta^1)\, d\theta^1 \\
&+ \left(\tilde{E}I_3^*(0)\, w_2'''(0) - \lambda\, Q_{ref}\, (L\phi_1'(0) - \phi(0)) \right) \delta w_2(0) \\
&+ \left(-\tilde{E}I_3^*(0)\, w_2''(0) + 2k_{Rf}\, w_2'(0) + L\lambda\, Q_{ref}\, \phi(0) \right) \delta w_2'(0) \\
&+ \left[\tilde{E}I_\omega^*(0)\phi_1'''(0) - \frac{2}{L}(1-\alpha)\,\tilde{E}I_\omega^*(0)\phi_1''(0) - \left(\frac{2}{L^2}(1-\alpha)^2\,\tilde{E}I_\omega^*(0) + GJ(0) \right)\phi_1'(0) \right] \delta\phi_1(0) \\
&+ \left[-\tilde{E}I_\omega^*(0)\phi_1''(0) + \left(\frac{2}{L}(1-\alpha)\,\tilde{E}I_\omega^*(0) + \frac{h_0^2}{4} 2k_{Rf} \right)\phi_1'(0) \right] \delta\phi_1'(0) \\
&+ \underline{\left(-\tilde{E}I_3^*(0)\, w_2'''(L) + k_T\, (w_2(L) - x_3^T\, \phi_1(L)) - \lambda\, Q_{ref}\, \phi_1(L) \right) \delta (w_2(L) - x_3^T\, \phi_1(L))} \\
&+ \tilde{E}I_3^*(0)\, w_2''(L)\, \delta w_2'(L) \\
&+ \underline{\left\{ -x_3^T\, \tilde{E}I_3^*(0)\, w_2'''(L) - \alpha^2\, \tilde{E}I_\omega^*(0)\phi_1'''(L) + \frac{2}{L}\alpha(1-\alpha)\,\tilde{E}I_\omega^*(0)\phi_1''(L) \right.} \\
&\qquad \underline{+ \left[\frac{2}{L^2}(1-\alpha)^2\,\tilde{E}I_\omega^*(0) + \left(1-\frac{h_0\, t_w^3}{3J(0)}(1-\alpha) \right) GJ(0) \right] \phi_1'(L)} \\
&\qquad \underline{\left. + \left(\lambda\, Q_{ref}\, (x_3^Q - x_3^T) + k_{R1} \right) \phi_1(L) \right\} \delta\phi_1(L)} \\
&+ \left(\alpha^2 \tilde{E}I_\omega^*(0)\phi_1''(L) - \frac{2}{L}\alpha(1-\alpha)\tilde{E}I_\omega^*(0)\phi_1'(L) \right) \delta\phi_1'(L)\ . \qquad (4.4.9)
\end{aligned}
$$

The particular grouping criterion that led to the writing of the underlined boundary terms in equation (4.4.9) warrants an explanation. By considering the variation $\delta\left(w_2(L) - x_3^T \phi_1(L) \right)$ of

the lateral displacement at the level of the translational restraint ($x_3 = x_3^T$), it is ensured that the natural boundary condition corresponding to $\delta\phi_1(L)$ involves only the torsional restraint stiffness k_{R1}, instead of both k_{R1} and k_T. Viewed from a complementary standpoint, this means that when $k_T = +\infty$ (see below), the values at $\theta^1 = L$ of the admissible variations $\delta(w_2 - x_3^T \phi_1)$ and $\delta\phi_1$ are independent – on the contrary, if the variations δw_2 and $\delta\phi_1$ were used, they would have to be related through $\delta w_2(L) = x_3^T \delta\phi_1(L)$.

Now, by virtue of the fundamental lemma of the calculus of variations, the vanishing of the first variation of Π_2 for all admissible δw_2 and $\delta\phi_1$ – *i.e.*, the criterion of Trefftz – leads us to the classical or strong form of the LTB archetypal problem, which may be phrased as follows (recall that, for the moment, we are assuming $k_{Rf}, k_{R1}, k_T \neq +\infty$; moreover, k_{Rf} and k_T are not simultaneously zero):

Archetypal problem.

Find $\lambda \in \mathbb{R}$ and real-valued functions $w_2, \phi_1 \in C^4[0, L]$, with $w_2 \neq 0$ or $\phi_1 \neq 0$, satisfying the differential equations

$$\tilde{E}I_3^*(0)\, w_2^{(4)}(\theta^1) - \lambda\, Q_{ref}\left((L-\theta^1)\phi_1''(\theta^1) - 2\phi_1'(\theta^1)\right) = 0 \tag{4.4.10}$$

$$\left(1-(1-\alpha)\frac{\theta^1}{L}\right)^2 \tilde{E}I_\omega^*(0)\,\phi_1^{(4)}(\theta^1) - \frac{4}{L}(1-\alpha)\left(1-(1-\alpha)\frac{\theta^1}{L}\right)\tilde{E}I_\omega^*(0)\,\phi_1'''(\theta^1)$$
$$-\left(1-\frac{h_0\, t_w^3}{3J(0)}(1-\alpha)\frac{\theta^1}{L}\right)GJ(0)\,\phi_1''(\theta^1) + \frac{h_0\, t_w^3}{3J(0)}\frac{1-\alpha}{L}GJ(0)\,\phi_1'(\theta^1)$$
$$-\lambda\, Q_{ref}\,(L-\theta^1)\, w_2''(\theta^1) = 0 \tag{4.4.11}$$

in the open interval $(0, L)$, together with the boundary conditions

$$w_2(0) = 0 \tag{4.4.12}$$

$$\tilde{E}I_3^*(0)\, w_2''(0) - 2k_{Rf}\, w_2'(0) - \lambda\, Q_{ref}\, L\,\phi_1(0) = 0 \tag{4.4.13}$$

$$\phi_1(0) = 0 \tag{4.4.14}$$

$$\tilde{E}I_\omega^*(0)\,\phi_1''(0) - \left(\frac{2}{L}(1-\alpha)\,\tilde{E}I_\omega^*(0) + \frac{h_0^2}{4}2k_{Rf}\right)\phi_1'(0) = 0 \tag{4.4.15}$$

$$\tilde{E}I_3^*(0)\, w_2'''(L) - k_T\left(w_2(L) - x_3^T\,\phi_1(L)\right) + \lambda\, Q_{ref}\,\phi_1(L) = 0 \tag{4.4.16}$$

$$w_2''(L) = 0 \tag{4.4.17}$$

$$x_3^T\,\tilde{EI}_3^*(0)\,w_2'''(L)+\alpha^2\,\tilde{EI}_\omega^*(0)\,\phi_1'''(L)-\frac{2}{L}\alpha(1-\alpha)\,\tilde{EI}_\omega^*(0)\,\phi_1''(L)$$

$$-\left[\frac{2}{L^2}(1-\alpha)^2\,\tilde{EI}_\omega^*(0)+\left(1-\frac{h_0\,t_w^3}{3J(0)}(1-\alpha)\right)GJ(0)\right]\phi_1'(L)$$

$$-\left((x_3^Q-x_3^T)\,\lambda\,Q_{ref}+k_{R1}\right)\phi_1(L)=0 \tag{4.4.18}$$

$$\alpha\,\tilde{EI}_\omega^*(0)\,\phi_1''(L)-\frac{2}{L}(1-\alpha)\,\tilde{EI}_\omega^*(0)\,\phi_1'(L)=0\ . \tag{4.4.19}$$

In the above list of boundary conditions, (4.4.12) and (4.4.14) are essential, while all the remaining ones are natural.

The modifications that must be incorporated into the strong form of the archetypal problem to account for rigid restraints are now discussed.

(i) If $k_{Rf}=+\infty$, the cantilever is fully built-in at the support and the natural boundary conditions (4.4.13) and (4.4.15) should be replaced by the corresponding essential ones:

$$w_2'(0)=0 \tag{4.4.20}$$

$$\phi_1'(0)=0\ . \tag{4.4.21}$$

(ii) Similarly, if $k_T=+\infty$, equation (4.4.16) should be replaced by

$$w_2(L)-x_3^T\,\phi_1(L)=0\ . \tag{4.4.22}$$

(iii) Finally, if $k_{R1}=+\infty$, the boundary condition (4.4.18) should be replaced by

$$\phi_1(L)=0 \tag{4.4.23}$$

and, in this particular case, the buckling problem clearly becomes independent of both x_3^Q and x_3^T.

The not unusual case of $N>1$ translational restraints at one cross-section, placed at the levels $x_3=x_3^{T.n}$ and with stiffnesses $k_{T.n}$, with $n=1,\cdots,N$, possibly combined with a torsional restraint with stiffness k_{R1}, can always be reduced to a single translational restraint with stiffness k_T^*, placed at the level $x_3=x_3^{T*}$, together with a torsional restraint with stiffness k_{R1}^*. If none of the restraints is rigid, then

$$k_T^*=\sum_{n=1}^{N}k_{T.n} \tag{4.4.24}$$

$$x_3^{T*}=\frac{\sum_{n=1}^{N}x_3^{T.n}\,k_{T.n}}{\sum_{i=1}^{n}k_{T.n}} \tag{4.4.25}$$

$$k_{\mathrm{R}1}^{*} = k_{\mathrm{R}1} + \sum_{n=1}^{N} \left(x_3^{T.n} - x_3^{T*} \right) x_3^{T.n} \, k_{T.n} \ . \tag{4.4.26}$$

If one, and only one, of the N translational restraints is perfectly rigid, say $k_{T.m} = +\infty$, then, with the customary algebraic conventions for the extended real line $\overline{\mathbb{R}}$ (*e.g.*, BOURBAKI 2007, ch. 4, § 4), equation (4.4.24) gives $k_T^{*} = +\infty$ and, after removing the $\frac{\infty}{\infty}$ indeterminacy, equation (4.4.25) yields $x_3^{T*} = x_3^{T.m}$. If two (or more) translational restraints are rigid, then $k_T^{*} = k_{\mathrm{R}x}^{*} = +\infty$ and x_3^{T*} becomes irrelevant.

Suppose that $k_T \neq +\infty$. Upon integrating twice the differential equation (4.4.10) and using the boundary conditions (4.4.16) and (4.4.17), together with the continuity properties of w_2, ϕ_1 and their derivatives, we get

$$\tilde{E} I_3^{*}(0) \, w_2''(\theta^1) - (L - \theta^1) \left[\lambda \, Q_{ref} \, \phi_1(\theta^1) - k_T \left(w_2(L) - x_3^T \, \phi(L) \right) \right] = 0 \ , \ \ 0 \leq \theta^1 \leq L \ . \tag{4.4.27}$$

In particular,

$$\tilde{E} I_3^{*}(0) \, w_2''(0) - \lambda \, Q_{ref} \, L \, \phi_1(0) + k_T \, L \left(w_2(L) - x_3^T \, \phi_1(L) \right) = 0 \ . \tag{4.4.28}$$

Now, suppose, in addition, that $k_{Rf} \neq +\infty$. It follows at once from (4.4.13) that

$$2 \, k_{Rf} \, w_2'(0) + k_T \, L \left(w_2(L) - x_3^T \, \phi_1(L) \right) = 0 \ . \tag{4.4.29}$$

The last-written equation, which involves only boundary terms, has a clear physical meaning – it is the global moment equilibrium equation about the axis through the origin O and along $\boldsymbol{e}_3$. We mention two immediate consequences:

(i) If $k_T = 0$, then $k_{Rf} \neq 0$ implies $w_2'(0) = 0$ – in the absence of a lateral translational restraint at the tip, any lateral bending restraint at the support ensures $w_2'(0) = 0$, as observed by TRAHAIR (1993, § 9.6.1.1).

(ii) If $k_{Rf} = 0$, then $k_T \neq 0$ implies $w_2(L) - x_3^T \, \phi_1(L) = 0$ – in the absence of a lateral bending restraint at the support, any translational restraint at the tip precludes the lateral deflection at its location.

By an appropriate change of variable, the above LTB problem may be converted into an equivalent one, posed on a fixed reference domain (*i.e.*, independent of the cantilever length) and written in non-dimensional form, which is a particularly adequate setting for carrying out systematic parametric studies – within the context of the archetypal problem being addressed, we cannot possibly agree with the assertion that it is "virtually impossible to non-dimensionalize the many parameters in tapered sections [members]" found in GALAMBOS (1998, p. 83).

Choosing the closed unit interval $[0,1]$ as the fixed reference domain, the change of variable is defined by the map $f:[0,L]\to[0,1]$, $f(\theta^1)=\theta^1/L=s$. Moreover, we set

$$\tilde{w}:[0,1]\to\mathbb{R}\ ,\quad \tilde{w}(s)=\frac{1}{L}\sqrt{\frac{\tilde{E}I_3^*(0)}{GJ(0)}}\ w_2(sL) \tag{4.4.30}$$

$$\tilde{\phi}:[0,1]\to\mathbb{R}\ ,\quad \tilde{\phi}(s)=\phi_1(sL)\ . \tag{4.4.31}$$

Finally, we introduce the map

$$x_3\mapsto\zeta(x_3)=\frac{2x_3}{\alpha h_0}\ , \tag{4.4.32}$$

which defines a non-dimensional vertical ordinate referred to (half) the cross-sectional depth at the tip, αh_0. The non-dimensional version of the archetypal problem is then stated as follows:

Archetypal problem (non-dimensional version).

Given the non-dimensional parameters

$$\gamma=\frac{\lambda Q_{ref}L^2}{\sqrt{\tilde{E}I_3^*(0)GJ(0)}} \tag{4.4.33}$$

$$\kappa_{\omega 0}=\frac{\pi}{L}\sqrt{\frac{\tilde{E}I_\omega^*(0)}{GJ(0)}} \tag{4.4.34}$$

$$\kappa_{J0}=\frac{h_0 t_w^3}{3J(0)} \tag{4.4.35}$$

$$\sigma_{Rf}=\frac{2k_{Rf}L}{\tilde{E}I_3^*(0)} \tag{4.4.36}$$

$$\sigma_{R1}=\frac{k_{R1}L}{GJ(0)} \tag{4.4.37}$$

$$\sigma_T=\frac{k_T L^3}{\tilde{E}I_3^*(0)} \tag{4.4.38}$$

$$\zeta_T=\zeta(x_3^T)=\frac{2x_3^T}{\alpha h_0} \tag{4.4.39}$$

$$\zeta_Q=\zeta(x_3^Q)=\frac{2x_3^Q}{\alpha h_0}\ , \tag{4.4.40}$$

where (i) $\sigma_{Rf},\sigma_{R1},\sigma_T\neq+\infty$ and (ii) σ_{Rf} and σ_T are not simultaneously zero, find $\gamma\in\mathbb{R}$ and $\tilde{w},\tilde{\phi}\in C^4[0,1]$, with $\tilde{w}\neq 0$ or $\tilde{\phi}\neq 0$, satisfying the differential equations

$$\tilde{w}^{(4)}(s)-\gamma\left((1-s)\tilde{\phi}(s)\right)''=0 \tag{4.4.41}$$

$$\left(\frac{\kappa_{\omega 0}}{\pi}\right)^2\left(1-(1-\alpha)s\right)^2\tilde{\phi}^{(4)}(s)-4\left(\frac{\kappa_{\omega 0}}{\pi}\right)^2(1-\alpha)\left(1-(1-\alpha)s\right)\tilde{\phi}'''(s)$$
$$-\left(1-\kappa_{J0}(1-\alpha)s\right)\tilde{\phi}''(s)+\kappa_{J0}(1-\alpha)\tilde{\phi}'(s)-\gamma(1-s)\tilde{w}''(s)=0 \tag{4.4.42}$$

in the open unit interval $(0,1)$, together with the boundary conditions

$$\tilde{w}(0)=0 \tag{4.4.43}$$

$$\tilde{w}''(0)-\sigma_{Rf}\,\tilde{w}'(0)-\gamma\,\tilde{\phi}(0)=0 \tag{4.4.44}$$

$$\tilde{\phi}(0)=0 \tag{4.4.45}$$

$$\tilde{\phi}''(0)-\left(2(1-\alpha)+\sigma_{Rf}\right)\tilde{\phi}'(0)=0 \tag{4.4.46}$$

$$\tilde{w}'''(1)-\sigma_T\left(\tilde{w}(1)-\frac{\kappa_{\omega 0}}{\pi}\alpha\zeta_T\,\tilde{\phi}(1)\right)+\gamma\,\tilde{\phi}(1)=0 \tag{4.4.47}$$

$$\tilde{w}''(1)=0 \tag{4.4.48}$$

$$\frac{\kappa_{\omega 0}}{\pi}\alpha\zeta_T\,\tilde{w}'''(1)+\frac{\kappa_{\omega 0}^2}{\pi^2}\alpha^2\tilde{\phi}'''(1)-2\frac{\kappa_{\omega 0}^2}{\pi^2}\alpha(1-\alpha)\tilde{\phi}''(1)$$
$$-\left(1+2\frac{\kappa_{\omega 0}^2}{\pi^2}(1-\alpha)^2-\kappa_{J0}(1-\alpha)\right)\tilde{\phi}'(1)$$
$$-\left(\frac{\kappa_{\omega 0}}{\pi}\alpha(\zeta_Q-\zeta_T)\gamma+\sigma_{R1}\right)\tilde{\phi}(1)=0 \tag{4.4.49}$$

$$\alpha\tilde{\phi}''(1)-2(1-\alpha)\tilde{\phi}'(1)=0\ . \tag{4.4.50}$$

The following non-dimensional counterparts of equations (4.4.20)-(4.4.23) should be used when σ_{Rf}, σ_{R1} and/or σ_T are infinitely large:

$$\tilde{w}'(0)=0 \tag{4.4.51}$$

$$\tilde{\phi}'(0)=0 \tag{4.4.52}$$

$$\tilde{w}(1)-\frac{\kappa_{\omega 0}}{\pi}\alpha\zeta_T\,\tilde{\phi}(1)=0 \tag{4.4.53}$$

$$\tilde{\phi}(1)=0\ . \tag{4.4.54}$$

The ordinary differential equations (4.4.41), (4.4.42) and the boundary conditions (4.4.44), (4.4.46)-(4.4.50) are the Euler-Lagrange equations and natural boundary conditions associated with the vanishing of the first variation of the functional

$$\begin{aligned}\tilde{\Pi}(\tilde{w},\tilde{\phi},\gamma) = {} & \frac{1}{2}\int_0^1 \tilde{w}''(s)^2\,ds + \frac{1}{2}\left(\frac{\kappa_{\omega 0}}{\pi}\right)^2 \int_0^1 \left(1-(1-\alpha)s\right)^2 \tilde{\phi}''(s)^2\,ds \\ & -2(1-\alpha)\left(\frac{\kappa_{\omega 0}}{\pi}\right)^2 \int_0^1 \left(1-(1-\alpha)s\right)\tilde{\phi}''(s)\tilde{\phi}'(s)\,ds \\ & +2(1-\alpha)^2\left(\frac{\kappa_{\omega 0}}{\pi}\right)^2 \int_0^1 \tilde{\phi}'(s)^2\,ds + \frac{1}{2}\int_0^1 \left(1-\kappa_{J0}(1-\alpha)s\right)\tilde{\phi}'(s)^2\,ds \\ & +\frac{\sigma_{Rf}}{2}\left(\tilde{w}'(0)^2 + \frac{\kappa_{\omega 0}^2}{\pi^2}\tilde{\phi}'(0)^2\right) + \frac{\sigma_{R1}}{2}\tilde{\phi}(1)^2 + \frac{\sigma_T}{2}\left(\tilde{w}(1) - \alpha\zeta_T\frac{\kappa_{\omega 0}}{\pi}\tilde{\phi}(1)\right)^2 \\ & -\gamma\int_0^1 (1-s)\tilde{w}''(s)\tilde{\phi}(s)\,ds + \frac{1}{2}\alpha\zeta_Q\frac{\kappa_{\omega 0}}{\pi}\gamma\tilde{\phi}(1)^2\ . \end{aligned} \tag{4.4.55}$$

For later convenience, we write (4.4.55) in the abbreviated form

$$\tilde{\Pi}(\tilde{w},\tilde{\phi},\gamma) = \tilde{A}(\tilde{w},\tilde{\phi}) - \gamma\,\tilde{B}(\tilde{w},\tilde{\phi})\ , \tag{4.4.56}$$

that is, $\tilde{A}(\tilde{w},\tilde{\phi})$ stands for the sum of the material terms in (4.4.55) (independent of γ), while $\tilde{B}(\tilde{w},\tilde{\phi})$ is the sum of the geometrical terms per unit value of γ.

In view of (4.4.30), it would have been more natural or, at any rate, more immediate to define the map

$$x_3 \mapsto \varepsilon(x_3) = \frac{x_3}{L}\sqrt{\frac{\tilde{E}I_3^*(0)}{GJ(0)}} \tag{4.4.57}$$

instead of $x_3 \mapsto \zeta(x_3)$ given by (4.4.32). Our choice was dictated by practical reasons, since (4.4.32) is easily visualised and conveys a clear perception of position (in relation to the cross-sectional depth at the tip). On the contrary, (4.4.57) is far from being intuitive. However, we shall have the occasion to use (4.4.57). Note the relationship

$$\varepsilon(x_3) = \alpha\frac{\kappa_{\omega 0}}{\pi}\zeta(x_3)\ . \tag{4.4.58}$$

4.4.3 Numerical solution

As in the illustrative example of the preceding chapter, the non-dimensional version of the archetypal problem is first converted into an inhomogeneous two-point boundary value

problem, which is then solved using the general-purpose code COLNEW,[11] an approach that was successfully applied to the LTB analysis of prismatic beams by REISSNER *et al.* (1987). The conversion is achieved by supplementing the original eigenproblem with the first-order ordinary differential equations

$$\tilde{\phi}_0'(s) = \gamma' = 0 \tag{4.4.59}$$

$$\begin{aligned}\vartheta'(s) = {} & \frac{1}{2}\tilde{w}''(s)^2 + \frac{1}{2}\left(\frac{\kappa_{\omega 0}}{\pi}\right)^2 \left(1-(1-\alpha)s\right)^2 \tilde{\phi}''(s)^2 \\ & -2(1-\alpha)\left(\frac{\kappa_{\omega 0}}{\pi}\right)^2 \left(1-(1-\alpha)s\right)\tilde{\phi}''(s)\tilde{\phi}'(s) \\ & +\frac{1}{2}\left(1+4(1-\alpha)^2\left(\frac{\kappa_{\omega 0}}{\pi}\right)^2 - \kappa_{J0}(1-\alpha)s\right)\tilde{\phi}'(s)^2\end{aligned} \tag{4.4.60}$$

and the boundary conditions

$$\vartheta(0) = \frac{\sigma_{Rf}}{2}\left(\tilde{w}'(0)^2 + \frac{\kappa_{\omega 0}^2}{\pi^2}\tilde{\phi}'(0)^2\right) \tag{4.4.61}$$

$$\vartheta(1) = 1 - \frac{\sigma_{R1}}{2}\tilde{\phi}(1)^2 - \frac{\sigma_T}{2}\left(\tilde{w}(1) - \alpha\zeta_T\frac{\kappa_{\omega 0}}{\pi}\tilde{\phi}(1)\right)^2 . \tag{4.4.62}$$

The first additional differential equation is just a statement of the fact that an eigenvalue, formally regarded as a function of s, is a constant. The second differential equation, together with the added boundary conditions, is equivalent to imposing the normalisation

$$\tilde{A}(\tilde{w},\tilde{\phi}) = 1 \tag{4.4.63}$$

and makes the eigenfunctions unique, up to sign. (Of course, when writing the boundary conditions (4.4.61)-(4.4.62) it was tacitly assumed that $\sigma_{Rf}, \sigma_{R1}, \sigma_T \neq +\infty$; the modifications required to deal with an infinitely large σ are obvious.) It should be noticed that (i) the augmented boundary value problem is non-linear, even though the original eigenproblem is linear, and (ii) the boundary conditions remain separated.

Since the parametric study reported in the next subsection requires the solution of chains of "nearby problems" (known as "homotopy chains" – DEUFLHARD 1979, p. 65), a relatively crude, but very effective, continuation strategy was implemented: the solution of a previous problem is used as the initial guess for the next one, having the same data except for a small increment in a single parameter, a possibility that is already encoded in COLNEW.

[11] A brief overview of COLNEW and its predecessor COLSYS is given in Appendix 1, at the end of chapter 3.

4.4.4 Parametric study

Richard Hamming summed up his views on scientific computing with the motto "the purpose of scientific computing is insight, not numbers" (HAMMING 1962). In the parametric study presented next, we will try to live up to Hamming's words and shed some light on the behaviour of restrained tapered I-beams. Each type of restraint is addressed separately – more specifically, we consider in succession the cases (i) $\sigma_T > 0$, with $\sigma_{Rx} = 0$ and $\sigma_{Rf} = +\infty$, (ii) $\sigma_{Rx} > 0$, with $\sigma_T = 0$ and $\sigma_{Rf} = +\infty$, and (iii) $\sigma_{Rf} > 0$, with $\sigma_T = \sigma_{Rx} = 0$. In order to focus on the effect of the restraints and its interplay with the degree of web tapering, the parametric study is restricted to the centroidal loading case ($\zeta_Q = 0$). Moreover, having previously remarked that the parameter κ_{J0} is relatively unimportant, we always set $\kappa_{J0} = 0.1$ (*vide supra*, chapter 2, note 58).

Built-in cantilevers ($\sigma_{Rf} = +\infty$) with a translational restraint at the tip ($\sigma_T > 0$, $\sigma_{R1} = 0$)

For selected values of the web taper ratio $\alpha = \frac{h(L)}{h_0}$ and for $0.1 \le \kappa_{\omega 0} = \frac{\pi}{L}\sqrt{\frac{\tilde{E}I_\omega^*(0)}{GJ(0)}} \le 2.5$, figure 4.4.3 shows:

(i) The non-dimensional buckling loads $\gamma_{cr} = \lambda_{cr} Q_{ref} L^2 / \sqrt{\tilde{E}I_3^*(0) GJ(0)}$ and $\gamma_b^{(2)}$, corresponding to the first (critical) and second buckling modes of cantilevers that are entirely free at the tip ($\sigma_T = k_T L^3 / (\tilde{E}I_3^*(0)) = 0$) – these results are presented for reference purposes;

(ii) The non-dimensional critical loads of cantilevers with a rigid translational tip restraint ($\sigma_T = +\infty$), located at the top flange ($\zeta_T = 2x_3^T / (\alpha h_0) = -1$), mid-depth ($\zeta_T = 0$) and bottom flange ($\zeta_T = 1$);

(iii) The percentage increase of the critical load factor, relative to the free-end case, due to the rigid restraint,

$$\Delta = \frac{\lambda_{cr}^{\text{rigidly restrained}} - \lambda_{cr}^{\text{free end}}}{\lambda_{cr}^{\text{free end}}} \times 100\% \ . \tag{4.4.64}$$

The results presented in this figure unveil the importance of the restraint location. Indeed, the effectiveness of the restraint in increasing the elastic buckling strength relative to the free-end case is greatest when it is located at the top flange ($\zeta_T = -1$). Moreover, the effectiveness of a top-flange restraint increases with the web-taper ratio α. It is also visible in figure 4.4.3 that the benefit of a top-flange restraint generally increases with $\kappa_{\omega 0}$ for a sufficiently large α. On the other hand, for moderate-to-high $\kappa_{\omega 0}$ values, a bottom flange

restraint is almost completely ineffective, especially when the taper is not very pronounced. The main issue in explaining these behavioural features is the distance, when buckling sets off, between the rotation centre of the tip cross-section in the free-end case (*i.e.*, without any restraint) and the location where the translational restraint is placed – the greater this distance, the more effective is the restraint. In order to back this assertion, we plot in figure 4.4.4, for selected values of α and $\kappa_{\omega 0}$, the percentage increase $\measuredangle$ defined by equation (4.4.64) *versus* $\varepsilon(x_3^{RC.\,free\,end} - x_3^T) = \frac{1}{L}\sqrt{\frac{\tilde{E}I_3^*(0)}{GJ(0)}}\,(x_3^{RC.\,free\,end} - x_3^T)$, where $x_3^{RC.\,free\,end}$ is the x_3-coordinate of the rotation centre in the free-end case and is given by

$$x_3^{RC.\,free\,end} = \left[\frac{w_{2.cr}(L)}{\phi_{1.cr}(L)}\right]^{free\,end} . \tag{4.4.65}$$

Observe that:

(i) $\measuredangle$ always increases with $\varepsilon(x_3^{RC.\,free\,end} - x_3^T)$.

(ii) For a given $\kappa_{\omega 0}$, the variation of $\measuredangle$ with $\varepsilon(x_3^{RC.\,free\,end} - x_3^T)$ is only mildly sensitive to the web taper ratio α. For a given α, the dependence of these plots on $\kappa_{\omega 0}$ is more pronounced, although this is not immediately perceived in figure 4.4.4.

Finally, notice that the critical load of a cantilever with a rigid translational restraint (even if located at the top flange) is always well below the second-mode buckling load of the same cantilever without the restraint – this is easily understood if the conjecture concerning the zeros of $\phi_{1.b}^{(n)}$ proves to be true.

Let us now turn to the influence of the restraint stiffness parameter $\sigma_T = k_T L^3 / (\tilde{E}I_3^*(0))$. We restrict ourselves to the case of a top-flange restraint ($\zeta_T = -1$). As shown in figure 4.4.5, there is a well-defined threshold beyond which a further increase in σ_T causes a negligible raise in buckling strength. Moreover, the ratio

$$r = \frac{\lambda_{cr}^{elastically\,restrained} - \lambda_{cr}^{free\,end}}{\lambda_{cr}^{rigidly\,restrained} - \lambda_{cr}^{free\,end}} \times 100\,\% \tag{4.4.66}$$

is practically independent of α and $\kappa_{\omega 0}$, and this is perhaps the dominant feature in this figure. It is therefore possible to state, with generality, that $\sigma_T = 10$ and $\sigma_T = 50$ guarantee $r = 60\%$ and $r = 90\%$, respectively. These figures provide useful quantitative guidelines for designing the tip translational restraint as far as its stiffness is concerned.

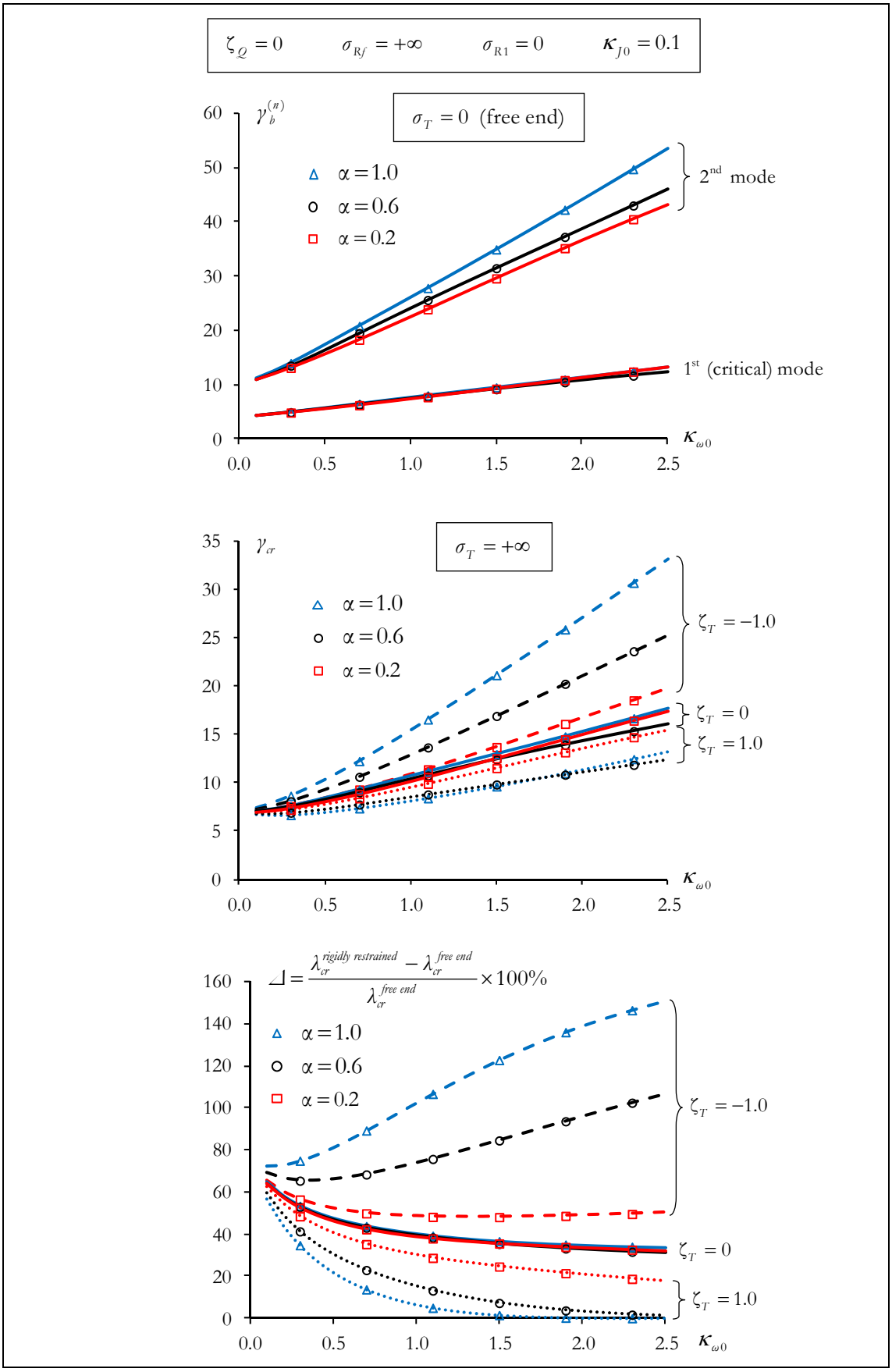

Figure 4.4.3: Effect of a rigid translational restraint at the tip

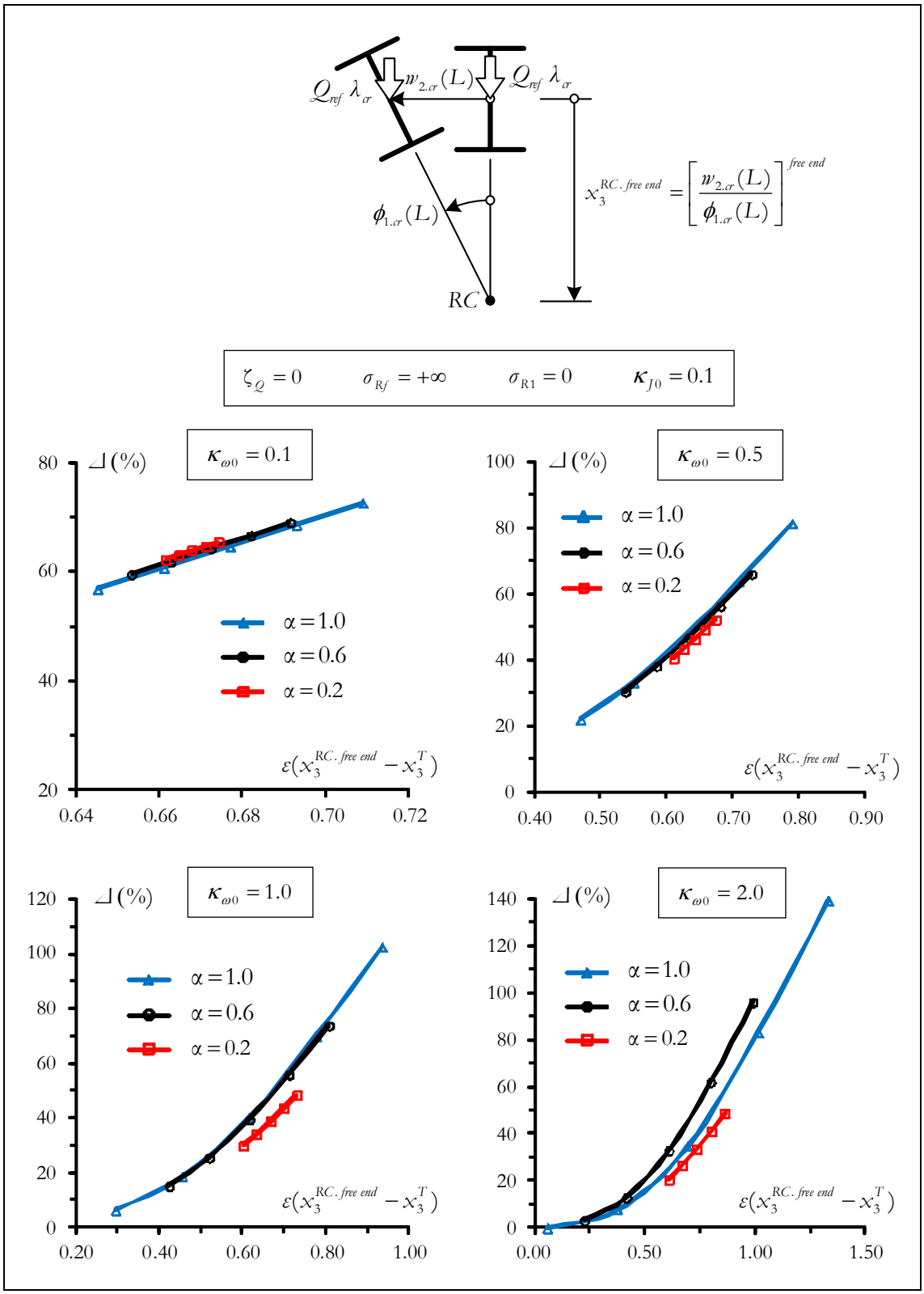

Figure 4.4.4: Influence of the distance between the rotation centre of the tip cross-section in the free-end case and the location of the translational restraint

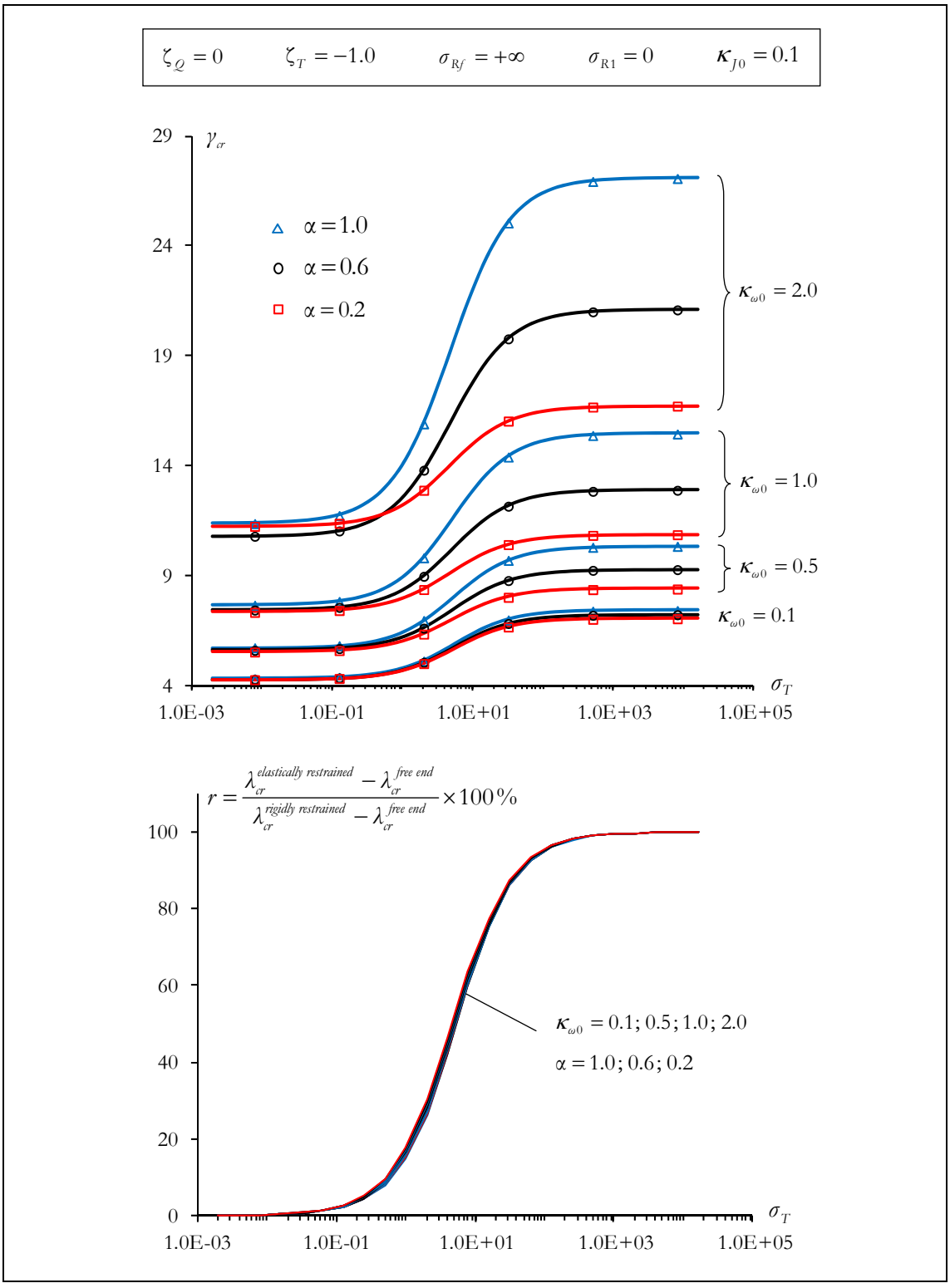

Figure 4.4.5: Effect of a linearly elastic top-flange translational restraint at the tip

Built-in cantilevers ($\sigma_{Rf}=+\infty$) with a torsional restraint at the tip ($\sigma_{R1}>0$, $\sigma_T=0$)

We now investigate the effect of a torsional restraint located at the tip of a built-in cantilever. The examination of figure 4.4.6, which concerns a perfectly rigid restraint (that is, $\sigma_{R1}=k_{R1}L/(GJ(0))=+\infty$), prompts the following observations:

(i) The critical load of a cantilever with a rigid torsional restraint is always well below the second-mode buckling load of the same cantilever with the tip entirely free – recall that the same was found in the case of a rigid translational restraint.

(ii) The critical load factor percentage increase $\measuredangle=(\lambda_{cr}^{\text{rigidly restrained}}-\lambda_{cr}^{\text{free end}})/\lambda_{cr}^{\text{free end}}$ due to the rigid torsional restraint generally grows with $\kappa_{\omega 0}$. However, the rate of growth gradually diminishes as the web-taper ratio α decreases. For $\alpha=0.2$, the percentage increase $\measuredangle$ remains comparatively constant.

The influence of the restraint stiffness parameter σ_{R1} is depicted in figure 4.4.7. Once again, there is a limit value beyond which further increases in σ_{R1} lead to imperceptible gains in buckling strength. As for the ratio (4.4.66), it now exhibits some sensitivity with respect to both α and $\kappa_{\omega 0}$. Nevertheless, it can be safely said that $\sigma_{R1}=10$ and $\sigma_{R1}=60$ guarantee at least $r=60\%$ and $r=90\%$, respectively.

Overhanging beam segments free at the tip ($\sigma_{R1}=\sigma_T=0$), with linearly elastic warping and minor axis bending restraints at the support ($0<\sigma_{Rf}<+\infty$)

Figure 4.4.8 shows the influence of the stiffness parameter $\sigma_{Rf}=2k_{Rf}L/(\tilde{E}I_3^*(0))$ in overhanging beam segments. For large $\kappa_{\omega 0}$ (segments with short span and/or slender cross-section at the support) and fixed σ_{Rf}, the non-dimensional critical load γ_{cr} does not increase monotonically with the web taper ratio α. As a matter of fact, for low values of σ_{Rf}, the trend is the opposite: γ_{cr} decreases as α increases. For large values of σ_{Rf}, γ_{cr} reaches a minimum at an intermediate value of α. At first glance, these findings seem to defy our intuition, even more so because the stepped model yields a steady increase of γ_{cr} with α (see the dashed lines in the bottom graphs of figure 4.4.8). However, this seeming paradox has an explanation, which is addressed next. The buckling strength of cantilevers/segments with large $\kappa_{\omega 0}$ (for illustration, we take $\kappa_{\omega 0}=2.0$ as reference throughout the discussion) depends to a large extent on the warping torsion (*i.e.*, torsion due to non-uniform warping) generated when buckling occurs. Non-uniform warping reflects itself in the membrane strains shown in figure 2.11.3 – in web-tapered I-beams,

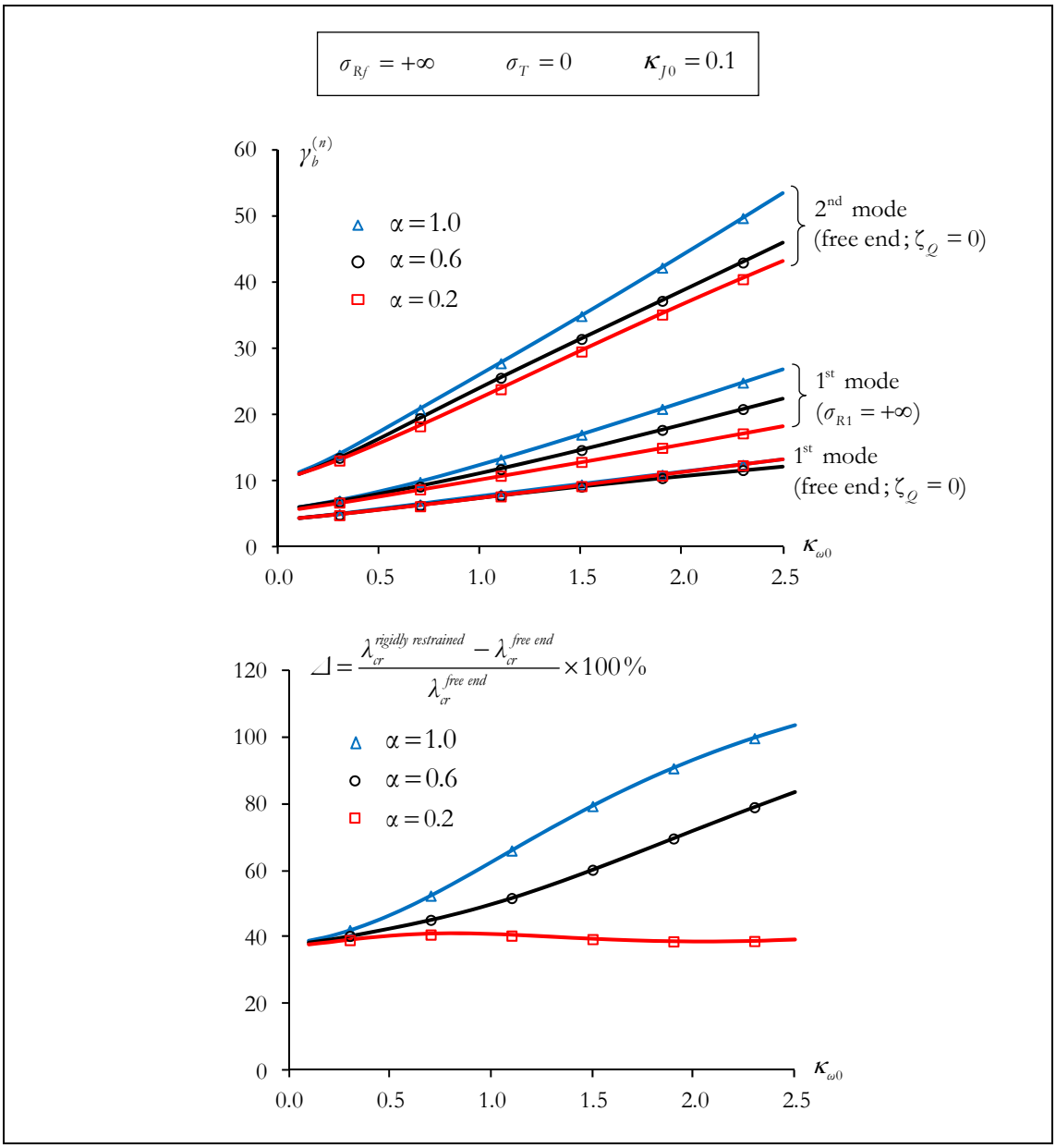

Figure 4.4.6: Effect of a rigid torsional restraint at the tip

these strains comprise two terms, one associated with $h\phi_1''$ (also present in prismatic members) and the other depending on $\tan\varphi\,\phi_1'$ (peculiar to tapered members). For warping to be uniform, it is required that

$$\frac{h(\theta^1)}{4}\phi_1''(\theta^1) - \tan\varphi\,\phi_1'(\theta^1) = 0\,,\ \forall\theta^1 \in [0, L] \tag{4.4.67}$$

or, in non-dimensional terms,

$$\big(1-(1-\alpha)s\big)\tilde{\phi}''(s) - 2(1-\alpha)\tilde{\phi}'(s) = 0\,,\ \forall s \in [0,1]\,. \tag{4.4.68}$$

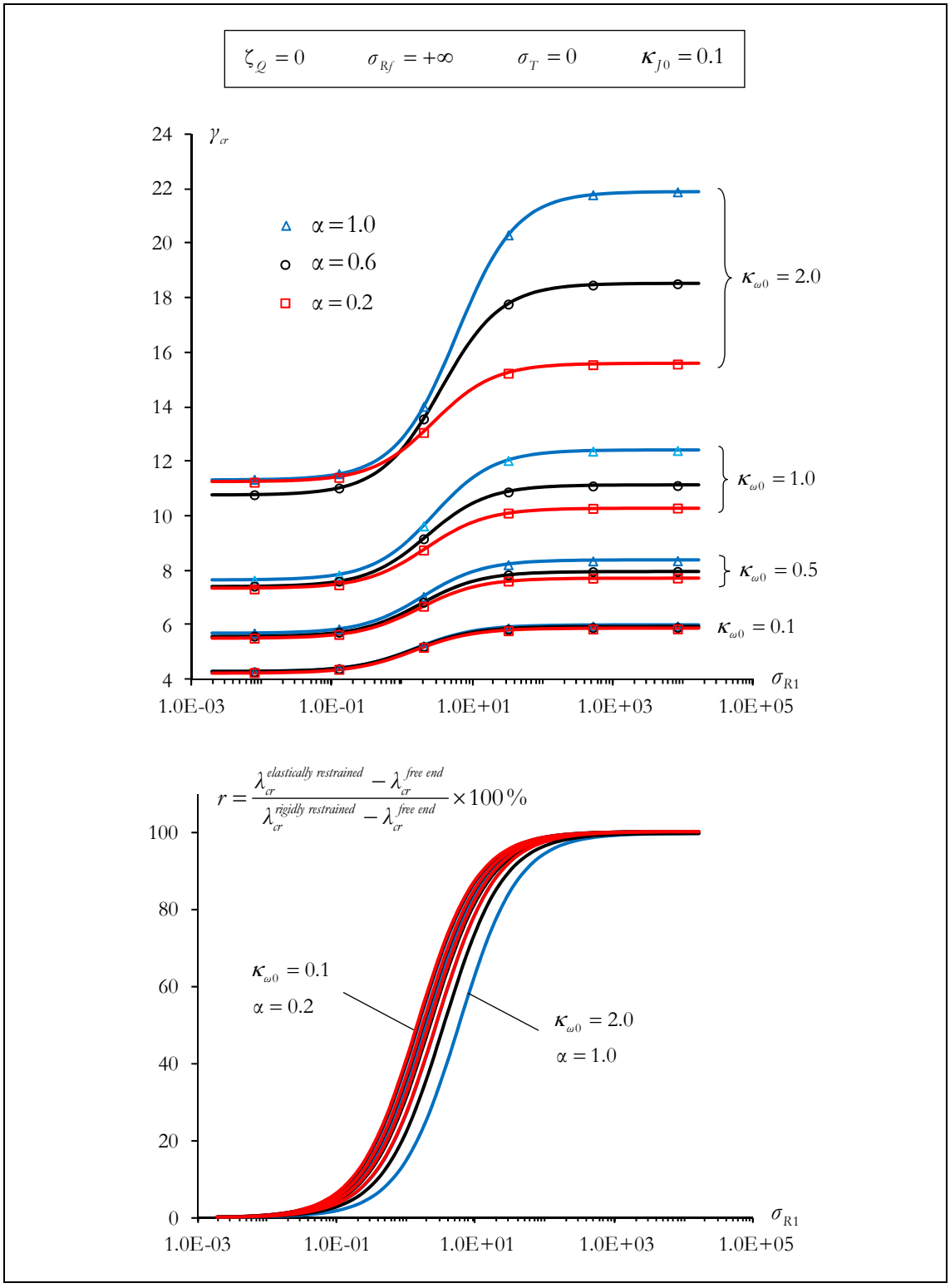

Figure 4.4.7: Effect of a linearly elastic torsional restraint at the tip

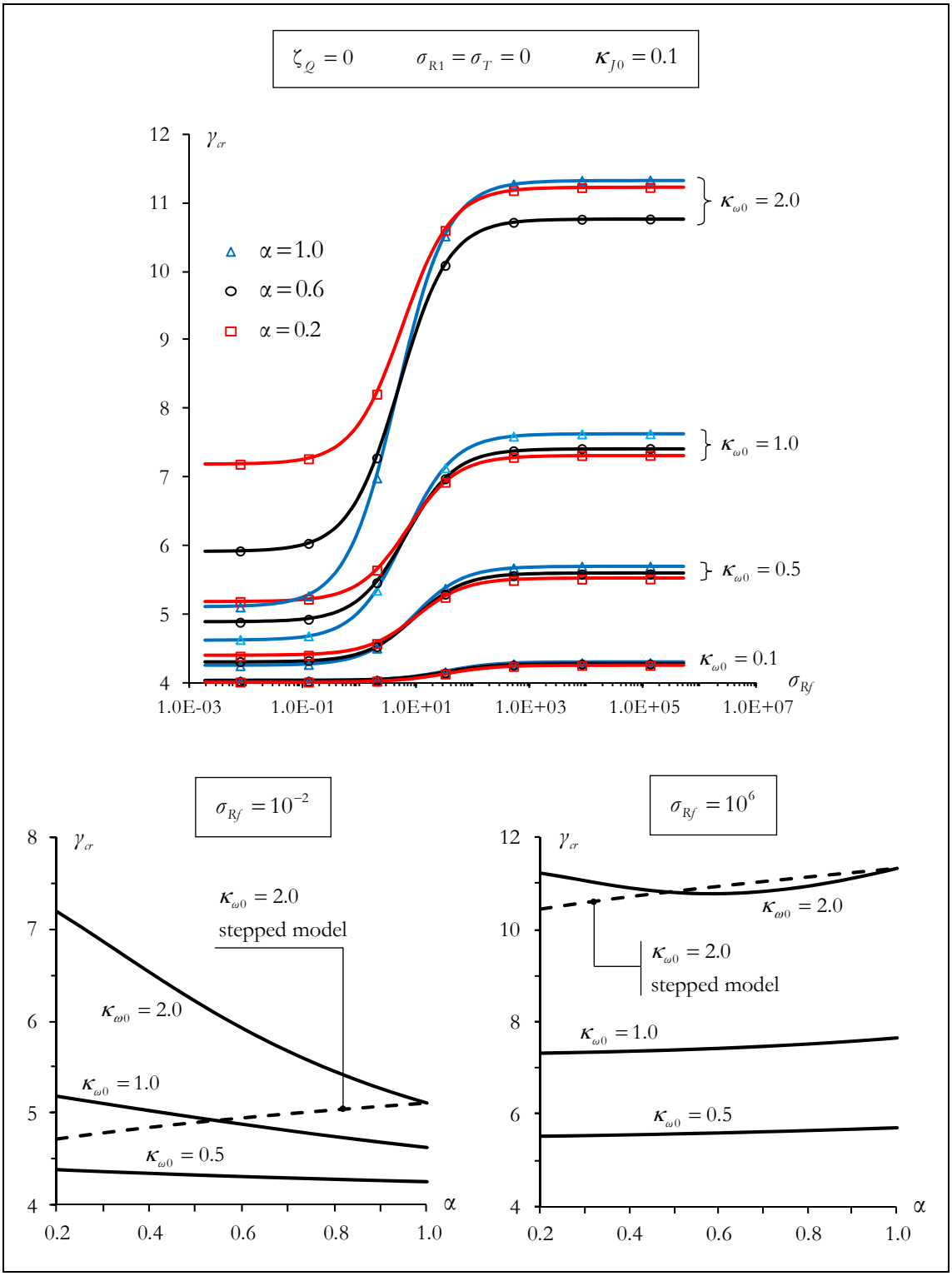

Figure 4.4.8: Effect of linearly elastic warping and minor axis bending restraints at the support

In prismatic beams, (4.4.67) and (4.4.68) become simply

$$\phi_1''(\theta^1) = 0\,,\ \forall \theta^1 \in [0, L] \tag{4.4.69}$$

$$\tilde{\phi}''(s) = 0\,,\ \forall s \in [0,1]\ . \tag{4.4.70}$$

Let us examine first the low σ_{Rf} case (say, $\sigma_{Rf} = 10^{-2}$), corresponding to a practically non-existent warping restraint at the support, and see how the preceding interpretative key applies. The graphs on the left-hand side of figure 4.4.9, concerning cantilevers with $\kappa_{\omega 0} = 2.0$, provide the basis for the ensuing discussion – they display (i) the critical buckling modes $(\tilde{w}_{cr}, \tilde{\phi}_{cr})$ associated with selected values of α, normalised so as to have $\tilde{A}(\tilde{w}_{cr}, \tilde{\phi}_{cr}) = 1$, and (ii) the corresponding non-dimensional lateral deflections $\tilde{w}_{cr} \pm \left(1-(1-\alpha)s\right)\frac{\kappa_{\omega 0}}{\pi}\tilde{\phi}_{cr}$ of the flange centroidal lines. The careful consideration of these graphs prompts the following observations:

(i) One need not be concerned with the lateral bending of the cantilevers, since $\tilde{w}_{cr}$ is practically independent of α.

(ii) In a prismatic member ($\alpha = 1$), the $\tilde{\phi}$-component of the critical buckling mode is almost linear (the L^2 norm of its second derivative, $\left\|\tilde{\phi}_{cr}''\right\|_{L^2} = \left(\int_0^1 \tilde{\phi}_{cr}''(s)^2\, ds\right)^{1/2}$, is very small, as shown in figure 4.4.10), indicating that warping is nearly uniform – this was already noted by TRAHAIR (1983) and leads to a low buckling strength.

(iii) Now, decrease α, starting from $\alpha = 1$. Up to a certain point (roughly $\alpha = 0.4 \sim 0.5$), the $\tilde{\phi}$-components of the critical buckling modes remain almost linear, and their (practically constant) slope gradually decreases (*e.g.*, see the case $\alpha = 0.6$ in figure 4.4.9). However, in view of (4.4.68), a linear $\tilde{\phi}_{cr}$ no longer means that warping is uniform, since the second term on the left-hand side of this equation, intrinsically associated with the web depth variation, does not vanish – notice the difference in lateral bending curvature between the top and bottom flange centroidal lines for $\alpha = 0.6$, which is clearly higher than in the prismatic case. There is thus some amount of warping torsion generated during buckling, responsible for the gradual increase in γ_{cr} with decreasing α observed in figure 4.4.8 (bottom left-hand corner).

(iv) When α drops below 0.4 (a situation typified by $\alpha = 0.2$ in figure 4.4.9), the normalised critical buckling modes $\tilde{\phi}_{cr}$ exhibit a more noticeable, even if still mild, curvature (as reflected in a higher L^2 norm of $\tilde{\phi}_{cr}''$ – see figure 4.4.10), so that both terms on the left-hand side of (4.4.68) are clearly non-zero. In the central portion of the span, these two terms have the same sign ($\tilde{\phi}_{cr}'$ and $\tilde{\phi}_{cr}''$ have opposite signs), thus reinforcing each other and leading to larger warping strains. Near the ends, on the contrary, they tend to cancel each other out ($\tilde{\phi}_{cr}'$ and $\tilde{\phi}_{cr}''$ have the same sign). The net effect, in this case, is to further increase γ_{cr} as α decreases.

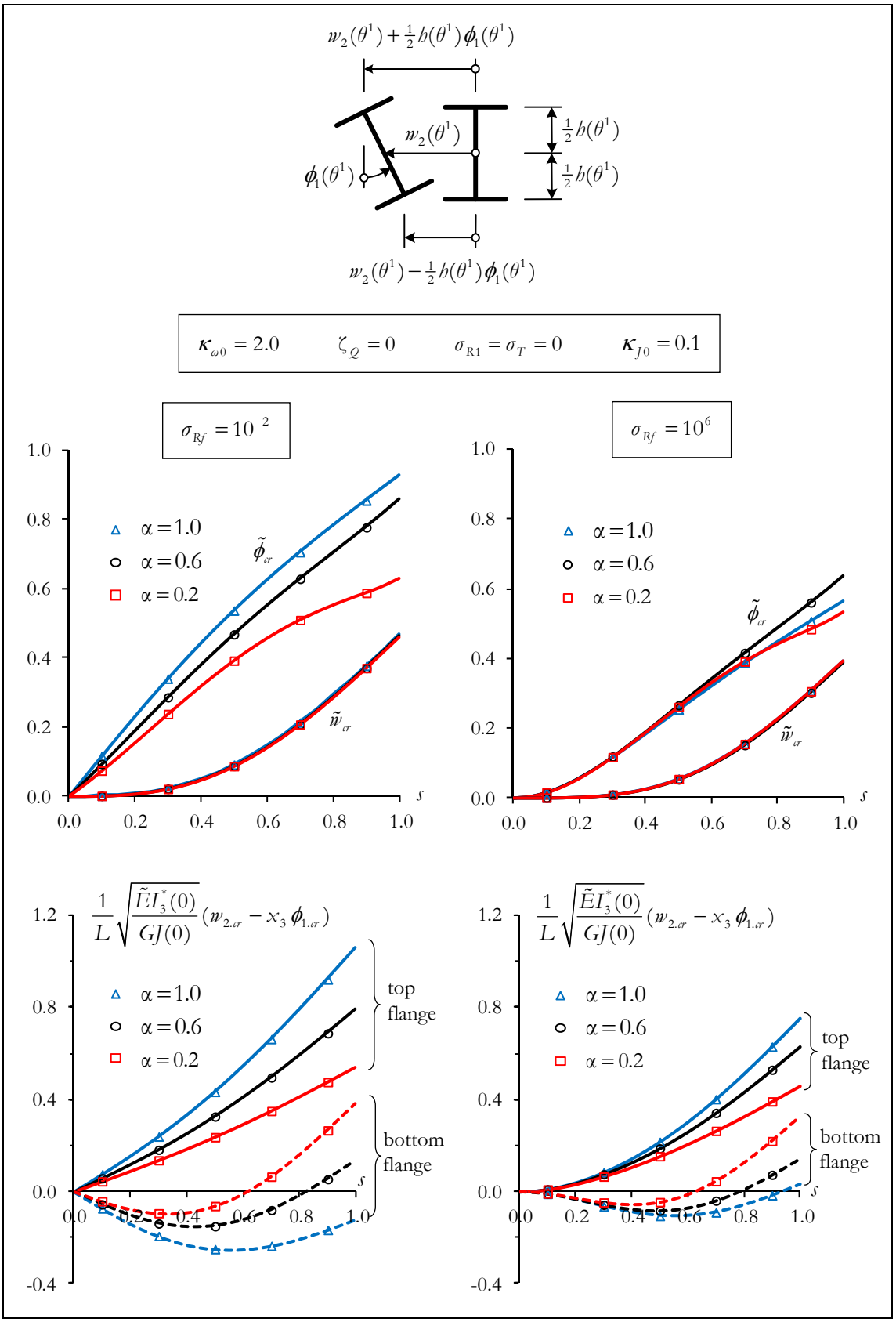

Figure 4.4.9: Critical buckling modes $(\tilde{w}_{cr}, \tilde{\phi}_{cr})$, normalised so as to have $\tilde{A}(\tilde{w}_{cr}, \tilde{\phi}_{cr})=1$, and corresponding non-dimensional lateral deflections of the flange centroidal lines

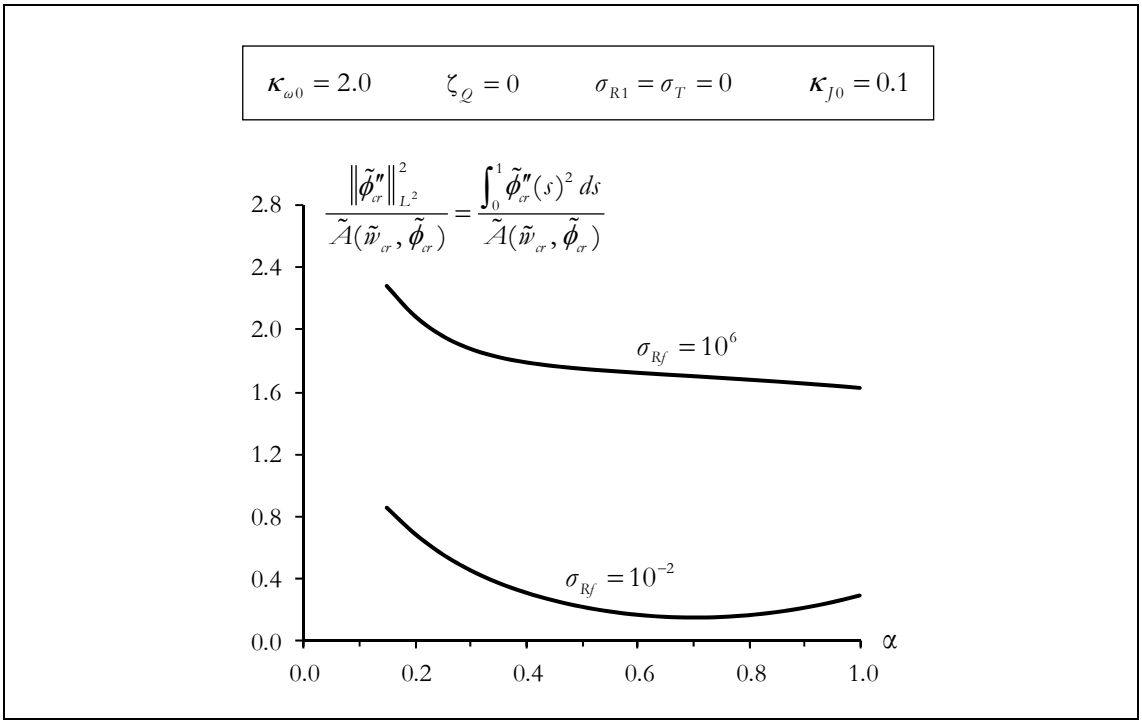

Figure 4.4.10: L^2 norm squared of $\tilde{\phi}''_{cr}$ per unit value of $\tilde{A}(\tilde{w}_{cr}, \tilde{\phi}_{cr})$

A closer look at the value at $(\tilde{w}_{cr}, \tilde{\phi}_{cr})$ of the material part of the non-dimensional energy functional (4.4.55) – *i.e.*, at $\tilde{A}(\tilde{w}_{cr}, \tilde{\phi}_{cr})$ – corroborates the above analysis. This functional is disassembled in its individual terms and, for ease of reference, the following notation is adopted:

$$\tilde{A}_3(\tilde{w}) = \frac{1}{2}\int_0^1 \tilde{w}''(s)^2\, ds \tag{4.4.71}$$

$$\tilde{A}_\omega(\tilde{\phi}) = \frac{1}{2}\left(\frac{\kappa_{\omega 0}}{\pi}\right)^2 \int_0^1 \left(1-(1-\alpha)s\right)^2 \tilde{\phi}''(s)^2\, ds \tag{4.4.72}$$

$$\tilde{A}_{\omega\psi}(\tilde{\phi}) = -2(1-\alpha)\left(\frac{\kappa_{\omega 0}}{\pi}\right)^2 \int_0^1 \left(1-(1-\alpha)s\right)\tilde{\phi}''(s)\tilde{\phi}'(s)\, ds \tag{4.4.73}$$

$$\tilde{A}_\psi(\tilde{\phi}) = 2(1-\alpha)^2\left(\frac{\kappa_{\omega 0}}{\pi}\right)^2 \int_0^1 \tilde{\phi}'(s)^2\, ds \tag{4.4.74}$$

$$\tilde{A}_{SV}(\tilde{\phi}) = \frac{1}{2}\int_0^1 \left(1-\kappa_{J0}(1-\alpha)s\right)\tilde{\phi}'(s)^2\, ds \tag{4.4.75}$$

$$\tilde{A}_{Rf}(\tilde{w}, \tilde{\phi}) = \frac{\sigma_{Rf}}{2}\left(\tilde{w}'(0)^2 + \left(\frac{\kappa_{\omega 0}}{\pi}\right)^2 \tilde{\phi}'(0)^2\right). \tag{4.4.76}$$

In figure 4.4.11, the percentage contribution of these individual terms to the aggregate total $\tilde{A}(\tilde{w}_{cr}, \tilde{\phi}_{cr})$ is plotted as a function of α. The observation of the top graph shows that:

(i) The ratio $\tilde{A}_3(\tilde{w}_{cr}) / \tilde{A}(\tilde{w}_{cr}, \tilde{\phi}_{cr})$ is independent of α and equal to 50%. In fact, this result can be easily proven. Since $\sigma_T = 0$, one has

$$\tilde{w}''(s) = \gamma\,(1-s)\,\tilde{\phi}(s)\ ,\quad 0 \le s \le 1\ , \tag{4.4.77}$$

which is just the non-dimensional version of equation (4.4.27). Therefore (recall that we are taking $\zeta_Q = 0$),

$$\gamma\,\tilde{B}(\tilde{w}, \tilde{\phi}) = \gamma \int_0^1 (1-s)\,\tilde{w}''(s)\,\tilde{\phi}(s)\,ds = \int_0^1 \tilde{w}''(s)^2\,ds = 2\,\tilde{A}_3(\tilde{w})\ . \tag{4.4.78}$$

The desired result now follows at once from the identity (LANGHAAR 1962, § 6.4)

$$\tilde{A}(\tilde{w}_{cr}, \tilde{\phi}_{cr}) = \gamma_{cr}\ \tilde{B}(\tilde{w}_{cr}, \tilde{\phi}_{cr})\ . \tag{4.4.79}$$

Note that this reasoning does not rest on any particular value or order of magnitude assumed for σ_{Rf}.

(ii) The ratio $\tilde{A}_\omega(\tilde{\phi}_{cr}) / \tilde{A}(\tilde{w}_{cr}, \tilde{\phi}_{cr})$ is always small, never exceeding 5%, and its dependence on α is very mild.

(iii) As α decreases, one notices a steady decay in the ratio $\tilde{A}_{SV}(\tilde{\phi}_{cr}) / \tilde{A}(\tilde{w}_{cr}, \tilde{\phi}_{cr})$ associated with Saint Venant torsion, which is compensated by an increase in $\left(\tilde{A}_{\omega\psi}(\tilde{\phi}_{cr}) + \tilde{A}_\psi(\tilde{\phi}_{cr})\right) / \tilde{A}(\tilde{w}_{cr}, \tilde{\phi}_{cr})$ (*i.e.*, an increase in the contribution of the terms involving the non-standard mechanical properties). The latter is mainly due to $\tilde{A}_\psi(\tilde{\phi}_{cr})$, whilst $\tilde{A}_{\omega\psi}(\tilde{\phi}_{cr}) / \tilde{A}(\tilde{w}_{cr}, \tilde{\phi}_{cr})$ remains always very small, oscillating between 0 and 3%.

Suppose now that σ_{Rf} is large (say, $\sigma_{Rf} = 10^6$), so that warping at the support is effectively prevented. Again, we may focus exclusively on the torsional behaviour at buckling, since lateral bending is unaffected by the web-taper ratio α. Near the support, and for the entire range of variation of α, the $\tilde{\phi}$-component of the critical buckling modes exhibits a substantial curvature and the flanges bend in opposite directions, as shown on the right-hand side of figure 4.4.9. Further away from the support, the shape of $\tilde{\phi}_{cr}$ depends on α: for moderate-to-high values of α (including the prismatic case), it is almost a straight line; for smaller α, however, the $\tilde{\phi}_{cr}$ display some curvature (this trend is reflected in figure 4.4.10). We therefore conclude that:

(i) In a prismatic member, warping is clearly non-uniform near the support, but nearly uniform throughout the remaining portion of the beam.

(ii) In a tapered member, both terms on the left-hand side of equation (4.4.68) are non-zero near the support, but since $\tilde{\phi}'_{cr}$ and $\tilde{\phi}''_{cr}$ have the same sign, they tend to cancel each

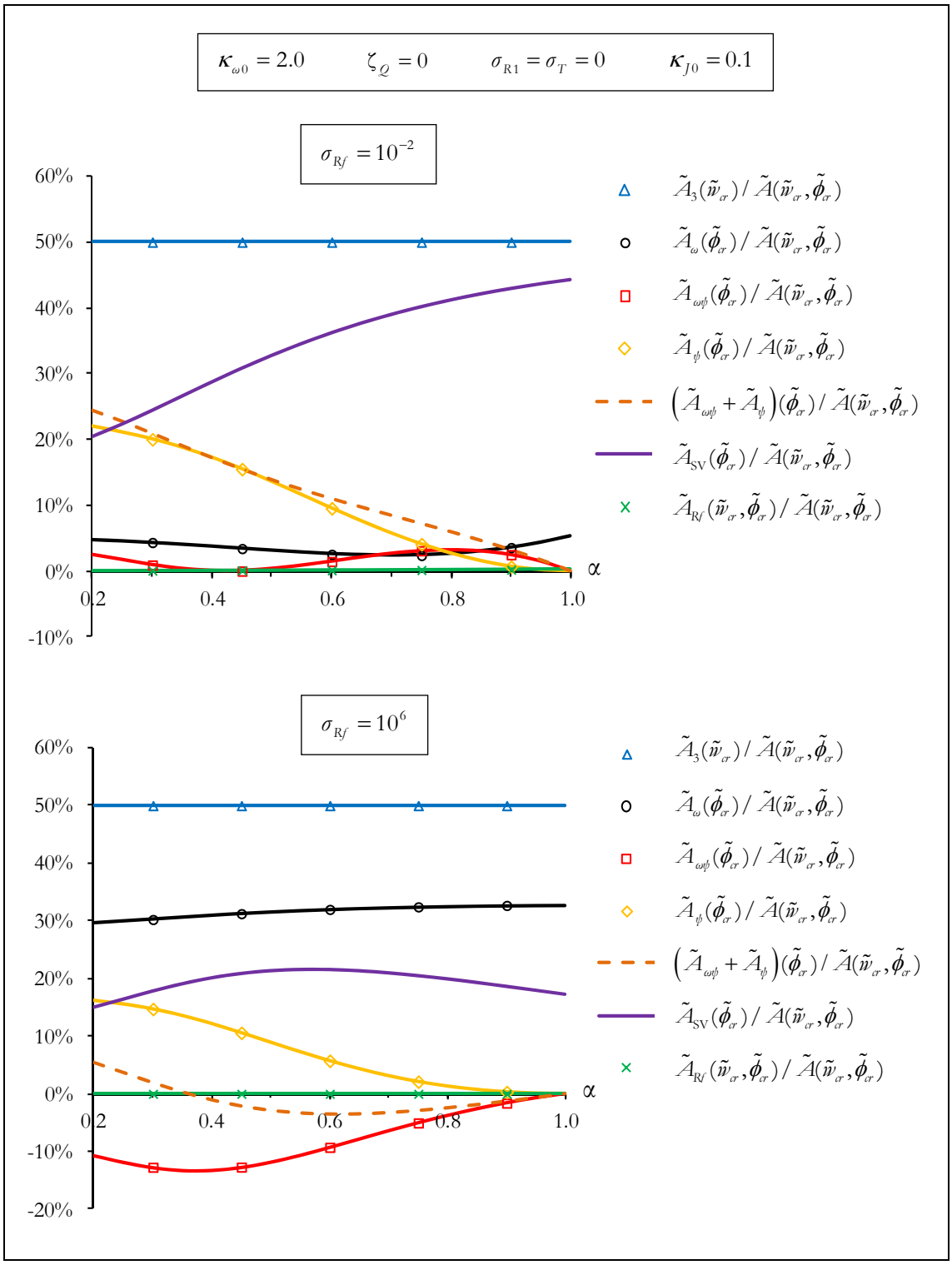

Figure 4.4.11: Contribution of the individual material terms (4.3.71)-(4.3.76), with $\tilde{w} = \tilde{w}_{cr}$ and $\tilde{\phi} = \tilde{\phi}_{cr}$, to the aggregate total $\tilde{A}(\tilde{w}_{cr}, \tilde{\phi}_{cr})$

other out, leading to the generation of a smaller amount of warping torsion in this beam segment, when compared with the prismatic case.

(iii) On the remaining portion of the beam, away from the support, the first term on the left-hand side of (4.4.68) is practically zero when α takes on moderate-to-high values; the effect of the second term (the one associated with the height variation), which is non-zero, turns out to be insufficient to compensate for item (ii), and the net result is a gradual decrease in γ_{cr} with decreasing α, at a slightly faster rate than predicted by the piecewise prismatic model (see figure 4.4.8).

(iv) For sufficiently low α, both terms on the left-hand side of (4.4.68) are non-zero away from the support, with $\tilde{\phi}'_{cr}$ and $\tilde{\phi}''_{cr}$ sharing the sign near the tip and having opposite signs in the central portion of the span. The overall effect is to raise the non-dimensional buckling load γ_{cr} as α decreases in the range $\alpha < 0.6$, as shown in figure 4.4.8.

The plot at the bottom of figure 4.4.11 corroborates the above analysis – indeed:

(i) The ratio $\tilde{A}_{\omega}(\tilde{\phi}_{cr}) / \tilde{A}(\tilde{w}_{cr}, \tilde{\phi}_{cr})$ is practically independent of α, but its contribution is now substantial, in stark contrast with the low σ_{Rf} case.

(ii) The ratio $\tilde{A}_{\omega\psi}(\tilde{\phi}_{cr}) / \tilde{A}(\tilde{w}_{cr}, \tilde{\phi}_{cr})$ is always negative for $0.2 \le \alpha < 1.0$. The sum $\left(\tilde{A}_{\omega\psi}(\tilde{\phi}_{cr}) + \tilde{A}_{\psi}(\tilde{\phi}_{cr})\right) / \tilde{A}(\tilde{w}_{cr}, \tilde{\phi}_{cr})$ reaches a minimum at $\alpha = 0.6$ (which virtually coincides with the minimum in the graph γ_{cr} *vs.* α for $\kappa_{\omega 0} = 2.0$ shown in figure 4.4.8) and is positive for $0.2 \le \alpha < 0.4$ (roughly agreeing with the domain where the values of γ_{cr} for $\kappa_{\omega 0} = 2.0$, yielded by the tapered model, are above those predicted by the stepped model).

REFERENCES

ACHOUR B. and ROBERTS T.M. (2000). Nonlinear strains and instability of thin-walled bars. *Journal of Constructional Steel Research*, **56**(3), 237-252.

ALWIS W.A.M. and WANG C.M. (1996). Wagner term in flexural-torsional buckling of thin-walled open-profile columns. *Engineering Structures*, **18**(2), 125-132.

ANDERSON J.M. and TRAHAIR N.S. (1972). Stability of monosymmetric beams and cantilevers. *Journal of the Structural Division – ASCE*, **98**(1), 269-286.

ANDRADE A. and CAMOTIM D. (2005). Lateral-torsional buckling of singly symmetric tapered beams: Theory and applications. *Journal of Engineering Mechanics – ASCE*, **131**(6), 586-597.

ANDRADE A., CAMOTIM D. and DINIS P.B. (2007a). Lateral-torsional buckling of singly symmetric web-tapered thin-walled I-beams: 1D model vs. shell FEA. *Computers & Structures*, **85**(17-18), 1343-1359.

ANDRADE A., CAMOTIM D. and PROVIDÊNCIA e COSTA P. (2007b). On the evaluation of elastic critical moments in doubly and singly symmetric I-section cantilevers. *Journal of Constructional Steel Research*, **63**(7), 894-908.

ANDRADE A., CAMOTIM D. and PROVIDÊNCIA P. (2010a). Discussion on the paper "Elastic flexural-torsional buckling of thin-walled cantilevers" by Lei Zhang and Geng Shu Tong [Thin-Walled Structures, **46**(1), 2008, 27-37]. *Thin-Walled Structures*, **48**(2), 184-186.

ANDRADE A., PROVIDÊNCIA P. and CAMOTIM D. (2010b). Elastic lateral-torsional buckling of restrained web-tapered I-beams. *Computers & Structures*, **88**(21-22), 1179-1196.

ARANTES E OLIVEIRA E.R. (1999). *Elementos da Teoria da Elasticidade* [Elements of the Theory of Elasticity]. Lisboa: IST Press.

ARGYRIS J.H., DUNNE P.C. and SCHARPF D.W. (1978a). On large displacement-small strain analysis of structures with rotational degrees of freedom. *Computer Methods in Applied Mechanics and Engineering*, **14**(3), 401-451.

ARGYRIS J.H., DUNNE P.C., MALEJANNAKIS G. and SCHARPF D.W. (1978b). On large displacement-small strain analysis of structures with rotational degrees of freedom. *Computer Methods in Applied Mechanics and Engineering*, **15**(1), 99-135.

ASGARIAN B., SOLTANI M. and MOHRI F. (2012). Lateral-torsional buckling of tapered thin-walled beams with arbitrary cross-sections. *Thin-Walled Structures*, in press.

ATTARD M.M. (1986). Nonlinear theory of non-uniform torsion of thin-walled open beams. *Thin-Walled Structures*, **4**(2), 101-134.

AUSTIN W.J., YEGIAN S. and TUNG T.P. (1957). Lateral buckling of elastically end-restrained beams. *Transactions of ASCE*, **122**, 374-409.

BABUSKA I. and OSBORN J. (1991). Eigenvalue problems. *Handbook of Numerical Analysis*, Volume 2: Finite Element Methods (Part 1), P.G. Ciarlet and J.L. Lions (Eds.). Amsterdam: Elsevier, 641-787.

BAZANT Z.P. and EL NIMEIRI M. (1973). Large-deflection spatial buckling of thin-walled beams and frames. *Journal of the Engineering Mechanics Division – ASCE*, **99**(6), 1259-1281.

BIRKHOFF G. and ROTA G.-C. (1989). *Ordinary Differential Equations* (4th edition). New York: Wiley.

BOISSONNADE N. and MUZEAU J.P. (2001). New beam finite element for tapered members. *Proceedings of the 8th International Conference on Civil and Structural Engineering Computing* (Vienna), B. Topping (Ed.). Vienna: Civil-Comp Press, 73-74 (full paper in CD-ROM proceedings).

BOURBAKI N. (2007). *Éléments de Mathématique – Topologie Générale (Chapitres 1 à 4)* [Elements of Mathematics – General Topology (Chapters 1 to 4)]. Berlin: Springer.

BRADFORD M.A. (1988). Lateral stability of tapered beam-columns with elastic restraints. *The Structural Engineer*, **66**(22), 376-382.

BRADFORD M.A. and CUK P.E. (1988). Elastic buckling of tapered monosymmetric I-beams. *Journal of Structural Engineering – ASCE*, **114**(5), 977-996.

BRAHAM M. (1997). Elastic lateral-torsional buckling of web tapered I-beams subjected to end moments. *Proceedings of 18th Czech-Slovak International Conference on Steel Structures and Bridges* (Brno), J. Melchner and J. Skyva (Eds.), 37-42.

BRAHAM M. and HANIKENNE D. (1993). Lateral buckling of web-tapered beams: An original design method confronted with a computer simulation. *Journal of Constructional Steel Research*, **27**(1-3), 23-36.

BRITISH STANDARDS INSTITUTION (2001). *Structural Use of Steelwork in Building – Part 1: Code of Practice for Design. Rolled and Welded Sections (BS 5950-1: 2000).*

BROWN T.G. (1981). Lateral-torsional buckling of tapered I-beams. *Journal of the Structural Division – ASCE*, **107**(4), 689-697.

BUTLER D.J. (1966). Elastic buckling tests on laterally and torsionally braced tapered I-beams. *Welding Journal Research Supplement*, **45**(1), 41.s-48.s.

CHAN S.L. (1990). Buckling analysis of structures composed of tapered members. *Journal of Structural Engineering – ASCE*, **116**(7), 1893-1906.

CIARLET P.G. (2000). *Mathematical Elasticity*, Volume 3: Theory of Shells. Amsterdam: Elsevier.

CODDINGTON E.A. and LEVINSON N. (1955). *Theory of Ordinary Differential Equations*. New York: McGraw-Hill.

COMO M. (1969). A basis for the linear theory of elastic stability of structures. *Meccanica*, **4**(1), 16-27

CULVER C.G. and PREG S.M. (1968). Elastic stability of tapered beam-columns. *Journal of the Structural Division – ASCE*, **94**(2), 455-470.

DEUFLHARD P. (1979). Nonlinear equation solvers in boundary value problem codes. *Codes for Boundary-Value Problems in Ordinary Differential Equations*, Lecture Notes in Computer Science 76, B. Childs, M. Scott, J.W. Daniel, E. Denman and P. Nelson (Eds.). Berlin: Springer, 40-66.

DUBAS P. (1984). Deux problèmes relatifs à l'instabilité par torsion des barres à section variable [Two problems concerning the torsional buckling of variable section bars]. *Verba Volant, Scripta Manent – Recueil de Témoignages et Contributions Techniques, en Hommage à Charles Massonnet, à l'Occasion de son Septantième Anniversaire*, 133-145.

DUPUIS G. (1969). Stabilité élastique des structures unidimensionelles [Elastic stability of one-dimensional structures]. *Zeitschrift für angewandte Mathematik und Physik*, **20**(1), 94-106.

FLINT A.R. (1951). The influence of restraints on the stability of beams. *The Structural Engineer*, **29**(9), 235-246.

GALAMBOS T.V. (Ed.) (1998). *Guide to Stability Design Criteria for Metal Structures* (5th edition). New York: Wiley.

GALÉA Y. (1986). Déversement des barres à section en I bissymétrique et hauteur d'âme linéairement variable [Lateral-torsional buckling of doubly-symmetric I-beams with linearly varying web depth]. *Revue Construction Métallique*, n. 2, 49-54.

GHOBARAH A.A. and TSO W.K. (1971). A non-linear thin-walled beam theory. *International Journal of Mechanical Sciences*, **13**(12), 1025-1038.

GJELSVIK A. (1981). *The Theory of Thin Walled Bars*. New York: Wiley.

GOODIER N.J. (1942). Torsional and flexural buckling of bars of thin-walled open section under compressive and bending loads. *Journal of Applied Mechanics – Transactions of the ASME*, **64**, A103-A107.

GOTO Y. and CHEN W.F. (1989). On the validity of Wagner hypothesis. *International Journal of Solids and Structures*, **25**(6), 621-634.

GUPTA P., WANG S.T. and BLANDFORD G.E. (1996). Lateral-torsional buckling of non-prismatic I-beams. *Journal of Structural Engineering - ASCE*, **122**(7), 748-755.

HAMMING R.W. (1962). *Numerical Methods for Scientists and Engineers*. New York: McGraw-Hill.

HOTCHKISS J.G. (1966). Torsion of rolled steel sections in building structures. *Engineering Journal – AISC*, **3**(1), 19-45.

KANG Y.J., LEE S.C. and YOO C.H. (1992). On the dispute concerning the validity of the Wagner hypothesis. *Computers & Structures*, **43**(5), 853-861.

KERENSKY O.A., FLINT A.R. and BROWN W.C. (1956). The basis for design of beams and plate girders in the revised British Standard 153. *Proceedings of the Institution of Civil Engineers*, **5**(Part III), 396-461.

KITIPORNCHAI S. and DUX P.F. (1982). Discussion on the paper "Wagner hypothesis in beam and column theory" by M. Ojalvo. *Journal of the Engineering Mechanics Division – ASCE*, **108**(3), 570-572.

KITIPORNCHAI S. and TRAHAIR N.S. (1972). Elastic stability of tapered I-beams. *Journal of the Structural Division – ASCE*, **98**(3), 713-728.

KITIPORNCHAI S. and TRAHAIR N.S. (1975). Elastic behavior of tapered monosymmetric I-beams. *Journal of the Structural Division – ASCE*, **101**(8), 1661-1678.

KITIPORNCHAI S., WANG C.M. and TRAHAIR N.S. (1987). Closure of the discussion on the paper "Buckling of monosymmetric I-beams under moment gradient". *Journal of Structural Engineering – ASCE*, **113**(6), 1391-1395.

KOITER W.T. (1963). Elastic stability and post-buckling behaviour. *Nonlinear Problems*, R.E. Langer (Ed.). Madison, Wisconsin: University of Wisconsin Press, 257-275.

KOITER W.T. (1965). The energy criterion of stability for continuous elastic bodies. *Proceedings of the Koninklijke Nederlandse Akademie van Wetenschappen*, **B68**, 178-202.

LANGHAAR H.L. (1962). *Energy Methods in Applied Mechanics*. New York: Wiley.

LEE L.H.N. (1956). Non uniform torsion of tapered I-beams. *Journal of the Franklin Institute*, **262**(July), 37-44.

LINDNER J. (1996) Influence of constructional details on the load carrying capacity of beams. *Engineering Structures*, **18**(10), 752-758.

LINDNER J. and GIETZELT R. (1983). Influence of end-plates on the ultimate load of laterally unsupported beams. *Instability and Plastic Collapse of Steel Structures*, L.J. Morris (Ed.). London: Granada, 538-546.

NETHERCOT D.A. (1973). Lateral buckling of tapered beams. *IABSE Publications*, **33-II**, 173-192.

OJALVO M. (1975). Discussion of "Warping and distortion at I-section joints", by P. Vacharajittiphan and N.S. Trahair. *Journal of the Structural Division – ASCE*, **101**(1), 343-345.

OJALVO M. (1981). Wagner hypothesis in beam and column theory. *Journal of the Engineering Mechanics Division – ASCE*, **107**(4), 669-677.

OJALVO M. (1983). Closure of the discussion on the paper "Wagner hypothesis in beam and column theory". *Journal of Engineering Mechanics – ASCE*, **109**(3), 924-932.

OJALVO M. (1987). Discussion on the paper "Buckling of monosymmetric I-beams under moment gradient" by S. Kitipornchai, C.M. Wang and N.S. Trahair. *Journal of Structural Engineering – ASCE*, **113**(6), 1387-1391.

OJALVO M. (1989). The buckling of thin-walled open-profile bars. *Journal of Applied Mechanics – Transactions of the ASME*, **56**(3), 633–638.

OJALVO M. (1990a). Closure of the discussion on the paper "The buckling of thin-walled open-profile bars". *Journal of Applied Mechanics – Transactions of the ASME*, **57**(2), 479–480.

OJALVO M. (1990b). *Thin-Walled Bars with Open Profiles*. Estes Park, Colorado: Olive Press.

OJALVO M. (2002). Towards resolving issues concerning torsional and lateral-torsional buckling of thin-walled open-profile bars. *Book of Abstracts of the 15th ASCE Engineering Mechanics Conference* (New York), A. Smyth (Ed.) (full paper in CD-ROM proceedings).

OJALVO M. (2007). Three hundred years of bar theory. *Journal of Structural Engineering – ASCE*, **133**(12), 1686-1689.

OJALVO M. and CHAMBERS R.S. (1977). Effect of warping restraints on I-beam buckling. *Journal of the Structural Division – ASCE*, **103**(12): 2351-2360.

PI Y.-L. and BRADFORD M.A. (2001). Effects of approximations in analyses of beams of open thin-walled cross-section – Part I: Flexural-torsional stability. *International Journal for Numerical Methods in Engineering*, **51**(7), 757-772.

PI Y.-L. and TRAHAIR N.S. (2000). Distortion and warping at beam supports. *Journal of Structural Engineering – ASCE*, **126**(11): 1279-1287.

PIGNATARO M., RIZZI N. and LUONGO A. (1991). *Stability, Bifurcation and Postcritical Behaviour of Elastic Structures*. Amsterdam: Elsevier.

PLUM C.M. and SVENSSON S.E. (1993). Simple method to stabilize I-beams against lateral buckling. *Journal of Structural Engineering – ASCE*, **119**(10), 2855-2870.

RAJASEKARAN S. (1994a). Equations for tapered thin-walled beams of generic open section. *Journal of Engineering Mechanics – ASCE*, **120**(8), 1607-1629.

RAJASEKARAN S. (1994b). Instability of tapered thin-walled beams of generic section. *Journal of Engineering Mechanics – ASCE*, **120**(8), 1630-1640.

REIS A.J.L. (1977). *Interactive Buckling in Elastic Structures*. Ph.D. Thesis, University of Waterloo, Canada.

REISSNER E., REISSNER J.E. and WAN F.Y.M. (1987). On lateral buckling of end-loaded cantilevers including the effect of warping stiffness. *Computational Mechanics*, **2**(2), 137-147.

RONAGH H., BRADFORD M. and ATTARD M. (2000a). Nonlinear analysis of thin-walled members of variable cross-section. Part I: Theory. *Computers & Structures*, **77**(3), 285-299.

RONAGH H., BRADFORD M. and ATTARD M. (2000b). Nonlinear analysis of thin-walled members of variable cross-section. Part II: Application. *Computers & Structures*, **77**(3), 301-313.

SILVA R.R. (1990). Discussion on the paper "The buckling of thin-walled open-profile bars" by M. Ojalvo. *Journal of Applied Mechanics – Transactions of the ASME*, **57**(2), 479.

SIMITSES G.J. and HODGES D.H. (2006). *Fundamentals of Structural Stability*. Oxford: Elsevier.

TAKABATAKE H. (1988). Lateral buckling of I-beams with web stiffeners and batten plates. *International Journal of Solids and Structures*, **24**(10), 1003-1019.

TEBEDGE N. (1972). *Applications of the Finite Element Method to Beam-Column Problems*. Ph.D. Thesis, Lehigh University.

TRAHAIR N.S. (1982). Discussion on the paper "Wagner hypothesis in beam and column theory" by M. Ojalvo. *Journal of the Engineering Mechanics Division – ASCE*, **108**(3), 575-578.

TRAHAIR N. (1983). Lateral buckling of overhanging beams. *Instability and Plastic Collapse of Steel Structures*, L.J. Morris (Ed.). London: Granada, 503-518.

TRAHAIR N.S. (1993). *Flexural-Torsional Buckling of Structures*. London: E & FN Spon.

TRAHAIR N.S. (2011). *Wagner's Beam Cycle*. Research Report R916, School of Civil Engineering, The University of Sydney.

TRAHAIR N.S. and NETHERCOT D.A. (1984). Bracing requirements in thin-walled structures. *Developments in Thin-Walled Structures 2*, J. Rhodes and A.C. Walker (Eds.). London: Elsevier, 93-130.

TREFFTZ E. (1930). Über die Ableitung der Stabilitätskriterien des elastischen Gleichgewichtes aus der Elastizitätstheorie endlicher Deformationen [On the derivation of stability criteria for elastic equilibrium from finite-deformation elasticity theory]. *Proceedings of the Third International Congress of Applied Mechanics* (Stockholm), Volume 3, 44-50.

TREFFTZ E. (1933). Zur Theorie der Stabilität des elastischen Gleichgewichts [On the theory of stability of elastic equilibrium]. *Zeitschrift für angewandte Mathematik und Mechanik*, **13**(2), 160-165.

VACHARAJITTIPHAN P. and TRAHAIR N.S. (1974). Warping and distortion at I-section joints. *Journal of the Structural Division – ASCE*, **100**(3), 547-564.

DE VILLE DE GOYET V. (1989). *L'Analyse Statique Non Linéaire par la Méthode des Éléments Finis des Structures Spatiales Formées de Poutres à Section Non Symétrique* [Finite Element Non-Linear Static Analysis of Spatial Structures Formed by Members with Non-Symmetrical Cross-Sections]. Ph.D. Thesis, University of Liège, Belgium.

VLASOV V.Z. (1961). *Thin-Walled Elastic Beams* [English translation of the 2nd Russian edition of 1959]. Jerusalem: Israel Program for Scientific Translation. French translation of the said Russian edition by G. Smirnoff (1962), *Pièces Longues en Voiles Minces*. Paris: Eyrolles.

WAGNER H. (1929). Verdrehung und Knickung von offenen Profilen. *Veröffentlichung zum 25jährigen Jubiläum, Technische Hochschule Danzig, 1904-1929*. Danzig: Verlag A.W. Kaffemann, 329-343. English translation by S. Reiss (1936), *Torsion and Buckling of Open Sections*, Technical Memorandum n. 807, National Advisory Committee for Aeronautics (NACA).

WAGNER H. and PRETSCHNER W. (1934). Verdrehung und Knickung von offenen Profilen. *Luftfahrtforschung*, **11**(6), 174-180. English translation by J. Vanier (1936), *Torsion and Buckling of Open Sections*, Technical Memorandum n. 784, National Advisory Committee for Aeronautics (NACA).

WEKEZER J. (1985). Instability of thin-walled bars. *Journal of Engineering Mechanics – ASCE*, **111**(7), 923-935.

WEMPNER G. (1972). *The Energy Criteria for Stability of Structures*. Research Report n. 119, University of Alabama in Huntsville Research Institute.

YANG Y.B. and MCGUIRE W. (1984). A procedure for analysing space frames with partial warping restraint. *International Journal for Numerical Methods in Engineering*, **20**(8): 1377-1398.

YANG Y.B. and YAU J.D. (1987). Stability of beams with tapered I-sections. *Journal of Engineering Mechanics – ASCE*, **113**(9), 1337-1357.

YURA J.A. (2001). Fundamentals of beam bracing. *Engineering Journal – AISC*, **38**(1), 11-26.

ZHANG L. and TONG G.S. (2008). Lateral buckling of web-tapered I-beams: A new theory. *Journal of Constructional Steel Research*, **64**(12), 1379-1393.

ZIEGLER H. (1952). Knickung gerader Stäbe unter Torsion [Buckling of straight bars under torsion]. *Zeitschrift für angewandte Mathematik und Physik*, **3**(2), 96-119.

ZIEGLER H. (1953). Linear elastic stability – A critical analysis of methods (2nd part). *Zeitschrift für angewandte Mathematik und Physik*, **4**(3), 167-185.

ZIEGLER H. (1956). On the concept of elastic stability. *Advances in Applied Mechanics 4*, H.L. Dryden and T. von Kármán (Eds.). New York: Academic Press, 351-403.

ZIEGLER H. (1968). *Principles of Structural Stability*. Waltham, Massachusetts: Blaisdell Publishing Company.

ZIEMIAN R.D. (Ed.) (2010). *Guide to Stability Design Criteria for Metal Structures* (6th edition). New York: Wiley.

Chapter 5

LATERAL-TORSIONAL BUCKLING OF STRIP BEAMS WITH LINEARLY TAPERED DEPTH

A SIMPLE PROBLEM, NOT SO SIMPLE (ANALYTICAL) ANSWER

Was du ererbt von deinen Vätern hast,
Erwirb es, um es zu besitzen.

JOHANN WOLFGANG VON GOETHE

I think that if in some case it is permissible to use unclear considerations, it is when one ought to establish a new principle, that does not logically follow from what is accepted already, and which is not in logical contradiction with other principles of science, but one cannot set this way when one has to solve a determined problem (of mechanics or of physics), which is posed mathematically in fully exact manner. This problem then becomes a problem of pure analysis and should be solved as such.[1]

ALEKSANDR MIKHAILOVICH LYAPUNOV

5.1 INTRODUCTION

Strip beams – that is, slender flexural members with narrow rectangular cross-section – are extensively used in civil, mechanical and aeronautical engineering. Owing to the ever present need to save weight and material in structural design, the use of tapered strip beams (*i.e.*, strip beams with a continuously varying depth and/or thickness) is particularly attractive. "Form ever follows function", as architect Louis Sullivan proclaimed.[2]

When loaded in the plane of greatest bending stiffness and if not adequately braced, a strip beam, either prismatic or tapered, is highly susceptible to lateral-torsional buckling (LTB), a bifurcation-type instability in which (i) the fundamental equilibrium path corresponds to shapes that are symmetric with respect to the plane of loading and (ii) the buckled states

[1] Translation from the Russian by Isaac Elishakoff (ELISHAKOFF 2005, p. 625).

[2] To put it more elaborately, function does not dictate form, it rather provides the discipline within which the designer finds the freedom to invent form (BILLINGTON 1997, p. 118).

are associated with non-symmetrical shapes – the beam deflects laterally (out-of-plane) and twists. The elastic LTB behaviour of prismatic strip beams has been extensively investigated since the pioneering studies of MICHELL (1899), PRANDTL (1899) and REISSNER (1904).[3] On the contrary, the LTB of tapered strip beams has received comparatively little attention, particularly if the focus is placed on analytical studies, *i.e.*, those that aim at obtaining exact closed-form solutions to the governing differential equations and, thereby, at establishing exact closed-form characteristic equations for the buckling loads (even if these characteristic equations are transcendental and do not admit closed-form solutions).[4] In fact, to the author's best knowledge, only FEDERHOFER (1931) and LEE (1959) have approached the subject from an analytical viewpoint. Federhofer considered cantilevers with constant thickness whose depth at a distance x from the clamped end is given by

$$h(x) = h_0 \left(1 - \frac{x}{L} \right)^n \quad \text{, with } 0 \le n \le 1 \text{ ,} \tag{5.1.1}$$

where L is the cantilever length and h_0 is the (maximum) depth at the clamped end – see figure 5.1.1. Observe that $n = 0$ defines a prismatic member, while $n = 1$ corresponds to a wedge-shaped one. Three types of transverse loading were addressed: (i) an uniformly distributed load, (ii) a point load applied at the free end and (iii) a distributed load whose magnitude q varies according to the same power law as the depth, that is,

$$q(x) = q_0 \left(1 - \frac{x}{L} \right)^n \text{ .} \tag{5.1.2}$$

In all three cases, the loads were applied at mid-depth. Federhofer showed that the governing differential equations are reducible to Bessel's equation, whose order depends on the parameter n and on the type of loading. Finding the buckling loads then amounts to finding the positive roots of certain Bessel functions of the first kind. As for Lee, he studied strip beams with constant thickness and linearly tapered depth under uniform moment.

---

[3] The strive for transparency in architectural design has led in recent years to an increasing use of glass panes as load-bearing elements and, consequently, to a renewed interest in this problem, as attested by LINDNER & HOLBERNDT (2006) and LUIBLE & CRISINEL (2005, 2006).

[4] It is generally believed that analytical solutions (in the above sense) exist for only relatively few, very simple buckling problems involving columns, beams and plates. The monographs by ELISHAKOFF (2005) and WANG *et al.* (2005) prove that there are, in fact, not just a few such solutions. However, as far as the LTB of tapered strip beams is concerned, the general belief is entirely warranted.

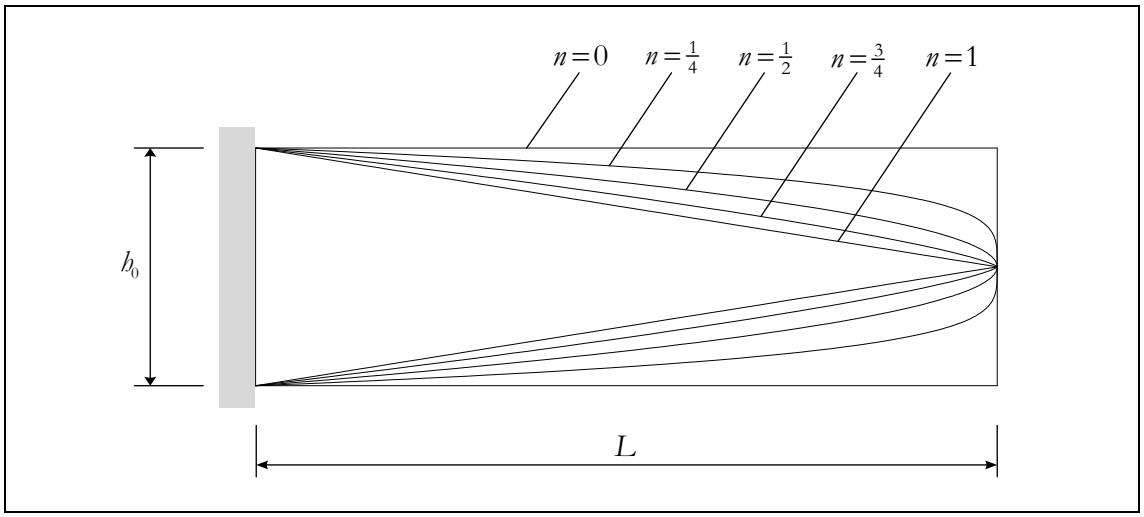

Figure 5.1.1: A sample of the class of strip beams investigated by FEDERHOFER (1931) – Side elevation

The beams were simply supported in the two principal bending planes, with the twist rotation prevented at both ends. The governing differential equation can be cast in the form of an Euler differential equation (*e.g.*, CODDINGTON & CARLSON 1997, § 6.3.2), whose general solution is expressible in terms of trigonometric and logarithmic functions. The buckling moments are then given by a closed-form expression.

This chapter can be roughly divided into three parts. The first part, comprising §§ 5.2-5.5, is a deeply revised and greatly expanded version of selected parts of the paper CHALLAMEL *et al.* (2007). It presents an analytical study on the elastic LTB of homogeneous strip beams with constant thickness and linearly tapered depth (prismatic beams being a special case). The beams are cantilevered and acted at the free end by a conservative point load, whose point of application may be vertically offset from the cross-section centroid. In § 5.2, the LTB problem is formulated as a Steklov-type eigenvalue problem, written in terms of a single dependent variable, namely the twist rotation of the cross-sections. The prismatic case is dealt with in § 5.3 – the specialised eigenproblem is cast in non-dimensional form, the general solution of the governing differential equation is found in terms of Bessel functions and the characteristic equation is obtained in closed-form. The tapered case (properly speaking) is the object of § 5.4. Once again, the eigenproblem is first cast in non-dimensional form. The general solution of the governing differential equation is now given in terms of Kummer's confluent hypergeometric function. The buckling loads correspond to the roots of the determinant of a 4×4 real matrix, whose entries are obtained in closed-

form. Section 5.5 addresses, in the restricted context of centroidal loading, the following question: of all tip-loaded, homogeneous and linearly tapered strip cantilevers with prescribed length, thickness, volume and elastic properties, which has the largest critical load?

In the second and third parts of the chapter, the problem described in § 5.2 is generalised along two different lines. First, in § 5.6, the analysis is extended to cantilevers (i) whose depth varies according to a non-increasing polygonal function of the distance to the support and (ii) which are subjected to an arbitrary number of independent conservative point loads, all acting in the same "downward" direction. However, instead of dealing with this extended problem in such general terms, a special case that "contains all the germs of generality" (to quote David Hilbert) is considered – a two-segment cantilever acted by two transverse loads, one applied at the free end and the other at the junction between segments. It is shown that the governing differential equations, cast in non-dimensional form, can be integrated in terms of confluent hypergeometric functions (Kummer and Tricomi functions) or Bessel functions, themselves special cases of confluent hypergeometric functions. It thus becomes possible to establish the exact characteristic equation for this structural system, which implicitly defines its stability boundary in the load-parameter space. This investigation was reported in the paper ANDRADE *et al.* (2012).

A beam-column that is bent in its plane of greatest stiffness and lacks adequate bracing may also experience out-of-plane buckling – the phenomenon is now called flexural-torsional buckling (FTB). The purpose of § 5.7 is the study of the elastic FTB behaviour of linearly tapered and cantilevered strip beam-columns acted by axial and transverse point loads applied at the centroid of the free-end section. For prismatic members, the governing differential equation can be integrated in closed-form by means of Kummer's confluent hypergeometric function. In the tapered case (strictly speaking), the analytical approach is fruitful only for certain ratios between the minimal and maximal depth of the beam-column. Indeed, the solution to the eigenproblem is obtained in the form of a Frobenius series, which is shown to converge in the interior of the domain and at the boundary if and only if $\frac{1}{2} < \frac{h_{min}}{h_{max}} < 1$. If such is the case, then the series solution can be used to set up the characteristic equation for the cantilever beam-column. Otherwise, the problem is solved numerically by means of a collocation procedure. The contents of this section, along with other material not included here, were published in the paper CHALLAMEL *et al.* (2010).

At this point, the sceptical reader might question the purpose of analytical investigations in this day and age of powerful numerical techniques and high-speed, large-capacity computers. At a philosophical level, the answer is found in Lyapunov's quotation at the beginning of the chapter. At a more utilitarian level, it is remarked that there are a number of important uses for analytical solutions:

(i) to gain physical insight into the roles played by the various geometrical and mechanical parameters; in particular, to elucidate those features of the solution that remain obscured in numerical analyses (a single numerical solution, based on assigned values of the parameters involved, does not reveal the whole physical and mathematical structures of the problem, nor does a collection of such solutions);

(ii) for preliminary design;

(iii) as benchmark solutions for verifying computational models.[5]

* * *

Since this chapter requires some familiarity with the rudiments of the theory of analytic maps of a real or complex variable, the following paragraphs contain a terse summary of the necessary prerequisites on this subject. For a systematic treatment, reference is made to KRANTZ & PARKS (2002) and CARTAN (1992).

A real or complex-valued (resp. complex-valued) map f defined on an open subset $\mathcal{D}$ of $\mathbb{R}$ (resp. of $\mathbb{C}$) is said to be real analytic (resp. complex analytic or holomorphic) on $\mathcal{D}$ if, for each point $x_0 \in \mathcal{D}$, there exists an open interval (resp. an open disk) centred at x_0, with positive radius $r(x_0)$ and contained in $\mathcal{D}$ such that, on this interval (resp. disk), $f(x)$ may be represented by a convergent series in powers of $x - x_0$:

$$f(x) = \sum_{n=0}^{+\infty} a_n (x - x_0)^n \quad \text{for } |x - x_0| < r(x_0) \ . \tag{5.1.3}$$

If such a representation exists, then it is unique. A map is said to be (real or complex) analytic at a point if it is (real or complex) analytic on some neighbourhood of that point. If f is defined on an arbitrary subset $\mathcal{A}$ of $\mathbb{R}$ or $\mathbb{C}$, not necessarily open, then f is said to be (real or complex) analytic on $\mathcal{A}$ if it is the restriction to $\mathcal{A}$ of an analytic map on an

[5] Verification is here understood as "the process of determining if a computational model obtained by discretizing a mathematical model of a physical event and the code implementing the computational model can be used to represent the mathematical model of the event with sufficient accuracy" (BABUSKA & ODEN 2004).

open set containing $\mathcal{A}$ (LANG 1999, p. 69). A complex analytic map on the whole of $\mathbb{C}$ is called an entire map.

It is true, but not immediately obvious, that the map defined by a convergent power series is (real or complex) analytic on the interior of the domain of convergence. Polynomials are therefore analytic maps on the whole of the real line or on the whole of the complex plane, and so is the exponential map $x \mapsto e^x$, defined for real or complex x by

$$e^x = \sum_{n=0}^{+\infty} \frac{1}{n!} x^n \quad .^6 \tag{5.1.4}$$

Let f be the (real or complex) map defined by the power series $\sum_{n=0}^{+\infty} a_n (x - x_0)^n$, with radius of convergence $r > 0$. Then f is differentiable (hence continuous) for $|x - x_0| < r$ and its derivative may be obtained by term-wise differentiation of the power series:

$$f'(x) = \sum_{n=1}^{+\infty} n\, a_n (x - x_0)^{n-1} \quad . \tag{5.1.5}$$

The derived series (5.1.5) has the same radius of convergence r as the original series. It follows that a (real or complex) analytic map on $\mathcal{D}$ is infinitely differentiable on $\mathcal{D}$ and all its derivatives are analytic on $\mathcal{D}$.

The sum and product of two analytic maps on $\mathcal{D}$ are also analytic on $\mathcal{D}$. Moreover, if f is analytic on $\mathcal{D}$ and $\mathcal{D}_1$ is the set of points in $\mathcal{D}$ where f does not vanish, then $1/f$ is analytic on $\mathcal{D}_1$. In particular, rational maps are analytic on the complement of the set of zeros of the denominator. Finally, if f is analytic on $\mathcal{D}$ and takes its values in $\mathcal{F}$ and if g is analytic on $\mathcal{F}$, then the composition $g \circ f$ is analytic on $\mathcal{D}$.

Every map of a complex variable that is differentiable on an open set $\mathcal{D} \subset \mathbb{C}$ is in fact analytic on $\mathcal{D}$, and hence infinitely differentiable on $\mathcal{D}$. The situation is entirely different in the case of a real variable: there exist differentiable maps whose derivatives are not differentiable; moreover, there exist infinitely differentiable maps which are not analytic (a classic example is given in CAMPOS FERREIRA 1987, pp. 417-418).

---

[6] The fundamental properties $e^{z+w} = e^z e^w$ and $(e^z)' = e^z$ of the exponential remain valid for every complex numbers z and w.

5.2 THE PROBLEM AND ITS MATHEMATICAL FORMULATION

We consider the LTB of a homogeneous and perfectly straight elastic strip cantilever, whose depth tapers linearly. The beam is clamped at its larger end and free at the smaller end, where a transverse point load is applied – see figure 5.2.1.

The beam is identified with its unloaded shape $\mathcal{B} \subset \mathcal{E}$, which is taken as the reference shape. To facilitate the geometrical description of $\mathcal{B}$, a fixed rectangular Cartesian frame $\left(O, \{\boldsymbol{e}_1, \boldsymbol{e}_2, \boldsymbol{e}_3\}\right)$ is adopted. The reference shape $\mathcal{B}$ is symmetrical relative to the planes passing through the origin O and spanned by $\{\boldsymbol{e}_1, \boldsymbol{e}_3\}$ and $\{\boldsymbol{e}_1, \boldsymbol{e}_2\}$. The beam axis lies on the intersection of these two planes and the cross-sections are orthogonal to it. Let $\hat{x}: \mathcal{E} \to \mathbb{R}^3$ denote the coordinate system associated with the adopted frame, that is, the map that assigns to each point X in $\mathcal{E}$ the ordered triplet $(x_1, x_2, x_3) \in \mathbb{R}^3$ defined by $x_i = (X - O) \cdot \boldsymbol{e}_i$, $i = 1, 2, 3$. The image of $\mathcal{B}$ under $\hat{x}$ is (see figure 5.2.1)

$$\hat{x}[\mathcal{B}] = \left\{ (x_1, x_2, x_3) \in \mathbb{R}^3 \;\middle|\; 0 \le x_1 \le L, -\frac{t}{2} \le x_2 \le \frac{t}{2}, -\frac{h(x_1)}{2} \le x_3 \le \frac{h(x_1)}{2} \right\}. \qquad (5.2.1)$$

Here, L is the length of the cantilever and t its (uniform) thickness. The map $h: [0, L] \to \mathbb{R}^+$ that describes the longitudinal variation of the cantilever depth is an affine map, defined by

$$h(x_1) = h_0 \left(1 - (1 - \alpha) \frac{x_1}{L} \right), \qquad (5.2.2)$$

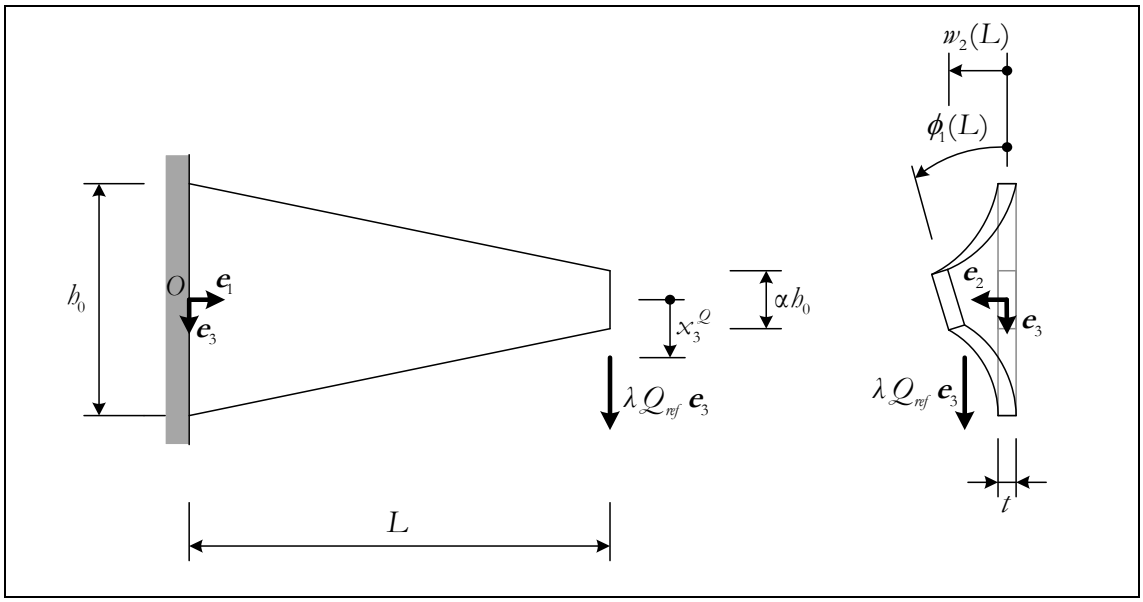

Figure 5.2.1: Linearly tapered strip cantilever – Reference and buckled shapes; applied load

with $0 < \alpha \leq 1$. It is assumed that $t \ll h_0 \ll L$. The parameter α will be called the taper ratio. Observe that $\alpha = 1$ defines a prismatic beam. Moreover, for fixed h_0 and L, the larger the taper ratio, the less pronounced the taper.

The elastic material constituting the beam is homogeneous and isotropic and the reference (unloaded) placement is assumed to correspond to a natural sate (CIARLET 1988, p. 118). This implies that, to within the first order with respect to the Green strain tensor, the behaviour of the material is governed by only two constants, *e.g.*, the Young modulus E and the shear modulus G (CIARLET 1988, th. 3.8-1).

The cantilever is acted at its free end by a conservative point load $\boldsymbol{Q} = Q\,\boldsymbol{e}_3$ applied to the material point whose reference place is $O + L\,\boldsymbol{e}_1 + x_3^Q\,\boldsymbol{e}_3$. (If $\left|x_3^Q\right| > \frac{\alpha h_0}{2}$, the point of application of the load is assumed to be connected to the end cross-section by a rigid rod, initially parallel to $\boldsymbol{e}_3$.) The magnitude Q of the applied load is deemed proportional to a single factor λ, and therefore one writes $Q = \lambda\, Q_{ref}$, where Q_{ref} is a positive reference magnitude. As shown schematically in figure 5.2.1, the load remains parallel to $\boldsymbol{e}_3$ throughout the deformation process.

It is required to find those values of λ, called buckling load factors, for which there exist, in addition to the fundamental equilibrium state (which corresponds to bending of the cantilever in its plane of greatest flexural rigidity), adjacent equilibrium states involving out-of-plane bending and torsion. It is further required to characterise the difference between adjacent and fundamental equilibrium shapes, *i.e.*, the buckling mode associated with a given buckling load factor.

Let Π_2 denote the second-order term of the change in total potential energy of the beam-load system from a fundamental equilibrium state (at constant load level λ). With $w_2(x_1)$ (resp. $\phi_1(x_1)$) representing the incremental displacement along $\boldsymbol{e}_2$ of the centroid (resp. the incremental twist rotation) of the cross-section at a distance x_1 from the support in the reference placement, one takes Π_2 in the form

$$\Pi_2(w_2, \phi_1, \lambda) = \frac{1}{2}\int_0^L EI_3(x_1)\, w_2''(x_1)^2\, dx_1 + \frac{1}{2}\int_0^L GJ(x_1)\, \phi_1'(x_1)^2\, dx_1$$
$$+ \lambda\, Q_{ref}\, L \int_0^L \left(\frac{x_1}{L} - 1\right) w_2''(x_1)\, \phi_1(x_1)\, dx_1 + \frac{1}{2}\lambda\, Q_{ref}\, x_3^Q\, \phi_1(L)^2\ , \qquad (5.2.3)$$

where the lateral bending and torsional rigidities vary with x_1 according to

$$EI_3(x_1) = \frac{E\,b(x_1)\,t^3}{12} = \frac{E\,b_0\,t^3}{12}\left(1-(1-\alpha)\frac{x_1}{L}\right) = EI_3(0)\left(1-(1-\alpha)\frac{x_1}{L}\right) \tag{5.2.4}$$

$$GJ(x_1) = \frac{G\,b(x_1)\,t^3}{3} = \frac{G\,b_0\,t^3}{3}\left(1-(1-\alpha)\frac{x_1}{L}\right) = GJ(0)\left(1-(1-\alpha)\frac{x_1}{L}\right) . \tag{5.2.5}$$

The first and second terms in the functional (5.2.3) represent the change in strain energy as given by the linear theory; the third term is the work of the stresses acting in the fundamental state due to the second-order components of the incremental deformation; finally, the fourth term is the negative of the second-order part of the work of the external loads (PIGNATARO *et al.* 1991, p. 230).

Observe that the effect of taper is accounted for merely by replacing a constant depth with a variable one in equations (5.2.4)-(5.2.5). It is thus assumed that taper does not further influence the computation of the cross-sectional rigidities EI_3 and GJ. There is theoretical (NADAI 1925, p. 203, and TRABUCHO & VIAÑO 1996, p. 799) and experimental (COLEMAN 1939 and LEE 1956) evidence in support of such an assumption. Nevertheless, it must be acknowledged that a recent asymptotic investigation of the linear in-plane bending behaviour of tapered strip beams (HODGES *et al.* 2008) showed that a correction for taper that explicitly involves b' should be included in the cross-sectional properties (axial and major bending rigidities) – see also BOLEY (1963).

A number of additional assumptions and simplifications are implicit in equations (5.2.3)-(5.2.5), namely:

(i) Transverse shear deformations are negligible. An analysis of the effects of transverse shear deformations on the lateral-torsional buckling of end-loaded prismatic strip cantilevers is given by REISSNER (1979).

(ii) The effect of restrained torsion warping may be ignored. In the case of prismatic strip beams, this assumption was shown to be legitimate by VOLOVOI *et al.* (1999).

(iii) Even discarding the influence of taper, the formula for $GJ(x_1)$ used in equation (5.2.5) is approximate and presupposes that the strip beam exhibits throughout its whole length a sufficiently large depth-to-thickness ratio (a similar remark was made in § 2.10.1 – for details, see TIMOSHENKO & GOODIER 1970, §§ 108-109).

(iv) The effect of bending curvature in the plane of greatest flexural rigidity prior to buckling is neglected. For end-loaded prismatic strip cantilevers, this effect is thoroughly discussed by HODGES & PETERS (1975) and REISSNER (1979, 1981).

The complete definition of the functional Π_2 still requires the specification of its domain. In particular, the class of admissible maps w_2 and ϕ_1 needs to be addressed, and this entails the characterisation of the following two properties: (i) the smoothness these maps must exhibit and (ii) the boundary conditions they must satisfy. For the integrals in (5.2.3) to make sense, an adequate smoothness requirement is that w_2 (resp. ϕ_1) be square-integrable on the interval $(0,L)$ and possess square-integrable first and second derivatives (resp. first derivative) on that interval.[7] However, with a view towards establishing the Euler-Lagrange equations associated with Π_2, one makes the more stringent requirement that w_2 (resp. ϕ_1) be four times (resp. twice) continuously differentiable on $[0,L]$ (*e.g.*, AXELSSON & BARKER 1984, ch. 2). In addition, w_2 and ϕ_1 must satisfy the essential boundary conditions

$$w_2(0) = 0 \tag{5.2.6}$$

$$w_2'(0) = 0 \tag{5.2.7}$$

$$\phi_1(0) = 0 \ . \tag{5.2.8}$$

The domain of the functional Π_2 is thus taken to be $\mathcal{D} = \mathcal{D}_1 \times \mathcal{D}_2 \times \mathbb{R}$, with

$$\mathcal{D}_1 = \left\{ w_2 \in C^4[0,L] \,\middle|\, w_2(0) = 0 \,,\, w_2'(0) = 0 \right\} \tag{5.2.9}$$

$$\mathcal{D}_2 = \left\{ \phi_1 \in C^2[0,L] \,\middle|\, \phi_1(0) = 0 \right\} \ . \tag{5.2.10}$$

Clearly, $\mathcal{D}_1$ and $\mathcal{D}_2$ are real linear spaces, with addition and multiplication by scalars defined in the usual point-wise manner.

Let δw_2 and $\delta\phi_1$ be admissible variations of w_2 and ϕ_1 (that is, differences between any two admissible maps w_2 or ϕ_1).[8] The first variation of Π_2 at (w_2, ϕ_1, λ) in the direction of $(\delta w_2, \delta\phi_1, 0)$, defined as

$$\delta\Pi_2(w_2, \phi_1, \lambda)[\delta w_2, \delta\phi_1, 0] = \frac{d}{da}\Pi_2(w_2 + a\,\delta w_2, \phi_1 + a\,\delta\phi_1, \lambda)\bigg|_{a=0} \quad (a \in \mathbb{R}) \,, \tag{5.2.11}$$

reads (Leibniz rule – *e.g.*, BARTLE 1967, th. 23.10 – is used to differentiate under the integral sign)

---

[7] By virtue of Sobolev's imbedding theorem, these conditions of square integrability imply that w_2 is continuously differentiable on $[0,L]$ and ϕ_1 is continuous on $[0,L]$ – *e.g.*, BREZIS 2011, pp. 213 and 217, or DACOROGNA 2004, remark 1.44(vii).

[8] Observe that the set of all admissible variations δw_2 (resp. $\delta\phi_1$) is the linear space $\mathcal{D}_1$ (resp. $\mathcal{D}_2$) itself.

$$\delta\Pi_2(w_2,\phi_1,\lambda)[\delta w_2,\delta\phi_1,0]=\int_0^L\Big[EI_3(x_1)\,w_2''(x_1)\,\delta w_2''(x_1)+GJ(x_1)\,\phi_1'(x_1)\,\delta\phi_1'(x_1)$$
$$+\lambda\,Q_{ref}\,L\left(\frac{x_1}{L}-1\right)\Big(\phi_1(x_1)\,\delta w_2''(x_1)+w_2''(x_1)\,\delta\phi_1(x_1)\Big)\Big]\,dx_1$$
$$+\lambda\,Q_{ref}\,x_3^Q\,\phi_1(L)\,\delta\phi_1(L)\ . \qquad (5.2.12)$$

Since the admissible maps w_2 and ϕ_1 (as well as their admissible variations) are smooth enough to allow integration by parts (*e.g.*, CAMPOS FERREIRA 1987, ch. 5, § 1, th. 18), one gets

$$\delta\Pi_2(w_2,\phi_1,\lambda)[\delta w_2,\delta\phi_1,0]=\int_0^L\left\{\Big(EI_3(x_1)\,w_2''(x_1)\Big)''+\lambda\,Q_{ref}\,L\left[\left(\frac{x_1}{L}-1\right)\phi_1(x_1)\right]''\right\}\delta w_2(x_1)\,dx_1$$
$$-\int_0^L\left[\Big(GJ(x_1)\,\phi_1'(x_1)\Big)'-\lambda\,Q_{ref}\,L\left(\frac{x_1}{L}-1\right)w_2''(x_1)\right]\delta\phi_1(x_1)\,dx_1$$
$$-\left[\Big(EI_3(x_1)\,w_2''(x_1)\Big)'+\lambda\,Q_{ref}\,L\left(\left(\frac{x_1}{L}-1\right)\phi_1(x_1)\right)'\right]\delta w_2(x_1)\Bigg|_0^L$$
$$+\left[EI_3(x_1)\,w_2''(x_1)+\lambda\,Q_{ref}\,L\left(\frac{x_1}{L}-1\right)\phi_1(x_1)\right]\delta w_2'(x_1)\Bigg|_0^L$$
$$+GJ(x_1)\,\phi_1'(x_1)\,\delta\phi_1(x_1)\Big|_0^L+\lambda\,Q_{ref}\,x_3^Q\,\phi_1(L)\,\delta\phi_1(L)\ . \qquad (5.2.13)$$

By virtue of the fundamental lemma of the calculus of variations (*e.g.*, DACOROGNA 2004, th. 1.24), the vanishing of $\delta\Pi_2$ for all admissible δw_2 and $\delta\phi_1$ – often referred to in the literature as the criterion of Trefftz (TREFFTZ 1930, 1933)[9] – leads to the classical or strong form of the LTB problem, which may be phrased as follows:

Problem 5.1.

Find $\lambda\in\mathbb{R}$ and real-valued maps w_2, ϕ_1 defined on the interval $[0,L]$, with

- $w_2\in C^4[0,L]$,
- $\phi_1\in C^2[0,L]$ and
- $w_2\neq 0$ or $\phi_1\neq 0$,

satisfying the differential equations

$$\left[EI_3(0)\left(1-(1-\alpha)\frac{x_1}{L}\right)w_2''(x_1)+\lambda\,Q_{ref}\,L\left(\frac{x_1}{L}-1\right)\phi_1(x_1)\right]''=0 \qquad (5.2.14)$$

[9] See also KOITER (1963, pp. 257-259) and WEMPNER (1972).

$$\left[GJ(0)\left(1-(1-\alpha)\frac{x_1}{L}\right)\phi_1'(x_1)\right]' - \lambda\, Q_{ref}\, L\left(\frac{x_1}{L}-1\right)w_2''(x_1) = 0 \qquad (5.2.15)$$

on the open interval $(0,L)$,[10] together with the boundary conditions

$$w_2(0) = 0 \qquad (5.2.16)$$

$$w_2'(0) = 0 \qquad (5.2.17)$$

$$\phi_1(0) = 0 \qquad (5.2.18)$$

$$\alpha EI_3(0)\, w_2''(L) = 0 \qquad (5.2.19)$$

$$\alpha EI_3(0)\, w_2'''(L) - EI_3(0)\frac{1-\alpha}{L} w_2''(L) + \lambda\, Q_{ref}\, \phi_1(L) = 0 \qquad (5.2.20)$$

$$\alpha GJ(0)\phi_1'(L) + \lambda\, Q_{ref}\, x_3^Q\, \phi_1(L) = 0\ . \qquad (5.2.21)$$

From a mathematical viewpoint, Problem 5.1 is a Steklov-type eigenproblem (BABUSKA & OSBORN 1991, p. 649) – the buckling load factors and the corresponding buckling modes are its eigenvalues and eigenfunctions. The characteristic space associated with a given buckling load factor λ is the set of all solutions (w_2,ϕ_1) of (5.2.14)-(5.2.21) for the given λ, including the trivial solution $(w_2,\phi_1)=(0,0)$. It is a subspace of the real vector space $C^0[0,L]\times C^0[0,L]$.

In fact, it suffices to consider eigenpairs with positive eigenvalues. Indeed, zero is not an eigenvalue (unloaded cantilevers do not buckle), as easily seen by direct inspection, and the eigenpairs with negative eigenvalues can be obtained from those with positive eigenvalues by symmetry considerations. For suppose that we are given two particular instances of Problem 5.1, labelled A and B, specified by the same $EI_3(0)$, $GJ(0)$, L, α and Q_{ref}, but having symmetrical x_3^Q. Then $\{\lambda,(w_2,\phi_1)\}$ is an eigenpair of A if and only if $\{-\lambda,(-w_2,\phi_1)\}$ is an eigenpair of B. Therefore, we may replace "$\lambda\in\mathbb{R}$" with "$\lambda\in\mathbb{R}^+$" in the statement of Problem 5.1 without loss of generality.

From an engineering viewpoint, the lowest positive eigenvalue is of particular interest. It is called the critical load factor and denoted by λ_{cr}. The corresponding buckling

[10] These are the Euler-Lagrange equations associated with Π_2. They form a mixed-order system of homogeneous linear ordinary differential equations with polynomial coefficients (of degree ≤ 1). The first equation can be solved for $v^{(4)}(x_1)$ since the corresponding coefficient does not vanish on $(0,L)$ – it is a positive constant if $\alpha=1$ and a first-degree polynomial with root $x_1 = L/(1-\alpha) > L$ if $0<\alpha<1$. Similarly, the second equation can be solved for $\phi''(x_1)$.

mode is labelled critical as well and written $(w_{2.cr}, \phi_{1.cr})$. One also speaks of the critical load and critical moment, defined as $Q_{cr} = Q_{ref}\,\lambda_{cr}$ and $M_{cr} = Q_{ref}\,L\,\lambda_{cr}$.

Integrating twice the differential equation (5.2.14), one obtains, for every x_1 in $(0, L)$,

$$\left[EI_3(0)\left(1-(1-\alpha)\frac{x_1}{L}\right) w_2''(x_1) + \lambda\, Q_{ref}\, L\left(\frac{x_1}{L}-1\right)\phi_1(x_1) \right]' = c_1 \tag{5.2.22}$$

$$EI_3(0)\left(1-(1-\alpha)\frac{x_1}{L}\right) w_2''(x_1) + \lambda\, Q_{ref}\, L\left(\frac{x_1}{L}-1\right)\phi_1(x_1) = c_1\, x_1 + c_2\ , \tag{5.2.23}$$

with $c_1, c_2 \in \mathbb{R}$. Since it is required that $w_2 \in C^4[0, L]$ and $\phi_1 \in C^2[0, L]$, it follows from the "principle of extension of identities" (BOURBAKI 2007a, p. 53, or DIEUDONNÉ 1960, th. 3.15.2) that these equations hold at $x_1 = 0$ and $x_1 = L$ as well. The boundary conditions (5.2.19)-(5.2.20) then imply $c_1 = c_2 = 0$ and lead to the conclusion that w_2'' and ϕ_1 are related through

$$w_2''(x_1) = -\frac{\lambda\, Q_{ref}\, L\left(\frac{x_1}{L}-1\right)}{EI_3(0)\left(1-(1-\alpha)\frac{x_1}{L}\right)}\phi_1(x_1) \tag{5.2.24}$$

on the interval $[0, L]$. Moreover, when taken together with (5.2.16) and (5.2.17), this equation shows that $\phi_1 = 0$ implies $w_2 = 0$. We are thus in a position to eliminate w_2 and write the buckling problem in terms of the single dependent variable ϕ_1 – in this sense, equation (5.2.24) may be regarded as a holonomic constraint (LANCZOS 1970, ch. 1, § 6). Problem 5.1 is thereby replaced with the following, which takes the form of a quadratic eigenproblem:

Problem 5.2.

Find $\lambda \in \mathbb{R}^+$ and $\phi_1 : [0, L] \to \mathbb{R}$, with $\phi_1 \in C^2[0, L]$ and $\phi_1 \neq 0$, satisfying the differential equation

$$EI_3(0)GJ(0)\left(1-(1-\alpha)\frac{x_1}{L}\right)^2 \phi_1''(x_1) - EI_3(0)GJ(0)\left(1-(1-\alpha)\frac{x_1}{L}\right)\frac{1-\alpha}{L}\phi_1'(x_1)$$
$$+\left[\lambda\, Q_{ref}\, L\left(\frac{x_1}{L}-1\right)\right]^2 \phi_1(x_1) = 0 \tag{5.2.25}$$

on the open interval $(0, L)$, together with the boundary conditions

$$\phi_1(0) = 0 \tag{5.2.26}$$

$$\alpha GJ(0)\phi_1'(L) + \lambda\, Q_{ref}\, x_3^{Q}\, \phi_1(L) = 0\ . \tag{5.2.27}$$

Once a buckling load factor λ and a corresponding buckling mode component ϕ_1 are known, the remaining buckling mode component w_2 can be obtained by solving the initial value problem defined by (5.2.24) and (5.2.16)-(5.2.17).

5.3 THE PRISMATIC CASE ($\alpha = 1$)

The specialisation of Problem 5.2 to the prismatic case ($\alpha = 1$) reduces to:

Problem 5.3.

Find $\lambda \in \mathbb{R}^+$ and $\phi_1 : [0, L] \to \mathbb{R}$, with $\phi_1 \in C^2[0, L]$ and $\phi_1 \neq 0$, satisfying the differential equation

$$EI_3(0)GJ(0)\phi_1''(x_1) + \left[\lambda Q_{ref} L\left(\frac{x_1}{L} - 1\right)\right]^2 \phi_1(x_1) = 0 \tag{5.3.1}$$

on the open interval $(0, L)$, together with the boundary conditions

$$\phi_1(0) = 0 \tag{5.3.2}$$

$$GJ(0)\phi_1'(L) + \lambda Q_{ref} x_3^Q \phi_1(L) = 0 \ . \tag{5.3.3}$$

By an appropriate change of independent variable, this problem may be posed on a fixed reference domain (*i.e.*, independent of the cantilever's length L) and written in non-dimensional form. Indeed, consider the map $f : [0, L] \to [0, 1]$ defined by $x_1 \mapsto 1 - \frac{x_1}{L}$ and let $s = f(x_1)$ denote the associated change of independent variable.[11] Moreover, define $\tilde{\phi} : [0, 1] \to \mathbb{R}$ such that $\phi_1 = \tilde{\phi} \circ f$ (that is, $\tilde{\phi} = \phi_1 \circ f^{-1}$). Clearly, ϕ_1 is twice continuously differentiable on $[0, L]$ if and only if $\tilde{\phi}$ is twice continuously differentiable on $[0, 1]$, with the chain rule yielding (*e.g.*, RUDIN 1976, th. 5.5)

$$\phi_1'(x_1) = \tilde{\phi}'\left(f(x_1)\right) f'(x_1) = -\frac{1}{L}\tilde{\phi}'(s) \tag{5.3.4}$$

$$\phi_1''(x_1) = -\frac{1}{L}\tilde{\phi}''\left(f(x_1)\right) f'(x_1) = \frac{1}{L^2}\tilde{\phi}''(s) \ . \tag{5.3.5}$$

Replace these results into equations (5.3.1)-(5.3.3). In addition, introduce the non-dimensional ratios

[11] Observe that f is a real analytic diffeomorphism. In particular, note that $f'(x_1) \neq 0$ for every x_1 in $(0, L)$, and this ensures that the leading coefficient in the transformed differential equation does not vanish on $(0, 1)$ – *vide infra*, equation (5.3.8).

$$\gamma = \frac{\lambda\, Q_{ref}\, L^2}{\sqrt{EI_3(0)\, GJ(0)}} \tag{5.3.6}$$

$$\varepsilon = \frac{x_3^Q}{L}\sqrt{\frac{EI_3(0)}{GJ(0)}}\ , \tag{5.3.7}$$

which will be referred to as the non-dimensional load and the load position parameter. In so doing, Problem 5.3 is brought into the following form:

Problem 5.4.

Find $\gamma \in \mathbb{R}^+$ and $\tilde{\phi} : [0,1] \to \mathbb{R}$, with $\tilde{\phi} \in C^2[0,1]$ and $\tilde{\phi} \neq 0$, satisfying the differential equation

$$\tilde{\phi}''(s) + \gamma^2 s^2\, \tilde{\phi}(s) = 0 \tag{5.3.8}$$

on the open interval $(0,1)$, together with the boundary conditions

$$\tilde{\phi}'(0) - \varepsilon\gamma\, \tilde{\phi}(0) = 0 \tag{5.3.9}$$

$$\tilde{\phi}(1) = 0\ . \tag{5.3.10}$$

The deceptively simple-looking differential equation (5.3.8) is a transformed version of Bessel's equation of order $\frac{1}{4}$, as first discussed systematically by LOMMEL (1871).[12] Its general solution on $(0,1)$ is

$$\tilde{\phi}(s) = \sqrt{s}\left(c_1 J_{\frac{1}{4}}\left(\frac{\gamma}{2}s^2\right) + c_2\, Y_{\frac{1}{4}}\left(\frac{\gamma}{2}s^2\right)\right) \ \text{, with } \gamma > 0 \text{ and } c_1, c_2 \in \mathbb{R}\ , \tag{5.3.11}$$

---

[12] Suppose that $\gamma > 0$. First, consider the change of dependent variable defined by $\tilde{\phi}(s) = \sqrt{s}\ \eta(s)$, $s \in (0,1)$. Then, consider the map $g : (0,1) \to (0, \frac{\gamma}{2})$, $s \mapsto \frac{\gamma}{2}s^2$ and let $z = g(s)$ denote the associated change of independent variable. Moreover, define $\tilde{\eta} : (0, \frac{\gamma}{2}) \to \mathbb{R}$ such that $\eta = \tilde{\eta} \circ g$. Therefore, on $(0,1)$, $\tilde{\phi}(s) = \sqrt{s}\ \tilde{\eta}\big(g(s)\big) = \sqrt{s}\ \tilde{\eta}(z)$ and

$$\tilde{\phi}'(s) = \gamma s^{3/2}\, \tilde{\eta}'(z) + \frac{1}{2} s^{-1/2}\, \tilde{\eta}(z)$$

$$\tilde{\phi}''(s) = \gamma^2 s^{5/2}\, \tilde{\eta}''(z) + 2\gamma s^{1/2}\, \tilde{\eta}'(z) - \frac{1}{4} s^{-3/2}\, \tilde{\eta}(z)\ .$$

Substituting these expressions into equation (5.3.8) and simplifying, one arrives at Bessel's equation

$$z^2\, \tilde{\eta}''(z) + z\ \tilde{\eta}'(z) + (z^2 - \nu^2)\, \tilde{\eta}(z) = 0\ ,$$

with $\nu = \pm\frac{1}{4}$. It's general solution on $(0, \frac{\gamma}{2})$ is

$$\tilde{\eta}(z) = c_1\, J_{1/4}(z) + c_2\, Y_{1/4}(z) \ \text{, with } c_1, c_2 \in \mathbb{R}\ .$$

Transforming back to the original variables s and $\tilde{\phi}$ leads to (5.3.11). On the positive real axis, $J_{1/4}$ and $Y_{1/4}$ form a numerically satisfactory fundamental pair of solutions of Bessel's equation in the sense of MILLER (1950) – see OLVER (1974, ch. 7, § 5.1) and OLVER & MAXIMON (2010, 10.2(iii)).

where $J_{1/4}$ and $Y_{1/4}$ are the Bessel functions of the first and second kinds of order $\frac{1}{4}$ (Bessel functions of the second kind are also known as Weber's or Neumann's functions).

* * *

It is convenient at this point to make a brief digression, the purpose of which is to define the Bessel functions of the first and second kinds and to establish the properties of these functions that will be needed below. It begins with a preliminary study of the gamma function.

For $x \in \mathbb{R}^+$, the gamma function Γ can be defined by Euler's integral of the second kind:

$$\Gamma(x) = \int_0^{+\infty} s^{x-1}\, e^{-s}\, ds \ . \tag{5.3.12}$$

Clearly, the above definition makes sense if and only if the improper integral converges – hence the restriction $x > 0$ (*e.g.*, CAMPOS FERREIRA 1987, pp 610 and 606).

Integrating by parts the second member of

$$\Gamma(x+1) = \int_0^{+\infty} s^{x}\, e^{-s}\, ds \tag{5.3.13}$$

yields

$$\Gamma(x+1) = \lim_{b\to+\infty} \int_0^{b} s^{x}\, e^{-s}\, ds = \lim_{b\to+\infty} \left(\left[-s^{x}\, e^{-s} \right]_0^{b} + x \int_0^{b} s^{x-1}\, e^{-s}\, ds \right)$$

$$= x \lim_{b\to+\infty} \int_0^{b} s^{x-1}\, e^{-s}\, ds = x\,\Gamma(x) \ , \tag{5.3.14}$$

since $b^x\, e^{-b} \to 0$ as $b \to +\infty$. Then, observing that

$$\Gamma(1) = \int_0^{+\infty} e^{-s}\, ds = 1 \ , \tag{5.3.15}$$

one concludes that $\Gamma(n+1) = n!$ for every non-negative integer n. The gamma function is thus seen to be an extension of the factorial function. (For a characterisation of Γ as an extension of the factorial function, see ANDREWS *et al.* 1999, th. 1.9.3, ARTIN 1931, th. 2.1, or BEALS & WONG 2010, th. 2.4.2. This characterisation was made the basis for the development of the theory of the gamma function in BOURBAKI 2007b, ch. 7.)

The functional equation $\Gamma(x+1) = x\,\Gamma(x)$ can be used to assign a meaning to $\Gamma(x)$ when $x < 0$, provided x is not a negative integer. Indeed, given $x < 0$, let N be the positive integer such that $-N < x \leq -N+1$. Then $x + N > 0$ and $\Gamma(x)$ is defined in terms of $\Gamma(x+N)$ by

$$\Gamma(x)=\frac{\Gamma(x+N)}{x(x+1)\cdots(x+N-1)}\,, \tag{5.3.16}$$

if $x\neq -N+1$. The gamma function is not defined for $x\in\mathbb{Z}_0^-$. The reciprocal $1/\Gamma(x)$ is defined for every $x\in\mathbb{R}$ if one agrees to set $1/\Gamma(x)=0$ when $x\in\mathbb{Z}_0^-$, since this is the limiting value of $1/\Gamma(x)$ at these points (see figure 5.3.1).

This discussion of the gamma function followed closely CODDINGTON & CARLSON (1997, p. 199) and SIMMONS (1991, pp. 351-353). More detailed treatments, which include the extension to the complex domain, are given in ANDREWS *et al.* (1999, ch. 1), BEALS & WONG (2010, ch. 2), BOURBAKI (2007b, ch. 7), ERDÉLYI *at al.* (1953a, ch. 1), HOCHSTADT (1971, ch. 3), LEBEDEV (1965, ch. 1), LUKE (1969, ch. 2), OLVER (1974, ch. 2, § 1), TEMME (1996, ch. 3), WANG & GUO (1989, ch. 3) or WHITTAKER & WATSON (1963, ch. 12). For a historical perspective on the gamma function, the interested reader is referred to DAVIS (1959) and DUTKA (1991).

In order to introduce the Bessel function of the first kind, consider the real power series

$$\sum_{n=0}^{+\infty}\frac{(-1)^n}{n!\,\Gamma(n+\nu+1)}\left(\frac{x}{2}\right)^{2n}\,, \tag{5.3.17}$$

where ν is an arbitrary real number. Using d'Alembert's test (*e.g.*, CAMPOS FERREIRA 1987, pp. 180-181) and the functional equation (5.3.14) of the gamma function, this series is easily seen to be absolutely convergent for every real number x – indeed, for arbitary $x\neq 0$, the

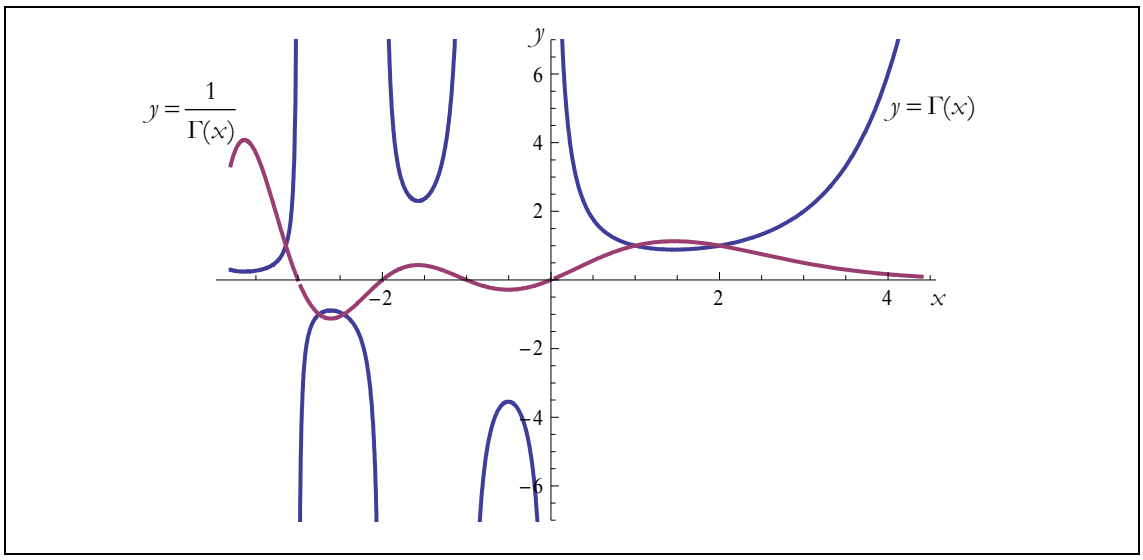

Figure 5.3.1: Gamma and reciprocal gamma functions

ratio of the absolute value of the $(n+1)^{\text{th}}$ term to that of the n^{th} term,

$$\frac{x^2}{4(n+1)\left|n+\nu+1\right|}\ , \tag{5.3.18}$$

tends to zero as $n \to +\infty$. It follows that the map assigning to each x in $\mathbb{R}$ the sum of the power series (5.3.17) is real analytic on the whole of $\mathbb{R}$. The Bessel function of the first kind of order $\nu \in \mathbb{R}$ is now defined to be the map $J_\nu : \mathbb{R}^+ \to \mathbb{R}$ determined by

$$J_\nu(x) = \left(\frac{x}{2}\right)^\nu \sum_{n=0}^{+\infty} \frac{(-1)^n}{n!\,\Gamma(n+\nu+1)} \left(\frac{x}{2}\right)^{2n} \ . \tag{5.3.19}$$

Being the product of two analytic maps, J_ν is itself a real analytic map on its domain. The particular case $J_{1/4}$ is plotted in figure 5.3.2.

For non-integer order ν, the canonical Bessel function of the second kind is defined as the following linear combination of J_ν and $J_{-\nu}$:

$$Y_\nu(x) = \frac{J_\nu(x)\cos(\nu\pi) - J_{-\nu}(x)}{\sin(\nu\pi)} \ , \ \nu \notin \mathbb{Z},\ x \in \mathbb{R}^+ . \tag{5.3.20}$$

Clearly, the map so defined is real analytic on $\mathbb{R}^+$. (If ν is an integer, a case that is of no concern here, the expression on the right-hand side of (5.3.20) is meaningless, a difficulty that is circumvented by replacing it with its limiting value, which is well-defined.) The graph of the particular case $Y_{1/4}$ is shown in figure 5.3.2, side by side with the graph of $J_{1/4}$.

The standard reference on Bessel functions is Watson's monumental treatise (WATSON 1944), but virtually every book dealing with special functions contains a chapter on Bessel functions – *e.g.*, ANDREWS *et al.* (1999, ch. 4), BEALS & WONG (2010, §§ 7.1), ERDÉLYI *at al.* (1953b, ch. 7), HOCHSTADT (1971, ch. 8), LEBEDEV (1965, ch. 5), OLVER

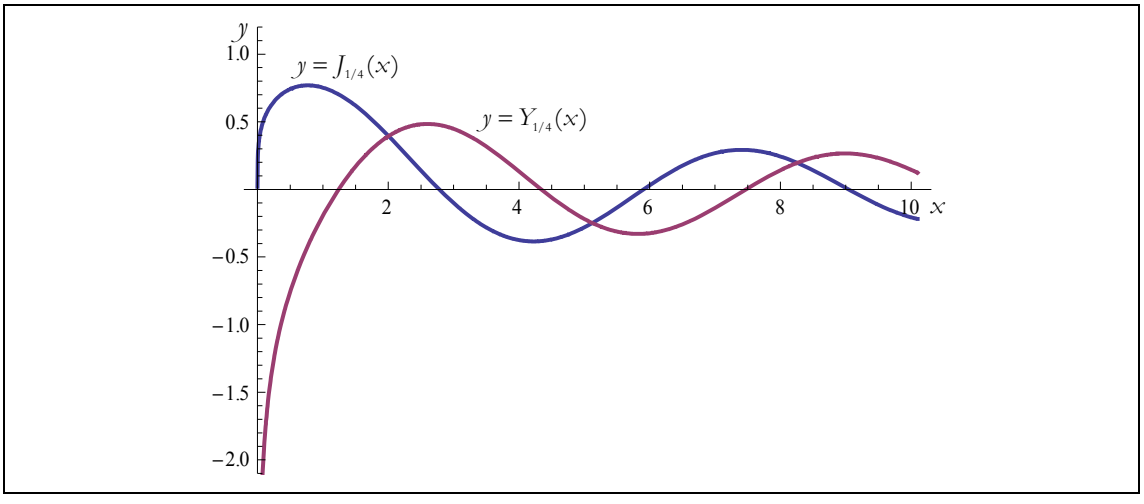

Figure 5.3.2: Bessel functions of the first and second kinds of order $\frac{1}{4}$

(1974, ch. 2, §§ 9-10 and ch. 7, §§ 4-8), TEMME (1996, ch. 9), WANG & GUO (1989, ch. 7) or WHITTAKER & WATSON (1963, ch. 17). The recently published *NIST Handbook of Mathematical Functions* includes an extensive collection of formulae on Bessel functions, presented in a readily accessible format (OLVER & MAXIMON 2010). The historical sketch in WATSON (1944), which concentrates primarily on the mathematical developments, is profitably supplemented by the account in DUTKA (1995) of the physical problems that motivated those developments.

* * *

Let us now return to Problem 5.4. Our present position is this: the general solution to the differential equation (5.3.8) on the interval $(0,1)$ has been found. The next step will be to set up the characteristic equation for the eigenvalues.

The definitions (5.3.19) and (5.3.20) make it possible to rewrite (5.3.11) in the form

$$\tilde{\phi}(s) = (c_1 + c_2) \sum_{n=0}^{+\infty} \frac{(-1)^n}{n!\,\Gamma\left(n+\frac{5}{4}\right)} \left(\frac{\gamma}{4}\right)^{2n+\frac{1}{4}} s^{4n+1}$$

$$- \sqrt{2}\, c_2 \left[\frac{\sqrt{2}}{\Gamma\left(\frac{3}{4}\right)\gamma^{\frac{1}{4}}} + \sum_{n=1}^{+\infty} \frac{(-1)^n}{n!\,\Gamma\left(n+\frac{3}{4}\right)} \left(\frac{\gamma}{4}\right)^{2n-\frac{1}{4}} s^{4n} \right], \tag{5.3.21}$$

with $0 < s < 1$, $\gamma > 0$ and $c_1, c_2 \in \mathbb{R}$. The two power series appearing on the right-hand side of (5.3.21) converge absolutely for every s in $\mathbb{R}$. Consequently, the right-hand side of (5.3.21) defines a family of real analytic maps of the variable s on the whole of $\mathbb{R}$. Since $\tilde{\phi}$ is required to be continuous on $[0,1]$, the "principle of extension of identities" implies that equation (5.3.21) must also hold at $s = 0$ and $s = 1$. This equation therefore defines the family of maps $[0,1] \to \mathbb{R}$ that (i) are twice continuously differentiable on $[0,1]$ – in fact, real analytic on $[0,1]$ – and (ii) satisfy the differential equation (5.3.8) on $(0,1)$. Moreover, term-by-term differentiation of the right-hand side of (5.3.21) yields

$$\tilde{\phi}'(s) = (c_1 + c_2) \left[\frac{2\sqrt{2}\,\gamma^{\frac{1}{4}}}{\Gamma\left(\frac{1}{4}\right)} + \gamma \sum_{n=1}^{+\infty} \frac{(-1)^n}{n!\,\Gamma\left(n+\frac{1}{4}\right)} \left(\frac{\gamma}{4}\right)^{2n-\frac{3}{4}} s^{4n} \right]$$

$$+ \sqrt{2}\,\gamma\, c_2 \sum_{n=0}^{+\infty} \frac{(-1)^n}{n!\,\Gamma\left(n+\frac{7}{4}\right)} \left(\frac{\gamma}{4}\right)^{2n+\frac{3}{4}} s^{4n+3}, \tag{5.3.22}$$

with $0 \le s \le 1$, $\gamma > 0$ and $c_1, c_2 \in \mathbb{R}$.

The boundary conditions (5.3.9) and (5.3.10) can now be written as

$$\left(c_1+c_2\right)\frac{2\sqrt{2}\,\gamma^{\frac{1}{4}}}{\Gamma\left(\frac{1}{4}\right)}+c_2\,\frac{2\varepsilon\gamma^{\frac{3}{4}}}{\Gamma\left(\frac{3}{4}\right)}=0 \tag{5.3.23}$$

$$c_1 J_{\frac{1}{4}}\left(\frac{\gamma}{2}\right)+c_2 Y_{\frac{1}{4}}\left(\frac{\gamma}{2}\right)=0 \tag{5.3.24}$$

and form a homogeneous linear system in the unknowns c_1 and c_2. For $\tilde{\phi}$ not to be identically zero, c_1 and c_2 cannot be simultaneously zero. Therefore, the determinant of the coefficient matrix of the system (5.3.23)-(5.3.24) must vanish:

$$\det\begin{bmatrix} J_{\frac{1}{4}}\left(\frac{\gamma}{2}\right) & Y_{\frac{1}{4}}\left(\frac{\gamma}{2}\right) \\ \frac{2\sqrt{2}\,\gamma^{\frac{1}{4}}}{\Gamma\left(\frac{1}{4}\right)} & \frac{2\sqrt{2}\,\gamma^{\frac{1}{4}}}{\Gamma\left(\frac{1}{4}\right)}+\frac{2\varepsilon\gamma^{\frac{3}{4}}}{\Gamma\left(\frac{3}{4}\right)} \end{bmatrix}=0\ . \tag{5.3.25}$$

This is the characteristic equation for the eigenvalues of Problem 5.4 – for a given load position parameter ε, a positive real number γ is an eigenvalue of Problem 5.4 if and only if it is a root of equation (5.3.25). In particular, one is primarily interested in the lowest positive root of (5.3.25), called the non-dimensional critical load and denoted by γ_{cr}, which yields the critical load factor λ_{cr} via (5.3.6).

For ε restricted to the range $-0.1\le\varepsilon\le 0.1$ of practical interest, the numerical computation of γ_{cr} was carried out with the mathematical software package Mathematica (WOLFRAM RESEARCH, INC. 2006). The starting point was the case $\varepsilon=0$ (centroidal loading), already treated by MICHELL (1899) and PRANDTL (1899), which amounts to finding the lowest positive root of $J_{-1/4}$ and leads to $\gamma_{cr}=\gamma_{cr}^{(0)}\cong 4.013$. This value was found to be an adequate initial guess for all subsequent computations with $\varepsilon\neq 0$. The results are summarised in table 5.3.1 and figure 5.3.3. The latter also shows the affine approximation $\varepsilon\mapsto 4.013\times(1+\varepsilon)$ proposed by Timoshenko in 1910 (see TIMOSHENKO & GERE 1961, eq. 6.24). This approximation, whose background is unknown to the author, practically coincides with the tangent line to the curve γ_{cr} *vs.* ε at the point $(\varepsilon,\gamma)=(0,\gamma_{cr}^{(0)})$. Indeed, consider the map $H:\mathbb{R}\times\mathbb{R}^+\to\mathbb{R}$ defined by

$$\begin{aligned} H(\varepsilon,\gamma) &= \left(\frac{2\sqrt{2}\,\gamma^{\frac{1}{4}}}{\Gamma\left(\frac{1}{4}\right)}+\frac{2\varepsilon\gamma^{\frac{3}{4}}}{\Gamma\left(\frac{3}{4}\right)}\right)J_{\frac{1}{4}}\left(\frac{\gamma}{2}\right)-\frac{2\sqrt{2}\,\gamma^{\frac{1}{4}}}{\Gamma\left(\frac{1}{4}\right)}Y_{\frac{1}{4}}\left(\frac{\gamma}{2}\right) \\ &= \frac{2\varepsilon\gamma^{\frac{3}{4}}}{\Gamma\left(\frac{3}{4}\right)}J_{\frac{1}{4}}\left(\frac{\gamma}{2}\right)+\frac{4\gamma^{\frac{1}{4}}}{\Gamma\left(\frac{1}{4}\right)}J_{-\frac{1}{4}}\left(\frac{\gamma}{2}\right), \end{aligned} \tag{5.3.26}$$

so that $H(\varepsilon,\gamma)=0$ is just a restatement of the characteristic equation (5.3.25). The map H is continuously differentiable on its domain, since the partial derivatives D_1H and D_2H, given by

$$D_1H(\varepsilon,\gamma)=\frac{2\gamma^{\frac{3}{4}}}{\Gamma\left(\frac{3}{4}\right)}J_{\frac{1}{4}}\left(\frac{\gamma}{2}\right) \tag{5.3.27}$$

$$\begin{aligned}D_2H(\varepsilon,\gamma)=&\frac{3\varepsilon}{2\Gamma\left(\frac{3}{4}\right)\gamma^{\frac{1}{4}}}J_{\frac{1}{4}}\left(\frac{\gamma}{2}\right)+\frac{\varepsilon\gamma^{\frac{3}{4}}}{2\Gamma\left(\frac{3}{4}\right)}\left(J_{-\frac{3}{4}}\left(\frac{\gamma}{2}\right)-J_{\frac{5}{4}}\left(\frac{\gamma}{2}\right)\right)\\&+\frac{1}{\Gamma\left(\frac{1}{4}\right)\gamma^{\frac{3}{4}}}J_{-\frac{1}{4}}\left(\frac{\gamma}{2}\right)+\frac{\gamma^{\frac{1}{4}}}{\Gamma\left(\frac{1}{4}\right)}\left(J_{-\frac{5}{4}}\left(\frac{\gamma}{2}\right)-J_{\frac{3}{4}}\left(\frac{\gamma}{2}\right)\right),\end{aligned} \tag{5.3.28}$$

exist and are continuous at each point (ε,γ) in $\mathbb{R}\times\mathbb{R}^+$ (*e.g.*, AVEZ 1983, ch. 2, § 3, or DIEUDONNÉ 1960, th. 8.9.1). Moreover, $H(0,\gamma_{cr}^{(0)})=0$ and $D_2H(0,\gamma_{cr}^{(0)})\neq 0$. It then follows from the implicit function theorem (*e.g.*, AVEZ 1983, ch. 3, § 5, or DIEUDONNÉ 1960, th. 10.2.1) that the tangent to the curve γ_{cr} *vs.* ε at the point $(\varepsilon,\gamma)=(0,\gamma_{cr}^{(0)})$ exists and its slope is $-D_1H(0,\gamma_{cr}^{(0)})/D_2H(0,\gamma_{cr}^{(0)})\cong 4.115$, which is very close to 4.013.

One further conclusion can be drawn from the foregoing analysis: if a given ε and a corresponding eigenvalue $\gamma>0$ are inserted into the system (5.3.23)-(5.3.24), the nullity of the resulting coefficient matrix is equal to 1. All the eigenvalues of Problem 5.4 are thus seen to be simple (*i.e.*, the associated characteristic space is one-dimensional).

$\varepsilon=\frac{x_3^Q}{L}\sqrt{\frac{EI_3(0)}{GJ(0)}}$	$\gamma_{cr}=\frac{\lambda_{cr}Q_{ref}L^2}{\sqrt{EI_3(0)GJ(0)}}$
–0.100	3.542
–0.075	3.669
–0.050	3.791
–0.025	3.906
0.000	4.013
0.025	4.111
0.050	4.202
0.075	4.285
0.100	4.361

Table 5.3.1: Prismatic strip cantilevers – Non-dimensional critical loads γ_{cr}

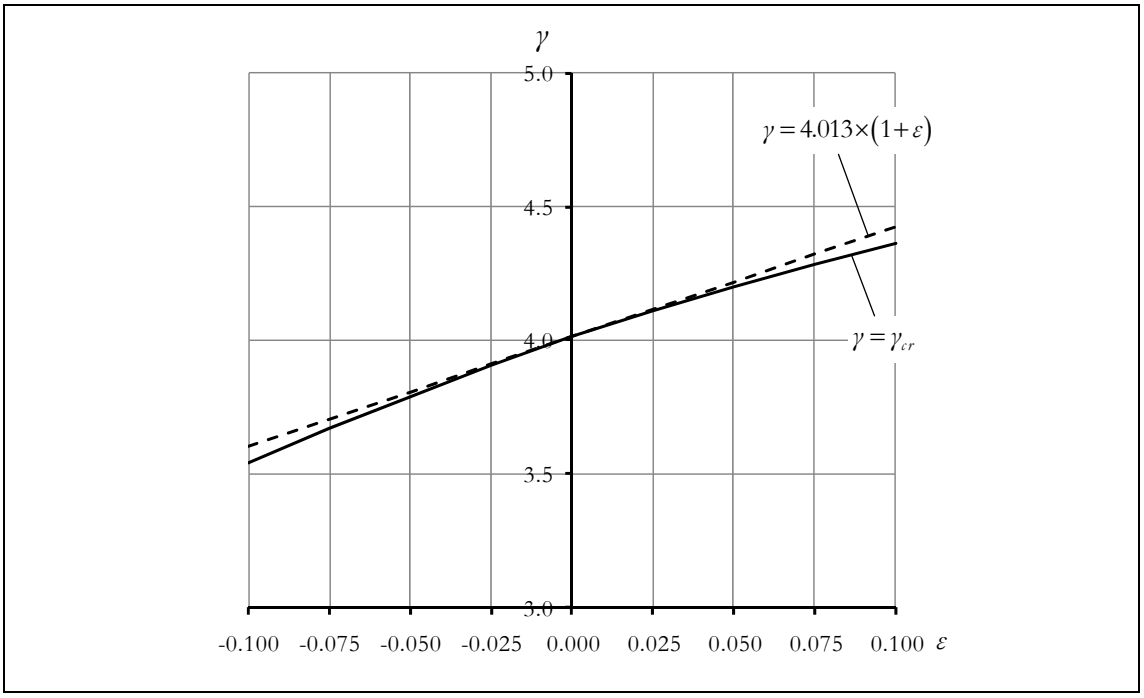

Figure 5.3.3: Prismatic strip cantilevers – Non-dimensional critical loads γ_{cr}

5.4 THE TAPERED CASE ($0 < \alpha < 1$)

In Problem 5.2, we now restrict the taper ratio α to lie in the open interval $(0,1)$. To cast this restricted version of Problem 5.2 in non-dimensional form, consider the map $f:[0,L]\to[\alpha,1]$, $x_1 \mapsto 1-(1-\alpha)\frac{x_1}{L}$ and let $s = f(x_1)$ denote the associated change of independent variable.[13] Moreover, define $\tilde{\phi}:[\alpha,1]\to\mathbb{R}$ such that $\phi_1 = \tilde{\phi}\circ f$. Clearly, $\phi_1 \in C^2[0,L]$ if and only if $\tilde{\phi}\in C^2[0,1]$ and one gets by the chain rule

$$\phi_1'(x_1) = \tilde{\phi}'\big(f(x_1)\big) f'(x_1) = -\frac{1-\alpha}{L}\tilde{\phi}'(s) \tag{5.4.1}$$

$$\phi_1''(x_1) = -\frac{1-\alpha}{L}\tilde{\phi}''\big(f(x_1)\big) f'(x_1) = \frac{(1-\alpha)^2}{L^2}\tilde{\phi}''(s)\ . \tag{5.4.2}$$

Introducing the non-dimensional load

$$\gamma = \frac{\lambda\, Q_{ref}\, L^2}{\sqrt{EI_3(0)GJ(0)}}\ , \tag{5.4.3}$$

which is identical with (5.3.6), and the load position parameter

[13] Once again, observe that (i) f is a real analytic diffeomorphism and, consequently, (ii) $f'(x_1)\neq 0$ for every x_1 in $(0,L)$.

$$\varepsilon = \frac{x_3^Q}{\alpha L}\sqrt{\frac{EI_3(0)}{GJ(0)}}\ , \tag{5.4.4}$$

which generalises (5.3.7), Problem 5.2, restricted so as to have $0<\alpha<1$, is brought into the following form:

Problem 5.5.

Find $\gamma \in \mathbb{R}^+$ and $\tilde{\phi}:[\alpha,1]\to\mathbb{R}$, with $\tilde{\phi}\in C^2[\alpha,1]$ and $\tilde{\phi}\neq 0$, satisfying the differential equation

$$\tilde{\phi}''(s)+\frac{1}{s}\tilde{\phi}'(s)+\frac{\gamma^2}{(1-\alpha)^4}\left(1-\frac{2\alpha}{s}+\frac{\alpha^2}{s^2}\right)\tilde{\phi}(s)=0 \tag{5.4.5}$$

on the open interval $(\alpha,1)$, together with the boundary conditions

$$\tilde{\phi}'(\alpha)-\frac{\varepsilon\gamma}{1-\alpha}\tilde{\phi}(\alpha)=0 \tag{5.4.6}$$

$$\tilde{\phi}(1)=0\ . \tag{5.4.7}$$

Equation (5.4.5) is a second-order homogeneous linear differential equation with a regular singular point at $s=0$ (which does not belong to the problem's domain of definition).[14] It is now shown that this equation is reducible to the canonical form known as Kummer's equation by means of elementary changes of variables. First, consider the change of dependent variable determined by

$$\tilde{\phi}(s)=s^{\sigma}e^{\tau s}\eta(s)=e^{\sigma\log(s)+\tau s}\eta(s)\ \ ,\ s\in(\alpha,1), \tag{5.4.8}$$

where σ and τ are complex constants. It should be noticed that the map $s\mapsto e^{\sigma\log(s)+\tau s}$ is real analytic and non-zero on $(\alpha,1)$. If $\tilde{\phi}$ is twice continuously differentiable on $(\alpha,1)$, then so is η; the converse is also true and

$$\tilde{\phi}'(s)=\sigma s^{\sigma-1}e^{\tau s}\eta(s)+\tau s^{\sigma}e^{\tau s}\eta(s)+s^{\sigma}e^{\tau s}\eta'(s) \tag{5.4.9}$$

$$\begin{aligned}\tilde{\phi}''(s)=&\left(\sigma(\sigma-1)s^{\sigma-2}e^{\tau s}+2\sigma\tau s^{\sigma-1}e^{\tau s}+\tau^2 s^{\sigma}e^{\tau s}\right)\eta(s)\\&+\left(2\sigma s^{\sigma-1}e^{\tau s}+2\tau s^{\sigma}e^{\tau s}\right)\eta'(s)+s^{\sigma}e^{\tau s}\eta''(s)\ .\end{aligned} \tag{5.4.10}$$

[14] The point $x=x_0$ is said to be a singular point of the second-order homogeneous linear differential equation $y''(x)+p(x)\,y'(x)+q(x)\,y(x)=0$ if either of the coefficient functions $x\mapsto p(x)$, $x\mapsto q(x)$ is not analytic at $x=x_0$. The singular point $x=x_0$ is said to be regular if the functions $x\mapsto(x-x_0)\,p(x)$ and $x\mapsto(x-x_0)^2\,q(x)$ are analytic at $x=x_0$ (*e.g.*, CODDINGTON & CARLSON 1997, p. 185, KRISTENSSON 2010, def. 2.4, OLVER 1974, ch. 5, § 4.1, SÁNCHEZ 1968, p. 145, SIMMONS 1991, pp. 184-185, TEMME 1996, def. 4.1, WANG & GUO 1989, p. 56, or WHITTAKER & WATSON 1963, pp. 194 and 197).

Substituting these expressions into equation (5.4.5) and simplifying, one gets

$$\eta''(s)+\left(A_0+\frac{B_0}{s}\right)\eta'(s)+\left(A_1+\frac{B_1}{s}+\frac{C_1}{s^2}\right)\eta(s)=0\ , \tag{5.4.11}$$

with

$$A_0=2\tau \tag{5.4.12}$$

$$B_0=1+2\sigma \tag{5.4.13}$$

$$A_1=\frac{\gamma^2}{(1-\alpha)^4}+\tau^2 \tag{5.4.14}$$

$$B_1=-\frac{2\alpha\gamma^2}{(1-\alpha)^4}+2\sigma\tau+\tau \tag{5.4.15}$$

$$C_1=\frac{\alpha^2\gamma^2}{(1-\alpha)^4}+\sigma^2\ . \tag{5.4.16}$$

Observe that equations (5.4.5) and (5.4.11) have essentially the same form. Next, choose

$$\sigma=i\frac{\alpha\gamma}{(1-\alpha)^2} \tag{5.4.18}$$

$$\tau=-i\frac{\gamma}{(1-\alpha)^2}\ , \tag{5.4.17}$$

so as to have $A_1=C_1=0$. Finally, consider the change of independent variable defined by the analytic homeomorphism (recall that $\gamma>0$, hence $A_0\neq 0$)

$$g:(\alpha,1)\to(-A_0\,\alpha,-A_0)=\left(i\frac{2\alpha\gamma}{(1-\alpha)^2},i\frac{2\gamma}{(1-\alpha)^2}\right),^{15}\quad s\mapsto\zeta=-A_0\,s=i\frac{2\gamma}{(1-\alpha)^2}s \tag{5.4.19}$$

and let $\tilde{\eta}:\mathcal{O}\to\mathbb{C}$, where $\mathcal{O}$ is an open subset of $\mathbb{C}$ containing $(-A_0\,\alpha,-A_0)$, be a differentiable (and hence analytic) map such that $\eta=\tilde{\eta}\circ g$. Then, on $(-A_0\,\alpha,-A_0)$, $\tilde{\eta}$ must satisfy the differential equation

$$\zeta\tilde{\eta}''(\zeta)+(b-\zeta)\tilde{\eta}'(\zeta)-a\,\tilde{\eta}(\zeta)=0\ , \tag{5.4.20}$$

with

$$a=\frac{B_1}{A_0}=\frac{1}{2} \tag{5.4.21}$$

$$b=B_0=1+i\frac{2\alpha\gamma}{(1-\alpha)^2}\ . \tag{5.4.22}$$

[15] In this context, the symbol (a,b), with $a,b\in\mathbb{C}$, stands for the set $\{\zeta\in\mathbb{C}\,|\,\zeta=(1-x)a+x\,b,\ 0<x<1\}$.

Equation (5.4.20) is known as Kummer's equation (KUMMER 1837), with parameters a and b. It is also known as the confluent hypergeometric equation, since it can be derived from the hypergeometric equation of Gauss by merging two of the latter's three regular singular points (see BUCHHOLZ 1953, § 1.1, or SLATER 1960, pp. 2-3).

The general solution of equation (5.4.20) is found by applying the method of Frobenius (FROBENIUS 1873, but see also BENDER & ORSZAG 2010, § 3.3, HENRICI 1977, § 9.6, INCE 1956, ch. 16, KRISTENSSON 2010, § 2.4, OLVER 1974, ch. 5, §§ 4-5, TEMME 1996, § 4.2.5, SÁNCHEZ 1968, app. A, and WHITTAKER & WATSON 1963, § 10.3). Accordingly, one seeks a formal solution of (5.4.20) near $z = 0$ in the form of a series of ascending powers of z (Frobenius series), say

$$\tilde{\eta}(z) = z^{m}\left(1+\sum_{n=1}^{+\infty} d_n z^n\right), \tag{5.4.23}$$

where the exponent m and the coefficients d_n are to be determined.[16] Assuming for the moment that term-by-term differentiation of the power series is permissible, the first and second derivatives of (5.4.23) are given by

$$\tilde{\eta}'(z) = z^{m-1}\left(m+\sum_{n=1}^{+\infty} d_n (m+n) z^n\right) \tag{5.4.24}$$

$$\tilde{\eta}''(z) = z^{m-2}\left(m(m-1)+\sum_{n=1}^{+\infty} d_n (m+n)(m+n-1) z^n\right). \tag{5.4.25}$$

Then, substituting (5.4.23)-(5.4.25) into the left-hand side of (5.4.20) and equating to zero the coefficient of each separate power of z, one obtains the indicial equation[17]

$$m(m+b-1) = 0\ , \tag{5.4.26}$$

---

[16] Let w be a fixed complex number. Unless indicated otherwise, the map $z \mapsto z^w$ of the complex variable z denotes the principal branch of the w^{th}-power function, defined on the slit complex plane $\mathbb{C}\setminus(-\infty,0]$ (*e.g.*, CONWAY 1978, ch. 3, § 2, or REMMERT 1991, ch. 5, particularly § 5). This principal branch is an analytic map on its domain, with derivative

$$\left(z^w\right)' = w z^{w-1}\ .$$

Moreover, it satisfies

$$z^{w_1+w_2} = z^{w_1} z^{w_2}$$

for every w_1 and w_2 in $\mathbb{C}$.

[17] The name "indicial equation" was coined by CAYLEY (1886). One also speaks of the indicial polynomial $P(m) = m(m+b-1)$.

with roots

$$m_1 = 0 \tag{5.4.27}$$

$$m_2 = 1 - b \ , \tag{5.4.28}$$

and the recurrence relation (with $d_0 = 1$)

$$(m+n)(m+b+n-1)d_n - (a+m+n-1)d_{n-1} = 0 \ \ , \ n = 1, 2, \cdots \ . \tag{5.4.29}$$

The root $m_1 = 0$ of the indicial equation leads to the following formal solution of equation (5.4.20):

$$\tilde{\eta}_1(z) = 1 + \frac{a}{b}z + \frac{a(a+1)}{b(b+1)}\frac{z^2}{2!} + \frac{a(a+1)(a+2)}{b(b+1)(b+2)}\frac{z^3}{3!} + \cdots + \frac{a(a+1)\cdots(a+n-1)}{b(b+1)\cdots(b+n-1)}\frac{z^n}{n!} + \cdots \tag{5.4.30}$$

(note that b is neither zero nor a negative integer). Using Pochhammer's symbol for the rising factorial, defined as

$$(a)_0 = 1 \qquad (a)_n = a(a+1)\cdots(a+n-1) = \prod_{k=0}^{n-1}(a+k) \ \ , \ \ n \in \mathbb{Z}^+ \ , \tag{5.4.31}$$

equation (5.4.30) is rewritten in the compact form

$$\tilde{\eta}_1(z) = \sum_{n=0}^{+\infty} \frac{(a)_n}{(b)_n}\frac{z^n}{n!} \ . \tag{5.4.32}$$

By d'Alembert's test, the above series is readily seen to be absolutely convergent for every $z \in \mathbb{C}$,[18] and so term-by-term differentiations are legitimate. Consequently, the formal solution $\tilde{\eta}_1$ is an actual solution of (5.4.20).

The entire function of the complex variable z defined by the series (5.4.32) is named after KUMMER (1836) and denoted $z \mapsto M(a, b, z)$.[19] The complex numbers a and b (with $b \notin \mathbb{Z}_0^-$), which are independent of z, are called the parameters of the function (for obvious reasons, a is the numeratorial parameter and b the denominatorial parameter) – in the present case, they are given by (5.4.21)-(5.4.22). Kummer's function belongs to the

---

[18] Indeed, set

$$u_n = \frac{(a)_n}{(b)_n}\frac{z^n}{n!} \ .$$

Then, for arbitrary $z \neq 0$, the ratio

$$\frac{|u_{n+1}|}{|u_n|} = \frac{|(a+n)z|}{|(n+1)(b+n)|}$$

tends to zero as $n \to +\infty$.

[19] The reader should be aware that several other notations are commonly used for this function – see DAALHUIS (2010, p. 322), ERDÉLYI *et al.* (1953a, p. 248) and SLATER (1960, p. 2).

class of confluent hypergeometric functions, which arise in a wide variety of fields of mathematical physics and probability theory[20] – for applications in structural mechanics, see LIU & XI (2002, ch. 2), MILISAVLJEVIC (1988), PANAYOTOUNAKOS (1995), POLIDORI & BECK (1996) and RAJ & SUJITH (2005). The theory of confluent hypergeometric functions is discussed at great length and detail in the monographs by BUCHHOLZ (1953), SLATER (1960) and TRICOMI (1954). More concise and selective treatments can be found in ANDREWS *et al.* (1999, ch. 4), BEALS & WONG (2010, ch. 6), ERDÉLYI *et al.* (1953a, ch. 6), HOCHSTADT (1971, ch. 7), KRISTENSSON (2010, ch. 7), LEBEDEV (1965, ch. 9, §§ 9-13), LUKE (1969, ch. 4), MEIXNER (1956, § 5), OLVER (1974, ch. 7, §§ 9-11), TEMME (1996, ch. 7), WANG & GUO (1989, ch. 6) or WHITTAKER & WATSON (1963, ch. 16). DAALHUIS (2010), POLYANIN & ZAITSEV (2003, Supplement S.2.7) and TRICOMI (1955) provide useful summaries of the theory.

Since b is not an integer, the root $m_2 = 1-b$ of the indicial equation leads to a second independent solution of equation (5.4.20) of the form

$$\begin{aligned}\tilde{\eta}_{I2}(\xi) &= \xi^{1-b}\left(1+\frac{1+a-b}{2-b}\xi+\frac{(1+a-b)(2+a-b)}{(2-b)(3-b)}\frac{\xi^2}{2!}+\cdots\right.\\ &\qquad\left.\cdots+\frac{(1+a-b)(2+a-b)\cdots(n+a-b)}{(2-b)(3-b)\cdots(n+1-b)}\frac{\xi^n}{n!}+\cdots\right)\\ &= \xi^{1-b}\sum_{n=0}^{+\infty}\frac{(1+a-b)_n}{(2-b)_n}\frac{\xi^n}{n!}\\ &= \xi^{1-b}\,M(1+a-b,\,2-b,\,\xi)\ . \end{aligned} \tag{5.4.33}$$

The general solution of (5.4.20) is thus

[20] Moreover, many transcendental functions that occur frequently enough to be given names can be expressed in terms of confluent hypergeometric functions. In view of the solution given for the prismatic case in the preceding section, the following relationship between Kummer's function and the Bessel function of the first kind (of arbitrary complex order ν) is particularly noteworthy (ERDÉLYI *et al.* 1953a, p. 265, HENRICI 1977, pp. 136-137, KRISTENSSON 2010, § 7.1.1, LEBEDEV 1965, p. 274, LUKE 1969, p. 213, OLVER & MAXIMON 2010, p. 228, TRICOMI 1954, p. 34):

$$J_\nu(\xi) = \frac{1}{\Gamma(1+\nu)}\left(\frac{\xi}{2}\right)^\nu e^{-i\xi}\,M\left(\frac{1}{2}+\nu,\,1+2\nu,\,2i\xi\right)\ ,\ \xi\in\mathbb{C}\setminus(-\infty,0]\,.$$

The right-hand side of the above identity is real-valued when $\nu\in\mathbb{R}$ and $\xi\in\mathbb{R}^+$, as it should (see the proposition in Appendix 2, at the end of this chapter).

$$\tilde{\eta}(\zeta) = c_1\, M(a,b,\zeta) + c_2\, \zeta^{1-b}\, M(1+a-b,2-b,\zeta) \quad \text{, with } c_1, c_2 \in \mathbb{C} \text{ .} \tag{5.4.34}$$

It should be noted that (5.4.32) and (5.4.33) form a numerically satisfactory fundamental pair of solutions in the sense of MILLER (1950) – see DAALHUIS (2010, 13.2(v)) and OLVER (1974, ch. 5, § 7.2).[21]

In turn, the general solution of (5.4.5) on the real interval $(\alpha,1)$ is

$$\tilde{\phi}(s) = s^{i\frac{\alpha\gamma}{(1-\alpha)^2}}\, e^{-i\frac{\gamma}{(1-\alpha)^2}s} \left[c_1\, M\left(\frac{1}{2}, 1+i\frac{2\alpha\gamma}{(1-\alpha)^2}, i\frac{2\gamma}{(1-\alpha)^2}s\right) \right.$$

$$\left. + c_2 \left(i\frac{2\gamma}{(1-\alpha)^2}s\right)^{-i\frac{2\alpha\gamma}{(1-\alpha)^2}} M\left(\frac{1}{2}-i\frac{2\alpha\gamma}{(1-\alpha)^2}, 1-i\frac{2\alpha\gamma}{(1-\alpha)^2}, i\frac{2\gamma}{(1-\alpha)^2}s\right) \right], \tag{5.4.35}$$

with $c_1, c_2 \in \mathbb{C}$. The right hand side of (5.4.35) defines a family of real analytic maps of the variable s on $\mathbb{R}\setminus\{0\}$. Arguing by continuity as in the paragraph following equation (5.3.21), one concludes that the above identity must also hold at $s=\alpha$ and $s=1$.

The differentiation of $\tilde{\phi}$, being a straightforward task that leads to a rather lengthy expression, is omitted – it suffices to say that use is made of the rule

$$\frac{d}{d\zeta} M(a,b,\zeta) = \sum_{n=1}^{+\infty} \frac{(a)_n}{(b)_n} \frac{\zeta^{n-1}}{(n-1)!} = \sum_{n=0}^{+\infty} \frac{(a)_{n+1}}{(b)_{n+1}} \frac{\zeta^n}{n!} = \frac{a}{b} \sum_{n=0}^{+\infty} \frac{(a+1)_n}{(b+1)_n} \frac{\zeta^n}{n!}$$

$$= \frac{a}{b} M(a+1,b+1,\zeta) \quad , b \notin \mathbb{Z}_0^- \ , \ \zeta \in \mathbb{C} \text{ .} \tag{5.4.36}$$

---

[21] In CHALLAMEL *et al.* (2007), an alternative fundamental pair of solutions of (5.4.20) was tacitly used, namely $\tilde{\eta}_1(\zeta) = M(a,b,\zeta)$ (as above) and $\tilde{\eta}_2(\zeta) = U(a,b,\zeta)$, where U denotes the principal branch of Tricomi's function (TRICOMI 1947). For non-integer values of b, $U(a,b,\zeta)$ is defined to be the following linear combination of $M(a,b,\zeta)$ and $\zeta^{1-b}\, M(1+a-b,2-b,\zeta)$:

$$U(a,b,\zeta) = \frac{\Gamma(1-b)}{\Gamma(1+a-b)} M(a,b,\zeta) + \frac{\Gamma(b-1)}{\Gamma(a)} \zeta^{1-b}\, M(1+a-b,2-b,\zeta) \quad , \zeta \in \mathbb{C}\setminus(-\infty,0] \text{ .}$$

Unless a is a non-positive integer (which would imply $1/\Gamma(a)=0$), $M(a,b,\zeta)$ and $U(a,b,\zeta)$ are linearly independent.

The right-hand side of the above equation is meaningless when b is an integer. Indeed,

(i) if $b \in \mathbb{Z}_0^-$, $M(a,b,\zeta)$ is undefined;

(ii) if $b=1$, $\Gamma(1-b)$ and $\Gamma(b-1)$ are undefined;

(iii) if $b = 2, 3, \cdots$, $M(1+a-b,2-b,\zeta)$ is undefined.

However, a limiting process, the details of which can be found in LEBEDEV (1965, § 9.10), yields a well-defined result, and this fact may be used to assign a meaning to $U(a,b,\zeta)$ whenever b is an integer.

According to OLVER (1974, ch. 7, § 10.5), $M(a,b,\zeta)$ and $U(a,b,\zeta)$ form a numerically satisfactory pair of solutions of Kummer's equation (5.4.20) for $a \neq 0, -1, -2, \cdots$, $\mathrm{Re}(b) \geq 1$ and $\mathrm{Re}(\zeta) \geq 0$.

The boundary conditions (5.4.6) and (5.4.7) now yield the homogeneous system of linear equations

$$a_{kl}\, c_l = 0 \quad (k,l = 1, 2) \ , \tag{5.4.37}$$

where

$$a_{11} = M\left(\frac{1}{2}, 1+i\frac{2\alpha\gamma}{(1-\alpha)^2}, i\frac{2\gamma}{(1-\alpha)^2}\right) \tag{5.4.38}$$

$$a_{12} = \left(i\frac{2\gamma}{(1-\alpha)^2}\right)^{-i\frac{2\alpha\gamma}{(1-\alpha)^2}} M\left(\frac{1}{2}-i\frac{2\alpha\gamma}{(1-\alpha)^2}, 1-i\frac{2\alpha\gamma}{(1-\alpha)^2}, i\frac{2\gamma}{(1-\alpha)^2}\right) \tag{5.4.39}$$

$$\begin{aligned} a_{21} = {} & i\frac{1}{(1-\alpha)\left(1+i\dfrac{2\alpha\gamma}{(1-\alpha)^2}\right)} M\left(\frac{3}{2}, 2+i\frac{2\alpha\gamma}{(1-\alpha)^2}, i\frac{2\alpha\gamma}{(1-\alpha)^2}\right) \\ & -\varepsilon\, M\left(\frac{1}{2}, 1+i\frac{2\alpha\gamma}{(1-\alpha)^2}, i\frac{2\alpha\gamma}{(1-\alpha)^2}\right) \end{aligned} \tag{5.4.40}$$

$$\begin{aligned} a_{22} = {} & \left(i\frac{2\alpha\gamma}{(1-\alpha)^2}\right)^{-i\frac{2\alpha\gamma}{(1-\alpha)^2}} \left[-\left(i\frac{2}{1-\alpha}+\varepsilon\right) M\left(\frac{1}{2}-i\frac{2\alpha\gamma}{(1-\alpha)^2}, 1-i\frac{2\alpha\gamma}{(1-\alpha)^2}, i\frac{2\alpha\gamma}{(1-\alpha)^2}\right)\right. \\ & \left. + \frac{\dfrac{4\alpha\gamma}{(1-\alpha)^2}+i}{1-\alpha-i\dfrac{2\alpha\gamma}{1-\alpha}} M\left(\frac{3}{2}-i\frac{2\alpha\gamma}{(1-\alpha)^2}, 2-i\frac{2\alpha\gamma}{(1-\alpha)^2}, i\frac{2\alpha\gamma}{(1-\alpha)^2}\right)\right] . \end{aligned} \tag{5.4.41}$$

Since both the coefficients (a_{kl}) and the unknowns (c_l) in this system are complex, we replace it with an equivalent one, with real coefficients and unknowns but twice the size:

$$\begin{cases} \mathrm{Re}(a_{kl})\,\mathrm{Re}(c_l) - \mathrm{Im}(a_{kl})\,\mathrm{Im}(c_l) = 0 \\ \mathrm{Im}(a_{kl})\,\mathrm{Re}(c_l) + \mathrm{Re}(a_{kl})\,\mathrm{Im}(c_l) = 0 \end{cases} \quad (k,l = 1, 2) \ , \tag{5.4.42}$$

where $\mathrm{Re}(\tilde{z})$ and $\mathrm{Im}(\tilde{z})$ stand for the real and imaginary parts of the complex number $\tilde{z}$.

For Problem 5.5 to have solutions $\tilde{\phi} \neq 0$, the determinant of the coefficient matrix of the system (5.4.42) must vanish. This condition provides the characteristic equation for the eigenvalues of Problem 5.5. In particular, given α (with $0 < \alpha < 1$) and ε, the corresponding non-dimensional critical load γ_{cr} is the lowest positive value of γ that makes the determinant vanish. Results for γ_{cr}, obtained with the mathematical software package Mathematica (WOLFRAM RESEARCH, INC. 2006), are presented in table 5.4.1 and plotted in

figure 5.4.1. These results were successfully benchmarked against shell finite element analyses – see CHALLAMEL *et al.* (2007) for details. It is also worth mentioning that the numerical results obtained by BAKER (1993) and MASSEY & MCGUIRE (1971) for the centroidal loading case ($\varepsilon = 0$) are in close agreement with those stemming from (5.4.42).

ε	γ_{cr}								
	$\alpha = 0.1$	$\alpha = 0.2$	$\alpha = 0.3$	$\alpha = 0.4$	$\alpha = 0.5$	$\alpha = 0.6$	$\alpha = 0.7$	$\alpha = 0.8$	$\alpha = 0.9$
–0.100	2.637	2.804	2.941	3.059	3.162	3.255	3.337	3.412	3.480
–0.075	2.646	2.823	2.972	3.101	3.218	3.323	3.420	3.509	3.592
–0.050	2.656	2.843	3.001	3.142	3.270	3.388	3.498	3.602	3.699
–0.025	2.665	2.861	3.030	3.182	3.321	3.451	3.573	3.689	3.800
0.000	2.674	2.879	3.058	3.219	3.369	3.510	3.643	3.771	3.894
0.025	2.682	2.897	3.084	3.255	3.415	3.565	3.709	3.848	3.982
0.050	2.691	2.914	3.110	3.290	3.458	3.618	3.771	3.919	4.063
0.075	2.699	2.930	3.134	3.322	3.499	3.667	3.829	3.985	4.137
0.100	2.708	2.946	3.158	3.354	3.538	3.714	3.883	4.047	4.206

Table 5.4.1: Linearly tapered strip cantilevers – Non-dimensional critical loads γ_{cr}

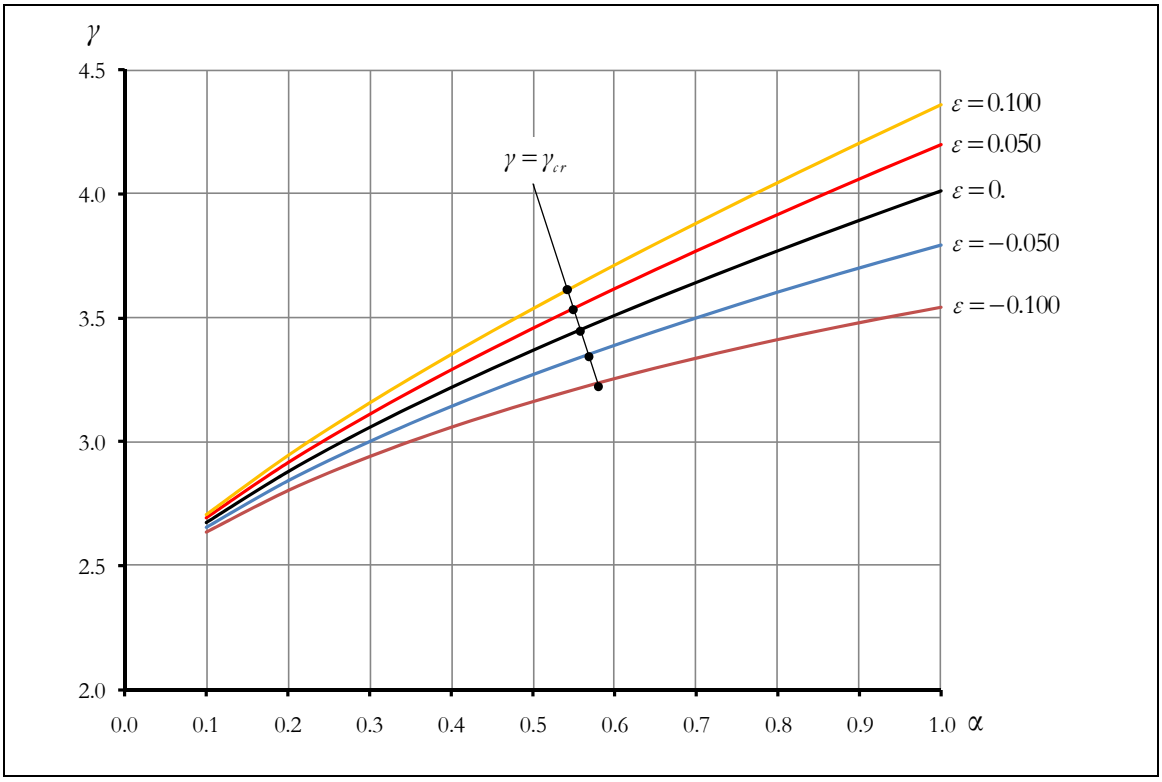

Figure 5.4.1: Linearly tapered strip cantilevers – Non-dimensional critical loads γ_{cr}

5.5 THE STRONGEST TIP-LOADED, LINEARLY TAPERED STRIP CANTILEVER

Throughout this section, the point load $\boldsymbol{Q}$ is taken to be applied at the centroid of the free-end section, *i.e.*, x_3^Q (and hence ε) is set equal to zero. With this restriction, we shall answer the following question: of all homogeneous linearly tapered strip cantilevers with prescribed length, thickness, volume and elastic properties, which has the largest critical load?

Let $\overline{h}$ denote the depth of the prismatic cantilever having the prescribed length, thickness and volume. Consider now a linearly tapered cantilever of equal length, thickness and volume, characterised by the taper ratio α. Its maximum depth $\hat{h}$ is given by

$$\hat{h} = \frac{2\overline{h}}{1+\alpha} \ . \tag{5.5.1}$$

For equal elastic constants, the ratio between the critical loads of the tapered and prismatic cantilevers, denoted by $\hat{Q}_{cr}$ and $\overline{Q}_{cr}$, is

$$\frac{\hat{Q}_{cr}}{\overline{Q}_{cr}} = \frac{\hat{h}}{\overline{h}}\frac{\hat{\gamma}_{cr}}{\overline{\gamma}_{cr}} = \frac{2\hat{\gamma}_{cr}}{(1+\alpha)\overline{\gamma}_{cr}} \ , \tag{5.5.2}$$

where $\hat{\gamma}_{cr}$ and $\overline{\gamma}_{cr} = \min\left\{\gamma > 0 \,\middle|\, J_{-1/4}(\gamma/2) = 0\right\} \cong 4.013$ are the non-dimensionl critical loads corresponding to $\hat{Q}_{cr}$ and $\overline{Q}_{cr}$, respectively. Figure 5.5.1 shows the variation of $\hat{Q}_{cr} / \overline{Q}_{cr}$

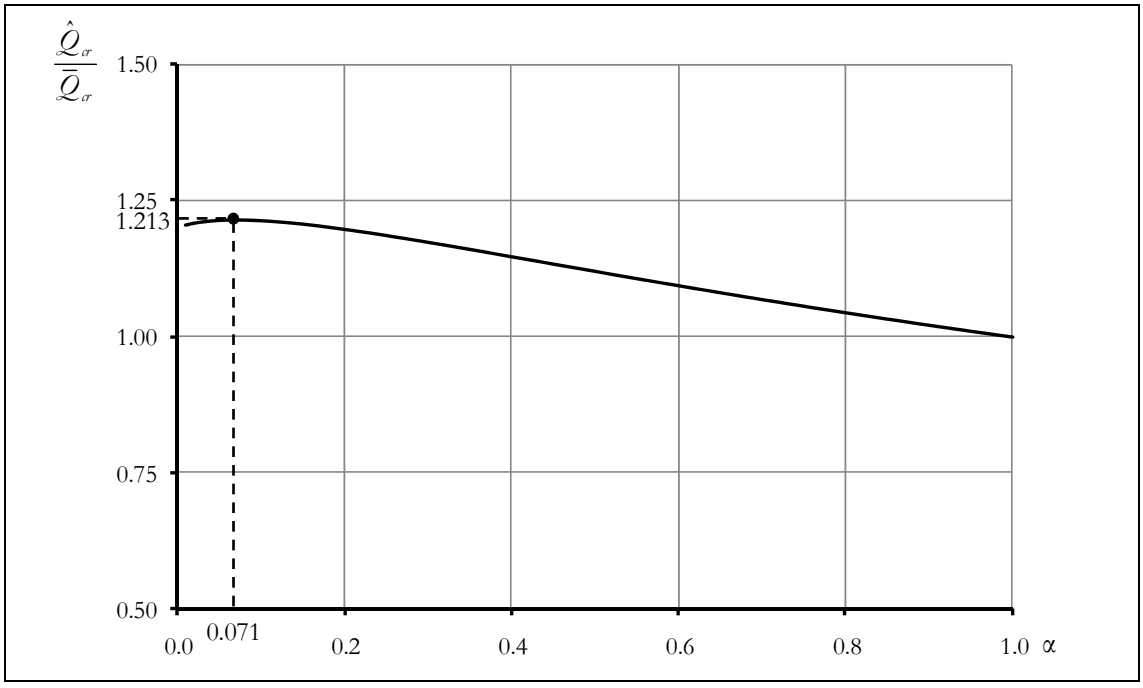

Figure 5.5.1: Variation of $\hat{Q}_{cr} / \overline{Q}_{cr}$ with the taper ratio α (for $\varepsilon = 0$)

with α, in the range $0 < \alpha \leq 1$. This variation is not monotonic, with $\hat{Q}_{cr} / \overline{Q}_{cr}$ reaching a maximum of $\cong 1.213$ at $\alpha \cong 0.071$. Therefore, as far as the elastic lateral-torsional buckling strength is concerned, this value of α defines the most efficient linearly tapered cantilever, whose critical load is 21.3% larger than that of its prismatic counterpart. Moreover, observe that $\hat{Q}_{cr} / \overline{Q}_{cr} > 1$ for $\alpha < 1$.

5.6 GENERALISATION 1: POLYGONALLY DEPTH-TAPERED CANTILEVERS WITH MULTIPLE TRANSVERSE POINT LOADS

Having solved a problem, one should not fail to look back at the completed solution, to re-examine the result and the path that led to it, to disentangle their essential features and to ask the question: "Can you use the result, or the method, for some other problem?" (POLYA 1973). In so doing, the author was led to consider the following generalisation of the problem discussed in §§ 5.2-5.4 – to describe analytically the elastic LTB behaviour of strip cantilevers (i) whose depth is given by a monotonically decreasing polygonal (*i.e.*, continuous and piecewise linear) function of the distance to the support and (ii) which are subjected to an arbitrary number of independent conservative point loads, all acting in the same "downward" direction.

The key to this generalised problem is the observation that there exists a positive integer N and a partition $0 = x_{1.0} < x_{1.1} < \cdots < x_{1.N} = L$ of the interval $[0, L]$ such that:

(i) on each closed interval $\left[x_{1.n-1}, x_{1.n}\right]$ $(n = 1, \cdots, N)$, the depth of the cantilever is given by an affine function, and

(ii) there are no loads applied at the cross-sections with abscissa in the open intervals $\left(x_{1.n-1}, x_{1.n}\right)$ $(n = 1, \cdots, N)$.

The new problem thus appears to be tractable by the methods used in §§ 5.2-5.4 – to wit, the elimination of the dependent variable w_2 and the reduction of the governing differential equation to a known canonical form by means of appropriately chosen changes of variables.

In this section, we shall discuss the special case depicted in figure 5.6.1, concerning a two-segment cantilever acted by two loads, one applied at the free end and the other at the junction between segments. This specialisation "contains all the germs of generality" (to quote David Hilbert).

To be precise, equation (5.2.1) remains valid, but the function $h:[0,L]\to\mathbb{R}^+$ that describes the variation of the cantilever's depth along its length is now defined by

$$h(x_1)=\begin{cases} h_0\left(1-(1-\beta)\dfrac{x_1}{\varrho L}\right) & \text{if } 0\le x_1\le \varrho L \\ h_0\left(\beta-(\beta-\alpha)\dfrac{x_1-\varrho L}{(1-\varrho)L}\right) & \text{if } \varrho L\le x_1\le L \end{cases}, \tag{5.6.1}$$

with $0<\varrho<1$ and $0<\alpha\le\beta\le 1$. Accordingly, the lateral bending and torsional rigidities of the cross-sections are given by

$$\begin{aligned} EI_3(x_1)=\frac{E\,h(x_1)\,t^3}{12} &= \begin{cases} \dfrac{E\,h_0\,t^3}{12}\left(1-(1-\beta)\dfrac{x_1}{\varrho L}\right) & \text{if } 0\le x_1\le \varrho L \\ \dfrac{E\,h_0\,t^3}{12}\left(\beta-(\beta-\alpha)\dfrac{x_1-\varrho L}{(1-\varrho)L}\right) & \text{if } \varrho L\le x_1\le L \end{cases} \\ &= \begin{cases} EI_3(0)\left(1-(1-\beta)\dfrac{x_1}{\varrho L}\right) & \text{if } 0\le x_1\le \varrho L \\ EI_3(0)\left(\beta-(\beta-\alpha)\dfrac{x_1-\varrho L}{(1-\varrho)L}\right) & \text{if } \varrho L\le x_1\le L \end{cases} \end{aligned} \tag{5.6.2}$$

$$\begin{aligned} GJ(x_1)=\frac{G\,h(x_1)\,t^3}{3} &= \begin{cases} \dfrac{G\,h_0\,t^3}{3}\left(1-(1-\beta)\dfrac{x_1}{\varrho L}\right) & \text{if } 0\le x_1\le \varrho L \\ \dfrac{G\,h_0\,t^3}{3}\left(\beta-(\beta-\alpha)\dfrac{x_1-\varrho L}{(1-\varrho)L}\right) & \text{if } \varrho L\le x_1\le L \end{cases} \\ &= \begin{cases} GJ(0)\left(1-(1-\beta)\dfrac{x_1}{\varrho L}\right) & \text{if } 0\le x_1\le \varrho L \\ GJ(0)\left(\beta-(\beta-\alpha)\dfrac{x_1-\varrho L}{(1-\varrho)L}\right) & \text{if } \varrho L\le x_1\le L \end{cases} \end{aligned} \tag{5.6.3}$$

The cantilever is acted by two conservative point loads, $\boldsymbol{Q}_1=\lambda_1\,\mathcal{Q}_{ref}\,\boldsymbol{e}_3$ and $\boldsymbol{Q}_2=\lambda_2\,\mathcal{Q}_{ref}\,\boldsymbol{e}_3$, where $\mathcal{Q}_{ref}$ is again a positive reference magnitude and λ_1, λ_2 are independent load factors, restricted to non-negative values. These loads are applied to the material points whose reference places are $O+L\,\boldsymbol{e}_1+x_3^{Q_1}\,\boldsymbol{e}_3$ and $O+\varrho L\,\boldsymbol{e}_1+x_3^{Q_2}\,\boldsymbol{e}_3$, as shown in figure 5.6.1, and remain parallel to $\boldsymbol{e}_3$ throughout the deformation process. The bending moment distribution in a fundamental equilibrium state is the real-valued map

$$M_2^f(x_1,\lambda_1,\lambda_2)=\begin{cases} \lambda_1\,\mathcal{Q}_{ref}\,(x_1-L)+\lambda_2\,\mathcal{Q}_{ref}\,(x_1-\varrho L) & \text{if } 0\le x_1\le \varrho L \\ \lambda_1\,\mathcal{Q}_{ref}\,(x_1-L) & \text{if } \varrho L\le x_1\le L \end{cases}. \tag{5.6.4}$$

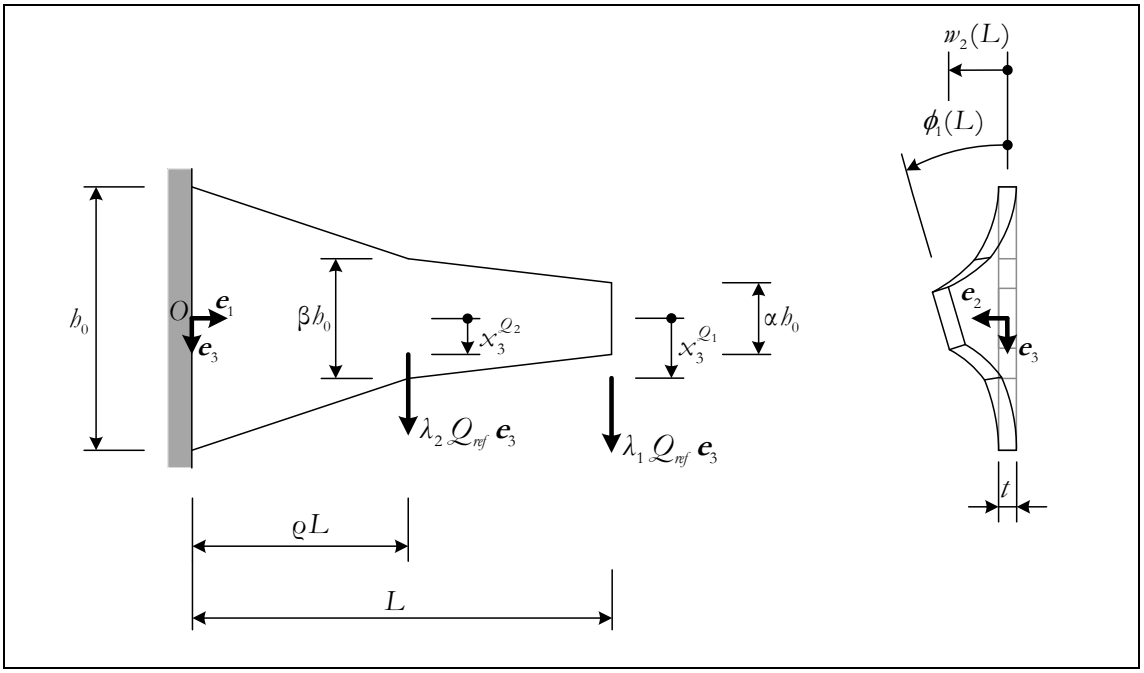

Figure 5.6.1: Two-segment strip cantilever acted by independent point loads applied at the free end and at the junction between segments

In the following, given a map defined on $[0,L]$, the subscripts "$-$" and "$+$" are used to indicate its restrictions to $[0,\varrho L]$ and $[\varrho L, L]$, respectively. Similarly, M_{2-}^f and M_{2+}^f denote the restrictions of the partial map $x_1 \mapsto M_2^f(x_1,\lambda_1,\lambda_2)$, obtained by holding λ_1 and λ_2 fixed, to $[0,\varrho L]$ and $[\varrho L, L]$. With these notational conventions, the functional Π_2, which represents, as the reader may recall, the second-order term of the change in total potential energy of the structural system from a fundamental equilibrium state at constant load, is given by

$$\begin{aligned}\Pi_2(w_2,\phi_1,\lambda_1,\lambda_2) = {} & \frac{1}{2}\int_0^{\varrho L} EI_{3-}(x_1)\,w_{2-}''(x_1)^2\,dx_1 + \frac{1}{2}\int_0^{\varrho L} GJ_-(x_1)\,\phi_{1-}'(x_1)^2\,dx_1 \\ & + \int_0^{\varrho L} M_{2-}^f(x_1,\lambda_1,\lambda_2)\,w_{2-}''(x_1)\,\phi_{1-}(x_1)\,dx_1 \\ & + \frac{1}{2}\int_{\varrho L}^{L} EI_{3+}(x_1)\,w_{2+}''(x_1)^2\,dx_1 + \frac{1}{2}\int_{\varrho L}^{L} GJ_+(x_1)\,\phi_{1+}'(x_1)^2\,dx_1 \\ & + \int_{\varrho L}^{L} M_{2+}^f(x_1,\lambda_1,\lambda_2)\,w_{2+}''(x_1)\,\phi_{1+}(x_1)\,dx_1 \\ & + \frac{1}{2}\lambda_1 Q_{ref}\,x_3^{Q_1}\,\phi_1(L)^2 + \frac{1}{2}\lambda_2 Q_{ref}\,x_3^{Q_2}\,\phi_1(\varrho L)^2\ . \end{aligned} \tag{5.6.5}$$

Regarding the domain of this functional, we require on physical grounds that w_2 (resp. ϕ_1) be continuously differentiable (resp. continuous) on $[0,L]$. Moreover, with a view towards

establishing the Euler-Lagrange equations associated with Π_2, w_{2-} (resp. w_{2+}) is required to be four times continuously differentiable on $[0,\varrho L]$ (resp. $[\varrho L, L]$) and ϕ_{1-} (resp. ϕ_{1+}) is required to be twice continuously differentiable on $[0,\varrho L]$ (resp. $[\varrho L, L]$). The essential boundary conditions to be satisfied are again (5.2.6)-(5.2.8). The domain of the functional Π_2 is thus taken to be $\mathcal{D}_1 \times \mathcal{D}_2 \times \mathbb{R}_0^+ \times \mathbb{R}_0^+$, with

$$\mathcal{D}_1 = \left\{ w_2 \in C^1[0,L] \,\middle|\, w_{2-} \in C^4[0,\varrho L],\, w_{2+} \in C^4[\varrho L, L],\, w_2(0) = 0,\, w_2'(0) = 0 \right\} \tag{5.6.6}$$

$$\mathcal{D}_2 = \left\{ \phi_1 \in C^0[0,L] \,\middle|\, \phi_{1-} \in C^2[0,\varrho L],\, \phi_{1+} \in C^2[\varrho L, L],\, \phi_1(0) = 0 \right\} . \tag{5.6.7}$$

Let δw_2 and $\delta\phi_1$ denote admissible variations of w_2 and ϕ_1 and form the first variation of Π_2 at $(w_2, \phi_1, \lambda_1, \lambda_2)$ in the direction of $(\delta w_2, \delta\phi_1, 0, 0)$. Then, integration by parts yields

$$\begin{aligned}
&\delta\Pi_2(w_2,\phi_1,\lambda_1,\lambda_2)[\delta w_2,\delta\phi_1,0,0] = \\
&= \int_0^{\varrho L} \left[\left(EI_3(x_1) w_{2-}''(x_1) \right)'' + \left(M_{2-}^f(x_1,\lambda_1,\lambda_2)\phi_{1-}(x_1) \right)'' \right] \delta w_{2-}(x_1)\, dx_1 \\
&\quad - \int_0^{\varrho L} \left[\left(GJ(x_1)\phi_{1-}'(x_1) \right)' - M_{2-}^f(x_1,\lambda_1,\lambda_2) w_{2-}''(x_1) \right] \delta\phi_{1-}(x_1)\, dx_1 \\
&\quad - \left[\left(EI_3(x_1) w_{2-}''(x_1) \right)' + \left(M_{2-}^f(x_1,\lambda_1,\lambda_2)\phi_{1-}(x_1) \right)' \right] \delta w_{2-}(x_1) \Big|_0^{\varrho L} \\
&\quad + \left(EI_3(x_1) w_{2-}''(x_1) + M_{2-}^f(x_1,\lambda_1,\lambda_2)\, \phi_{1-}(x_1) \right) \delta w_{2-}'(x_1) \Big|_0^{\varrho L} \\
&\quad + GJ(x_1)\phi_{1-}'(x_1)\delta\phi_{1-}(x_1) \Big|_0^{\varrho L} \\
&\quad + \int_{\varrho L}^{L} \left[\left(EI_3(x_1) w_{2+}''(x_1) \right)'' + \left(M_{2+}^f(x_1,\lambda_1,\lambda_2)\phi_{1+}(x_1) \right)'' \right] \delta w_{2+}(x_1)\, dx_1 \\
&\quad - \int_{\varrho L}^{L} \left[\left(GJ(x_1)\phi_{1+}'(x_1) \right)' - M_{2+}^f(x_1,\lambda_1,\lambda_2) w_{2+}''(x_1) \right] \delta\phi_{1+}(x_1)\, dx_1 \\
&\quad - \left[\left(EI_{3+}(x_1) w_{2+}''(x_1) \right)' + \left(M_{2+}^f(x_1,\lambda_1,\lambda_2)\phi_{1+}(x_1) \right)' \right] \delta w_{2+}(x_1) \Big|_{\varrho L}^{L} \\
&\quad + \left(EI_3(x_1) w_{2+}''(x_1) + M_{2+}^f(x_1,\lambda_1,\lambda_2)\, \phi_{1+}(x_1) \right) \delta w_{2+}'(x_1) \Big|_{\varrho L}^{L} \\
&\quad + GJ(x_1)\phi_{1+}'(x_1)\delta\phi_{1+}(x_1) \Big|_{\varrho L}^{L} \\
&\quad + \lambda_1 Q_{ref}\, x_3^{Q_1}\, \phi_1(L)\delta\phi_1(L) + \lambda_2 Q_{ref}\, x_3^{Q_2}\, \phi_1(\varrho L)\delta\phi_1(\varrho L) .
\end{aligned} \tag{5.6.8}$$

The criterion of Trefftz, combined with the fundamental lemma of the calculus of variations, now leads to the following classical statement of the problem of finding the buckling load factors and the buckling modes for the cantilever shown in figure 5.6.1:

Problem 5.6.

Find non-negative real numbers λ_1, λ_2 and functions $w_2, \phi_1 : [0,L] \to \mathbb{R}$, with

- w_2 continuously differentiable on $[0,L]$,
- $w_{2-} = w_2 \big| [0,\varrho L]$ (resp. $w_{2+} = w_2 \big| [\varrho L, L]$) four times continuously differentiable on $[0,\varrho L]$ (resp. $[\varrho L, L]$),
- ϕ_1 continuous on $[0,L]$,
- $\phi_{1-} = \phi_1 \big| [0,\varrho L]$ (resp. $\phi_{1+} = \phi_1 \big| [\varrho L, L]$) twice continuously differentiable on $[0,\varrho L]$ (resp. $[\varrho L, L]$) and
- $w_2 \neq 0$ or $\phi_1 \neq 0$,

satisfying the differential equations

$$\left(EI_3(x_1)\, w_2''(x_1)\right)'' + \left(M_2^f(x_1,\lambda_1,\lambda_2)\, \phi_1(x_1)\right)'' = 0 \tag{5.6.9}$$

$$\left(GJ(x_1)\, \phi_1'(x_1)\right)' - M_2^f(x_1,\lambda_1,\lambda_2)\, w_2''(x_1) = 0 \tag{5.6.10}$$

on each open interval $(0, \varrho L)$ and $(\varrho L, L)$, together with the boundary conditions

$$w_2(0) = 0 \tag{5.6.11}$$

$$w_2'(0) = 0 \tag{5.6.12}$$

$$\phi_1(0) = 0 \tag{5.6.13}$$

$$\alpha\, EI_3(0)\, w_2''(L) = 0 \tag{5.6.14}$$

$$\alpha\, EI_3(0)\, w_2'''(L) - EI_3(0) \frac{\beta - \alpha}{(1-\varrho)L}\, w_2''(L) + \lambda_1\, Q_{ref}\, \phi_1(L) = 0 \tag{5.6.15}$$

$$\alpha\, GJ(0)\, \phi_1'(L) + \lambda_1\, Q_{ref}\, x_3^{Q_1}\, \phi_1(L) = 0 \tag{5.6.16}$$

and the jump conditions

$$\beta\, EI_3(0)\left(w_{2+}''(\varrho L) - w_{2-}''(\varrho L)\right) = 0 \tag{5.6.17}$$

$$\beta\, EI_3(0)\left(w_{2+}'''(\varrho L) - w_{2-}'''(\varrho L)\right) - EI_3(0)\left(\frac{\beta-\alpha}{(1-\varrho)L} w_{2+}''(\varrho L) - \frac{1-\beta}{\varrho L} w_{2-}''(\varrho L)\right)$$

$$-\lambda_1\, Q_{ref}\, (1-\varrho)\, L\left(\phi_{1+}'(\varrho L) - \phi_{1-}'(\varrho L)\right) - \lambda_2\, Q_{ref}\, \phi_1(\varrho L) = 0 \tag{5.6.18}$$

$$\beta\, GJ(0)\left(\phi_{1+}'(\varrho L) - \phi_{1-}'(\varrho L)\right) - \lambda_2\, Q_{ref}\, x_3^{Q_2}\, \phi_1(\varrho L) = 0\ . \tag{5.6.19}$$

From a mathematical viewpoint, Problem 5.6 is a two-parameter eigenproblem – an eigenvalue is an ordered pair $(\lambda_1, \lambda_2) \in \mathbb{R}_0^+ \times \mathbb{R}_0^+$ for which there exist functions w_2 and ϕ_1 with the specified smoothness, not both identically zero, that satisfy (5.6.9)-(5.6.19). In fact, we shall consider only eigenvalues with $\lambda_1 > 0$. Indeed, (i) it can be seen by direct inspection that $(0, 0)$ is not an eigenvalue and (ii) eigenvalues of the form $(0, \lambda_2)$, with $\lambda_2 > 0$, can be found by ignoring the unloaded segment, which merely undergoes a rigid-body displacement – the problem reduces itself to that of a tip-loaded, linearly tapered cantilever with length ϱL and taper ratio β, already discussed.

The question now arises whether it is again possible to eliminate w_2 from the buckling problem. We shall see that the answer is affirmative. From (i) the differential equation (5.6.9), which holds on $(0, \varrho L)$ and $(\varrho L, L)$, (ii) the smoothness required of the functions w_2 and ϕ_1, (iii) the boundary conditions (5.6.14)-(5.6.15) and (iv) the jump conditions (5.6.17)-(5.6.18), one infers that w_2 is twice continuously differentiable on $[0, L]$ and, on this interval, w_2'' is related to ϕ_1 through

$$w_2''(x_1) = -\frac{M_2^f(x_1, \lambda_1, \lambda_2)}{EI_3(x_1)} \phi_1(x_1) \ . \tag{5.6.20}$$

Moreover, when taken together with (5.6.11)-(5.6.12), this equation shows that $\phi_1 = 0$ implies $w_2 = 0$. Therefore, as in § 5.2, the buckling problem can be written in terms of the single dependent variable ϕ_1.

The above considerations lead to the replacement of Problem 5.6 with:

Problem 5.7.

Find $\lambda_1 \in \mathbb{R}^+$, $\lambda_2 \in \mathbb{R}_0^+$ and $\phi_1 : [0, L] \to \mathbb{R}$, with

- ϕ_1 continuous on $[0, L]$,
- $\phi_{1-} = \phi_1 \big| [0, \varrho L]$ (resp. $\phi_{1+} = \phi_1 \big| [\varrho L, L]$) twice continuously differentiable on $[0, \varrho L]$ (resp. on $[\varrho L, L]$) and
- $\phi_1 \neq 0$,

satisfying the differential equation

$$\left(GJ(x_1)\phi_1'(x_1)\right)' + \frac{M_2^f(x_1, \lambda_1, \lambda_2)^2}{EI_3(x_1)} \phi_1(x_1) = 0 \tag{5.6.21}$$

on each open interval $(0, \varrho L)$ and $(\varrho L, L)$, together with the boundary conditions

$$\phi_1(0) = 0 \tag{5.6.22}$$

$$\alpha GJ(0)\,\phi_1'(L)+\lambda_1 Q_{ref}\,x_3^{Q_1}\,\phi_1(L)=0 \tag{5.6.23}$$

and the jump condition

$$\beta GJ(0)\big(\phi_{1+}'(\varrho L)-\phi_{1-}'(\varrho L)\big)-\lambda_2 Q_{ref}\,x_3^{Q_2}\,\phi_1(\varrho L)=0\ . \tag{5.6.24}$$

Once an eigenvalue (λ_1,λ_2) and a corresponding eigenfunction component ϕ_1 are known, the remaining eigenfunction component w_2 can be obtained by solving the initial value problem formed by (5.6.20) and (5.6.11)-(5.6.12).

Four different cases can be distinguished in Problem 5.7 according to the shape of the cantilever (that is, according to the type of function h):

(i) prismatic cantilever ($\alpha=\beta=1$);

(ii) cantilever whose depth is a strictly decreasing function of the distance to the support ($0<\alpha<\beta<1$);

(iii) cantilever consisting of a depth-tapered segment adjacent to the support, followed by a prismatic segment ($0<\alpha=\beta<1$);

(iv) cantilever consisting of a prismatic segment adjacent to the support, followed by a depth- tapered segment ($0<\alpha<\beta=1$).

Case (i) was thoroughly analysed in CHALLAMEL & WANG (2010) and will not be addressed here. Case (ii) will be discussed in detail. It includes, as a special instance, the case of a linearly tapered cantilever subjected to intermediate and tip forces – β ceases to be an independent parameter, being given in terms of α and ϱ by $\beta=1-(1-\alpha)\varrho$. For cases (iii) and (iv), only a brief sketch of the solution will be presented.

5.6.1 The case $0<\alpha<\beta<1$

We begin by casting Problem 5.7, restricted so as to have $0<\alpha<\beta<1$ (see figure 5.6.1), in non-dimensional form. To this end, consider the homeomorphism $f:[0,L]\to[\alpha,1]$ defined by

$$f(x_1)=\begin{cases}1-(1-\beta)\dfrac{x_1}{\varrho L} & \text{if } 0\le x_1\le \varrho L\\[2ex] \beta-(\beta-\alpha)\dfrac{x_1-\varrho L}{(1-\varrho)L} & \text{if } \varrho L\le x_1\le L\end{cases} \tag{5.6.25}$$

and let $s=f(x_1)$ denote the associated change of independent variable. Observe that the restriction of f to $[0,\varrho L]$ (resp. to $[\varrho L,L]$) is a real analytic diffeomorphism onto

$[\beta, 1]$ (resp. $[\alpha, \beta]$). Define $\tilde{\phi} : [\alpha, 1] \to \mathbb{R}$ such that $\phi_1 = \tilde{\phi} \circ f$ and let $\tilde{\phi}_-$ (resp. $\tilde{\phi}_+$) denote the restriction of $\tilde{\phi}$ to $[\alpha, \beta]$ (resp. $[\beta, 1]$).[22] Clearly, ϕ_1 is continuous on $[0, L]$ if and only if $\tilde{\phi}$ is continuous on $[\alpha, 1]$. Moreover, $\phi_{1-} = \phi_1 \big| [0, \varrho L]$ (resp. $\phi_{1+} = \phi_1 \big| [\varrho L, L]$) is twice continuously differentiable on $[0, \varrho L]$ (resp. $[\varrho L, L]$) if and only if $\tilde{\phi}_+ = \tilde{\phi} \big| [\beta, 1]$ (resp. $\tilde{\phi}_- = \tilde{\phi} \big| [\alpha, \beta]$) is twice continuously differentiable on $[\beta, 1]$ (resp. $[\alpha, \beta]$), with the chain rule yielding

$$\phi'_{1-}(x_1) = -\frac{1-\beta}{\varrho L} \tilde{\phi}'_+(s) \tag{5.6.26}$$

$$\phi'_{1+}(x_1) = -\frac{\beta-\alpha}{(1-\varrho) L} \tilde{\phi}'_-(s) \tag{5.6.27}$$

$$\phi''_{1-}(x_1) = \left(\frac{1-\beta}{\varrho L} \right)^2 \tilde{\phi}''_+(s) \tag{5.6.28}$$

$$\phi''_{1+}(x_1) = \left(\frac{\beta-\alpha}{(1-\varrho) L} \right)^2 \tilde{\phi}''_-(s) \ . \tag{5.6.29}$$

Then, with the introduction of the non-dimensional loads

$$\gamma_1 = \frac{\lambda_1 Q_{ref} L^2}{\sqrt{EI_3(0) GJ(0)}} \qquad \gamma_2 = \frac{\lambda_2 Q_{ref} L^2}{\sqrt{EI_3(0) GJ(0)}} \ , \tag{5.6.30}$$

the load position parameters

$$\varepsilon_1 = \frac{x_3^{Q_1}}{\alpha L} \sqrt{\frac{EI_3(0)}{GJ(0)}} \qquad \varepsilon_2 = \frac{x_3^{Q_2}}{\beta L} \sqrt{\frac{EI_3(0)}{GJ(0)}} \tag{5.6.31}$$

and the shorthand symbol

$$\overline{\beta} = 1 - \frac{1-\beta}{\varrho} \ ,^{23} \tag{5.6.32}$$

Problem 5.7, with $0 < \alpha < \beta < 1$, is brought into the following form:

---

[22] The subscripts "$-$" and "$+$" have therefore slightly different meanings (but the same underlying spirit) when applied to functions defined on different intervals. This is unlikely to cause confusion.

[23] Recall that the continuous function $x_1 \mapsto h(x_1)$ is defined in equation (5.6.1) by two expressions, one valid for $0 \le x_1 \le \varrho L$ and the other for $\varrho L \le x_1 \le L$. Suppose now that the domain of validity of the former expression is extended to the whole interval $[0, L]$ (and the codomain of h is extended to $\mathbb{R}$) – then one would have $h(L) = \overline{\beta} h_0$. Clearly, it is possible to have $\overline{\beta} \le 0$.

Problem 5.8.

Find scalars $\gamma_1 \in \mathbb{R}^+$, $\gamma_2 \in \mathbb{R}_0^+$ and functions $\tilde{\phi}_- : [\alpha, \beta] \to \mathbb{R}$, $\tilde{\phi}_+ : [\beta, 1] \to \mathbb{R}$, with

- $\tilde{\phi}_- \in C^2[\alpha, \beta]$,
- $\tilde{\phi}_+ \in C^2[\beta, 1]$ and
- $\tilde{\phi}_- \neq 0$ or $\tilde{\phi}_+ \neq 0$,

satisfying

$$\tilde{\phi}_-''(s) + \frac{1}{s}\tilde{\phi}_-'(s) + \frac{(1-\varrho)^4 \gamma_1^2}{(\beta-\alpha)^4}\left(1 - \frac{2\alpha}{s} + \frac{\alpha^2}{s^2}\right)\tilde{\phi}_-(s) = 0 \tag{5.6.33}$$

on (α, β),

$$\tilde{\phi}_+''(s) + \frac{1}{s}\tilde{\phi}_+'(s) + \frac{\varrho^4}{(1-\beta)^4}\left[(\gamma_1+\gamma_2)^2 - \frac{2(\gamma_1+\gamma_2)(\overline{\beta}\gamma_1+\beta\gamma_2)}{s} + \frac{(\overline{\beta}\gamma_1+\beta\gamma_2)^2}{s^2}\right]\tilde{\phi}_+(s) = 0 \tag{5.6.34}$$

on $(\beta, 1)$ and

$$\tilde{\phi}_-'(\alpha) - \frac{\varepsilon_1(1-\varrho)\gamma_1}{\beta-\alpha}\tilde{\phi}_-(\alpha) = 0 \tag{5.6.35}$$

$$\tilde{\phi}_+(1) = 0 \tag{5.6.36}$$

$$\tilde{\phi}_+(\beta) - \tilde{\phi}_-(\beta) = 0\ . \tag{5.6.37}$$

$$(1-\overline{\beta})\tilde{\phi}_+'(\beta) - \frac{\beta-\alpha}{1-\varrho}\tilde{\phi}_-'(\beta) - \varepsilon_2\gamma_2\,\tilde{\phi}_-(\beta) = 0\ . \tag{5.6.38}$$

Observe that (5.6.37) ensures that the function $\tilde{\phi}$ defined by piecing together $\tilde{\phi}_-$ and $\tilde{\phi}_+$ (that is, $\tilde{\phi} : [\alpha, 1] \to \mathbb{R}$ is defined by setting $\tilde{\phi}(s) = \tilde{\phi}_-(s)$ if $s \in [\alpha, \beta]$ and $\tilde{\phi}(s) = \tilde{\phi}_+(s)$ if $s \in [\beta, 1]$) is meaningful. Moreover, it is continuous (see the "pasting lemma" in MUNKRES 2000, pp. 108-109).

The differential equations (5.6.33) and (5.6.34) are of the same form as (5.4.5) and they are likewise reducible to Kummer's equation (5.4.20) in the manner described in the paragraph following equation (5.4.7). The parameters involved in the relevant changes of variables are given in table 5.6.1, using the notation of the said paragraph. Since the parameter A_0 in both columns of this table is never zero, the reduction processes for equations (5.6.33) and (5.6.34) are always well-defined.

Reduction of (5.6.33) to Kummer's equation	Reduction of (5.6.34) to Kummer's equation
$\sigma = i\,\dfrac{(1-\varrho)^2\alpha\gamma_1}{(\beta-\alpha)^2}$	$\sigma = i\,\dfrac{\varrho^2(\overline{\beta}\gamma_1+\beta\gamma_2)}{(1-\beta)^2}$
$\tau = B_1 = -i\,\dfrac{(1-\varrho)^2\gamma_1}{(\beta-\alpha)^2}$	$\tau = B_1 = -i\,\dfrac{\varrho^2(\gamma_1+\gamma_2)}{(1-\beta)^2}$
$A_0 = -i\,\dfrac{2(1-\varrho)^2\gamma_1}{(\beta-\alpha)^2} \quad (\neq 0)$	$A_0 = -i\,\dfrac{2\varrho^2(\gamma_1+\gamma_2)}{(1-\beta)^2} \quad (\neq 0)$
$b = B_0 = 1+i\,\dfrac{2(1-\varrho)^2\alpha\gamma_1}{(\beta-\alpha)^2} \quad (\notin \mathbb{Z}_0^-)$	$b = B_0 = 1+i\,\dfrac{2\varrho^2(\overline{\beta}\gamma_1+\beta\gamma_2)}{(1-\beta)^2} \quad (\notin \mathbb{Z}_0^-)$
$A_1 = C_1 = 0$	$A_1 = C_1 = 0$
$a = \dfrac{1}{2}$	$a = \dfrac{1}{2}$

Table 5.6.1: Parameters involved in the reduction of equations (5.6.33) and (5.6.34) to Kummer's equation

One now turns to the general solution of Kummer's equation with parameters a and b as given in the above table. As in § 5.4, Kummer's function $z \mapsto M(a,b,z)$ is always well-defined (since $b \notin \mathbb{Z}_0^-$) and can be adopted for member of a fundamental pair of solutions. However, unlike the situation in § 5.4, we may have $b=1$ in the second column of table 5.6.1 (when $\overline{\beta}\gamma_1+\beta\gamma_2=0$), in which case $z^{1-b}M(1+a-b,2-b,z)$ fails to provide a suitable second independent solution – indeed, $M(a,b,z)=z^{1-b}M(1+a-b,2-b,z)$ if $b=1$. In order to treat every possible case in a unified manner, the principal branch $z \mapsto U(a,b,z)$, $z \in \mathbb{C}\setminus(-\infty,0]$, of Tricomi's function is chosen as the second independent solution to Kummer's equation (*vide supra*, note 21) – on the one hand, the definition of $U(a,b,z)$ places no restriction whatsoever on the complex parameters a and b; on the other hand, $M(a,b,z)$ and $U(a,b,z)$ are linearly independent when $a \neq 0,-1,-2,\cdots$ and, in addition, they form a numerically satisfactory pair of solutions when $\mathrm{Re}(b) \geq 1$ and $\mathrm{Re}(z) \geq 0$ (OLVER 1974, p. 259), which is always the case.

The general solutions of the differential equations (5.6.33) and (5.6.34), on (α,β) and $(\beta,1)$, respectively, can therefore be written as

$$\tilde{\phi}_-(s) = s^{i\frac{(1-\varrho)^2\alpha\gamma_1}{(\beta-\alpha)^2}} e^{-i\frac{(1-\varrho)^2\gamma_1}{(\beta-\alpha)^2}s}\left[c_1 M\left(\frac{1}{2}, 1+i\frac{2(1-\varrho)^2\alpha\gamma_1}{(\beta-\alpha)^2}, i\frac{2(1-\varrho)^2\gamma_1}{(\beta-\alpha)^2}s\right)\right.$$
$$\left. + c_2 U\left(\frac{1}{2}, 1+i\frac{2(1-\varrho)^2\alpha\gamma_1}{(\beta-\alpha)^2}, i\frac{2(1-\varrho)^2\gamma_1}{(\beta-\alpha)^2}s\right)\right] \qquad (5.6.39)$$

$$\tilde{\phi}_+(s) = s^{i\frac{\varrho^2(\overline{\beta}\gamma_1+\beta\gamma_2)}{(1-\beta)^2}} e^{-i\frac{\varrho^2(\gamma_1+\gamma_2)}{(1-\beta)^2}s}\left[c_3 M\left(\frac{1}{2}, 1+i\frac{2\varrho^2(\overline{\beta}\gamma_1+\beta\gamma_2)}{(1-\beta)^2}, i\frac{2\varrho^2(\gamma_1+\gamma_2)}{(1-\beta)^2}s\right)\right.$$
$$\left. + c_4 U\left(\frac{1}{2}, 1+i\frac{2\varrho^2(\overline{\beta}\gamma_1+\beta\gamma_2)}{(1-\beta)^2}, i\frac{2\varrho^2(\gamma_1+\gamma_2)}{(1-\beta)^2}s\right)\right], \qquad (5.6.40)$$

with $c_k \in \mathbb{C}$, $k = 1, \cdots, 4$.

By continuity, it is easily seen that equation (5.6.39) (resp. (5.6.40)) must also hold at $s = \alpha$ and $s = \beta$ (resp. $s = \beta$ and $s = 1$). It thereby defines the family of functions on $[\alpha, \beta]$ (resp. $[\beta, 1]$) whose members (i) are twice continuously differentiable on $[\alpha, \beta]$ (resp. $[\beta, 1]$) – in fact, real analytic on $[\alpha, \beta]$ (resp. $[\beta, 1]$) – and (ii) satisfy the differential equation (5.6.33) (resp. (5.6.34)) on (α, β) (resp. $(\beta, 1)$). The differentiation formulae (5.4.36) and (*e.g.*, DAALHUIS 2010, eq. (13.3.22))

$$\frac{d}{dz}U(a, b, z) = -aU(a+1, b+1, z) \quad , \; z \in \mathbb{C} \setminus (-\infty, 0] \, , \qquad (5.6.41)$$

now yield

$$\tilde{\phi}_-'(s) = i\frac{(1-\varrho)^2\gamma_1}{(\beta-\alpha)^2} s^{i\frac{(1-\varrho)^2\alpha\gamma_1}{(\beta-\alpha)^2}} e^{-i\frac{(1-\varrho)^2\gamma_1}{(\beta-\alpha)^2}s}\left\{c_1\left[\left(\frac{\alpha}{s}-1\right)M\left(\frac{1}{2}, 1+i\frac{2(1-\varrho)^2\alpha\gamma_1}{(\beta-\alpha)^2}, i\frac{2(1-\varrho)^2\gamma_1}{(\beta-\alpha)^2}s\right)\right.\right.$$
$$\left. + \frac{1}{1+i\frac{2(1-\varrho)^2\alpha\gamma_1}{(\beta-\alpha)^2}} M\left(\frac{3}{2}, 2+i\frac{2(1-\varrho)^2\alpha\gamma_1}{(\beta-\alpha)^2}, i\frac{2(1-\varrho)^2\gamma_1}{(\beta-\alpha)^2}s\right)\right]$$
$$+ c_2\left[\left(\frac{\alpha}{s}-1\right)U\left(\frac{1}{2}, 1+i\frac{2(1-\varrho)^2\alpha\gamma_1}{(\beta-\alpha)^2}, i\frac{2(1-\varrho)^2\gamma_1}{(\beta-\alpha)^2}s\right)\right.$$
$$\left.\left. - U\left(\frac{3}{2}, 2+i\frac{2(1-\varrho)^2\alpha\gamma_1}{(\beta-\alpha)^2}, i\frac{2(1-\varrho)^2\gamma_1}{(\beta-\alpha)^2}s\right)\right]\right\} \quad , \; \alpha \le s \le \beta \, . \qquad (5.6.42)$$

$$\tilde{\phi}_+'(s) = i\frac{\varrho^2}{(1-\beta)^2}\, s^{\,i\frac{\varrho^2(\bar{\beta}\gamma_1+\beta\gamma_2)}{(1-\beta)^2}}\, e^{-i\frac{\varrho^2(\gamma_1+\gamma_2)}{(1-\beta)^2}s}$$

$$\times\left\{c_3\left[\left(\frac{\bar{\beta}\gamma_1+\beta\gamma_2}{s}-(\gamma_1+\gamma_2)\right)M\left(\frac{1}{2},1+i\frac{2\varrho^2(\bar{\beta}\gamma_1+\beta\gamma_2)}{(1-\beta)^2},i\frac{2\varrho^2(\gamma_1+\gamma_2)}{(1-\beta)^2}s\right)\right.\right.$$

$$\left.+\frac{\gamma_1+\gamma_2}{1+i\dfrac{2\varrho^2(\bar{\beta}\gamma_1+\beta\gamma_2)}{(1-\beta)^2}}M\left(\frac{3}{2},2+i\frac{2\varrho^2(\bar{\beta}\gamma_1+\beta\gamma_2)}{(1-\beta)^2},i\frac{2\varrho^2(\gamma_1+\gamma_2)}{(1-\beta)^2}s\right)\right]$$

$$+c_4\left[\left(\frac{\bar{\beta}\gamma_1+\beta\gamma_2}{s}-(\gamma_1+\gamma_2)\right)U\left(\frac{1}{2},1+i\frac{2\varrho^2(\bar{\beta}\gamma_1+\beta\gamma_2)}{(1-\beta)^2},i\frac{2\varrho^2(\gamma_1+\gamma_2)}{(1-\beta)^2}s\right)\right.$$

$$\left.\left.-(\gamma_1+\gamma_2)\,U\left(\frac{3}{2},2+i\frac{2\varrho^2(\bar{\beta}\gamma_1+\beta\gamma_2)}{(1-\beta)^2},i\frac{2\varrho^2(\gamma_1+\gamma_2)}{(1-\beta)^2}s\right)\right]\right\}\quad,\ \beta\le s\le 1\ . \tag{5.6.43}$$

The substitution of (5.6.39)-(5.6.40) and (5.6.42)-(5.6.43) into the boundary and jump conditions (5.6.35)-(5.6.38) leads to the linear system

$$a_{kl}\,c_l = 0 \quad (k,l=1,\cdots,4) \tag{5.6.44}$$

with coefficients

$$a_{11} = \frac{1}{\dfrac{2(1-\varrho)^2\alpha\gamma_1}{(\beta-\alpha)^2}-i}M\left(\frac{3}{2},2+i\frac{2(1-\varrho)^2\alpha\gamma_1}{(\beta-\alpha)^2},i\frac{2(1-\varrho)^2\alpha\gamma_1}{(\beta-\alpha)^2}\right)$$

$$-\frac{\varepsilon_1(\beta-\alpha)}{1-\varrho}M\left(\frac{1}{2},1+i\frac{2(1-\varrho)^2\alpha\gamma_1}{(\beta-\alpha)^2},i\frac{2(1-\varrho)^2\alpha\gamma_1}{(\beta-\alpha)^2}\right) \tag{5.6.45}$$

$$a_{12} = -i\,U\left(\frac{3}{2},2+i\frac{2(1-\varrho)^2\alpha\gamma_1}{(\beta-\alpha)^2},i\frac{2(1-\varrho)^2\alpha\gamma_1}{(\beta-\alpha)^2}\right)$$

$$-\frac{\varepsilon_1(\beta-\alpha)}{1-\varrho}U\left(\frac{1}{2},1+i\frac{2(1-\varrho)^2\alpha\gamma_1}{(\beta-\alpha)^2},i\frac{2(1-\varrho)^2\alpha\gamma_1}{(\beta-\alpha)^2}\right) \tag{5.6.46}$$

$$a_{13} = a_{14} = a_{21} = a_{22} = 0 \tag{5.6.47}$$

$$a_{23} = M\left(\frac{1}{2},1+i\frac{2\varrho^2(\bar{\beta}\gamma_1+\beta\gamma_2)}{(1-\beta)^2},i\frac{2\varrho^2(\gamma_1+\gamma_2)}{(1-\beta)^2}\right) \tag{5.6.48}$$

$$a_{24} = U\left(\frac{1}{2},1+i\frac{2\varrho^2(\bar{\beta}\gamma_1+\beta\gamma_2)}{(1-\beta)^2},i\frac{2\varrho^2(\gamma_1+\gamma_2)}{(1-\beta)^2}\right) \tag{5.6.49}$$

$$a_{31} = \beta^{\,i\frac{(1-\varrho)^2\alpha\gamma_1}{(\beta-\alpha)^2}}\, e^{-i\frac{(1-\varrho)^2\beta\gamma_1}{(\beta-\alpha)^2}}\, M\left(\frac{1}{2},1+i\frac{2(1-\varrho)^2\alpha\gamma_1}{(\beta-\alpha)^2},i\frac{2(1-\varrho)^2\beta\gamma_1}{(\beta-\alpha)^2}\right) \tag{5.6.50}$$

$$a_{32}=\beta^{i\frac{(1-\varrho)^2\alpha\gamma_1}{(\beta-\alpha)^2}}e^{-i\frac{(1-\varrho)^2\beta\gamma_1}{(\beta-\alpha)^2}}U\left(\frac{1}{2},1+i\frac{2(1-\varrho)^2\alpha\gamma_1}{(\beta-\alpha)^2},i\frac{2(1-\varrho)^2\beta\gamma_1}{(\beta-\alpha)^2}\right)\Bigg] \tag{5.6.51}$$

$$a_{33}=-\beta^{i\frac{\varrho^2(\overline{\beta}\gamma_1+\beta\gamma_2)}{(1-\beta)^2}}e^{-i\frac{\varrho^2\beta(\gamma_1+\gamma_2)}{(1-\beta)^2}}M\left(\frac{1}{2},1+i\frac{2\varrho^2(\overline{\beta}\gamma_1+\beta\gamma_2)}{(1-\beta)^2},i\frac{2\varrho^2\beta(\gamma_1+\gamma_2)}{(1-\beta)^2}\right) \tag{5.6.52}$$

$$a_{34}=-\beta^{i\frac{\varrho^2(\overline{\beta}\gamma_1+\beta\gamma_2)}{(1-\beta)^2}}e^{-i\frac{\varrho^2\beta(\gamma_1+\gamma_2)}{(1-\beta)^2}}U\left(\frac{1}{2},1+i\frac{2\varrho^2(\overline{\beta}\gamma_1+\beta\gamma_2)}{(1-\beta)^2},i\frac{2\varrho^2\beta(\gamma_1+\gamma_2)}{(1-\beta)^2}\right) \tag{5.6.53}$$

$$a_{41}=\beta^{i\frac{(1-\varrho)^2\alpha\gamma_1}{(\beta-\alpha)^2}}e^{-i\frac{(1-\varrho)^2\beta\gamma_1}{(\beta-\alpha)^2}}\Bigg[\varepsilon_2\gamma_2\,M\left(\frac{1}{2},1+i\frac{2(1-\varrho)^2\alpha\gamma_1}{(\beta-\alpha)^2},i\frac{2(1-\varrho)^2\beta\gamma_1}{(\beta-\alpha)^2}\right)$$
$$+\frac{(1-\varrho)\gamma_1}{(\beta-\alpha)\left(\frac{2(1-\varrho)^2\alpha\gamma_1}{(\beta-\alpha)^2}-i\right)}M\left(\frac{3}{2},2+i\frac{2(1-\varrho)^2\alpha\gamma_1}{(\beta-\alpha)^2},i\frac{2(1-\varrho)^2\beta\gamma_1}{(\beta-\alpha)^2}\right)\Bigg] \tag{5.6.54}$$

$$a_{42}=\beta^{i\frac{(1-\varrho)^2\alpha\gamma_1}{(\beta-\alpha)^2}}e^{-i\frac{(1-\varrho)^2\beta\gamma_1}{(\beta-\alpha)^2}}\Bigg[\varepsilon_2\gamma_2\,U\left(\frac{1}{2},1+i\frac{2(1-\varrho)^2\alpha\gamma_1}{(\beta-\alpha)^2},i\frac{2(1-\varrho)^2\beta\gamma_1}{(\beta-\alpha)^2}\right)$$
$$-i\frac{(1-\varrho)\gamma_1}{(\beta-\alpha)}U\left(\frac{3}{2},2+i\frac{2(1-\varrho)^2\alpha\gamma_1}{(\beta-\alpha)^2},i\frac{2(1-\varrho)^2\beta\gamma_1}{(\beta-\alpha)^2}\right)\Bigg] \tag{5.6.55}$$

$$a_{43}=-\frac{\varrho(\gamma_1+\gamma_2)}{(1-\beta)\left(\frac{2\varrho^2(\overline{\beta}\gamma_1+\beta\gamma_2)}{(1-\beta)^2}-i\right)}\beta^{i\frac{\varrho^2(\overline{\beta}\gamma_1+\beta\gamma_2)}{(1-\beta)^2}}e^{-i\frac{\varrho^2\beta(\gamma_1+\gamma_2)}{(1-\beta)^2}}$$
$$\times M\left(\frac{3}{2},2+i\frac{2\varrho^2(\overline{\beta}\gamma_1+\beta\gamma_2)}{(1-\beta)^2},i\frac{2\varrho^2\beta(\gamma_1+\gamma_2)}{(1-\beta)^2}\right) \tag{5.6.56}$$

$$a_{44}=i\frac{\varrho(\gamma_1+\gamma_2)}{1-\beta}\beta^{i\frac{\varrho^2(\overline{\beta}\gamma_1+\beta\gamma_2)}{(1-\beta)^2}}e^{-i\frac{\varrho^2\beta(\gamma_1+\gamma_2)}{(1-\beta)^2}}U\left(\frac{3}{2},2+i\frac{2\varrho^2(\overline{\beta}\gamma_1+\beta\gamma_2)}{(1-\beta)^2},i\frac{2\varrho^2\beta(\gamma_1+\gamma_2)}{(1-\beta)^2}\right)\Bigg]\,. \tag{5.6.57}$$

As in § 5.5, the system (5.6.44), with complex coefficients and unknowns, is unfolded into

$$\begin{cases}\mathrm{Re}(a_{kl})\,\mathrm{Re}(c_l)-\mathrm{Im}(a_{kl})\,\mathrm{Im}(c_l)=0\\ \mathrm{Im}(a_{kl})\,\mathrm{Re}(c_l)+\mathrm{Re}(a_{kl})\,\mathrm{Im}(c_l)=0\end{cases}\quad(k,l=1,\cdots,4)\,. \tag{5.6.58}$$

The characteristic equation for the eigenvalues of Problem 5.8 is now obtained by equating to zero the determinant of the coefficient matrix of (5.6.58), which is a necessary and sufficient condition for this system to have non-trivial solutions – and thus for having

$\tilde{\phi}_- \neq 0$ or $\tilde{\phi}_+ \neq 0$. Given α, β, ϱ, ε_1 and ε_2, the characteristic equation defines a family of curves in (the first quadrant of) the non-dimensional load plane (γ_1, γ_2). Amongst these curves, the most important from a practical standpoint is that which is first intersected by a ray emanating from the origin, called the "stability boundary" (HUSEYIN 1970, 1978, § 2.5) or "buckling envelope" (CHILVER 1972, p. 54).

The stability boundary of linear, conservative systems such as those under examination in this work cannot have convexity towards the origin. This general result, which was first established independently by PAPKOVITCH (1934) and SCHAEFER (1934), is based on the extremum properties of the Rayleigh quotient and applies to finite-dimensional and continuous systems alike.[24] Its usefulness lies in the ability to construct polygonal lower bounds to the stability boundary once a number of points on it are known.

5.6.2 The case $0 < \alpha = \beta < 1$

The scope of Problem 5.7 is now limited by the restriction $0 < \alpha = \beta < 1$. We will thus be looking at cantilevers consisting of a depth-tapered segment adjacent to the support and a prismatic segment, with forces applied at the tip and at the junction between the two segments (see figure 5.6.2).

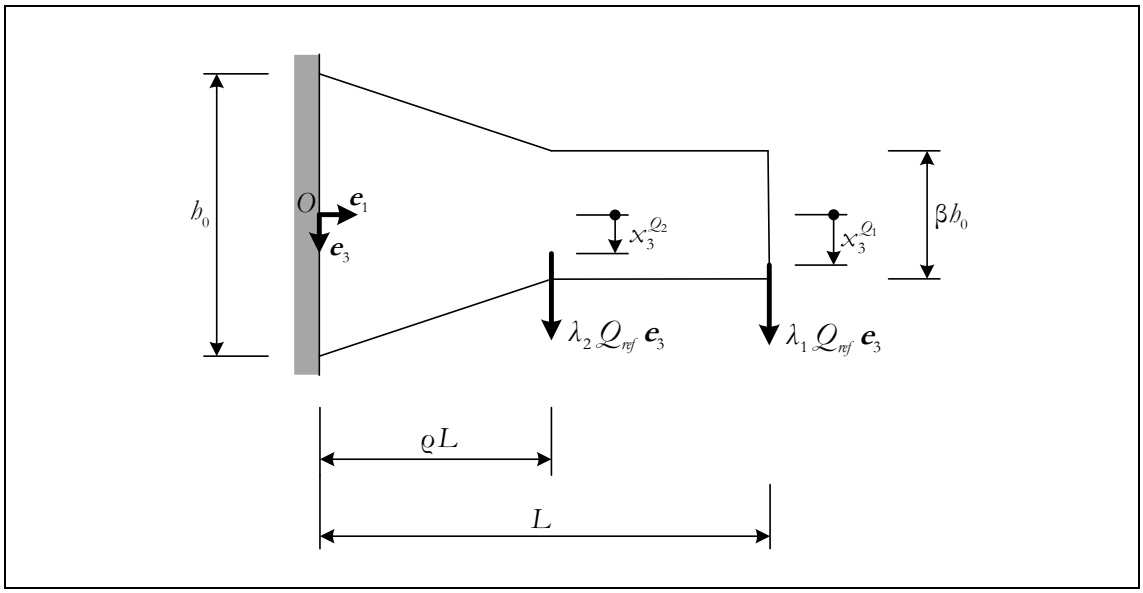

Figure 5.6.2: Two-segment strip cantilever with $0 < \alpha = \beta < 1$

[24] It can also be viewed as a corollary to a theorem obtained by HUSEYIN & ROORDA (1971) for finite-dimensional dynamical systems and extended to continuous systems by MASUR (1972).

Consider the homeomorphism $f:[0,L]\to[0,1]$ defined by

$$f(x_1)=\begin{cases}1-(1-\beta)\dfrac{x_1}{\varrho L} & \text{if } 0\le x_1\le \varrho L\\[2ex] \beta-\beta\dfrac{x_1-\varrho L}{(1-\varrho)L} & \text{if } \varrho L\le x_1\le L\end{cases} \tag{5.6.59}$$

and let $s=f(x_1)$ denote the associated change of independent variable. Moreover, define $\tilde{\phi}:[0,1]\to\mathbb{R}$ such that $\phi_1=\tilde{\phi}\circ f$ (that is, $\tilde{\phi}=\phi_1\circ f^{-1}$) and denote its restrictions to $[0,\beta]$ and to $[\beta,1]$ by $\tilde{\phi}_-$ and $\tilde{\phi}_+$, respectively. Finally, define the parameters γ_1, γ_2, ε_1, ε_2 and $\overline{\beta}$ as in (5.6.30)-(5.6.32) – with $\alpha=\beta$, of course. It is then a simple matter to see that the restricted Problem 5.7 can be cast in the following non-dimensional form:

Problem 5.9.

Find scalars $\gamma_1\in\mathbb{R}^+$, $\gamma_2\in\mathbb{R}_0^+$ and functions $\tilde{\phi}_-:[0,\beta]\to\mathbb{R}$, $\tilde{\phi}_+:[\beta,1]\to\mathbb{R}$, with

- $\tilde{\phi}_-\in C^2[0,\beta]$,
- $\tilde{\phi}_+\in C^2[\beta,1]$ and
- $\tilde{\phi}_-\neq 0$ or $\tilde{\phi}_+\neq 0$,

satisfying

$$\tilde{\phi}_-''(s)+\frac{(1-\varrho)^4\gamma_1^2}{\beta^6}s^2\,\tilde{\phi}_-(s)=0 \tag{5.6.60}$$

on $(0,\beta)$,

$$\tilde{\phi}_+''(s)+\frac{1}{s}\tilde{\phi}_+'(s)+\frac{\varrho^4}{(1-\beta)^4}\left[(\gamma_1+\gamma_2)^2-\frac{2(\gamma_1+\gamma_2)(\overline{\beta}\gamma_1+\beta\gamma_2)}{s}\right.$$

$$\left.+\frac{(\overline{\beta}\gamma_1+\beta\gamma_2)^2}{s^2}\right]\tilde{\phi}_+(s)=0 \tag{5.6.61}$$

on $(\beta,1)$ and

$$\tilde{\phi}_-'(0)-\frac{\varepsilon_1(1-\varrho)\gamma_1}{\beta}\tilde{\phi}_-(0)=0 \tag{5.6.62}$$

$$\tilde{\phi}_+(1)=0 \tag{5.6.63}$$

$$\tilde{\phi}_+(\beta)-\tilde{\phi}_-(\beta)=0\ . \tag{5.6.64}$$

$$\left((1-\overline{\beta})\tilde{\phi}_+'(\beta)-\frac{\beta}{1-\varrho}\tilde{\phi}_-'(\beta)\right)-\varepsilon_2\gamma_2\,\tilde{\phi}_-(\beta)=0\ . \tag{5.6.65}$$

Equation (5.6.60) is of the same form as (5.3.8). Its general solution on $(0,\beta)$ is

$$\tilde{\phi}_{-}(s)=\sqrt{s}\left(c_1 J_{\frac{1}{4}}\left(\frac{(1-\varrho)^2\gamma_1}{2\beta^3}s^2\right)+c_2 Y_{\frac{1}{4}}\left(\frac{(1-\varrho)^2\gamma_1}{2\beta^3}s^2\right)\right), \tag{5.6.66}$$

with $\gamma_1>0$ and $c_1, c_2\in\mathbb{R}$. Using (5.3.19) and (5.3.20), this can be rewritten as

$$\tilde{\phi}_{-}(s)=(c_1+c_2)\sum_{n=0}^{+\infty}\frac{(-1)^n}{n!\,\Gamma\left(n+\frac{5}{4}\right)}\left(\frac{(1-\varrho)^2\gamma_1}{4\beta^3}\right)^{2n+\frac{1}{4}}s^{4n+1}$$

$$-\sqrt{2}\,c_2\left[\frac{\sqrt{2}\,\beta^{\frac{3}{4}}}{\Gamma\left(\frac{3}{4}\right)\sqrt{1-\varrho}\,\gamma_1^{\frac{1}{4}}}+\sum_{n=1}^{+\infty}\frac{(-1)^n}{n!\,\Gamma\left(n+\frac{3}{4}\right)}\left(\frac{(1-\varrho)^2\gamma_1}{4\beta^3}\right)^{2n-\frac{1}{4}}s^{4n}\right]. \tag{5.6.67}$$

Equation (5.6.61) is identical with (5.6.34) and its general solution on $(\beta,1)$ is therefore given by (5.6.40).

The remainder of the solution process follows a now familiar path and warrants no further elaboration.

5.6.3 The case $0<\alpha<\beta=1$

In order to deal with the case $0<\alpha<\beta=1$, shown schematically in figure 5.6.3, consider the change of variable $s=f(x_1)$ determined by the homeomorphism $f:[0,L]\to[\alpha,1+\varrho]$,

$$f(x_1)=\begin{cases}1+\varrho-\dfrac{x_1}{L} & \text{if } 0\le x_1\le \varrho L\\[2ex] 1-(1-\alpha)\dfrac{x_1-\varrho L}{(1-\varrho)L} & \text{if } \varrho L\le x_1\le L\end{cases}. \tag{5.6.68}$$

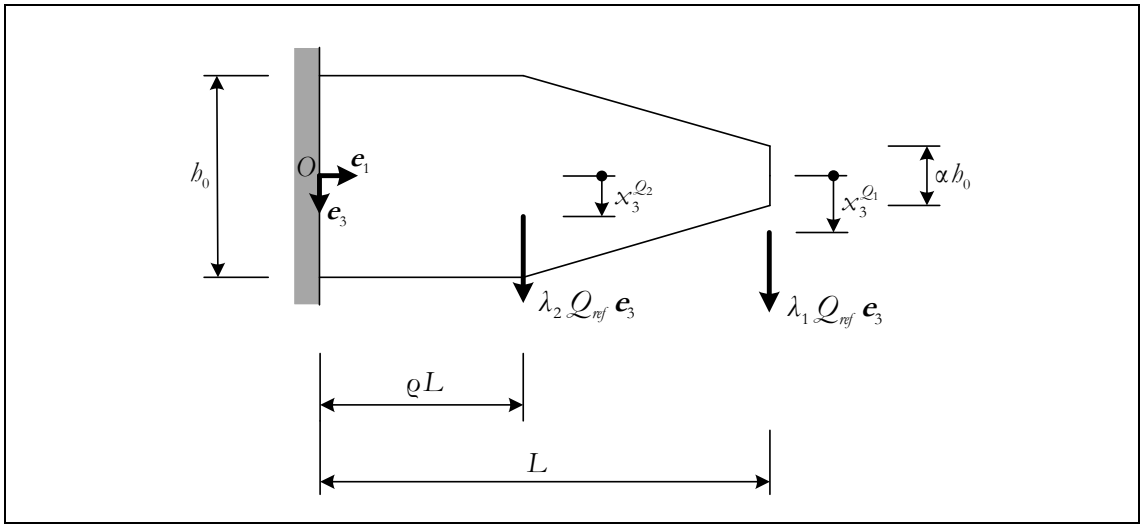

Figure 5.6.3: Two-segment strip cantilever with $0<\alpha<\beta=1$

As usual, define $\tilde{\phi}:[\alpha,1+\varrho]\to\mathbb{R}$ such that $\phi_1=\tilde{\phi}\circ f$ and denote its restrictions to $[\alpha,1]$ and to $[1,1+\varrho]$ by $\tilde{\phi}_-$ and $\tilde{\phi}_+$, respectively. Defining the parameters γ_1, γ_2, ε_1 and ε_2 as in (5.6.30)-(5.6.31) – with $\beta=1$, of course –, it is easily seen that Problem 5.7, under the restriction $0<\alpha<\beta=1$, is brought into the following form:

Problem 5.10.

Find scalars $\gamma_1\in\mathbb{R}^+$, $\gamma_2\in\mathbb{R}_0^+$ and functions $\tilde{\phi}_-:[\alpha,1]\to\mathbb{R}$, $\tilde{\phi}_+:[1,1+\varrho]\to\mathbb{R}$, with

- $\tilde{\phi}_-\in C^2[\alpha,1]$,
- $\tilde{\phi}_+\in C^2[1,1+\varrho]$ and
- $\tilde{\phi}_-\neq 0$ or $\tilde{\phi}_+\neq 0$,

satisfying

$$\tilde{\phi}_-''(s)+\frac{1}{s}\tilde{\phi}_-'(s)+\frac{(1-\varrho)^4\gamma_1^2}{(1-\alpha)^4}\left(1-\frac{2\alpha}{s}+\frac{\alpha^2}{s^2}\right)\tilde{\phi}_-(s)=0 \tag{5.6.69}$$

on $(\alpha,1)$,

$$\tilde{\phi}_+''(s)+\left[\varrho\gamma_1+\gamma_2-(\gamma_1+\gamma_2)s\right]^2\tilde{\phi}_+(s)=0 \tag{5.6.70}$$

on $(1,1+\varrho)$ and

$$\tilde{\phi}_-'(\alpha)-\frac{\varepsilon_1(1-\varrho)\gamma_1}{1-\alpha}\tilde{\phi}_-(\alpha)=0 \tag{5.6.71}$$

$$\tilde{\phi}_+(1+\varrho)=0 \tag{5.6.72}$$

$$\tilde{\phi}_+(1)-\tilde{\phi}_-(1)=0\ . \tag{5.6.73}$$

$$\left(\tilde{\phi}_+'(1)-\frac{1-\alpha}{1-\varrho}\tilde{\phi}_-'(1)\right)-\varepsilon_2\gamma_2\,\tilde{\phi}_-(1)=0\ . \tag{5.6.74}$$

Equation (5.6.69) is identical with (5.6.33) (with $\beta=1$, of course). As for equation (5.6.70), it can be reduced to the same form as (5.3.8) or (5.6.60). Indeed, perform the shift

$$s\mapsto\xi=s-\frac{\varrho\gamma_1+\gamma_2}{\gamma_1+\gamma_2} \tag{5.6.75}$$

and define, on the interval $\left(\frac{(1-\varrho)\gamma_1}{\gamma_1+\gamma_2},\frac{\gamma_1+\varrho\gamma_2}{\gamma_1+\gamma_2}\right)$, a new real-valued function η such that $\tilde{\phi}_+(s)=\eta(\xi)$. Then η satisfies on its domain the differential equation

$$\eta''(\xi)+(\gamma_1+\gamma_2)^2\xi^2\eta(\xi)=0\ , \tag{5.6.76}$$

whose general solution is given by (*vide supra*, note 12)

$$\eta(\tilde{z}) = \sqrt{\tilde{z}}\left(c_3\, J_{\frac{1}{4}}\left(\frac{\gamma_1+\gamma_2}{2}\tilde{z}^2 \right) + c_4\, Y_{\frac{1}{4}}\left(\frac{\gamma_1+\gamma_2}{2}\tilde{z}^2 \right) \right) \quad \text{, with } c_3, c_4 \in \mathbb{R} \ . \tag{5.6.77}$$

The general solution of (5.6.70) on $(1, 1+\varrho)$ is therefore

$$\tilde{\phi}_+(s) = \sqrt{s - \frac{\varrho\gamma_1+\gamma_2}{\gamma_1+\gamma_2}} \left[c_3\, J_{\frac{1}{4}}\left(\frac{\left(\varrho\gamma_1+\gamma_2-(\gamma_1+\gamma_2)s\right)^2}{2(\gamma_1+\gamma_2)} \right) \right.$$

$$\left. + c_4\, Y_{\frac{1}{4}}\left(\frac{\left(\varrho\gamma_1+\gamma_2-(\gamma_1+\gamma_2)s\right)^2}{2(\gamma_1+\gamma_2)} \right) \right] \quad \text{, with } c_3, c_4 \in \mathbb{R} . \tag{5.6.78}$$

The remainder of the solution process is now an uneventful repetition of known techniques.

5.6.4 Illustrative examples

Illustrative example 1

As a first illustration of the foregoing theory, consider the family of strip cantilevers shown in figure 5.6.4, whose depth tapers linearly between h_0 at the support ($x_1 = 0$) and αh_0 at the free end ($x_1 = L$) and which are subjected to conservative loads applied to the centroids of the free-end section and of an intermediate section defined by the abscissa $x_1 = \varrho L$. The depth of the latter section is βh_0, with $\beta = 1-(1-\alpha)\varrho$. For reference purposes, the prismatic case ($\alpha = 1.0$) is also included (see CHALLAMEL & WANG 2010).

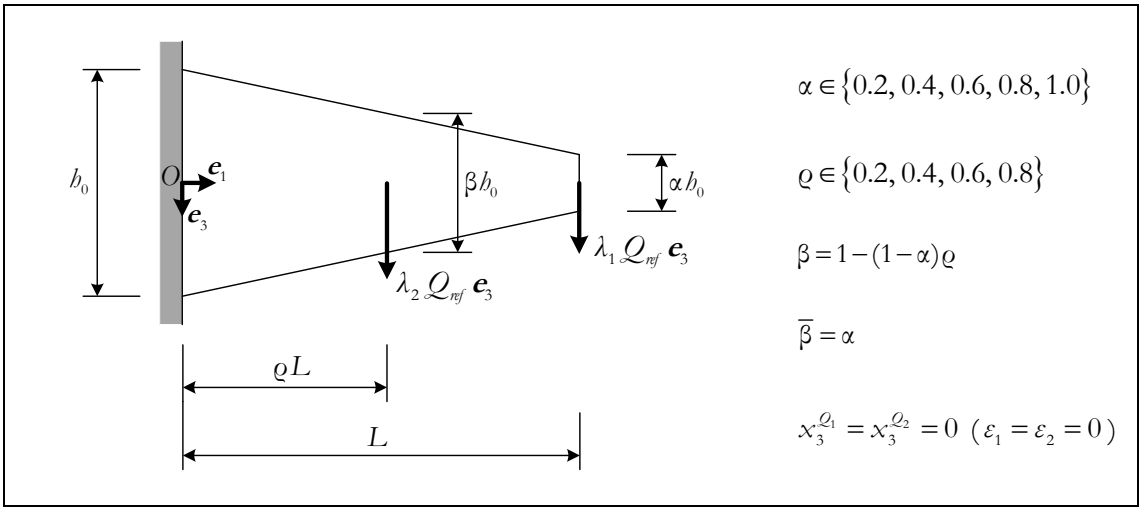

Figure 5.6.4: Illustrative example 1

Each combination of values assigned to the parameters α and ϱ determines a specific non-dimensional LTB problem and, in particular, a specific stability boundary in (the first quadrant of) the non-dimensional load plane (γ_1, γ_2). To obtain (a number of points on) such a stability boundary, the following procedure was adopted:

(i) First, set $\gamma_2 = 0$ and compute the critical value of the non-dimensional load γ_1, which shall be denoted $\gamma_{1.u}$ (the subscript "*u*" stands for "uncoupled load case" and, for the sake of notational simplicity, the subscript "*cr*" is omitted). This provides the point $(\gamma_{1.u}, 0)$ where the stability boundary intersects the positive γ_1 semi-axis.

(ii) Repeat the previous step with the roles of γ_1 and γ_2 reversed, so as to obtain the point $(0, \gamma_{2.u})$ where the stability boundary intersects the positive γ_2 semi-axis.[25]

(iii) For fixed values of γ_1 in the open interval $(0, \gamma_{1.u})$, compute the lowest positive value of γ_2 that satisfies the characteristic equation. Each combination thus obtained corresponds to a point on the stability boundary.

(iv) As a check, reverse the roles of γ_1 and γ_2 in the previous step.

All the computations were carried out with the mathematical software package Mathematica (WOLFRAM RESEARCH, INC. 2006). The values $\gamma_{1.u}$ and $\gamma_{2.u}$ are collected in table 5.6.2 – observe that $\gamma_{1.u}$ is obviously independent of ϱ. The stability boundaries are sketched in figure 5.6.5 on the basis of 41 points with equally spaced abscissas. Notice that the γ_1- and γ_2-axes were normalised through division by $\gamma_{1.u}$ and $\gamma_{2.u}$, respectively. As theoretically predicted, the stability boundaries do not exhibit convexity towards the origin. The Dunkerley-type lower bounds (*e.g.*, TARNAI 1995, 1999)

$$\frac{\gamma_1}{\gamma_{1.u}} + \frac{\gamma_2}{\gamma_{2.u}} = 1 \ , \quad 0 \le \gamma_1 \le \gamma_{1.u} \ , \quad 0 \le \gamma_2 \le \gamma_{2.u} \ , \tag{5.6.79}$$

are also shown in figure 5.6.5 (dashed lines). For fixed α, these lower bounds become more accurate as ϱ increases – in fact, Dunkerley's line (5.6.79) would be exact in the limiting case $\varrho = 1$ (both loads applied at the free-end section). For low values of ϱ (intermediate load applied relatively close to the support), the accuracy of Dunkerley's line as an approximation to the stability boundary is poor. In the limiting case $\varrho = 0$ ("intermediate" load applied at the support), $\gamma_{2.u}$ would become infinitely large and the stability boundary would degenerate into the vertical line $\gamma_1 = \gamma_{1.u}$. For fixed ϱ, the normalised

[25] Recall the remark made in the paragraph following the statement of Problem 5.6.

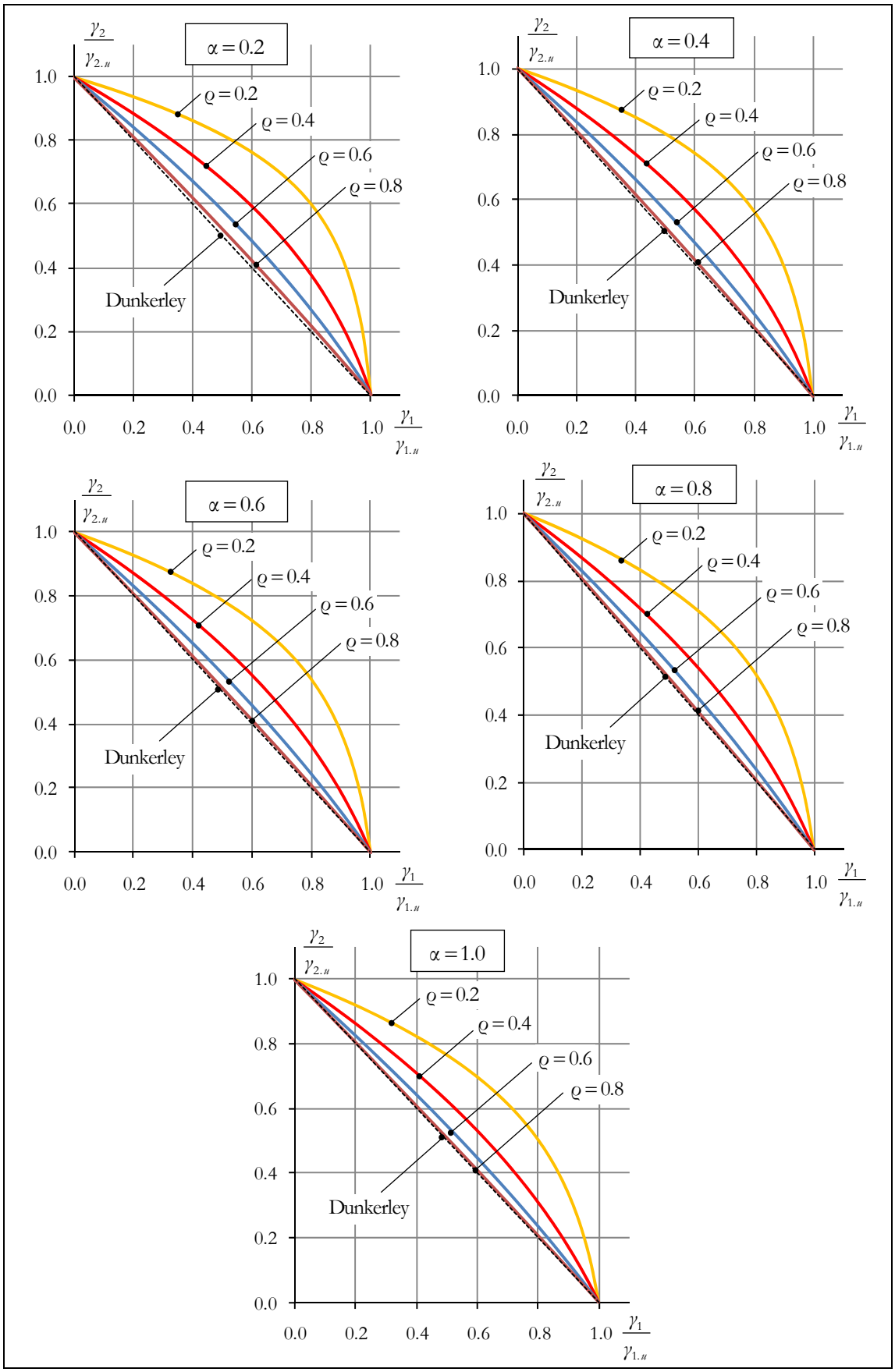

Fig. 5.6.5: Illustrative example 1 – Stability boundaries

α	$\gamma_{1.u}$	$\gamma_{2.u}$			
		$\varrho = 0.2$	$\varrho = 0.4$	$\varrho = 0.6$	$\varrho = 0.8$
0.2	2.879	95.52	22.61	9.438	4.931
0.4	3.219	96.75	23.25	9.900	5.309
0.6	3.510	97.95	23.88	10.34	5.652
0.8	3.771	99.14	24.49	10.75	5.970
1.0	4.013	100.3	25.08	11.15	6.270

Table 5.6.2: Illustrative example 1 – Non-dimensional critical loads $\gamma_{1.u}$ and $\gamma_{2.u}$ for the uncoupled load cases

stability boundaries corresponding to decreasing values of α are arranged in order, from the inner-most to the outer-most, and closely grouped together (particularly so if ϱ is large).

Illustrative example 2

The second illustrative example concerns two-segment cantilevers acted by a single load applied at the centroid of the free-end section ($\gamma_2 = 0, \varepsilon_1 = 0$) – see figure 5.6.6. The length of the first segment (adjacent to the support) relative to the total length of the cantilever takes on the values $\varrho = 0.3$, $\varrho = 0.5$ and $\varrho = 0.7$. For each ϱ, the parameter α characterising the depth of the free-end section is assigned the fixed value 0.2, while the parameter β defining the depth at the junction between segments varies from 0.2 $(= \alpha)$ to 1.0. We will thus be looking at a gradual transition between the two extreme cases discussed in §§ 5.6.2-5.6.3.

The non-dimensional critical loads $\gamma_{1.u}$ are graphically displayed in figure 5.6.7(a). These graphs are indeed continuous at $\beta = \alpha = 0.2$ and $\beta = 1.0$. Moreover, for $\beta = 1 - \varrho(1 - \alpha)$, when the cantilevers reduce to a single linearly tapered segment loaded at the tip, we obtain $\gamma_{1.u} \cong 2.879$, in perfect agreement with the result reported in § 5.4. As expected, for fixed ϱ (resp. fixed β), the non-dimensional critical load $\gamma_{1.u}$ is an increasing function of β (resp. of ϱ). Figure 5.6.7(b) is far more interesting – it displays, for each ϱ, the ratio between the critical load $\lambda_{1.u} Q_{ref}$ and the cantilever volume V, non-dimensionalised by the multiplicative factor $3L^3 / (t^2 \sqrt{EG})$, *versus* the parameter β. The ratio $\lambda_{1.u} Q_{ref} / V$ is a measure of the efficiency of each cantilever geometry with respect to LTB. The maximum

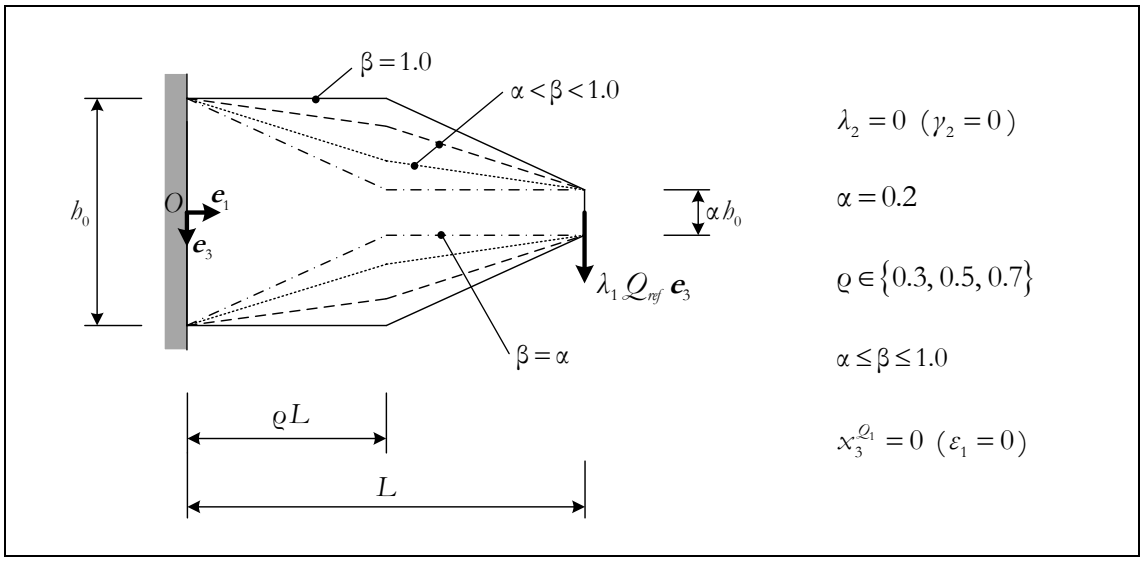

Figure 5.6.6: Illustrative example 2

achievable efficiency is found to be practically independent of ϱ (for the three values of ϱ considered in this study). However, as ϱ increases, this maximum occurs for progressively lower values of β. These β values are always larger than those corresponding to a single linearly tapered segment (*i.e.*, larger than $1-(1-\alpha)\varrho$), even if marginally so for $\varrho = 0.7$, which means that the optimal shape is always convex.

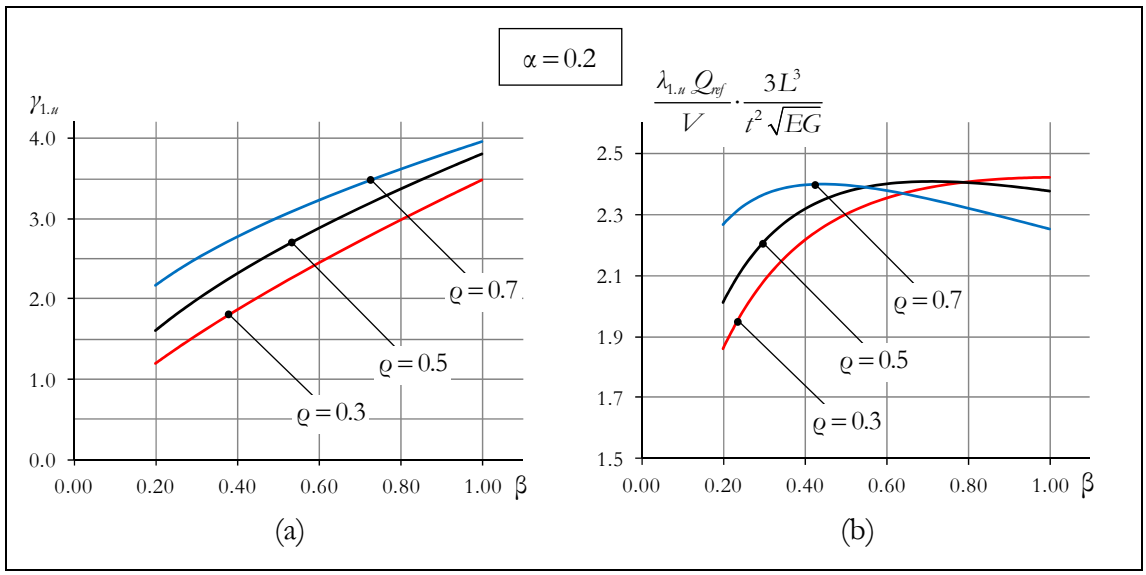

Figure 5.6.7: Illustrative example 2 – Non-dimensional (a) critical loads and (b) critical load-to-volume ratios

* * *

In both examples, some of the analytical solutions were compared with the results of shell finite element analyses. An excellent agreement was found in all cases, thus corroborating the mathematical model described at the beginning of this section and confirming the correctness of the analytical results. The details of the comparison are given in the paper ANDRADE *et al.* (2012).

5.7 GENERALISATION 2: CANTILEVERED BEAM-COLUMNS

In this section, we turn once again to the linearly tapered strip cantilevers described in § 5.2, which are now acted by two conservative point loads (see figure 5.7.1) – a transverse load $\boldsymbol{Q} = \lambda_1 \, Q_{ref} \, \boldsymbol{e}_3$ and an axial compressive load $\boldsymbol{P} = -\lambda_2 \, P_{ref} \, \boldsymbol{e}_1$, where Q_{ref}, P_{ref} are positive reference magnitudes and λ_1, λ_2 are independent load factors, restricted to non-negative values.[26] As shown in figure 5.7.1, these loads are applied at the centroid of the free-end section and always retain their original direction. Our purpose is to study analytically (to the extent that the analytical approach is feasible) the flexural-torsional buckling (FTB) behaviour of such a class of beam-columns.

The functional Π_2 is now defined by

$$\Pi_2(w_2, \phi_1, \lambda_1, \lambda_2) = \frac{1}{2}\int_0^L EI_3(x_1)\, w_2''(x_1)^2 \, dx_1 + \frac{1}{2}\int_0^L GJ(x_1)\, \phi_1'(x_1)^2 \, dx_1$$

$$+\lambda_1 \, Q_{ref} \, L \int_0^L \left(\frac{x_1}{L} - 1 \right) w_2''(x_1)\, \phi_1(x_1) \, dx_1 - \frac{1}{2}\, \lambda_2 \, P_{ref} \int_0^L w_2'(x_1)^2 \, dx_1 \quad , \tag{5.7.1}$$

where $EI_3(x_1)$ and $GJ(x_1)$ are given by (5.2.4)-(5.2.5). This definition neglects both the amplification of the in-plane bending moments by the axial load and the effect of the in-plane bending curvature on the FTB strength. The domain of Π_2 is taken as $\mathcal{D}_1 \times \mathcal{D}_2 \times \mathbb{R}_0^+ \times \mathbb{R}_0^+$, with

$$\mathcal{D}_1 = \left\{ w_2 \in C^4\left[0, L\right] \,\middle|\, w_2(0) = 0 \,,\, w_2'(0) = 0 \right\} \tag{5.7.2}$$

$$\mathcal{D}_2 = \left\{ \phi_1 \in C^2\left[0, L\right] \,\middle|\, \phi_1(0) = 0 \right\} \,. \tag{5.7.3}$$

[26] Due to symmetry, reversing the direction of the load $\boldsymbol{Q}$ does not change the problem, and so the condition $\lambda_1 \geq 0$ is no restriction at all. As for the condition $\lambda_2 \geq 0$, it is not essential for the ensuing analysis (as the reader may easily verify) and could very well be omitted – however, in the case $\lambda_2 < 0$, we would no longer be dealing with a beam-column, strictly speaking, but with a "tensioned beam", less susceptible to buckling.

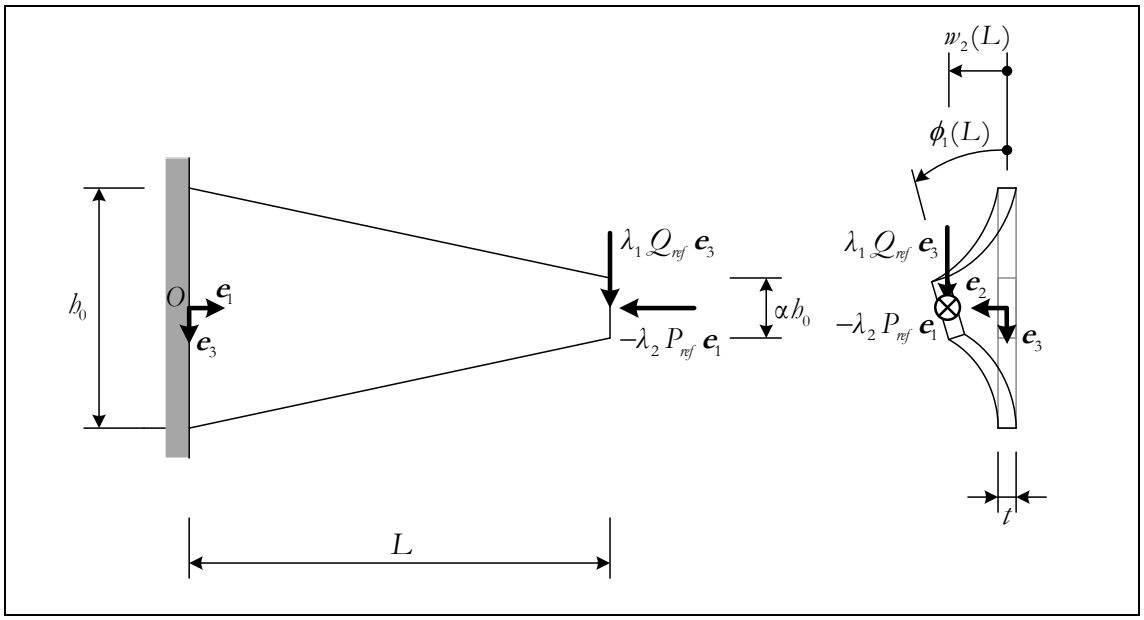

Figure 5.7.1: Linearly tapered cantilevered strip beam-column – Reference and buckled shapes; applied loads

Within this framework, it is straightforward to see that the criterion of Trefftz and the fundamental lemma of the calculus of variations jointly lead to the following classical statement of the beam-column FTB problem:

Problem 5.11.

Find non-negative real numbers λ_1, λ_2 and functions $w_2, \phi_1 : [0, L] \to \mathbb{R}$, with

- $w_2 \in C^4[0, L]$,
- $\phi_1 \in C^2[0, L]$ and
- $w_2 \neq 0$ or $\phi_1 \neq 0$,

satisfying the differential equations

$$\left[EI_3(0)\left(1-(1-\alpha)\frac{x_1}{L}\right)w_2''(x_1) + \lambda_2 P_{ref} w_2(x_1) + \lambda_1 Q_{ref} L\left(\frac{x_1}{L}-1\right)\phi_1(x_1)\right]'' = 0 \quad (5.7.4)$$

$$\left[GJ(0)\left(1-(1-\alpha)\frac{x_1}{L}\right)\phi_1'(x_1)\right]' - \lambda_1 Q_{ref} L\left(\frac{x_1}{L}-1\right)w_2''(x_1) = 0 \quad (5.7.5)$$

on the open interval $(0, L)$, together with the boundary conditions

$$w_2(0) = 0 \quad (5.7.6)$$

$$w_2'(0) = 0 \quad (5.7.7)$$

$$\phi_1(0) = 0 \quad (5.7.8)$$

$$\alpha EI_3(0)w_2'''(L)-EI_3(0)\frac{1-\alpha}{L}w_2''(L)+\lambda_2 P_{ref}\,w_2'(L)+\lambda_1 Q_{ref}\,\phi_1(L)=0 \quad (5.7.9)$$

$$\alpha EI_3(0)w_2''(L)=0 \quad (5.7.10)$$

$$\alpha GJ(0)\phi_1'(L)=0\ . \quad (5.7.11)$$

This is again a two-parameter eigenproblem, just as Problem 5.6.

The integration of equations (5.7.4)-(5.7.5), together with the use of the boundary conditions (57.9)-(5.7.11), leads to

$$EI_3(0)\left(1-(1-\alpha)\frac{x_1}{L}\right)w_2''(x_1)+\lambda_2 P_{ref}\left(w_2(x_1)-w_2(L)\right)+\lambda_1 Q_{ref}L\left(\frac{x_1}{L}-1\right)\phi_1(x_1)=0 \quad (5.7.12)$$

$$\lambda_1 Q_{ref}L\left(\frac{x_1}{L}-1\right)w_2'(x_1)-\lambda_1 Q_{ref}\left(w_2(x_1)-w_2(L)\right)-GJ(0)\left(1-(1-\alpha)\frac{x_1}{L}\right)\phi_1'(x_1)=0\ . \quad (5.7.13)$$

Consider now the map $f:[0,L]\to[0,1]$ defined by $x_1\mapsto 1-\frac{x_1}{L}$ and let $s=f(x_1)$ denote the associated change of independent variable. Moreover, introduce the functions $\tilde{w},\tilde{\phi}:[0,1]\to\mathbb{R}$ such that $w_2=L(\tilde{w}\circ f)$ and $\phi_1=\tilde{\phi}\circ f$. Equations (5.7.12)-(5.7.13) are thereby brought into the form

$$\left(\alpha+(1-\alpha)s\right)\tilde{w}''(s)+\frac{\lambda_2 P_{ref}L^2}{EI_3(0)}\left(\tilde{w}(s)-\tilde{w}(0)\right)-\frac{\lambda_1 Q_{ref}L^2}{EI_3(0)}s\,\tilde{\phi}(s)=0 \quad (5.7.14)$$

$$\frac{\lambda_1 Q_{ref}L^2}{GJ(0)}\left[s\,\tilde{w}'(s)-\left(\tilde{w}(s)-\tilde{w}(0)\right)\right]+\left(\alpha+(1-\alpha)s\right)\tilde{\phi}'(s)=0\ . \quad (5.7.15)$$

The former equation shows that $\tilde{\phi}(s)$ is given by

$$\tilde{\phi}(s)=\frac{EI_3(0)\left(\alpha+(1-\alpha)s\right)\tilde{w}''(s)+\lambda_2 P_{ref}L^2\left(\tilde{w}(s)-\tilde{w}(0)\right)}{\lambda_1 Q_{ref}L^2 s} \quad (5.7.16)$$

on the open interval $(0,1)$. The incorporation of this result into equation (5.7.15) yields the third-order linear differential equation

$$\frac{EI_3(0)}{L^2}\left(\alpha+(1-\alpha)s\right)^2 s\,\tilde{w}'''(s)-\frac{EI_3(0)}{L^2}\alpha\left(\alpha+(1-\alpha)s\right)\tilde{w}''(s)$$
$$+\left[\frac{\lambda_1^2 Q_{ref}^2 L^2}{GJ(0)}s^2+\lambda_2 P_{ref}\left(\alpha+(1-\alpha)s\right)\right]\left[s\,\tilde{w}'(s)-\left(\tilde{w}(s)-\tilde{w}(0)\right)\right]=0\ . \quad (5.7.17)$$

Then, by defining $\eta:[0,1]\to\mathbb{R}$, $\eta(s)=\tilde{w}(s)-\tilde{w}(0)$ and the non-dimensional loads[27]

[27] Observe that (5.7.18) is identical with (5.3.6) and (5.6.30$_1$).

$$\gamma_1 = \frac{\lambda_1 \, Q_{ref} \, L^2}{\sqrt{EI_3(0)\,GJ(0)}} \tag{5.7.18}$$

$$\gamma_2 = \frac{\lambda_2 \, P_{ref} \, L^2}{EI_3(0)} \ , \tag{5.7.19}$$

equation (5.7.17) is reduced to the non-dimensional form

$$\begin{aligned} &\big(\alpha+(1-\alpha)s\big)^2 \, s\,\eta'''(s) - \alpha\big(\alpha+(1-\alpha)s\big)\,\eta''(s) + \\ &\quad + \Big[\gamma_1^2 \, s^2 + \gamma_2\big(\alpha+(1-\alpha)s\big)\Big]\big(s\,\eta'(s)-\eta(s)\big) = 0 \ . \end{aligned} \tag{5.7.20}$$

This equation suggests one further manipulation: with the introduction of the function $\tilde{\eta}:[0,1]\to\mathbb{R}$ defined by $\tilde{\eta}(s) = s\,\eta'(s) - \eta(s)$, one obtains the second-order differential equation

$$\begin{aligned} &\big(\alpha+(1-\alpha)s\big)^2 \, \tilde{\eta}''(s) - \big(2\alpha+(1-\alpha)s\big)\big(\alpha+(1-\alpha)s\big)\frac{1}{s}\tilde{\eta}'(s) \\ &\quad + \Big[\gamma_1^2 \, s^2 + \gamma_2\big(\alpha+(1-\alpha)s\big)\Big]\tilde{\eta}(s) = 0 \ . \end{aligned} \tag{5.7.21}$$

It remains to specify the two boundary conditions to which equation (5.7.21) is subjected. At $s=0$ (*i.e.*, at the cantilever's tip), one has, by definition, $\eta(0)=0$ and hence $\tilde{\eta}(0)=0$. At $s=1$ (*i.e.*, at the clamped end), the condition $\tilde{w}'(1)=0$ yields $\eta'(1)=0$ and, consequently, $\tilde{\eta}(1)=\eta'(1)-\eta(1)=-\eta(1)$. Moreover, by virtue of equation (5.7.16) and continuity considerations, the condition $\tilde{\phi}(1)=0$ implies $\tilde{w}''(1)+\gamma_2\big(\tilde{w}(1)-\tilde{w}(0)\big)=0$ or, which is the same, $\eta''(1)+\gamma_2\,\eta(1)=0$. Therefore, one concludes that $\tilde{\eta}'(1)-\gamma_2\,\tilde{\eta}(1)=0$.

To sum up, the non-dimensional version of the two-parameter eigenproblem governing the FTB of the strip beam-columns of figure 5.7.1 may be phrased as follows:

Problem 5.12.

Find $\gamma_1, \gamma_2 \in \mathbb{R}_0^+$ and $\tilde{\eta}:[0,1]\to\mathbb{R}$, with $\tilde{\eta}\in C^3[0,1]$ and $\tilde{\eta}\neq 0$, satisfying

$$\begin{aligned} &\big(\alpha+(1-\alpha)s\big)^2 \, \tilde{\eta}''(s) - \big(2\alpha+(1-\alpha)s\big)\big(\alpha+(1-\alpha)s\big)\frac{1}{s}\tilde{\eta}'(s) \\ &\quad + \Big[\gamma_1^2 \, s^2 + \gamma_2\big(\alpha+(1-\alpha)s\big)\Big]\tilde{\eta}(s) = 0 \ . \end{aligned} \tag{5.7.22}$$

on the open interval $(0,1)$, together with the boundary conditions

$$\tilde{\eta}(0) = 0 \tag{5.7.23}$$

$$\tilde{\eta}'(1) - \gamma_2\,\tilde{\eta}(1) = 0 \ . \tag{5.7.24}$$

An eigenvalue is an ordered pair $(\gamma_1^2, \gamma_2) \in \mathbb{R}_0^+ \times \mathbb{R}_0^+$ for which the boundary value problem (5.7.22)-(5.7.24) admits non-trivial (*i.e.*, not identically zero) solutions $\tilde{\eta} \in C^3[0,1]$.

5.7.1 Prismatic beam-columns ($\alpha = 1$)

For prismatic beam-columns ($\alpha = 1$), the uncoupled load cases offer no difficulty whatsoever:

(i) When $\lambda_2 = 0$ (or, equivalently, when $\gamma_2 = 0$), we have the lateral-torsional buckling problem investigated in § 5.3, with $\varepsilon_Q = 0$. The buckling values of the non-dimensional transverse load γ_1 are twice the positive roots of the Bessel function of the first kind of order $-\frac{1}{4}$, $J_{-1/4}$.

(ii) When $\lambda_1 = 0$ (or, equivalently, when $\gamma_1 = 0$), we have the well-known Euler problem of column buckling (EULER 1744, 1759).[28] The buckling values of the non-dimensional compressive load γ_2 are $\frac{n\pi^2}{4}$, where n is a positive integer.

One is therefore left with:

Problem 5.13.

Find $\gamma_1, \gamma_2 > 0$ and $\tilde{\eta}: [0,1] \to \mathbb{R}$, with $\tilde{\eta} \in C^3[0,1]$ and $\tilde{\eta} \neq 0$, satisfying the differential equation

$$\tilde{\eta}''(s) - \frac{2}{s}\tilde{\eta}'(s) + (\gamma_1^2 s^2 + \gamma_2)\tilde{\eta}(s) = 0 \tag{5.7.25}$$

on the open interval $(0,1)$, together with the boundary conditions

$$\tilde{\eta}(0) = 0 \tag{5.7.26}$$

$$\tilde{\eta}'(1) - \gamma_2 \tilde{\eta}(1) = 0 \ . \tag{5.7.27}$$

It is possible to bring equation (5.7.25) into a familiar form through a judiciously chosen change of independent variable. Indeed, consider the map $g: (0,1) \to (0,1)$, $s \mapsto s^2$ and let $z = g(s)$ denote the associated change of variable. Moreover, define $y: (0,1) \to \mathbb{R}$ such that, on $(0,1)$, $\tilde{\eta} = y \circ g$. The differential equation (5.7.25) is thereby transformed into

$$y''(z) - \frac{1}{2z}y'(z) + \left(\frac{\gamma_1^2}{4} + \frac{\gamma_2}{4z}\right) y(z) = 0 \ , \quad z \in (0,1) \ , \tag{5.7.28}$$

[28] See TRUESDELL (1960, § 28 and ch. 4F) for an excellent analysis of Euler's work on column buckling.

which is of the same form as equation (5.4.5). It is then a simple matter to see that the general solution of equation (5.7.25) on $(0,1)$ may be written as

$$\tilde{\eta}(s) = s^3 e^{-i\frac{\gamma_1}{2}s^2}\left[c_1 M\left(\frac{5}{4} + i\frac{\gamma_2}{4\gamma_1}, \frac{5}{2}, i\gamma_1 s^2\right) + c_2 (i\gamma_1 s^2)^{-\frac{3}{2}} M\left(-\frac{1}{4} + i\frac{\gamma_2}{4\gamma_1}, -\frac{1}{2}, i\gamma_1 s^2\right)\right], \tag{5.7.29}$$

with $c_1, c_2 \in \mathbb{C}$. By continuity, this solution extends to $s = 0$ and $s = 1$.

The boundary condition (5.7.26) implies $c_2 = 0$ and one then concludes from the proposition in Appendix 2 (at the end of this chapter) that the constant c_1 must be real-valued for all positive values of γ_1. The boundary condition (5.7.27) now leads to the characteristic equation

$$e^{-i\frac{\gamma_1}{2}}\left[(3 - \gamma_2 - i\gamma_1) M\left(\frac{5}{4} + i\frac{\gamma_2}{4\gamma_1}, \frac{5}{2}, i\gamma_1\right) + \left(-\frac{\gamma_2}{5} + i\gamma_1\right) M\left(\frac{9}{4} + i\frac{\gamma_2}{4\gamma_1}, \frac{7}{2}, i\gamma_1\right)\right] = 0\ , \tag{5.7.30}$$

which may be written in the more compact form

$$e^{-i\frac{\gamma_1}{2}} M\left(\frac{1}{4} + i\frac{\gamma_2}{4\gamma_1}, \frac{1}{2}, i\gamma_1\right) = 0\ . \tag{5.7.31}$$

A detailed proof of the equivalence between equations (5.7.30) and (5.7.31), which is by no means obvious, is given in Appendix 3, at the end of this chapter. Moreover, it follows once again from the proposition in Appendix 2 that left-hand side of equation (5.7.31) is real-valued for all positive values of γ_1. It is worth noting that MILISAVLJEVIC (1988) arrived at exactly the same characteristic equation using a direct equilibrium approach.

As in § 5.6, the characteristic equation (5.7.31) defines a family of curves in the first quadrant of the (γ_1^2, γ_2) half-plane, the first of which is (part of) the beam-column's stability boundary. This stability boundary intersects the γ_1^2 semi-axis and the positive γ_2 semi-axis at the points $(\gamma_{1.u}^2, 0)$ and $(0, \gamma_{2.u})$, with $\gamma_{1.u}^2 \cong 16.101$ (the square of twice the lowest positive root of $J_{-1/4}$) and $\gamma_{2.u} = \frac{\pi^2}{4}$. To obtain additional points on the stability boundary, choose a fixed value for γ_2 in the open interval $\left(0, \frac{\pi^2}{4}\right)$ and solve the

characteristic equation for its the lowest positive root γ_1.[29] The results of these calculations are presented in table 5.7.1 and plotted in figure 5.7.2. The comparison with the numerical results reported by MARTIN (1951) shows an excellent agreement. Moreover, it can be seen that Dunkerley's line

$$\left(\frac{\gamma_1}{\gamma_{1.u}}\right)^2 + \frac{\gamma_2}{\gamma_{2.u}} = 1 \ , \quad 0 \le \gamma_1^2 \le \gamma_{1.u}^2 \ , \quad 0 \le \gamma_2 \le \gamma_{2.u} \ , \tag{5.7.32}$$

provides a rather accurate lower bound for the stability boundary. In view of the quite good accuracy of equation (5.7.32), as well as of its simplicity and elegance, the use of additional correction factors or exponents, as suggested for instance by DIMAGGIO *et al.* (1952, eq. (15)[30]), seems hardly justifiable.

$\gamma_2 = \frac{\lambda_2 P_{ref} L^2}{EI_{3.0}}$	$\gamma_1^2 = \frac{\lambda_1^2 Q_{ref}^2 L^4}{EI_{3.0} GJ_0}$	
	Present work	MARTIN (1951)
0.000	16.101	16.101
0.290	14.458	14.478
1.012	10.108	10.125
1.568	6.475	6.355
1.942	3.878	3.885
2.174	2.200	2.176
2.311	1.184	1.156
2.389	0.597	0.598
2.436	0.240	0.244
$\frac{\pi^2}{4}$	0.000	0.000

Table 5.7.1: Prismatic cantilevered strip beam-columns – Non-dimensional critical loads

[29] Of course, the roles of γ_1 and γ_2 can be reversed in this procedure, if only for verification purposes.

[30] The cited equation is patently misprinted – the symbols p and q should be interchanged.

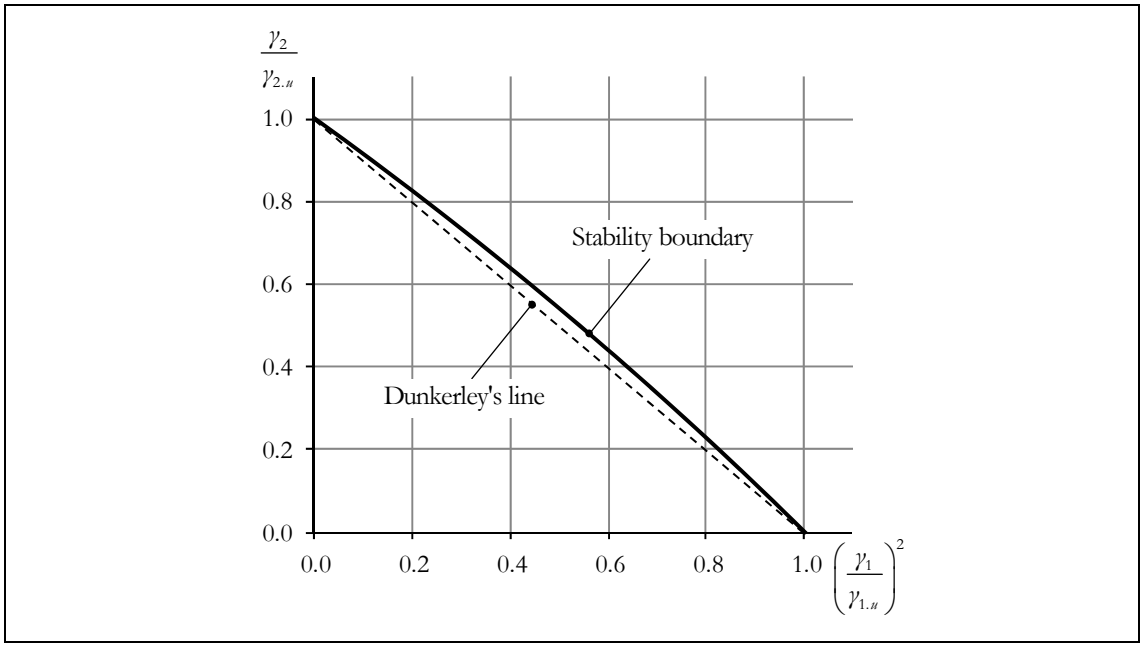

Figure 5.7.2: Prismatic cantilevered strip beam-column – Stability boundary

5.7.2 Tapered beam-columns ($0<\alpha<1$)

Frobenius series solution

In Problem 5.12, we now restrict the taper ratio α to lie in the open interval $(0,1)$. Equation (5.7.22) can then be cast in the form

$$\tilde{\eta}''(s)-\left(\frac{2}{s}-\frac{1}{s+\dfrac{\alpha}{1-\alpha}}\right)\tilde{\eta}'(s)+\left[\frac{\dfrac{\gamma_1^2}{(1-\alpha)^2}s^2}{\left(s+\dfrac{\alpha}{1-\alpha}\right)^2}+\frac{\dfrac{\gamma_2}{1-\alpha}}{s+\dfrac{\alpha}{1-\alpha}}\right]\tilde{\eta}(s)=0\ , \tag{5.7.33}$$

making it clear that $s=0$ and $s=-\frac{\alpha}{1-\alpha}$ are regular singular points (*vide supra*, note 14) – while the latter falls outside the domain of the problem, the former coincides with one of the boundary points. Although the above equation cannot be solved in closed-form, it is possible (i) to obtain an explicit series representation for its general solution, relative to the singularity at the origin, and (ii) to show that it converges for sufficiently small s (*e.g.*, CODDINGTON & CARLSON 1997, ch. 6, or INCE 1956, ch. 16). If the boundary point $s=1$ lies in the domain of convergence, this series solution can be used to set up the characteristic equation for the tapered beam-column.

For the sake of convenience, we rewrite equation (5.7.33) in the more concise form

$$\tilde{\eta}''(s)+F(s)\,\tilde{\eta}'(s)+G(s,\gamma_1,\gamma_2)\,\tilde{\eta}(s)=0\ . \tag{5.7.34}$$

At $s=0$, the functions $s \mapsto s\,F(s)$ and $s \mapsto s^2\,G(s,\gamma_1,\gamma_2)$ may be expanded in the power series

$$s\,F(s) = \sum_{n=0}^{+\infty} f_n\,s^n = -2 + \frac{1-\alpha}{\alpha}\,s - \left(\frac{1-\alpha}{\alpha}\right)^2 s^2 + \cdots \tag{5.7.35}$$

$$s^2\,G(s,\gamma_1,\gamma_2) = \sum_{n=0}^{+\infty} g_n(\gamma_1,\gamma_2)\,s^n = \frac{\gamma_2}{\alpha}s^2 - \frac{(1-\alpha)\,\gamma_2}{\alpha^2}\,s^3 + \left(\frac{\gamma_1^2}{\alpha^2} + \frac{(1-\alpha)^2\,\gamma_2}{\alpha^3}\right)s^4 - \left(\frac{2(1-\alpha)\,\gamma_1^2}{\alpha^3} + \frac{(1-\alpha)^3\,\gamma_2}{\alpha^4}\right)s^5 + \cdots\,. \tag{5.7.36}$$

Using d'Alembert's test (*e.g.*, CAMPOS FERREIRA 1987, pp. 180-181), their radius of convergence is found to be

$$R = \lim\left|\frac{f_n}{f_{n+1}}\right| = \lim\left|\frac{g_n(\gamma_1,\gamma_2)}{g_{n+1}(\gamma_1,\gamma_2)}\right| = \frac{\alpha}{1-\alpha} \tag{5.7.37}$$

(*i.e.*, the radius of convergence is determined by the distance between the two regular singular points).

The indicial equation of (5.7.33), relative to $s=0$, is given by

$$m^2 + (f_0 - 1)\,m + g_0 = 0\ , \tag{5.7.38}$$

with $f_0 = -2$ and $g_0 = 0$, as can be seen from (5.7.35)-(5.7.36) by direct inspection. Its roots are $m_1 = 3$ and $m_2 = 0$. Since $(m_1 - m_2)$ is a positive integer, equation (5.7.33) has two independent solutions of the form

$$\tilde{\eta}_1(s) = s^{m_1}\left(1 + \sum_{n=1}^{+\infty} a_n\,s^n\right) \tag{5.7.39}$$

$$\tilde{\eta}_2(s) = c\,\tilde{\eta}_1(s)\log(s) + s^{m_2}\sum_{n=0}^{+\infty} b_n\,s^n \tag{5.7.40}$$

on the interval $0 < s < R = \frac{\alpha}{1-\alpha}$, and the series converge for $|s| < R = \frac{\alpha}{1-\alpha}$ (CODDINGTON & CARLSON 1997, th. 6.10). The real constant c in (5.7.40) may happen to be zero, in which case $\tilde{\eta}_2$ will have the same form as $\tilde{\eta}_1$. The general solution of (5.7.33) on $(0,1)$ is then $\tilde{\eta}(s) = c_1\,\tilde{\eta}_1(s) + c_2\,\tilde{\eta}_2(s)$, with $c_1, c_2 \in \mathbb{R}$.

Let us first compute $\tilde{\eta}_1$ by applying the method of Frobenius (*vide supra*, § 5.4, particularly the paragraph including equations (5.4.23) through (5.4.29)). We simply insert equation (5.7.39) into equation (5.7.33) and equate to zero the coefficient of each power of s. This leads to the recursive relation (with $a_0 = 1$)

$$\Big[(m_1+n)^2+(f_0-1)(m_1+n)+g_0\Big]a_n=-\sum_{k=0}^{n-1}\Big[(m_1+k)f_{n-k}+g_{n-k}\Big]a_k\ ,\ n=1,2,\cdots\ , \tag{5.7.41}$$

which can be rewritten as

$$P(m_1+n)\,a_n=-\sum_{k=0}^{n-1}\Big[(m_1+k)f_{n-k}+g_{n-k}\Big]a_k\ , \tag{5.7.42}$$

where

$$P(m)=m^2+(f_0-1)m+g_0 \tag{5.7.43}$$

is the indicial polynomial. Since $P(m_1+n)\neq 0$ for all n, one obtains from (5.7.42) the coefficients a_n $(n=1,2,\cdots)$ of the series (5.7.39), expressed in terms of α, γ_1 and γ_2. As a matter of fact, the first three coefficients are given by

$$a_1=-\frac{3(1-\alpha)}{4\alpha} \tag{5.7.44}$$

$$a_2=\frac{6(1-\alpha)^2-\alpha\gamma_2}{10\alpha^2} \tag{5.7.45}$$

$$a_3=-\frac{\Big(4(1-\alpha)^2-\alpha\gamma_2\Big)(1-\alpha)}{8\alpha^3} \tag{5.7.46}$$

and, for $n\geq 4$, one has the recursion relation (with $a_0=1$)

$$\alpha^2(n+3)\,n\,a_n=\alpha(1-\alpha)(n+2)(1-2n)\,a_{n-1}+\Big((1-\alpha)^2(1-n)(1+n)-\alpha\gamma_2\Big)a_{n-2}$$
$$-\gamma_2\,\alpha\,a_{n-3}-\gamma_1\,a_{n-4}\ . \tag{5.7.47}$$

We now turn to the solution $\tilde{\eta}_2$ and we tentatively apply once again the method of Frobenius – that is, we set $c=0$ and $b_0=1$ in equation (5.7.40) and repeat the procedure of the foregoing paragraph. Since this turns out to be successful,[31] there is a second independent Frobenius series solution to equation (5.7.33). However, this second solution will not be needed in the following. Indeed, because $\tilde{\eta}_1(s)\to 0$ and $\tilde{\eta}_2(s)\to b_0=1$ when $s\to 0^+$, the boundary condition $\tilde{\eta}(0)=0$ implies $c_2=0$ and we are left solely with $\tilde{\eta}(s)=c_1\,\tilde{\eta}_1(s)$.

---

[31] Because $P(m_2+3)=0$, it is generally impossible to obtain b_3 from the equation

$$P(m_2+3)\,b_3=-\sum_{k=0}^{2}\Big((m_2+k)f_{3-k}+g_{3-k}\Big)b_k\ ,$$

in which case the recursive determination of the coefficients b_n of the second Frobenius series breaks down. However, in the particular problem under examination, the right-hand side of the above equation vanishes. It follows that b_3 can be assigned any value whatsoever and the remaining coefficients $b_4, b_5, \cdots$ can be computed without any further difficulties. As BENDER & ORSZAG (2010, p. 72) suggestively put it, "the recursion relation has successfully jumped the hurdle" at $n=m_1-m_2=3$.

If $R = \frac{\alpha}{1-\alpha} > 1$ (*i.e.*, if $\alpha > \frac{1}{2}$), then $\tilde{\eta}_1$ converges at $s = 1$, and so does its derivative. It is therefore legitimate to introduce $\tilde{\eta} = c_1 \tilde{\eta}_1$ into the boundary condition (5.7.24), a procedure that yields the characteristic equation

$$\sum_{n=1}^{+\infty} n\, a_n + (3 - \gamma_2)\left(1 + \sum_{n=1}^{+\infty} a_n \right) = 0 \ , \tag{5.7.48}$$

valid for tapered beam-columns with $\frac{1}{2} < \alpha < 1$. Since no closed-form expression can be found for the sum of the two series appearing in this equation, one is forced, for all practical purposes, to replace them by the partial sums corresponding to a number N of terms chosen so as to ensure the desired accuracy of the computed solutions. In other words, equation (5.7.48) is replaced by

$$\sum_{n=1}^{N} n\, a_n + (3 - \gamma_2)\left(1 + \sum_{n=1}^{N} a_n \right) = 0 \ . \tag{5.7.49}$$

For sufficiently high values of α (say, $\alpha \geq 0.6$), the stability boundary can be obtained with good accuracy – say, at least four correct significant digits in the computation of one of the non-dimensional loads, for a given value of the other – with a moderate number N of terms ($N \leq 80$, to be specific). A typical example of the observed oscillatory convergence behaviour is presented in figure 5.7.3. When α is close to (but above) $\frac{1}{2}$, convergence becomes extremely slow and a similar level of accuracy requires N in the thousands. Figure 5.7.4 shows the stability boundaries for selected values of α, computed with the number N of terms indicated. For reference purposes, the prismatic case ($\alpha = 1.0$) is also displayed.

Numerical solution by a collocation-based procedure

For $0 < \alpha \leq \frac{1}{2}$, the characteristic equation (5.7.48) ceases to be valid and one is forced to use a numerical approach.[32] As in previous chapters, the eigenproblem (5.7.22)-(5.7.24) is converted into an inhomogeneous two-point boundary value problem, which is then solved using the general-purpose code COLNEW (BADER & ASCHER 1987),[33] an approach that has been successfully applied to the lateral-torsional buckling analysis of prismatic and

[32] Needless to say, the numerical approach can also be used when $\frac{1}{2} < \alpha \leq 1$.

[33] A brief overview of COLNEW and its predecessor COLSYS is given in Appendix 1, at the end of chapter 3.

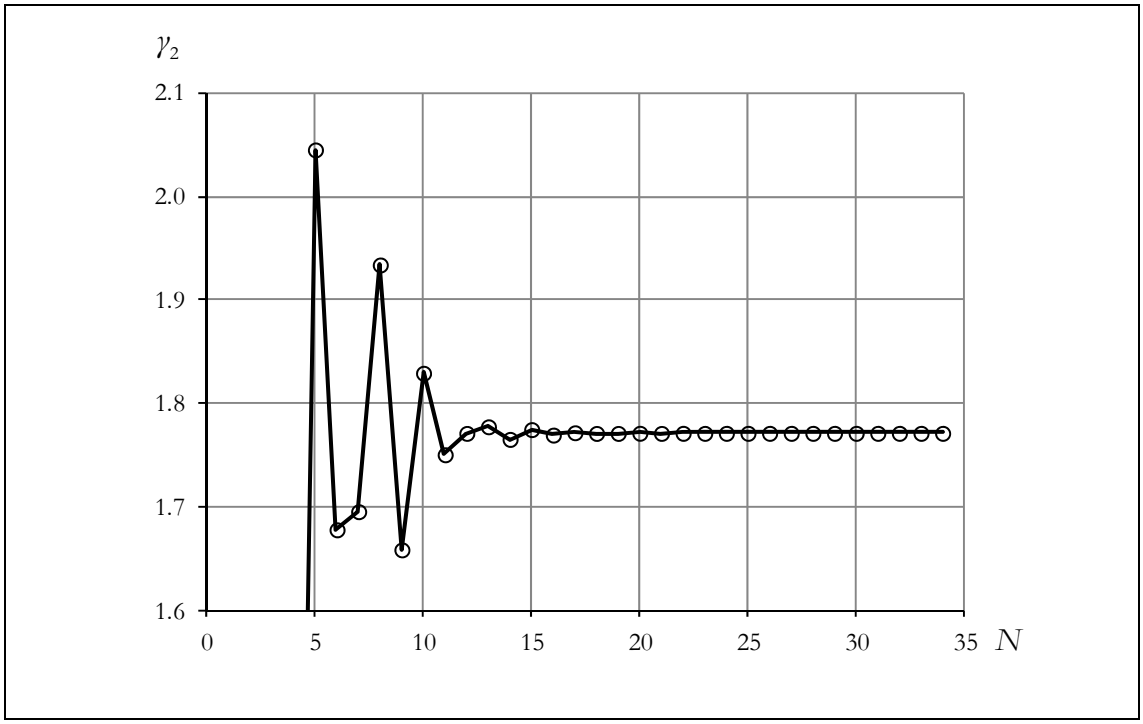

Figure 5.7.3: Convergence of the Frobenius series solution – $\alpha = 0.75$, $\gamma_1 = 1.854\ (\cong \frac{1}{2}\gamma_{1.u})$

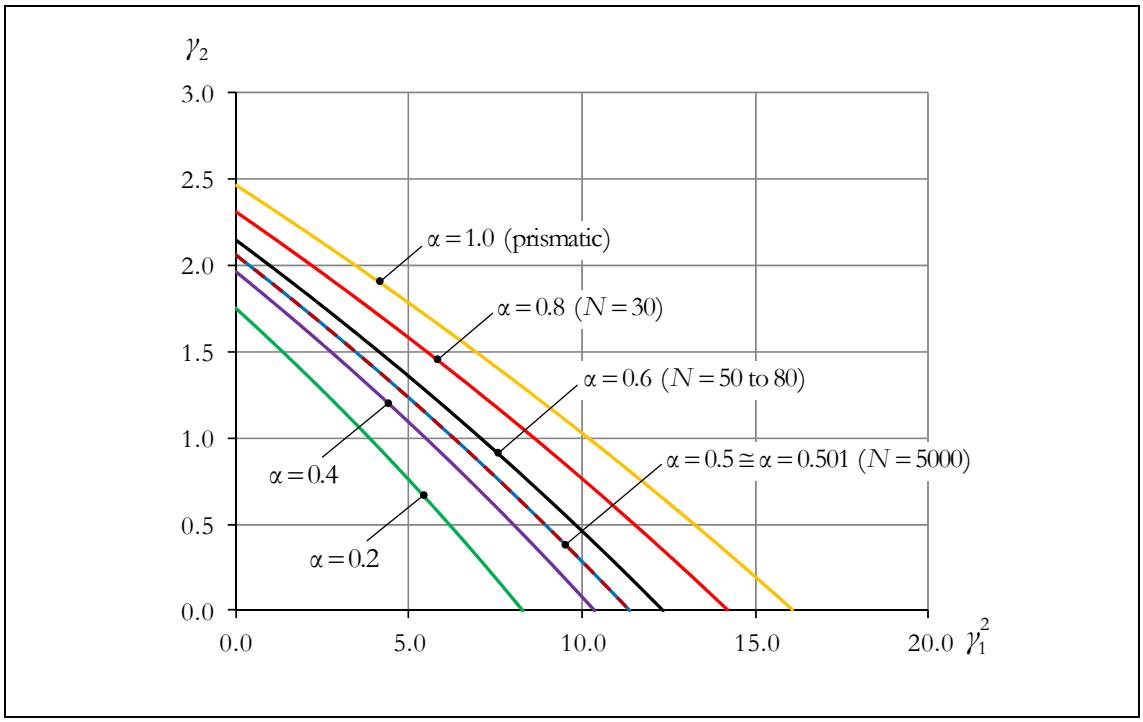

Figure 5.7.4: Linearly tapered cantilevered strip beam-columns – Stability boundaries

tapered beams (REISSNER *et al.* 1987 and ANDRADE *et al.* 2006, 2010). The required conversion is achieved in the following way:

(i) For the computation of the critical value of γ_n ($n=1$ or $n=2$), corresponding to a given fixed value of the other non-dimensional load, the differential equation

$$\tilde{\eta}_0'(s) = (\gamma_n)' = 0 \tag{5.7.50}$$

is added to the original problem. It is readily recognized that (5.7.50) is just an implicit statement of the fact that γ_n, formally interpreted as a function of s, is a constant.

(ii) In order to have a unique eigenfunction $\tilde{\eta}$ (up to sign), one adds the differential equation

$$\vartheta'(s) = \tilde{\eta}(s)^2 \ , \ \ 0 < s < 1 \tag{5.7.51}$$

and the boundary conditions

$$\vartheta(0) = 0 \tag{5.7.52}$$

$$\vartheta(1) = 1 \ . \tag{5.7.53}$$

This is equivalent to imposing the normalisation condition

$$\int_0^1 \tilde{\eta}(s)^2 \, ds = 1 \tag{5.7.54}$$

upon the eigenfunctions.

It should be noticed that (i) the enlarged boundary value problem is non-linear and (ii) the boundary conditions remain separated. Another important feature to appreciate is the fact that there is no need to modify COLNEW in order to deal with the regular singularity at the boundary point $s=0$, as the discretisation method involves collocation at Gaussian points and so the left-hand side of equation (5.7.22) is never evaluated at an end point (AUZINGER *et al.* 2006).

Since the construction of stability boundaries for different values of the taper ratio α requires the solution of chains of "nearby" problems (known as "homotopy chains" – DEUFLHARD 1979, p. 65), a simple continuation strategy was implemented: γ_m ($m \neq n$) and α are taken as the continuation parameters and the solution of a previous problem is adopted as the initial guess for a subsequent one, having the same data except for a small increment in a single continuation parameter, a possibility that is already encoded in COLNEW. The continuation process can start with one of the uncoupled load cases and $\alpha = 1$, for which there are known analytical solutions. The results obtained for $0 < \alpha \leq \frac{1}{2}$

are plotted in figure 5.7.4. For $\frac{1}{2} < \alpha \leq 1$, the collocation and Frobenius series solutions virtually coincide with one another.

* * *

The analytical and numerical solutions presented above were compared with the results of shell finite element analyses and an excellent agreement was found in all cases – the details can be found in CHALLAMEL *et al.* (2010). Moreover, (i) the results concerning $\gamma_2 = 0$ (beam lateral-torsional buckling) are in perfect agreement with those obtained previously in § 5.4 and (ii) the results concerning $\gamma_1 = 0$ (column flexural buckling) are in perfect agreement with those presented by DINNIK (1932), who obtained the general solution to the governing differential equation in terms of Bessel functions.

In accordance with the theorem of Papkovitch-Schaefer, the stability boundaries in in the first quadrant of the $\left(\gamma_1^2, \gamma_2\right)$ half-plane, shown in figure 5.7.4, never exhibit convexity towards the origin. They are therefore bounded from below by the corresponding Dunkerley's lines (5.7.32), which can be seen to be quite accurate. In fact, equation (5.7.32) is precisely the approximation proposed by GATEWOOD (1955) for this problem. Moreover, the ratio

$$\frac{\gamma_{1.u}}{\gamma_{2.u}} = \frac{\lambda_{1.u}\, Q_{ref}}{\lambda_{2.u}\, P_{ref}} \sqrt{\frac{EI_{3.0}}{GJ_0}} \tag{5.7.55}$$

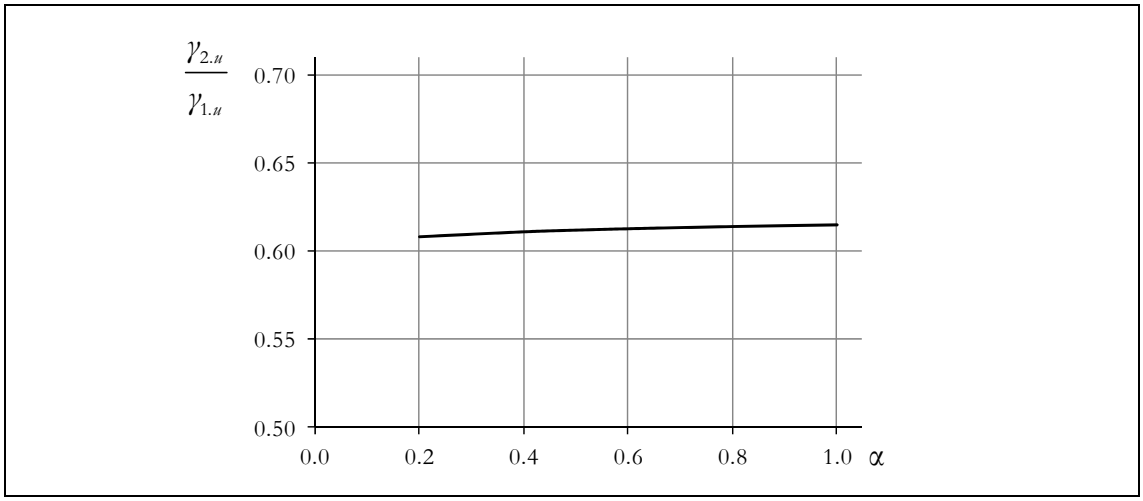

Figure 5.7.5: Linearly tapered cantilevered strip beam-columns – Ratio $\gamma_{2.u} / \gamma_{1.u}$ *vs.* α

is practically independent of α over the range $0.2 \le \alpha \le 1.0$, as shown in figure 5.7.5. We can take $\gamma_{2.u} / \gamma_{1.u} \cong 0.612$ (with relative errors less than 0.6%) and approximate Dunkerley's line by

$$\left(\frac{\gamma_1}{\gamma_{1.u}} \right)^2 + \frac{\gamma_2}{0.612 \gamma_{1.u}} = 1 \ , \ 0 \le \gamma_1^2 \le \gamma_{1.u}^2 \ , \ 0 \le \gamma_2 \le 0.612 \gamma_{1.u} \ , \tag{5.7.56}$$

which requires the sole knowledge of $\gamma_{1.u}$.

APPENDIX 2

In this appendix, one proves the following result:

Proposition. Let there be given a function $u:\mathbb{R}\to\mathbb{R}$ and real numbers A and B, with $2A\notin\mathbb{Z}_0^-$. The function defined on $\mathbb{R}$ by

$$f(t)=e^{-iu(t)}\,M\big(A+iB,2A,i2u(t)\big) \tag{A2.1}$$

is real-valued.

Proof. First, observe that for every $a,z\in\mathbb{C}$ and $b\in\mathbb{R}$ (excluding $b=0,-1,-2,\ldots$), one has

$$\overline{M(a,b,z)}=M(\overline{a},b,\overline{z})\ , \tag{A2.2}$$

where the superposed bar denotes complex conjugation. Indeed, by definition, $M(a,b,z)$ is given by the sum of the absolutely convergent series (recall equations (5.4.30) and (5.4.32))

$$M(a,b,z)=1+\frac{a}{b}z+\frac{a(a+1)z^2}{b(b+1)2!}+\frac{a(a+1)(a+2)z^3}{b(b+1)(b+2)3!}+\ldots\ . \tag{A2.3}$$

Therefore, using the basic properties of complex conjugation, one finds

$$\begin{aligned}\overline{M(a,b,z)}&=\overline{1+\frac{a}{b}z+\frac{a(a+1)z^2}{b(b+1)2!}+\frac{a(a+1)(a+2)z^3}{b(b+1)(b+2)3!}+\ldots}\\&=1+\frac{\overline{a}}{b}\overline{z}+\frac{\overline{a}(\overline{a}+1)\overline{z}^2}{b(b+1)2!}+\frac{\overline{a}(\overline{a}+1)(\overline{a}+2)\overline{z}^3}{b(b+1)(b+2)3!}+\ldots=M(\overline{a},b,\overline{z})\ .\end{aligned} \tag{A2.4}$$

The application of this result, together with the identity $\overline{e^{z}}=e^{\overline{z}}$, to the conjugate of $f(t)$ yields

$$\overline{f(t)}=e^{iu(t)}\,M\big(A-iB,2A,-i2u(t)\big)\ . \tag{A2.5}$$

Finally, using Kummer's first theorem (*e.g.*, DAALHUIS 2010, eq. (13.2.39)), one obtains

$$\begin{aligned}\overline{f(t)}&=e^{iu(t)}\,e^{-i2u(t)}\,M\big(2A-(A-iB),2A,i2u(t)\big)\\&=e^{-iu(t)}\,M\big(A+iB,2A,i2u(t)\big)=f(t)\end{aligned} \tag{A2.6}$$

and the conclusion $f(t)\in\mathbb{R}$ follows immediately.

The above proof is a minor generalisation of an unpublished note by B.M. Milisavlevich.

APPENDIX 3

In this appendix, one shows that equations (5.7.30) and (5.7.31) are equivalent. Indeed, by setting

$$a = \frac{1}{4} + i\,\frac{\gamma_2}{4\gamma_1} \tag{A3.1}$$

$$b = \frac{3}{2} \tag{A3.2}$$

$$z = i\,\gamma_1 \tag{A3.3}$$

in the recurrence relation (*e.g.*, DAALHUIS 2010, eq. (13.3.13))

$$(a+1)z\,M(a+2,b+2,z)+(b+1)(b-z)\,M(a+1,b+1,z)-b(b+1)\,M(a,b,z)=0\ , \tag{A2.4}$$

one finds

$$\left(-\frac{\gamma_2}{5}+i\,\gamma_1\right)M\left(\frac{9}{4}+i\,\frac{\gamma_2}{4\gamma_1},\frac{7}{2},i\,\gamma_1\right)+\left(3-i\,2\gamma_1\right)M\left(\frac{5}{4}+i\,\frac{\gamma_2}{4\gamma_1},\frac{5}{2},i\,\gamma_1\right)$$
$$-3\,M\left(\frac{1}{4}+i\,\frac{\gamma_2}{4\gamma_1},\frac{3}{2},i\,\gamma_1\right)=0 \tag{A3.5}$$

and the insertion of this result into equation (5.7.30) leads to

$$e^{-i\frac{\gamma_1}{2}}\left[(-\gamma_2+i\,\gamma_1)M\left(\frac{5}{4}+i\,\frac{\gamma_2}{4\gamma_1},\frac{5}{2},i\,\gamma_1\right)+3\,M\left(\frac{1}{4}+i\,\frac{\gamma_2}{4\gamma_1},\frac{3}{2},i\,\gamma_1\right)\right]=0\ . \tag{A3.6}$$

Using the recurrence relation (A3.4) once again, now with

$$a = -\frac{3}{4} + i\,\frac{\gamma_2}{4\gamma_1} \tag{A3.7}$$

$$b = \frac{1}{2} \tag{A3.8}$$

$$z = i\,\gamma_1 \tag{A3.9}$$

one obtains

$$(-\gamma_2+i\,\gamma_1)M\left(\frac{5}{4}+i\,\frac{\gamma_2}{4\gamma_1},\frac{5}{2},i\,\gamma_1\right)+(3-i\,6\gamma_1)M\left(\frac{1}{4}+i\,\frac{\gamma_2}{4\gamma_1},\frac{3}{2},i\,\gamma_1\right)$$
$$-3\,M\left(-\frac{3}{4}+i\,\frac{\gamma_2}{4\gamma_1},\frac{1}{2},i\,\gamma_1\right)=0 \tag{A3.10}$$

and equation (A3.6) is thus brought into the form

$$e^{-i\frac{\gamma_1}{2}}\left[i\,6\gamma_1 M\left(\frac{1}{4}+i\frac{\gamma_2}{4\gamma_1},\frac{3}{2},i\,\gamma_1\right)+3M\left(-\frac{3}{4}+i\frac{\gamma_2}{4\gamma_1},\frac{1}{2},i\,\gamma_1\right)\right]=0\ . \tag{A3.11}$$

Finally, the recurrence relation (*e.g.*, DAALHUIS 2010, eq. (13.3.4))

$$b\,M(a,b,z)-b\,M(a-1,b,z)-z\,M(a,b+1,z)=0\ , \tag{A3.12}$$

with

$$a=\frac{1}{4}+i\,\frac{\gamma_2}{4\gamma_1} \tag{A3.13}$$

$$b=\frac{1}{2} \tag{A3.14}$$

$$z=i\,\gamma_1\ , \tag{A3.15}$$

gives

$$M\left(\frac{1}{4}+i\frac{\gamma_2}{4\gamma_1},\frac{1}{2},i\,\gamma_1\right)-M\left(-\frac{3}{4}+i\frac{\gamma_2}{4\gamma_1},\frac{1}{2},i\,\gamma_1\right)$$
$$-i\,2\gamma_1 M\left(\frac{1}{4}+i\frac{\gamma_2}{4\gamma_1},\frac{3}{2},i\,\gamma_1\right)=0\ . \tag{A3.16}$$

The incorporation of this identity into equation (A3.11) yields the desired result:

$$e^{-i\frac{\gamma_1}{2}}M\left(\frac{1}{4}+i\,\frac{\gamma_2}{4\gamma_1},\frac{1}{2},i\,\gamma_1\right)=0\ . \tag{A3.17}$$

REFERENCES

ANDRADE A., CHALLAMEL N., PROVIDÊNCIA P. and CAMOTIM D. (2012). Lateral-torsional stability boundaries for polygonally depth-tapered strip cantilevers under multi-parameter point load systems – An analytical approach. *Journal of Applied Mechanics – Transactions of the ASME*, in press.

ANDRADE A., PROVIDÊNCIA P. and CAMOTIM D. (2006). Lateral-torsional buckling analysis of web-tapered I-beams using finite element and spline collocation methods. *Book of Abstracts of the 3rd European Conference on Computational Mechanics – Solids, Structures and Coupled Problems in Engineering* (Lisbon), C.A. Mota Soares *et al.* (Eds.). Dordrecht, The Netherlands: Springer, 680 (full paper in CD-ROM Proceedings).

ANDRADE A., PROVIDÊNCIA P. and CAMOTIM D. (2010). Elastic lateral-torsional buckling of restrained web-tapered I-beams. *Computers & Structures*, **88**(21-22), 1179-1196.

ANDREWS G.E., ASKEY R. and ROY R. (1999). *Special Functions*. Encyclopedia of Mathematics and its Applications, Volume 71. Cambridge: Cambridge University Press.

ARTIN E. (1931). *Einführung in die Theorie der Gammafunktion*. Leipzig: Teubner. English translation by M. Butler (1964), *The Gamma Function*. New York: Holt, Rinehart and Winston.

AUZINGER W., KARNER E., KOCH O. and WEINMÜLLER E. (2006). Collocation methods for the solution of eigenvalue problems for singular ordinary differential equations. *Opuscula Mathematica*, **26**(2), 229-241.

AVEZ A. (1983). *Calcul Différentiel* [Differential Calculus]. Paris: Masson.

AXELSSON O. and BARKER V.A. (1984). *Finite Element Solution of Boundary Value Problems – Theory and Computation*. Orlando, Florida: Academic Press.

BABUSKA I. and ODEN J.T. (2004). Verification and validation in computational engineering and science: Basic concepts. *Computer Methods in Applied Mechanics and Engineering*, **193**(36-38), 4057–4066.

BABUSKA I. and OSBORN J. (1991). Eigenvalue problems. *Handbook of Numerical Analysis*, Volume 2: Finite Element Methods (Part 1), P.G. Ciarlet and J.L. Lions (Eds.). Amsterdam: Elsevier, 641-787.

BADER G. and ASCHER U. (1987). A new basis implementation for a mixed order boundary value ODE solver. *SIAM Journal on Scientific and Statistical Computing*, **8**(4), 483-500.

BAKER G. (1993). Lateral buckling of nonprismatic cantilevers using weighted residuals. *Journal of Engineering Mechanics – ASCE*, **119**(10), 1899-1919.

BARTLE R.G. (1967). *The Elements of Real Analysis*. New York: Wiley.

BEALS R. and WONG R. (2010). *Special Functions – A Graduate Text*. Cambridge: Cambridge University Press.

BENDER C.M. and ORSZAG S.A. (2010). *Advanced Mathematical Methods for Scientists and Engineers I – Asymptotic Methods and Perturbation Theory*. New York: Springer.

BILLINGTON D.P. (1997). *Robert Maillart – Builder, Designer, and Artist*. Cambridge: Cambridge University Press.

BOLEY B.A. (1963). On the accuracy of the Bernoulli-Euler theory for beams of variable section. *Journal of Applied Mechanics – Transactions of the ASME*, **30**, 373-378.

BOURBAKI N. (2007a). *Éléments de Mathématique – Topologie Générale (Chapitres 1 à 4)* [Elements of Mathematics – General Topology (Chapters 1 to 4)]. Berlin: Springer.

BOURBAKI N. (2007b). *Éléments de Mathématique – Fonctions d'Une Variable Réelle: Théorie Élémentaire* [Elements of Mathematics – Functions of One Real Variable: Elementary Theory]. Berlin: Springer.

BREZIS H. (2011). *Functional Analysis, Sobolev Spaces and Partial Differential Equations*. New York: Springer.

BUCHHOLZ H. (1953). *Die konfluente hypergeometrische Funktion*. Berlin: Springer. English translation by H. Lichtbau and K. Wetzel (1969), *The Confluent Hypergeometric Function, with Special Emphasis on its Applications*. New York: Springer.

CAMPOS FERREIRA J. (1987). *Introdução à Análise Matemática* [Introduction to Mathematical Analysis]. Lisboa: Fundação Calouste Gulbenkian.

CARTAN H. (1992). *Théorie Élémentaire des Fonctions Analytiques d'Une ou Plusieurs Variables Complexes* [Elementary Theory of Analytic Functions of One or Several Complex Variables] (6^{e} édition). Paris: Hermann.

CAYLEY A. (1886). On linear differential equations. *Quarterly Journal of Pure and Applied Mathematics*, **21**, 321-331. Reprinted in *The Collected Mathematical Papers of Arthur Cayley*, Volume 12, 1897. Cambridge: Cambridge University Press, 394-402.

CHALLAMEL N., ANDRADE A. and CAMOTIM D. (2007). An analytical study on the lateral-torsional buckling of linearly tapered cantilever strip beams. *International Journal of Structural Stability and Dynamics*, **7**(3), 441-456.

CHALLAMEL N., ANDRADE A., CAMOTIM D. and MILISAVLEVICH B.M. (2010). Flexural-torsional buckling of cantilever strip beam-columns with linearly varying depth. *Journal of Engineering Mechanics – ASCE*, **136**(6), 787-800.

CHALLAMEL N. and WANG C.M. (2010). Exact lateral-torsional buckling solutions for cantilevered beams subjected to intermediate and end transverse point loads. *Thin-Walled Structures*, **48**(1), 71-76.

CHILVER A.H. (1972). The elastic stability of structures. *Stability – Fourteen Special Lectures Presented at the University of Waterloo from October 1970 to September 1971* (SM Study n.º 6), H.H.E. Leipholz (Ed.). Solid Mechanics Division, University of Waterloo, Canada, 41-61.

CIARLET P.G. (1988). *Mathematical Elasticity*, Volume 1: Three-Dimensional Elasticity. Amsterdam: North-Holland.

CODDINGTON E.A. and CARLSON R. (1997). *Linear Ordinary Differential Equations*. Philadelphia: Society for Industrial and Applied Mathematics (SIAM).

COLEMAN R.P. (1939). *The Frequency of Torsional Vibration of a Tapered Beam*. Technical Note n. 697, National Advisory Committee for Aeronautics (NACA).

CONWAY J.B. (1978). *Functions of One Complex Variable* (2nd edition). New York: Springer.

DAALHUIS A.B.O. (2010). Confluent hypergeometric functions. *NIST Handbook of Mathematical Functions*, F.W.J. Olver, D.W. Lozier, R.F. Boisvert and C.W. Clark (Eds.). New York: Cambridge University Press, 321-349.

DACOROGNA B. (2004). *Introduction to the Calculus of Variations*. London: Imperial College Press.

DAVIS P.J. (1959). Leonhard Euler's integral: A historical profile of the gamma function. *The American Mathematical Monthly*, **66**(10), 849-869. Reprinted in *The Chauvenet Papers – A Collection of Prize-Winning Expository Papers in Mathematics*, Volume 2, J.C. Abbott (Ed.), 1978. Washington, D.C.: The Mathematical Association of America, 332-351.

DEUFLHARD P. (1979). Nonlinear equation solvers in boundary value problem codes. *Codes for Boundary-Value Problems in Ordinary Differential Equations*, Lecture Notes in Computer Science 76, B. Childs, M. Scott, J.W. Daniel, E. Denman and P. Nelson (Eds.). Berlin: Springer, 40-66.

DIEUDONNÉ J. (1960). *Foundations of Modern Analysis*. New York: Academic Press.

DIMAGGIO F., GOMZA A., THOMAS W.E. and SALVADORI M.G. (1952). Lateral buckling of beams in bending and compression. *Journal of the Aeronautical Sciences*, **19**(8), 574-576.

DINNIK A. (1932). Design of columns of varying cross section. *Transactions of the ASME*, **54**, Paper nº. APM-54-16, 165-171.

DUTKA J. (1991). The early history of the factorial function. *Archive for History of Exact Sciences*, **43**(3), 225-249.

DUTKA J. (1995). On the early history of Bessel functions. *Archive for History of Exact Sciences*, **49**(2), 105-134.

ELISHAKOFF I. (2005). *Eigenvalues of Inhomogeneous Structures – Unusual Closed-Form Solutions*. Boca Raton, Florida: CRC.

ERDÉLYI A., MAGNUS W., OBERHETTINGER F. and TRICOMI F.G. (1953a). *Higher Transcendental Functions*, Volume 1. New York: McGraw-Hill.

ERDÉLYI A., MAGNUS W., OBERHETTINGER F. and TRICOMI F.G. (1953b). *Higher Transcendental Functions*, Volume 2. New York: McGraw-Hill.

EULER L. (1744). Additamentum I. De curvis elasticis. *Methodus Inveniendi Lineas Curvas Maximi Minimive Proprietate Gaudentes, sive Solutio Problematis Isoperimetrici Lattissimo Sensu Accepti* [A Method of Finding Curved Lines Enjoying Properties of Maximum or Minimum, or Solution of Isoperimetric Problems in the Broadest Accepted Sense]. Lausanne & Geneva: Marcum-Michaelem Bousquet & Socios, 245-310. Reprinted in *Leonhardi Euleri Opera Omnia*, Series Prima (Opera Mathematica), Volume 24, C. Carathéodory (Ed.), 1952. Zurich: Orell Füssli, 231-297. Annotated English translation by W.A. Oldfather, C.A. Ellis and D.M. Brown (1933), Leonhard Euler's elastic curves, *Isis*, **20**(1), 72-160.

EULER L. (1759). Sur la force des colonnes [On the strength of columns]. *Mémoires de l'Académie Royale des Sciences et Belles Lettres*, Berlin, **13**, 252-282. Reprinted in *Leonhardi Euleri Opera Omnia*, Series Secunda (Opera Mechanica et Astronomica), Volume 17, C. Blanc and P. Haller (Eds.), 1982. Zurich: Orell Füssli, 89-118. Partial english translation (§§ 1-18) and introductory study by J.A. Van den Broek (1947), Euler's classic paper "On the strength of columns", *American Journal of Physics*, **15**(4), 309-318.

FEDERHOFER K. (1931). Neue Beiträge zur Berechnung der Kipplasten gerader Stäbe [New contributions to the calculation of the lateral-torsional buckling loads of straight bars]. *Sitzungsberichte der Akademie der Wissenschaften in Wien*, **140**, 237-270.

FROBENIUS G. (1873). Ueber die Integration der linearen Differentialgleichungen durch Reihen [On the integration by series of linear differential equations]. *Journal für die reine und angewandte Mathematik*, **76**, 214-235.

GATEWOOD B.E. (1955). Buckling loads for beams of variable cross section under combined loads. *Journal of the Aeronautical Sciences*, **22**(4), 281-282.

HENRICI P. (1977). *Applied and Computational Complex Analysis*, Volume 2: Special Functions, Integral Transforms, Asymptotics, Continued Fractions. New York: Wiley.

HOCHSTADT H. (1971). *The Functions of Mathematical Physics*. New York: Wiley.

HODGES D.H., HO J.C. and YU W. (2008). The effect of taper on section constants for in-plane deformation of an isotropic strip. *Journal of Mechanics of Materials and Structures*, **3**(3), 425-440.

HODGES D.H. and PETERS D.A. (1975). On the lateral buckling of uniform slender cantilever beams. *International Journal of Solids and Structures*, **11**(12), 1269-1280.

HUSEYIN K. (1970). The elastic stability of structural systems with independent loading parameters. *International Journal of Solids and Structures*, **6**(5), 677-691.

HUSEYIN K. (1978). *Vibrations and Stability of Multiple Parameter Systems*. Alphen aan den Rijn, the Netherlands: Noordhoff.

HUSEYIN K. and ROORDA J. (1971). The loading-frequency relationship in multiple eigenvalue problems. *Journal of Applied Mechanics – Transactions of the ASME*, **38**(4), 1007-1011.

INCE E.L. (1956). *Ordinary Differential Equations*. New York: Dover.

KOITER W.T. (1963). Elastic stability and post-buckling behaviour. *Nonlinear Problems*, R.E. Langer (Ed.). Madison, Wisconsin: University of Wisconsin Press, 257-275.

KRANTZ S.G. and PARKS H.R. (2002). *A Primer of Real Analytic Functions* (2nd edition). Boston: Birkhäuser.

KRISTENSSON G. (2010). *Second Order Differential Equations – Special Functions and Their Classification*. New York: Springer.

KUMMER E.E. (1836). Über die hypergeometrische Reihe $1+\frac{\alpha.\beta}{1.\gamma}x+\frac{\alpha(\alpha+1)\beta(\beta+1)}{1.2.\gamma(\gamma+1)}x^2+\frac{\alpha(\alpha+1)(\alpha+2)\beta(\beta+1)(\beta+2)}{1.2.3.\gamma(\gamma+1)(\gamma+2)}x^3+\cdots$. *Journal für die reine und angewandte Mathematik*, **15**, 39-83 and 127-172. Reprinted in *Ernst Eduard Kummer Collected Papers*, Volume 2: Function Theory, Geometry and Miscellaneous, A. Weil (Ed.), 1975. Berlin: Springer, 75-166. English translation by H. Nagaoka (1891), On the hypergeometric series …, K. Yamakawa (Ed.), *Memoirs on Infinite Series*. Tokyo: The Tokio Mathematical and Physical Society.

KUMMER E.E. (1837). De integralibus quibusdam definitis et seriebus infinitis [On certain definite integrals and infinite series]. *Journal für die reine und angewandte Mathematik*, **17**, 228-242. Reprinted in *Ernst Eduard Kummer Collected Papers*, Volume 2: Function Theory, Geometry and Miscellaneous, A. Weil (Ed.), 1975. Berlin: Springer, 196-210.

LANCZOS C. (1970). *The Variational Principles of Mechanics* (4th edition). Toronto: University of Toronto Press.

LANG S. (1999). *Complex Analysis* (4th edition). New York: Springer.

LEBEDEV N.N. (1965). *Special Functions and their Applications*. Englewood Cliffs, New Jersey: Prentice-Hall.

LEE L.H.N. (1956). Non-uniform torsion of tapered I-beams. *Journal of the Franklin Institute*, **262**(July), 37-44.

LEE L.H.N. (1959). On the lateral buckling of a tapered narrow rectangular beam. *Journal of Applied Mechanics – Transactions of the ASME*, **26**, 457-458.

LINDNER J. and HOLBERNDT T. (2006). Zum Nachweis von stabilitätsgefährdeten Glasträgern unter Biegebeanspruchung [Stability design of glass beams subjected to bending]. *Stahlbau*, **75**(6), 488-498.

LIU G.R. and XI Z.C. (2002). *Elastic Waves in Anisotropic Laminates*. Boca Raton, Florida: CRC Press.

LOMMEL E. (1871). Zur Theorie der Bessel'schen Functionen [On the theory of Bessel functions]. *Mathematische Annalen*, **3**, 475-487.

LUIBLE A. and CRISINEL M. (2005). Stability of load carrying elements of glass. *Proceedings of the 4th European Conference on Steel and Composite Structures – EUROSTEEL 2005* (Maastricht, The Netherlands), B. Hoffmeister and O. Hechler (Eds.). Aachen: Druck und Verlagshaus Mainz, 2.4:9-16 (Volume B).

LUIBLE A. and CRISINEL M. (2006). Lateral torsional buckling of glass beams. *Progress in Steel, Composite and Aluminium Structures – Proceedings of the XI International Conference on Metal Structures* (Rzeszów, Poland), M. Gizejowski *et al.* (Eds.). London: Taylor & Francis, 971-978.

LUKE Y.L. (1969). *The Special Functions and their Approximations*, Volume 1. San Diego, California: Academic Press.

MARTIN H.C. (1951). Elastic instability of deep cantilever struts under combined axial and shear loads at the free end. *Proceedings of the 1st U.S. National Congress of Applied Mechanics* (Chicago), 395-402.

MASSEY C. and MCGUIRE P.J. (1971). Lateral stability of nonuniform cantilevers. *Journal of the Engineering Mechanics Division – ASCE*, **97**(EM3), 673-686.

MASUR E.F. (1972). Discussion on the paper "The loading-frequency relationship in multiple eigenvalue problems" by K. Huseyin and J. Roorda. *Journal of Applied Mechanics – Transactions of the ASME*, **39**(2), 635-636.

MEIXNER J. (1956). Spezielle Funktionen der mathematischen Physik [The special functions of mathematical physics]. *Handbuch der Physik*, Volume I: Mathematical Methods 1, S. Flügge (Ed.). Berlin: Springer, 147-217.

MICHELL A.G.M. (1899). Elastic stability of long beams under transverse forces. *Philosophical Magazine*, **48**, 198-309.

MILISAVLJEVIC B.M. (1988). Lateral buckling of a cantilever beam with imperfections. *Acta Mechanica*, **74**(1-4), 123-137.

MILLER J.C.P. (1950). On the choice of standard solutions for a homogeneous linear differential equation of the second order. *The Quarterly Journal of Mechanics and Applied Mathematics*, **3**(2), 225-235.

MUNKRES J.R. (2000). *Topology* (2nd edition). Upper Saddle River, New Jersey: Prentice-Hall.

NADAI A. (1925). *Elastische Platten* [Elastic Plates]. Berlin: Julius Springer.

OLVER F.W.J. (1974). *Asymptotics and Special Functions*. New York: Academic Press.

OLVER F.W.J. and MAXIMON L.C. (2010). Bessel functions. *NIST Handbook of Mathematical Functions*, F.W.J. Olver, D.W. Lozier, R.F. Boisvert and C.W. Clark (Eds.). New York: Cambridge University Press, 215-286.

PANAYOTOUNAKOS D.E. (1995). Classes of solutions in the problem of stability analysis in bars with varying cross-section and axial distributed loading. *International Journal of Solids and Structures*, **32**(21), 3229-3236.

PAPKOVITCH P.F. (1934). Ein allgemeiner Satz über die Stabilität Elastischer Systeme unter Gleichzeitiger Wirkung von mehren Belastung [A general theorem on the stability of elastic systems under the simultaneous effect of several loads]. *Proceedings of the 4th International Congress of Applied Mechanics* (Cambridge), 231-232.

PIGNATARO M., RIZZI N. and LUONGO A. (1991). *Stability, Bifurcation and Postcritical Behaviour of Elastic Structures*. Amsterdam: Elsevier.

POLIDORI D.C. and BECK J.L. (1996). Approximate solutions for non-linear random vibration problems. *Probabilistic Engineering Mechanics*, **11**(3), 179-185.

POLYA G. (1973). *How to Solve It – A New Aspect of Mathematical Method* (2nd edition). Princeton, New Jersey: Princeton University Press.

POLYANIN A.D. and ZAITSEV V.F. (2003). *Handbook of Exact Solutions for Ordinary Differential Equations* (2nd edition). Boca Raton, Florida: Chapman & Hall/CRC.

PRANDTL L. (1899). *Kipp-Erscheinungen – Ein Fall von instabilem elastischem Gleichgewicht* [Lateral-Torsional Buckling Phenomena – A Case of Unstable Elastic Equilibrium]. Dissertation, Ludwig-Maximilians-Universität München. Reprinted in *Ludwig Prandtl Gesammelte Abhandlungen zur angewandten Mechanik, Hydro- und Aerodynamik* [Ludwig Prandtl Collected Works on Apllied Mechanics, Hydro- and Aerodynamics], Volume 1, W. Tollmien, H. Schlichting and H. Görtler (Eds.), 1961. Berlin: Springer, 10-74.

RAJ A. and SUJITH R.I. (2005). Closed-form solutions for the free longitudinal vibration of inhomogeneous rods. *Journal of Sound and Vibration*, **283**(3–5), 1015–1030.

REISSNER E. (1979). On lateral buckling of end-loaded cantilever beams. *Zeitschrift für angewandte Mathematik und Physik*, **30**(1), 31-40.

REISSNER E. (1981). On the effect of shear center location on the values of axial and lateral cantilever buckling loads for singly symmetric cross-section beams. *Zeitschrift für angewandte Mathematik und Physik*, **32**(2), 182-188.

REISSNER E., REISSNER J.E. and WAN F.Y.M. (1987). On lateral buckling of end-loaded cantilevers including the effect of warping stiffness. *Computational Mechanics*, **2**(2), 137-147.

REISSNER H. (1904). Über die Stabilität der Biegung [On the stability of beams]. *Sitzungsberichte der Berliner Mathematischen Gesellschaft*, **3**, 53-56.

REMMERT R. (1991). *Theory of Complex Functions*. New York: Springer.

RUDIN W. (1976). *Principles of Mathematical Analysis* (3rd edition). Tokyo: McGraw-Hill.

SÁNCHEZ D.A. (1968). *Ordinary Differential Equations and Stability Theory – An Introduction*. New York: Dover.

SCHAEFER H. (1934). Angenäherte Berechnung des kleinsten Eigenwertes zusammengesetzter Systeme [Approximate calculation of the smallest eigenvalue of composite systems]. *Zeitschrift für angewandte Mathematik und Mechanik*, **14**(6), 367-368.

SIMMONS G.F. (1991). *Differential Equations with Applications and Historical Notes* (2nd edition). Singapore: McGraw-Hill.

SLATER L.J. (1960). *Confluent Hypergeometric Functions*. Cambridge: Cambridge University Press.

TARNAI T. (1995). The Southwell and the Dunkerley theorems. *Summation Theorems in Structural Stability* (CISM Courses and Lectures n. 354), T. Tarnai (Ed.). Wien: Springer, 141-185.

TARNAI T. (1999). Summation theorems concerning critical loads of bifurcation. *Structural Stability in Engineering Practice*, L. Kollár (Ed.). London: E & FN Spon, 23-58.

TEMME N.M. (1996). *Special Functions – An Introduction to the Classical Functions of Mathematical Physics*. New York: Wiley.

TIMOSHENKO S.P. and GERE J.M. (1961). *Theory of Elastic Stability* (2nd edition). Tokyo: McGraw-Hill.

TIMOSHENKO S.P. and GOODIER J.N. (1970). *Theory of Elasticity* (3rd edition). New-York: McGraw-Hill.

TRABUCHO L. and VIAÑO J.M. (1996). Mathematical modeling of rods. *Handbook of Numerical Analysis*, Volume 4: Finite Element Methods (Part 2) – Numerical Methods for Solids (Part 2), P.G. Ciarlet and J.L. Lions (Eds.). Amsterdam: Elsevier, 487-974.

TREFFTZ E. (1930). Über die Ableitung der Stabilitätskriterien des elastischen Gleichgewichtes aus der Elastizitätstheorie endlicher Deformationen [On the derivation of stability criteria for elastic equilibrium from finite-deformation elasticity theory]. *Proceedings of the Third International Congress of Applied Mechanics* (Stockholm), Volume 3, 44-50.

TREFFTZ E. (1933). Zur Theorie der Stabilität des elastischen Gleichgewichts [On the theory of stability of elastic equilibrium]. *Zeitschrift für angewandte Mathematik und Mechanik*, **13**(2), 160-165.

TRICOMI F.G. (1947). Sulle funzioni ipergeometriche confluent [On confluent hypergeometric functions]. *Annali di Matematica Pura ed Applicata*, **36**(4), 141-175.

TRICOMI F.G. (1954). *Funzioni Ipergeometriche Confluenti* [Confluent Hypergeometric Functions]. Roma: Edizioni Cremonese.

TRICOMI F.G. (1955). Konfluente hypergeometrische Funktionen – Zusammenfassender Bericht [Confluent hypergeometric functions – Summary report]. *Zeitschrift für angewandte Mathematik und Physik*, **6**(4), 257-274.

TRUESDELL C. (1960). The rational mechanics of flexible or elastic bodies, 1638-1788. *Leonhardi Euleri Opera Omnia*, Series Secunda (Opera Mechanica et Astronomica), Volume 11/2. Zurich: Orell Füssli.

VOLOVOI V.V., HODGES D.H., BERDICHEVSKY V.L. and SUTYRIN V.G. (1999). Asymptotic theory for static behavior of elastic anisotropic I-beams. *International Journal of Solids and Structures*, **36**(7), 1017-1043.

WANG C.M., WANG C.Y. and REDDY J.N. (2005). *Exact Solutions for Buckling of Structural Members*. Boca Raton, Florida: CRC.

WANG Z.X. and GUO D.R. (1989). *Special Functions*. Singapore: World Scientific.

WATSON G.N. (1944). *A Treatise on the Theory of Bessel Functions* (2nd edition). Cambridge: Cambridge University Press.

WEMPNER G. (1972). *The Energy Criteria for Stability of Structures*. Research Report n. 119, University of Alabama in Huntsville Research Institute.

WHITTAKER E.T. and WATSON G.N. (1963). *A Course of Modern Analysis* (4th edition, 8th reprint). Cambridge: Cambridge University Press.

WOLFRAM RESEARCH, INC. (2006). *Wolfram Mathematica 6.2*. Champaign, Illinois.

Chapter 6

SUMMARY AND CONCLUSIONS.

RECOMMENDATIONS FOR FUTURE RESEARCH

What we call the beginning is often the end
And to make an end is to make a beginning.
The end is where we start from.

T. S. ELIOT

Hofstadter's Law: It always takes longer than you expect,
even when you take into account Hofstadter's Law.

DOUGLAS R. HOFSTADTER

6.1 SUMMARY AND CONCLUSIONS

The object of the present thesis was the development of one-dimensional models for the linear static, dynamic and lateral-torsional buckling analysis of tapered thin-walled bars with open cross-sections. Moreover, we endeavoured to supply physical interpretations for the key behavioural features implied by these models, in order to shed light into the roles played by the various geometrical and mechanical parameters, with particular emphasis on those that are peculiar to the tapered case. Bearing this in mind, one now presents an outline of the contents of the thesis and a statement of conclusions, emphasizing the main original findings reported and how they contribute to further the state-of-the-art knowledge.

In chapter 2, a linear one-dimensional model for the stretching, bending and twisting of prismatic thin-walled bars with open cross-sections under general static loading conditions was presented. Its most distinctive and novel features may be summarised as follows:

(i) Thin-walled bars are basically regarded as internally constrained membrane shells.

(ii) The internal constraints extend to the tapered case the classical assumptions of Vlasov's prismatic bar theory. This extension is achieved in such a way as to retain an intrinsic geometrical meaning, *i.e.*, independent of the choice of parametrisation.

(iii) The internal constraints are treated consistently as *a priori* restrictions, of a constitutive nature, on the possible deformations of the middle surface of the bar. The membrane forces are decomposed additively into active and reactive parts, and the constitutive dependence of the active membrane forces on the membrane strains reflects the maximal symmetry compatible with the assumed internal constraints. Stress resultants are likewise split into active and reactive categories: while the normal force, bending moments and bimoment are purely active, the shear forces are purely reactive and the torque is partly active and partly reactive.

(iv) In tapered bars, and from the point of view of kinematics, the constraints give rise to an additional (non-standard) basic membrane strain mode, which is absent in prismatic bars – its amplitude is the rate of twist. As a consequence, the model features additional stiffness terms associated with the torsional behaviour, whose physical significance was illustrated through examples.

(v) From the point of view of statics, the counterpart of the preceding item is the contribution of the active membrane forces to the total torque, which is absent in prismatic bars.

(vi) There are exceptions to the statements in items (iv) and (v) – for instance, the additional basic strain mode and the contribution of the membrane forces to the total torque vanish in tapered bars whose middle surface is cut out from a cylindrical one.

(vii) The classical model of Vlasov for prismatic bars is obtained as a special case.

By virtue of the above peculiar traits, there are some striking contrasts with stepped (*i.e.*, piecewise prismatic) models in dealing with restrained torsion warping. As a consequence, whenever torsional effects are involved, the structural behaviour predicted by our model is generally at odds with that obtained using an assembly of prismatic segments obeying Vlasov's theory, regardless of the number of segments (*i.e.*, even when their length tends to zero). The physical causes at the root of these discrepancies were illustrated through concrete examples, showing that stepped models exhibit several important mechanical shortcomings. Moreover, since the discrepancies may be significant, one

concludes that the use of stepped models to simulate the spatial behaviour of tapered thin-walled bars with open cross-sections is inadequate except in special cases.

The illustrative examples also showed that the approach to non-uniform torsion pioneered by Timoshenko (and further developed by Weber and the Bleiches) – *i.e.*, regarding each plated component of the bar as an Euler-Bernoulli member undergoing stretching and bending –, when correctly applied to the tapered case, is entirely compatible with ours.

One further point deserves to be mentioned. It was shown that the developed one-dimensional model fits nicely into the unifying framework of a Tonti diagram. Indeed, the field equations relating the generalised displacements to the applied bar loads can be viewed as the combination of three sets of equations, arguably of a more fundamental nature: kinematical equations (connecting generalised displacements and strains), constitutive equations (relating the active stress resultants to the generalised strains) and equilibrium equations (establishing the final link between the active stress resultants and the applied bar loads).

The above remarks and conclusions carry over, almost word by word, to the dynamical case addressed in chapter 3, in which the contributions of rotatory inertia and torsion-warping inertia were fully taken into account. Moreover, fitting the model into the framework of a Tonti diagram required the definition of generalised velocities and momentum densities – with these quantities, the kinetic energy can be written in a very simple and compact form.

In chapter 4, we derived a linearised one-dimensional model for the elastic lateral-torsional buckling of singly symmetric tapered thin-walled beams with open cross-sections, loaded in the plane of greatest bending stiffness (symmetry plane). The adopted kinematical description precludes the model from capturing any local or distortional instability phenomena. Moreover, the effect of the pre-buckling deflections was ignored. Using an archetypal problem that "contains all the germs of generality", it was shown how the presence of linearly elastic or rigid discrete restraints, which may have a translational, torsional, minor axis bending and/or warping nature, can be accommodated in the one-dimensional lateral-torsional buckling model. Once again, it was concluded that it is generally incorrect to replace a tapered thin-walled beam with a piecewise prismatic model.

The discrepancies are particularly striking when warping torsion plays an important role in resisting buckling. Indeed, in the analysis of overhanging segments free at the tip and with linearly elastic warping and minor axis bending restraints at the support, it was found that for a large $\kappa_{\omega 0} = \frac{\pi}{L}\sqrt{\frac{\tilde{E}I_{\omega}^{*}(0)}{GJ(0)}}$ (short span and/or slender cross-section at the support) and a fixed restraint stiffness parameter $\sigma_{Rf} = 2k_{Rf}\,L/(\tilde{E}I_{3}^{*}(0))$, the non-dimensional critical load $\gamma_{cr} = \lambda_{cr}\,Q_{ref}\,L^{2}/\sqrt{\tilde{E}I_{3}^{*}(0)GJ(0)}$ does not increase monotonically with the web-taper ratio $\alpha = h(L)/h_{0}$. For low values of σ_{Rf}, the non-dimensional critical load γ_{cr} decreases as α increases. For large values of σ_{Rf}, on the other hand, γ_{cr} reaches a minimum at an intermediate value of α. The lateral-torsional buckling behaviour of built-in cantilevers with a translational or a rotational restraint at the tip was also the object of a detailed parametric investigation, whence the following conclusions were drawn:

(i) The critical load of a cantilever with a rigid restraint at the tip (either translational or torsional) is well below the second-mode buckling load of the same cantilever without the restraint.

(ii) The main factor in explaining the effectiveness of a rigid translational restraint in increasing the buckling strength is the distance between the rotation centre of the cross-section in the free-end case and the location of the translational restraint – the greater the distance, the more effective is the restraint.

(iii) There is a well-defined threshold beyond which the outcome, in terms of buckling strength, of further increases in the stiffness of the restraints is negligible.

In Chapter 5, there was a change of tone. The focus shifted from the construction and understanding of models, together with the analysis of illuminating special cases, to the analytical treatment of problems that are formulated from the onset in precise mathematical terms. The ordinary differential equations governing the lateral-torsional buckling of strip beams with varying depth were integrated exactly, in closed form, using confluent hypergeometric functions (Kummer and Tricomi functions). It was then possible to establish exact characteristic equations for the buckling loads, even though these characteristic equations are transcendental and do not have closed-form solutions. For strip beam-columns, the analytical approach, by means of the method of Frobenius, was found to be successful only in the range $\frac{1}{2} < \frac{h_{min}}{h_{max}} \leq 1$.

On several occasions, scattered throughout the thesis, we had to choose a numerical method for solving eigenproblems in ordinary differential equations. In this choice, we

departed from the usual approach adopted among the structural engineering community, which consists in the use of the finite element method in one of its many versions. Instead, the eigenproblems were first reformulated as standard inhomogeneous two-point boundary value problems, which were then solved using the easily available, widely documented, reliable and efficient general-purpose code COLNEW. The possibility of combining the use of COLNEW with a simple continuation strategy greatly facilitated the solution of chains of "nearby" problems (homotopy chains). In the buckling problems involving strip beam-columns, the presence of a regular singularity in the governing differential equation posed no difficulty whatsoever.

6.2 PUBLICATIONS

Part of the research work reported in this thesis has already been disseminated among the scientific community through the following publications:

(I) Research articles and discussions in international scientific journals

1. Challamel N., Andrade A. and Camotim D. (2007). An analytical study on the lateral-torsional buckling of linearly tapered cantilever strip beams. *International Journal of Structural Stability and Dynamics*, **7**(3), 441-456.
2. Andrade A., Camotim D. and Providência P. (2010). Discussion on the paper "Elastic flexural-torsional buckling of thin-walled cantilevers" by Lei Zhang and Geng Shu Tong [Thin-Walled Structures, **46**(1), 2008, 27–37]. *Thin-Walled Structures*, **48**(2), 184-186.
3. Challamel N., Andrade A., Camotim D. and Milisavlevich B.M. (2010). On the flexural-torsional buckling of cantilever strip beam-columns with linearly varying depth. *Journal of Engineering Mechanics – ASCE*, **136**(6), 787-800.
4. Andrade A., Providência P. and Camotim D. (2010). Elastic lateral-torsional buckling of restrained web-tapered I-beams. *Computers & Structures*, **88**(21-22), 1179-1196.
5. Andrade A., Challamel N., Providência P. and Camotim D. (2012). Lateral-torsional stability boundaries for polygonally depth-tapered strip cantilevers under multi-parameter point load systems – An analytical approach. *Journal of Applied Mechanics – Transactions of the ASME*, in press.

(II) Communications at international conferences, published in the corresponding proceedings

1. Andrade A., Providência P. and Camotim D. (2006). Lateral-torsional buckling analysis of web-tapered I-beams using finite element and spline collocation methods. *Book of Abstracts of the 3rd European Conference on Computational Mechanics – Solids, Structures and Coupled Problems in Engineering*, C.A. Mota Soares *et al.* (Eds.), Lisbon, 5-9 June, Springer, 680 (full paper in CD-ROM Proceedings).
2. Andrade A., Providência P. and Camotim D. (2008). Lateral-torsional buckling of elastically restrained web-tapered I-beams. *Book of Abstracts of the Inaugural International Conference of the ASCE Engineering Mechanics Institute (EM 2008)*, Minneapolis, 18-21 May, 47 (full paper in USB flash drive Proceedings).
3. Andrade A., Challamel N., Providência P. and Camotim D. (2012). An analytical study on the elastic lateral-torsional buckling of polygonally depth-tapered strip cantilevers under multi-parameter point load systems. USB key drive *Proceedings of the 2012 Joint Conference of the Engineering Mechanics Institute and the 11th ASCE Joint Specialty Conference on Probabilistic Mechanics and Structural Reliability (EMI/PMC 2012)*, Notre Dame University, Indiana, 17-20 June.

Additional publications, dealing mostly with the material presented in chapters 2 and 3, are currently under preparation.

6.3 RECOMMENDATIONS FOR FUTURE RESEARCH

One immediate task lies ahead: to perform a more extensive comparison between the predictions of the developed one-dimensional models and the results of higher-dimensional finite element analyses (and, desirably, of experimental investigations as well) other than the (fairly limited) ones indicated at the end of § 4.2. This would allow a more comprehensive assessment of the merits, limitations and range of applicability of the one-dimensional models.

Once this task is completed, there is a wealth of challenging open problems for future research. One possible direction in which the models of chapters 2-4 can be extended, or modified, is to consider tapered thin-walled bars with closed cross-sections or with cross-sections combining closed cells and open branches. The extension into the

materially non-linear range can also be envisaged. With specific reference to chapter 4, the development of torsional and/or flexural-torsional buckling models for thin-walled columns and beam-columns is also particularly relevant. While the column case seems fairly straightforward and should not entail major theoretical developments beyond those presented in this thesis, the analysis of tapered beam-columns will require careful consideration of the effects of the pre-buckling deflections, namely (i) the amplification, due to the axial compressive force, of the primary bending moments and deflections, and (ii) the influence of the in-plane curvature on the flexural-torsional buckling strength.

The starting point in the development of the one-dimensional models of chapters 2 through 4 was a membrane shell theory (the parent theory in the induced-constraint approach, as we have called it). A significant contribution would be to investigate the consequences of starting from a more general shell theory, including both membrane and flexural behaviours – for instance, Koiter's shell theory. The need for the *ad hoc* addition of the term U_{SV} to the membrane strain energy would most likely disappear, thus increasing the inner consistency of the models. Moreover, the rather artificial gap currently existing between chapters 2-4 and chapter 5 would probably be bridged.

One of the fundamental assumptions (internal constraints) underpinning the one-dimensional models developed in chapters 2-4 is the absence of in-plane cross-sectional deformations (distortion). However, when the cross-sections are very slender or when there is incomplete cross-sectional support, significant distortion may occur unless adequate stiffening is provided. The extension of the models to account for this added behavioural complexity would be of major interest.

In a one-dimensional frame model, a joint is usually regarded as the *locus* where certain continuity conditions between the bars are to be specified. Therefore, the modelling of joints is inextricably interwoven with the modelling of the connected bars. Regarding the specification of the aforementioned continuity conditions, the incorporation of out-of-plane warping and in-plane cross-sectional deformations in the bar model poses major difficulties. Therefore, one further possible avenue of research is the investigation of the warping transmission and distortion at joints connecting non-aligned tapered thin-walled bars and exhibiting different stiffening configurations.

The analytical solutions obtained in chapter 5 should find an interesting and rather useful field of application in shape optimisation studies.

Finally, the development of rational design guidelines for tapered thin-walled members (columns, beams and beam-columns) is a subject of great practical relevance and, therefore, well worthy of a considerable research effort.